

Towards the development of a novel vaccine for *Trichuris* *trichiura*

A thesis submitted to The University of Manchester for
the degree of
Doctor of Philosophy (PhD)
in the Faculty of Biology, Medicine and Health

2019

Ayat Tariq Zawawi

School of Biological Sciences
Division of Infection, Immunity and Respiratory
Medicine

ProQuest Number: 28301589

All rights reserved

INFORMATION TO ALL USERS

The quality of this reproduction is dependent on the quality of the copy submitted.

In the unlikely event that the author did not send a complete manuscript and there are missing pages, these will be noted. Also, if material had to be removed, a note will indicate the deletion.



ProQuest 28301589

Published by ProQuest LLC (2020). Copyright of the Dissertation is held by the Author.

All Rights Reserved.

This work is protected against unauthorized copying under Title 17, United States Code
Microform Edition © ProQuest LLC.

ProQuest LLC
789 East Eisenhower Parkway
P.O. Box 1346
Ann Arbor, MI 48106 - 1346

Table of Contents

List of Figures.....	8
List of Tables.....	11
Abstract	14
Declaration	15
Copyright statement.....	15
Acknowledgements	17
Chapter One.....	18
Introduction.....	18
1.1 Human soil-transmitted helminths.....	19
1.2 <i>Trichuris trichiura</i> in humans	19
1.3 <i>Trichuris muris</i> in mice as a model of human trichuriasis	20
1.4 The lifecycle of <i>Trichuris</i> spp.....	20
1.5 <i>Trichuris</i> genome structure and shared antigens.....	21
1.6 Immune responses to <i>T. muris</i> infection	24
1.6.1 Elements contributing to resistance/susceptibility to <i>T. muris</i> infection	24
1.6.2 Acquired immunity to <i>T. muris</i>	26
1.6.3 Cytokines associated with resistance/susceptibility to <i>T. muris</i> infection	27
1.6.4 Other sources of Th2 cytokines	29
1.6.5 B-cells and production of IgG antibodies	31
1.7 Mechanisms of <i>T. muris</i> expulsion.....	31
1.7.1 Epithelial cell turnover	32
1.7.2 Intestinal muscle hyper-contractility	32
1.7.3 Goblet cells and mucus production	33
1.8 Experimental <i>Trichuris</i> vaccine candidates.....	35
1.9 Epitope-based vaccine against trichuriasis	37
1.10 Immunoinformatics and epitope prediction	39
1.10.1 B-cell epitopes prediction	39
1.10.2 T-cell epitopes prediction	40
1.11 Virus-like particle (VLP) as a promising vaccine delivery system	41
1.11.1 Key features of VLP which bestow promise as a vaccine delivery system.....	42
1.11.2 VLPs and the induction of humoral and cellular immune responses	43
1.12 Hepatitis B core (HBc) particle as a promising VLP platform	48

1.13 Thesis aim and objectives.....	50
Chapter Two.....	51
2.1 Mice	52
2.2 Parasite	52
2.2.1 Maintenance of <i>T. muris</i> Life Cycle.....	52
2.2.2 <i>Trichuris muris</i> Passage.....	52
2.2.3 Egg preparation.....	52
2.2.4 Assessment of egg infectivity.....	53
2.2.5 Preparation of Excretory/Secretary (E/S) Antigen	53
2.3 <i>In vivo</i> evaluation of mice vaccinated with 25 µg of pre-mixed VLPs (HBc-H ₁₁₂₋₁₂₈ , HBc-CBD ₃₆₋₅₂ , HBc-CBD ₁₂₄₃₋₁₂₅₉ , and HBc-CLSP ₁₄₃₋₁₅₈)	53
2.4 <i>In vivo</i> evaluation of mice vaccinated with 25 µg of pre-mixed VLPs (HBc-H ₁₁₂₋₁₂₈ , HBc-CBD ₂₄₁₋₂₅₇ , HBc-CLSP ₁₄₃₋₁₅₈ and HBc-CLSP ₃₉₈₋₄₁₆) emulsified with an equal volume of AddaVax™ adjuvant	53
2.5 <i>In vivo</i> evaluation of mice vaccinated with 50 µg of pre-mixed VLPs (HBc-CBD ₁₂₄₃₋₁₂₅₉ , HBc-CBD ₂₄₁₋₂₅₇ , HBc-CLSP ₁₄₃₋₁₅₈ and HBc-CLSP ₃₉₈₋₄₁₆)	54
2.6 Worm Burden	54
2.7 Serum collection and preparation	54
2.8 Mouse tail bleeding	54
2.9 Isolation and stimulation of cells	55
2.9.1 Isolation and stimulation of cells from mesenteric lymph nodes (MLN)	55
2.9.2 Isolation and stimulation of mouse bone marrow-derived Macrophages (BMDMs)	55
2.9.3 Isolation and stimulation of mouse bone marrow-derived Dendritic cells (BMDCs)	56
2.10 Flow Cytometry	57
2.10.1 BMDC and BMDM staining	57
2.11 Cytometric Bead Array (CBA)	58
2.12 Mouse Inflammation Cytometric Bead Array (CBA).....	58
2.13 LEGENDplex	58
2.14 ELISA measurement of <i>T. muris</i> -specific IgM, IgG1, and IgG2c	59
2.15 ELISA measurement of VLP-specific IgM, IgG1, and IgG2c ELISA	59
2.16 Semi-Dry western blot.....	60
2.17 Histology.....	60
2.17.1 Haematoxylin and Eosin staining of paraffin sections.....	60
2.17.2 Goblet cell staining of paraffin sections	61

2.17.3	Quantification of histological staining	61
2.18	HBC-insert plasmid construction.....	61
2.19	HBC-HP ₁₋₅₁₂ and HBC-mosaic plasmid construction	62
2.20	Transformation	69
2.21	Plasmid purification: QIAprep spin miniprep kit	69
2.22	DNA sequencing	69
2.23	Small-scale VLP expression	69
2.24	Large-scale VLP expression	70
2.25	Preparation of cell lysate	70
2.26	Stage 1 purification using StrepTrap™ affinity chromatography	70
2.27	Stage 2 purification using size exclusion chromatography (SEC)	71
2.29	10% Sodium Dodecyl Sulfate Polyacrylamide Gel Electrophoresis (SDS-PAGE)	71
2.30	Designed VLPs construction and solubility	71
2.31	ELISA-based endotoxin detection assay	72
2.32	Circular Dichroism spectropolarimeter (CD)	72
2.33	Transmission Electron microscopy (TEM)	72
2.34	Labelling VLPs with Fluorescein dye	73
2.35	Fluorescein-conjugated VLP internalisation and localisation in APCs using an Amnis ImageStreamX cytometer	73
2.36	Prediction of Physicochemical Properties	73
2.37	Procedures to reduce Endotoxin (LPS) contamination	73
2.38	Protein storage	74
2.39	Statistical analysis	74
	Chapter Three	75
3.1	Introduction.....	76
3.2	Aim and objectives	77
3.3	Methods.....	77
3.3.1	Search strategy	77
3.3.2	Construction of an epitope training set	79
3.3.3	Prediction of MHC-II T-cell epitopes	80
3.3.4	Evaluation and statistical analysis.....	80
3.4	Results	81
3.5	Discussion	85

3.5.1	Evaluation of available MHC-II binding prediction tools.....	85
3.5.2	Updates of the available <i>in silico</i> prediction tools	88
3.5.3	Applications of MHC-II prediction tools	88
3.6	Summary	89
Chapter Four		91
4.1	Introduction.....	92
4.2	Aim and objectives	92
4.2	Methods and results.....	93
4.2.1	Data acquisition and identification of potential virulent proteins	93
4.2.2	Identification of non-homologous proteins to human and mouse with high expression levels	93
4.2.3	Prediction of <i>Trichuris</i> MHC-II T-cell binding epitopes.....	94
4.2.4	Conservation and allergens	94
4.3	Discussion	108
4.3.1	The choice of secreted proteins as vaccine candidates	108
4.3.2	<i>Trichuris</i> proteins selected for epitope prediction	109
4.4	Summary	112
Chapter Five.....		113
5.1	Introduction.....	114
5.2	Aim and objectives	114
5.3	Results	115
5.3.1	Prediction of the recombinant VLP protein's physicochemical properties	115
5.3.2	Design of the native VLP (HBc-Ag)	119
5.3.3	Cloning and expression of the native VLP (HBc-Ag)	119
5.3.4	Purification of the native VLP (HBc-Ag)	120
5.3.5	Cloning and expression of HBc-Ag containing <i>Trichuris</i> antigens	121
5.3.6	Purification of VLP recombinant proteins	125
5.3.7	Endotoxin levels of the purified VLP recombinant proteins	127
5.3.8	Circular dichroism (CD) spectroscopy	128
5.3.9	Characterisation of VLP recombinant protein assembly by TEM	130
5.4	Discussion	133
5.4.1	Selection of <i>E. coli</i> for expressing VLP recombinant proteins.	133
5.4.2	Insertion capacity and solubility of the native VLP (HBc-Ag)	134

5.4.3 Assessing VLP recombinant proteins' structure, stability and assembly	134
5.5 Summary	135
Chapter Six.....	138
6.1 Introduction	139
6.2 Aim and objectives	140
6.3 Results	141
6.3.1 Activation of BMDCs by VLPs.....	141
6.3.2 Inflammatory cytokine production by BMDCs after stimulation with VLPs	144
6.3.3 Inflammatory cytokine production by BMDMs after stimulation with VLPs	146
6.3.4 Uptake of fluorescein-conjugated VLPs by BMDCs.....	149
6.3.5 Direct visualisation of VLP association and co-localization in APCs	151
6.4 Discussion	157
6.4.1 Dendritic cell activation by VLPs	157
6.4.2 Macrophage activation by VLPs.....	160
6.5 Summary	161
Chapter Seven	162
7.1 Introduction	163
7.2 Aim and objectives	164
7.3 Results	165
7.3.1 Experimental protocol for <i>in vivo</i> evaluation of vaccinating mice with 25 µg of pre-mixed VLPs expressing <i>Trichuris</i> MHC-II T-cell epitopes (HBc-H ₁₁₂₋₁₂₈ , HBc-CLSP ₁₄₃₋₁₅₈ , HBc-CBD ₁₂₄₃₋₁₂₅₉ , and HBc-CBD ₂₄₁₋₂₅₇)	165
7.3.2 Experimental protocol for <i>in vivo</i> evaluation of vaccinating mice with 25 µg of pre-mixed VLPs + <i>Trichuris</i> MHC-II T-cell epitopes (HBc-H ₁₁₂₋₁₂₈ , HBc-CLSP ₁₄₃₋₁₅₈ , HBc-CLSP ₃₉₈₋₄₁₆ , and HBc-CBD ₂₄₁₋₂₅₇) formulated with AddaVax™ adjuvant	179
7.3.3 Experimental protocol for <i>in vivo</i> evaluation of vaccinating mice with 50 µg of pre-mixed VLPs + <i>Trichuris</i> MHC-II T-cell epitopes (HBc-CBD ₁₂₄₃₋₁₂₅₉ , HBc-CBD ₂₄₁₋₂₅₇ , HBc-CLSP ₁₄₃₋₁₅₈ , and HBc-CLSP ₃₉₈₋₄₁₆).....	184
7.4 Discussion	206
7.4.1 Protection and immune responses to the VLPs+ T-cell epitopes vaccine candidates	206
7.4.2 VLP-based vaccines against parasite infections.....	210
7.5 Summary	211
Chapter Eight	213

2.11	Identification of novel <i>Trichuris</i> MHC-II T-cell epitopes as promising vaccine candidates 215	
2.12	VLP (HBc-Ag) as a promising vaccine delivery system	217
2.13	Identification of a novel VLP-based vaccine against trichuriasis	218
2.14	Prospects and challenges for anti- <i>Trichuris</i> vaccine design	219
2.15	Conclusions and future perspectives	221
References	222
Appendices Chapter 3:	261
Appendices Chapter 4:	271
Supplementary Table 4.1 Percentage conservation of the <i>T. muris</i> MHC-II T-cell epitopes (CLSP ₂₂₂₋₂₃₇ , CLSP ₄₃₃₋₄₅₀ , CLSP ₁₄₃₋₁₅₈ , CLSP ₄₂₄₋₄₄₃) to homologous <i>T. trichiura</i> proteins.....	271	
Appendices Chapter 7:	274
Appendix 7.1 Serum parasite-specific responses following vaccination of mice with VLPs expressing <i>Trichuris</i> T-cell epitopes.....	274
Appendix 7.2 Serum VLP+ T-cell epitope-specific responses following vaccination of mice with VLPs expressing <i>Trichuris</i> T-cell epitopes.....	277
Appendix 7.3 The cellular immune responses following vaccination of mice with VLPs expressing <i>Trichuris</i> T-cell epitopes and infection	278
Appendix 7.4 Crypt hyperplasia following vaccination of mice with VLPs expressing <i>Trichuris</i> T-cell epitopes	281
Appendix 7.5 Goblet cells hyperplasia in mice vaccinated with VLPs expressing <i>Trichuris</i> T- cell epitopes.....	283

Word count: 66.878

List of Figures

Figure 1.1 <i>Trichuris muris</i> life cycle.	21
Figure 1.2 Immune profiles during <i>Trichuris muris</i> infection.	34
Figure 1.3 Reverse Vaccinology (RV) strategy.	38
Figure 1.4 Key features of virus-like particle (VLP) as a promising vaccine delivery system.	43
Figure 1.5 The different immune responses induced by VLPs	47
Figure 1.6 A schematic representation of the HBc-Ag capsid arrangement as carriers for foreign epitopes (1QGT, Protein Data Bank).	48
Figure 2.1 The complete sequence of the native VLP (HBc-Ag) construct.	63
Figure 2.2: DNA construction for HBc-Ag inserted in N -terminally T7-tagged pET-17b vector from Novagen.	63
Figure 3.1 A PRISMA flow diagram of the systematic review screening process for restricted MHC-II T-cell bioinformatics prediction tools.	78
Figure 3.2 NetMHC-II 2.2 and IEDB tools performance.	83
Figure 4.1 The flow diagram of reverse vaccinology approach to identify potential vaccine candidates (MHC-II T-cell epitopes) from the <i>T. muris</i> genome.	95
Figure 5.1 SDS-PAGE analysis of the native VLP (HBc-Ag) after small-scale expression.	120
Figure 5.2 The native VLP (HBc-Ag) purification profile and SDS-PAGE analysis.	121
Figure 5.3 Protocol used for VLP recombinant proteins cloning, expression and purification	122
Figure 5.4 SDS-PAGE analysis of VLP recombinant proteins (HBc-CBD ₃₆₋₅₂ , HBc-CBD ₁₂₄₃₋₁₂₅₉ , HBc-CBD ₂₄₁₋₂₅₇ and HBc-H ₁₁₂₋₁₂₈) after small-scale expression.	123
Figure 5.5 SDS-PAGE analysis of VLP recombinant proteins (HBc-CLSP ₄₃₃₋₄₅₀ , HBc-CLSP ₂₂₂₋₂₃₇ , HBc-CLSP ₁₄₃₋₁₅₈ , HBc-CLSP ₄₂₄₋₄₄₃ and HBc-CLSP ₃₉₈₋₄₁₆) after small-scale expression..	123
Figure 5.6 SDS-PAGE analysis of HBc-Pfam ₂₅₆₋₂₇₃ after small-scale expression.	124
Figure 5.7 SDS-PAGE analysis of HBc-HP ₁₋₅₁₂ after small-scale expression.	124
Figure 5.8 SDS-PAGE analysis of HBc-mosaic after small-scale expression.	125
Figure 5.9 The VLP recombinant proteins (HBc-H ₁₁₂₋₁₂₈ , HBc-CBD ₃₆₋₅₂ , HBc-CBD ₁₂₄₃₋₁₂₅₉ and HBc-CBD ₂₄₁₋₂₅₇ , HBc-CLSP ₄₃₃₋₄₅₀ , HBc-CLSP ₁₄₃₋₁₅₈ , and HBc-CLSP ₃₉₈₋₄₁₆) purification profile and SDS-PAGE analysis.	126
Figure 5.10 The recombinant proteins (HBc-CLSP ₂₂₂₋₂₃₇ , and HBc-CLSP ₄₂₄₋₄₄₃) purification profile and SDS-PAGE analysis.	127
Figure 5.11 The secondary structure composition of the native VLP (HBc-Ag) and VLPs expressing <i>Trichuris</i> MHC-II T-cell epitopes.	129
Figure 5.12 Electron microscopy of negatively stained VLP recombinant proteins.	132
Figure 6.1 Representative gating strategy of mouse bone marrow-derived DCs (BMDCs) analysed by flow cytometry.	142
Figure 6.2 Phenotypic activation of BMDCs stimulated with VLPs compared to ES and LPS as positive controls.	143
Figure 6.3 Inflammatory cytokines production by mouse bone marrow-derived DCs (BMDCs) in response to VLPs.	145

Figure 6.4 Representative gating strategy for mouse bone marrow-derived macrophages (BMDMs) purity.....	147
Figure 6.5 Inflammatory cytokines productions by mouse bone marrow-derived macrophages (BMDMs) in response to VLPs.....	148
Figure 6.6 Uptake of VLPs by mouse bone marrow-derived DCs (BMDCs) analysed by flow cytometry.....	150
Figure 6.7 Representative images of fluorescein-conjugated VLPs internalisation in the BMDCs.	153
Figure 6.8 Representative images of fluorescein-conjugated VLPs internalisation in the BMDMs.	154
Figure 6.9 Representative images of fluorescein-conjugated VLPs co-localization in the BMDCs.	155
Figure 6.10 Representative images of fluorescein-conjugated VLPs co-localization in the BMDMs..	159
Figure 7.1 Experimental schedule and worm burden of mice vaccinated and challenged with a <i>T. muris</i> infection.....	166
Figure 7.2 Parasite-specific IgM, IgG1 and IgG2c serum antibodies levels at day 14.....	168
Figure 7.3 VLPs-specific IgM serum antibody levels at day 14 post-infection.....	170
Figure 7.4 Parasite-specific cytokine production by mesenteric lymph node cells from mice vaccinated with VLPs+ T-cell epitopes and control mice.....	172
Figure 7.5 The correlation of worm burden with parasite-specific Th2 and anti-inflammatory cytokine production from mice vaccinated with VLPs+ T-cell epitopes	173
Figure 7.6 Cytokine production by mesenteric lymph node cells from mice vaccinated with VLPs+ T-cell epitopes and control mice.	174
Figure 7.7 Changes in intestinal pathology in <i>T. muris</i> infected mice vaccinated with VLPs+ T-cell epitopes and control mice..	176
Figure 7.8 Quantification of goblet cell numbers in <i>T. muris</i> infected mice vaccinated with VLPs+ T-cell epitopes and control mice.....	178
Figure 7.9 Experimental schedule and worm burden of mice vaccinated and challenged with a <i>T. muris</i> infection.	180
Figure 7.10 Western blots of serum of vaccinated mice and control groups against <i>T. muris</i> ES..	182
Figure 7.11 Western blots of serum IgG from vaccinated mice and control groups specific for VLPs+ T-cell epitopes proteins.	183
Figure 7.12 Experimental schedule and worm burden of mice vaccinated and challenged with a <i>T. muris</i> infection.	186
Figure 7.13 Parasite-specific IgM and IgG1 serum antibodies levels at day -1.....	188
Figure 7.14 Parasite-specific IgM, IgG1 and IgG2c serum antibodies levels at day 14 post-infection.	189
Figure 7.15 Pre-mixed VLPs+ T-cell epitopes-specific IgM and IgG1 serum antibodies levels at day -1.	191
Figure 7.16 Pre-mixed VLP+ T-cell epitope-specific IgM, IgG1 and IgG2c levels at day -1.	192

Figure 7.17 Native VLP (HBc-Ag) and VLP+ T-cell epitope-specific IgM levels at day 14 post-infection (p.i.).....	193
Figure 7.18 Native VLP (HBc-Ag) and VLP+ T-cell epitope-specific IgG1 levels at day 14 post-infection (p.i.).....	194
Figure 7.19 Native VLP (HBc-Ag) and VLP+ T-cell epitope-specific IgG2c levels at day 14 post-infection (p.i.).....	195
Figure 7.20 Parasite-specific cytokine production by mesenteric lymph node cells from mice vaccinated with VLPs+ T-cell epitopes and control mice.....	198
Figure 7.21 Cytokine production by mesenteric lymph node cells from mice vaccinated with VLPs+ T-cell epitopes and control mice.	199
Figure 7.22 Cytokine production by mesenteric lymph node cells from mice vaccinated with VLPs+ T-cell epitopes and control mice.	200
Figure 7.23 Changes in intestinal pathology in <i>T. muris</i> infected mice vaccinated with VLPs+ T-cell epitopes and control mice.	202
Figure 7.24 Quantification of goblet cell numbers in <i>T. muris</i> infected mice vaccinated with VLPs+ T-cell epitopes and control mice.	204
Figure 7.25 Isolated lymphoid follicle-like structures' in <i>T. muris</i> infected mice vaccinated with VLPs+ T-cell epitopes and control mice.....	215
Figure 8.1 Reverse vaccinology strategy used to identify epitope-based vaccine against trichuriasis infection.....	217
Supplementary Figure 7.1 Parasite-specific IgG1 serum antibody levels at day -1	275
Supplementary Figure 7.2 Parasite-specific IgM, IgG1 and IgG2c serum antibodies levels at day 14 post-infection.....	276
Supplementary Figure 7.3 VLPs-specific IgM serum antibody levels at day 14 post-infection.	277
Supplementary Figure 7.4 Parasite-specific cytokine production by mesenteric lymph node cells from mice vaccinated with VLPs+ T-cell epitopes and control mice.....	279
Supplementary Figure 7.5 Cytokine production by mesenteric lymph node cells from mice vaccinated with VLPs+ T-cell epitopes and control mice.....	280
Supplementary Figure 7.6 Changes in intestinal pathology in <i>T. muris</i> infected mice vaccinated with VLPs+ T-cell epitopes and control mice.....	282
Supplementary Figure 7.7 Quantification of goblet cell numbers in <i>T. muris</i> infected mice vaccinated with VLPs+ T-cell epitopes and control mice.....	284

List of Tables

Table 2.1 Flow cytometry panel.....	57
Table 2.2 List of MHC-II T-cell epitope sequences and primers used to amplify the target.....	65
Table 2.3 The complete sequences of the selected antigen constructs obtained from GeneArt.....	66
Table 3.1 List of Keywords used in this review.....	79
Table 3.2 List of MHC-II epitope prediction tools and their number of publication, number of citations using Google Scholar, the online availability, last update, and community.....	82
Table 3.3 The sensitivity and probability of predicting MHC-II T-cell epitopes using SYFPEITHI, IEDB, NetMHC-II 2.2, and Rankpep prediction tools.....	84
Table 4.1 The prediction scores of MHC-II T-cell epitope (CBD1243-1259) containing three overlapping peptides predicted from chitin-binding domain containing protein (TMUE_s0281000600) using the IEDB prediction tool.....	97
Table 4.2 List of 219 identified <i>Trichuris</i> MHC-II T-cell peptides.....	98
Table 4.3 List of 10 <i>Trichuris</i> MHC-II T-cell epitopes which have potential as vaccine candidates.....	107
Table 5.1 The schematics design and physicochemical properties of the VLP recombinant constructs.....	116
Table 5.2 Endotoxin concentration of the purified VLP recombinant proteins determined by EndoLISA detection assay.....	128
Table 5.3 Summary of the VLP recombinant protein properties.....	132
Table 5.4: Summary of biophysical analysis of VLP constructs reported in the literature.....	139
Supplementary Table 3.1 List of websites and sources used to screen for MHC class I and II <i>in silico</i> prediction tools.....	261
Supplementary Table 3.2 MHC-II T-cell epitopes dataset used to evaluate the MHC-II <i>in silico</i> prediction tools used in this review.....	262
Supplementary Table 3.3 List of MHC class I and II and HLA binders peptides <i>in silico</i> prediction tools.....	269
Supplementary Table 4.1 Percentage conservation of the <i>T. muris</i> MHC-II T-cell epitopes (CLSP ₂₂₂₋₂₃₇ , CLSP ₄₃₃₋₄₅₀ , CLSP ₁₄₃₋₁₅₈ , CLSP ₄₂₄₋₄₄₃) to homologous <i>T. trichiura</i> proteins.....	271
Supplementary Table 4.2 Percentage conservation of the <i>T. muris</i> MHC-II T-cell epitopes (CBD ₃₆₋₅₂ and CBD ₁₂₄₃₋₁₂₅₉) to homologous <i>T. trichiura</i> proteins.....	272
Supplementary Table 4.3 Percentage conservation of the <i>T. muris</i> MHC-II T-cell epitope (CBD ₂₄₁₋₂₅₇) to homologous <i>T. trichiura</i> proteins.....	273
Supplementary Table 4.4 Percentage conservation of the <i>T. muris</i> MHC-II T-cell epitope (Pfam ₂₅₆₋₂₇₃) to homologous <i>T. trichiura</i> proteins.....	273
Supplementary Table 4.5 Percentage conservation of the predicted <i>T. muris</i> MHC-II T-cell epitope (H ₁₁₂₋₁₂₈) to homologous <i>T. trichiura</i> proteins.....	273

List of Abbreviations

aa	Amino acid
AAM	Alternatively activated macrophages
Ag	Antigen
ANN	Artificial neural network
ANOVA	Analysis of variance
APC	Antigen-presenting cell
BLAST	Basic local alignment search tool
BMDCs	Bone marrow-derived dendritic cells
BMDMs	Bone marrow-derived macrophages
BSA	Bovine serum albumin
CD	Cluster of differentiation
CD	Circular dichroism
CV	Column volume
DCs	Dendritic cells
dDCs	Dermal dendritic cells
DNA	Deoxyribonucleic acid
DNase	Deoxyribonuclease
<i>E. coli</i>	<i>Escherichia coli</i>
EDTA	Ethylene diamine tetra acetic acid
ELISA	Enzyme linked immunosorbent assay
EM	Electron microscopy
ES	Excretory-secretory
EV	Extracellular vesicle
fDCs	Follicular dendritic cells
Fig	Figure
FN-γ	Interferon gamma
GM-CSF	Granulocyte-macrophages colony stimulating
H&E	Hematoxylin and eosin stain
HBc-Ag	Hepatitis B core antigen
HBc-CBD	Hepatitis B core-chitin-binding domain
HBc-CLSP	Hepatitis B core-chymotrypsin-like serine protease
HBc-HP	Hepatitis B core-hypothetical protein
HBs-Ag	Hepatitis B surface antigen
HLA	Human leukocyte antigen
HMM	Hidden Markov models
hrs	Hours
IEDB	Immune epitope database and analysis
Ig	Immunoglobulin (e.g. IgM, IgG)
IL	Interleukin (e.g. IL-10)
ILC	Innate lymphoid cells
imDCs	Immature dendritic cells
IPTG	Isopropyl-β-D-1-thiogalactopyranoside
KDa	Kilodaltons
KO	Knockout mouse
LB	Luria Bertani broth
LCs	Langerhans cells
LNs	Lymph nodes
LPS	Lipopolysaccharide
MCP-1	Monocyte chemoattractant protein-1

M-CSF	Macrophage colony-stimulating factor
MHC	Major histocompatibility complex
Min	Minute
MIP	Macrophage inflammatory proteins
MIR	Major immunodominant region
MLAs	Machine learning algorithms
MLN	Mesenteric lymph node
Mw	Molecular weight
NTDs	Neglected tropical diseases
ON	Over-night
p.i.	Post-infection
PAMPs	Pathogen-associated molecular pattern motifs
PBS	Phosphate buffered saline
PBS-T	0.05% v/v Tween 20 in PBS
PCR	Polymerase chain reaction
PRRs	Pattern-recognition receptors
QM	Quantitative matrices
RELMβ	Resistin-like molecule β
RPMI	Roswell park memorial institute medium
RT	Room temperature
RV	Reverse Vaccinology
s.c	Subcutaneous
SCID	Severe combined immunodeficiency
SDS-PAGE	Sodium dodecyl sulphate-polyacrylamide gel electrophoresis
SEC	Size exclusion chromatography
SEM	Standard error of mean
SLPI	Secretory leukocyte protease inhibitor
spp	Species
STH	Soil-transmitted helminth
SVM	Support vector machine
T. muris	<i>Trichuris muris</i>
T. spiralis	<i>Trichinella spiralis</i>
T. trichiura	<i>Trichuris trichiura</i>
TB	Tuberculosis
TCR	T cell receptor
TEM	Transmission electron microscopy
Th	T helper cell (e.g. Th1, Th2 and Th17)
TLR	Toll-like receptors
TNF	Tumour necrosis factor
Treg	Regulatory T-cell
TSLP	Thymic stromal lymphopoietin
Tween 20	Polyoxyethylene (20) sorbitan monolaurate
U	Units
UniProt	Universal protein resource database
VLP	Virus-like particles
WAP	Whey acidic protein
WHO	World Health Organization
WT	Wild type

Abstract

Trichuris trichiura (whipworm) is a soil-transmitted helminth parasite that affects around 500 million people worldwide, resulting in disability and poor child development, especially in areas of poor hygiene and sanitation. The ideal vaccine to protect against *T. trichiura* in humans would include protein epitopes that elicit a protective T helper cell type 2 immune response. Herein, we used bioinformatics tools to identify candidate histocompatibility complex class II (MHC-II) molecule T-cell epitopes from known *Trichuris muris* proteins selected using inclusion and exclusion criteria. *T. muris* is the murine whipworm that is closely related to the human pathogen making it a relevant model parasite. A number of prediction tools are available for the identification of peptides that bind to MHC-II molecules. The lack of standardised methodology and the difficulty of MHC-II epitope prediction make the selection of an appropriate prediction tool difficult. This study reports a systematic review to choose the most appropriate tools to predict MHC-II epitopes. Subsequently, up to fifteen epitopes were predicted, from the selected *T. muris* proteins and expressed on Hepatitis B core antigen virus-like particles VLP (HBc-Ag). VLPs expressing *Trichuris* MHC-II T-cell epitopes were tested *in vitro* to address whether they could activate and be taken up by antigen-presenting cells (APCs).

VLPs expressing T-cell epitopes efficiently stimulated both antigen-presenting cells (dendritic cells and macrophages) to produce a broad range of pro-inflammatory and anti-inflammatory cytokines and were internalised and well co-localized in the lysosomes of both APCs.

I also immunised mice with VLPs+ T-cell epitopes prior to infection with *T. muris* to test the protective immune response *in vivo*. Notably, upon challenge infection, mice vaccinated with the VLPs+ T-cell epitopes showed a significantly reduced worm burden in the caecum and colon. Immunisation of mice with VLPs+ T-cell epitopes followed by infection induced *T. muris*-specific IgM and IgG2c antibody responses. High levels of VLPs+ T-cell epitopes-specific IgM and IgG2c, were also induced after challenge infections. The protection of mice by VLPs+ T-cell epitopes was also characterised by the production of mesenteric lymph node (MLN)-derived Th2 cytokines. The predicted epitopes identified using the right combination of immunoinformatics and immunogenicity screening tools have the potential to bring *T. trichiura* to a vaccine trial.

Declaration

I declare that no portion of the work referred to in the thesis has been submitted in support of an application for another degree or qualification of this or any other university or other institute of learning.

Copyright statement

- i. The author of this thesis (including any appendices and/or schedules to this thesis) owns certain copyright or related rights in it (the "Copyright") and s/he has given The University of Manchester certain rights to use such Copyright, including for administrative purposes.
- ii. Copies of this thesis, either in full or in extracts and whether in hard or electronic copy, may be made only in accordance with the Copyright, Designs and Patents Act 1988 (as amended) and regulations issued under it or, where appropriate, in accordance with licensing agreements which the University has from time to time. This page must form part of any such copies made.
- iii. The ownership of certain Copyright, patents, designs, trademarks and other intellectual property (the "Intellectual Property") and any reproductions of copyright works in the thesis, for example graphs and tables ("Reproductions"), which may be described in this thesis, may not be owned by the author and may be owned by third parties. Such Intellectual Property and Reproductions cannot and must not be made available for use without the prior written permission of the owner(s) of the relevant Intellectual Property and/or Reproductions.
- iv. Further information on the conditions under which disclosure, publication and commercialisation of this thesis, the Copyright and any Intellectual Property and/or Reproductions described in it may take place is available in the University IP Policy (see <http://documents.manchester.ac.uk/DoculInfo.aspx?DocID=24420>), in any relevant Thesis restriction declarations deposited in the University Library, The University Library's regulations (see <http://www.library.manchester.ac.uk/about/regulations/>) and in The University's policy on Presentation of Theses.

I dedicate this PhD thesis to:

my husband, Waleed Gazzaz

and

my children, Khalid and Salam

for their eternal love and support

Acknowledgements

First and foremost, I would like to express my sincere gratitude to my great supervisor Professor Kathryn Else for her continuous support, encouragement, for her patience, motivation, and immense knowledge. Her guidance helped me in all the time of research and writing of this thesis. I could not have imagined having a better advisor and mentor for my PhD journey. Besides my supervisor, I would like to thank my co-supervisors: Professor Jeremy Derrick and Professor Andy Brass for their insightful comments and encouragement. Without them precious support, it would not be possible to conduct this research.

Not to forget my colleagues for their wonderful collaboration. You supported me greatly and were always willing to help me. I would particularly like to thank: Iris Mair, Ruth Forman, Munirah Albaqshi, Leena Binmahfouz, Murtala Jibril, Faisal Minshawi, Angela Thistlethwaite, and Larisa Logunova.

A big and warm thank to my precious family, my amazing parents (Tarek and Salam), and my brothers (Islam and Mustafa). They have been my true inspiration and motivation to pursue my PhD studies. Finally, I would like to thank King Abdul Aziz University in Jeddah for funding this research.

Last but not least; I would like to thank my beloved husband Waleed Gazzaz and my beloved children (Khalid and Salam), for their patience, full support, and unconditional love.

Chapter One

Introduction

1.1 Human soil-transmitted helminths

Soil-transmitted helminths (STHs) are nematode worms that are transmitted to humans via faecal-contaminated soil (Jourdan et al., 2018). The four most prevalent STHs worldwide are the Hookworms *Necator americanus* and *Ancylostoma duodenale*, the roundworm *Ascaris lumbricoides*, together with the whipworm *Trichuris trichiura* (Brooker et al., 2006; WHO, 2005). Since 1980, the global health community have focused their research on ascariasis and neglected trichuriasis, despite the fact that trichuriasis is the second most common STH infection after ascariasis (John and Ralph, 1989). *Trichuris trichiura* is highly distributed throughout moist tropic and subtropic areas in the developing world, with the highest prevalence in sub-Saharan Africa, East Asia, India, China and South America (Bethony et al., 2006; Moser et al., 2015). Around 477 million people are estimated to be infected with *Trichuris* infection, with the highest intensity of infection seen in school-aged children (Alexander and Blackburn, 2019; Pullan et al., 2014).

1.2 *Trichuris trichiura* in humans

The whipworm *T. trichiura* has a simple, direct life cycle. Humans are the primary host, although some animals, such as lemurs, monkeys, and pigs have also been reported to carry the *T. trichiura* worms (Stephenson et al., 2000). Population-based studies demonstrate that the majority of people harbour asymptomatic light infection with less than 100 worms, while relatively fewer people have heavy chronic infections with more than 10,000 worms (Nokes et al., 1991; Stephenson et al., 2000). High-intensity chronic infections are associated with colitis, nutritional disturbances, growth retardation and *Trichuris* dysentery syndrome (TDS), which is characterised by rectal prolapse and chronic iron deficiency anaemia as a result of bleeding lesions (Khuroo et al., 2010).

There are several factors that affect the severity and intensity of infection, including environmental conditions, such as changes in climate and season (Brooker et al., 2006; Crompton and Savioli, 1993); demographic factors, such as the host's general health, gender, age and immunogenetics (Bundy et al., 1987; Williams-Blangero et al., 2002); and socioeconomic factors, such as education, occupation, sanitation, poverty, behaviour and household clustering (Drake et al., 2000; Montresor et al., 1998). The highest intensity of infection is seen in school-aged children (5–15 years of age) infected with *Trichuris* and *Ascaris*, while adults often carry the highest hookworm loads (Bundy et al., 1987a; 1987b; Nokes et al., 1991). These intensity/age profiles confirm that the prevalence and intensity of *T. trichiura* infection are age-related (Bundy et al., 1987a; 1988). The decrease in worms observed with age could be a result of less exposure to the parasites (behavioural changes) or development of acquired immunity (Anderson and May, 1985; Bundy et al., 1985; Quihui et al., 2006).

The primary method of preventing STH infections is enhancing individuals' health and standard of living. This can be done by improving sanitation and encouraging better health and hygiene behaviour and attitudes through educational programmes (Pullan et al., 2014). However, the cost of providing clean food and water and ensuring adequate sanitation makes it difficult for many developing countries to implement such initiatives (Farrell et al., 2018). Therefore, the World Health Organisation (WHO), in collaboration with several countries' ministries of health, are implementing global mass drug administration (MDA) programmes to reduce the worm burden of all at-risk

people, including preschool- and school-aged children and pregnant and breastfeeding women, living in areas in which STH infection is endemic (Farrell et al., 2018; Freeman et al., 2019; WHO, 2015). The WHO recommends periodic preventive treatment with either mebendazole or albendazole once annually and, occasionally, twice annually to prevent and reduce morbidity (Anto and Nugraha, 2019; Becker et al., 2018; Mehta, 2013; WHO, 2013). Although this preventive chemotherapy strategy is the most common and effective method to control the spread of STHs, several studies have shown that both drugs have low efficacy against *Trichuris* infections compared to *Ascaris* and hookworm infections (Patel et al., 2019; Speich et al., 2015; Turner et al., 2016). Also, field studies carried out in Myanmar, Vietnam and Zanzibar have shown that repeated treatment prevents hosts from developing acquired immunity at an earlier age, and the development of anthelmintic-resistant parasites (Albonico et al., 2003; Dunn et al., 2019; Flohr et al., 2007; Mrus et al., 2018). For these reasons and its massive annual cost, MDA alone is unlikely to provide a long-term solution for STH infection. Thus, there is considerable interest in developing vaccines against STHs, as these have the potential to be cost-effective, long-term immunological control strategies for controlling the outcome of drug therapy and reinfection (Becker et al., 2018; Dixon et al., 2008).

There is still no licensed vaccine against any human STH. However there are two hookworm vaccine candidates undergoing clinical trials (Diemert et al., 2017; Nagel and Diemert, 2018), and several pre-clinical vaccine candidates for *Schistosoma* species (spp) (Hotez et al., 2019) and *Ascaris* spp (Gazzinelli-Guimaraes et al., 2018; Tsuji et al., 2004). Comparatively, little progress has been made towards developing a vaccine for *T. trichiura*, although several pre-clinical studies have shown promising results, as discussed in section 1.8 (Briggs et al., 2018; Dixon et al., 2010).

1.3 *Trichuris muris* in mice as a model of human trichuriasis

Trichuris muris is the most useful experimental animal model used by immunologists to understand the host-parasite interaction and immune response to *Trichuris* infection as *T. muris* and *T. trichiura* are genetically, morphologically, antigenically, physiologically and epidemiologically similar (Foth et al., 2014; Hurst and Else, 2013; Klementowicz et al., 2012; Roach et al., 1988). Thus *T. muris* in the mouse is a well-defined model to investigate vaccine design.

1.4 The lifecycle of *Trichuris* spp

The host becomes infected upon ingesting food or soil contaminated with embryonated eggs (the infected stage). These eggs hatch in the host's large intestine and release larvae. The larvae penetrate the epithelial cells at the base of the crypts, feed and moult to L2, L3, L4 and finally to the adult stage (Stephenson et al., 2000). As adults, the anterior part of the worm body is embedded within epithelial cells, leaving the posterior end free into the lumen of the large intestine to facilitate mating and oviposition (Tilney et al., 2005). In humans, adult parasites usually take 60 to 70 days after infection to develop in the caecum. After copulation with males, females begin to oviposit between 3,000 and 20,000 unembryonated eggs per day in the caecum. Later, these eggs will pass with stool. Under moist, warm soil in the shade, the eggs will develop into the embryonated infective stage within 15 to 30 days. The lifespan of the *T. trichiura* adults is around one year. The

life cycle of *T. muris* in mice is similar to that of *T. trichiura* in humans, with adult worms developing 32 days post-infection (p.i.) (Klementowicz et al., 2012) (Figure 1.1).

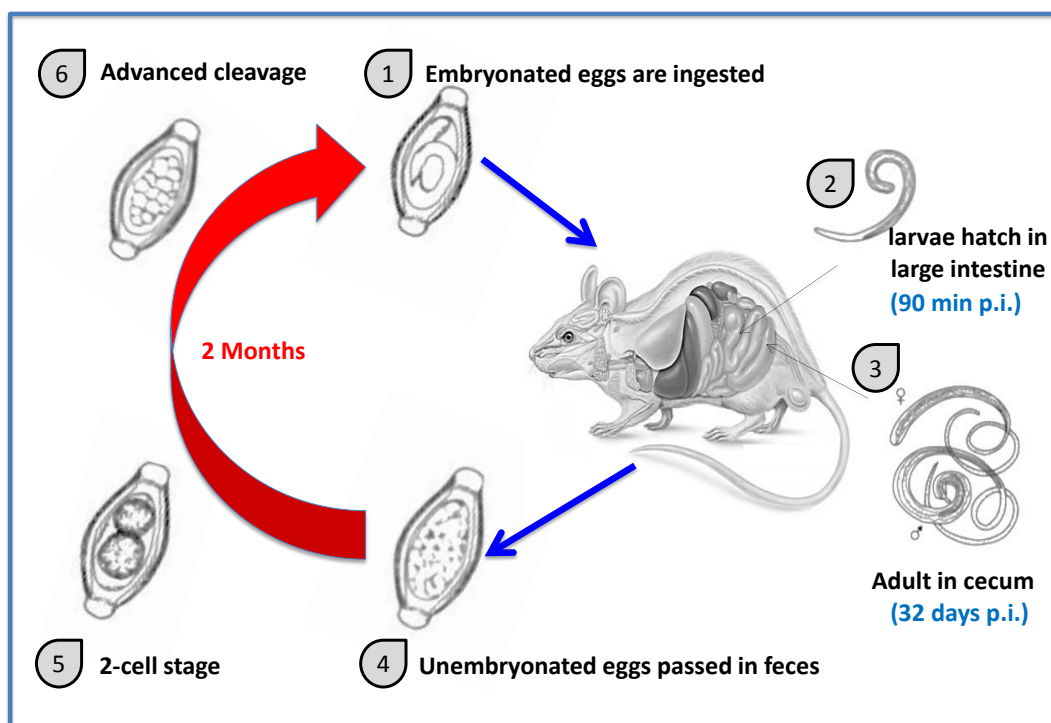


Figure 1.1 *Trichuris muris* life cycle. Infection occurs when the host (mice) ingests soil-contaminated food with the infective stage (Embryonated eggs) which hatches in the large intestine 90 min post infection (p.i.) and release larvae (L1) and undergoes three moults (L2-L4) in 22 days post infection. Finally, adult worms develop from infective eggs 32 days p.i. The female and male adult worms live in the cecum, with the anterior region embedded in the mucosa and posterior end free into the lumen to facilitate mating and oviposition. Female worms then release unembryonated eggs that pass in the faeces of the host to the soil where they develop and mature to the infective stage (Embryonated eggs) in 2 months.

1.5 *Trichuris* genome structure and shared antigens

Foth et al., Jex et al., Mitreva et al., Santos et al., Leroux et al., along with the recent Consortium report provided substantial genomic information for clade I parasitic nematodes (2014b; 2014; 2011; 2016; 2018; 2019). In 2014, Foth et al. sequenced the whole genome of *T. muris* using multiple parasites (1 male and 11 females) of the Edinburgh strain and then used it as a reference map to sequence a single *T. trichiura* male from an infected patient in Ecuador. The *T. muris* genome was found to be assembled into a 1,123 kb scaffold with an N50 of 1,580 kb and a total size of 85.00 Mb, whereas *T. trichiura* was assembled into a 3,711 kb scaffold with an N50 of only 71.2 kb and a total size of 75.18 Mb (Foth et al., 2014). Interestingly *T. muris* has specific chromosome-level synteny across nematode genera (Foth et al., 2014). The intrachromosomal rearrangement is found in other nematode lineages and is a hallmark of nematodes' genome evolution (Desjardins et al., 2013; Ghedin et al., 2007). In total, 11,004 and 9,650 genes were predicted in *T. muris* and *T. trichiura*, respectively, and the majority of *Trichuris* genes were orthologues for both species. Also, 2,350 genes of *T. trichiura* and 3,817 genes of *T. muris* appeared to be species-specific and were particularly enriched in hypothetical proteins with

unknown function, extracellular proteins, proteases and protease inhibitors (Foth et al., 2014). Furthermore, to investigate the immune response and the roles of T-helper (Th1 and Th2), Foth et al. characterised the gene expression in the caeca and mesenteric lymph nodes (MLNs) of chronically infected mice using RNA sequencing (RNA-Seq) (2014). Both tissues exhibited an upregulation of specific genes consistent with a Th1 response (Foth et al., 2014).

A recent comparative study of over 50 parasitic nematode genomes conducted based on 36 published genomes observed gene count expansion of proteases and protease inhibitors in all parasitic nematodes and platyhelminth families, which are involved in host tissue penetration and migration, immunomodulation and modification of the host environment (Consortium, 2019). The trypsin inhibitors have notably expanded as the most abundant protease inhibitor across parasitic nematodes and platyhelminths (Consortium, 2019; Jex et al., 2018; Zarowiecki and Berriman, 2015).

Transcripts of the anterior region of *T. muris* were dominated by chymotrypsin A-like serine proteases and by protease inhibitors, including secretory leukocyte peptidase inhibitors (SLPIs) (Foth et al., 2014). Chymotrypsin A-like serine proteases are more abundant in both *Trichuris* genomes, in terms of both gene number and gene expression, compared to other protease families and far higher than in other nematodes (Foth et al., 2014). These proteases are known to degrade the mucus barrier in the host's intestine by inhibiting intestinal mucins, Muc2 in particular (Drake et al., 1994; Foth et al., 2014; Hasnain et al., 2012). Chymotrypsin A-like serine proteases are also thought to play a role as an anticoagulant by regulating blood clotting in the host and in digesting host tissue, such as fibrinogen (Jex et al., 2014). Jex et al. sequenced the whole genome of a single adult male and a single adult female pig worm (*T. suis*) (2014). Interestingly, chymotrypsin A-like serine proteases were also upregulated in the stichosomes of *T. suis* species and exhibited high homology with *Schistosoma mansoni* serine protease 1 (SP1) and human kallikrein (Golias et al., 2007), which play a critical role in inhibiting inflammation (Jex et al., 2014).

The *T. muris* genome contains 44 genes that encode SLPI-like proteins, which are the most abundant protease inhibitors in the anterior region of *T. muris*, while *T. trichiura* contains 20 such genes and *Trichinella spiralis* contains 23 such genes (Foth et al., 2014). Host SLPI-like proteins are predominantly secreted by epithelial cells at mucosal sites, and they exhibit anti-inflammatory and antimicrobial properties and play a role in modulating inflamed intestinal tissue in the host (Williams et al., 2006). These proteins are also similar to the mesocentin protein of *Caenorhabditis elegans*, which plays a role in the development of the nervous system (Bénard et al., 2006).

Transcripts for DNase II-like proteins, which are known to be involved in mediation of DNA apoptosis in hosts, were also highly expressed in the anterior region of *T. muris*, similar to *T. spiralis* and *C. elegans* (Lai et al., 2009; Leroux et al., 2018; Liu et al., 2008). Three male-specific encoding proteins were also expressed: major sperm protein (MSP), which plays a role in the amoeboid locomotion of nematode sperm, and proteins with casein-kinase-related and epidermal-growth-factor-like domains that have roles in male mating functions (Hu et al., 2006; Leroux et al., 2018; Tarr and Scott, 2005). Chitin-binding domains that are associated with the

eggshell formation in *C. elegans* were also upregulated in female *T. muris* whipworms (Foth et al., 2014; Johnston et al., 2010). These proteins are also predominantly expressed in *T. trichiura*, *T. suis*, *Nippostrongylus brasiliensis* and *Heligmosomoides polygyrus* (Jex et al., 2014; Santos et al., 2016; Vannella et al., 2016). The transcriptional landscape of both larval stages (L2 and L3) is similar to adult worms' anterior region, except that high levels of ribosomal proteins, collagen and fibronectin-related proteins are expressed in the larval stages as a result of fast growth and cuticle synthesis (Foth et al., 2014; Johnston et al., 2010).

Santos et al. (2016) reported the first transcriptomic exploration of the adult stage of *T. trichiura* worms obtained from infected Ecuadorian children using next-generation sequencing technology and a *de novo* assembly strategy. Among the 40 most highly expressed protein-encoding genes of *T. trichiura*, a set of sequences that code vitellogenins, chitin-binding proteins and hypothetical proteins were identified as potential molecules for the development of a trichuriasis vaccine (Santos et al., 2016). Also, of the 40 most highly expressed protein-encoding genes of *T. trichiura*, 26 protein-coding genes were identified to be highly expressed and conserved among the adult stages of the three *Trichuris* species (*T. suis*, *T. muris*, and *T. trichiura*) (Caffrey et al., 2018; Ghedin, 2014; Howe et al., 2015; Santos et al., 2016). The *de novo* assembled transcriptome of *T. trichiura* also predicted 20 transcripts that code for proteins with immunomodulatory properties (Santos et al., 2016).

Using the nano-LC/mass spectrometry approach, it was also demonstrated that *Trichinella spiralis* shared 12 proteins in *T. trichiura* adult worm fractions (Santos et al., 2013). Among the homology identified proteins are macrophage migration inhibitory factor homologue (MIFH), fructose-bisphosphate aldolase (FBPA) and heat shock protein 70 (Santos et al., 2013). These proteins are known to have immunomodulatory effects that could lead to the development of novel drugs for allergic and autoimmune diseases (Hauet-Broere et al., 2006; Maizels and Yazdanbakhsh, 2003; Marques et al., 2008).

The anterior region of the *Trichuris* worm has a secretory gland and a storage organ called stichostome, which consists of a row of stichocytes along the oesophagus and serves as a rich source of excretory/secretory (ES) proteins (Lightowlers and Rickard, 1988). Such ES products are produced in the stichosome and are thought to be released through the anterior ends of adult whipworms embedded in the colonic mucosa to facilitate worm feeding (Jenkins and Wakelin, 1977; Lightowlers and Rickard, 1988; Wakelin and Selby, 1973). Due to intimate nature of the host-parasite interaction, extensive studies across many helminth spp have investigated the ES components that play a role in immunomodulation and inducing Th2-skewed immune response (Harnett and Harnett, 2017; McSorley et al., 2013). For example, proteomic analysis of ES proteins isolated from *T. suis* and *Trichinella pseudospiralis* at various life stages revealed that the most abundant classes were proteases, protease inhibitors and uncharacterised proteins (Leroux et al., 2018; Wang et al., 2017). In a different study, Tritten et al. (2017) sequenced *T. muris* ES microRNA (miRNA) isolated from vesicles/particles of the same size as exosomes using polymer precipitation and analysed the protein profiles by liquid chromatography-tandem mass

spectrometry. Most miRNA targets identified in *T. muris* exosome-like vesicles were conserved across nematodes and mouse miRNAs, which may reflect host-parasite interactions. Furthermore, comparison of *T. muris*-derived proteins and published nematode protein secretomes revealed a high degree of conservation at the functional level (Tritten et al., 2017). Tritten and co-workers (2017) also identified trypsin domains in the secretomes of *T. muris* that could have similar biological functions to the serine proteases. More recently, Eichenberger et al. (2018a) reported proteomic and genomic analyses of *T. muris* ES and extracellular vesicle (EV) fractions purified using OptiPrep. As expected, proteases (including serine proteases), trypsin domain-containing proteins and protease inhibitors were among the most abundant proteins found in the ES fractions of adult *T. muris* worms (Eichenberger et al., 2018b). Trypsin or trypsin-like domain proteins involved in proteolysis were also well represented in the *T. muris* EV fractions (Shears et al., 2018a). Also, the RNA content of EVs fractions characterised using the Illumina HiSeq platform demonstrated that hypothetical proteins with “unknown function” are among the most abundant domains in the mRNA transcripts mapping of *T. muris* genes (Eichenberger et al., 2018b).

Collectively, the wealth of information in genomics and proteomics provided an incentive to develop a vaccine for trichuriasis based on new methods.

1.6 Immune responses to *T. muris* infection

The type of immune response generated against *T. muris* is critical in promoting either susceptibility or resistance to infection. Thus, the vaccine candidate needs to be presented to the host's immune system in a manner that stimulates an appropriate protective immune response to infection. For *Trichuris*, this response is generally a Th2-dependent immune response, whereas a Th1 response is associated with chronic infection and increased immunopathology (Hurst and Else, 2013).

1.6.1 Elements contributing to resistance/susceptibility to *T. muris* infection

Studies conducted with inbred and gene knockout (KO) mice have greatly contributed to our knowledge of the importance of certain elements in relation to resistance/susceptibility to *T. muris* infection, including genetic background, gender, infection dose and parasite strain (Else, 2003; Hayes et al., 2014; Klementowicz et al., 2012).

First, it has been shown that there is considerable variation in the persistence of *T. muris* infection between mouse strains as well as within the same strain (Wakelin, 1967; Worley et al., 1962). The genetic background of the mouse strain plays a vital role in determining the protective immune response to infection (Klementowicz et al., 2012). For example, mice with a BALB/c genetic background are resistant to infection and rapidly expel parasites, while AKR and B10.BR strains are susceptible to infection (Else et al., 1993a; Else et al., 1992; Else and Wakelin, 1988). Also, the slower-responding C57BL/6 mouse strain is normally resistant to infection when infected with a high-dose of *T. muris* eggs; mice were able to expel the worms by day 21 p.i., and full protection was observed by day 28 p.i. (Bancroft et al., 2001; Cliffe et al., 2005; D'elia et al., 2009). Such variation in immune response between different mouse strains has helped in understanding the

different immune responses generated against *T. muris* and subsequent parasite expulsion (Zhan et al., 2014).

Second, several studies have clearly demonstrated that the gender of the host affects the immune response to *T. muris* infection. For example, Bancroft et al. (2000) showed that male and female interleukin 4 (IL-4) deficient mice with a BALB/c background responded differently to worm expulsion; males developed a chronic infection, while females expelled the *Trichuris* worms (Bancroft et al., 2000). This difference in expulsion kinetics is thought to be IL-13 dependent, as treating IL-4 deficient female mice with anti-IL-13 antibodies led to the development of chronic infection while administration of recombinant IL-13 enabled male IL-4 deficient mice to expel worms. This study thus highlighted the critical role of the Th2 cytokine (IL-13) in driving worm expulsion (Bancroft et al., 2000). Further research has revealed that sex hormones may play a role in the gender differences in worm expulsion. This can be explained as the male-related hormone dihydrotestosterone seems to decrease the ability of dendritic cells (DCs) to activate T-cells and promotes T-cell differentiation towards a Th1-type immune response via IL-18-dependent mechanisms in male IL-4 deficient mice. In contrast, the female-associated hormone 17-β-estradiol (E2) enhances the generation of a Th2 immune response *in vitro* (Hepworth et al., 2010).

Third, the infective dose can profoundly influence hosts' susceptibility or resistance to *T. muris* infection (Bancroft et al., 1994). It has been demonstrated that a low-dose of *Trichuris* infection (10–40 eggs) favours the development of a long-lasting chronic infection associated with a Th1 immune response, whereas a high-dose (200–400 eggs) favours the development of worm expulsion associated with a Th2 immune response in most laboratory strains, including C57BL/6 and BALB/c mice (Bancroft et al., 1994; Wakelin, 1973). Bancroft et al. (2001) also demonstrated that the fate of a secondary infection depends on the level of the primary infection. Interestingly, BALB/K mice were able to develop a protective immunity when infected with a high-dose of *T. muris* followed by a low-dose, whereas mice were susceptible to a high-dose if a low-dose was administered first (Bancroft et al., 2001). BALB/K and C57BL/6 mice were also able to develop protective immunity after administration of a repeated 'trickle' of low-dose infections (Bancroft et al., 2001). In contrast, susceptible AKR mice and immuno-compromised strains, such as severe combined immunodeficient (SCID) mice, were unable to expel high or low doses of *Trichuris* infections (Bancroft et al., 2001).

Fourth, *T. muris* isolates can influence the hosts' immune response to infection (Klementowicz et al., 2012). Most inbred mouse strains, including B10.BR, CBA and C57BL/10, are susceptible to a high-dose of the Sobreda (S) isolate and resistant to the Edinburgh (E) and Japan (J) isolates (Bellaby et al., 1996; D'elia et al., 2009; Koyama and Ito, 1996). S-isolate-infected mice developed Th1 immunity characterised by production of high levels of interferon gamma (IFN-γ), secretion of anti-parasite serum IgG2c and an increased number of regulatory T cells (Tregs) in the gut (Bellaby et al., 1996; D'elia et al., 2009; Johnston et al., 2005; Koyama and Ito, 1996). On the other hand, E- and J-isolate-infected mice developed Th2 immunity characterised by the production of high levels of IL-5 and secretion of anti-parasite serum IgG1 (Bellaby et al., 1996; D'elia et al., 2009). The *T. muris* E isolate was used in all the *in vivo* experiments conducted in the current thesis.

Overall, *T. muris* is a helpful tool for understanding the components involved in the mediation of susceptibility/resistance to *Trichuris* infection, and it serves as a model of cytokine-mediated immunity to all gastrointestinal nematodes (Cliffe and Grencis, 2004).

1.6.2 Acquired immunity to *T. muris*

In the context of acquired immune responses, Wakelin was the first researcher who demonstrated that more than 70% of outbred Schofield mice expelled *T. muris* and developed protective immunity to primary and secondary infections, with only 30% of the mice were susceptible to infection (Wakelin, 1967). Immunity was completely suppressed by administration of an immunosuppressive agent (cortisone acetate) (Selby and Wakelin, 1973). Subsequently, several studies revealed that immunity can be transferred by antiserum and mesenteric lymph node cells (MLNCs) taken from infected animals and highlighted the importance of T-cells in mediating *T. muris* expulsion (Else and Grencis, 1991; Lee et al., 1983; Selby and Wakelin, 1973). For example, Yoichi showed that congenitally athymic (nude) mice were susceptible to *T. muris* infection unless they received thymus, MLNC or spleen cells, while phenotypically normal mice were resistant to *T. muris* infection (1991). This and similar studies confirm that immunity to *T. muris* is thymus-dependent.

Serial studies subsequently highlighted the role of CD4+ T helper cells and CD8+ cytotoxic T-cells in mediating cellular protective immunity against *T. muris* (Humphreys et al., 2004). For instance, Koyama et al. (1995) depleted CD4+ and CD8+ T-cells *in vivo* in BALB/c mice. Depletion of CD4+ T-cells, but not CD8+ T-cells, resulted in suppression of worm expulsion, suggesting that CD4+ T-cells, and not CD8+ T-cells, mediate protective immunity against *T. muris* infection (Koyama et al., 1995). Also, Else and Grencis (1996b) demonstrated that adoptive transfer of pure populations of CD4+ T-cells protected SCID mice from *T. muris* infection in the complete absence of antibodies and B-cells. Another study demonstrated that CD4+ T-cells are localised at the site of infection (large intestinal mucosa) to confer protection against larval stages of *T. muris* (Betts and Else, 2000; Svensson et al., 2010). Interestingly, inhibition of the molecules necessary for activated CD4+ T-cell migration to the gut-associated lymphoid tissue, including the gut homing receptors (β 7 and α E integrins) and the gut homing ligand MAdCAM-1, completely abrogated the ability of transferred CD4+ T-cells to confer resistance in SCID mice (Betts and Else, 2000). Furthermore, CD4+ T-cells localization to the site of infection is dependent on the Gai-coupled receptors; however, neutralization of the most abundantly expressed chemokine receptors (CCR6 and CXCR3) by CD4+ T cells in the MLN, which are involved in gut homing by T-cells, did not prevent expulsion of worms (Svensson et al., 2010). Humphreys and Grencis (2002) also demonstrated that C57BL/6 mice become more susceptible to infection with age due to a decreased ability of CD4+ T-cells to respond to stimulation *in vitro* and were less able to proliferate and polarise into Th2 cells.

Collectively, the studies described in this section and others confirm the role of CD4+ T lymphocytes in the development of protective immunity against *T. muris*.

1.6.3 Cytokines associated with resistance/susceptibility to *T. muris* infection

Based on cytokine production patterns, naïve CD4+ T-cells can be differentiated into four subsets: T helper 1 (Th1), T helper 2 (Th2), T helper 17 cells (Th17) and regulatory T-cells (Treg) (Harrington et al., 2005; Street and Mosmann, 1991). Early studies comparing susceptible versus resistant mouse strains to *T. muris* infection provided initial evidence that both Th1 and Th2 are associated with susceptibility and resistant immune responses to *T. muris* infections (Else et al., 1994; Grencis, 2001; Koyama et al., 1995; Scott and Kaufmann, 1991). It is now well documented that resistance to *T. muris* infection is promoted by generation of a Th2 immune response and secretion of the Th2 cytokines IL-4, IL-5, IL-6, IL-9, IL-10 and IL-13 and tumor necrosis factor α (TNF- α), whereas susceptibility to infection is promoted by generation of a Th1 immune response and production of the Th1-associated cytokines IFN- γ and IL-18 (Bancroft et al., 2001; Dixon et al., 2010; Gause, 2003; Licona-Limon et al., 2017). In humans, host susceptibility and susceptibility to reinfection have also been linked to whole-blood cytokine responses. Susceptible individuals infected with *T. trichiura* are characterised by poor Th2 response and a negative association between IL-5 and IL-13 responses and infection, suggesting that humans exhibit a protective Th2 response, similar to mice (Faulkner et al., 2002; Jackson et al., 2004a; Turner et al., 2002).

One of the Th2 cytokines produced in response to resistance to infection, IL-5, is involved in the inducing eosinophilia during *T. muris* and *T. trichiura* infection (Else and Grencis, 1991; Jackson et al., 2004b; Svensson et al., 2011). However, IL-5 appeared not to be essential for worm expulsion, as treatment with anti-IL-5 monoclonal antibodies had no effect on worm clearance in resistant BALB/k mice (Betts and Else, 1999). Furthermore, no difference in worm expulsion was observed following infection in CCL11-deficient and CCL11 IL-5 double-deficient mice (Dixon et al., 2006). Therefore, despite being a useful Th2 cytokine hallmark of helminth infection, IL-5 is not thought to play a critical role in mediating worm expulsion.

Several studies have also assessed the importance of IL-4 and IL-13 in promoting *T. muris* expulsion. IL-4 and IL-13 share a sequence homology and functions associated with type 2 responses (Rao and Avni, 2000). For example, early studies demonstrated that both IL-4 and IL-13 KO mice are susceptible to *T. muris* infection (Bancroft et al., 1998). Administration of an IL-4 complex to susceptible AKR mice resulted in the development of a Th2 response and enabled worm expulsion, and blocking IL-4 function in resistant BALB/k mice prevented the generation of a protective immune response (Else et al., 1994; Grencis, 1993). Other studies have highlighted the several effector functions of IL-4 in mast cell (Lorentz et al., 2000), goblet cell responses (Dabbagh et al., 1999), and stimulation of intestinal muscle hypercontractility (Akiho et al., 2002). Bancroft et al. (2000) found that IL-4/- mice with a BALB/c background were able to expel *T. muris* worms through IL-13-mediated responses, inferring that IL-13 plays a prominent role in *Trichuris* infection. However, an earlier study showed that IL-13 KO mice failed to expel *T. muris* worms despite generating a Th2 response involving the production of IL-4, IL-5 and IL-9 and high levels of serum IgG1 and IgE p.i. (Bancroft et al., 1998). Other studies have provided evidence that IL-13 plays a role in increasing epithelial cell turnover and producing mucins to promote worm expulsion (Bancroft et al., 2000; Bancroft et al., 1998; Hasnain et al., 2011a).

Another cytokine that plays a major role in resistance to *T. muris* is IL-9. An early study by Faulkner et al. (1998) demonstrated that the MLNs of resistant BALB/K mice express high levels of IL-9 as early as day 4 p.i. compared to susceptible AKR mice (Faulkner et al., 1998). Furthermore, treating AKR mice with an IL-9 complex resulted in a reduction in worm survival (Faulkner et al., 1998). Moreover, the importance of IL-9 has been illustrated in the stimulation of intestinal smooth muscle contractility, which drives *T. muris* expulsion but not goblet cell hyperplasia and mucosal mast cell protease-1 production (Khan et al., 2003; Richard et al., 2000). Thus, impaired IL-9 expression often results in chronic helminth infection (Li et al., 2017). Collectively, these findings clearly confirm the central role of Th2 response in protective immunity to trichuriasis.

The regulatory molecule IL-10, which is produced by Tregs, B-cells and DCs, has been shown to play a role in both resistance and survival during *T. muris* infection (Schopf et al., 2002). Mice deficient in IL-10 were susceptible to *T. muris* infection characterised by elevated levels of IFN- γ and TNF- α , and they displayed fatal intestinal pathology (Schopf et al., 2002). However, both IL-10 and transforming growth factor- β (TGF- β) can be detected in the large intestine during *T. muris* infection, and seem to play a role in regulating immunity to *T. muris* infection (Collison et al., 2010; Veldhoen et al., 2008). In another study, an increasing number of Foxp3+ regulatory T-cells during chronic infection was found to be advantageous for the host as this minimised gut damage (D'elia et al., 2009). However, Treg cells are not considered to be critical for protection (Worthington et al., 2013).

It has been further demonstrated that the role of TNF- α in susceptibility/resistance to *Trichuris* infection is context-dependent, with high levels of TNF- α detected in susceptible hosts during Th1 response (Artis et al., 1999a; Hayes et al., 2007). Hayes et al. (2007) showed that mice deficient in TNF- α receptor (p55/p75) with a C57BL/6 background are susceptible to *T. muris* infection, but that this phenotype can be restored by IL-13 administration. *In vivo* treatment of resistant C57BL/6 mice with anti-TNF- α monoclonal antibodies significantly prevented worm expulsion without altering the magnitude of the type 2 response compared to control mice treated with PBS (Artis et al., 1999a). Furthermore, female susceptible BALB/c IL-4 KO mice (in which expulsion is mediated by IL-13) that were infected with *T. muris* and treated with recombinant TNF- α were able to clear the infection (Artis et al., 1999a). This suggests that TNF- α plays a role in IL-13-mediated anti-*T. muris* effector responses (Artis et al., 1999a). Although TNF- α may enhance either Th1 or Th2 during an ongoing immune response to *T. muris* infection, it is not necessary for developing immunity.

Equally importantly, IL-12, IL-18 and IFN- γ are associated with Th1 response and the development of susceptibility to infection (Bancroft et al., 2004; Belladonna et al., 2002). In one study, *in vivo* treatment of resistant mice with recombinant IL-12 promoted the development of chronic intestinal nematode infection (Bancroft et al., 1997). In contrast, IL-12 KO mice have been reported to be capable of expelling *T. muris* parasites, regardless of whether they were administered a high- or low-dose infection (Bancroft et al., 2001; Helmby et al., 2001). Helmby et al. (2001) also suggested that IL-18 promotes the development of *Trichuris* chronic infection by down-regulating IL-13. Furthermore, Else et al. (1994) provided the first evidence of the critical role of IFN- γ in developing chronic infection, as depletion of IFN- γ in susceptible AKR mice resulted in the expulsion of the

parasite. Collectively, Th1 cytokines (IL-12, IL-18 and IFN- γ) are hallmarks of a type 1 immune response, whereas Th2 cytokines (IL-4, IL-5, IL-9 and IL-13) are hallmarks of a type 2 immune response and the generation of worm expulsion in *T. muris* infection.

1.6.4 Other sources of Th2 cytokines

The key factors that are essential for generation of a protective Th2 immune response have not been fully characterised, with many different cell types implicated, including mast cells, eosinophils, natural killer cells (NKs), innate lymphoid cells (ILCs), dendritic cells (DCs), basophils and macrophages (Grencis et al., 2014).

Increased numbers of mast cells and eosinophils are typical in helminth infection and during *T. muris* infection (Mukai et al., 2016), but neither cell type has been shown to play a critical role in protective immunity against *T. muris* (Betts and Else, 1999; Knight et al., 2000). For example, Hepworth et al. (2012) demonstrated that mice deficient in mast cells were characterised by increased worm burden and decreased levels of epithelial IL-25, IL-33 and thymic stromal lymphopoitin (TSLP) following *T. muris* infection. Furthermore, Svensson et al. (2001) demonstrated that eosinophils accumulate faster and in greater numbers in the MLNs of *T. muris*-resistant BALB/c mice compared to susceptible AKR mice. However, mice deficient in eosinophils (Δ dblGATA-1 mice) were still able to expel *T. muris* (Svensson et al., 2011). Collectively, these data suggest that mast cells and eosinophils do not play a critical role in parasite expulsion within this infection system.

It has also been hypothesised that NK T-cells may play an essential role in driving Th2 responses that produce protective immunity against *T. muris* (Hepworth and Grencis, 2009). However, depletion of NK1.1+ cells in resistant mice (B10.BR) by anti-NK1.1 monoclonal antibody injection failed to induce the mice to develop susceptibility (Koyama, 2002). This implies that, in the presence of *T. muris*, NKs are not involved in the induction of Th2 response and the development of parasite expulsion.

New insights highlight that the role of the ILCs, which are mainly driven by IL-25 and IL-33 production, is associated with Th2 response and development of resistance to *T. muris* infection (Humphreys et al., 2008; Minutti et al., 2017; Saenz et al., 2010; Spencer et al., 2014). Mice deficient in either cytokine (IL-25 or IL-33) exhibit delayed worm expulsion, while treating susceptible mice during the early stages of infection with either recombinant IL-25 or IL-33 promoted Th2 immunity and worm expulsion (Fallon et al., 2006; Humphreys et al., 2008; Owyang et al., 2006). Chronically infected IL-25-deficient mice developed severe infection associated with heightened expression of IFN- γ and IL-17 and a significant reduction in IL-4 and IL-13 Th2 cytokines (Owyang et al., 2006). However, there is limited evidence regarding the role of Th17 in protection against *T. muris* infection (Bouchery et al., 2014).

Intestinal epithelial cells (IECs) are able to sense *T. muris* infection and initiate Th2 cell-mediated immunity through the release of TSLP, IL-25 and IL-33, which promotes the development, proliferation and activation of ILC2s, basophils, mast cells, eosinophils and DCs in the early phases of infection (Taylor et al., 2009; Zaph et al., 2007).

The kinetics of DCs may also be important for regulation of intestinal immune responses by processing antigens, migrating to MLNs upon activation and priming naïve T-cells that subsequently drive adaptive immunity (Joeris et al., 2017). Intestinal DCs can be classified into three distinct subsets based on their expression of CD11b and CD103 and either interferon regulatory factor 4 or 8 (IRF4 or IRF8) (Joeris et al., 2017). There is some controversy about the importance of DCs in triggering Th2 responses during *T. muris* infection. For example, there is evidence that the IL-27 produced by DCs during *T. muris* infection directly suppresses CD4+ T-cell proliferation and Th2 cytokine production and promotes the development of susceptibility and a Th1 immune response (Artis et al., 2004a; Bancroft et al., 2004). Furthermore, depletion of CD11c+ DC cells during *T. muris* infection resulted in normal expression of Th2 cytokines (IL-4 and IL-5) and expulsion of *Trichuris* worms, suggesting that DCs were not involved in priming CD4+ T-cells (Perrigoue et al., 2009). However, it was previously reported that DCs mobilise to the site of infection via epithelial chemokine production more quickly in resistant mice than in susceptible ones (Bowcutt et al., 2014; Cruickshank et al., 2009). Also, recent studies demonstrated a dominant role for IRF4-dependent CD11b+ DCs in the induction of Th2 immunity, notably during infection with *T. muris* (Demiri et al., 2017; Mayer et al., 2017). Another study found that IRF8-dependent CD103+ DCs promoted *T. muris* chronicity by generating type 1 immunity with helper CD4+ T-cells and cytotoxic CD8+ T-cells (Luda et al., 2016).

It has, however, been suggested that basophils are more important than DCs for priming CD4+ T-cells. Data indicates that basophils expressing major histocompatibility molecules (MHC) class II in draining LNs upon activation of the immune system play an important role in promoting Th2-dependent immunity to *T. muris* by producing TSLP and IL-4, which facilitate DC-mediated development (Perrigoue et al., 2009; Sokol et al., 2009; Webb et al., 2019; Wynn, 2009). For example, Siracusa et al. (2001) demonstrated that TSLPR KO mice exhibited impaired *Trichuris* worm expulsion due to a decreased number of basophils and decreased levels of IL-5 and IL-13 during acute *T. muris* infection. However, adoptive transfer of basophils into TSLPR KO mice led to a reduction in worm numbers (Siracusa et al., 2011).

Because macrophages exhibit diverse biological functions such as antigen-presenting cells (APCs), phagocytosis, production of cytokines and in tissue repair, it is not easy to predict their role in immunity to *T. muris* infection (Faz-Lopez et al., 2016; Noel et al., 2004). However, alternatively activated macrophages (AAMs) have been reported to have several roles in type 2 immune responses induced by IL-4 and IL-13 in intestinal nematode infections (Faz-Lopez et al., 2016; Kreider et al., 2007). Specifically, AAMs are involved in tissue remodelling, repairing the tissue affected by large extracellular nematodes, limiting of damage and inflammatory responses, and smooth muscle hypercontractility to promote nematode expulsion (Kreider et al., 2007; Zhao et al., 2008). Interestingly, larger numbers of macrophages were found accumulated in the lamina propria of resistant BALB/c mice to *T. muris* infection compared to susceptible AKR mice (Little et al., 2005). However, Bowcutt et al. (2011) found that using a cell-specific targeting strategy, arginase-1 deficiency in macrophages had no effect on resistance to *T. muris* infection, suggesting that macrophages have a possible arginase-independent role in the immune response to *T. muris*.

1.6.5 B-cells and production of IgG antibodies

The role of B-cells and B-cell-derived antibodies in mediating immune responses to *T. muris* has received a great amount of attention. However, it has been postulated that the role of B-cells in the immune response to *Trichuris* infection is context-dependent (Sahputra et al., 2019; Sorobetea et al., 2018). The number of B-cells is significantly elevated in both *T. muris*-resistant and susceptible mice strains (Else and Grencis, 1991), with a marked increase in the production of anti-*T. muris* antibodies (IgA and IgG subclasses) in MLNs as early as 14 and 21 days p.i. (Blackwell and Else, 2001; Koyama et al., 1999). It was also found that parasite-specific IgE was negatively correlated with infection intensity and positively correlated with age, suggesting that IgE is associated with protection (Faulkner et al., 2002; Turner et al., 2002).

It is widely accepted that IgG1 is correlated with the development of Th2 response in resistance and IgG2 is correlated with the development of Th1 response in susceptibility to *T. muris* infection (Blackwell and Else, 2002). An early study by Lee et al. (1983) showed that transfer of enriched T-cell populations from MLNCs, but not B-cell enriched populations from *T. muris*-infected animals, to naïve recipients transferred immunity to infection. It has also been demonstrated that adaptive transfer of only CD4+ T-cells purified from BALB/c donor mice to SCID mice (which are deficient in B- and T-cells) was sufficient to expel *T. muris* worms, suggesting that antibodies are not essential for expulsion (Else and Grencis, 1996). However, a different study demonstrated that μMT mice on a C57BL/6 background which are not able to produce B-cells did not expel *T. muris* worms efficiently (Blackwell and Else, 2001). When these animals were reconstituted with B-cells, however, they were able to expel most of the worms; expulsion was associated with Th2 response and production of a high level of specific anti-*T. muris* antibodies (Blackwell and Else, 2001). Furthermore, the adoptive transfer of serum from resistant mice provided high levels of protection to susceptible strains of mice (Blackwell and Else, 2001; Selby and Wakelin, 1973). Early studies have also shown that parasite-specific IgG1 is involved in the memory response of the adaptive immune system in resistant strains following primary infection (Else et al., 1993a). A recent study supported the role for B-cells in the generation of protective immunity to *T. muris* infection and suggested that the Th2 type immune response is dependent on the host's genetic background and is independent of antibodies (Sahputra et al., 2019).

Taken together, the findings of the above-mentioned studies suggest that B-cells might play a role in stimulating the generation and/or polarisation of T-cell responses by either cytokine secretion or antigen presentation. This is probably most effective in mice with secondary *T. muris* infection (Sorobetea et al., 2018).

1.7 Mechanisms of *T. muris* expulsion

Once adaptive immunity has been stimulated in the local lymph nodes (LNs), activated effector cells must home back to the site of the infection 'large intestine' where worms expulsion can take place (Sorobetea et al., 2018). A variety of Th2 regulated immune-mediated mechanisms are characterised for *T. muris* expulsion including epithelial cell turn over (Cliffe and Grencis, 2004;

Cliffe et al., 2005), increased muscle hyper-contractility (Khan et al., 2003), goblet cell hyperplasia and production of mucins (Artis et al., 2004b).

1.7.1 Epithelial cell turnover

Mucosal layers come into contact with early larval stages of *T. muris* at the start of the infection and/or adult stage during the reproductive phase of infection. This first line of defence is controlled by the Th2 response (Artis et al., 1999b). Because of the intimate relationship between parasites and the epithelial cells located on the surface of the intestine, it is reasonable to suggest that intestinal epithelial cells are an intrinsic barrier to infection (Cliffe and Grencis, 2004).

Susceptible AKR mice with chronic infection are characterised by crypt hyperplasia under the immune control by the pro-inflammatory cytokine IFN- γ , to regulate epithelial cell proliferation and apoptosis (Artis et al., 1999b; Cliffe et al., 2005). Crypt hyperplasia has also been observed in mice protected from infection by subcutaneous (s.c) immunisation with ES emulsified with Freund's incomplete adjuvant (ES/FIA) and PBS/FIA, followed by *Trichuris* infection (Dixon et al., 2010). However, no such dramatic changes were observed in the guts of naturally resistant mice. It has been demonstrated that increased epithelial turnover, which results in short crypts, is an essential mechanism of expulsion in natural resistance BALB/c mice, as it physically forces worms out, leading them to move from the base to the tip of crypts before being shed into the lumen (Cliffe et al., 2005). Cliffe and co-workers (2005) also highlighted the importance of this mechanism using IL-4 KO and IL-13 KO mice and demonstrated that acceleration of epithelial cell turnover is IL-13-dependent but IL-4-independent. Furthermore, treating both AKR and SCID mice with anti-CXCL10 antibodies (IFN- γ -induced protein 10) associated with a Th1 response, resulted in earlier up-regulation in epithelial cell turnover and worm expulsion (Cliffe et al., 2005).

Bell and Else (2001) also demonstrated that the indoleamine 2, 3-dioxygenase (IDO) enzyme gene was up-regulated in the gut during chronic *T. muris* infection. The authors also demonstrated an increase in the rate of colonic epithelial cell turnover after treating susceptible SCID mice with an IDO inhibitor that leads to parasite expulsion, suggesting that IDO may also play a direct role in controlling epithelial cell turnover (Bell and Else, 2011). Taken together, the findings described above highlight the role of epithelial cell turnover as a major mechanism of *T. muris* expulsion.

1.7.2 Intestinal muscle hyper-contractility

It has been suggested that increased contractility of the smooth muscle cells lining the wall of the intestine may be an essential mechanism for *T. muris* and *T. spiralis* expulsion (Khan et al., 2003; Khan et al., 2005; Khan et al., 2001). Studies have shown that muscle contraction is an immune-mediated mechanism controlled by IL-4, IL-13 and IL-9 Th2 cytokines (Akiho et al., 2002; Khan et al., 2003). For example, Khan et al. (2003) showed that blocking IL-9 via antibody treatment or immunisation with the OVA-IL-9 complex during *T. muris* infection significantly decreased colonic muscle hypercontractility and inhibited worm expulsion. Another study also showed that treating susceptible AKR mice chronically infected with *T. muris* with the immunosuppressive drug dexamethasone resulted in a partially normalised IFN- γ level and muscle contractility (Motomura et

al., 2010). Thus, smooth muscle hypercontractility appears to be an important immune-mediated mechanism for the expulsion of gastrointestinal parasites.

1.7.3 Goblet cells and mucus production

The extrinsic physical barrier comprised of goblet cells and mucins is known to assist in parasite expulsion under the control of Th2 cytokines (IL-13 and IL-9 and IL-22) (Artis et al., 2004b; Leung, 2013; Turner et al., 2013). It has been demonstrated that the number of goblet cells increases in both susceptible and resistant mice during *T. muris* infection compared to uninfected naïve mice (Artis et al., 2004b; Cliffe and Grencis, 2004; Datta et al., 2005; Owyang et al., 2006). Goblet cells produce different defensive compounds, including glycoprotein mucin (the major protein component of mucus), which acts as a sticky blanket that inhibits the motility and feeding of *T. muris* and mediates worm expulsion (Hasnain et al., 2011b; Hasnain et al., 2010; McGuckin et al., 2011). However, the type of mucin produced by intestinal goblet cells differs between resistant and susceptible mice (Hasnain et al., 2011a; Hasnain et al., 2010). Muc2 was only up-regulated in resistant mice (BALB/c, C57BL/6). Moreover, Muc2-deficient mice showed delayed parasite expulsion compared to resistant wild-type C57BL/6 mice (Hasnain et al., 2010). Hasnain et al. (2012) also demonstrated that serine protease, the main protein secreted by *T. muris*, has the ability to make the mucus barrier more porous by degrading Muc2. Interestingly, Muc5ac, which is a mucin that is not normally expressed in the intestinal tract, was detected in resistant animals before *T. muris* expulsion and was associated with the production of IL-13 (Hasnain et al., 2011b; Hasnain et al., 2010). Mice deficient in Muc5ac were susceptible to *Trichuris* infection despite the robust Th2 effector response and remained highly susceptible to *T. muris* infection even after treatment with an IFN- γ neutralising antibody, which further enhanced the Th2 response (Hasnain et al., 2010). These findings suggest that certain mucins can have a direct effect on worm expulsion.

Goblet cells produce resistin-like molecule β (RELM β), which is associated with the production of Th2 cytokines (IL-13) in animals that are resistant to *T. muris* infection (Artis et al., 2004b; Nair et al., 2008). RELM β are also known to prevent lumen-dwelling worms from feeding and growing and block their motility and attachment to the host's epithelium (Artis et al., 2004b; Herbert et al., 2009). However, Nair et al. (2008) showed that RELM β KO mice exhibited reduced intestinal inflammation and were able to expel acute *T. muris* infection, suggesting that RELM β does not play an essential role in the generation of Th2 response in resistant mice (Nair et al., 2008).

In summary, ejection of *T. muris* worms relies on a combination of physiological mechanisms, including increased epithelial cell turnover, increased muscle contractility, goblet cell hyperplasia and production of the mucins summarised in Figure 1.2.

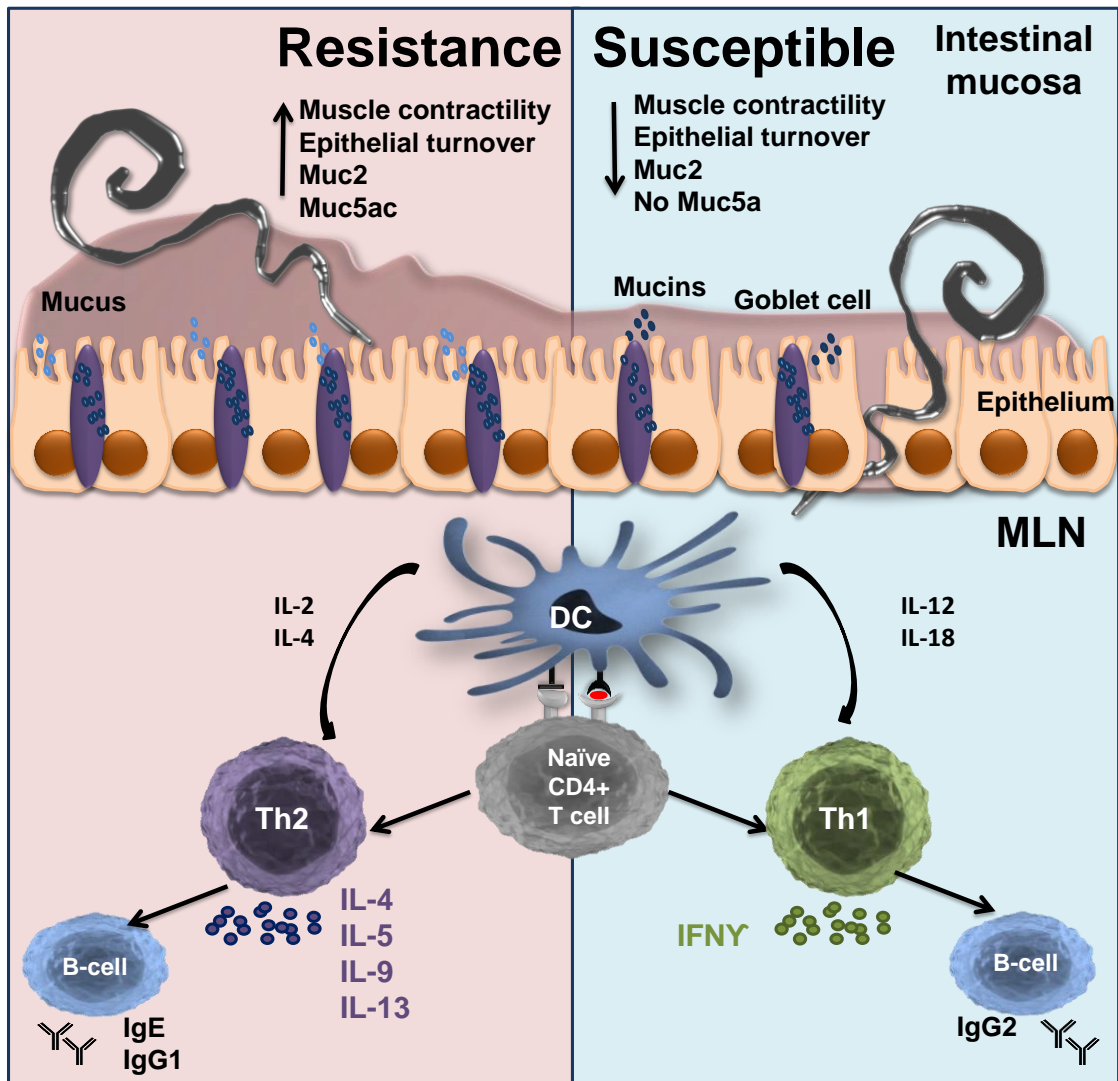


Figure 1.2 Immune profiles during *Trichuris muris* infection. During resistance to *T. muris* infection, whipworms traverse through the epithelium. Damaged epithelial cells release alarmins such as IL-25 and IL-33 that activate innate lymphoid type 2 cells (ILC2) or antigen-presenting cells such as the dendritic cells (DCs) or macrophages. These alarmins, together with helminth-derived products, promote a Th2 immune response. Activated DCs, migrate to the draining lymph nodes where they induce differentiation and polarisation of naïve CD4+ T-cells to Th2-cells. Th2 cells subsequently secrete Th2 cytokines (IL-4, IL-5, IL-9, and IL-13) which drive the activation of B-cells and induces isotype switching to IgE and IgG1. Furthermore, the activation of Th2 response results in the stimulation of anti-helminth responses, including increase epithelial cell turnover and muscle contractility. In addition to inducing goblet cell hyperplasia and the secretion of Muc5ac and Muc2 mucins that result in thickening of the mucus layer, which have a direct detrimental effect on worm expulsion. In contrast, in susceptibility, *T. muris* parasites significantly damage the epithelium as they migrate, causing the release of damage signals that stimulate the activation of innate cells present in the tissue. Activated DCs induce differentiation and polarisation of naïve T-cells to Th1-cells, which secrete Th1 cytokines, including IFN- γ . Th: T-helper, IL: interleukin, immunoglobulin: Ig, IFN- γ : interferon gamma.

1.8 Experimental *Trichuris* vaccine candidates

Vaccines are one of the most cost-effective and well-established interventions to control and prevent infectious diseases in both the human medicine and veterinary fields (Lombard et al., 2007). It is now clear that to produce effective immunisations, it requires long-term stimulation of both the humoral and cellular arms of the immune system to a specific region of the pathogen to produce effector and memory cells to avoid subsequent re-infection (Clem, 2011). STHs have complex genomes, proteomes, and correspondingly complex immunomes (Foth et al., 2014). This complexity represents a great challenge for the development of an effective vaccine (De Sousa and Doolan, 2016). Thus, the availability of an effective vaccine to most helminth infections does not exist. However, the development of vaccines for helminth infections has progressed through generations; the earliest vaccines included attenuated or irradiation-killed parasites, subsequent subunit vaccines contained excretory/secretory (ES) products, ES fractions and extracellular vesicles (EVs), and most recently using purified recombinant parasite antigens (Bain, 1999; Briggs et al., 2018; Dixon et al., 2010; Kifle et al., 2017; Shears et al., 2018a).

Conventional vaccines, such as live attenuated and whole inactivated vaccines, include weakened or killed microorganisms or their derivatives, such as detoxified toxins (Sinha and Bhattacharya, 2006). Such vaccines have reduced the morbidity of major infectious diseases such as smallpox, poliovirus and diphtheria, but they have not eliminated existing or newly emerging diseases (Arnon and Ben-Yedidya, 2003). Irradiated larval vaccines, for example, have been commercially available since 1959 for *Ancylostoma caninum* and bovine lungworm, *Dictyocaulus viviparus*, in animals (Bain, 1999; Miller, 1978). Despite the fact that they have been used for treating animals, these vaccines are not stable and cannot be used against human parasites (Schneider et al., 2011).

One of the first attempts at a non-living vaccine for *T. trichiura* was conducted on the mouse model *T. muris*, using adult and larval worm somatic antigens to stimulate protective immunity in infected animals (Wakelin and Selby, 1973). Vaccination of mice with *T. muris* somatic antigens that were isolated from NIH mice and emulsified in Freund's incomplete adjuvant stimulated protective immunity and a 92% reduction in worm burden after infection (Wakelin and Selby, 1973). Wakelin and Selby (1973) also demonstrated that soluble antigens from the anterior region of adult worms were shown to more effectively stimulate immunity than antigens prepared from the posterior region. Hence, *T. muris* adult worm homogenate and ES products from both adult and larval stages have been utilised as early stages of vaccine development to *T. trichiura* (Jenkins and Wakelin, 1977; 1983). For example, there was only sufficient protection against *T. muris* in several susceptible mouse strains that were administered with homogenised adult antigens combined with cholera toxin as an oral vaccine (Robinson et al., 1995). However, full protection in all the tested mice strains was achieved through s.c. vaccination with adult antigens emulsified in Freund's adjuvant (Robinson et al., 1995). Jenkins and colleagues (1983) also showed that vaccinating NIH mice subcutaneously with 100 µg of ES without adjuvant was more effective than intraperitoneal vaccination; s.c. vaccination resulted in about 70% reduction in worm burden of a high-dose infection at day 9 post-infection (p.i.) compared to 33% for intraperitoneal vaccination. More recently, Dixon et al. (2010) showed that s.c. vaccination of naturally susceptible AKR mice with 100 µg of *T. muris* ES emulsified with Freund's incomplete adjuvant (IFA) induced expulsion of a

high-dose infection. This study also described priming of the immune response to s.c. vaccination as occurring in peripheral LNs (Dixon et al., 2010).

Interest in identifying host protective material in EV components within helminth secretions has increased recently (Eichenberger et al., 2018a; Eichenberger et al., 2018b; Hansen et al., 2015; Tritten and Geary, 2018). For example, Coakley et al. (2017) showed that intraperitoneal vaccination of mice with *H. polygyrus* exosome-like vesicles (ELVs) prior to infection resulted in a significant reduction in *H. polygyrus* worm burden and egg output. Also, Shears et al. (2018a; 2018b) showed that vaccinating C57BL/6 mice with either ES fractions or EVs isolated from *T. muris* without an adjuvant and prior to infection with a low-dose of *T. muris* eggs significantly reduced the worm burden compared to the PBS-injected group.

Notwithstanding these achievements, developing a subunit vaccine based on native antigens has many manufactory complications, such as cost, time consumption, difficulty of purifying large quantities of worm antigens and control over differences in batches to develop a commercially stable vaccine (Geldhof et al., 2007; Hewitson and Maizels, 2014). To overcome these and other crucial limitations and ensure that safer and more reliable vaccines are developed, new approaches are being considered, especially after the failure of anti-helminthic drugs (Terry et al., 2014). Such approaches include recombinant, DNA and epitope-based vaccines (Patronov and Doytchinova, 2013). Recombinant vaccines may contain secreted or extracted fractions from the pathogen or synthetic peptides or proteins that can lead to a protective immune response produced by genetic engineering technology, and expressed in a heterologous expression system (Noon and Aroian, 2017). Of the most successful recombinant vaccines are the two against hookworm disease caused by *Necator americanus*, which consist of aspartic protease-1 (Na-APR-1) and glutathione-S-transferase-1 (Na-GST-1). These vaccines are currently in phase 1 of clinical trials (Diemert et al., 2018; Diemert et al., 2017; Hotez et al., 2013).

Gomez-Samblas et al. (2017) have also identified a vaccine candidate against some helminth parasites, including *T. muris*, based on recombinant serine/threonine phosphatase 2A from the nematode *Angiostrongylus costaricensis* (rPP2A), which is formulated as a lipopeptide and conjugated with a self-adjuvant oleic-vinyl sulfone (OVS). Interestingly, intranasal immunisation of AKR mice with the vaccine candidate prior to *T. muris* challenge showed a marked reduction in the number of nematode eggs and adults. The immunised mice also developed a combined Th17/Th9 response orchestrated by the cytokines IL-25, IL-17 and IL-9 (Gomez-Samblas et al., 2017). The same vaccine candidate has also been tested in lambs and was found to provide significant protection against the ovine helminth *Haemonchus contortus* and *Teladorsagia circumcincta* infection (Mohamed Fawzi et al., 2013).

More recently, Briggs et al. (2018) developed two vaccines against trichuriasis based on *T. muris* whey acidic protein (rTm-WAP49) and *T. muris* WAP fragment fusion protein (rTm-WAP-F8+Na-GST-1) formulated with Montanide ISA 720 adjuvant. Vaccinating AKR mice with the vaccine candidates three times at two-week intervals prior to *T. muris* challenge induced a partial reduction in worm burden (48% and 38%, respectively) (Briggs et al., 2018). The authors also showed that both humoral and cellular immune responses were induced and characterised by elevated antigen-

specific IgG1 and IgG2c antibodies and Th2 (IL-4, IL-9 and IL-13) cytokines in the draining inguinal LNs, draining mesenteric LNs and spleens of vaccinated mice (Briggs et al., 2018). Despite these promising results, subunit vaccines require substantial adjuvant and often do not provide sufficient protective cellular immunity compared with other vaccine approaches (Arnon and Ben-Yedidya, 2003).

Recent advances in helminth genomics and proteomics have made available a wealth of information for the development of DNA and epitope-based vaccines to induce immune responses with less risk than conventional vaccines (Gurunathan et al., 2000; Loukas and Giacomin, 2016). For example, the *Ascaris suum* vaccine composed of gene-encoding *A. suum* enolase (As-enol-1) that was amplified, cloned and expressed in Marc-145 cells resulted in a 61.13% reduction ($P < 0.05$) in larvae recovery in Kunming mice (Chen et al., 2012). In addition, a recent study tested the efficacy of a naked DNA vaccine approach without adjuvant that used the serine protease (Ts-NBLsp) of *T. spiralis* larvae (Xu et al., 2017). Vaccinating Kunming mice twice with 60 µg of the vaccine candidate resulted in a 77.93% reduction in muscle larvae following *T. spiralis* infection and promoted both type 1 and type 2 immune responses (Xu et al., 2017). More recently, Sun et al. (2019) demonstrated that intranasal vaccination of BALB/c mice with *T. spiralis* serine protease (rTsSP) cDNA cloned and expressed in *E. coli* and coupled with cholera toxin B subunit (CTB) resulted in a 71.10% adult and 62.10% larva reduction after challenge.

The emergence of pathogen genomic sequencing and recombinant DNA technology enabled the development of a methodology called Reverse Vaccinology (RV), which relies on genomic data and bioinformatics analysis to identify critical antigens derived from the pathogen genome with minimum risk (De Sousa and Doolan, 2016; Del Tordello et al., 2017). The vaccine against *Neisseria meningitidis* serogroup B, which is the primary cause of sepsis and meningitis in children and young adults, was the first vaccine created with the RV approach to be approved for humans (Dretler et al., 2018; Pizza et al., 2000). The success of RV for *N. meningitidis* and the significant developments in immunoinformatic tools have prompted researchers to apply RV to develop epitope-based vaccines against a variety of parasites, including *Plasmodium falciparum* (Pance, 2019), *Onchocerca volvulus* (Shey et al., 2019), *Cystic echinococcosis* (Pourseif et al., 2018), *Leishmania infantum* (Dias et al., 2018), and *T. spiralis* (Gu et al., 2016; Wei et al., 2011). For example, Dias et al. (2018) developed an epitope-based vaccine against leishmaniasis based on CD4+ and CD8+ T-cell epitopes derived from three different *L. infantum* proteins predicted using the NetCTLpan *in silico* prediction tool. Interestingly, following *L. infantum* promastigote challenge, vaccinating mice with the epitope-based vaccine candidate significantly reduced the parasite burden in several organs compared to control groups (Dias et al., 2018).

1.9 Epitope-based vaccine against trichuriasis

Based on the promising results of the epitope-based vaccines, the present study developed epitope-based vaccines for *Trichuris* based on the RV strategy. The RV approach comprises five major steps, which can be thought of as a funnelling process (Figure 1.3). The first step is the identification of secreted, upregulated and conserved proteins from the pathogen genome that can elicit a protective immune response (Khan et al., 2006). Second, after selecting a set of proteins

derived from the whole genome, immunoinformatic tools are used to identify potential highly immunogenic epitopes that have a high probability of stimulating an appropriate immune response to the pathogen components by mapping the protein sequence (Terry et al., 2014; Vaishnav et al., 2015). Because the expression frequencies of proteins differ, it is necessary to select multiple epitopes from different proteins. This allows the pathogen to be identified at different developmental stages, increasing the chance of antigen coverage and inducing greater immune response (Thomas and Luxon, 2013). However, not every epitope derived from a protein should be included; one should select only epitopes in sufficiently high concentrations to stimulate a protective immune response (De Groot et al., 2002b). In addition, the selected epitopes need to cover the highly polymorphic nature of the MHC to ensure that the T-cell epitope-based vaccine has good coverage in the human population (De Groot et al., 2002a; De Groot and Berzofsky, 2004; Soria-Guerra et al., 2015). Further, it is important to consider the human genome and human microbiome genomes to avoid an allergic response (IgA response) (Hotez et al., 2016; Moise et al., 2011). Third, these epitopes can then be cloned and expressed on any platform, such as bacteria, yeast or viruses. Fourth, the vaccine candidates will be tested through *in vitro* immunogenicity studies (Moise et al., 2011). Finally, having identified lead antigens to include in the vaccine, the vaccine needs to be tested in the preclinical stage (animal testing) and then in the clinical stage (human testing) (Urban et al., 2007).

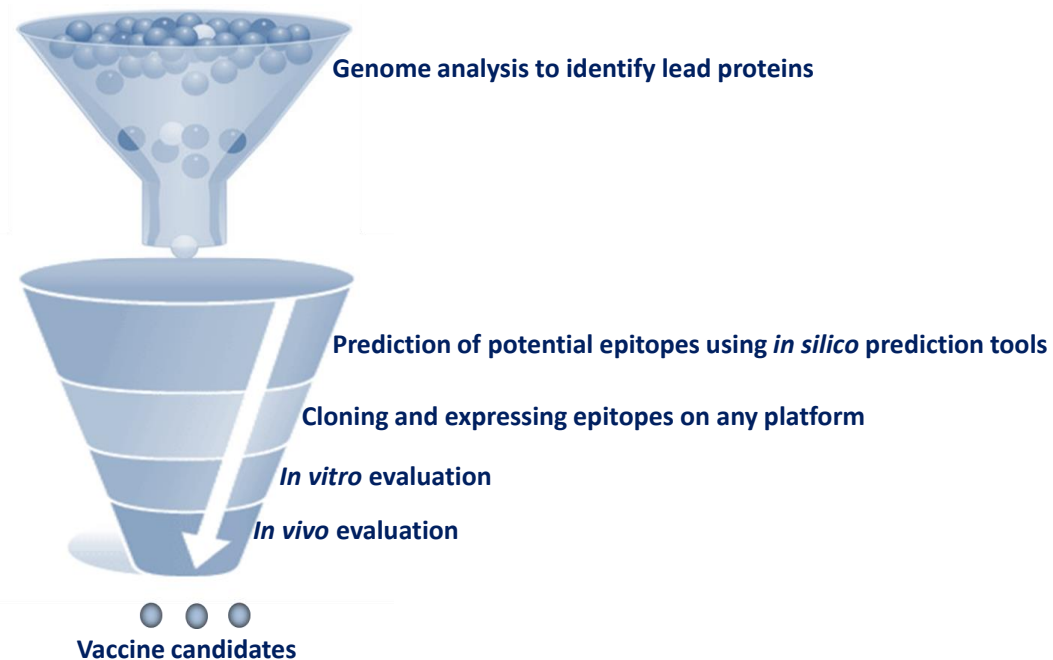


Figure 1.3 Reverse Vaccinology (RV) strategy. The epitope-based vaccine strategy comprises five steps; First, identifying genes from the pathogen genome that encode proteins with promising vaccine antigen properties. Second, *in silico* immunoinformatic tools are then used to predict specific epitopes by mapping protein sequence. Third, these epitopes need to be cloned and expressed on any vaccine platform. Fourth, *in vitro* assays are then used to evaluate the vaccine candidates in inducing a specific immune response. Fifth, the vaccine candidates are then evaluated *in vivo* for immunogenicity and protection in mice before testing in man. Adapted from Moise et al. (2011).

1.10 Immunoinformatics and epitope prediction

Immunoinformatic approaches, such as those involving epitope prediction tools, are powerful methods for analysing immunological data that combine genetics sequence analysis, proteomics and mathematical models to better understand how the whole immune system function (Bambini and Rappuoli, 2009; Lund, 2005). New applications of bioinformatics have increased the number of diseases that can be prevented by vaccination and dramatically reduced the time and resources involved in experimental and laboratory-based studies for discovery research and vaccine development (Comber and Philip, 2014; Lund, 2005; Sidney et al., 2013). Combining systems biology approaches with bioinformatics tools may ultimately lead to the development of optimised gene therapy and vaccines against pathogens such as *T. trichiura* (De Sousa and Doolan, 2016; Del Tordello et al., 2017).

Epitopes are immunogenic regions of proteins that induce a more selective, specific and potent immune response than that induced by a whole protein (Huang and Honda, 2006; Kao and Hodges, 2009; Richard Ag et al., 2002). For instance, Alves-Silva et al. (2017) demonstrated that vaccination of mice with *Leishmania amazonensis* NH36 protein reduced footpad lesion sizes by 55%. However, vaccination of mice with the two domains (F1 and F3) containing the most potent CD4+ and CD8+ T-cell epitopes as a recombinant chimera induced more robust reductions in size (82%) and the parasite load of skin lesions (Alves-Silva et al., 2017).

Depending on the structure of epitopes and their integration with a paratope, epitopes can be classified as either linear or nonlinear. Linear (continuous) epitopes are the primary structure of linear sequences of amino acids that are recognised by T-cell receptors (TCRs), while nonlinear (discontinuous) epitopes are three-dimensional proteins recognised by B-cells in their native structure (Huang and Honda, 2006; Richard Ag et al., 2002). Also, based on their respective receptors, epitopes are categorised as B- or T-cell epitopes (Yang and Yu, 2009).

1.10.1 B-cell epitopes prediction

B-cell epitopes can be conformational and linear peptides, but more than 90% are conformational epitopes that are recognised by B-cell receptors or antibodies. They can take the form of small, complete chemical compounds or large compounds like lipids, nucleotides, glycans and proteins (Horsfall et al., 1991; Richard Ag et al., 2002). Based on the immune response elicited by B-cell epitopes, they are classified as either class 1, which inhibit antigen function, or class 2, which destroy the organism (Sollner et al., 2008). Each class should be predicted separately.

The complex conformational (nonlinear) structure of B-cell epitopes, the generality of antigenicity and the small database for training antigen-antibody complexes make the performance of B-cell epitope prediction tools very poor compared to that of T-cell epitope prediction tools (Ponomarenko and Bourne, 2007; Reitmaier, 2007). Again, because it is difficult to predict the 3D structure of proteins, there are few B-cell epitope databases and software, and the few that do exist exhibit low accuracy (Yang and Yu, 2009). Therefore, B-cell synthetic vaccines have not achieved much success, and none have been licensed for human use (Palatnik-De-Sousa et al., 2018).

1.10.2 T-cell epitopes prediction

T-cell epitopes are linear peptides that are recognised by T-cells via TCRs and presented on the surface of APCs, such as DCs, macrophages or B-cells (Nielsen et al., 2010b). Foreign molecules are taken up by APCs and cleaved into peptides, which bind to MHC I or II in mice and human leukocyte antigen (HLA) in humans to induce an immune response in the host (Backert and Kohlbacher, 2015; Münz, 2012).

Epitope prediction tools can be classified into several categories, including predictors of peptides that bind transporters associated with antigen processing (TAPs), predictors of the proteasomal cleavage site, predictors of MHC binding sites and predictors of T- and B-cell epitopes (Patronov and Doytchinova, 2013). Of these approaches, MHC-peptide binding is the most selective one at determining T-cell epitopes (Sanchez-Trincado et al., 2017).

MHC-I molecules present short peptides (8–11 amino acids) with a unique motif sequence of two main anchor residues, usually located at the amino and carboxy termini pools of the peptide ligand, that are recognised by CD8+ T cytotoxic cells (Elliott et al., 1991; Rötzschke et al., 1991). In contrast, MHC-II molecules present longer peptides (12–25 amino acids) with three main anchor residues located at positions 1, 6 and 9 that are recognised by CD4+ T helper cells (Brown et al., 1993; Madden, 1995; Wieczorek et al., 2017). Because the MHC-II groove is open at both ends (unlike the MHC-I binding groove, which is closed at both ends), MHC-II CD4+ T-cell epitope prediction tools have much lower accuracy compared to MHC-I tools (Godkin et al., 2001; Yang and Yu, 2009).

Given the fundamental roles of CD4+ T-cells in anti-*Trichuris* protective immunity (Bouchery et al., 2014), defining a set of MHC-II T-cell epitopes for protection while excluding extraneous and dangerous whole proteins using immunoinformatic tools can lead to the development of a novel epitope-based vaccine to *Trichuris* infection. However, more than 50 MHC-II epitope prediction tools are currently available, and not all are equivalent (Brusic et al., 2004; De Groot and Moise, 2007; Yang and Yu, 2009; Zhang et al., 2012). For example, some of the tools are qualitative, such as RankPep (Reche et al., 2002), while others are quantitative, such as the immune epitope database and analysis (IEDB) tool (Wang et al., 2008). Furthermore, the sensitivity (inclusion and identification of a large proportion of ligands efficiency) and specificity (exclusion of irrelevant sequences efficiency) of each epitope prediction tool varies (Patronov and Doytchinova, 2013). It has been suggested that the limited performance of some prediction tools is due to the limited training dataset used to evaluate the tools (Chaves et al., 2012; Hegde et al., 2018; Lin Hh, 2008; Wang et al., 2008). Thus, choosing an *in silico* prediction tool is a critical step when designing an epitope-based vaccine (Yang and Yu, 2009). Therefore, the current study provides a systematic review of the available bioinformatics tools for prediction of MHC-II T-cell epitopes and compares the performance of the tools in predicting MHC-II T-cell epitopes. Previous reviews in this area have evaluated different T-cell epitope prediction tools (Gowthaman and Agrewala, 2007; Lin et al., 2008), but non to my knowledge have been conducted in a systematic way using the outlined criteria and the same training sets described in Chapter 3.

After predicting and selecting a set of epitopes, it is important to note that they are short peptides, which usually cannot fold autonomously and will probably lose their original biological activity. As a result, epitopes may display low solubility, immunogenicity and physiochemical instability compared to full proteins (Ryadnov, 2012; Usmani et al., 2018). Therefore, the predicted MHC-II T-cell epitopes need to be expressed in a practical and safe vaccine delivery system, such as virus-like particles (VLPs), to ensure that an epitope-based vaccine can promote a protective immune response (Sanchez-Trincado et al., 2017).

1.11 Virus-like particle (VLP) as a promising vaccine delivery system

VLPs are non-infectious, highly organised spheres that self-assemble from virus-derived envelopes and/or capsid proteins. They possess the immunostimulatory and self-adjuvanting properties of natural viruses but do not contain genetic material (Choi et al., 2018; Zeltins, 2013). VLPs can be naturally formed during infection or genetically engineered and produced on a large scale (Mohsen et al., 2018). Since the beginning of the 1980s, more than 100 types of VLPs have been successfully used to produce vaccines against foreign epitopes or the viruses from which they are derived, including hepatitis E and B viruses (Pumpens and Grens, 2001), human adenovirus virus (Villegas-Mendez et al., 2010), human papillomavirus (Roden et al., 2018), influenza virus (Pushko et al., 2005), and *Enterobacteri*a phage Qbeta (QP) (Cielens et al., 2000).

VLPs feature remarkably highly immunostimulatory activity and therefore are effective for use in vaccine delivery (El-Sayed and Kamel, 2018), drug delivery (Ma et al., 2012), allergen immunotherapy (Anzaghe et al., 2018) and diagnostic activities (Schwarz et al., 2017). Vaccines for hepatitis B (Recombivax and Engerix) (Haber et al., 2018) and human papillomavirus (Gardasil® and Cervarix®) (Elliott and Chan, 2018; Monie et al., 2008) are four examples of human licenced VLP-based vaccines.

Furthermore, VLPs can overcome B-cell tolerance and induction of self-specific antibodies and therefore have been widely used as self-antigen carriers for the development of therapeutic vaccines against chronic diseases, such as arthritis (Röhn et al., 2006), hypertension (Ambühl et al., 2007), asthma (Akache et al., 2016), and cancer (Costa et al., 2018). VLPs have also been used to develop highly immunogenic and protective vaccines against parasitic infectious diseases. For example, RTS, S (Mosquirix) was the first licensed VLP-based vaccine generated against parasitic disease (Hawkes, 2015). It is composed of three tandem repeat (R) and cell (T) epitopes from the circumsporozoite protein of the *P. falciparum* malaria parasite, which are displayed on hepatitis B surface particles (HBs-Ag) (S), co-expressed in *Saccharomyces cerevisiae* (S) and reconstituted with an AS01 adjuvant (Pance, 2019). Furthermore, *Toxoplasma gondii* (Guo et al., 2019), *T. spiralis* (Lee et al., 2016), and *Clonorchis sinensis* vaccine (Lee et al., 2017) are still restricted to small-scale fundamental research (Schwarz et al., 2017).

Even though there are several VLP-based vaccines on the market, several challenges should be considered when developing a novel VLP-based vaccine (Mohsen et al., 2018). Some are related to the VLP platform, and others are related to particular vaccines (Mohsen et al., 2018). Challenges specific to VLP-based vaccine platforms include choosing the VLP platform and choosing the

expression system (Mohsen et al., 2018). Challenges specific to particular vaccines include selecting the most immunogenic antigen or epitope for an effective vaccine, inducing a sufficient immune response to produce protection and attracting industrial interest in producing the vaccine (Kawano et al., 2018; Mohsen et al., 2018).

1.11.1 Key features of VLP which bestow promise as a vaccine delivery system

VLPs can overcome the disadvantages of the soluble antigens that have been widely used in numerous vaccine approaches, including poor safety, instability and poor immunogenicity (Chackerian, 2007; Mohsen et al., 2018). Figure 1.4 summarises the key features of VLPs. For example, the non-replicating nature of non-infectious VLPs represents a safer alternative to attenuated viruses in vaccine development (D'argenio and Wilson, 2010; Ludwig and Wagner, 2007). Although VLPs lack the genetic material packaged within particles, they usually package different natural immune modulators (e.g. nucleic acids such as ssRNA and dsRNA) from host cells in the expression process, which facilitates internalisation by APCs by engaging different pathogen recognition receptors (Mohsen et al., 2018).

The high stability of VLPs (i.e. their ability to withstand several different conditions during production and distribution) can improve the utility of vaccines by reducing the costs associated with longer shelf-life and cold storage (Jeong and Seong, 2017). Another key feature of VLPs is their ability to display different-size antigens on their surface via chemical crosslinking or genetic fusion (Fogarty and Swartz, 2018; Patel and Swartz, 2011). However, the choice of method will impact the overall stability and immunogenicity of VLP-based vaccines (Mohsen et al., 2018). Furthermore, VLPs can be produced in different expression systems, including bacteria, yeast, plant, insect and mammalian cells, providing flexibility during manufacturing (Makarkov et al., 2019; Shirbaghaee and Bolhassani, 2016; Ulmer et al., 2006). However, the host component may have an unknown effect on the immunogenicity of VLP-based vaccines, and therefore it is essential to carefully select an expression vector when designing new vaccines (Mohsen et al., 2018). Another major advantage of using VLPs as vaccine delivery systems is their ability to activate both humoral and cellular immune responses through various means, as summarised in Figure 1.5 (D'argenio and Wilson, 2010; Grgacic and Anderson, 2006). In general, the interaction of the VLP with the immune system depends on the nano-particles size and the surface geometry (Shirbaghaee and Bolhassani, 2016; Tao et al., 2018).

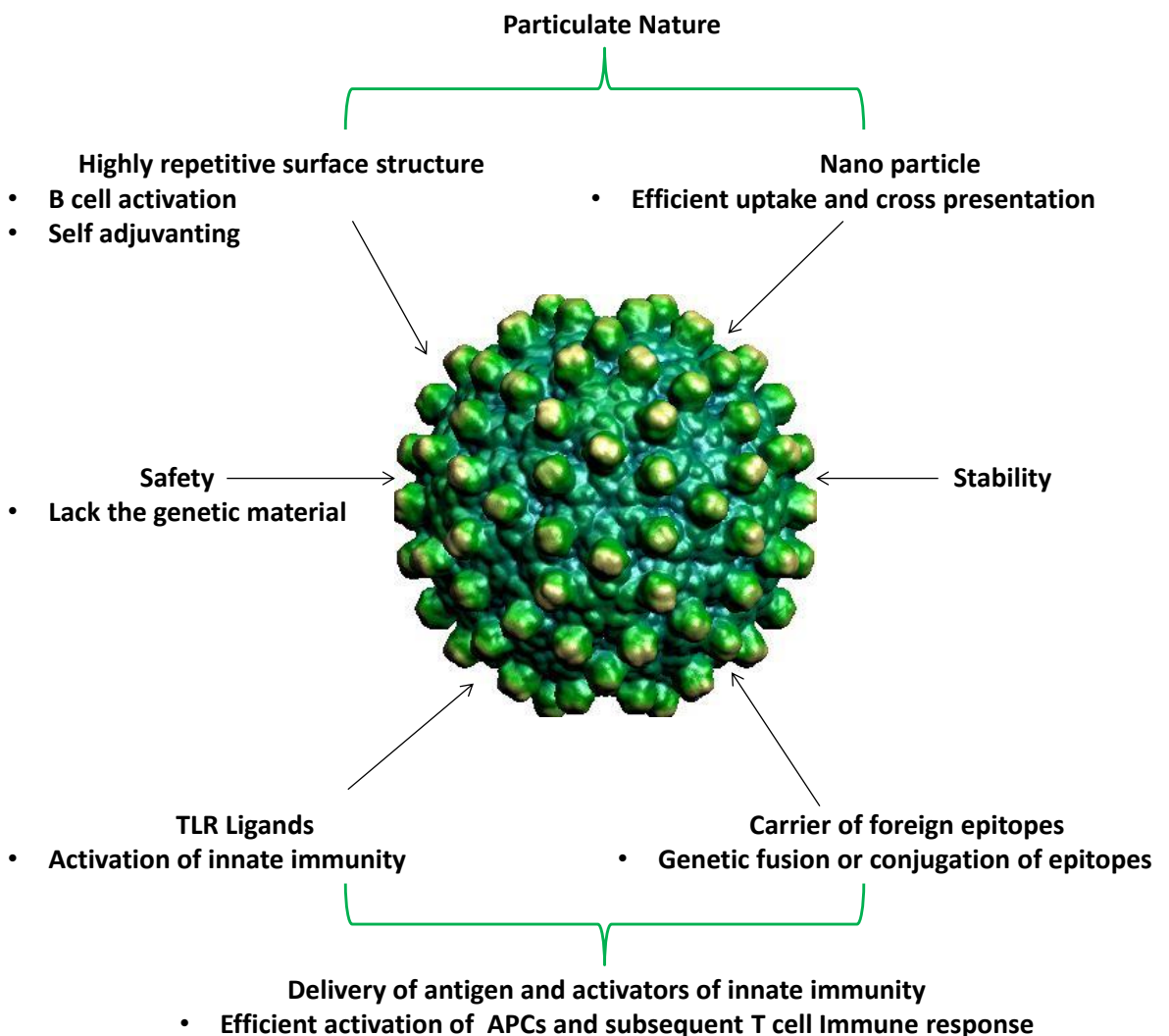


Figure 1.4 Key features of virus-like particle (VLP) as a promising vaccine delivery system. VLPs are self-assembled, non-replicated viruses that lack the genetic material. The well-defined geometry, small size and the repetitive structure on the VLP surface allow efficient uptake by antigen-presenting cells for processing and cross-presentation by MHC-II and MHC-I that can lead to strong cellular and humoral immune responses without the use of an adjuvant. VLPs have the ability to carry a variety of foreign antigens with high stability compared to the soluble antigens; therefore, VLPs have shown dramatic effectiveness as a drug and a vaccine delivery platform. Adapted from Crisci et al. (2012).

1.11.2 VLPs and the induction of humoral and cellular immune responses

Several steps are important for generating potent protective immune responses, including antigen uptake and processing by APCs, trafficking to LNs and activation of APCs for effective T-cell priming and activation of B-cells (Jennings and Bachmann, 2008). Uptake of antigens by APCs depends on several antigen-associated properties, including surface charge, size and shape, that impact the immune responses that are relevant to the outcome of vaccination (Gause et al., 2017). For example, VLPs have large surfaces with charged, hydrophobic properties, which facilitates interaction with APCs (Bachmann and Jennings, 2010).

Studies have also shown that the nano size (20–200 nm in diameter) of VLPs influences immunogenicity through two mechanisms: first, it allows for free draining from periphery to

secondary lymphoid organs, and second, it facilitates interaction with different APCs (Gomes et al., 2017b). For example, Manolova et al. (2008) showed that bacteriophage Qb-VLPs can be detected in C57BL/6 mice footpads for at least 40 minutes post-injection and at drainage LNs 2 hours post-injection without assistance from migratory APCs at the site of injection. After 48 hours post-injection, VLPs were detected distributed in the sub-capsular space, cortex and paracortex of the draining LNs, and some were detected inside B-cell follicles, while larger particles were retained at the injection site and needed to be transported into the LNs by migratory APCs (Manolova et al., 2008). A more recent study showed that Qb-VLPs can reach popliteal LNs in mouse footpads less than 10 minutes post-injection (Mohsen et al., 2017a). Other than free lymphatic drainage, VLPs can be actively transported from the intradermal injection site to the drainage LNs via specialised cells such as skin-derived macrophages, dermal DCs and Langerhans cells (Bousarghin et al., 2005; Fausch et al., 2003; Keller et al., 2010; Ruedl et al., 2002).

Furthermore, natural IgM bind strongly to the VLPs repetitive surfaces through multivalent, high-avidity interactions that facilitate trafficking of bound entities to lymphoid organs, which leads to recruitment and activation of complement component 1q (C1q) and the classical pathway of the complement cascade (Bachmann and Jennings, 2010; Link et al., 2012). Link et al. (2012) demonstrated that Qb-VLP accumulated on murine splenic follicle dendritic cells (FDCs) via B-cells *in vivo* in the absence of prior immunity (specific IgM Abs). The authors also reported that natural IgM and C1q bound directly to the surface of Qb-VLP and led to activation of the classical complement cascade. However, deficiency in IgM and C1q led to complete failure of Qb-VLP deposition on FDCs, suggesting that natural IgM Abs and complement components were required to mediate the capture and transport of VLPs (Link et al., 2012).

The pattern of distribution of VLPs in LNs also facilitates the interaction of VLPs with different APCs (DCs, macrophages and B-cells) that are essential for activating innate and adaptive immune responses against those particles (Mohsen et al., 2018; Plummer and Manchester, 2011). Following uptake by APCs, VLPs will reach the endosomal-lysosomal compartments, where they are processed and degraded into peptides (Keller et al., 2010; Storni and Bachmann, 2004). These peptides are presented to the T-cells as exogenous antigens on MHC-II molecule and then activate CD4+ T-cells. They can also be cross-presented as endogenous antigens on MHC-I molecules and activate CD8+ T-cells (Keller et al., 2010; Storni and Bachmann, 2004). For instance, immunisation of mice with T4 phage-VLP that display *Yersinia pestis* antigens (F1mutV) induced balanced Th1 and Th2 immune responses (Tao et al., 2013). The fact that the VLP size appears to be favourable for uptake by DCs and subsequent processing and presentation by both MHC I and II and direct promotion of DC maturation and migration have led some researchers to describe VLPs as 'self-adjuvanting' immunogen delivery systems (Kushnir et al., 2012). However, some VLP-based vaccines must be formulated with potent adjuvants in order to induce efficient immune responses (Hill et al., 2018). Targeting DCs is another promising strategy that can further enhance the vaccine efficacy (Franco et al., 2011).

Following uptake of VLPs by professional APCs in the T-cell zone, VLPs subsequently provide signals to naïve B-cells to initiate a specific class-switched antibody response (Wykes et al., 1998).

VLP-induced monocyte activation is demonstrated by upregulation of cell surface markers (MHC-II, CD80 and CD86). Furthermore, maturation of naïve B-cells into effector cells (plasma cells) and memory B-cells and production of antibodies requires ‘help’ from T helper cells in the form of release of pro-inflammatory cytokines, particularly those associated with a Th2 response (IL-4, IL-5, IL-6, IL-9, IL-13 and TNF- α), and an anti-inflammatory cytokine (IL-10) (Ding et al., 2010; Lenz et al., 2003; Siegrist and Aspinall, 2009; Speth et al., 2008). For example, Mohsen et al. (2017a) demonstrated that LN-resident APCs (DCs and macrophages) efficiently took up Q β -VLPs characterised by strong expression of MHC-II. Furthermore, two-photon microscopy confirmed the co-localisation of VLPs in popliteal draining LNs (Mohsen et al., 2017a). Another study analysed phagocytosis of exogenous HBc-VLPs by bone-marrow-derived DCs (BMDCs) using immunofluorescence and confocal laser scanning microscopy (CLSM) (Ding et al., 2010). Phenotypic analysis revealed that the HBc-VLP-pulsed BMDCs significantly increased BMDCs’ surface markers (CD80, CD86 and MHC-II) compared to untreated BMDCs (Ding et al., 2010). Furthermore, the cytokine expression of HBc-VLP-pulsed BMDCs identified by RT-PCR and electrophoresis on 1.2% agarose gels confirmed that IL-12 (p40) and IFN- γ were secreted, unlike the control groups (Ding et al., 2010). Other studies have confirmed that macrophages are activated in response to VLPs characterised by the secretion of the proinflammatory cytokines TNF- α , IL-6 and IL-1 β , unlike unstimulated cells (Lenz et al., 2003; Wahl-Jensen et al., 2005).

A key feature of successful VLP-based vaccines is their ability to induce strong and long-lasting humoral immune responses, often without adjuvants (Mohsen et al., 2018). Overall, the stimulation of B-cells by VLPs and the induction of IgM antibodies can be mediated by T-cell-dependent and -independent immune responses (Fehr et al., 1998; Liu et al., 2012; Milich et al., 1997a; Zeltins, 2013). The immune response induced by VLPs is based on the highly repetitive surface patterns on the VLPs and the B-cell epitopes at the tip of the spikes of VLPs directly enhance the immunogenicity of VLPs by cross-linking B-cell receptors (BCRs) and inducing B-cell proliferation, antibody production and costimulatory molecules (Bessa et al., 2012; Milich et al., 1997a).

Early research on hepatitis B core antigen (HBc-Ag), as an example of a VLP, showed that it binds specifically to the BCR on naïve murine B-cells, induces B7.1 and B7.2 costimulatory molecules *in vitro* and *in vivo* and primes T cell-independent antibody production (Bachmann et al., 1993; Fehr et al., 1998; Milich, 1999; Milich et al., 1997a; Milich and McLachlan, 1986). Although the production of specific HBc-Ag antibodies occurs through a T-cell-independent pathway, HBc-Ag stimulates an HBc-Ag specific T-cell immune response (IL-2 production) efficiently *in vivo* (Lee et al., 2009; Milich et al., 1987a; Milich et al., 1987b; Schödel et al., 1994). Bessa et al. (2012) demonstrated that intranasal administration of the Q β -VLPs in C57BL/6 mice resulted in strong splenic B-cell responses as the VLPs bind to B-cells via the BCR and then are transported from the lung to splenic B-cell follicles. More recently, Hong et al. (2018) vaccinated different genetically modified mice with Qb-VLP as a model antigen. They demonstrated that the B-cells were sufficient to initiate prompt naïve CD4+ T-cell activation, proliferation and differentiation without DCs in response to VLP via direct interactions and TLR signalling-mediated cytokine production (Hong et al., 2018). These results suggest that B-cells might be the dominant APCs for VLP responses and are directly involved in the stimulation of CD4+ T-cells (Hong et al., 2018). Not only are B-cells the primary

APC for HBc-Ag VLP, but also the specific subset of splenic B1a- and B1b-cells are the most efficient presenters to naïve CD4+ T-cells (Lee et al., 2009).

Another crucial feature of the humoral response elicited by the repetitive structure of VLPs is pathogen-associated molecular pattern motifs (PAMPs). These motifs directly trigger the immune system recognised by pattern-recognition receptors (PRRs) such as Toll-like receptors (TLR7 or TLR9) in host B-cells, which promote isotype switching (Clingan and Matloubian, 2013; Jegerlehner et al., 2007; Plummer and Manchester, 2011). Finally, the fact that the physical properties of the VLPs play an important role in activating B-cells and inducing long-lasting antibody responses suggests that immunisation with low doses of VLPs will be sufficient to elicit a robust immune response (Crisci et al., 2013). To conclude, the highly immunogenic properties of VLPs based on the viral fingerprint retained from the parental viruses, including the size and surface geometry and the ability to present foreign antigens on their surface have tremendous potential for enhancing vaccine immunity.

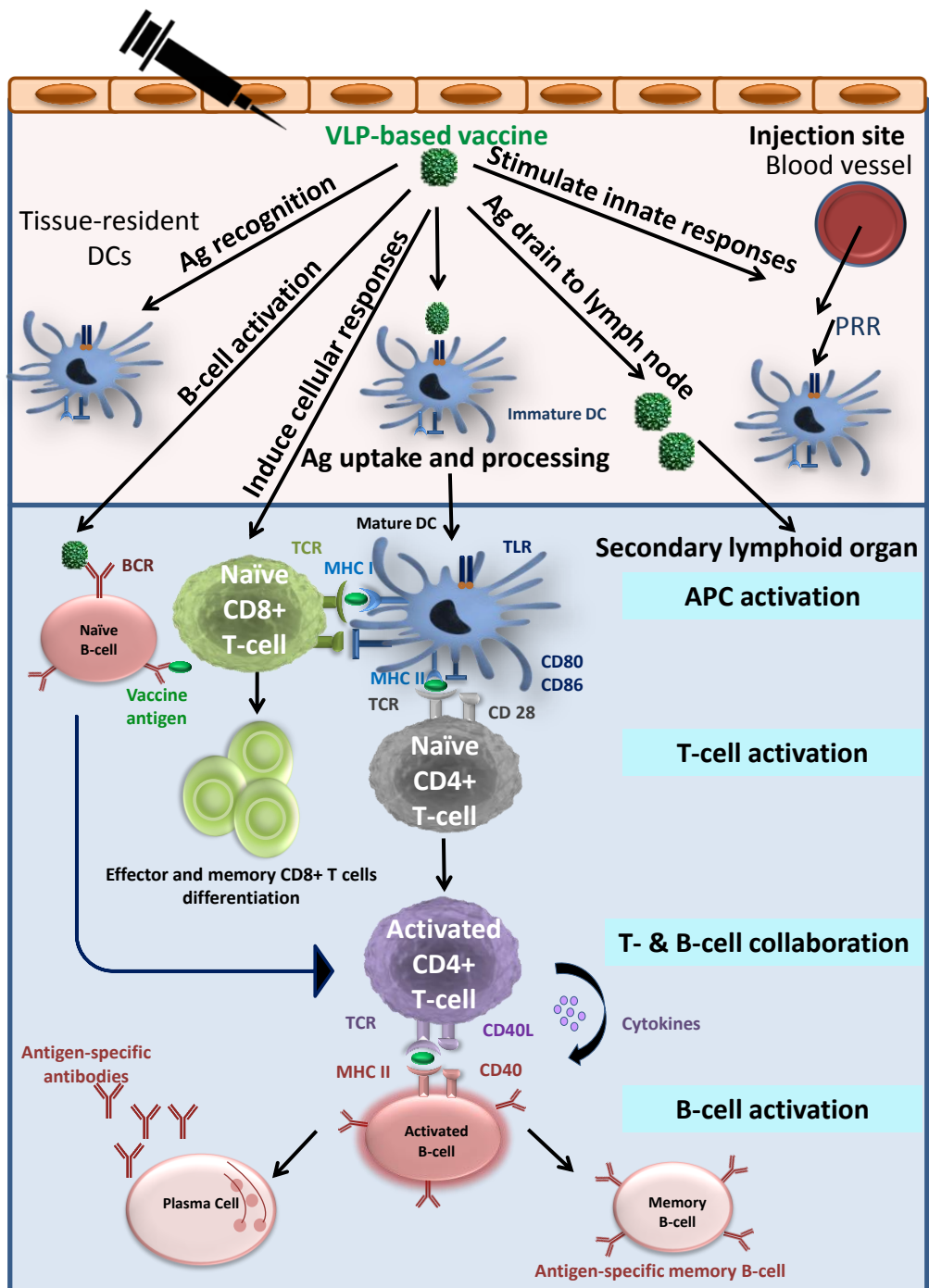


Figure 1.5 The different immune responses induced by VLPs. The repetitive surface structure of the VLP makes it recognised as pathogen-associated geometric patterns PAMPs by pathogen-recognition receptors (PRR) expressed by DCs that stimulate the innate immune system. Furthermore, the nanoparticle size of the VLP facilitate free intro into the lymph nodes and/or uptake of by the APC near the injection site that leads to migration to the secondary lymphoid organs. Upon reaching the lymph nodes, APCs uptake VLPs were they will be processed and presented by MHC-II and MHC-I pathways, which eventually leads to T-cell activation of both CD8+ and CD4+ T-cells. Following the T-cell activation, proliferation and differentiation, T-cells interact with native B-cells and produce cytokines that stimulate B-cell activation and differentiation into plasma cells which secretes VLPs specific antibodies into the circulation and the differentiation into VLPs specific memory B-cells. Most of these memory cells will migrate to the bone marrow and will only be activated after re-encounter with the same VLP vaccine. The native B-cells can also be activated directly by the VLPs through T-cell independent mechanism. Adapted from (Tao et al., 2018).

1.12 Hepatitis B core (HBc) particle as a promising VLP platform

Although it is now well documented that the VLPs induce strong immune responses, some VLPs elicit weak T-cell responses. Therefore, choosing the right VLP is critical when designing a VLP-based vaccine (Fuenmayor et al., 2017). HBc particles were first described as a promising VLP carrier of foreign immunological epitopes in the mid-1980s (Chanock et al., 1987). Now, HBc particles are the most flexible and promising VLP for displaying foreign peptide sequences (Pumpens and Grens, 2001).

HBV is an enveloped virus that contains an icosahedral core (HBc-Ag) and is surrounded by an HBV surface antigen (HBsAg) embedded in the lipid envelope, which has been used as a vaccine carrier (Cao et al., 2019; Howard, 1986; Seeger and Mason, 2000). Electron cryomicroscopy, image reconstruction and X-ray crystallography images have revealed that HBc particles are organised into two amphipathic α helical hairpins. This results in the formation of a dimer with four helix-forming spikes on the surface. This can assemble into a small or large capsid composed of a triangulation number $T = 3$ subunit or $T = 4$ packings comprised of 180 or 240 core proteins, respectively. The icosahedral repeat unit in the $T = 4$ capsid consists of four subunits (A, B, C and D) that form two dimers, as shown in Figure 1.6. The $T = 3$ capsid consists of three subunits (A, B and C) that form trimers. In general, HBc capsids are characterised by a hydrophobic core that stabilises folded monomers with a Cys61 residue, which forms an intradimer disulfide bridge between two monomers but is not essential for capsid formation (Böttcher and Nassal, 2018; Böttcher et al., 2006; Böttcher et al., 1997; Cao et al., 2019; Crowther et al., 1994).

HBc-core particles have several features that make them attractive carriers for foreign epitopes (Clarke et al., 1987). For example, they have a high level of expression and efficiency in different homologous and heterologous expression systems, including various mammalian cell cultures (Netter et al., 2001), virus expression systems (Villegas-Mendez et al., 2010), insect cell lines such as Spodoptera cells (Brandenburg et al., 2005) and plants cells like transgenic *Nicotiana benthamiana* plants (Makarkov et al., 2019). Also, they have high levels of expression and efficiency in bacteria, such as *Escherichia coli* (Wang et al., 2016), *Acetobacter* (Schröder et al., 1991) and *Salmonella* (Schödel et al., 1990), and in yeast like *Pichia pastoris* (Li et al., 2007). Another feature is the ability of HBc-Ag polypeptides to induce strong B-cell, T-helper and cytotoxic T lymphocyte immune responses to foreign epitopes in addition to their dual roles as a T cell-dependent and independent antigen (Chisari and Ferrari, 1995; Milich and McLachlan, 1986; Qiao et al., 2016; Roose et al., 2013). Previously, a variety of studies have observed that immunising mice with full-length HBc-Ag primed Th1 immune response, as measured by the production of specific anti-HBc IgG2c and IgG2b and a high level of IFN- γ and low level of IL-4. In contrast, immunising mice with HBc-Ag lacking the C-terminal arginine-rich domain (HBcAg₁₄₄, and HBcAg₁₄₉) primed Th2 immune response, as evidenced by the production of specific anti-HBc IgG1 and low levels of IgG2c and IgG2b as well as the release of a high levels of IL-4 and low levels of IFN- γ (Milich et al., 1997b; Riedl et al., 2002; Sominskaya et al., 2013). The VLP used in this study is based on HBc-Ag lacking the C-terminal arginine-rich domain.

To display the target antigens on the surface of HBc-Ag with high density, the antigens can be genetically inserted at different sites within the virus structure or fused by chemical techniques, such as chemical crosslinkers (Akhras et al., 2017; Frietze et al., 2016; Howarth and Brune, 2018). As a carrier, HBc-Ag has a high capacity for insertion and display of foreign epitopes in three different regions with high flexibility: the N- and C-terminal regions and the central part, which is called the major immunodominant region (MIR), at the tip of the spike between amino acids 78 and 79 (Pumpens et al., 1995; Pumpens and Grens, 2002). The MIR has a surprisingly high capacity for insertion (up to 238 amino acids) and can induce a high level of specific B- and T-cell immune responses. In contrast, the N- and C-terminus regions failed to accept 120-aa-long fragments (Koletzki et al., 1999; Kratz et al., 1999). C-terminus insertion, which occurs at the 144, 149 and 156 positions, has a capacity of only 100 amino acids and is able to induce only moderate specific immunogenicity (Pumpens and Grens, 2001; Yoshikawa et al., 1993). Furthermore, epitope insertion in the N-terminal region has been shown to provide a high level of specific antibodies to different inserted epitopes with a vector capacity of around 50 aa in length (Pumpens and Grens, 2001).

Because recombinant HBc-Ag VLPs are generally easy to purify, they have been widely used for displaying foreign immunodominant peptides and proteins in vaccines developed for both infectious and non-infectious diseases (Janssens et al., 2010). A number of HBV VLP-based vaccines are currently available on the market, and others are still in clinical and preclinical trials. For example, an influenza virus vaccine composed of influenza matrix protein 2 (M2e) fused with HBc-Ag, which induced protection against a lethal challenge with various influenza A virus subtypes in animal models, is currently in phase I of its clinical trial (Keshavarz et al., 2019).

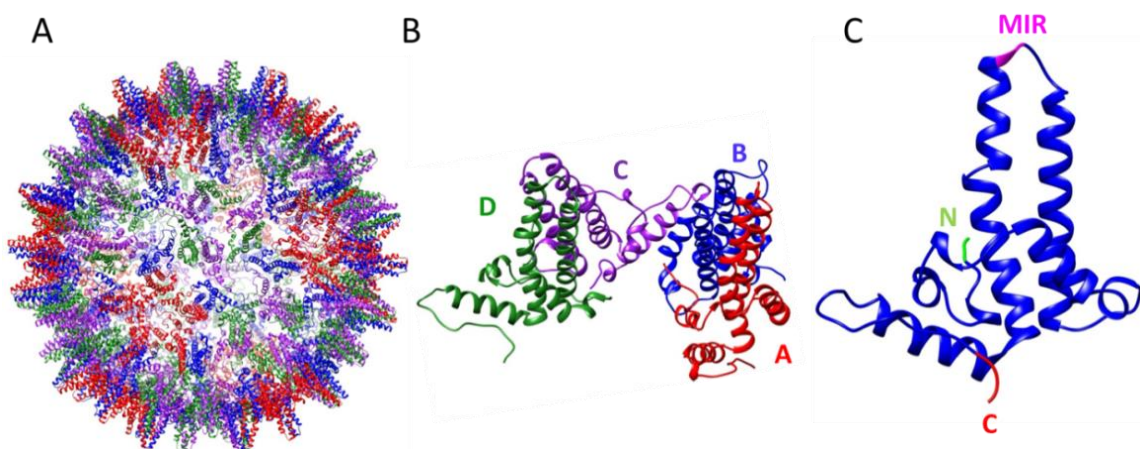


Figure 1.6 A schematic representation of the HBc-Ag capsid arrangement as carriers for foreign epitopes (1QGT, Protein Data Bank). (A) Surface representation of the Three-Dimensional full assembly of HBc-Ag. (B) The crystal structure of two HBc-Ag dimers structure made up of 4 subunits. Subunits A, B, C, and D are shown in red, blue, purple and green respectively. (C) The crystal structure of HBc-Ag monomer of subunit B. The Major Immunodominant Region (MIR) is highlighted in pink, the C- terminus region is highlighted in red and the N- terminus region is highlighted in green. Chimera was used for capsid structure assembly <https://www.cgl.ucsf.edu/chimera/>.

1.13 Thesis aim and objectives

Trichuris trichiura is the second most common STH infection and remains a neglected disease. However, no effective human-licensed vaccine is available (Loukas and Giacomin, 2016). The aim of this thesis is to develop a novel epitope-based vaccine against trichuriasis based on an RV approach that overcomes the limitations of conventional approaches to vaccine development. *T. trichiura* and *T. muris* are closely related at the genetic and proteome level (Foth et al., 2014). Thus, testing of VLPs that express *Trichuris* MHC-II T-cell epitopes in an animal model of trichuriasis enables testing of their ability to drive a protective immune response in a relevant system.

The overall aim of the thesis was split into five objectives, each of which is explored in one of the subsequent chapters:

Chapter 3: To assess available MHC-II restricted T-cell epitope *in silico* prediction tools to select the top MHC class II *in silico* prediction tools.

Chapter 4: To identify a set of *Trichuris* MHC-II T-cell epitopes vaccine candidates based on the reverse vaccinology approach.

Chapter 5: To design, clone, express and purify novel constructs based on VLP (HBc-Ag) expressing *Trichuris* MHC-II T-cell epitopes.

Chapter 6: To determine the ability of mouse bone marrow-derived dendritic cells (BMDCs) and mouse bone marrow-derived macrophages (BMDMs) to function as primary APCs for the native VLP (HBc-Ag) and for VLPs expressing *Trichuris* MHC-II T-cell epitopes.

Chapter 7: To evaluate various VLPs expressing different *Trichuris* MHC-II T-cell epitopes as potential vaccine candidates *in vivo* in a murine model of *Trichuris* infection.

Chapter Two

Materials and methods

2.1 Mice

Male C57BL/6 male mice were purchased from Envigo (Bicester, UK) at age 6-8 weeks. Severe combined immunodeficient (SCID) mice used to maintain the life cycle of *T. muris* were bred at the Biological Sciences Facilities at the University of Manchester. The mice were fed autoclaved food and water and were maintained under specific pathogen-free conditions. All animal experiments were approved by the University of Manchester Animal Welfare and Ethical Review Board and performed under the regulation of the Home Office Scientific Procedures Act (1986), and the Home Office approved licence 70/8127.

2.2 Parasite

2.2.1 Maintenance of *T. muris* Life Cycle

The E isolate of *T. muris* discovered in Edinburgh zoo in 1954 was used to maintain the life cycle of *T. muris*.

2.2.2 *Trichuris muris* Passage

Around 150-200 infective *Trichuris* eggs were administered to SCID mice by oral gavage using a blunt-tip needle. Mice were euthanised by CO₂ asphyxiation after 42 days as this is the time when eggs are fully mature, and egg-laying is maximal. The caecum and the first part of the colon were removed and opened lengthways and washed three times in pre-warmed at 37°C Phosphate Buffered Saline (PBS) (1.37 M NaCl, 27 M KCl, 100 mM Na₂HPO₄, and 18 mM KH₂PO₄) supplemented with (100 U/ml) penicillin and (100 µg/ml) streptomycin (Sigma-Aldrich). Live worms were removed with fine forceps under a microscope. The worms were then placed in 6-well plates (Costar, Corning Corporation, NY, USA) containing pre-warmed medium (RPMI-1640) obtained from (Sigma-Aldrich) supplemented with (100 U/ml) penicillin and (100 µg/ml) streptomycin. The plates were then incubated in a humid environment at 37°C for four hours. Following the 4 hrs incubation, the supernatant was collected and replaced with a fresh RPMI medium (supplemented as before) and incubated for overnight. The supernatant containing E/S and eggs from 4 hrs and overnight culture were harvested for the preparation of Excretory/Secretary (E/S) antigens. Eggs were harvested from 4 hrs and overnight medium by centrifugation at 720 x g for 5 minutes. Pellets were then re-suspended in distilled water and filtered through 100 µm nylon strainer (Falcon, BD Biosciences, Oxford, UK) into 75 cm tissue culture flasks. The tissue culture flasks were then kept at room temperature (RT) in the dark for 6-8 weeks to allow eggs embryonation and were monitored regularly under the microscope. Tissue culture flasks containing embryonated eggs were kept at 4°C for the next infection.

2.2.3 Egg preparation

An aliquot of eggs was taken from a stock tissue culture flask and centrifuged at 448 x g with deceleration 3 and acceleration 9 for 15 min. The pellet was then re-suspended in Milli-Q water and eggs mixed continually using a magnetic stirrer. A high dose infection was prepared by counting 150-200 *T. muris* embryonated eggs in a total volume of 200 µl under 10X objective microscope.

2.2.4 Assessment of egg infectivity

To assess the infectivity of each egg batch, 200-250 embryonated eggs were given by oral gavage to three SCID mice. Day 12 post-infection (p.i.), mice were sacrificed, and the worm burden was assessed (see below). The infectivity was calculated as; the mean number of larvae established divided by the number of embryonated eggs administrated.

2.2.5 Preparation of Excretory/Secretary (E/S) Antigen

Excretory/Secretary (E/S) antigen was prepared as described by (Else and Wakelin, 1989). The supernatant harvested after 4 hrs and overnight culture during the passage were filtered using a 0.22 µm filter (Millex filter, Millipore Corporation) obtained from (Fisher Scientific UK), and then concentrated to 5 ml using Centriprep YM-10 tubes (Millipore Corporation, MA, USA) at 400 x g for 30 minutes at 4°C. The protein was then dialysed against three changes of 5 Litres PBS for 72 hours at 4°C using molecular weight cut off 12-14000 Dalton tubes. Following dialysis, the four hour and overnight E/S were stored at -80°C for further analysis. The four hour E/S was used for stimulating mesenteric lymph nodes, and BMDC and the overnight E/S was used in the ELISA assay. The protein concentration in the ON and 4 hrs ES was determined using a NanoDrop spectrophotometer.

2.3 *In vivo* evaluation of mice vaccinated with 25 µg of pre-mixed VLPs (HBc-H₁₁₂₋₁₂₈, HBc-CBD₃₆₋₅₂, HBc-CBD₁₂₄₃₋₁₂₅₉, and HBc-CLSP₁₄₃₋₁₅₈)

30 male, C57BL/6 (6 weeks old) were divided randomly into three groups: 10 mice in each group were inoculated subcutaneously (s.c) with 200 µl of sterile PBS as a negative control and with 200 µl of 25 µg native VLP (HBc-Ag). The vaccinated mouse group was administrated with 200 µl of 25 µg pre-mixed VLP (HBc-Ag) proteins (HBc-H₁₁₂₋₁₂₈, HBc-CBD₃₆₋₅₂, HBc-CBD₁₂₄₃₋₁₂₅₉, and HBc-CLSP₁₄₃₋₁₅₈) at a 1:1:1:1 ratio. All experimental groups were vaccinated on one abdominal site at (day -20) and were boosted with the same dose at (day -10) in the other abdominal site. At day 10 post vaccination, 5 mice of each group were challenged orally with a high dose of *T. muris* (150 eggs) per mouse. Mice were sacrificed 14 days after challenge infection by an overdose of CO₂.

2.4 *In vivo* evaluation of mice vaccinated with 25 µg of pre-mixed VLPs (HBc-H₁₁₂₋₁₂₈, HBc-CBD₂₄₁₋₂₅₇, HBc-CLSP₁₄₃₋₁₅₈ and HBc-CLSP₃₉₈₋₄₁₆) emulsified with an equal volume of AddaVax™ adjuvant

20 male, C57BL/6 (6 weeks old) were divided randomly into 4 groups: 5 mice were inoculated s.c with overnight ES antigens emulsified with an equal volume of AddaVax™ (InvivoGen) to achieve a vaccine dose of 100 µg ES in 100 µl AddaVax™ as a positive control. The negative group was inoculated s.c with 200 µl of sterile PBS/AddaVax. Alternatively, 5 mice were vaccinated with 200 µl of 100 µl 25 µg VLP (HBc-Ag) added to 100 µl AddaVax™. The vaccinated mouse group was administrated with 200 µl of 25 µg pre-mixed VLP +T-cell epitopes (HBc-H₁₁₂₋₁₂₈, HBc-CBD₂₄₁₋₂₅₇, HBc-CLSP₁₄₃₋₁₅₈ and HBc-CLSP₃₉₈₋₄₁₆) at a 1:1:1:1 ratio mixed 1:1 with AddaVax. All experimental groups were vaccinated in one abdominal site at (day -35) and were boosted with the same dose at (day -14) in the other abdominal site. At day 9 post the last vaccination, blood was collected from the tail vein, and serum samples were separated and stored at -20°C. At day 10 post vaccination,

mice were challenged orally with a high dose of *T. muris* (150 eggs) per mouse. Mice were sacrificed 14 days after challenge infection by an overdose of CO₂.

2.5 *In vivo* evaluation of mice vaccinated with 50 µg of pre-mixed VLPs (HBc-CBD₁₂₄₃₋₁₂₅₉, HBc-CBD₂₄₁₋₂₅₇, HBc-CLSP₁₄₃₋₁₅₈ and HBc-CLSP₃₉₈₋₄₁₆)

44 male, C57BL/6 (6 weeks old) were divided randomly into 4 groups: 11 mice were inoculated s.c with overnight ES antigens emulsified with an equal volume of Alum-an aluminium salt adjuvant (Hogenesch, 2013) obtained from Thermo Scientific to achieve a vaccine dose of 100 µg ES in 100 µl Alum as a positive control. The negative group was inoculated s.c with 200 µl of sterile PBS. Alternatively, 11 mice were vaccinated with 200 µl of 50 µg VLP (HBc-Ag). The vaccinated mouse group was administrated with 200 µl of 50 µg pre-mixed VLPs + T-cell epitopes (HBc-CBD₁₂₄₃₋₁₂₅₉, HBc-CBD₂₄₁₋₂₅₇, HBc-CLSP₁₄₃₋₁₅₈ and HBc-CLSP₃₉₈₋₄₁₆). All experimental groups were vaccinated in the scruff of the neck at (day -20) and were boosted with the same dose at (day -10) in the same site. At day 9 post the last vaccination, blood was collected from the tail vein, and sera samples were separated and stored at -20°C. At day 10 post vaccination, mice were challenged orally with a high dose of *T. muris* (150 eggs) per mouse. Mice were sacrificed 14 days after challenge infection by an overdose of CO₂.

2.6 Worm Burden

Worm burdens in the caecum and proximal colon were assessed at day 14 p.i. using the method described by (Else and Wakelin, 1990b). For L2 and L3 larval counts, at autopsy caecae and proximal colons were removed and stored at -20°C for a minimum of 24 hrs to aid the epithelial cell scrape. The frozen gut was cut lengthways in a petri dish filled with distal water and shaken to remove the gut contents, then placed in a new Petri dish filled with fresh distal water. In order to remove the epithelial layer together with the larvae, the gut lining was scraped gently using watchmaker's forceps. Worms were then counted under a stereo microscope. All worm counts were performed in a blinded manner.

2.7 Serum collection and preparation

At autopsy, blood samples were collected from mice by cardiac puncture into a 1.5 ml Eppendorf tube and left at room temperature until clotted. The blood was then centrifuged 2 times each time for 6 min at 250 x g. The sera was then collected into a new labelled tube and stored at -20°C for further analysis.

2.8 Mouse tail bleeding

Mice were first placed on a 37°C heating box for up to 5 minutes before restraining using a suitable mouse restrainer chamber. The tail vein was then punctured using a 20 gauge (G) needle and a 75 µl volume of blood collected using a capillary tube. The puncture site was then compressed with tissue to stop the bleeding.

2.9 Isolation and stimulation of cells

2.9.1 Isolation and stimulation of cells from mesenteric lymph nodes (MLN)

MLN were harvested from mice into 5 ml RPMI-1640 medium obtained from (Sigma-Aldrich, St Louis, MO) supplemented with 10% foetal calf serum (FCS), 1% L-Glutamine (Invitrogen Ltd., UK), and 1% penicillin/streptomycin (Invitrogen Ltd., UK). A cell suspension was made by forcing the MLN through a 70 µm cell strainer filter into a petri dish using a 2 ml syringe plunger under sterile conditions. Cells were pelleted by centrifuging at 300 x g for 5 min at 4°C. After that, the cell pellet was resuspended in 1 ml red blood cell lysing buffer containing 8.3 g/L ammonium chloride (Sigma-Aldrich, St Louis, MO) for 90 seconds to lyse red blood cells. The volume was increased to 2 ml using complete RPMI© medium, and the cellular suspension washed two times by adding 10 ml RPMI© medium and centrifuging at 250 x g at 4°C for 5 min. The cells were counted on a Casy Cell counter (Schärfe System, Reutlingen, Germany) and an appropriate amount of RPMI© medium added to give 5×10^6 cells/ml.

2.9.2 Isolation and stimulation of mouse bone marrow-derived Macrophages (BMDMs)

BMDMs were generated from the tibia and femurs of 6–8 week old male naïve C57BL/6 mice. First, tissue was removed from the bones, then the ends of the bones were trimmed. The bone marrow was flushed out from the bone into a petri dish with complete medium consisting of Dulbecco's Modified Eagle's Medium (DMEM) – high glucose (Sigma-Aldrich) supplemented with 5% heat-inactivated FCS (Hyclone, Logan, UT), 100 µg/mL penicillin and 100 µg/mL streptomycin (Sigma-Aldrich), and Eagle's minimum essential medium (MEM) non-essential amino acid solution (Sigma-Aldrich). The cell suspension was then washed using a 21 G needle and drawn into a syringe and filtered through a 70 µm nylon cell strainer (Sigma-Aldrich) to remove clumps of cells and tissue debris. Following centrifugation at 300 xg for 10 minutes, red blood cells (RBCs) were lysed with 1 ml RBCs lysing buffer Hybri-MAX (Sigma-Aldrich) for 2 minutes at room temperature. Complete media was then added to stop the reaction. Following centrifugation, the cell pellet was re-suspended in complete media and counted using a CASY-1 Cell Counter. 25×10^6 cells were plated into 25 ml complete media supplemented with macrophage colony-stimulating factor (M-CSF) (eBioscience) at 0.1 mg/ml in a T75 cell culture flask and incubated at 37°C with 5% CO₂. Fresh complete media supplemented with M-CSF at 0.1 mg/ml was added after 3 days. BMDMs were then recovered on day 8 to assess purity by FACS and for stimulation with VLP recombinant protein by adding 5 ml accutase solution (Sigma-Aldrich) for 5 min at 37°C.

BMDMs purity: Following centrifugation at 300 x g for 10 minutes, 1×10^6 /ml cells were stained with F4/80, CD11b, and CD11c antibodies for 30 minutes on ice, before washing, fishing and acquiring using an LSRII flow cytometer (Becton Dickinson Biosciences, Oxfordshire).

BMDMs stimulation assays: BMDMs on day 8 were harvested, and cell concentration was adjusted to 1×10^6 /ml. Cells were incubated with 10 µg/ml VLP (HBc-Ag), VLPs + T-cell epitopes (HBc-H₁₁₂₋₁₂₈, HBc-CBD₁₂₄₃₋₁₂₅₉, HBc-CBD₂₄₁₋₂₅₇, HBc-CLSP₁₄₃₋₁₅₈, and HBc-CLSP₃₉₈₋₄₁₆) overnight at 37°C. ES at a final concentration 50 µg/ml and lipopolysaccharide (LPS) at final concentration 0.1 µg/ml

were used as positive controls, and untreated macrophages were used as a negative control. After 24 hours, the supernatants were harvested separately and stored at -20°C until analysed by LEGENDplex for cytokine content.

Evaluation of VLP uptake by BMDMs: BMDMs on day 8 were collected at 1×10^6 /ml and incubated with fluorescein-conjugated VLP each separately (HBc-Ag, HBc-H₁₁₂₋₁₂₈, HBc-CBD₂₄₁₋₂₅₇, and HBc-CLSP₃₉₈₋₄₁₆) at a final concentration 10 µg/ml for overnight culture at 37°C. Fluorescein-conjugated bovine serum albumin (BSA) at a final concentration 10 µg/ml was used as a positive control. Next day, the non-adherent macrophages were removed, and cells were stained with cell surface markers and analysed on an LSRII flow cytometer (Becton Dickinson Biosciences, Oxfordshire). The supernatants were harvested separately and stored at -20°C until analysed by LEGENDplex for cytokine content.

2.9.3 Isolation and stimulation of mouse bone marrow-derived Dendritic cells (BMDCs)

BMDCs were generated from the tibia and femurs of 6-8 week old male naïve C57BL/6 mice. First, tissues were removed from the bones, then the ends of the bones were trimmed. The bone marrow was flushed out from the bone into a petri dish with complete medium consisting of RPMI 1640© (Sigma-Aldrich) supplemented with 5% heat-inactivated FCS (Hyclone, Logan, UT), 100 µg/mL penicillin and 100 µg/mL streptomycin (Sigma-Aldrich), 2 mM L-Glutamine (Sigma-Aldrich), and 50 µM β-mercaptoethanol (Gibco). The cell suspension was then washed using a 21 G needle and drawn into a syringe and filtered through a 60-100 µm nylon cell strainer (Sigma-Aldrich). Following centrifugation at 300 x g for 10 minutes, RBCs were lysed with 1 ml RBCs lysing buffer Hybri-MAX (Sigma-Aldrich) for 2 minutes at room temperature. Complete RPMI 1640 media was then added to stop the reaction. Following centrifugation, the cell pellet was re-suspended in complete RPMI 1640 media and counted using a CASY-1 Cell Counter. 40 µl (1×10^7 /ml) cells were added to the centre of 2 ml complete RPMI 1640 supplemented with granulocyte-macrophage colony-stimulating factor (GM-CSF), at 20 ng/ml to give a final cell concentration of 2×10^5 in a 6 well plate, and incubated at 37°C with 5% CO₂. Fresh complete RPMI 1640 supplemented with GM-CSF at 20 ng/ml was added after 3 days. 2 ml of the media were then replaced with fresh complete RPMI 1640 supplemented with GM-CSF at 20 ng/ml after 6 days incubation.

BMDCs purity: Following centrifugation at 300 x g for 10 minutes, 1×10^6 /ml cells were stained with CD11b, CD11c and F4/80 antibodies for 30 minutes on ice, before washing, fishing and acquiring using an LSRII flow cytometer (Becton Dickinson Biosciences, Oxfordshire).

BMDCs stimulation assays: BMDCs on day 8 were harvested, and cell concentration adjusted to 1×10^6 /ml. Cells were incubated with 10 µg/ml VLP (HBc-Ag), VLPs + T-cell epitopes (HBc-H₁₁₂₋₁₂₈, HBc-CBD₁₂₄₃₋₁₂₅₉, HBc-CBD₂₄₁₋₂₅₇, HBc-CLSP₁₄₃₋₁₅₈, and HBc-CLSP₃₉₈₋₄₁₆) for overnight at 37°C. ES at a final concentration 50 µg/ml and LPS at final concentration 0.1 µg/ml were used as positive controls, and untreated BMDCs were used as a negative control. After 24 hours, the supernatants were harvested separately and stored at -20°C until analysed by CBA for cytokine content.

2.10 Flow Cytometry

2.10.1 BMDC and BMDM staining

After overnight incubation with VLPs, ES or LPS, 1×10^6 BMDCs and BMDMs were washed 3X in PBS and treated for 20 min on ice with FcR-blocking reagent (Anti-Mouse CD16/CD32 eBiolegend) in PBS FACS buffer (1X PBS, 2% FCS, 0.05% sodium azite). Live/Dead (Zombie UV™) was then added for 20 min at 4°C in the dark. Blocked cells were then subsequently stained with cell surface markers CD11c (BV605), CD11b (FITC), CD40 (PE-Cy7), CD80 (PerCp/cy5.5), CD86 (APC), F4/80 Alexa (Fluor® 700) and MHC class II I-Ab (BV650) from Biolegend in 100 µl PBS FACS buffer for 30 min at 4°C followed by washing with 2 ml PBS FACS buffer. After washing, cells were resuspended in PBS FACS buffer for FACS analysis. At least 30.000 gated events were acquired per sample. Greater than 95% of live dendritic cells and macrophages measured by Zombie UV™ were positive. Dendritic cells were greater than 95% pure, with less than 1% of cells being positive for the macrophage marker F4/80. Cells and fluorescence intensity were acquired using an LSRII flow cytometer (Becton Dickinson Biosciences, Oxfordshire) and analysed using FlowJo X software (Tree Star, Inc. COMPNAY, ADDRESS). The flow cytometry panel is summarised in Table 2.1.

Table 2.1 Flow cytometry panel.

Antibody	Fluorochrome	Clone	Stock Concentration mg/ml	Concentration used	Catalogue number
Anti-mouse F4/80	PE	BM8	0.2	1:1000	123110
Anti-mouse CD45	Alexa Fluor® 700	30-F11	0.5	1:300	103127
Anti-mouse I-A/I-E	Brilliant Violet 650™	M5/114.1 5.2	0.2	1:100	107639
Anti-mouse/human CD11b	FITC	M1/70	0.5	1:200	101205
Anti-mouse CD11c	Brilliant Violet 605™	N418	0.2	1:200	117334
Anti-mouse CD40	PE/Cy7	3/23	0.2	1:200	124622
Anti-mouse CD45	Alexa Fluor® 700	30-F11	0.5	1:100	103128
Anti-mouse CD80	PE/Cy5	16-10A1	0.2	1:100	104712
Anti-mouse CD86	APC	GL-1	0.2	1:100	105012
Live/dead stain	Zombie UV™ Fixable	NA	NA	1:1000	423107

All anti-mouse antibodies were obtained from Biolegend (UK). NA: not available.

2.11 Cytometric Bead Array (CBA)

To analyze the cellular immune responses, 5×10^6 /ml MLN cells from mice vaccinated with VLP (HBc-Ag), VLPs + T-cell epitopes, ES and PBS with and without *T. muris* infection were stimulated with ConA at 5 µg/ml and the supernatants were collected after 24 hrs; or with 4 hrs E/S at 50 µg/ml and the supernatant collected after 48 hrs. The concentrations of IFN-γ, TNF, IL-4, IL-5, IL-6, IL-9, IL-10, IL-13, and IL-17A in the supernatants were measured by cytometric bead array according to the manufacturer's instructions from the Mouse/Rat Soluble Protein Flex Set System kit (BD Biosciences Pharmingen, Oxford, UK). CBA data was analysed on a MACSQuant analyser with FCAP array software and the CBA analysis software package (BD Biosciences).

2.12 Mouse Inflammation Cytometric Bead Array (CBA)

To analyse the cellular immune responses, 1×10^6 /ml BMDMs were incubated with 10 µg/ml VLP (HBc-Ag), VLPs + T-cell epitopes (HBc-H₁₁₂₋₁₂₈, HBc-CBD₁₂₄₃₋₁₂₅₉, HBc-CBD₂₄₁₋₂₅₇, HBc-CLSP₁₄₃₋₁₅₈, and HBc-CLSP₃₉₈₋₄₁₆), 0.1 µg/ml LPS, and 50 µg/ml ES and the supernatants were collected after 24 hrs. The concentrations of TNF, IL-6, IL-10, IL-13, IL17, IL-12p70, IL-1β, Monocyte Chemoattractant Protein-1 (MCP-1), macrophage inflammatory proteins (MIP) and RANTES (CCL5) in the supernatants were measured by CBA according to the manufacturer's instructions from the Mouse/Rat soluble protein flex set system kit (BD Biosciences Pharmingen, Oxford, UK). In brief, cell supernatants and standards were diluted 1:1 in assay buffer then 12.5 µl was added to each well. CBA beads were then vortexed for 30 seconds, and 12.5 µl was added to each well. CBA beads were incubated with cell supernatants for 1 hrs at 40 x g on a plate shaker at RT followed by washing with washing buffer. Beads were then conjugated with streptavidin-PE for 1 hour and washed prior to sample reading using FACSVerse (FACSuite v1.6) and analysed with MACSQuant analyser with FCAP array software and the CBA analysis software package (BD Biosciences).

2.13 LEGENDplex

The supernatants from BMDCs, cultured at 1×10^6 /ml and incubated with or without VLP (HBc-Ag), and VLPs + T-cell epitopes (HBc-H₁₁₂₋₁₂₈, HBc-CBD₁₂₄₃₋₁₂₅₉, HBc-CBD₂₄₁₋₂₅₇, HBc-CLSP₁₄₃₋₁₅₈, and HBc-CLSP₃₉₈₋₄₁₆) at (10 µg/ml), LPS (0.1 µg/ml), or ES (50 µg/ml), were harvested after 24 hours. Inflammatory cytokines including; IL- 1β, IL-6, IL-10, IL-12p70, IL-17A, IL-23, IL-27, CCL2 (MCP-1), IL1-β, IFN-γ, TNF-α, and GM-CSF were analysed using a LEGENDplex™ mouse inflammatory cytokine panel kit from Biolegend according to the manufacturer's instruction. In brief, cell supernatants and standards were diluted 1:1 in assay buffer then 10 µl was added to each well. Legendplex beads were then vortexed for 30 seconds, and 5 µl was added to each well. Legendplex beads were incubated with cell supernatants for 2 hrs at 40 x g on a plate shaker at RT followed by washing with washing buffer. Beads were then conjugated with streptavidin-PE for 30 min and washed prior to sample reading using FACSVerse (FACSuite v1.6) and analysed with BioLegend's LEGENDplexTM Data Analysis Software.

2.14 ELISA measurement of *T. muris*-specific IgM, IgG1, and IgG2c

To analyse the *T. muris* specific antibody (IgM, IgG1, and IgG2c) responses of vaccinated mice, serial dilutions of mice sera were assessed using the ELISA-based assay. 96 well flat-bottomed ELISA plates (Immulon IV plates-Dynatech- Canada) were coated with 50 µl/well of the overnight *T. muris* E/S antigen at 5 µg/ml in 0.5 M carbonate-bicarbonate buffer, pH 9.6 for overnight at 4°C. The next day, the plates were washed 5 times with PBS Tween-20 (PBS-T20) (0.05% Tween 20, Sigma-Aldrich) and incubated for 1 hour at 37°C with 100 µl/well of 3% BSA (Sigma-Aldrich) in PBS-T20 to block non-specific binding. After 1 hour, plates were washed 5 times with PBS-T20. The sera were diluted from 1:20 to 1:2560 in PBS-T20 and then 50 µl of each dilution was added to the plates and incubated for 1 hour at 37°C followed by washing 5 times with PBS-T20. Subsequently, 50 µl of Biotinylated rat anti-mouse IgG1 (Clone: A85-1, BD Biosciences, 1:500) or IgG2a/c (Clone: R19-15, BD Biosciences, 1:100) or Biotinylated rat anti-mouse IgM (Clone: 11/41, BD Biosciences, 1:500) was added to the plates and the plates were incubated for 1 hour at room temperature. The plates were then washed 5 times with PBS-T20. After that, 75 µl/well of SA-POD (Streptavidin-Peroxidase - Sigma-Aldrich - 1:1000) was added to the plates and incubated for 1 hour at room temperature followed by 5 washes with PBS-T20. 100 µl/well of TMB ELISA substrate (3, 3', 5, 5'-tetramethylbenzidine- Thermo) was then added to the plates for colour development. Finally, 50 µl/well of the stop solution 0.003% (H₂SO₄) (2N sulphurine acids- R&D) was added to stop the colour development. Plates were read using a Dynex MRX11 plate reader (DYNEX Technologies) at 450 nm with a reference of 570 nm. Data were analysed by using the GraphPad Prism7 software.

2.15 ELISA measurement of VLP-specific IgM, IgG1, and IgG2c ELISA

All sera were individually collected, and levels of IgM, IgG1 and IgG2c specific for VLP (HBc-Ag) and VLPs expressing MHC-II T-cell epitopes were determined by ELISA. 96 well flat-bottomed ELISA plates (Immulon IV plates-Dynatech- Canada) were coated with 50 µg/well of the purified VLP (HBc-Ag) and with VLPs + MHC-II T-cell epitopes at 1 µg/ml in 0.5 M carbonate-bicarbonate buffer pH 9.6 for overnight at 4°C. The next day, plates were washed 5 times with PBS Tween-20 (PBS-T20) (0.05% Tween 20, Sigma-Aldrich) and incubated for 1 hour at 37°C with 100 µl/well of 3% BSA in PBS to block non-specific binding. The sera were diluted from 1:20 to 1:2560 in PBS-T20 and then 50 µl of each dilution was added to the plates and incubated for 1 hour at 37°C followed by washing 5 times with PBS-T20. Subsequently, 50 µl Biotinylated rat anti-mouse IgG1 (Clone: A85-1, BD Biosciences, 1:500) or IgG2c (Clone: R19-15, BD Biosciences, 1:100) or Biotinylated rat anti-mouse IgM (Clone: 11/41, BD Biosciences, 1:500) was added to the plates and the plates were incubated for 1 hour at room temperature. The plates were then washed 5 times with PBS-T20. 75 µl/well of SA-POD (Streptavidin-Peroxidase- Roch- 1:1000) was added to the plates and incubated for 1 hour at room temperature followed by 5 washes with PBS-T20. 100µl/well of TMB ELISA substrate (3, 3', 5, 5'-tetramethylbenzidine- Thermo) was then added to the plates. Finally, 50 µl/well of the stop solution 0.003% (H₂SO₄) (2N sulphurine acids- R&D) was added to stop the colour development. Plates were read using a Dynex MRX11 plate reader (DYNEX Technologies) at 450 nm with a reference of 570 nm. Data were analysed by using the GraphPad Prism7 software.

2.16 Semi-Dry western blot

ON E/S or purified VLP recombinant proteins were first separated by the NuPAGE 10% Bis-Tris Pre-Cast gels Sodium Dodecyl Sulfate Polyacrylamide Gel Electrophoresis (SDS-PAGE) as described in section 2.15.11 (Life Technologies). Gels were placed next to a 0.45 µm nitrocellulose membrane (Bio-Rad), and an electrical current caused the separated proteins to transfer onto the membrane using a Bio-Rad Transblot SD Semi-Dry transfer cell at 25 V constant voltages for 10 min in Tris-Glycine Transfer Buffer 1XTBS (Bio-Rad). The membranes were then cut into strips, and each strip was blocked with 3 ml of 5% w/v nonfat dry milk (Cell Signaling) in 1XTBST Tris Buffered Saline with Tween 20 at room temperature for 1 hour followed by washing three times for 10 min each with 3 ml of 1XTBST. The membranes were then incubated overnight in mouse serum diluted at (1:80) pooled from individuals within mouse groups. The next day, the membranes were washed three times with 1XTBST, and peroxidase affiniPure F (ab')₂ Fragment goat anti-mouse IgM, µ chain specific (Jackson Immuno Research) was added at a 1:10,000 or anti-mouse IgG, HRP-linked antibody (Cell Signaling) at a 1:3,000 dilution, and incubated at room temperature for 1 hour. After three washes with 1XTBST, membranes were incubated with 10 ml of clarity western ECL substrate (Bio-Rad) (5 ml Reagent A and 5 ml Reagent B) for 1 min at room temperature to visualise the target protein. Detection was carried out using the ChemiDoc MP Imager system (BIO-RAD, UK).

2.17 Histology

A 1 cm segment of the cecum was removed and placed in pre-labelled histology cassettes and fixed at room temperature in Neutral buffered formalin (NBF) fixative (4% v/v formaldehyde (BDH), 0.154 M NaCl (Sigma-Aldrich), 2% v/v glacial acetic acid (BDH), 1.37 mM hexadecyl trimethylammonium bromide (Sigma-Aldrich) overnight, prior to processing and embedding in paraffin (Histocentre2, Shandon). For histochemical analysis, 5 µm thick serial sections were cut using microtome and collected onto pre-labelled gelatine coated glass slides and allowed to dry for overnight at 37°C. Slides were then dewaxed in citroclear (TCS Biosciences) for 10 mins, followed by a five minute rehydration step through a series of washes with decreased serial dilutions of ethanol (100%, 100%, 90%, 70%, and 50%) (Fisher Scientific), followed by five minutes incubation in dH₂O.

2.17.1 Haematoxylin and Eosin staining of paraffin sections

Hematoxylin and Eosin staining was performed to measure the crypt length. Rehydrated sections were stained with hematoxylin solution (Sigma-Aldrich) for 4 minutes, followed by washing in tap water for 5 mins. Slides were differentiated with 1% acid alcohol (1% HCl in 70% alcohol) for 2 seconds to remove excess dye, followed by washing in tap water for 5 mins. Slides were then treated with eosin (Sigma-Aldrich) for 30 seconds, followed by washing in tap water for 5 minutes. Sections were then dehydrated through a series of washes with increased serial dilutions of ethanol (50%, 70%, 90%, and then 100%). Finally, slides were cleared with citroclear for 5 mins and mounted and coverslipped using DEPEX mounting media (BDH Laboratory Supplies).

2.17.2 Goblet cell staining of paraffin sections

Periodic acid–Schiff staining (PAS) was performed to identify mucus-secreting cells (goblet cells). Slides were stained in 1% alcian blue (Sigma-Aldrich) in 3% acetic acid (pH2.5) for 15 minutes followed by washing in distilled water. Slides were then treated with 1% periodic acid (Sigma-Aldrich) for 5 minutes and then washed in distilled water followed by a wash in tap water for 5 minutes, then another rinse in distilled water. Slides were then treated with Schiff's reagent (Sigma-Aldrich) for 10 minutes and then washed in distilled water, followed by a wash in tap water for 5 minutes, then another rinse in distilled water. Slides were then treated with Mayer's haematoxylin (Sigma-Aldrich) for 3 minutes and followed by tap water. Slides were then treated with 5% acetic acid (Sigma-Aldrich) for 20 seconds, then another rinse in distilled water. Sections were dehydrated through a series of washes with increased serial dilutions of ethanol (50%, 70%, 90%, and then 100%). Slides were then cleared with citroclear for 5 mins and mounted and coverslipped using DEPEX mounting media (BDH Laboratory Supplies). Goblet cells were stained blue (acid mucins) with grey/blue nuclei.

2.17.3 Quantification of histological staining

Stained slides of proximal colon sections were scanned using 3D Histech Pannoramic 250 flash slide scanner. Photographs of the sections were taken at 100X magnification using panoramic viewer version 1.15.4 software. Twenty crypt lengths from 60 measurements were determined per mouse using ImageJ software. The number of goblet cells was determined as the total number of PAS-positive cells in 60 randomly selected crypts in three fields of view from each section.

2.18 HBc-insert plasmid construction

The native VLP (HBc-Ag) obtained from (pmK-RQ) vector was first placed in a pET17b vector between the NdeI (CATATG) and Xhol (CTCGAG) restriction sites. Figure 2.1 shows the details of the HBc construct. The fusion of each MHC-II T-cell epitope was obtained by melting and annealing oligonucleotide primers obtained from (Eurofins) containing restriction sites (BamHI + EcoRI) obtained from (Eurofins). To anneal forward and reverse primers, 2 µg of each oligonucleotide primer was added to the annealing buffer (10 mM Tris, 50mM NaCl, 1 mM EDTA, pH 7.5-8.0) in a total volume of 50 µl and placed on a 90-95°C hot block for 5-10 minutes. The hot block with the tube was removed from the heat source and placed on the bench allowing for slow cooling (annealing) at 37°C for 45 minutes. Table 2.2 lists the complete sequences of the MHC-II T-cell epitopes and primers of the constructs.

The insertion was made at the MIR to generate higher immunogenicity. The insert was subjected to ligation with Rapid Ligase, and the resulting fragments were inserted into the (pET-17b) vector previously digested with (BamHI + EcoRI) restriction enzymes (Fig 2.2). The ligation mixture comprised of 2 µl (25 ng/m) vector added to 1 µl (75 ng/ml) insert DNA, 2 µl of 5X Ligase Buffer, 1 µl Rapid DNA Ligase (Roche Diagnostic), and Milli-Q water to a total volume of 10 µl and incubated at 37°C for 2 hours.

2.19 HBc-HP₁₋₅₁₂ and HBc-mosaic plasmid construction

The HBc-HP₁₋₅₁₂ and HBc-mosaic DNA sequence were codon optimised in *E. coli* and synthesised by GeneArt. The synthesised DNA obtained from the (pmK-RQ) vector was placed in a pET17b vector between the NdeI (CATATG) and XhoI (CTCGAG) restriction sites. The synthesised DNA obtained in the (pmK-RQ) vector was first purified using the QIAprep Spin Miniprep extraction kit following the original protocol provided by (Qiagen - USA). After the purification, the vector was then linearized by restriction digests (PstI and BglIII). The digested DNA was confirmed by mixing the DNA with a loading buffer (Bioline- Germany) and then submitted to 0.5% (w/v) agarose gel electrophoresis (Bioline- Germany) with Tris- Acetate- EDTA (TAE) with ethidium bromide (Sigma-Aldrich). The DNA was then extracted from the gel and purified using the QIAquick PCR Purification Kit following the original protocol provided by (Qiagen-USA). The concentration of the DNA was measured using a Nano-Drop spectrophotometer. The DNA was then subjected to ligation with Rapid Ligase, and the resulting fragments were inserted into the (pET-17b) vector previously digested with (BamHI + EcoRI) restriction enzymes as mentioned before. Table 2.3 lists the complete sequences of the HBc-HP₁₋₅₁₂ and HBc-mosaic constructs.

CATATG GACATTGACCCTTACAAAGAATTGGCGCGACAGTGGAACTGTTGAGCTTCCTCCCTCTG AT 1. TTTTCCCCTCCGTGCAGATCTGCTGGATA CGGCCTCCGCCCTTATCGCAAGCGTTGGAGAGTC CAGAACATTGTTACCCGCATCATACTGCTCTGCAGGAATCCTGTGTTGGGGTGAGTTAATGAC TCTGGCAACGTGGTGGGAATAACCTTGAGGACGGCGGTGGCGGTAGCGGGGGCGGCGGCGG GGATCC CCG GCGAATT C GGCGGTGGCGGTAGCGGGGTGGCGGTTGCAGATCTGGTGGTAAACTATGTGAACA CGAATATGGGCTAAAAATTGGCAGCTGCTCTGGTTCACATTAGCTGCTGACCTTGTCGGGA AACGGTCTGGAGTACCTGGTAGCTCGGGCTGGATTGGACACCGCCAGCTTACGGCCCCCA AACGCTCCGATCTTAAGTACGCTGCCGAAACCACCGTGGTGGTAGCGGCAGGTTACCGGT AAGC TT GGCGGTGGC TGGAGCCATCCGCAGTTGAAAAATAACTCGAG	582. H MetDIDPYKEFGATVELLSFLPSDFFPSVRDLDTASALYREALESPFHCSPEHCSPHHTALRQAILCWGE L MetT L ATWGN N LED GGGGSGGGGS PAEF GGGGSGGGGS RDLVNVNTN M et GLKIRQLLWFHIS CLTFGRETVLEYLVSGVWIRT PPAYRP PNAPI STLPET TVVGSGG GTGKL GGGWSHPQFEKTAAL E
His MetGluThrAspIleAspProTyrLysGluPheGlyAlaThrValGluLeuLeuSerPheLeuP ro 1. SerAspPhePheProSerValArgAspLeuLeuAspThrAlaSerAlaLeuTyrArgGluAlaLeuG luSerProGluHisCysSerProHisHisThrAlaLeuArgGlnAlaIleLeuCysTrpGlyGluLe uMetGluThrThrLeuAlaThrTrpValGlyAsnAsnLeuGluAsp Gly Gly Gly Gly Gly Gly Ser Pro Ala Glu Phe Gly Gly Gly Ser Gly Gly Gly Gly Ser Pro Ala Tyr Arg Pro Pro Asn Ala Pro Ile Leu Ser Thr Leu Pro Glu Thr Thr Val Val Gly Ser Gly Gly Thr Gly Lys Leu Gly Gly Gly Trp Ser His Pro Gln Phe Glu Lys Ser Thr Pro Leu Gl u 202.	

Figure 2.1 The complete sequence of the native VLP (HBc-Ag) construct. Bases marked in red are restriction sites; NdeI (**CATATG**), XbaI (**CTCGAG**), BamHI (**GGATCC**), EcoRI (**GAATTC**), KpnI (**GGTACC**) and HindIII (**AAGCTT**) with short bases (GGT) in between in the C-terminus. Bases marked in green (**CCGGCG**) and (**PAEF**) are short bases between the Major Immunodominant Region (MIR) BamH1 and EcoR1 restriction sites. Yellow marked bases are artificial linker regions (4xGS4xGS) before and (4xGS4xGS) after the MIR restriction site to enhance the flexibility of the fusion proteins. Orange bases (**TGGAGCCATCCGCAGTTGAAAAA**) and (**WSHPQFEK**) are the Strep-tag, and the pink bases (**AAA**) are the stop codon.

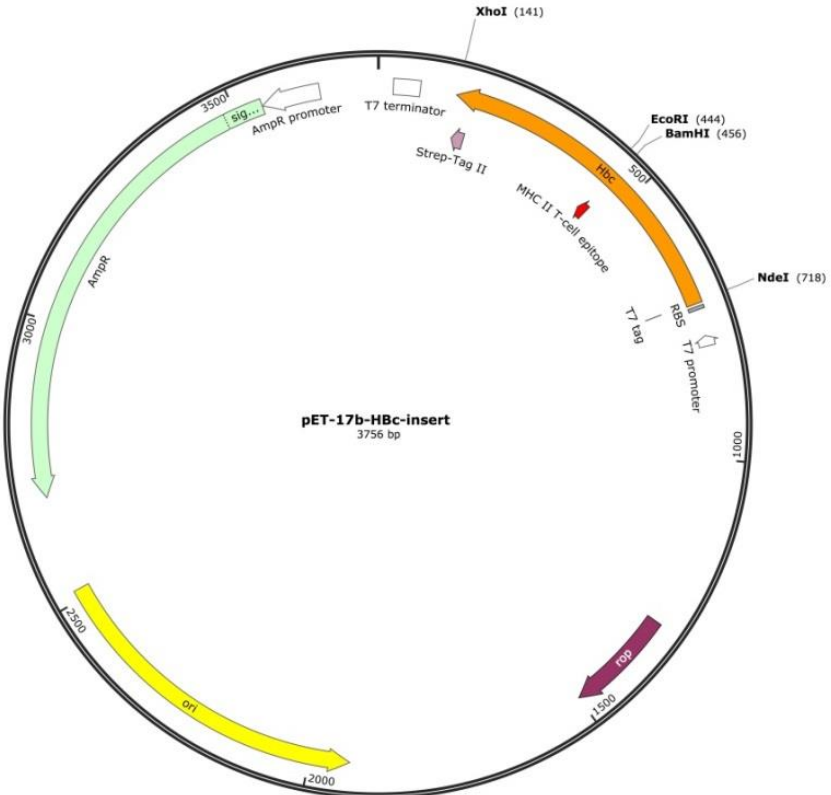


Figure 2.2: DNA construction for HBc-Ag inserted in N-terminally T7-tagged pET-17b vector from Novagen. HBc-Ag indicates the full sequence of HBc-Ag. Twenty-two amino acids as an MHC T-cell epitope for *Trichuris* were inserted in the MIR of the HBc-Ag. The cloning site for the MHC-II T-cell epitopes is BamH1 and EcoR1. Ampicillin: Ampicillin resistance gene. Ori: vector origin of replication.

Table 2.2 List of MHC-II T-cell epitope sequences and primers used to amplify the target.

Protein (Uniprot ID number)	Epitope name amino acid sequence	Primers sequence
Chitin-binding domain containing protein (A0A0N5E6C6)	CBD ₃₆₋₅₂ RPRLLKIKWSPTAASTA	Forward BamHI primer: GATCCtttccgccccgcgcctgctgaaaattaaatggagcccaccgcggcgacccgcgattcatG
		Reverse EcoRI primer: AATTCatgaatcgccgtgctcgccgcggctggctccatthaatttcagcaggcgccggcgccgaaaG
Chitin-binding domain containing protein (A0A0N5E6C6)	CBD ₁₂₄₃₋₁₂₅₉ PAGVVYQCTMPRYTLCV	Forward BamHI primer: GATCCaacctgccgcggcggtgttatcagtgcaccatgccgcgtataacccttgtgcG
		Reverse EcoRI primer: AATTCgacagggatagcgcggcatggtaactgatacaccacgcggccggcaggttG
Chitin-binding domain containing protein (A0A0N5DK22)	CBD ₂₄₁₋₂₅₇ GRTTPVTSAPTTVTTER	Forward BamHI primer: GATCCtgcaccggccgaccaccccggtgaccagcgcgcgaccaccgtgaccaccgaacgcagcccgG
		Reverse EcoRI primer: AATTCgggctgcgttcggttcacggtggtcggcgctggcacccgggtggcgccggcaatG
Pfam-B 9093 domain containing protein (A0A0N5E6W6)	Pfam 256-273 NFGEYWFTKPVGSVSYKV	Forward BamHI primer: GATCCgaatttaacttggcaatattggttaccaaaccggggcagcgtgagctataaagtgcgtgcG
		Reverse EcoRI primer: AATTCgacgcactttagctcacgtgcacccaccggttggtaaaccatattcccaaagttaatG
Chymotrypsin-like serine proteases (A0A0N5DEK1)	CLSP ₄₃₃₋₄₅₀ SKLRVYAGSPRSRIR	Forward BamHI primer: GATCCgaaaaagcaactgcgcgttatgcggcagccgcgttagccgcattcgccgcG
		Reverse EcoRI primer: AATTCggcgcgcaatgcggctaaagcgcggctgcccgcatacgcgcagttgttccattttttttG
Chymotrypsin-like serine proteases (A0A0N5E3X0)	CLSP ₂₂₂₋₂₃₇ MEKKRKYLGSPLVCF	Forward BamHI primer: GATCCaaaaaaaaatggaaaaaaaaacgcaaatatctggcagccgcgtggtgctttgtgcgcG
		Reverse EcoRI primer: AATTCgacgcacaagcacccagcggctgccagatattgcgtttttccattttttttG
Chymotrypsin-like serine proteases (A0A0N5DUC1)	CLSP ₁₄₃₋₁₅₈ AILQLAKPVFSNTVR	Forward BamHI primer: GATCCggcgtggcgttgcagctggcggaaaccgggtgcgttagcaacaccgtgcgcacgattG
		Reverse EcoRI primer: AATTCaattcgccgcacgggtttgctaaacggcaccgggttgcagaatgcgcacgcccG

Chymotrypsin-like serine proteases (A0A0N5DUC1)	CLSP ₄₂₄₋₄₄₃ CTGSLYASARANFTRTVLTS	BamHI Fw: <i>GATCCgtgatttgacccggcagcctgtatgcgagcgccgcgcgaacttaccgcaccgtgtacca</i> <i>gcgcgagcG</i> Reverse EcoRI primer: <i>AATTcgctcgcgctggtcagcacggtgccggtaaagtgcgcgcgcgtcgcatacaggctgccggtaa</i> <i>aatcacG</i>
Chymotrypsin-like serine proteases (A0A0N5DUC1)	CLSP ₃₉₈₋₄₁₆ SDHQEGYPVSPSVHIVSLA	Forward BamHI primer: <i>GATCCcatgtgagcgatcatcaggaaggctatccgtgagcccagcgtgcatattgtgagcctggcgaaaggcG</i> Reverse EcoRI primer: <i>AATTcgccaggctacaatatgcacgctcggctcaccggatagccttcgtatgcgtcacatgG</i>
Hypothetical protein (A0A0N5DRU5)	H ₁₁₂₋₁₂₈ GARKFLPIYQKAVAEK	Forward BamHI primer: <i>GATCCaaaggcggcgccgcaaattctgccattatcagaaagcggtggcggaaaaaaa</i> <i>gaagtgcG</i> Reverse EcoRI primer: <i>AATTccacttc</i> <i>ttttctccgccaccgtttctgataaatcggcagaaatttgcgcgcgcgccttG</i>

The restriction sites and the two extra amino acids bases are coloured in green and red, respectively.

Table 2.3 The complete sequences of the selected antigen constructs obtained from GeneArt.

Synthetic Protein	Protein amino acid Sequence
HBc-Hypothetical protein (HBc-HP₁₋₅₁₂) (A0A0N5DRU5) Molecular weight: 55.29kDa	<p>HMDIDPYKEFGATVELLSFLPSDFPPSVDLLTASALYREALESPEHCSPHTALRQAILCWGELMTLATWGNNELEDGGGGSGGGSGGGGGGGELGLVAAGHKDECDCIKGVPGYEKSHLDYAGKFKGARKFLPIYEKAVAEKEVLIKGGPGACDYEPCECRHKRGVEDCGCLKGVGPGYEKSYLDYAGKFKGARKFLPIYQKAVAEKEVLIKGGPGACDYEPCECRHKRGLKDCGCCKGVGPGYEKSYLDYDGKFKGARKFLPIYEKAVAEKEVLIKGVPGACDWEPCECRHKRGLKDCGCLKGVGPGYEKSYLDYAGKFKGARKFLPIYEKAVAEKEVLIKGGPGARDGCKHMGLIKIRQLLWFHISCLTFRET VLEYLVSFGVWIRTPPAYRPPNAPISTLPETTVVGSGGGTGKLGGGWSHPQFEKLE</p> <p>HisMetAspIleAspProTyrLysGluPheGlyAlaThrValGluLeuLeuSerPheLeuProSerAspPhePheProSerValArgAspLeuLeuAspThrAlaSerAla1. LeuTyrArgGluAlaLeuGluSerProGluHisCysSerProHisHisThrAlaLeuArgGlnAlaIleLeuCysTrpGlyGluLeuMetThrLeuAlaThrTrpValGlyAsnAsnLeuGluAspGlyGlyGlyGlySerGlyGlyGlySerGlyGlyGlyGlyGlyGluLeuGlyLeuValAlaAlaGlyHisLysAspGluCysAspCysIleLysGlyValGlyProGlyTyrGluLysSerHisLeuAspTyrAlaGlyLysPheLysGlyGlyAlaArgLysPheLeuProIleTyrGluLysAlaValAlaGluGluLysGluValLeuIleLysGlyGlyProGlyAlaCysAspTyrGluProCysGluCysArgHisLysArgGlyValGluAspCysGlyCysLeuLysGlyValGlyProGlyTyrGluLysSerTyrLeuAspTyrAlaGlyLysPheLysGlyGlyAlaArgLysPheLeuProIleTyrGlnLysAlaValAlaGluGluLysGluValLeuIleLysGlyGlyProGlyAlaCysAspTyrGluProCysGluCysArgHisLysArgGlyLeuLysAspCysGlyCysCysLysGlyValGlyProGlyTyrGluLysSerTyrLeuAspTyrAspGlyLysPheLysGlyGlyAlaArgLysPheLeuProIleTyrGluLysAlaValAlaGluGluLysGluValLeuValLysGlyGlyProGlyAlaCysAspTrpGluProCysGluCysArgHisLysArgGlyLeuLysAspCysGlyCysLeuLysGlyValGlyProGlyTyrGluLysSerTyrLeuAspTyrAlaGlyLysPheLysGlyGlyAlaArgLysPheLeuProIleTyrGluLysAlaValAlaGluGluLysGluValLeuValLysGlyGlyProGlyAlaCysAspTrpGluProCysGluCysArgHisLysArgGlyLeuLysAspCysGlyCysLeuLysGlyValGlyProGlyTyrGluLysSerTyrLeuAspTyrAlaGlyLysPheLysGlyGlyAlaArgLysPheLeuProIleTyrGluLysAlaValAlaGluGluLysGluValLeuIleLysGlyGlyProGlyAlaCysAspTrpGluProCysGluCysArgHisLysMetGlyLeuLysIleArgGlnLeuLeuTrpPheHisIleSerCysLeuThrPheGlyArgGluThrValLeuGluTyrLeuValSerPheGlyValTrpIleArgThrProProAlaTyrArgProProAsnAlaProIleLeuSerThrLeuProGluThrThrValValGlySerGlyGlyLysLeuGlyGlyGlyTrpSerHisProGlnPheGluLysLeuGlu512.</p>
HBc-Hypothetical protein (A0A0N5DRU5) + CLSP₃₉₈₋₄₁₆ +	<p>HMDIDPYKEFGATVELLSFLPSDFPPSVDLLTASALYREALESPEHCSPHTALRQAILCWGELMTLATWGNNELEDGGGGSGGGSGGGGGGGELGLVAAGHKDECDCIKGVPGYEKSHLDYAGKFKGARKFLPIYEKAVAEKEVLIKGGPGACDYEPCECRHKRGVEDCGCLKGVGPGYEKSYLDYAGKFKGARKFLPIYQKAVAEKEVLIKGGPGACDWEPCECRHKRGLKDCGCCKGVGPGYEKSYLDYDGKFKGARKFLPIYEKAVAEKEVLIKGVPGACDWEPCECRHKRGLKDCGCLKGVGPGYEKSYLDYAGKFKGARKFLPIYEKAVAEKEVLIKGGPGARDGCKHGGGGELAKSKLDRVYAGSPRFSRIFGGGSGGGGGGGGELIVRKTFRVPFPFRPRLLKIKWSPTAASTAIHPRWTMRENAAVILLVLIALAAFGEAGYSCEGKSNGDYGDPAEPCSSRYFSCVNGKAIGRQCPRGLYFHPGLDKCDWPHGITACSNVQEKETFRCPAENGDPDPEHQCSAKFWRCTNGKAEPYAMGLKIRQLLWFHISCLTFRET VLEYLVSFGVWIRTPPAYRPPNAPISTLPETTVVGSGGGTGKLGGGWSHPQFEKLE</p>

Chitin binding domain A0A0N5DK22 (HBc-mosaic) Molecular weight: 77.70 kDa	HisMetAspIleAspProTyrLysGluPheGlyAlaThrValGluLeuLeuSerPheLeuProSerAspPhePheProSerValArg 1. AspLeuLeuAspThrAlaSerAlaLeuTyrArgGluAlaLeuGluSerProGluHisCysSerProHisHisThrAlaLeuArgGlnAlaIleLeuCysTrpGlyGluLeu MetThrLeuAlaThrTrpValGlyAsnAsnLeuGluAspGlyGlyGlySerGlyGlyGlySerGlyGlyGlyGlyGluLeuGlyLeuValAlaAlaGly HisLysAspGluCysAspCysIleLysGlyValGlyProGlyTyrGluLysSerHisLeuAspTyrAlaGlyLysPheLysGlyGlyAlaArgLysPheLeuProIleTyr GluLysAlaValAlaGluGluLysGluValLeuIleLysGlyGlyProGlyAlaCysAspTyrGluProCysGluCysArgHisLysArgGlyValGluAspCysGlyCys LeuLysGlyValGlyProGlyTyrGluLysSerTyrLeuAspTyrAlaGlyLysPheLysGlyAlaArgLysPheLeuProIleTyrGlnLysAlaValAlaGluGlu LysGluValLeuIleLysGlyGlyProGlyAlaCysAspTyrGluProCysGluCysArgHisLysArgGlyLeuLysAspCysGlyCysCysLysGlyValGlyProGly TyrGluLysSerTyrLeuAspTyrAspGlyLysPheLysGlyGlyAlaArgLysPheLeuProIleTyrGluLysAlaValAlaGluGluLysGluValLeuValLysGly GlyProGlyAlaCysAspTrpGluProCysGluCysArgHisLysArgGlyLeuLysAspCysGlyCysLeuLysGlyValGlyProGlyTyrGluLysSerTyrLeuAsp TyrAlaGlyLysPheLysGlyGlyAlaArgLysPheLeuProIleTyrGluLysAlaValAlaGluGluLysGluValLeuValLysGlyGlyProGlyAlaCysAspTrp GluProCysGluCysArgHisLysArgGlyLeuLysAspCysGlyCysLeuLysGlyValGlyProGlyTyrGluLysSerTyrLeuAspTyrAlaGlyLysPheLysGly GlyAlaArgLysPheLeuProIleTyrGluLysAlaValAlaGluGluLysGluValLeuIleLysGlyProGlyAlaArgAspCysGlyCysLysHisGlyGlyGly GlySerGlyGlyGlySerGlyGlyGlyGlyGlyGluLeuAlaLysSerLysLeuArgValTyrAlaGlySerProArgPheSerArgIleArgGlyGlyGlyGly SerGlyGlyGlySerGlyGlyGlyGlyGlyGluLeuIleValArgLysThrPheArgValGlyProPheProArgLeuLeuIleLysTrpSerPro ThrAlaAlaSerThrAlaIleHisProArgTrpThrMetGlyArgGluAsnAlaLysValAlaIleLeuLeuAlaLeuAlaLeuAlaPheGlyGluAlaGlyTyr SerCysGluGlyLysSerAsnGlyAspTyrGlyAspProAlaGluProCysSerSerArgTyrPheSerCysValAsnGlyLysAlaIleGlyArgGlnCysProArgGly LeuTyrPheHisProGlyLeuAspLysCysAspTrpProHisGlyIleThrAlaCysSerAsnValGlnGluLysGluThrPheArgCysProAlaGluAsnGlyAspTyr ProAspProGluHisGlnCysSerAlaLysPheTrpArgCysThrAsnGlyLysAlaGluProTyrAlaMetGlyLeuLysIleArgGlnLeuLeuTrpPheHisIleSer CysLeuThrPheGlyArgGluThrValLeuGluTyrLeuValSerPheGlyValTrpIleArgThrProProAlaTyrArgProProAsnAlaProIleLeuSerThrLeu ProGluThrThrValValGlySerGlyGlyGlyThrGlyLysLeuGlyGlyGlyTrpSerHisProGlnPheGluLysLeuGlu
--	--

Bases marked in Blue are hypothetical protein, purple residues are the CLSP₃₉₈₋₄₁₆ epitope, and the green residues are chitin-binding domain-containing protein (A0A0N5DK22). Yellow marked residues are artificial linker regions (**4GS4GS5G**) to enhance the flexibility of the fusion proteins. The orange bases are the StrepTag (**WSHP**).

2.20 Transformation

The recombinant plasmid containing the epitope insert was first transformed into XL-I Blue supercompetent cells and Lemo21 (DE3) competent cells for small-scale expression obtained from (New England Biolabs) by heat-shock transformation. The recombinant plasmid containing the synthesised protein insert was transformed into Ultracompetent cells (XL10-Gold) obtained from (Agilent Technologies) by heat-shock transformation. For this, 1 μ l of the DNA mixture was added into 50 μ l of the heat shock competent cells in a falcon tube and placed on ice for 30 mins. The tube was then transferred into a 42°C water bath for 45 secs and then transferred to the ice for 2 mins. 250 μ l of the Luria-Bertani (LB) Broth were then added to the transformation mixture and incubated at 37° C for 1 hour. 250 μ l of the transformation mixture was then added to the LB plate containing the appropriate antibiotic (Ampicillin or Kanamycin) and incubated at 37°C for overnight.

2.21 Plasmid purification: QIAprep spin miniprep kit

The recombinant plasmid DNA was purified using the original protocol that is provided by (Qiagen-USA). Briefly, the bacterial cell pellet was resuspended in 250 μ l Buffer P1 and transferred to microcentrifuge tubes. After that, 250 μ l Buffer P2 was added to the tubes and mixed thoroughly by inverting the tube 4–6 times, followed by adding 350 μ l Buffer N3 and mixing immediately. The tubes were then centrifuged in a table-top microcentrifuge for 10 min at 8,000 $\times g$. To wash the QIAprep 2.0 spin column, 0.75 ml Buffer PE was added, followed by centrifugation. Finally, to elute the DNA, the QIAprep 2.0 column was placed in a clean 1.5 ml microcentrifuge tube, and 55 μ l of Milli-Q water was added to the centre of each column, let stand for 3 min and centrifuged for 1 min. The concentration of the DNA was measured using a NanoDrop spectrophotometer, and the nucleotide sequence was verified by DNA sequencing (GATC- Biotech, Germany).

2.22 DNA sequencing

The correct insert nucleotide sequence was verified by DNA sequencing (GATC-Biotech, Germany) using the Sanger Supremerun service. DNA was eluted in Milli-Q water and chipped in a hydrated form. T7 Promoter primer was provided by the (GATC-Biotech, Germany). The DNA sequence results were provided in FASTA format and were analysed using SnapGene.

DNA concentrations were assessed using a NanoDrop spectrophotometer. Briefly, 1 μ l of Milli-Q water was first used to calibrate the spectrophotometer followed by sample buffer to clean it before loading 1 μ l of the sample. To calculate the DNA concentration, 1 μ l Milli-Q water was used as a blank, and absorption reading was conducted at 260 nm and 280 nm and the ratio between two.

2.23 Small-scale VLP expression

For small expression of the confirmed inserts, a single colony was picked from the overnight LB agar plate and inoculated into 50 mL LB broth medium supplemented with 50 μ L of 100 μ g/mL of the appropriate antibiotic (Ampicillin or Kanamycin) and incubated at 37°C for overnight in a shaker incubator to obtain a saturated culture. Next day, 400 μ L of the incubated cells were added to 4 mL LB broth containing 4 μ L of 100 μ g/mL of the appropriate antibiotic (Ampicillin or Kanamycin) and incubated for 3-4 hours until the optical density OD600 reached 0.6-0.8. The optical density was measured using spectrophotometer at 600nm wavelength. Once the OD600 reached 0.6-0.8,

flasks were chilled at 4°C for 30 mins then induced by Isopropyl-β-D-1-thiogalactopyranoside (IPTG) at a final concentration of 0.4 mM and incubated for 3-4 hours to induce recombinant protein expression. Tubes were then centrifuged at 16,000 x g for 10 minutes at 4°C. Cells were disrupted by ultra-sonication on ice using Banddelin (Sonoplus) 35% amplitude (Am) for 5 seconds on and 10 seconds off for 5-7 mins, and the supernatant containing soluble recombinant protein was harvested by centrifugation at 16,000 x g for 10 minutes at 4°C.

2.24 Large-scale VLP expression

For the overexpression of soluble proteins, the native VLP (HBc-Ag) and the VLPs + T-cell epitopes (HBc-CBD₃₆₋₅₂, HBc-CBD₁₂₄₃₋₁₂₅₉, HBc-CBD₂₄₁₋₂₅₇, HBc-CLSP₄₃₃₋₄₅₀, HBc-CLSP₂₂₂₋₂₃₇, HBc-CLSP₁₄₃₋₁₅₈, HBc-CLSP₄₂₄₋₄₄₃, HBc-CLSP₃₉₈₋₄₁₆ and HBc-H₁₁₂₋₁₂₈) were transformed into ClearColi-BL21 (DE3) electrocompetent cells obtained from (Lucigen) and incubated overnight at 37°C. Next day, 40 ml of the transformed cells at a starting optical density (0.1 OD₆₀₀) were inoculated into 2 L (2x LB) liquid media supplemented with 100 µg/mL ampicillin for 3-4 hours. Once the OD₆₀₀ reached 0.6-0.8, flasks were chilled at 4°C for 30 mins then induced by IPTG at a final concentration of 0.4 mM. The culture was then grown by continuous shaking for 12-16 hours at 16°C. The cells were then harvested by centrifugation at 6,000 x g for 20 mins at 4°C using Sorvall RC-5C plus with the Sorvall SLC -300 rotor. Cell pellets were then stored rapidly at -80°C after flash freezing in liquid nitrogen until needed.

2.25 Preparation of cell lysate

The cells from the large-scale expression were first thawed and then resuspended at a ratio (4 ml/gram cells) in Strep-Tag washing buffer (100 mM Tris-HCl, 150 mM NaCl, 1 mM EDTA, pH 8). 1 tablet of cOmplete TM EDTA- Free Protease Inhibitor Cocktail (Sigma-Aldrich) was added per 50 mls of the resuspended cells along with 5 µg/ml DNase I (Sigma-Aldrich). The cell suspension was then disrupted by ultra-sonication on ice using Banddelinuw 3200 (Sonoplus) amplitude (Am) in 35% for 5 sec on and 10 sec off for 5-8 minutes. The supernatant containing soluble recombinant protein was harvested following centrifugation at 18,900 x g for 40 mins at 4°C in 50 ml Nalgene PC tubes using Sorvall RC Plus with the Fiber-Lite F21 8x50y rotor. Finally, the soluble supernatant was filtered through 0.22 µm pore size filters.

2.26 Stage 1 purification using StrepTrap™ affinity chromatography

The soluble native VLP (HBc-Ag) and the soluble VLP expressing *Trichuris* MHC-II T-cell epitopes were purified by 5 ml affinity column chromatography using StrepTrap™ column prepacked with StrepTactin Sepharose for purifying Strep(II)-tag proteins by following the manufacturer's protocol provided by GE Healthcare. The binding/wash buffer used was the (100 mM Tris-HCl, 150 mM NaCl, 1 mM EDTA, pH 8) and the elution buffer was the lysis buffer supplemented with 2.5 mM desthiobiotin (GE Healthcare). Briefly, the column was first equilibrated with 5 CV (column volume) washing buffer using a hydrostatic pump at a rate of 1ml/min. To regenerate the column, 10 CV 0.5 mM NaOH was used at 2 ml/min followed by 10 CV H₂O, 5 CV binding buffer, loading the samples to the column at a rate of 1 ml/min followed by a 10 CV binding buffer. 5 CV elution buffer was then

applied at 1 ml/min. The purification fractions were collected and concentrated to 0.5 ml using centrifugal Vivaspin concentrator (20 ml MWCO 10,000) at 6,000 x g at 4°C.

2.27 Stage 2 purification using size exclusion chromatography (SEC)

The native VLP (HBc-Ag) and the VLP recombinant proteins were further purified by SEC separation (Superose 6, 10/300 GL) using the AKTA FPLC device (GE Healthcare). The column was first equilibrated with 1.5 CV PBS buffer at pH 7.4 with a flow rate (0.5 ml/min) by following the original protocol provided by (GE, Healthcare, US). Purified VLPs were first concentrated to 0.5 ml using Vivaspin concentrator (MWCO 10.000 kDa), then loaded onto a 5 ml loop. Purification was performed at a flow rate of 0.2 ml/min, and 0.5 ml fractions were collected into a 96 well block. The purified proteins were visualised using SDS-PAGE analysis. The data for chromatograms in VLPs purification were obtained from UNICORN software associated with ÄKTA purifier, and the graphs were plotted using Excel.

The protein concentrations were assessed using a NanoDrop Spectrophotometer. Briefly, 1 µl of Milli-Q water was first used to calibrate the spectrophotometer followed by sample buffer to clean it before loading 1 µl of the sample and the protein absorbance measured at 280 nm. The molecular mass, the number of amino acids, and the extinction coefficient estimated from the protein sequence using the ExPASy ProtParam tool were used to measure the concentration of the purified VLP recombinant proteins (Gasteiger et al., 2005).

2.29 10% Sodium Dodecyl Sulfate Polyacrylamide Gel Electrophoresis (SDS-PAGE)

The SDS-PAGE analysis of the total protein fraction before purification and the pellet after first and the second purification was carried out to confirm the presence of the recombinant protein. The samples were mixed with 4X Laemmli Loading Buffer (Bioline) containing 5% of 2-mercaptoethanol (Sigma-Aldrich) in a total volume of 20 µl. Before loading, the samples were boiled at 90°C on a hot plate for 3 mins, and 15 µl of the sample was loaded on to NuPAGE 10% Bis-Tris Pre-Cast gels (Life Technologies) and electrophoresed for 60 min at 160 V. 8 µl of the Bio-Rad using 1X MES running buffer containing 50 mM MES, 50 mM Tris-base, 0.1% SDS, 1 mM EDTA, pH 7.3 and obtained from NuPAGE gels, Invitrogen. The precision plus protein unstained protein standard was used as a reference ladder (Bio-Rad). The precision plus protein stained protein standard (Bio-Rad) was used as a reference ladder if the gel was used for western blot. The gel surface was washed with Milli-Q water after separation was complete and then stained with instant blue protein stain (Expedeon) if not used for Western Blot.

2.30 Designed VLPs construction and solubility

The translation of the DNA vaccine (nucleotide) sequence into a protein sequence (amino acids) was conducted by <http://web.expasy.org/translate/>. The Vendruscolo Lab, CamSol method Software, Centre for Misfolding Diseases (University of Cambridge) was then used to predict the solubility of the constructs based on the protein sequence (One score per residue) using <http://www-mvsoftware.ch.cam.ac.uk/index.php/camsolintrinsic>. Proteins with scores ≥ 1 are considered highly soluble, whereas scores ≤ -1 poorly soluble ones (Sormanni et al., 2017;

Sormanni et al., 2015). Finally, the synthesised DNA was ordered from <https://www.thermofisher.com/uk/en/home.html>.

2.31 ELISA-based endotoxin detection assay

The level of endotoxin in all the purified VLPs was measured with an ELISA-based endotoxin detection assay (Hyglos) following the manufacturer protocol provided by from Biotech. Briefly, purified VLPs were diluted in 10 fold steps and endotoxin standard (*E. coli* 055: B5) was diluted to (500 EU/ml, 50 EU/ml, 5 EU/ml, 0.5 EU/ml, and 0.05 EU/ml) using endotoxin-free water provided with the kit. 100 µl of the VLPs, standard dilutions and endotoxin-free water as negative control were added in duplicate into the microtiter wells pre-coated with LPS-binding phage recombinant protein. 20 µl of binding buffer was then added to the wells and incubated for 90 minutes at 37°C in the dark followed by washing 3 times with washing buffer. Finally, 150 µl/well of assay reagent substrate was added to the plate. Plate fluorescence signals were read at time 0 mins and after incubation for 90 mins using microplate fluorescence reader (FLx800™) supplied by BioTek Instruments. To calculate the endotoxin levels in the VLPs, the values at time 0 min were subtracted from 90 mins values, and the endotoxin standards were used to draw a 4 parameter logistic, nonlinear curve to back-calculate the endotoxin levels.

2.32 Circular Dichroism spectropolarimeter (CD)

The secondary structure of VLP recombinant proteins was examined using Circular Dichroism Spectropolarimeter (JASCO, J-810, Tokyo, Japan) using Spectra Manager software (Greenfield, 2006). The sample was first equilibrated with nitrogen gas for 10 minutes, and the Peltier temperature controller was brought to 20°C. After that, 180 µl of 0.5 mg/ml protein was loaded into a 0.5 mm UV-quartz cell cuvette then placed into the spectropolarimeter holder. All circular dichroism (CD) experiments were performed in a 0.2 mm path-length cuvette in the 260nm-190nm wavelength range, 0.5-sec response, 1 nm bandwidth, 10 accumulations (the number of scans) and 0.5 cm cell length. To wash cuvettes between samples, 5% Decon was used first, followed by 1 M Nitric acid and finally with Milli-Q H₂O. PBS buffer was used as blank, and the results were extracted from the protein containing spectra. DichroWeb was then used to interpret the results (Whitmore and Wallace, 2009).

2.33 Transmission Electron microscopy (TEM)

The presence and assembly of the purified VLP proteins were verified by transmission electron microscopy with negative staining. First, the proteins were dialysed from PBS to 1X TRIS buffer using Slide-A-Lyser MINI Dialysis Devices, 10K MWCO, 0.5 ml, 25/PK (Thermo Scientific). After that, 10 µl of the VLPs at 0.5 mg/ml was loaded onto a carbon-coated grid (JEOL, Tokyo, Japan), and left to stand for 5 min. Grids were then stained with 3% uranyl acetate (UA) for 1 min, and then the excess drained. The grid was then examined directly under FEI Tecnai 12 Biotwin Transmission Electron Microscope operating at 120 kV at magnifications ranging from 6000x to 100,000x.

2.34 Labelling VLPs with Fluorescein dye

To assess virus-like particles uptake by BMDCs and BMDMs, VLPs were labelled with Fluorescein dye following the manufacturer's protocol of Lightning-Link® Fluorescein Conjugation Kit obtained from (Expedeon- Innova Biosciences). Briefly, 10 µl of VLPs (HBc-Ag, HBc-H₁₁₂₋₁₂₈, HBc-CBD₂₄₁₋₂₅₇, and HBc-CLSP₃₉₈₋₄₁₆) at 1 mg/ml concentration were added to 1 µl LL-modifier reagent and mixed gently to give a final concentration of 0.9 mg/ml. The mixture was then added to a glass vial of Lightning-Link® mix and incubated for 3 hours @ RT (20-25°C) in the dark. 1 µl LL-quencher FD reagent was then added to quench the reaction. Free fluorescein dye was separated from the VLPs proteins by dialysis into PBS. Fluorescence intensity was examined using LSRII flow cytometer (Becton Dickinson Biosciences, Oxfordshire) and was analysed using FlowJo X software (Tree Star, Inc. COMPNAY, ADDRESS). The fluorescein-conjugated VLPs were then stored at -20 °C freezer to be used for the *in vitro* assays.

2.35 Fluorescein-conjugated VLP internalisation and localisation in APCs using an Amnis ImageStreamX cytometer

BMDCs and BMMs on day 8 were collected at 1X10⁶/ml and incubated with 10 µg/ml with fluorescein-conjugated VLP separately (HBc-Ag, HBc-H₁₁₂₋₁₂₈, HBc-CBD₂₄₁₋₂₅₇, and HBc-CLSP₃₉₈₋₄₁₆) for overnight at 37°C in 5% CO₂. Fluorescein-conjugated BSA and fluorescein-conjugated dextran at a final concentration 10 µg/ml were used as positive controls, and unstimulated BMDCs were used as a negative control. Next day, cells were incubated with 50 mM Lysotracker dye obtained from (Invitrogen) for 45 min prior to harvesting to visualise the lysosomal localisation of fluorescein-conjugated VLPs by ImageStreamX cytometry. A total of 5000 events were collected per sample. A Brightfield-1 filter was employed to image dendritic cells and macrophages, a fluorescein isothiocyanate (FITC-488 nm) filter to image fluorescein-conjugated VLPs, and an (APC-592 nm) filter to image lysosomes. The data were analysed using IDEAS software version 6.2.187.0. To correct spectral overlaps, a compensation matrix was applied to all the data after the acquisition. The degree of co-localization between green fluorescent conjugated VLPs (FITC) and Lysotracker was quantitatively measured by the Bright Detail Similarity (BDS-R3) on a cell-by-cell basis. A Bright Detail Similarity value of 1.0 indicates a high degree of similarity between two images in the same spatial location (correlated) and a value around 0 has no significant similarity (uncorrelated).

2.36 Prediction of Physicochemical Properties

The physico-chemical properties of the purified proteins were characterised using Expasy ProtParam server (<http://expasy.org/cgi-bin/protparam>) deduced from the protein sequence. This server was used to determine the molecular weight, the number of amino acids and the extinction coefficient and the GRAVY (a hydropathic index) (Gasteiger et al., 2005).

2.37 Procedures to reduce Endotoxin (LPS) contamination

To prevent endotoxin contamination, all the containers used for purifying the proteins were cleaned with virkon then distilled water then filled with 1 M NaOH, and allowed to soak for 24 hours before

use. All the buffers and water were UV sterilised and filtered with a 0.22 µm strainer filter and autoclaved before use.

2.38 Protein storage

The purified protein samples were aliquoted into 450 µl, cryofreezed with liquid nitrogen and stored at -80°C freezer to be used for *in vivo* and *in vitro* assays.

2.39 Statistical analysis

Statistical analyses were performed using Graph Pad Prism, version 7.00 software. In all tests, * $P \leq 0.05$, ** $P \leq 0.01$ *** $P \leq 0.001$, **** $P \leq 0.0001$ were considered statistically significant and were determined using the Kruskal–Wallis non-parametric ANOVA for comparing multiple groups.

Chapter Three

Systematic review and evaluation of MHC-II restricted T-cell epitope prediction tools

3.1 Introduction

Immunoinformatics approaches, including epitope prediction tools, are powerful bioinformatics tools that analyse immunological data by combining genetics sequence analysis, proteomics and mathematical models. In addition, they dramatically reduce the time, cost and effort involved in experimental and laboratory-based studies (Comber and Philip, 2014; Khalili et al., 2014; Lund, 2005; Sidney et al., 2013). Combinations of systems biology approaches and bioinformatics tools is very promising and may ultimately lead to the development of an epitope-based vaccine against microbial pathogens based on the reverse vaccinology (RV) approach (Brusic and Petrovsky, 2005; Yan, 2010). For example, the *P. falciparum* (RTS,S) vaccine, which contains three tandem repeat and T-cell epitopes identified from the circumsporozoite protein using *in silico* prediction tools, displayed on hepatitis B surface particiles (HBs-Ag) that were co-expressed in *Saccharomyces cerevisiae* and reconstituted with an AS01 adjuvant, is currently undergoing a clinical trial (Pance, 2019).

It is well documented that CD4+ T-cells play essential roles in the development of protective immunity against *Trichuris* spp, which is driven by type 2 cytokines (Bouchery et al., 2014). Initiation of an antigen-specific immune response requires antigenic peptides to be presented to CD4+ T-cells in the context of MHC class II molecules in mice and HLA molecules in humans (Dhanda et al., 2017). MHC class II peptides are 12–25 amino acids in length, and they have three main anchor residues located at positions 1, 6 and 9 that bind to CD4+ T-cells (Patronov and Doytchinova, 2013). Unlike MHC-I molecules' peptide-binding groove, which is closed at both ends, the groove in MHC-II molecules is open at both ends. For this reason, MHC-II CD4+ T-cell epitope prediction tools have much lower accuracy compared to MHC-I tools (Godkin et al., 2001; Yang and Yu, 2009). Therefore, selection of an appropriate MHC class II prediction tool is a critical first step in the development of an epitope-based vaccine against *T. trichiura* (Usmani et al., 2018).

MHC prediction models can be broadly divided into two groups: sequence-based approaches, which analyse amino acid sequences, and structure-based approaches, which analyse the three-dimensional structures of proteins (Dhanda et al., 2017). Sequence-based approaches include binding motifs, artificial neural networks (ANNs), support vector machines (SVMs), and Hidden Markov Models (HMMs), while structure-based approaches include threading algorithms, homology modelling, peptide docking, simulations, binding energy, and molecular dynamics (Patronov and Doytchinova, 2013). The sensitivity (i.e. the inclusion and efficiency of identifying a large proportion of ligands) and specificity (i.e. the efficiency of exclusion of irrelevant sequences) of each epitope prediction tool vary. For instance, motif-based approaches define peptide binding motifs in each MHC class I and II binding peptide that contain anchor residues, which are frequently occurring amino acids that interact with specific anchor positions in the polymorphic pockets of specific MHC alleles (Vivona et al., 2008). However, the absence of motifs in some MHC binders and the potential for secondary anchor residues to be located at nonconserved positions can limit the specificity and sensitivity of motif-based approaches compared to other tools (Brusic et al., 2004). This shortcoming has led to the development of quantitative matrices (QMs) and machine learning algorithms (MLAs), such as ANNs and SVMs (Martin et al., 2003; Meister et al., 1995; Wang et al., 2008). Although QMs assume that each amino acid in a peptide independently contributes to each

position at which an MHC binds, instead of anchor positions and residues, they cannot handle nonlinear data (Lafuente and Reche, 2009). MLA approaches can more accurately predict MHC binders as they can handle both linear and non-linear data (Dönnes and Elofsson, 2002; Singh and Mishra, 2008).

Comparison of different *in silico* prediction tools remains a complex task for many reasons, including inadequate documentation of the datasets used for model building, lack of availability of the training dataset used to evaluate the tools, and lack of a unified output format, which makes combining the results of several servers complicated (Soria-Guerra et al., 2015). Furthermore, there is no standardised methodology to compare the utility of prediction tools. To overcome these challenges and enable selection of an appropriate prediction tool for predicting *Trichuris* MHC-II T-cell epitopes, this chapter provides a systematic review of the available bioinformatics tools to evaluate the performance of the tools. Previous reviews have evaluated different T-cell epitope prediction tools (Gowthaman and Agrewala, 2007; Lin et al., 2008), but none to my knowledge have been conducted systematically using the criteria outlined below.

3.2 Aim and objectives

The overall aim of this chapter was to select the top MHC class II *in silico* prediction tools. This aim was achieved via two objectives:

- To identify the available MHC class II *in silico* prediction tools by conducting a systematic review based on defined inclusion/exclusion criteria.
- To evaluate the sensitivity and probability of predicting MHC-II T-cell epitopes using a unique protein training set to select the top MHC class II *in silico* prediction tools.

3.3 Methods

3.3.1 Search strategy

A protocol was designed to identify the bioinformatics tools that can predict MHC-II T-cell epitopes in accordance with the well-defined Preferred Reporting Items for Systematic Reviews and Meta-Analyses (PRISMA) (Moher et al., 2010). The search was limited to the English language and used the search terms shown in Table 3.1. A list of the search terms was first used in December 2015 on Google and other websites (Supplementary Table 3.1) to screen for MHC class I and II *in silico* prediction tools. The number of citations (>200), number of publications (>200), online availability, last update and community were considered to determine whether the tools would be selected for further analysis. The number of publications and citations for each tool were obtained from Google Scholar. In the case of duplicate citations, the highest number of citations was used. A flow diagram of the systematic review screening process for MHC-II T-cell bioinformatics prediction tools is shown in Figure 3.1.



PRISMA Flow Diagram

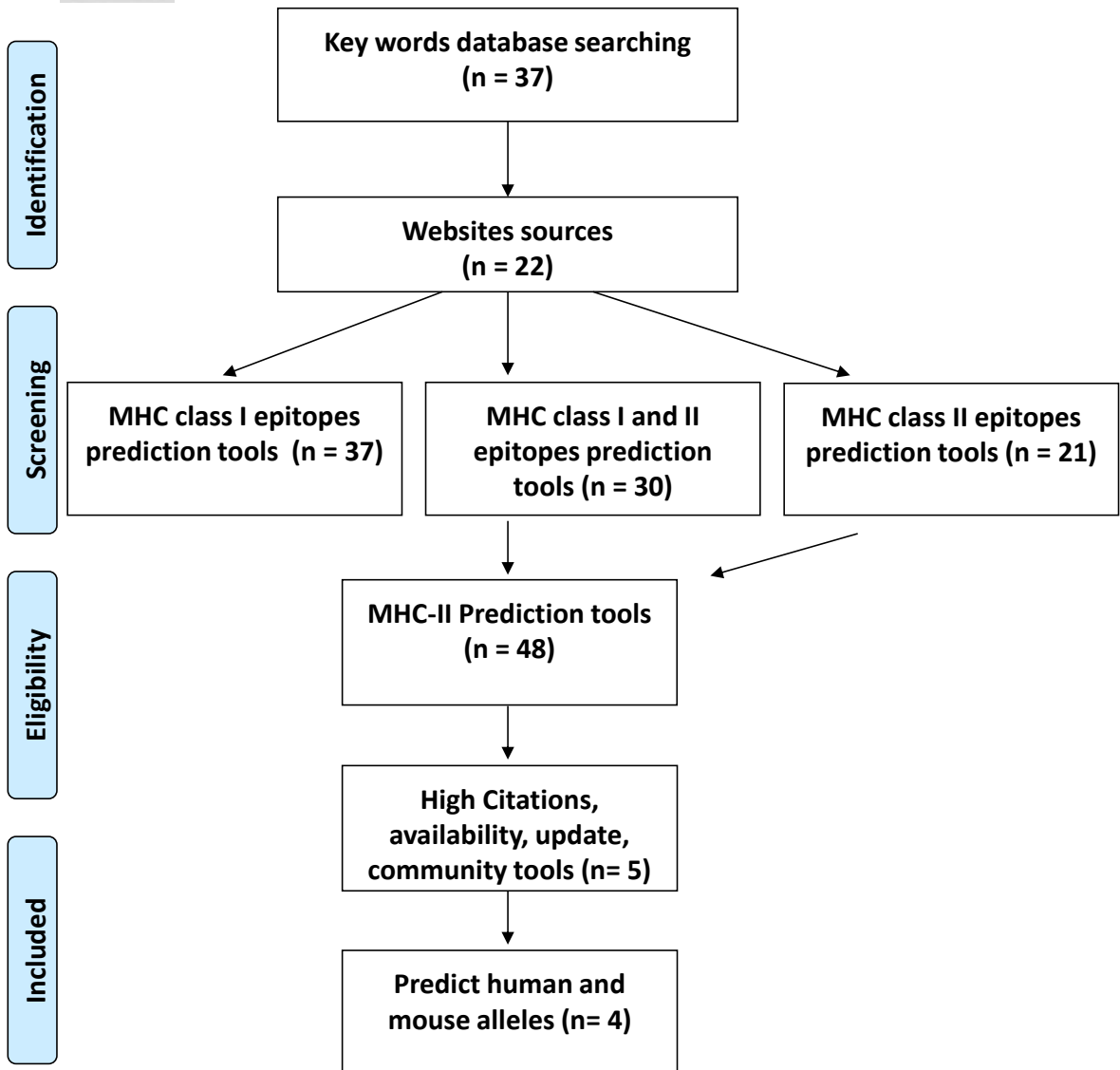


Figure 3.1 A PRISMA flow diagram of the systematic review screening process for restricted MHC-II T-cell bioinformatics prediction tools. A list of search terms was used in Google website and other website sources to screen for MHC class I and II *in silico* prediction tools. Aspects relating to the number of citations (>200), number of publications, online availability, last update and community were used as inclusion/exclusion criteria to select the top MHC-II *in silico* prediction tools. n= number of key words, websites sources and *in silico* prediction tools.

Table 3.1 List of Keywords used in this review.

Keywords
Computational vaccinology
<i>In silico</i> vaccine
Peptide-based vaccine
T cell epitope vaccine
Epitope prediction algorithms
Binding affinity prediction
Bioinformatics prediction tools
Immunoinformatics prediction tools
<i>In silico</i> peptide docking assay
<i>In silico</i> tools for vaccine design
<i>In silico</i> epitope prediction
<i>In silico</i> design of epitope-based vaccines
T cell epitope identification
T cell epitope prediction
Prediction of CTL epitopes
T cell epitope prediction methods
T cell epitope prediction tools
Application of Epitope Driven Vaccine Design
Major histocompatibility complex prediction
MHC prediction
MHC prediction methods
MHC class II epitope prediction
MHC class I epitope prediction
MHC class II epitope prediction tools
MHC class I epitope prediction tools
MHC binding prediction
MHC class I binding prediction
MHC class II binding prediction
Prediction of MHC peptide binding
Identification of MHC binding motifs
Epitope prediction software
T cell epitope database
Databases for T cell epitopes
MHC database
Major histocompatibility complex database
Database for MHC ligands and peptide motifs
Epitope Analysis

3.3.2 Construction of an epitope training set

To evaluate the performance of the tools, a literature search for MHC-II CD4+ T-cell peptide binding datasets was performed using the search terms ‘universal T-cell epitopes’ and ‘MHC class II T-cell epitopes’ on Google Scholar in December 2015. These datasets included epitopes with publicly available sequences that the literature had experimentally validated to be immunogenic in mice. Care was taken to exclude the training datasets used for tool development.

In order to find the optimal set of epitopes, two different sets of epitopes were analysed. The first set was composed of a publicly available series of peptide sequences from 15 different proteins

that can bind to MHC class II molecules. The second set included one untested protein of *T. muris*, which served as a control to evaluate the performance of the tools. Collectively, the training dataset was composed of 145 epitopes from 16 different proteins (Supplementary Table 3.2).

3.3.3 Prediction of MHC-II T-cell epitopes

Full-length sequences of proteins containing T-cell epitopes were obtained from the Universal Protein Resource (UniProt) database <http://www.uniprot.org> in FASTA format. The Immune Epitope Database (IEDB), NetMHC-II 2.2, Rankpep and SYFPEITHI tools were used to predict T-cell epitopes for mouse strains with I-Ab and I-Ad mouse alleles.

Each tool applied a different prediction method and scoring system to generate the predictions output. For instance, the IEDB tool used the consensus method for prediction, which combines the NN-align, SMM-align, combinatorial library and Sturniolo methods (Wang et al., 2008), while the NetMHC 2.2 tool uses ANNs (Nielsen and Lund, 2009).

The output of the IEDB and NetMHC 2.2 tools (the binding affinities) were expressed as half-maximal inhibitory concentration IC₅₀ (nM) values. Epitopes that bind with an affinity of <50 nM are considered to have high affinity, those that bind with <500 nM have an intermediate affinity and those that bind with <5000 nM have a low affinity (Nielsen and Lund, 2009). All epitopes with high or intermediate affinity are considered ‘true binders’, while epitopes with low affinity are considered ‘nonbinders’. No known T-cell epitope has an IC₅₀ value of >5000 nM (Wang et al., 2008).

The scoring system of the SYFPEITHI prediction tool depends on whether peptide amino acids frequently occur in anchor positions. Optimal anchor residues are given the value 15 and scores of -1 or -3 points are given to amino acids that have a negative effect on epitopes’ binding ability at a certain sequence position. Epitopes that bind strongly are among the top 2% of all peptides predicted in 80% of all predictions results (Rammensee et al., 1999).

The Rankpep tool uses position-specific scoring matrices (PSSMs) to predict MHC-II T-cell epitopes (Reche et al., 2002). A high peptide score percentage indicates that the epitope is likely to bind to the set of aligned peptides that bind to a given MHC-II molecule (Reche et al., 2002). The peptide lengths in all the resulting sets were based on the complex of 15 mer core region peptides of MHC class II molecules.

3.3.4 Evaluation and statistical analysis

Using the training set of epitopes, the performance of the four MHC-II epitope prediction tools, selected through our inclusion/exclusion criteria, were assessed as weak, intermediate or high binders. The prediction results were classified into two categories, true positive (TP) and false negative (FN), based on the threshold values (Altman and Bland, 1994). In addition, the evaluation assessed sensitivity (TP/[TP+FN]) and probability (TP/total). Nonparametric Spearman correlation and Bland-Altman analyses were performed to show the relationship and agreement between the scores derived from the NetMHC-II 2.2 and IEDB tools. The level of significance was set at p <

0.05 for the correlation test. All statistical analyses were performed using the software package GraphPad Prism version 6 for Windows.

3.4 Results

Based on a list of search terms used on Google and other websites, 88 servers that predict T-cell epitopes based on MHC class I and II binding were identified (Supplementary Table 3.3). Off the 88 tools, only 48 tools that can predict MHC-II epitopes were identified (Table 3.2). Since our primary focus was MHC-II T-cell epitope prediction tools, only those tools were further evaluated based on the inclusion criteria. The top five tools that met the inclusion criteria were IE�DB, SYPEITHI, NetMHC-II 2.2, Rankpep and ProPred. They were then scanned for the ability to predict MHC-II T-cell epitopes in two mouse alleles, I-Ab and I-Ad. The ProPred tool was excluded from further analysis because it only predicts HLA-DR binding sites. The four epitope prediction tools that met all the selection criteria were subsequently evaluated using the epitope training set to calculate the sensitivity and probability with which they could predict MHC II T-cell epitopes.

Using the epitope training set (Supplementary Table 3.2), it was observed that IE�DB and NetMHC-II 2.2 tools have high levels of sensitivity (~78.00%) and probability (~17.00%) for predicting MHC-II T-cell binding epitopes with high affinities, while Rankpep and SYFPETHI exhibited low sensitivity (10.61% and 8.33%, respectively). Collectively, the data indicate that the best prediction tools across all MHC-II T-cell prediction servers considered in this study are IE�DB and NetMHC-II 2.2 (Table 3.3).

Statistically significant differences were found when correlating the scores returned by the NetMHC-II 2.2 and IE�DB tools for MHC I-Ab ($p < 0.0001$; $r = 0.78$, 95% CI = 0.66–0.86) and MHC I-Ad ($p = 0.0071$; $r = 0.46$, 95% CI = 0.13–0.70), as shown in Figure 3.2 (A and B). A Bland-Altman plot compares the average affinity of peptide binding predicted by NetMHC-II 2.2 and IE�DB plotted against the difference in peptide-binding affinity scores given by the two tools for the prediction of MHC-II T-cell epitopes from I-Ab and I-Ad alleles (Figure 3.2 C, and D). The two tools were more likely to agree for peptides with high-affinity scores (<50 nM) than those with intermediate and low-affinity scores (<500 and <5000 nM, respectively). In addition, the majority of scores are distributed symmetrically around the mean, indicating no systematic bias. In general, the statistical evidence suggests that the NetMHC-II 2.2 and IE�DB tools are able to predict peptides with high-affinity binding scores equally well. Also, the predictions with high-affinity binding scores are mainly estimated for MHC (I-Ab) molecules than MHC (I-Ad), as shown in Figure 3.2 (C and D).

Collectively, the work in this chapter has systematically reviewed and evaluated available MHC-II cell epitope prediction tools and included two such tools to use in the project going forward.

Table 3.2 List of MHC-II epitope prediction tools and their number of publication, number of citations using Google Scholar, the online availability, last update, and community.

Prediction Tool	No of publication	No of Citation	Availability	Last Update in 2015	Community
IEDB	440	1550	Yes	12/2015	National Institute of Allergy and Infectious Diseases
NetMHCII 2.2	363	202	Yes	03/02/2012	Center for Biological Sequence analysis CBS
NNAlign (NetMHCII-2.0)	163	13	Yes	17/03/2015	CBS
NetMHCIIpan 3.1	83	156	Yes	17/11/2015	CBS, IMMI, and LIAI.
PickPocket 1.1	26	26	Yes	01/05/2015	CBS, IMMI, and LIAI.
ProPred	715	544	Yes	07/06/2002	Raghava's Group
FDR4	12	1	Yes	07/12/2014	Raghava's Group
HLAPRED	63	91	Yes	NA	Raghava's Group
HLA-DR4 Pred	563	124	Yes	27/09/2014	Raghava's Group
MHC2Pred	114	55	Yes	07/12/2014	Raghava's Group
IMHC	1	5	No	NA	Raghava's Group
MHC Bench	53	7	Yes	11/03/2014	Raghava's Group
IL4pred	3	5	Yes	NA	Raghava's Group
IFNepitope	17	4	Yes	07/12/2014	Raghava's Group
IL-10Pred	1	16	Yes	NA	Raghava's Group
Tmhcpred	4	NA	Yes	NA	Raghava's Group
MULTIPRED2	40	33	Yes	22/07/2014	Bioinformatics Core at Cancer Vaccine Center, Dana-Farber Cancer Institute.
PREDBALB/c	47	50	Yes	NA	Bioinformatics Core at Cancer Vaccine Center, Dana-Farber Cancer Institute.
RANKPEP	709	272	Yes	16/12/2015	Bioinformatics Core at Cancer Vaccine Center, Dana-Farber Cancer Institute.
MHCMIR 1.0	41	13	Yes	29/04/2015	Laboratory of data mining and intelligent information processing.
MHC2SKpan-1.0.	6	4	Yes	NA	Laboratory of data mining and intelligent information processing.
TEPIPOPEpan	35	27	Yes	11/12/2014	Laboratory of data mining and intelligent information processing.
MetaMHC	21	13	NA	NA	Laboratory of data mining and intelligent information processing.
MetaMHCIIpan	4	1	NA	NA	Laboratory of data mining and intelligent information processing.
MHC2MIL	7	4	Yes	NA	Laboratory of data mining and intelligent information processing.
MultiRTA	38	26	NA	NA	NA
EpiTOP	?	13	Yes	NA	Faculty of Pharmacy Medical University of Sofia
EpiDOCK	29	17	Yes	NA	Faculty of Pharmacy Medical University of Sofia
VaxiJen	185	141	Yes	NA	Faculty of Pharmacy Medical University of Sofia
Vaxign	3	132	Yes	NA	University of Michigan Medical School
MHCpred	387	58	Yes	11/05/2011	Faculty of Pharmacy Medical University of Sofia

PREDIVAC	26	13	Yes	27/11/2014	University of Queensland
MHC-BPS	40	32	NA	11/12/ 2014	Bioinformatics and Drug Design Group, Department of Pharmacy, National University of Singapore
SYFPEITHI	3,280	2013	Yes	27 /08/2012	Applied Bioinformatics Group at University of Tuebingen
SVMHC	385	260	Yes	NA	Applied Bioinformatics Group at University of Tuebingen
EpiToolKit 2.0	43	20	Yes	NA	Applied Bioinformatics Group at University of Tuebingen
OptiTope	33	34	Yes	NA	Applied Bioinformatics Group at the University of Tuebingen
SNEPV2	83	31	Yes	NA	Applied Bioinformatics Group at University of Tuebingen
FRED	1	16	Yes	NA	Applied Bioinformatics Group at University of Tuebingen
POPI2.0	221	82	Yes	NA	Institute of Bioinformatics, National Chaio Tung University
EpiMatrix (iVAX)	1,010	115	NA	2014	EpiVax
Epitopemap	34	1	Yes	NA	Damien Farrell (web2py platform)
Hotspot Hunter	36	19	No	NA	NA
TEpredict	290	14	Yes	26/08/2012	Russian Foundation for Basic Research grant
EpDis	1	0	Yes	24/06/ 2016	Bioinformatics Research Group
SVRMHC	125	83	Yes	NA	Biolead
POPI2.0	134	85	Yes	11/12/2009	Institute of Bioinformatics, National Chaio Tung University
PepCrawler	30	32	Yes	01/02/2016	BioInfo3D Group

NA: Not available.

Table 3.3 The sensitivity and probability of predicting MHC-II T-cell epitopes using SYFPEITHI, IEDB, NetMHC-II 2.2, and Rankpep prediction tools.

Server	Sensitivity	Probability
SYFPEITHI	8.33%	7.63%
IEDB	77.87%	15.68%
NETMHCI	77.87%	19.42%
RANKPEP	10.61%	6.25%

Using a handcrafted training set of proteins, the sensitivity as TP/(TP+FN) and the probability as TP/total of MHC-II T-cell epitopes prediction were calculated.

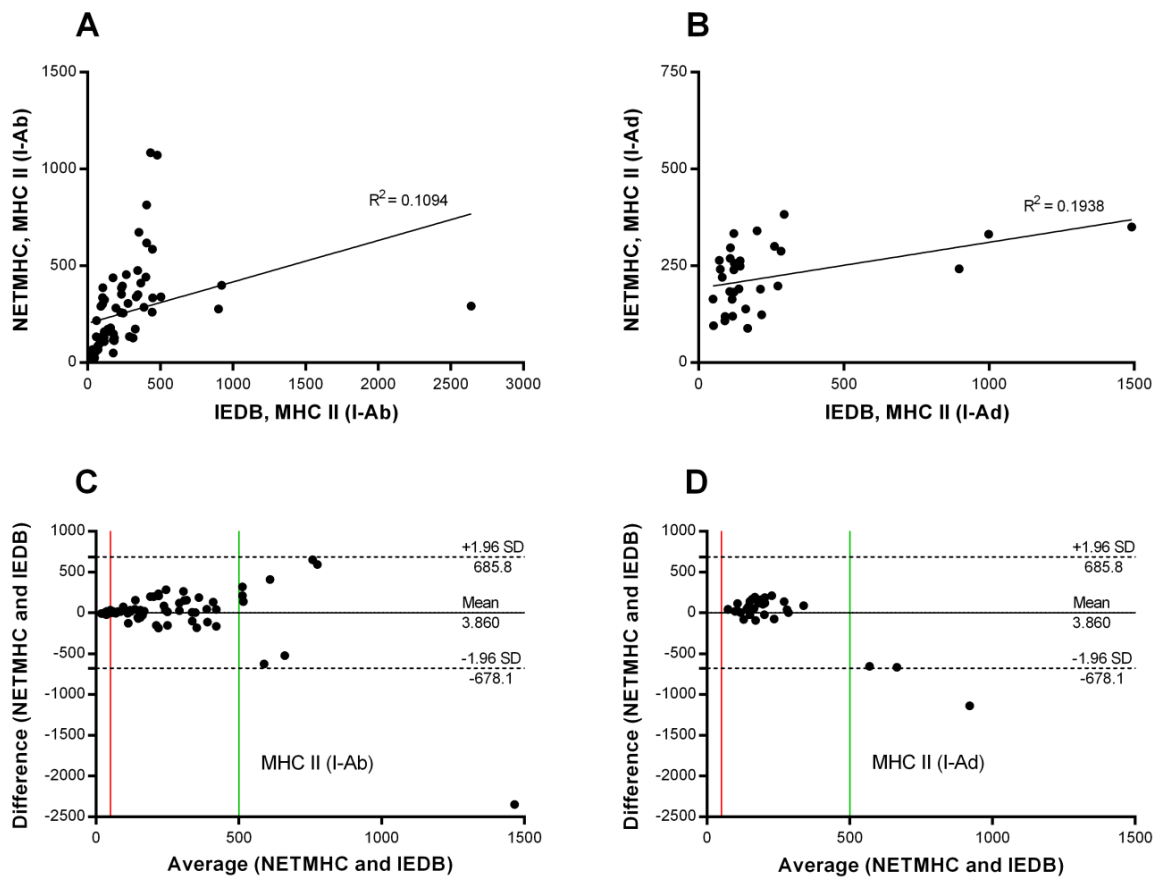


Figure 3.2 NetMHC-II 2.2 and IEDB tools performance. (A) The correlation score of the NetMHC-II 2.2 and IEDB tools for predicting MHC-II (I-Ab) epitopes. (B) The correlation score of the NetMHC-II 2.2 and IEDB tools for predicting MHC-II (I-Ad) epitopes. (C) The Bland-Altman plot of the difference and average of NetMHC-II 2.2 and IEDB prediction of MHC-II (I-Ab) epitopes and (D) in predicting MHC-II (I-Ad) epitopes. The red line means 50 nM and the green line means 500 nM.

3.5 Discussion

Prediction of which protein epitopes are potential vaccine candidates using immunoinformatics tools is a powerful strategy for development of epitope-based vaccines (Rasmussen et al., 2016). There are more than 80 computer-based prediction tools for identifying peptides that bind to MHC class I and II molecules, but not all are equivalent; some epitope prediction tools may fail to predict all significant epitopes (Yang and Yu, 2009). The performance of *in silico* prediction tools is affected by several factors. For example, MHC-II CD4+ T-cell epitope prediction tools have much lower accuracy than MHC-I tools because the MHC-I binding groove is closed, while the MHC-II groove is open at both ends (Godkin et al., 2001; Yang and Yu, 2009). Also, the use of a limited training dataset to evaluate the tools may affect performance (Hegde et al., 2018; Lin Hh, 2008; Wang et al., 2008). It was suggested that the low performance of MHC class II prediction tools is not due only to poor algorithm performance; the genetic diversity of human populations present further significant challenge (Paul et al., 2015). Thus, choosing the best bioinformatics tool to predict MHC class II T-cell epitopes is critical when designing epitope-based vaccines (Pappalardo et al., 2015; Schumacher et al., 2017). This chapter presents a systematic review of existing MHC-II restricted T-cell epitope prediction tools and evaluated four tools intended to establish the most appropriate bioinformatics tools currently available for predicting *Trichuris* MHC-II T-cell epitopes.

Four tools met the inclusion/exclusion criteria and were further analysed to determine the specificity and probability with which they can predict MHC class II T-cell epitopes. The IE3DB and NetMHC-II 2.2 tools achieved similarly high levels of sensitivity and probability of predicting binding epitopes with high affinities, while Rankpep and SYFPETHI exhibited low sensitivity. Each tool applies different methods of prediction; the IE3DB tool uses a quantitative consensus method that combines the strengths of various methods (Wang et al., 2008); the NetMHC-II 2.2, another quantitative tool, uses an NN-align algorithm and weight matrix (Nielsen and Lund, 2009); and both SYFPEITHI (Rammensee et al., 1999) and Rankpep (Reche et al., 2002) are qualitative tools that use motif PSSMs. All the tools were ‘user-friendly’, but the IE3DB tool has features that the other three do not, including a browser to input protein sequence formats in a national centre for biotechnology information (NCBI) database, seven different prediction methods and an easy method of downloading the prediction output into an Excel spreadsheet. In contrast, SYFPETHI is limited to specific alleles compared to the three other tools.

3.5.1 Evaluation of available MHC-II binding prediction tools

Several studies have compared the performance of different MHC class II peptide binding prediction tools (Borrás-Cuesta et al., 2000; Gowthaman and Agrewala, 2007; Lin et al., 2008), but the comparison presented in this chapter is different for two main reasons. First, the MHC-II prediction tools were selected in a systematic way using inclusion/exclusion criteria. Second, a unique dataset was used for comparison.

Because training sets of peptides were used for the development of epitope prediction tools, it is important to evaluate their performance using unique sets that do not overlap with the original training set (Murugan and Dai, 2005; Nielsen et al., 2004; Yasser et al., 2008). However, some

published studies which have aspired to evaluate the performance of T-cell epitope prediction tools have used training datasets that are similar to the original training sets (Yasser et al., 2008). Therefore, to more rigorously assess the relative performance of the available prediction tools, this study excluded training datasets and introduced new peptides to the tools.

Gowthaman and Agrewala (2007) evaluated the performance of six class II binding peptide prediction tools (ProPred, MHC2Pred, Rankpep, SVMHC, MHCpred and MHC-BPS) and concluded that none can be efficiently used to predict which epitopes are crucial for vaccination. However, the limited number of peptides, HLA class II alleles and prediction methods (matrix-based methods and SVM) used to evaluate the tools limited the significance of their results (Gowthaman and Agrewala, 2007).

Other published comparisons claim that the IEDB tool, using the consensus method, is the gold standard tool since it appears to be the strongest predictor of MHC binding epitopes amongst the other online available tools (Wang et al., 2008). For example, Wang et al. (2008) evaluated the performance of nine MHC class II peptide binding tools (consensus, SYFPEITHI, Rankpep, average relative binding [ARB], ProPred, SMM-align, SVRMHC, MHC2Pred and MHCpred) for different human and animal alleles using a comprehensive three datasets. The first is an unpublished experimental dataset of 10,017 peptide-binding affinities for 16 MHC class II molecules, and it was used to evaluate the binding affinities of the prediction tools. The second consists of 29 structures associated with 14 different MHC class II molecules extracted from the Protein Data Bank (PDB), and it was used to evaluate the ability of prediction tools to locate the 9-mer core of epitopes. The third dataset consists of 664 peptides experimentally tested in a C57BL/6 (H-2b) strain of laboratory mouse for CD4+ T-cell activation (Wang et al., 2008). The IEDB tool using consensus method outperformed all other MHC class II prediction methods in terms of sensitivity in predicting binding affinity and T-cell activation, followed by Rankpep, SMM-align and ProPred. It was suggested that the increased epitope prediction accuracy of the consensus method is attributed to the combination of the top performance methods and access to the most comprehensive online database (Salimi et al., 2010; Wang et al., 2008). It was also suggested that the great performance of the SMM-align tool can be attributed to its utilisation of the IEDB dataset (Wang et al., 2008). This would confirm that the size of the training set is an important factor contributing to better performance (Wang et al., 2008). Furthermore, comparison of the predicted 9-mer core with the true cores extracted from crystal structures revealed that the ProPred tool was able to most accurately predict cores, followed by SYFPEITHI and SMM-align (Wang et al., 2008). The fact that the ProPred tool is based on the TEPIPOPE database of experimental assays further confirms that the performance of the tool is directly affected by the type of training database applied (Wang et al., 2008). However, this study did not assess the performance of the consensus approach for predicting 9-mer cores that interact with the binding groove of the MHC class II molecule.

Ogishi and Yotsuyanagi demonstrated that integration of MHC class II *in vitro* binding and naturally eluted ligands derived from mass spectrometry (MS) data can improve the predictive performance of the NetMHCII and NetMHCIIpan tools regarding identification of T-cell epitopes (Ogishi and

Yotsuyanagi, 2019). Another study also suggested that the poor performance of the SYFPEITHI matrix-based MHC-binding prediction tool is due to the fact that it helps locate epitopes in known target proteins but does not predict epitopes in unknown proteins (Pelte et al., 2004). The results of their study agree with those of the present study, which found that the SYFPEITHI tool has low accuracy for predicting MHC-II T-cell epitopes. Another study also reported that the SYFPEITHI server is a poor predictor of MHC-I peptide binding affinity compared to SMM-QMs and ANN-based methods (Peters et al., 2006).

De Groot and Martin (2009) compared the EpiMatrix tool to other MHC class II prediction tools, including IEDB and SYFPEITHI, using MHC class II-peptide complex crystal structures extracted from the Protein Data Bank (PDB). EpiMatrix was 5% better than the IEDB tool using the ARB method of prediction and 9% better than SYFPEITHI (De Groot and Martin, 2009). However, EpiMatrix was not evaluated in this study or similar studies comparing epitope prediction algorithms because it is a commercial tool that is limited to commercial users and selected academic collaborators.

A different study compared the performance of 21 HLA class II binding affinity tools using a dataset of 103 peptides from four independent studies (Lin et al., 2008). However, this study did not compare the performance of the tools for predicting MHC-II binding affinity peptides. Lin et al. (2008) suggested that the NetMHCIIpan server, which is based on a combination of binding ligand and structure-based methods, ProPred, consensus and MULTIPRED (SVM), were the best predictors. Another study conducted by Ivan et al. (2011) has also identified NetMHCII and NetMHCIIpan as the best publicly available MHC class II epitope predictors compared to ProPred, Rankpep and EpiTOP.

A more recent study by Zhao and Sher (2018) evaluated the MHC-II prediction tools hosted on the IEDB analysis resource server using newly available, untested data of both synthetic and naturally processed epitopes. Among the 18 predictors that were benchmarked, an ANN-based approach, NN-align (NetMHCII2), outperformed all other tools, including NetMHCIIpan and the consensus method for both MHC class I and class II predictions (Zhao and Sher, 2018). Furthermore, Andreatta et al. (2018) created an automated platform to benchmark six commonly used MHC class II peptide binding prediction tools using 59 datasets that were newly entered into the IEDB database and had not yet been made public to prevent biased assessment of the available prediction tools. Their evaluation suggested that NetMHCIIpan is currently the most accurate tool, followed by NN-align and the IEDB (consensus) tool (Andreatta et al., 2018). Despite differences in the datasets used for comparison, these studies agree with the comparison study in this chapter, which found that the IEDB (consensus) and NETMHC-II 2.2 (ANN) tools are among the best MHC-II prediction tools. NetMHCIIpan was not included in this study because it did not meet the inclusion criteria. Collectively, I recommend the use of IEDB and NETMHC-II 2.2 prediction tools in any MHC class II epitope prediction study to reduce the experimental cost of identifying epitopes. However, the output of these tools needs to be carefully evaluated *in vitro* and *in vivo* before they are used to bring an epitope-based vaccine to trial.

3.5.2 Updates of the available *in silico* prediction tools

During the time period covered by this systematic review, the available *in silico* prediction tools have been improved and updated. For example, the performance of MHC-II peptide binding prediction tools (NetMHCII and NetMHCIIpan) was recently improved using a dataset of quantitative MHC peptides extracted from the IEDB (Jensen et al., 2018; Jurtz et al., 2017).

Moreover, the IEDB Analysis Resource developed an online tool called TepiTool, which provides a set of step-by-step instructions for how to predict MHC class I and class II epitopes, including which alleles to include, which lengths to consider and which cut-offs should be considered relevant (Paul et al., 2016). TepiTool uses the consensus, NN-align, SMM-align (also known as NetMHCII-1.1, version 1.1), Sturniolo and combinatorial library prediction algorithms to examine hundreds of alleles from different species, including humans, chimpanzees, bovines, gorillas, macaques, mice and pigs (Paul et al., 2016). More recently, an allele-integrated deep learning framework named Allele-Integrated MHC (AI-MHC) was developed to improve class I and class II HLA binding predictions by allowing the tool to be trained on effectively larger datasets (Sidhom et al., 2018). Also, in 2017, the VacSol pipeline was introduced for rapidly and efficiently identifying vaccine candidates from the whole proteomes of bacterial pathogens (Rizwan et al., 2017). The pipeline screens for proteome analysis using several well-known tools (BLAST, PfTools2.3, PSORTb3.0, HMMTOP 2.0, DEG 10.0, VFDB, ABCPred, ProPred-I, ProPred and UniProt-SwissProt) for prediction of B- and T-cell epitopes, subcellular protein localisation and transmembrane topology (Rizwan et al., 2017).

All the above-mentioned MHC-II binding prediction tools apply indirect methods to predict T-helper epitopes. However, there are a few direct methods for predicting cytokine-specific peptides that can induce IL-4 (Dhanda et al., 2013a), IL-10 (Nagpal et al., 2017) and IFN-gamma production (Dhanda et al., 2013b). Immune recognition of peptides by T-cells depends on the formation of a ternary complex ‘sandwich’ consisting of protein peptides between MHC and TCR. Most of the current research focuses on evaluating the MHC-facing agretopes. However, the JanusMatrix and Reptope tools evaluate both TCR-facing and MHC-facing peptides in a single analysis to improve the selection of vaccine antigens (He et al., 2014; Moise et al., 2013; Ogishi and Yotsuyanagi, 2019). Also, ITCell was introduced in 2018 to predict T-cell epitopes based on information about the three stages of the immune response pathway: antigen cleavage, MHC-II presentation and TCR recognition (Schneidman-Duhovny et al., 2018). Using benchmarks, it was found that the ITCell method had better accuracy than the NetMHCIIpan single-stage epitope prediction algorithm (Schneidman-Duhovny et al., 2018).

3.5.3 Applications of MHC-II prediction tools

The IEDB and NetMHC-II prediction tools have become widely used for developing epitope-based vaccines against many parasites, including *Plasmodium falciparum* (Singh et al., 2010), *Trypanosoma brucei* (Teh-Poot et al., 2014), *Echinococcus granulosus* (Ma et al., 2013), *Leishmania infantum* (Agallou et al., 2014; Dias et al., 2018), and *Onchocerca volvulus* (Shey et al., 2019). Also, in an effort to identify helminth immunomodulatory proteins, Homan and Bremel (2018)

used IEDB approaches to predict MHC-I and II binding epitopes from secreted proteins from 17 helminth spp and common co-infections (*P. falciparum*, *Mycobacterium tuberculosis* and *H. pylori*). Not only were MHC binding epitopes predicted but also amino acid motifs (T-cell-exposed motifs [TCEMs]) with a high likelihood of being recognised by T-cell receptors and eliciting Treg responses were identified (Homan and Bremel, 2018). TCEMs were found to be shared to a high degree across helminth species and with *P. falciparum* and *M. tuberculosis* when these contribute to co-infection (Homan and Bremel, 2018).

Despite its inferior performance, the SYFPEITHI tool has been used to predict T-cell epitopes from the nematode parasite *Trichinella spiralis*. For example, Gu et al. (2016) used this tool to predict a set of 12 CD4+ T-cell epitopes from a *T. spiralis* paramyosin protein (Ts-Pmy). Five of the epitopes significantly induced splenocyte proliferation and secretion of the Th2 cytokines IL-4 and IL-5 in splenocytes from mice vaccinated with recombinant Ts-Pmy protein (rTs-Pmy) (Gu et al., 2016). In addition, splenocytes from mice vaccinated with individual synthesised peptides emulsified with an ISA50 V2 adjuvant stimulated with the corresponding peptides induced strong T-cell proliferation and secretion of a mix of Th1 and Th2 cytokines (Gu et al., 2016). However, this study was limited as it did not assess protective immunity to the parasite.

Given that all MHC class II T-cell epitope prediction tools provide false positives and false negatives to varying degrees, it is recommended that multiple bioinformatics tools be combined to predict MHC class II T-cell epitopes. For example, Agallou et al. (2017) developed a multi-peptide-based nanovaccine against leishmaniasis based on *Leishmania* cysteine protease A (CPA160-189) co-encapsulated with monophosphoryl lipid A (MPLA) in Poly(D,L-lactic-co-glycolide) (PLGA) nanoparticles. The potential MHC class I and II binding epitopes derived from the *L. infantum* CPA protein were predicted by three *in silico* analysis tools: SYFPEITHI, BIMAS and NetMHCII (Agallou et al., 2014). Subcutaneous vaccination of BALB/c mice with the vaccine candidate induced specific anti-CPA160-189 cellular and humoral immune responses characterised by the production of high levels of IL-2, IFN- γ and TNF α cytokines and IgG1/IgG2c antibodies (Agallou et al., 2017). Furthermore, the vaccinated mice displayed significantly reduced hepatic (48%) and splenic (90%) parasite load prior to *L. infantum* promastigote challenge (Agallou et al., 2017).

In summary, almost every aspect of the field of immunoinformatics is rapidly expanding, including the design of epitope-based vaccines. Accurate prediction of MHC II T-cell epitopes using *in silico* prediction tools is a critical first step in the development of an epitope-based vaccine. Therefore, a systematic review and evaluation of the available MHC class II *in silico* prediction tools was conducted in this chapter to determine which ones have the best predictive ability.

3.6 Summary

- Based on a list of search terms used on Google and other websites, 44 servers that can predict MHC-II peptides were identified.
- Aspects relating to the number of citations (>200), number of publications (>200), online availability, last update and community were used as inclusion/exclusion criteria to select

the top MHC-II *in silico* prediction tools. The five tools that met the inclusion criteria were IEDB, SYPEITHI, NetMHC-II 2.2, Rankpep and ProPred.

- A unique training data set was used to evaluate the performance of the top tools. The IEDB and NetMHC-II 2.2 tools exhibited similarly high levels of sensitivity and probability for predicting epitopes with strong affinities, while the Rankpep and SYFPETHI prediction tools exhibited low sensitivity.

Chapter Four

Trichuris MHC-II T-cell epitope prediction

4.1 Introduction

Designing a vaccine for a neglected tropical parasite, such as *T. trichiura*, is one of the most challenging tasks for medical scientists. Although anthelmintic treatments for *Trichuris* infections exist, the available drugs have low efficacy and are threatened by drug resistance (Mrus et al., 2018; Patel et al., 2019). Thus, as with all neglected tropical infectious diseases (NTDs), control and prevention of trichuriasis are superior to a cure (Briggs et al., 2018). Therefore, developing a vaccine would be the most effective method to control *Trichuris* infections (Dixon et al., 2010). However, while many research scientists have put substantial effort into developing such a vaccine, there is currently no licensed vaccine against *Trichuris*, as much work must be done to improve the specificity, sensitivity and safety of candidate vaccines (Blair and Diemert, 2015).

The advent of the genome era has provided new effective strategies for vaccine development (Del Tordello et al., 2017). The reverse vaccinology (RV) approach, in particular, which relies on both genome information and the tremendous advances in immunological and bioinformatics tools, has been used to develop epitope-based vaccines (Bambini and Rappuoli, 2009). One of the advantages of the RV approach is that every antigen encoded in the *Trichuris* genome can be screened using immunoinformatics-based software to determine its ability to induce an immune response (De Sousa and Doolan, 2016; Del Tordello et al., 2017). Thus, it can overcome some of the limitations of conventional methods of screening vaccine candidates (Arnon and Ben-Yedidya, 2003; Capecchi et al., 2004; Moise et al., 2011).

There are several challenges that can arise when screening for potential vaccine candidates, such as identifying immunogenic candidates in a large-scale genome and choosing a suitable animal model for testing immunogenicity and protective immunity (Thomas and Luxon, 2013). To address these challenges, a set of *Trichuris* proteins can be selected from the genomes of *T. trichiura* and its murine equivalent, *T. muris*, based on selected parameters associated with antigenic peptides that would provide protection against trichuriasis in C57BL/6 mice.

Designing vaccines based on multi-stage antigens has been an effective strategy for complex pathogens, such as *M. tuberculosis* and *Plasmodium* (Cabrera-Mora et al., 2016; Mosavat et al., 2016). Therefore, the ultimate goal of this study is to design a novel multi MHC class II T-cell epitope-based vaccine predicted from multi-stage *Trichuris* proteins, which will likely induce effective protective immunity, using the RV approach. The T-cell epitopes will then be incorporated into a VLP to generate a candidate vaccine against human trichuriasis.

4.2 Aim and objectives

The overall aim of this chapter was to identify novel MHC-II T-cell epitopes from the *Trichuris* genome as promising vaccine candidates using an RV approach. This chapter addressed the following two objectives as part of the overall aim:

- To identify a set of proteins from the *Trichuris* genome based on inclusion/exclusion criteria to select proteins with the high potential to be lead antigens in the development of an anti-*Trichuris* vaccine.

- To predict the most conserved and antigenic *Trichuris* MHC-II T-cell epitopes from the selected proteins using the IEDB prediction tool identified in Chapter 3.

4.2 Methods and results

4.2.1 Data acquisition and identification of potential virulent proteins

The stichosome in the whipworm anterior region secrete ES products which have been suggested to trigger the host immune response and induce host immunity after infection (Dixon et al., 2010; Shears et al., 2018b). Furthermore, previous research conducted by Dixon et al., (2008) and Else et al., (1990), showed that antibody recognition of high molecular weight proteins in both *T. muris* adult and larval ES correlated with resistance to *T. muris* infection. To increase the chance of antigen coverage to induce a strong immune response, secreted and surface-exposed proteins in L2, L3, male and female adult worms' anterior region were selected for this study as potential vaccine candidates based on published information (Foth et al., 2014).

The 85-Mb genome (~11,004 protein-encoding genes) of *T. muris* and the 73-Mb genome (~9650 protein-coding genes) of *T. trichiura* sequenced by Foth et al. (2014) served as rich sources of potential vaccine candidates and therefore were used as starting points (Foth et al., 2014). From the whole genome of the *Trichuris*, 637 proteins expressed in L2, L3, male and female adult worms' anterior region were selected. Of the total of 637 proteins, only proteins that possess signal peptides and do not exhibit transmembrane domains were included, resulting in a sample of 156 proteins.

Full-length sequences of the *Trichuris* proteins were obtained from the Universal Protein Resource (UniProt) database in FASTA format <http://www.uniprot.org/>.

4.2.2 Identification of non-homologous proteins to human and mouse with high expression levels

To eliminate autoimmune reactions when tested in mice and humans, the proteins identified in the previous step were checked to determine their homology with human and mouse proteins using the basic local alignment search tool (BLAST), which is available online in the UniProt database <https://www.uniprot.org/blast/>. All proteins with any degree of homology with humans or mice were excluded, leaving 60 candidate proteins.

Of these, only upregulated proteins in L2, L3 and adult worms' anterior region were selected based on their transcript expression level. Based on the high-throughput transcriptome data generated from the RNA of *T. muris* and Gene Ontology (GO) term enrichment analyses, a transcriptional upregulation in a particular protein refers to (≥ 10 Log₂ (normalised read count) transcript expression level (Foth et al., 2014). Of the 60 selected proteins, only 27 proteins were selected to predict *Trichuris* MHC-II T-cell epitopes.

4.2.3 Prediction of *Trichuris* MHC-II T-cell binding epitopes

Since antibodies are not essential for protection against *Trichuris* infection and protective immunity is mediated by CD4+ T-cells, not CD8+ T-cells, the selected proteins were screened to predict MHC-II T-cell epitopes rather than B-cell epitopes (Else and Grencis, 1996; Koyama et al., 1995).

All 27 selected proteins were screened to predict T-cell MHC class II epitopes using the IEDB (consensus method) prediction tool (Wang et al., 2008).

There are many different human MHC (human leukocyte antigen [HLA]) alleles, and the distributions of particular types are associated with different populations. The analysis was carried out to predict the binding affinity to the MHC class II allele I-Ab mouse strain and the 11 most prevalent human class II HLA allele supertypes (Nielsen et al., 2010a; Nielsen and Lund, 2009; Wang et al., 2008; Wang et al., 2010).

The predicted peptide output (i.e. binding affinity) of the NN-align and SMM-align methods was expressed as IC50 (nM) values. IC50 values of <50 nM indicate high affinity, values of <500 nM indicate intermediate affinity and values of <5000 nM indicate low affinity. The median percentile rank (%) of three prediction methods (combinatorial library, SMM-align and Sturniolo) was also used to generate the rank for the consensus method. A small numbered percentile rank (%) indicates that a peptide has a high binding affinity to MHC class II alleles (Wang et al., 2008). The consensus method was used to select only those peptides with a low median percentile rank according to three different prediction methods to reduce the chance of failure during prediction.

Table 4.1 shows examples of the prediction scores of three peptides predicted from the *T. muris* chitin-binding domain-containing protein (TMUE_s0281000600). The (PAGVYYQCTMPRYTL) peptide, for example, has high and intermediate binding to H2-lab and to the HLA-DRB1*01:01, HLA-DRB1*03:01, HLA-DRB1*04:01, HLA-DRB1*07:01, HLA-DRB1*08:02, HLA-DRB1*11:01, HLA-DRB1*13:02, HLA-DRB1*15:01, HLA-DRB3*01:01 and HLA-DRB3*02:02 alleles. The two other peptides have high and intermediate binding affinity to H2-lab and only seven human alleles. Due to the large volume of data, the prediction scores for the rest of the predicted *Trichuris* MHC-II T-cell peptides are presented in the enclosed CD. To cover common global alleles, peptides were selected based on their ability to bind to at least three different human alleles. Table 4.2 lists the MHC-II T-cell peptides with high or intermediate binding affinity to the mouse I-Ab allele and at least three different human alleles that were selected for further analysis.

4.2.4 Conservation and allergens

One of the critical steps in the development of an effective vaccine is the identification of a conserved antigen from the genome to overcome antigenic variation and reduce the chance of immune escape (Khan et al., 2006). To assess how well the predicted MHC-II T-cell peptides were conserved within the *T. trichiura* genome, the IEDB conservancy analysis tool was used. This tool calculates the degree of conservancy (i.e. similarity) of a peptide within a specified protein sequence (Bui et al., 2007). Only peptides that are >70% conserved with at least one homologous *T. trichiura* protein were selected for further analysis. Of the 219 MHC-II T-cell peptides, only 33

(shown in red in Table 4.2) met these criteria. The conservancy analysis results of the 33 MHC-II peptides are shown in Supplementary Tables 4.1–4.6. For example, the three overlapping peptides predicted from the *T. muris* hypothetical protein (A0A0N5DRU5) that cover the H₁₁₂₋₁₂₈ epitope and used in the first *in vivo* study in Chapter 7, have more than 86% conservation across eight different *T. trichiura* homologous proteins (Supplementary Table 4.6). The conservation of all the predicted MHC-II peptides is presented in the enclosed CD.

The 33 MHC-II peptides were then assessed for the prediction of IgE epitopes and allergenic potential using the AllerTOP v.2.0 server <http://www.ddg-pharmfac.net/AllerTOP/> (Dimitrov et al., 2014). All the 33 MHC-II T-cell peptides were predicted to have no allergenic potential.

Table 4.3 lists the final set of 10 potential *Trichuris* MHC-II T-cell epitopes containing 33 overlapping peptides that emerged as promising vaccine candidates after application of the selection criteria detailed in Figure 4.1. These epitopes, which were predicted from a Pfam domain-containing protein (B_9093-A0A0N5E6W6), hypothetical protein (A0A0N5DRU5), chymotrypsin-like serine proteases (A0A0N5DEK1, A0A0N5E3X0 and A0A0N5DUC1) and chitin-binding domain-containing proteins (A0A0N5DK22 and A0A0N5E6C6), will be fused into VLPs as potential vaccine candidates in Chapter 5.

A flow diagram of the RV approach used in this study to identify potential vaccine candidates from *Trichuris* genome is shown in Figure 4.1.

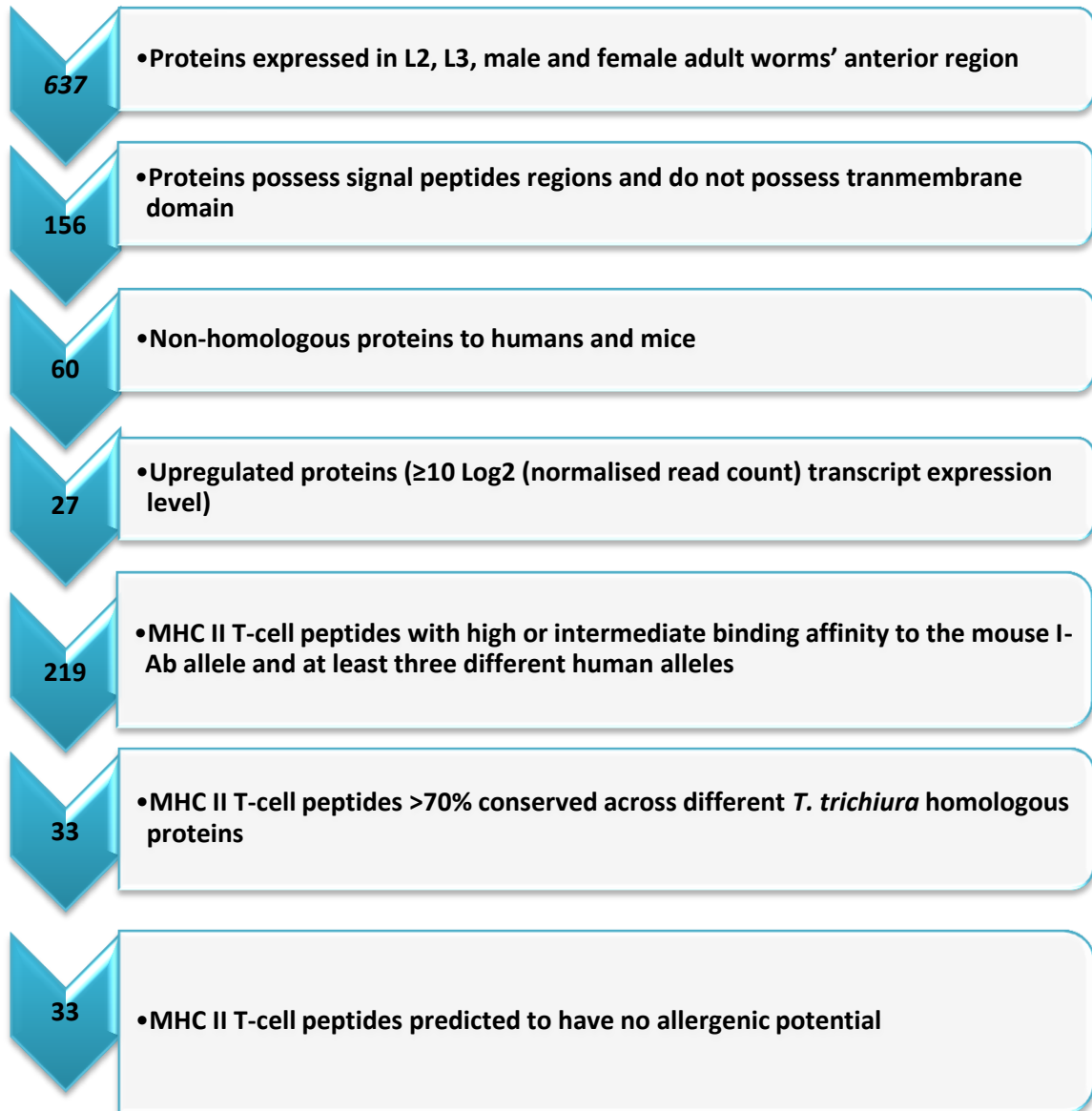


Figure 4.1 The flow diagram of reverse vaccinology approach to identify potential vaccine candidates (MHC-II T-cell epitopes) from the *T. muris* genome. The number on the blue arrow represents the number of proteins or epitopes selected for the next step.

Table 4.1 The prediction scores of MHC-II T-cell epitope (CBD₁₂₄₃₋₁₂₅₉) containing three overlapping peptides predicted from chitin-binding domain containing protein (TMUE_s0281000600) using the IEDB prediction tool (Wang et al., 2008).

Allele	Prediction method	Peptide sequence		
		PAGVYQCTMPRYTL	AGVYQCTMPRYTLC	GVVYQCTMPRYTLCV
H2-lab	% rank	14	14	18
	smm	X	X	X
	nn	389	390	400
HLA-DRB1 01:01	% rank	26	25	26
	smm	169	174	174
	nn	32	29	20
HLA-DRB1 03:01	% rank	1	1	5
	smm	X	X	X
	nn	306	X	X
HLA-DRB1 04:01	% rank	5	5	10
	smm	436	436	X
	nn	94	114	160
HLA-DRB1 07:01	% rank	6	6	6
	smm	248	246	238
	nn	32	34	30
HLA-DRB1 08:02	% rank	7	8	10
	smm	X	X	X
	nn	308	252	428
HLA-DRB1 11:01	% rank	1	1	1
	smm	193	198	193
	nn	44	35	23
HLA-DRB1 13:02	% rank	X	X	X
	smm	X	X	X
	nn	X	X	X
HLA-DRB1 15:01	% rank	8	8	8
	smm	X	X	X
	nn	82	81	71
HLA-DRB3 01:01	% rank	9	X	X
	smm	X	X	X
	nn	324	X	X
HLA-DRB3 02:02	% rank	4	X	X
	smm	150	X	X
	nn	52	X	X
HLA-DRB4 01:01	% rank	X	X	X
	smm	X	X	X
	nn	X	X	X

X: Non-binding peptide.

Table 4.2 List of 219 identified *Trichuris* MHC-II T-cell peptides.

Protein Groups	UniProt Protein ID (WormBase ParaSite ID)	Peptide sequence	Number of Hits	Conservation %
WAP domain containing protein	A0A0N5DEU3 (TMUE_s0004017900)	ASPQYETFPVAQAGK	4	33.33%
		SPQYETFPVAQAGKP	4	33.33%
		KKNLIVWSKPDANNR	7	46.67%
		KNLIVWSKPDANNRL	7	46.67%
		NLIVWSKPDANNRLL	7	46.67%
		KDDSSTWAISKAPKL	6	46.67%
		DDSSTWAISKAPKLF	6	46.67%
		DSSTWAISKAPKLFC	6	46.67%
		SSTWAISKAPKLFCM	6	53.33%
		STWAISKAPKLFCMG	7	46.67%
Deoxyribonuclease (DNase) II	A0A0N5DMY6 (TMUE_s0030007700)	NVAIVYNDHPPLTPK	10	53.33%
		VAIVYNDHPPLTPKP	10	60.00%
		AIVYNDHPPLTPKPP	8	53.33%
		IVYNDHPPLTPKPPV	7	46.67%
		WAKTVAYESPNIYFS	8	53.33%
		AKTVAYESPNIYFSN	8	53.33%
		KTVAYESPNIYFSNK	7	46.67%
		YSSFMTVALATTLTM	6	66.67%
		SSFMTVALATTLMW	6	66.67%
		DPERTRWGHSSAASK	4	40%
		MEKKRKYLGSPLVCF	7	73.33%
		EKKRKYLGSPLVCFV	7	80%
		SVQTRTLNYFAPLNA	7	46.67%
Chymotrypsin-like serine protease	A0A0N5DE40 (TMUE_s0003007500)	VQTRTLNYFAPLNAF	7	53.33%
		QTRTLNYFAPLNAFL	9	60%
		TRTLNYFAPLNAFLP	9	60%
		RTLNYFAPLNAFLPG	9	66.67%
		TLNYFAPLNAFLPGG	8	66.67%
		LNYFAPLNAFLPGGT	7	66.67%
		MEKKRKYLGSPLVCF	7	73.33%
		EKKRKYLGSPLVCFV	7	80%
		SVQTRTLNYFAPLNA	7	46.67%
		VQTRTLNYFAPLNAF	7	53.33%

	PPIRPELQITRPVPS	8	40.00%
	PIRPELQITRPVPST	8	40.00%
	IRPELQITRPVPSTS	8	40.00%
	RPELQITRPVPSTSS	8	40.00%
	PELQITRPVPSTSSS	7	46.67%
	ELQITRPVPSTSSSD	7	46.67%
	LQITRPVPSTSSDE	7	46.67%
	LDVSKKVVYVAPGAL	6	60%
	DVSKKVVYVAPGALP	6	53.33%
	VSKKVVYVAPGALPI	7	46.67%
	SKKVVYVAPGALPIC	7	53.33%
	KKVVYVAPGALPICM	7	53.33%
	KVVYVAPGALPICMA	7	46.67%
	VVYVAPGALPICMAP	5	53.33%
A0A0N5DEI6 (TMUE_s0004005300)	AQYMLPWNAIIATQI	8	60.00%
	QYMLPWNAIIATQIR	7	60.00%
	YMLPWNAIIATQIRG	6	60.00%
	MLPWNAIIATQIRGS	6	66.67%
	LPWNAAIIATQIRGSV	7	60.00%
A0A0N5DUC1 (TMUE_s0069001100)	NFLCLAFTACLVTAAC	5	40%
	FLCLAFTACLVTAAL	5	40%
	LCLAFATACLVTAALA	5	40%
	CLAFTACLVTAALAI	4	40%
	LAFTACLVTAALAAIE	4	46.67%
	AFTACLVTAALAAIEC	4	46.67%
	AILQLAKPVFSNTV	11	80%
	ILQLAKPVFSNTVR	10	80%
	LSDQLSSSYSSSSSS	4	66.67%
	SDQLSSSYSSSSSE	3	66.67%
	DQLSSSYSSSSSEH	4	60.00%
	QLSSSYSSSSSEHI	4	60.00%
	LSSSYSSSSSEHIS	4	66.67%
	SDHQEGYPVSPSVH	4	86.67%
	DHQEGYPVSPSVHIV	4	86.67%

	HQE ^G PVSPSVHIVS	5	86.67%
	QEG ^G PVSPSVHIVSL	5	86.67%
	E ^G YPVSPSVHIVSLA	5	93.33%
	E ^V ICTGSLYASARAN	4	53.33%
	VICTGSLYASARANF	7	60.00%
	I ^C TGSLYASARANFT	8	66.67%
	C ^T GSLYASARANFTR	9	73.33%
	T ^G SLYASARANFTRT	9	73.33%
	G ^S LYASARANFTRTV	10	73.33%
	SLYASARANFTRTVL	9	66.67%
	L ^Y ASARANFTRVLT	6	66.67%
	Y ^A SARANFTRV LTS	5	73.33%
	SNFMVYMGSVRSFAA	8	46.67%
	NFMVYMGSVRSFAAG	8	53.33%
	F ^M VYMGSVRSFAAGG	7	46.67%
	KWLPIYRISTKPIMA	12	40%
	WLPIYRISTKPIMAH	12	40%
	LPIYRISTKPIMAH	12	40%
	PIYRISTKPIMAHHS	12	40%
	IYRISTKPIMAHSA	11	40%
	YRISTKPIMAHHSAL	8	40%
	GVCEHGLSAAAPVRI	6	40%
	VCEHGLSAAAPVRIL	6	40%
	CEHGLSAAAPVRILS	6	40%
	EHGLSAAAPVRILSP	6	40%
	HGLSAAAPVRILSPQ	7	40%
	GLSAAAPVRILSPQE	5	46.67%
	QYGIYDFTPEKAHLN	4	46.67%
	YGIYDFTPEKAHLND	4	53.33%
	GIYDFTPEKAHLNDI	4	53.33%
	IYDFTPEKAHLNDIN	4	40%
AOA0N5E1M5 (TMUE_s0144000100)	WNNRYGINIASPSDI	9	40%
	NNRYGINIASPSDIS	10	40%
	NRGYGINIASPSDISV	9	46.67%

		RYGINIASPSDISVY	10	53.33%
		YGINIASPSDISVYL	9	60%
Protease Inhibitor	A0A0N5DEK1 (TMUE_s0004007100)	AADCFSKYEHAPAAA	5	60.00%
		ADCFSKYEHAPAAAK	5	60.00%
		DCFSKYEHAPAAKS	6	46.67%
		CFSKYEHAPAAKS	6	40%
		AKSKLRLVYAGSPRFS	8	80%
		KSKLRLVYAGSPRFSR	9	86.67%
		SKLRLVYAGSPRFSRI	9	86.67%
		KLRVYAGSPRFSRIR	9	86.67%
		LLLLLFRRWAVAPKP	7	33.33%
		LLLLLFRRWAVAPKPN	7	33.33%
Chitin-binding domain containing protein (PF01607)	A0A0N5E3R5 (TMUE_s0186000600)	LLLLFRWAVAPKPNV	7	33.33%
		LLLFRWAVAPKPNVP	7	33.33%
		LNILRWYFNPATRTC	8	46.67%
		NILRWYFNPATRTCE	8	53.33%
		ILRWYFNPATRTCEI	8	46.67%
		LRWYFNPATRTCEIF	6	46.67%
		RPRLLKIKWSPTAAS	11	100.00%
		PRLLKIKWSPTAAST	11	93.33
		RLLKIKWSPTAASTA	11	86.67
		LLKIKWSPTAASTAI	10	33.33%
	A0A0N5E6C6 (TMUE_s0281000600)	LKIKWSPTAASTAIH	7	40%
		LGSLHYIRRPPMPIR	10	40%
		GSLHYIRRPPMPIRY	10	46.67%
		SLHYIRRPPMPIRYE	10	46.67%
		LHYIRRPPMPIRYES	8	53.33%
		HYIRRPPMPIRYESP	6	60.00%
		PAGVVYQCTMPRYTL	10	86.67%
		AGVVYQCTMPRYTLC	8	60.00%
		GVVYQCTMPRYTLCV	8	72.00%
		QQVDDISVVTSPPVTT	7	40%
		QVDDISVVTSPPVTT	8	40%
		VDDISVVTSPPVTTS	8	40%

		DDISVVTSPPVTTSD	8	40%
		DISVVTSPPVTTSDS	8	60.00%
		ISVVTSPPVTTSDSV	8	66.67%
Cystatin domain containing protein	A0A0N5DK22 (TMUE_s0018008000)	GRTTPVTSAPTVTT	5	100.00%
		RTTPVTSAPTVTTE	5	93.33%
		TTPVVTSAPTTVTER	5	86.67%
Pfam-B 9093 domain containing protein	A0A0N5E055 (TMUE_s0122001300)	AFALFGFASGAPAAV	7	33.33%
		FALFGFASGAPAAVD	7	33.33%
		ALFGFASGAPAAVDT	7	33.33%
		LFGFASGAPAAVDTA	6	33.33%
		FGFASGAPAAVDTAS	6	33.33%
Thioredoxin 8 domain containing protein	A0A0N5E6W6 (TMUE_s0327000100)	NFGEYWFTKPVGSVS	5	80%
		FGEYWFTKPVGSVSY	5	80%
		GEYWFTKPVGSVSYK	5	73.33%
		EYWFTKPVGSVSYKV	5	73.33%
	A0A0N5E4A5 (TMUE_s0201000900)	LLVTLGYFQFSTALG	6	53.33%
		LVTLGYFQFSTALGD	6	46.67%
		VTLGYFQFSTALGDI	6	40%
		TLGYFQFSTALGDIC	6	46.67%
		LGYFQFSTALGDCS	6	46.67%
		LPAVVVNPSGIPIA	5	26.67%
Myoglobin	A0A0N5DPB5 (TMUE_s0037005600)	PAVVVVNPSGIPIAK	5	33.33%
		AVVVVNPSGIPIAKY	5	26.67%
		VVVVNPSGIPIAKYT	4	26.67%
		ALLALSFAAVGTYAS	6	20%
		LLALSFAAVGTYASS	6	26.67%
		LALSFAAVGTYASSA	7	26.67%
		ALSFAAVGTYASSAS	5	20%
		LSFAAVGTYASSASI	6	20%
		SFAAVGTYASSASIV	6	26.67%
		FAAVGTYASSASIVK	7	26.67%
		AAVGTYASSASIVKD	7	26.67%
		AVGTYASSASIVKDQ	6	26.67%
		HVGLTELKGAKPILL	6	40%

		VGLTELKGAKPILLK	6	40%
		GLTELKGAKPILLKF	7	40%
		LTELKGAKPILLKFM	8	33.33%
Poly cysteine and histidine tailed protein isoform	A0A0N5DW69 (TMUE_s0083002300)	DGYEPHSVAPANVHI	4	53.33%
		GYEPHSVAPANVHIP	4	53.33%
Hypothetical protein	A0A0N5DVH8 (TMUE_s0077002200)	MIAALPLSLAALLLA	7	53.33%
		SLAALLLASVSAVTN	8	46.67%
		LAALLLASVSAVTNE	8	46.67%
	A0A0N5DPK5 (TMUE_s0038007500)	TVEQYMRIFYKSSSAT	6	26.67%
		VEQYMRIFYKSSSATK	8	40%
		EQYMRIFYKSSSATKT	8	40%
		QYMRIFYKSSSATKTT	8	40%
		YMRIFYKSSSATKTTT	8	40%
		MRIYKSSSATKTTHL	8	46.67%
	A0A0N5DN19 (TMUE_s0031002800)	RSKILAAKPDESFAA	4	33.33%
		SKILAAKPDESFAAR	4	40%
	A0A0N5DI21 (TMUE_s0012009900)	MRTLYILAASALALV	9	40%
		RTLTYILAASALALVW	9	40%
		TLYILAASALALVWT	9	40%
		LYIILAASALALVWTV	9	40%
		YILAASALALVWTVY	9	40%
		ALALVWTVYAAPIPD	6	46.67%
		LALVWTVYAAPIPDQ	6	46.67%
		ALVWTVYAAPIPDQV	6	46.67%
		LVWTVYAAPIPDQVG	6	46.67%
		VWTVYAAPIPDQVGA	6	40%
	A0A0N5DRU4 (TMUE_s0052001000)	MQFYYLVVFAGLAAA	7	46.67%
		QFYYLVVFAGLAAAG	7	46.67%
		FYYLVVFAGLAAAGH	7	46.67%
		YYLVVFAGLAAAGHW	7	46.67%
		YLVVFAGLAAAGHWK	6	40%
		LVVFAGLAAAGHWKC	6	46.67%
	A0A0N5DDM9	MHVYLVILLAGAAAA	9	53.33%

	(TMUE_s0002011300)	HVYLVILLAGAAAAN	9	46.67%
		VYLVILLAGAAAANY	9	46.67%
		YLVILLAGAAAANYC	9	46.67%
		LVILLAGAAAANYCD	9	46.67%
A0A0N5DDM8 (TMUE_s0002011200)		MHVYLVILLAGAAAA	9	53.33%
		HVYLVILLAGAAAAN	9	46.67%
		VYLVILLAGAAAANY	9	46.67%
		YLVILLAGAAAANYC	9	46.67%
		LVILLAGAAAANYCD	9	46.67%
		VILLAGAAAANYCDC	7	46.67%
	A0A0N5DLK1 (TMUE_s0024002900)	RKFLPIYQQKASSAK	5	53.33%
		KFLPIYQQKASSAKE	5	53.33%
A0A0N5DRU5 (TMUE_s0052001100)		FLPIYQQKASSAKEV	5	53.33%
		MQFYWLVLFAGLVAAA	6	53.33%
		QFYWLVLFAGLVAAG	6	53.33%
		FYWLVLFAGLVAAGH	6	53.33%
		YWLVLFAGLVAAGHK	6	60%
		WLVLFAGLVAAGHKD	6	53.33%
		GARKFLPIYQKAVAE	7	86.67%
		ARKFLPIYQKAVAE	8	73.33%
		RKFLPIYQKAVAEK	8	73.33%

MHC-II T-cell peptides with high and intermediate affinity binding to (I-Ab) mouse strain and for human allele supertypes (HLA-DRB1*01:01, HLA-DRB1*03:01, HLA-DRB1*04:01, HLA-DRB1*07:01, HLA-DRB1*08:02, HLA-DRB1*11:01, HLA-DRB1*13:02, HLA-DRB1*15:01, HLA-DRB3*01:01, HLA-DRB3*02:02, and HLA-DRB4*01:01) predicted using the IEDB prediction tool (Wang et al., 2008). Number of hits is the number of alleles that bind to the MHC-II T-cell peptides with high or intermediate binding affinity. Conservation % is between *T. muris* peptides and *T. trichiura* homology proteins. The 33 peptides that have high or intermediate binding affinity to (I-Ab) mouse allele and to at least 3 different human alleles and with >70% conservation in *T. trichiura* homology proteins are in red colour.

Table 4.3 List of 10 *Trichuris* MHC-II T-cell epitopes which have potential as vaccine candidates.

<i>T. muris</i> proteins (UniProt ID)	Epitope name	Peptide sequence	Amino acid position	The sequence of the protein in FASTA format
Chymotrypsin-like serine protease (A0A0N5DEK1)	Chymotrypsin-like serine protease epitope (CLSP ₄₃₃₋₄₅₀)	AKSKLRYAGSPRFS KSKLRYAGSPRFSR SKLRYAGSPRFSRI KLRYAGSPRFSRIR	433-447 434-448 435-449 436-450	MLYKHCWILLPLICLA FGQNPRTAPCGMPSLYGGQSIQAYLDNK SQNLVL PWTGRMNSS ALILT AGSCFRHTL RKGPKHFKVYAGL DRLRLFLNHGEKS KARSIRIMP YNTANENI WNGVALVTLKKPFVN KQISPVC VAAERRLDEEV RMAPGSV CRGQFPE LANLGGLCSH HERADSEKSLGGPLVCLVN GRAYQYGVYLSQLITRKAL SVHK QALHF YGHITT VLEDDQQ TASRIIQLGSSGKPTKSSESAPSISSESESTE ECGQ QPPSTSM PRPNR PPPH CARPPR SHVSPPRPNHV SPPRNHV STPRPNHV SLP RNHV SPPR PPSPPR RVACDT RTFGRS VESYVIGNA QDMF PWNV IITS KV RGSTR CIGSLV HRG DERQL VN GTDV VL TAA DCFSKYEHAPA AAKSKLRYAGSPRFSRIR RRG NKV KIANV LLYGLP WGNK QDNV VPCL APRESL PPHASCYV THDKREH RIDE E IIMTRNAQCLSAGE REKA ANFRGICAIE EKK KH VQLGSPMVCIVYGRAYQYGVYLNQLSLQINNKVKQNLGFYAEINIVHESIGLITTKE DQWSTQTVPALNQGNRPNVCPWPGGNINAVPLPTPLPNAEY PSSS LEIVGKVILPSLPK YDMSNKTIA TTHEH ILVR DKV IGE SAIAGG VT KG CANIAGNDMAEIPGVSGSFVT GSCT MG GSEGHFGQ QSSH LPGAS GVH IFIV SGK SIEAL CTG TL V RPGEI Y SDEV V T ASRCV KSMA APNYRVYVG SLLPRKMTVEQ LGKTLV E VGGI FATP FYAAYNE LKEMG MVT LKL KHRV KVI QGVQS FPL PYSSTGASS RMQC YVSG V CQHGM PVRV QYQ LLT PTEC GRHL GKS YLP NMV MYC GVGQKEI LQY PVG SP LVCESS QW TQFGI YDHT VRT STV H RVAN V KMPEH NEI ALFM KI GDDVARV QT QTT S
Chymotrypsin-like serine protease (A0A0N5E3X0)	Chymotrypsin-like serine protease epitope (CLSP ₂₂₂₋₂₃₇)	MEKKRKYLG SPLVCF EKKRKYLG SPLVCFV	222-236 223-237	MQR LIA LLPIVA WVS LLTEQVHS FECGYPRA FGGQLSSYVQDKD GLTF PWTVAI IRSY G KYLC LG SIVPE ETD SA KSKN SSNI I LTAG NCLR KSHG K SWG KPK RYAVVAG ISRY SFFSR GEKTHAKY VRIT QFKT GGNDQI WDGV AALY LKKPLIF GK YI SPV CLAL PSF QP SEK MECY VTQY SNK RNFN ED P VGV V P G A Q C D F G Q F P E L A R V G G I C A I K K MEKKRKYLG SPLVCF VR GR AFQYGIYL SELV LSD RL SVQ TRTL NYF APLN A FL PGGT PEL QP II LGKPD GDSS SSS S EEKH C E L RPSR KPERPSS SASYT SSSA EEND GPAN VIL PPIR PEL QIT R PVP STSS SDV KAPV R PPTFI KKD E TSSPSY SSS SASS S D E QRL P T RPA I P V P P D Y P T HPI P I P P R P NY P P P P D Y P T A P I HPI P I P P R P N Y P P P P P A R Q P R C G D T S VLG KRL DLY VH GKN SPT SF PWD ALIA T K MIG TVK CLG S LI HSD SAEK PANAS DL LITSGYCFHQERYGQWLDVSKV VV VAPG AL PICMA I GSQPSPTALCYY SRF YKSAD RIYEELAQFH QP RRCLET KYK T P G FEG LCTREP K RR TVQQGA PLIC IENG QAAQ YGVY LTPMMSK YENVKHWFGFYSEM RVVYHAL SDDR IN RV PEN I P VTH QQP FN
Chymotrypsin-like serine protease	Chymotrypsin-like serine protease	AILQLAKPVFSNTV ILQLAKPVFSNTVR	143-157 144-158	MNFL CLAFTACLV TAALAIE CGDV SYARL TPMDY ALNT NGQKLT FPWS VV LQRK AVV PPW CLATII IQPDQ HTT KSNH SSYV LTAGDC FRNN VLKHYSK FSHF HVFG VTKY SSFT DGTR YEIKSGKL HLQ QHAEGP I RSGV AILQLAKPVFSNTVR P ICLP P RQH PPLD STCFMSVY

(A0A0N5DUC1)	epitope (CLSP ₁₄₃₋₁₅₈)			HKQQNIIDEVDAPLIFGANC GefNAVLHKAKGYCSYYPPRQHVTLGSPLMCIVGVKVFQYGVYTTEFQNYIQGKSQYEKLGFFNSVHDAARETI AELPDRPAATEMPPLSDQLSSYS SSSSEHISSSFSDSQSKEQC PPHCGQSDGSTEEIPTHPELPSSPEKPEAPLPA PLPKPI PQPIPQPEQPEGNVPSIDDL YPSMPESSDAHAHV SDHQEGYPVSPSVHIVSLA EGKP EVI CTGSLYASARANFTRTVLTS ASCVWSRVVSNFVYMGSVRSFAAGGHGKWLPIYRIS TKPIMAHHSALKMMGVGVVKLKKPVSAKG VGFQMPDMFDYATENSQCFVAGVCEHGLSA AAPVRILSPQECRSRLRGKFYPNIEYCALMRKGAMMKVVGAA LVCR TDLEWQWIQYGIYD FTPEKAHLNDINSKNIKTQEIGIFMKVQGGIKFVKRKEADELLGLYK
	Chymotrypsin-like serine protease epitope (CLSP ₄₂₄₋₄₄₃)	CTGSLYASARANFTR	424-438	
		TGSLYASARANFTRT	425-439	
		GSLYASARANFTRTV	426-440	
		YASARANFTRTVLTS	429-443	
	Chymotrypsin-like serine protease epitope (CLSP ₃₉₈₋₄₁₆)	SDHQEGYPVSPSVHI	398-412	
		DHQEGYPVSPSVHIV	399-413	
		HQEGYPVSPSVHIVS	400-414	
		QEGYPVSPSVHIVSL	401-415	
		EGYPVSPSVHIVSLA	402-416	
Pfam domain-containing protein (B_9093) (A0A0N5E6W6)	Pfam domain-containing protein epitope (Pfam ₂₅₆₋₂₇₃)	NFGEYWFTKPVGSVS	256-270	MQWTSILFVAFGCLQFSAVFSDRCNAESSTSYYDYKKVQAERVYWKVKRERTVAAGCV LDSGEKLDNFNTYRTDFLLRCDRINETAVVLTpvkCIMHGQELDRGSSVQQGSFIYTCL EEGGRIGLVITGCVGDKSVVVKFGETFMRKSFLFCMVGEGTRVIHKAVGCVIGGQVNINH KTINIGKYWYKCSRGNNGVQVEVMGCVDSTGKQIDAGDKYRDGGFLFHCKSVGSAVNIV FAGCIAREFGVLKEF NFGEYWFTKPVGSVSYKVACAGDEKS VVPQVVQCIANMDQGRMVL KVGECAKYG TDRMFTCMRKDGTVVARLVTIEEHALSFQTYTAIEGDQCPLPPK
		FGEYWFTKPVGSVSY	257-271	
		GEYWFTKPVGSVSYK	258-272	
		EYWFTKPVGSVSYKV	259-273	
Hypothetical protein (A0A0N5DRU5)	Hypothetical epitope (H ₁₁₂₋₁₂₈)	GARKFLPIYQKAVAE	112-126	MQFYWLVLFLAGLVAAGHKDECDCIKGVGPGYEKSHLDYAGKFGGARKFLPIYEKAVAEE KEVLIKGGPGACDYEPCECRHKRGVEDCGCLKGVGP GYEKSYLDYAGKFKG GARKFLPIY QKAVAEKEVLIKGGPGACDYEPCECRHKRGLKDCGCCKGVGP GYEKSYLDYDGKFKGGA RKFLPIYEKAVAEEKEV LVKGGPGACDW EPCECRHKRGLKDCGCLKGVGP GYEKSYLDY GKF KGGARKFLPIYEKAVAEEKEV LVKGGPGACDW EPCECRHKRGLKDCGCLKGVGP GYEKSYLDYAGKFKGGARKFLPIYEKAVAEEKEVLIKGGPGARD CGCKH
		ARKFLPIYQKAVAE	113-127	
		RKFLPIYQKAVAEEK	114-128	
Chitin-binding domain containing protein (PF01607) (A0A0N5E6C6)	Chitin-binding domain containing protein epitope (CBD ₃₆₋₅₂)	PRLLKIKWSPTAAST	36-50	MRFVVHPKLATQVASFLGGSSCSIVRKTFRVGPFP RPRLLKIKWSPTAASTAIH PRWTMG RENAKVAILLVLIAA FGEAGYSCEGKSNGDYGDPAEPCSSRYFSCVNGKAIGRQCP RG LYFHPGLDKCDWPHGITACSNVQEKE TFRCPAENGDPDPEHQCSAKFWRCTNGKAEPYA CMNGQVFDERLARCSPASGKCAFCLHQPKGQYRWT EEEVCSP EYLEC VENY GRTTVKRP NDLFNDET KLCQPKSEVAECNPQPLLHN EHE DGGHHLAAGIGVPKARPLAPAVVPSPH PAAR SVHSCTS PRATGRCTGEYEGCDHGKPVRLCAVGLVYFEEYGGC VEP THSPECPKT VRQASKFHCTDRPGAKLARGRCKPEYVHCMGAI A VRQWCAPDEVFDQ QSECSVHVAL TDD CTPAAEPHSHSQTHDTHSIANSICS KEDRQLRRRALEQCSKYYVQCDDHSGDQVRSCSN GIYDEM YDRCLPPDLSNCHKVDGIPFYPLNRRKRIERSLRHGRQNSMFNPLFKGDGL PQIHSAQIGIPQLELRDEELRANENLPRRETHFGLNKHV KMEMEVGGETIPLPGGEVAQ VPSIAAASQGRTAVIANLEG LNFDEG PRTAATAVPLIEQNLM PQTGDGIVVPSLDVAQ QV
	Chitin-binding	PAGVVYQCTMPRYTL	1243- 1257	

	domain containing protein epitope (CBD ₁₂₄₃₋₁₂₅₉)	AGVVYQCTMPRYTLC	1244-1258	QQIAVPQANVHAPPQEDLPEPPVGYGAVPPPPVDNVVETPAQWQQPPQADVQFGRPLP APQEYVPVTTPFGVTPVFANPPAGPQGMPQAIVPRKVSNDALGPIKPGSFCANQKDGVY SYGPCRIRDYAVCRGKREIRLSCAIGEIFDPYLFVCTSNEYGYQCALTMTTTTIAPTPS SDVPSTVCLNKADGFYAIAPCSRIFYGCFNGLYQLYQCQFGEVYSQIQHRCIVPGLSCLG AMQTPKAPLGTFFPGTSLPRFCASFEIWSDCASPCGEATCGLLNPPTCGRPKPGCVCR PGYVRLSQSRMCPQEVCLQYTLTNRGLDQTYCRFRPDGLYPYPPGRVCDQRYLRCRGGA IDAQLCQRGEVFDPDKSQCISERACRAPEPSAGGLDSYFCRGKPGSAYNLPGKTCFTIYY LCSDGTVSGFKCPNGYVFDLHLGCVPPSHCDDGPLDNLYCAGKRDGSYTFGNYKCFPI YYTCISGRANFAICRSVDEDLNFNHYCVPRNSCLGSLHYIRRPPMPIRYESPFNLSGSF DPSFCVNQPDGAYPIVECTSPYLVCINSVTTIHYCFPGEIFARVNL PAGVVYQCTMPRYT LCVPTYPQPYPPFTTATTTVAPTVNNLCAAPAVDGQLHPLSNNPCERHYINCTGGSFL LTCPDRTVFNSTSLLCQPNFACLVQPPPDRQLCLDRPNGFYFTLCSQYYLYCQDGIGW VQTCLNPHWAFNGQTMQCAPRHSVAGCRPAGLHHMPNRPGLSALDMRCQTLGDRGYEIT PCQSDFIVCNMGFGDVRSCGSNMVFYGEQQRCARTSEVPACRAKGGSILCLGKPDGAYPF APCSQFYIWRSESYVERCGPRQIFSALQSCVDITSIASCLAQSDPPAQSDPSHQCTT PGVOSIGQCLPSFHVCTPLGVLIIVQCGRGDFDEHLRVCVPAACGRSQVPAANAAAPV IVTNPPTLADSADLVGFTNLNDGLYPIANDCRRFVQCSHTGVHVRNCPDGRVFNMMDPR DPHCDLPRNVPACQQVDDISVVTSPPVTSVDVSNCVDKADGFYRHMTDCTRFIQCFRR RSFVLRCATGLVFNPLINVCFPRRVPDFCNIRMEDTAADTPMDSICSQAQDGAFVRDPST CSAYYRCVHGKAHRFNC PANL VFNTRNNVCDYPTRVPECSP
		GVVYQCTMPRYTLCV	1245-1259	
Chitin-binding domain containing protein (PF01607) (AOA0N5DK22)	Chitin-binding domain containing protein (CBD ₂₄₁₋₂₅₇)	GRTTPVTSAPTTVTT	241-255	MAQLLALVFLSSLLELHASVQHSEFLKRCAHIPDGNYPISPCSHNYLACTGARGLIRTCP SGLIYDPLRNCEVKTNVPSCCVPTTTTPQSDVPSTTEQQTFDCSGLLPGDYPLRPNSC LQQYFTCDADSVGVVRVCPCNSLYFDPVNRCNFFNNIASCSGSTTPPTTATTTLGPTLPP VQFDCSSRDPDFYPNPARQCGSIYYACTGGQARRLFCGSGLAYDVITRACQSPDNTYACT GRTTPVTSAPTTVTTTER SPIDCVTLPNGIYPNPASACSRIFVCSRDGIAERFVCPGQLYF DPARQSCQRFDNIDFACTGVTTTTTPPTTATTTPQMPFDSSLADGLYLPNPTSICSTFY YICSGSVARRQNCPAGLYYDPEMQQCNSFGNIFVCTGTRQTTATTMLVTATSAPGLDC TNLPNGIYPNPRSQCSPIFYFYCTNGFTYEHRCLEDDLFNPELKICDRYSNIFFCTGTRST PPTTPPTTPQSDVPNCFLPNGYNPNPAAQCSNIFFTCSNGKATIRICPLETFFDPEL QLCLAFNDVPVCTGTPRTTTATTTPLSDVTPFFQCSNRPNGNYPLGPCEQVYVSCVD GTPSLRECPPNLFYDFTINECDIYRIPSCGGQRTTPISDVTITIPTPPPEFDCTRLAD GKYPNPRNVCHSNFYVCAGGRTSKMLCPAGLVYDANLQQCVFYRRPPPCVKTLPVSN
		RTTPVTSAPTTVTTE	242-256	
		TTPVTSAPTTVTTTER	243-257	

The 33 MHC-II T-cell peptides were predicted from 7 different *Trichuris* proteins based on their binding ability to bind to at least 3 human alleles and the mouse I-Ab allele and with > 70% conservation in homologous *T. trichiura* proteins. 10 epitopes containing overlapping peptides highlighted in yellow colour were subsequently used for inclusion in VLPs as potential vaccine candidates.

4.3 Discussion

As it infects more than 540 million people worldwide, trichuriasis is one of the world's most important neglected infectious diseases (Pullan et al., 2014). Existing anthelmintic treatments are trusted, but the increasing rates of drug resistance and re-infection pose significant threats to public health (Zhan et al., 2014). Developing a vaccine is the most desirable and cost-effective approach to control *Trichuris* infection, and thus the search for an efficient vaccine against *Trichuris* infection has been ongoing for many years (Dixon et al., 2010). To date, researchers have focused on designing vaccines against *Trichuris* infection based on ES products or EVs, ES or EV fractions and, most recently, the *T. muris* whey acidic protein (WAP) (Briggs et al., 2018; Dixon et al., 2008; Shears et al., 2018a; Zhan et al., 2014). However, this is the first study to identify a set of novel MHC-II T-cell epitopes from the *Trichuris* genome that may induce cross-protection act not only against *T. muris* but also against *T. trichiura* using the RV approach.

Since the advent of immunoinformatics tools for prediction of antigenic epitopes and protein analysis, promising epitope-based vaccines have been developed against several parasites. For example, Gu et al. (2017) developed a multi-epitope vaccine against *T. spiralis* infection based on CD4+ T-cell epitopes and B-cell epitopes predicted from *T. spiralis* paramyosin protein (Ts-Pmy) that were expressed as a soluble recombinant protein (rMEP) in *Escherichia coli*. Mice immunised with the rMEP exhibited 55.4% muscle larval reduction, while those immunised with paramyosin recombinant protein (rTs-Pmy) prior to *T. spiralis* infection exhibited only 34.4% reduction. Protection was associated with the production of high levels of anti-rMEP-specific IgG1/IgG2c antibodies and the secretion of IFN- γ , IL-4 and IL-5 cytokines (Gu et al., 2017).

Based on the promising results of Gu et al.'s study and others, the present study designed a multi epitope-based vaccine against *Trichuris* infection. However, since CD4+ T-cells, not B-cells, protect against *Trichuris* infection (Else and Grencis, 1996; Koyama et al., 1995), only MHC-II T-cell epitopes were predicted from different *Trichuris* proteins. The selected epitopes will be fused into VLPs, which will serve as a vaccine delivery system.

4.3.1 The choice of secreted proteins as vaccine candidates

Proteins are the first choice for vaccine candidates for many researchers because proteins can be easily identified and produced in large quantities for inclusion in commercial vaccines (Hein and Harrison, 2005). In addition, many secreted proteins found in parasite ES products have different antigenic properties, suggesting that they are great vaccine targets (Dalton et al., 2003; Zarowiecki and Berriman, 2015). For example, proteins secreted from *Leishmania* spp have been found to play an important role in the host-parasite interaction, generating a strong immune response and protection against infection in mice (John et al., 2012; Santarém et al., 2007). Another study indicated that boosting bacillus Calmette-Guerin (BCG)-immunised guinea pigs with a purified recombinant *Mycobacterium tuberculosis* major secreted protein (30-kDa protein) significantly boosted the animals' cell-mediated and humoral immune responses and enhanced protection against tuberculosis compared to non-boosted BCG-immunised animals (Horwitz et al., 2005).

Based on the fact that ES proteins secreted from both adult and larval *T. muris* elicit strong immunity and protection against infection in mice (Dixon et al., 2010; Shears et al., 2018b), only secreted, surface exposed and highly expressed proteins were selected for this study as they should have a great immunogenic potential during infection and consequently induce protection as vaccine candidates.

4.3.2 *Trichuris* proteins selected for epitope prediction

From the whole parasite genome, 10 epitopes containing 33 overlapping peptides were identified. CBD₃₆₋₅₂, CBD₁₂₄₃₋₁₂₅₉, and CBD₂₄₁₋₂₅₇ epitopes were predicted from two different chitin-binding domain-containing proteins, and the H₁₁₂₋₁₂₈ epitope was predicted from a hypothetical protein. In addition, the CLSP₄₃₃₋₄₅₀, CLSP₂₂₂₋₂₃₇, CLSP₁₄₃₋₁₅₈, CLSP₄₂₄₋₄₄₃ and CLSP₃₉₈₋₄₁₆ epitopes were predicted from three different chymotrypsin-like serine proteases, and the Pfam₂₅₆₋₂₇₃ epitope was predicted from a Pfam B domain-containing protein.

Although several studies have provided rich information about the host-parasite interaction, the precise biological function of each *Trichuris* protein is unclear (Zarowiecki and Berriman, 2015). Several studies have demonstrated that chitin-binding domain genes are highly expressed in *Caenorhabditis elegans*, *N. brasiliensis*, *H. polygyrus*, *Ascaris lumbricoides*, *Ancylostoma ceylanicum*, and *Anopheles gambiae* insects (Foor, 1967; Shen and Jacobs-Lorena, 1998; Tjoelker et al., 2000; Vannella et al., 2016; Wei et al., 2016). In the nematode *C. elegans*, chitin-binding domain-containing proteins are highly expressed in adults, larvae and pharynx cells, suggesting that they have different functional roles (Veronica et al., 2001). Specifically, they are thought to be associated with eggshell formation and early single-cell developmental stages, such as secretion of the chitinous eggshell following fertilisation, maintenance of the osmotic/permeability barrier in the middle layer of the eggshell, polar-body extrusion and initiation of single-cell embryo (zygote) polarisation (Johnston et al., 2006, 2010; Nance, 2005; Zhang et al., 2005). Several studies have also suggested that the acidic mammalian chitinase (AMCase) that constitutively degrades chitin substrates in the mouse gastrointestinal environment are critical initiators of protective type 2 responses to intestinal nematodes (Ohno et al., 2016; Zhu et al., 2004). For example, Vannella et al. (2016), demonstrated that, following infection with *N. brasiliensis* and *H. polygyrus*, AMCase-deficient mice developed impaired type 2 immunity as well as reduced mucus production and decreased intestinal expression of the signature type 2 response genes which regulate T-cell homing. Taken together, these results suggest that AMCase may play a role in priming protection against gastrointestinal nematode infections.

There is little published research on Pfam B domain-containing proteins. Nevertheless, based on the BLAST analyses conducted in this study, they appear to have homologues in other parasites, including *T. trichiura*, *T. suis*, *Trichinella* spp, *Ancylostoma ceylanicum*, *Diploscapter pachys*, *Caenorhabditis* spp, *Strongyloides* spp, *Enterobius vermicularis*, *Ascaris* spp, *Brugia malayi* and others.

Hypothetical proteins, also known as uncharacterised proteins, are noticeably transcriptionally upregulated in various stages and sexes in *Trichuris* spp and other nematode genomes (Foth et al.,

2014; Hunt et al., 2016; Jex et al., 2014; Leroux et al., 2018). Also, the RNA content of *T. muris* EV fractions, which are characterised using the Illumina HiSeq platform, showed that hypothetical proteins with unknown function are among the most abundant domains in *T. muris* (Eichenberger et al., 2018b). Shears et al. (2018a) also suggested that hypothetical proteins isolated from *T. muris* ES and EV proteins are promising vaccine candidates. Thus, vaccinating C57BL/6 mice with EVs isolated from *T. muris* ES without an adjuvant prior to infection with a low-dose of *T. muris* eggs induced significant protection characterised with low worm burden and a high level of IgG1 anti-parasite antibodies against soluble ES proteins (Shears et al., 2018a).

Chymotrypsin-like serine proteases could also be promising vaccine candidates, given that the most abundant proteases in the anterior region of *T. muris* are chymotrypsin A-like serine proteases (Foth et al., 2014). These proteases have also been found as conserved in the secretomes of more than 40 helminth spp (Consortium, 2019; Cuesta-Astroza et al., 2017). For example, *Strongyloides stercoralis* (Marcilla et al., 2012), *Necator americanus* (Cantacessi et al., 2010), *A. caninum* (Zhan et al., 2003), *Trichinella pseudospiralis* (Xu et al., 2017), *T. spiralis* (Wei et al., 2011), and *T. suis* (Cantacessi et al., 2011) express high levels of chymotrypsin-like serine proteases, which have thus been proposed to play an essential role in inducing the host immune response. Interestingly, the chymotrypsin-like serine protease (TMUE_s0003007500) and hypothetical proteins (TMUE_s0038007500 and TMUE_s0031002800) identified in this study were among the secreted proteins with signal peptides in *T. muris* ES products (Eichenberger et al., 2018b), confirming that these proteins play a role in the secretory pathway.

Trichuris spp, like other helminth parasites, secrete different proteinases, such as serine, cysteine and metalloproteases, to overcome the host tissue barrier or obtain essential nutrients for survival (Hewitson and Maizels, 2014; Izvekova and Frolova, 2017; Viney, 2017). Although the biological functions of the genes encoding proteases or peptidases remain unclear, helminth serine proteases seem to play a central role in either the invasion process or modulation of the host immune response to enhance the survival in the host (Balasubramanian et al., 2010; Santos et al., 2013; Gomez-Fuentes et al., 2019; Toubarro et al., 2010; Yang et al., 2015). For example, *Strongyloides* spp, like many other helminth parasites, produce proteases to break down the host tissue to facilitate migration to the gut and to digest the host tissue to acquire food (Viney, 2017). Also, *T. muris* secretes serine proteases, which are involved in degrading host intestinal mucins 2 (Muc2) polymers within the mucus barrier facilitating mating and egg laying, increasing the host's susceptibility to *T. muris* infection (Drake et al., 1994; Hasnain et al., 2012). Chymotrypsin-like (S1) serine proteases are also upregulated in the stichosome of *T. suis* (Jex et al., 2014). It has also been suggested that some *T. suis* chymotrypsin-like serine proteases assist in digesting components of the host, such as blood, serum and tissue (Jex et al., 2014).

Interestingly, immunising BALB/c mice with a recombinant vaccine based on the serine protease gene (TspSP-1.2) encoding a 35.5 kDa protein from *T. spiralis* muscle larvae prior to challenging the mice with *T. spiralis* infective larvae induced a partial reduction in intestinal adult worms and muscle larvae (Wang et al., 2013). Furthermore, when the serum from mice vaccinated with TspSP-1.2 was added to a human colon carcinoma cell line (HCT-8 cells) monolayer overlaid with

infective larvae for 1 hour at 37°C, the invasion rate of the infective larvae into the cell monolayer was partially prevented (Wang et al., 2013). Another study showed that vaccinating BALB/c mice with a recombinant serine protease of adult *Trichinella spiralis* (Ts-Adsp) formulated with an alum adjuvant prior to *T. spiralis* challenge induced a reduction in worm burden (Feng et al., 2013). The results indicated that both humoral and cellular immune responses were induced to serine proteases, as demonstrated by the elevated levels of specific anti-rTs-Adsp IgG and IgE antibodies and mixed Th1 (IFN-γ and IL-2) and Th2 (IL-4, IL-10 and IL-13) cytokines (Feng et al., 2013). Moreover, vaccinating Kunming mice twice with serine proteases from new-born *T. spiralis* (Ts-NBLsp) larvae as a naked DNA vaccine prior to challenging the mice with *T. spiralis* muscle larvae (ML) led to a 77.93% reduction in ML and boosted anti-Ts-NBLsp-specific IgG responses (Xu et al., 2017). In another study, Ren et al. (2018) demonstrated that vaccinating BALB/c mice with recombinant *T. spiralis* 31 kDa protein (rTs31) containing a domain of a trypsin-like serine protease prior to challenging the mice with *T. spiralis* larvae elicited a significant humoral response and protection, as demonstrated by the 56.93% reduction in adult worms at day 6 p.i. and 53.50% reduction in muscle larvae at day 42 p.i.. More recently, Sun et al. (2019) demonstrated that intranasal vaccination of BALB/c mice with *T. spiralis* serine protease (rTsSP) coupled with cholera toxin B subunit (CTB) resulted in a 71.10% adult and 62.10% larva reduction after challenge. Collectively, these studies suggest that *Trichuris* chymotrypsin-like serine protease could be a promising protein candidate for inclusion in a vaccine for trichuriasis.

In 2018, Shears et al. fractionated *T. muris* ES using a combination of size exclusion chromatography (Superose 12) and gel filtration chromatography (Superdex 75), to identify a set of potential immunogenic candidates using mass spectrometry. Interestingly, C57BL/6 mice vaccinated with the ES fraction induced high antibody responses. In addition, stimulating infection-primed MLN lymphocytes from C57BL/6 mice with ES fractions for 42 hours induced a high level of Th2 cytokines (IL-9 and IL-13) in the supernatant (Shears et al., 2018b). Interestingly, some of the proteins identified in this chapter were identified in Shears et al.'s report, including a WAP domain containing protein (TMUE_s0004017900), Deoxyribonuclease (DNase) II (TMUE_s0030007700), chymotrypsin-like serine proteases (TMUE_s0191000800, TMUE_s0003007500, TMUE_s0004005300, TMUE_s0069001100, and TMUE_s0004007100), chitin-binding domain containing protein (TMUE_s0281000600 and s0018008000), cystatin-domain containing protein (TMUE_s0122001300), myoglobin (TMUE_s0027006900), a poly cysteine and histidine tailed protein isoform (TMUE_s0083002300), and hypothetical proteins (TMUE_s0077002200, TMUE_s0038007500, TMUE_s0031002800, TMUE_s0012009900, TMUE_s0002011300). Notably, the chymotrypsin-like serine proteases TMUE_s0191000800 and TMUE_s0003007500; the chitin-binding domain containing protein TMUE_s0281000600; and the hypothetical proteins TMUE_s0038007500, TMUE_s0031002800, and TMUE_s0012009900, which were selected to predict the MHC-II T-cell epitopes, were identified in the most immunogenic ES fractions (Shears et al., 2018b). Most importantly, the final set of selected epitopes identified in this chapter included three MHC-II T-cell epitopes predicted from these proteins: CLSP₂₂₂₋₂₃₇, which was predicted from the chymotrypsin-like serine protease TMUE_s0191000800, and CBD₃₆₋₅₂ and CBD₁₂₄₃₋₁₂₅₉, which were predicted from the chitin-binding domain-containing protein TMUE_s0281000600.

A better understanding of the biological function of *Trichuris* proteins might shed new light on host-parasite interactions, which will help identify potential vaccine candidates. Certainly, the RV approach facilitated screening for *Trichuris* immunogenic candidates by reducing the required time and effort. Otherwise, screening would be difficult to carry out experimentally due to the complicated genome and variations in immune responses. The provided framework for identifying potential epitope vaccine candidates within the *T. muris* and *T. trichiura* genomes could be used in future studies to identify epitope-based vaccine candidates against other parasites.

4.4 Summary

- Based on the RV approach, a set of proteins were identified from the *Trichuris* genome using inclusion and exclusion criteria. A *T. muris* genome was used as a reference genome and short-listed proteins according to their secretion pathway and expression level. The selected proteins were then checked to determine their homology with *T. trichiura*, human and mouse proteins using the BLAST tool. After short-listing, 27 proteins were selected as suitable vaccine targets.
- The selected vaccine target proteins were then used to predict MHC-II T-cell epitopes as promising vaccine antigen candidates using the IEDB *in silico* prediction tools and subsequently the predicted peptides were screened for allergenicity and conservancy, resulting in a final set of 10 *Trichuris* MHC-II T-cell epitopes containing 33 overlapping peptides.

Chapter Five

**Design of HBc-Ag VLP expressing
Trichuris MHC-II T-cell epitopes**

5.1 Introduction

Virus-like particles (VLPs) are viral structural proteins that have an intrinsic ability to self-assemble into viral capsids, but they possess the immunostimulatory and self-adjuvanting properties of natural viruses (Grgacic and Anderson, 2006; Whitacre et al., 2009). Over the years, many VLP-based vaccines have been engineered to display foreign pathogenic antigens and have proven to be more immunogenic than recombinant protein-based vaccines (Jennings and Bachmann, 2008; Roldao et al., 2010). Some of these VLP-based vaccines are used worldwide, such as the hepatitis B virus (HBV) vaccine (GlaxoSmithKline's Engerix®) (Keatinggm, 2003) and the human papillomavirus vaccine (Cervarix®) (McKeage and Romanowski, 2011). While the anti-malaria vaccine (RTS, S/AS01) is in clinical development (Dobano et al., 2019), and many others are undergoing pre-clinical evaluation, such as the human immunodeficiency virus (HIV) and influenza vaccines (Franco et al., 2011; Song et al., 2011). Also, several VLP-based vaccine candidates are under investigation, including those against *Trichinella spiralis* and *Clonorchis sinensis* (Lee et al., 2017; Lee et al., 2016).

Several types of VLPs have been used for vaccine development, one of the most promising of which is the HBV core particle (HBc-Ag) (Chisari and Ferrari, 1995; Qiao et al., 2016; Roose et al., 2013). This is a self-assembling viral capsid that can induce potent B-cell and T-cell dependent and independent immune responses without the need for an adjuvant (Milich et al., 1988; Milich and McLachlan, 1986). HBc-Ag VLP displaying foreign epitopes has been used as a promising vaccine carrier against several diseases, including Crohn's disease (Guan et al., 2009), Anthrax (Yin et al., 2008), hand-foot-and-mouth disease (Huo et al., 2017), hepatitis B and C (Sominskaya et al., 2010), malaria caused by *Plasmodium falciparum* (Nardin et al., 2004), and toxoplasmosis caused by *T. gondii* (Guo et al., 2019). Furthermore, HBc-Ag VLP displaying large foreign antigens has been used as a promising vaccine carrier for diseases such as *Mycobacterium tuberculosis* (Yin et al., 2011) and Lyme disease (Nassal et al., 2008). These studies confirm that HBc-Ag VLP is a safe, efficient and economical vaccine delivery platform that can display antigens of different sizes and be inexpensively produced in different expression systems.

5.2 Aim and objectives

The overall aim of this chapter was to design and purify HBc-Ag VLPs expressing novel *Trichuris* MHC-II T-cell epitopes. To achieve this aim, the current chapter addressed the following objectives:

- To design, clone and express a native VLP (HBc-Ag) construct that can be used as a base construct to insert *Trichuris* MHC-II T-cell epitopes.
- To design, clone and express novel constructs based on VLP (HBc-Ag) expressing the following *Trichuris* MHC-II T-cell epitopes: CLSP₄₃₃₋₄₅₀, CLSP₂₂₂₋₂₃₇, CLSP₁₄₃₋₁₅₈, CLSP₄₂₄₋₄₄₃, CLSP₃₉₈₋₄₁₆, Pfam₂₅₆₋₂₇₃, H₁₁₂₋₁₂₈, CBD₃₆₋₅₂, CBD₁₂₄₃₋₁₂₅₉, and CBD₂₄₁₋₂₅₇.
- To design, clone and express novel constructs based on VLP (HBc-Ag) expressing larger amino acid sequences in order to enhance the immunogenicity of the construct. The first construct design, named HBc-mosaic, provides a single expression system that can display multiple *Trichuris* epitopes (hypothetical protein A0A0N5DRU5 + CLSP₃₉₈₋₄₁₆ epitope + chitin-binding domain-containing protein A0A0N5DK22). The second construct,

named HBc-HP₁₋₅₁₂, is based on VLP (HBc-Ag) expressing the *Trichuris* hypothetical protein (A0A0N5DRU5).

- To purify VLP recombinant proteins by Strep-Tag affinity chromatography and size exclusion chromatography (SEC).
- To assess the endotoxin contamination of VLP recombinant proteins using the EndoLISA endotoxin detection assay.
- To assess VLP recombinant proteins' structure and assembly by circular dichroism (CD) spectroscopy and transmission electron microscopy (TEM).

5.3 Results

5.3.1 Prediction of the recombinant VLP protein's physicochemical properties

The physicochemical properties derived from the primary structure of each VLP–antigen fusion (e.g. the molecular mass and isoelectric point) were identified using the Expasy ProtParam server (Gasteiger et al., 2005) to assist in the identification of stable vaccine candidates (Cox and Onraedt, 2012; Jain et al., 2015). Table 5.1 details the design and derived physicochemical properties of the VLP recombinant constructs. The *in vivo* half-life of all the proteins expressed and purified in *E. coli* was estimated to be >10 hours by the Expasy ProtParam server (Varshavsky, 1997). A hydropathic index, the GRAVY, was also calculated. Positive GRAVY values indicated hydrophobicity, and negative GRAVY values indicated hydrophilicity (Kyte and Doolittle, 1982). All the constructs have negative values, suggesting that they are soluble.

Table 5.1 The schematics design and physicochemical properties of the VLP recombinant constructs.

VLP recombinant protein name	Schematic picture of the construct	Number of resides inserted in the native HBc-Ag	Total number of resides in the whole construct	Molecular mass (kDa)	Extinction coefficient	GRAVY index	Estimated half-life in <i>E. coli</i> <i>in vivo</i>
HBc-Ag		0	203	21.82	3495	-0.177	>10 hours
HBc-HP ₁₋₅₁₂		309	512	55.29	7575	-0.422	>10 hours
HBc-mosaic		520	723	77.16	10818	-0.442	>10 hours

HBc-Pfam₂₅₆₋₂₇₃		9	212	22.84	4355	-0.165	>10 hours
HBc-HP₁₁₂₋₁₂₈		8	211	22.66	3967	-0.069	>10 hours
HBc-CLSP₄₃₃₋₄₅₀		11	214	23.13	3656	-0.242	>10 hours
HBc-CLSP₂₂₂₋₂₃₇		12	215	23.27	3669	-0.220	>10 hours
HBc-CLSP₁₄₃₋₁₅₈		11	214	22.85	3507	-0.078	>10 hours

HBc- CLSP₄₂₄₋₄₄₃	<p>CLSP₄₂₄₋₄₄₃</p> <p>1 148 152 159</p> <p>HBc-Ag GGG Strep-Tag</p>	13	216	23.06	3669	-0.085	>10 hours
HBc- CLSP₃₉₈₋₄₁₆	<p>CLSP₃₉₈₋₄₁₆</p> <p>1 148 152 159</p> <p>HBc-Ag GGG Strep-Tag</p>	14	217	23.17	3656	-0.163	>10 hours
HBc- CBD₃₆₋₅₂	<p>CBD₃₆₋₅₂</p> <p>1 148 152 159</p> <p>HBc-Ag GGG Strep-Tag</p>	8	211	22.62	4057	-0.173	>10 hours
HBc- CBD₁₂₄₃₋₁₂₅₉	<p>CBD₁₂₄₃₋₁₂₅₉</p> <p>1 148 152 159</p> <p>HBc-Ag GGG Strep-Tag</p>	15	218	23.45	3967	-0.129	>10 hours
HBc- CBD₂₄₁₋₂₅₇	<p>CBD₂₄₁₋ 257</p> <p>1 148 152 159</p> <p>HBc-Ag GGG Strep-Tag</p>	10	213	22.71	3520	-0.187	>10 hours

Number of residues inserted in the native HBc-Ag, the total number of residues in the expressed construct, the molecular mass, extinction coefficient (Kyte and Doolittle, 1982), grand average of hydropathicity (GRAVY index) (Kyte and Doolittle, 1982), and the estimated half-life in *E. coli* (Varshavsky, 1997) were characterised using Expasy ProtParam server (Gasteiger et al., 2005).

5.3.2 Design of the native VLP (HBc-Ag)

The design of VLPs expressing *Trichuris* MHC-II T-cell epitopes was based on the original HBc-Ag, which consists of a 183-residue sequence (GenBank AAK62975.1). Three important modifications were made to the native VLP (HBc-Ag) used in this study. First, arginine-rich residues in the C-terminal domain (150–183 aa) act as RNA-binding sites, which are required for capsid stability and RNA encapsidation, but not for structural assembly (Birnbaum and Nassal, 1990; Gallina et al., 1989; Nassal, 1992). Therefore, these sequences were truncated, leaving the N-terminal domain (148 aa) without disturbing the assembly of the structure. Second, to enhance the flexibility of insertion of foreign epitopes and improve folding, short linkers (4xGS3xGS) were inserted before and after the major immunodominant region (MIR) region (Chen et al., 2013; Janssens et al., 2010). Finally, to facilitate purification of the recombinant constructs using Strep-Tag affinity chromatography, the Strep-Tag sequence (WSHPQFEK) and glycine-rich (GGG) flexible linkers were inserted at the C-terminus as described in Chapter 2 (Figure 2.1).

5.3.3 Cloning and expression of the native VLP (HBc-Ag)

The first objective was to verify that the native VLP (HBc-Ag) construct could be cloned, expressed, purified and used as a base construct to insert *Trichuris* MHC-II T-cell epitopes. Thus, first, the pET17b plasmid vector system was digested using NdeI and XbaI restriction enzymes to ligate the native VLP (HBc-Ag) to construct a recombinant plasmid. The VLP (HBc-Ag) construct was synthesised (GeneArt) and cloned into the pET17b expression vector for recombinant expression in *Escherichia coli*. The construct was verified by DNA sequencing and subsequently transformed into *E. coli* Lemo21 (DE3) competent cells for small-scale expression by isopropyl β-D-1-thiogalactopyranoside (IPTG) induction. Lemo21 (DE3) chemically competent *E. coli* cells are a BL21(DE3)-derived strain that is suitable for tuneable T7-driven expression of routine and challenging proteins under the control of IPTG (Kuipers et al., 2017). After 14–16 hours, cells were harvested and disrupted by sonication, and the cell lysate was collected in the supernatant after centrifugation. Monitoring by SDS-PAGE revealed that the native VLP (HBc-Ag) is soluble; a band at the expected molecular mass of approximately 22 kDa was observed in both the cell lysate (total protein [TP]) and the soluble protein (SP) (Figure 5.1).

For large-scale expression, the native VLP (HBc-Ag) construct was transformed into ClearColi-BL21 (DE3) electrocompetent cells for overnight growth and IPTG induction at 16°C.

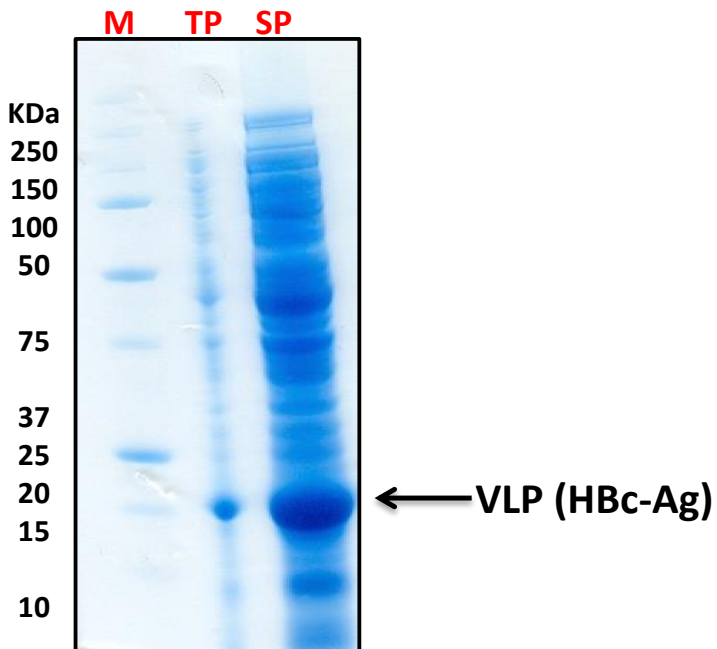


Figure 5.1 SDS-PAGE analysis of the native VLP (HBc-Ag) after small-scale expression. SDS-PAGE (10% gels) stained with Coomassie blue. M: protein marker (Precision Plus protein standard, unstained, Bio-Rad). Lanes 'TP' and 'SP' represent cell lysate (total protein) after sonication and soluble protein supernatant after centrifugation, respectively. A band corresponding to the estimated molecular mass from the HBc-Ag protein sequence (~22 kDa) is present in both the TP and SP lanes is indicated by the arrow.

5.3.4 Purification of the native VLP (HBc-Ag)

The presence of a C-terminal affinity Strep-Tag at the end of the pET17b vector facilitates purification of the native VLP (HBc-Ag). The HBc-Ag was purified by Strep-Tag affinity chromatography using StrepTrap HP, as shown in Figure 5.2 (B, Lane 1). The eluted fractions were then concentrated to 0.5 ml using a Vivaspin concentrator (MWCO 10.000 kDa). Next, the proteins were subjected to a second round of purification performed by SEC. The SEC chromatogram of the purified native VLP (HBc-Ag) revealed the purity of the protein; a clear single peak was eluted in fractions of 7–10 ml, as shown in Figure 5.2 (A). The 120 dimers ($T=4$) fused via dimer-dimer interactions to assemble into the HBc-Ag ($2 \times 120 \times 22 = 5.2$ MDa). SDS-PAGE analyses also indicate the presence of a single band of the VLP (HBc-Ag) monomer, with an expected molecular mass of ~22 kDa, as shown in Figure 5.2 (B, Lane 2). Purifying the VLP recombinant protein using two different methods was essential to remove contaminants and transfer the protein to a more physiologically appropriate vaccine buffer (1X PBS PH7.4).

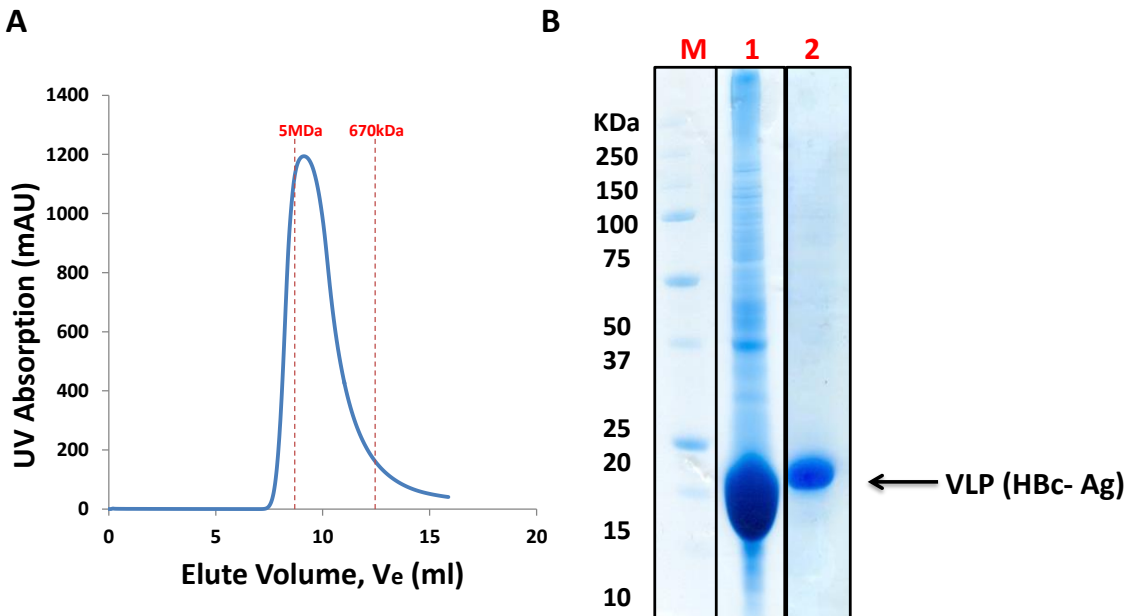


Figure 5.2 The native VLP (HBc-Ag) purification profile and SDS-PAGE analysis. (A) Chromatogram of the native VLP (HBc-Ag) purified by SEC. Separation was carried out on a Superose 6, 10/300 GL (GE Healthcare), at a flow rate of 0.2 ml/min. HBc-Ag was eluted in 0.5 ml fraction and a sample of the SEC elution peak was analysed on SDS-PAGE. Vertical red lines indicate the elution volume of mass standards, from left to right: 2MDa, 670kDa. HBc-Ag was eluted in a single peak at elution voulme= 7 ml. (B) Purification monitored by SDS-PAGE (10% gel) stained with Coomassie blue. M: protein marker (Precision Plus protein standard, unstained, Bio-Rad); Lane 1: HBc-Ag after Strep-Tag affinity purification using the StrepTrap HP, and Lane 2: HBc-Ag after SEC purification. The arrow represents HBc-Ag band that corresponds to the estimated molecular mass of ~22 kDa.

5.3.5 Cloning and expression of HBc-Ag containing *Trichuris* antigens

Foreign epitope sequences can be inserted and displayed in three different regions on HBc particles: the N- and C-terminal regions and the MIR at the tips of the spike (position 79/80) (Pumpens and Grens, 1999, 2001). The MIR has been identified as a superior site as it allows for insertion of up to 238 amino acid residues and thus can induce a stronger immune response in mice compared to the N- and C- termini (Koletzki et al., 1999; Kratz et al., 1999; Schödel et al., 1992). Therefore, all the target antigens were inserted in the MIR of the native VLP (HBc-Ag).

The processes of cloning, expressing and purifying VLP recombinant protein is divided into six steps (Figure 5.3). The process of expression of VLPs with *Trichuris* MHC-II T-cell epitopes was similar to that for expressing native VLP (HBc-Ag), except the MHC-II T-cell epitope primers were annealed and the resulting ligation was inserted into linearised VLP (HBc-Ag) in the MIR before expression and transformation into Lemo21 (DE3) competent cells for small-scale expression in order to monitor the proteins' solubility. The MHC-II T-cell epitope sequences and primers used to amplify the target can be found in Chapter 2 (Table 2.2).

Visualisation of protein solubility by SDS PAGE revealed that the VLP recombinant proteins (HBc-CBD₃₆₋₅₂, HBc-CBD₁₂₄₃₋₁₂₅₉, HBc-CBD₂₄₁₋₂₅₇, HBc-CLSP₄₃₃₋₄₅₀, HBc-CLSP₂₂₂₋₂₃₇, HBc-CLSP₁₄₃₋₁₅₈, HBc-CLSP₄₂₄₋₄₄₃, HBc-CLSP₃₉₈₋₄₁₆, and HBc-H₁₁₂₋₁₂₈) were found to be expressed as soluble

products. A band with the expected molecular mass (approximately 22 kDa) was present in both the crude lysates and soluble proteins after centrifugation (Figures 5.4 and 5.5). Also, the total cell lysate showed a wide range of proteins prior to sonication and centrifugation (Figures 5.4 and 5.5, TP lanes). However, HBc-Pfam₂₅₆₋₂₇₃ did not give a band in the soluble protein (Fig 5.6), suggesting that it was insoluble when overexpressed in *E. coli*.

Larger amino acid sequences (HBc-HP₁₋₅₁₂, and HBc-mosaic) were also inserted in the MIR of the native VLP (HBc-Ag). The full genetic sequences of the constructs can be found in Chapter 2 (Table 2.3). The CamSol method (Sormanni et al., 2015) was used to predict whether large foreign antigens were compatible with the VLP assembly (Frietze et al., 2016; Joshi et al., 2013). Although the software predicted that HBc-HP₁₋₅₁₂ and HBc-mosaic could be soluble, the two constructs were insoluble when expressed in *E. coli* (Figures 5.7 and 5.8). Therefore, they were not purified further.

The constructs identified as soluble were transformed into ClearColi-BL21 (DE3) electrocompetent cells for overnight growth and IPTG induction for large-scale expression.

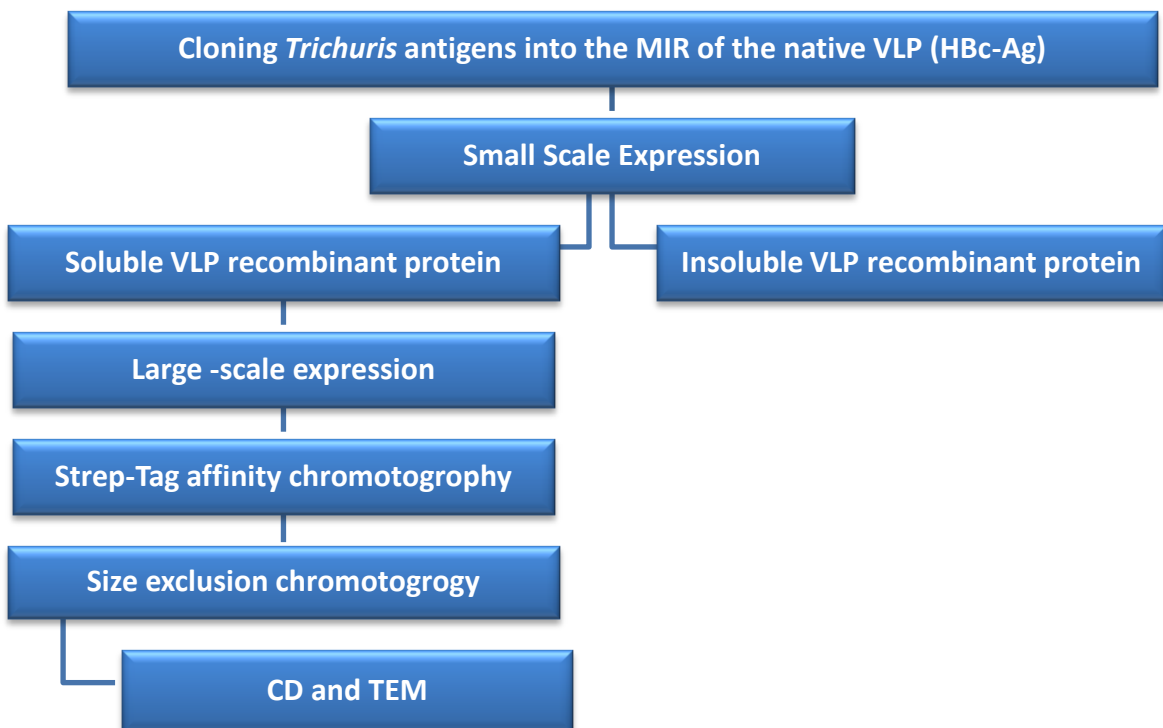


Figure 5.3 Protocol used for VLP recombinant proteins cloning, expression and purification.
First, the *Trichuris* antigen was cloned into the MIR of the VLP (HBc-Ag). The correct construct confirmed by the DNA sequencing were expressed after IPTG induction for small-scale expression to assess the solubility. Only soluble proteins were then expressed for large-scale expression. The VLP recombinant proteins were then purified twice using Strep-Tag affinity and SEC. Finally, the VLP recombinant protein structure and assembly were assessed using CD and TEM analysis tools.

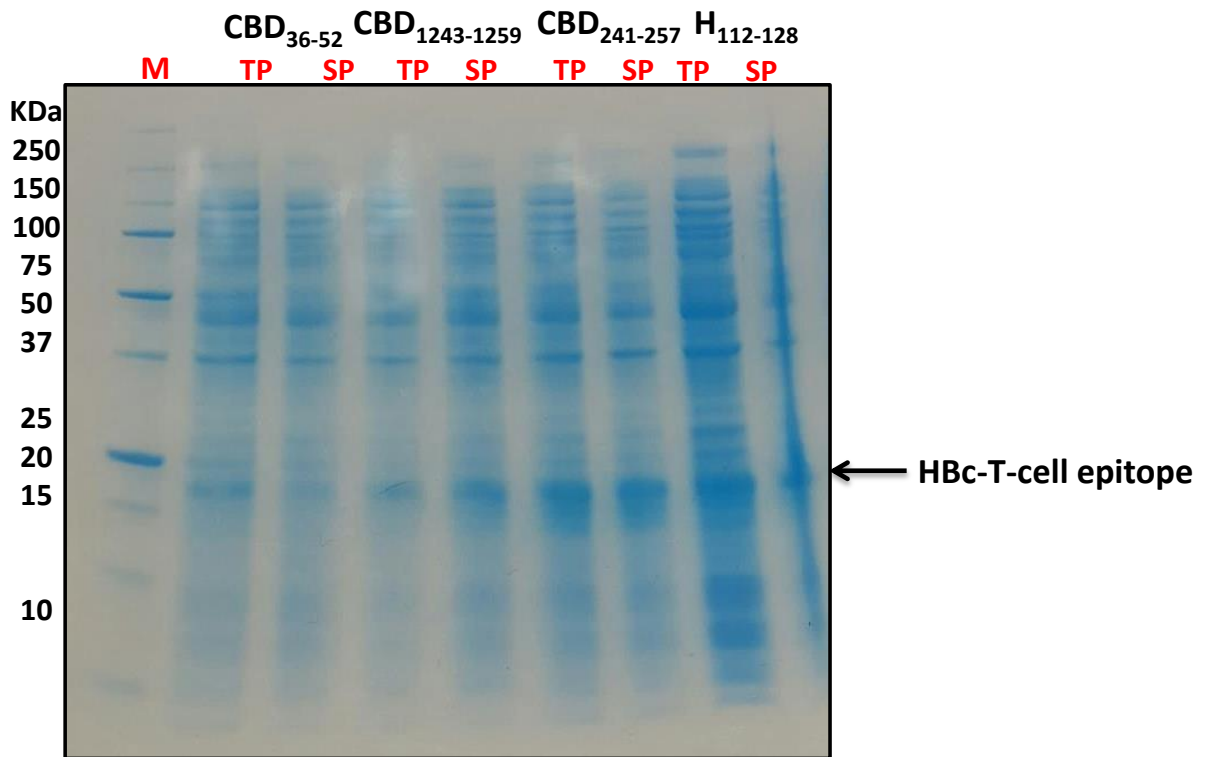


Figure 5.4 SDS-PAGE analysis of VLP recombinant proteins (HBc-CBD₃₆₋₅₂, HBc-CBD₁₂₄₃₋₁₂₅₉, HBc-CBD₂₄₁₋₂₅₇ and HBc-H₁₁₂₋₁₂₈) after small-scale expression. Solubility was ascertained by SDS-PAGE (10% gel) stained with Coomassie blue. M: protein marker (Precision Plus protein standard, unstained, Bio-Rad). Lanes 'TP' and 'SP' represent cell lysate (total protein) after sonication and soluble protein supernatant after centrifugation, respectively. The arrow represents the VLP recombinant protein band in the TP and SP that corresponds to the estimated molecular mass of ~22 kDa estimated from the protein sequence.

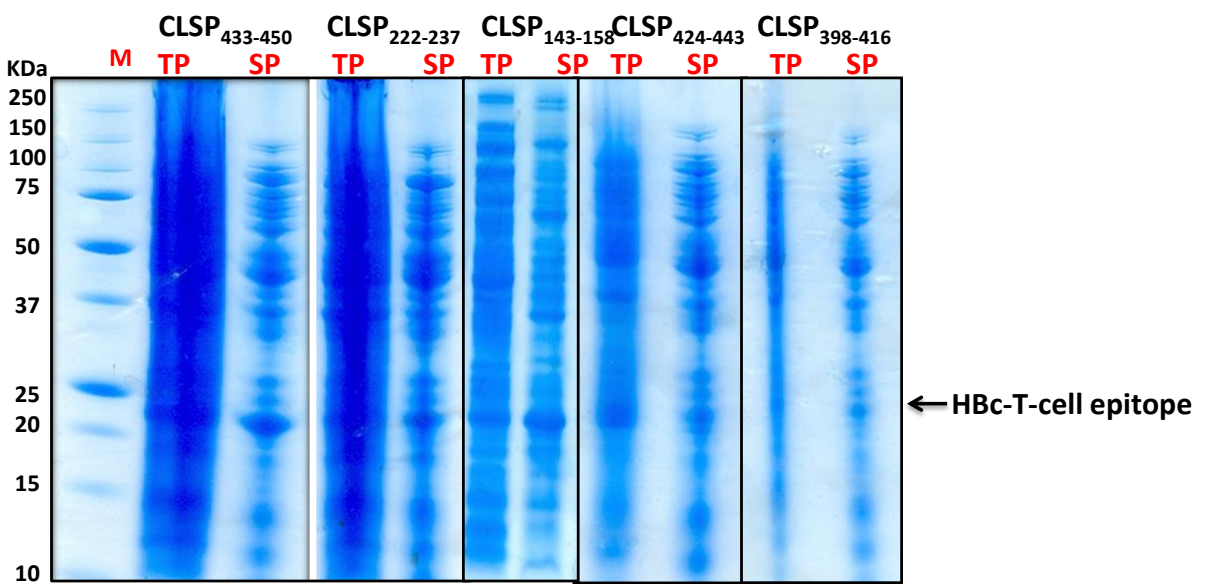


Figure 5.5 SDS-PAGE analysis of VLP recombinant proteins (HBc-CLSP₄₃₃₋₄₅₀, HBc-CLSP₂₂₂₋₂₃₇, HBc-CLSP₁₄₃₋₁₅₈, HBc-CLSP₄₂₄₋₄₄₃ and HBc-CLSP₃₉₈₋₄₁₆) after small-scale expression. Solubility was ascertained by SDS-PAGE (10% gel) stained with Coomassie blue. M: protein marker (Precision Plus protein standard, unstained, Bio-Rad). Lanes 'TP' and 'SP' represent cell lysate (total protein) after sonication and soluble protein supernatant after centrifugation, respectively. The arrow represents the VLP recombinant protein band in the TP and SP that corresponds to the estimated molecular mass of ~22 kDa estimated from the protein sequence.

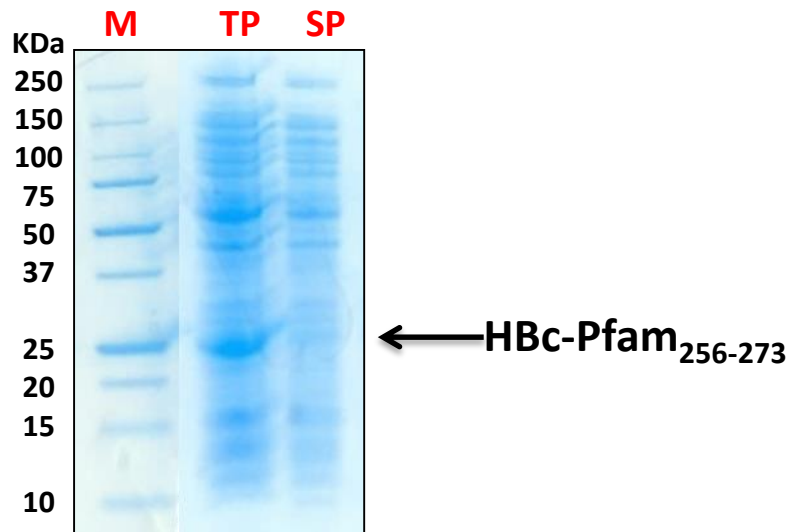


Figure 5.6 SDS-PAGE analysis of HBc-Pfam₂₅₆₋₂₇₃ after small-scale expression. Solubility was ascertained by SDS-PAGE (10% gel) stained with Coomassie blue. M: protein marker (Precision Plus protein standard, unstained, Bio-Rad). Lanes 'TP' and 'SP' represent cell lysate (total protein) after sonication and soluble protein after centrifugation, respectively. The arrow represents the HBc-Pfam₂₅₆₋₂₇₃ band in the TP that corresponds to the estimated molecular mass of ~22 kDa estimated from the protein sequence.

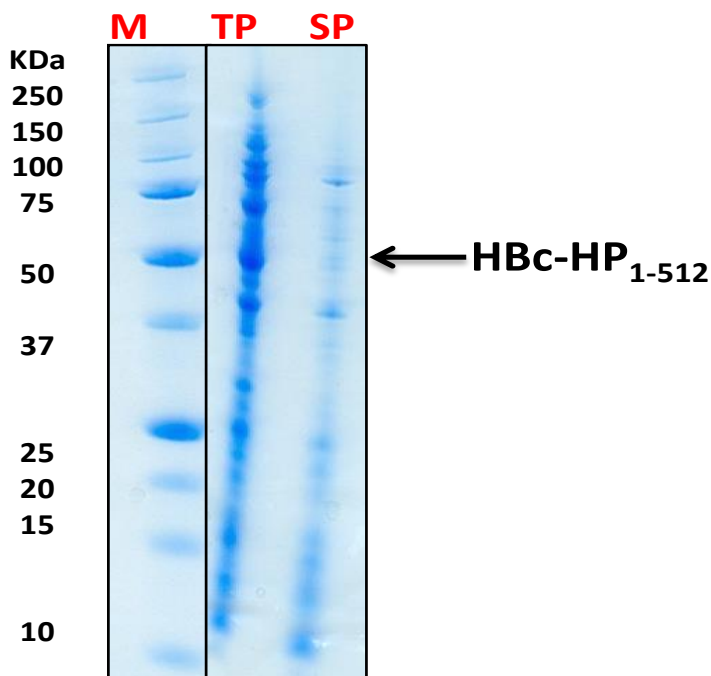


Figure 5.7 SDS-PAGE analysis of HBc-HP₁₋₅₁₂ after small-scale expression. Solubility was ascertained by SDS-PAGE (10% gel) stained with Coomassie blue. M: protein marker (Precision Plus protein standard, unstained, Bio-Rad). Lanes 'TP' and 'SP' represent cell lysate (total protein) after sonication and soluble protein after centrifugation, respectively. The arrow represents the HBc-HP₁₋₅₁₂ band in the TP that corresponds to the estimated molecular mass of ~55.29 kDa estimated from the protein sequence.

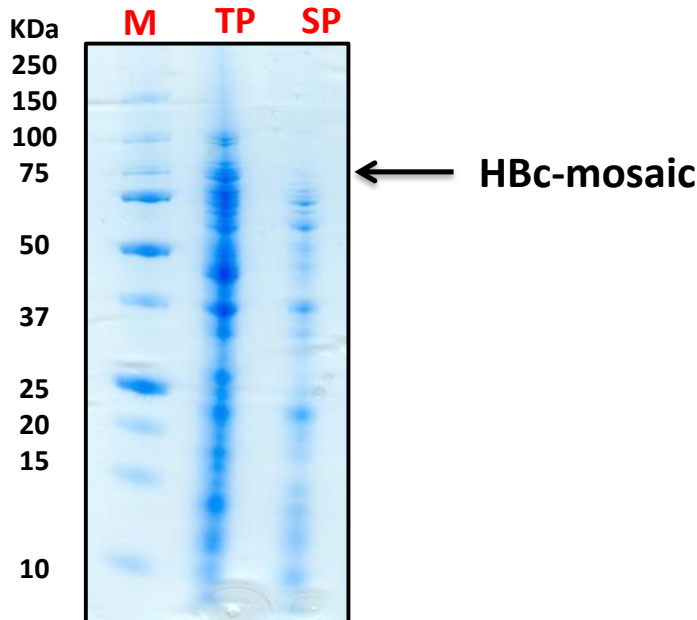


Figure 5.8 SDS-PAGE analysis of HBc-mosaic after small-scale expression. Solubility was ascertained by SDS-PAGE (10% gel) stained with Coomassie blue. M: protein marker (Precision Plus protein standard, unstained, Bio-Rad); TP: total protein (cell lysate) after sonication; SP: soluble protein after centrifugation. The arrow represents the HBc-mosaic band in the TP that corresponds to the estimated molecular mass of ~77.70 kDa estimated from the protein sequence.

5.3.6 Purification of VLP recombinant proteins

The VLP recombinant proteins HBc-H₁₁₂₋₁₂₈ (Fig 5.9 B, Lane 1), HBc-CBD₃₆₋₅₂ (D), HBc-CBD₁₂₄₃₋₁₂₅₉ (F), and HBc-CBD₂₄₁₋₂₅₇ (H), HBc-CLSP₄₃₃₋₄₅₀ (J), HBc-CLSP₁₄₃₋₁₅₈ (L), and HBc-CLSP₃₉₈₋₄₁₆ (N) were successfully purified by Strep-Tag affinity chromatography using the StrepTrap HP. The eluted fractions were then concentrated using a Vivaspin concentrator (MWCO 10.000 kDa). A second round of purification with SEC was performed to produce a homologous population of folded VLPs. Monitoring the SEC chromatogram of the purified VLP recombinant proteins revealed the purity of the proteins, which featured a clear single peak in fractions 7–10 ml (Fig 5.9 A, C, E, G, I, K and M). The SDS-PAGE analyses also revealed a single band, confirming the purity of the protein monomer with an expected molecular mass of ~22 kDa (Fig 5.9 B, D, F, H, J, L and N, Lane 2). However, two defined peaks were observed in the SEC profiles of HBc-CLSP₂₂₂₋₂₃₇ and HBc-CLSP₄₂₄₋₄₄₃ (Fig 5.10 A and C), suggesting that these two VLP recombinant proteins were not assembled properly. The apparent small difference in the molecular mass of the native HBc-Ag and HBc expressing *Trichuris* MHC-II T-cell epitopes is due to the small number of residues inserted in the HBc-Ag. It was also observed that HBc-Ag, HBc-H₁₁₂₋₁₂₈, HBc-CBD₂₄₁₋₂₅₇, HBc-CLSP₁₄₃₋₁₅₈, and HBc-CLSP₃₉₈₋₄₁₆ exhibited adequate expression, with an average yield of 8 mg per 2L culture. However, HBc-CBD₃₆₋₅₂, HBc-CBD₁₂₄₃₋₁₂₅₉, HBc-CLSP₄₃₃₋₄₅₀ and HBc-CLSP₁₄₃₋₁₅₈ had an expression with an average yield of 4 mg per 2L culture, while HBc-CLSP₂₂₂₋₂₃₇ and HBc-CLSP₄₂₄₋₄₄₃ had an expression with an average yield <4 mg per 2L culture.

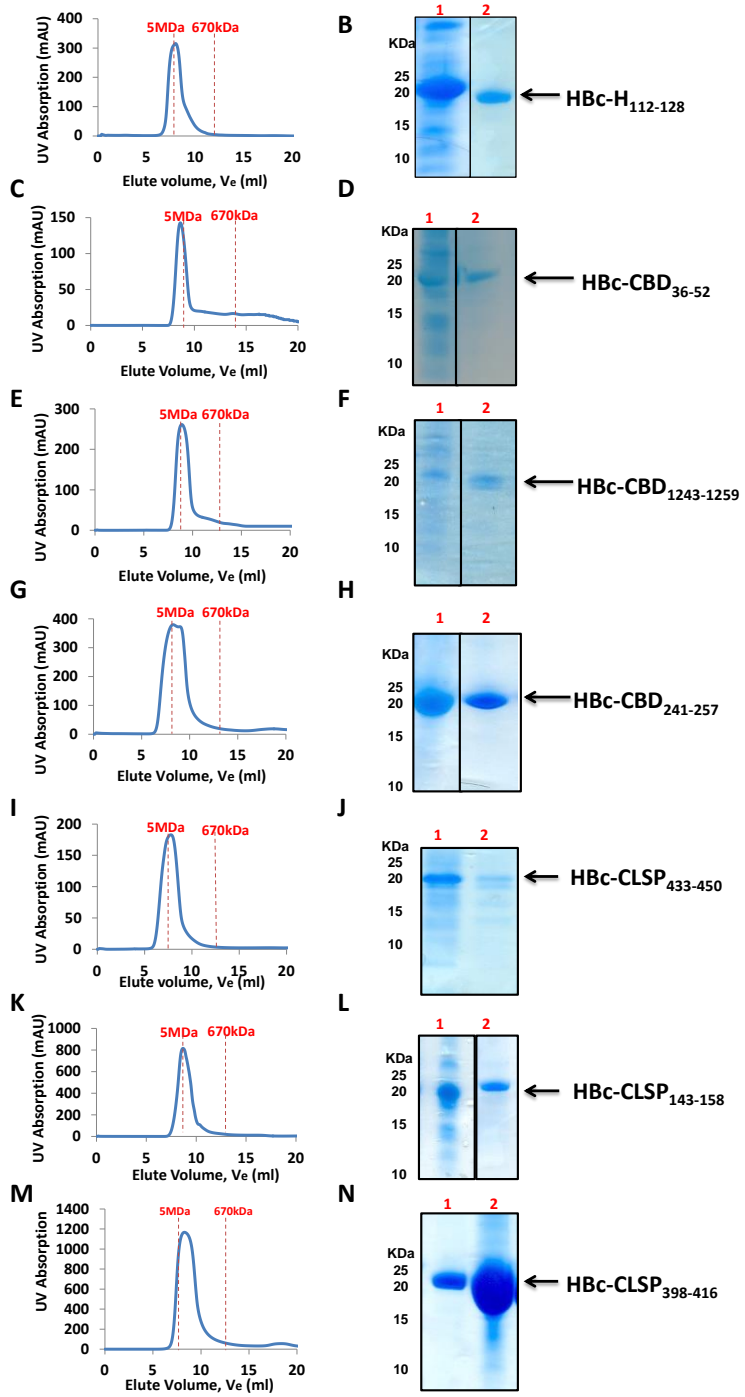


Figure 5.9 The VLP recombinant proteins ($\text{HBc-H}_{112-128}$, HBc-CBD_{36-52} , $\text{HBc-CBD}_{1243-1259}$ and $\text{HBc-CBD}_{241-257}$, $\text{HBc-CLSP}_{433-450}$, $\text{HBc-CLSP}_{143-158}$, and $\text{HBc-CLSP}_{398-416}$) purification profile and SDS-PAGE analysis. Left: Chromatogram of the VLP recombinant proteins purified using SEC. Separation was carried out on a Superose 6, 10/300 GL (GE Healthcare), at a flow rate of 0.2 ml/min. VLP recombinant proteins were eluted in 0.5 ml fraction and a sample of SEC the elution peak was visualised by SDS-PAGE. Vertical red lines indicate the elution volume of mass standards, from left to right: 2MDa, 670kDa. Right: Purification visualised by SDS-PAGE (10% gel) analysis stained with Coomassie blue. M: protein marker (Precision Plus protein standard, unstained, Bio-Rad); Lane 1: VLP recombinant protein after Strep-Tag affinity purification using the StrepTrap HP, and Lane 2: VLP recombinant protein after SEC purification. The arrow represents VLP recombinant protein monomer with an expected molecular mass of ~22 kDa.

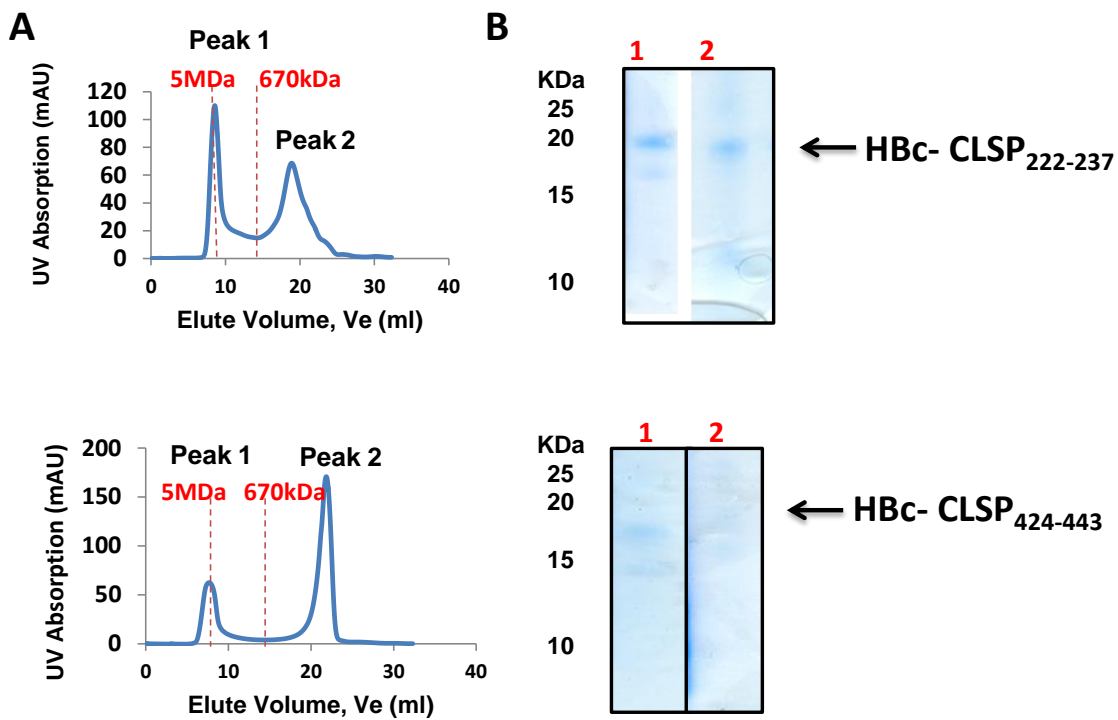


Figure 5.10 The recombinant proteins (HBc-CLSP₂₂₂₋₂₃₇**, and **HBc-CLSP₄₂₄₋₄₄₃**) purification profile and SDS-PAGE analysis.** Left: Chromatogram of the VLP recombinant proteins purified using SEC. Separation was carried out on a Superose 6, 10/300 GL (GE Healthcare), at a flow rate of 0.2 ml/min. VLP recombinant proteins were eluted in 0.5 ml fraction and a sample of the SEC elution peak 1 was visualised by SDS-PAGE. Vertical red lines indicate the elution volume of mass standards, from left to right: 5MDa, 670kDa. Right: Purification visualised by SDS-PAGE (10% gel) stained with Coomassie blue. M: protein marker (Precision Plus protein standard, unstained, Bio-Rad); Lane 1: VLP recombinant protein after Strep-Tag affinity purification using the StrepTrap HP, and Lane 2: VLP recombinant protein after SEC purification. The arrow represents VLP recombinant protein monomer with an expected molecular mass of ~22 kDa.

5.3.7 Endotoxin levels of the purified VLP recombinant proteins

Gram-negative *E. coli* bacteria are a widely preferred prokaryotic expression system for producing vaccines and therapeutic products because of their rapid growth, high efficacy and ease of culture (Kyriakopoulos and Kontoravdi, 2013). However, overexpression of VLPs in *E. coli* introduces an increased risk of lipopolysaccharide (LPS) contamination. LPS, also known as an endotoxin, is the primary element in the outer membranes of gram-negative bacteria. It consists of a hydrophobic domain (lipid A), an oligosaccharide (core) and a polysaccharide (O-antigen) (Liu et al., 1997). When LPS is recognised by TLR4, a strong inflammatory response is induced, which can lead to septic shock (Raetz and Whitfield, 2002; Shimazu et al., 1999). It is therefore, essential to prevent endotoxin contamination when developing a vaccine or drug intended for human use.

VLPs have a large surface area, which increases their susceptibility to LPS contamination and can trap endotoxin within the VLP structure. Therefore, all the procedures and methods used to purify the proteins, such as cleaning the containers and chromatography columns with 1 M NaOH prior to purification and use of two different methods to purify the recombinant proteins, were specifically designed to eliminate endotoxin contamination (Petsch and Anspach, 2000; Reichelt et al., 2006). Furthermore, to purify VLP recombinant proteins with minimal endotoxic activity, *E. coli* (ClearColi

BL21) electrocompetent cells were used in this study (Huang et al., 2017). The ClearColi strain contains seven genetic deletions within the lipid A synthesis pathway and thus lacks all the carbohydrate decorations that are usually attached to LPS to produce a genetically modified LPS (Lipid IVA) (Mamat et al., 2013). The Lipid IVA is sufficient for cell viability but is incapable of interacting with TLR4 receptors and inducing an endotoxic response in humans (Miroux and Walker, 1996; Rosano and Ceccarelli, 2014).

The manufacturer of Lucigen ClearColi cells indicated in the user manual that the standard methods used to measure endotoxin levels, such as the Limulus amebocyte lysate (LAL) assay, were unable to discriminate between the modified (Lipid IVA) and unmodified LPS (Lipid A). <https://www.lucigen.com/faq-clearcoli.htm>. The LAL assay relies on blood cells (amoebocytes) extracted from the horseshoe crab, *Limulus Polyphemus*, to detect endotoxins (Novitsky, 1998). Therefore, LPS contamination was tested using the EndoLISA endotoxin detection assay, which relies on a recombinant bacteriophage protein (Factor C) that is activated upon contact with endotoxins, facilitating reliable quantification of the degree of enzyme activity as a surrogate measurement of LPS activation (Grallert et al., 2011). However, as with the LAL assay, there were no assurances that the EndoLISA would be capable to differentiate between the modified and unmodified LPS (Lipid IVA and Lipid A).

Endotoxin limits are expressed as international endotoxin units (IUs or EU). According to the United States Pharmacopeia (USP) and the United States Food and Drug Administration (FDA), the recommended endotoxin level in recombinant subunits and polysaccharide vaccines is < 20 EU/ml (~3 ng/ml) and < 10 EU/ml (~1.5 ng/ml) for gene vector vaccines (Brito and Singh, 2011). The level of endotoxins in purified VLP recombinant proteins was unacceptably high (~100 ng/ml), as shown in Table 5.2. The fact that specific measures were taken into consideration when purifying the proteins to minimise LPS contamination suggests that the EndoLISA detection assay, like the LAL assay, cannot discriminate between modified and unmodified LPS.

Table 5.2 Endotoxin concentration of the purified VLP recombinant proteins determined by EndoLISA detection assay.

VLP Recombinant Protein	ng/ml
HBc-CBD ₃₆₋₅₂	47.07
HBc-CBD ₁₂₄₃₋₁₂₅₉	56.13
HBc-H ₁₁₂₋₁₂₈	108.9
HBc-CLSP ₄₃₃₋₄₅₀	154.2

5.3.8 Circular dichroism (CD) spectroscopy

Circular dichroism (CD) spectroscopy was used to examine the composition of the secondary structure to verify that the folding of the native VLP (HBc-Ag) and VLPs expressing *Trichuris* MHC-

II T-cell epitopes was correct. Then, the VLP recombinant proteins' CD spectra were analysed using DichroWeb software to estimate the percentages of secondary structures (Whitmore and Wallace, 2009). The native VLP (HBc-Ag) was calculated to be composed of 33% α -helices, 11% β -strands, 22% turns and 32% disordered structures (Figure 5.11 A). Similar values were obtained for the HBc-CSLP₃₉₈₋₄₁₆ (Fig 5.11 B), HBc-CBD₂₄₁₋₂₅₇ (C), HBc-CBD₁₂₄₃₋₁₂₅₉ (D), HBc-CLSP₁₄₃₋₁₅₈ (E) and HBc-H₁₁₂₋₁₂₈ (F). However, there was a notable difference in the composition of the secondary structure of HBc-CBD₃₆₋₅₂ (Fig 5.11 G). The differences in the secondary structures of the native VLP (HBc-Ag), H₁₁₂₋₁₂₈ and HBc-CBD₃₆₋₅₂ were probably caused by aggregation.

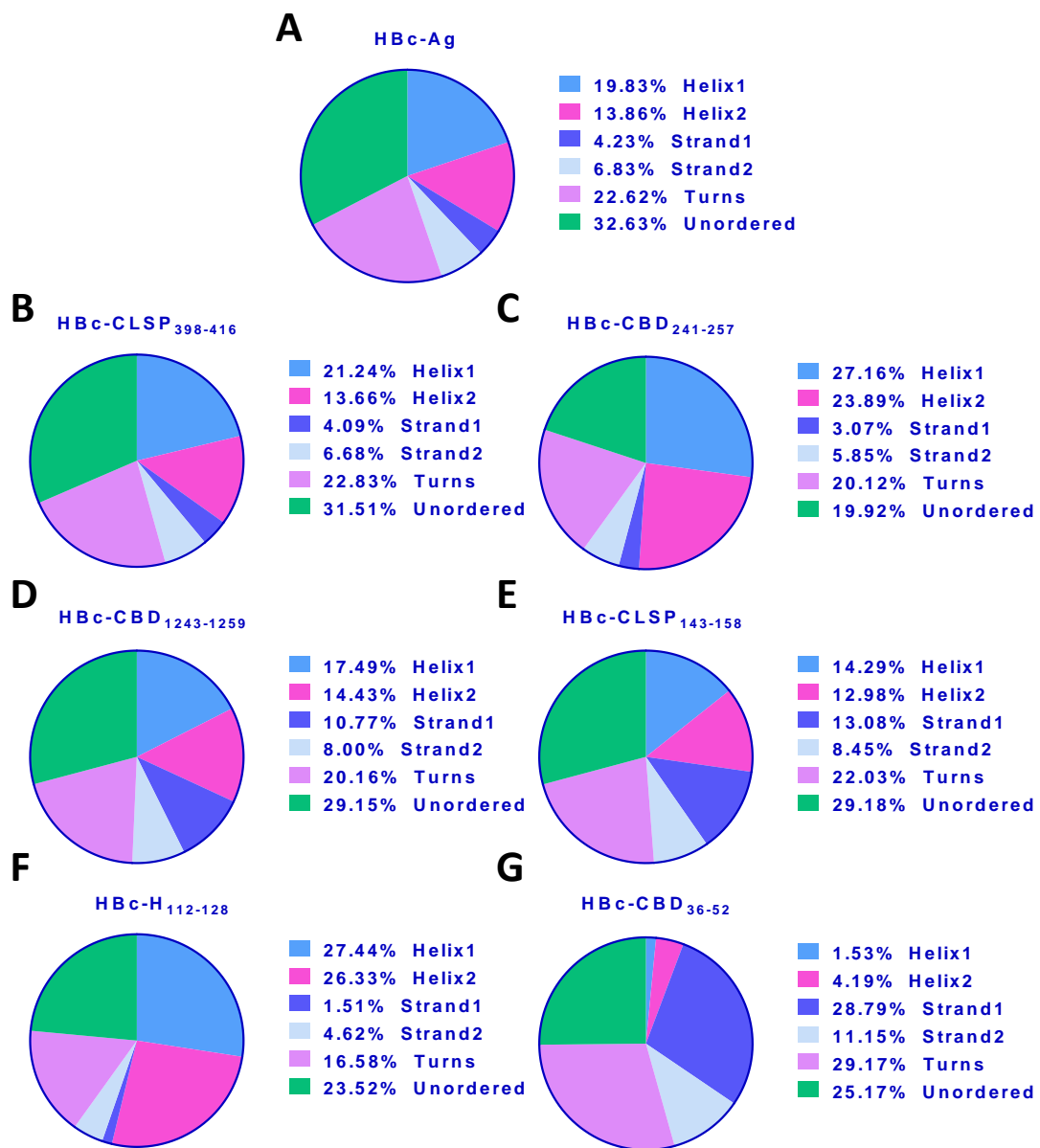
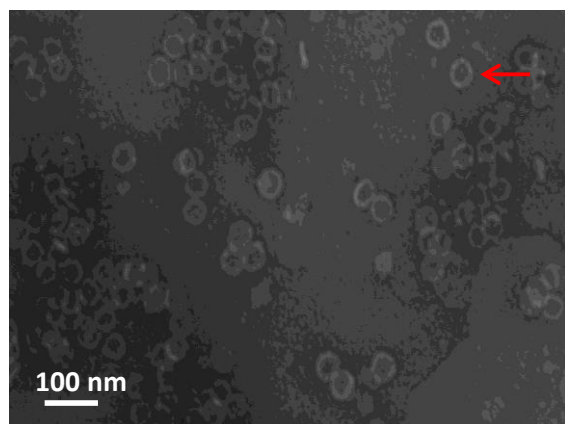


Figure 5.11 The secondary structure composition of the native VLP (HBc-Ag) and VLPs expressing *Trichuris* MHC-II T-cell epitopes. Circular dichroism (CD) spectroscopy was used to examine the secondary structure composition of the native VLP (HBc-Ag) (A) and VLPs expressing *Trichuris* T-cell epitopes HBc-CSLP₃₉₈₋₄₁₆ (B), HBc-CBD₂₄₁₋₂₅₇ (C), HBc-CBD₁₂₄₃₋₁₂₅₉ (D), HBc-CLSP₁₄₃₋₁₅₈ (E) HBc-H₁₁₂₋₁₂₈ (F) and HBc-CBD₃₆₋₅₂ (G) at 0.5 mg/ml. The secondary structure composition calculated using DichroWeb software and plotted using GraphPad software (Whitmore and Wallace, 2009).

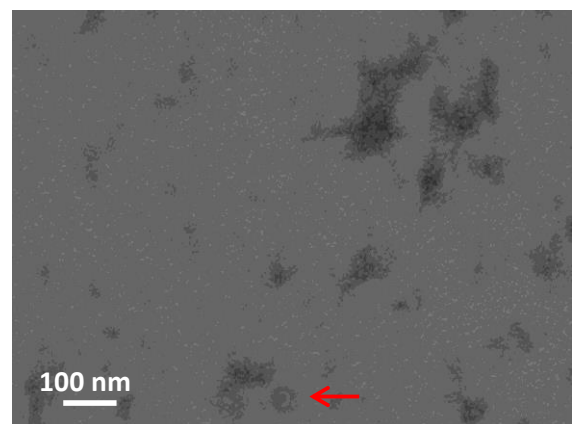
5.3.9 Characterisation of VLP recombinant protein assembly by TEM

The self-assembly of the purified VLP recombinant proteins was verified by TEM with negative staining. Within the resolution limits of TEM, native VLP (HBc-Ag) particles appeared to be uniform and spherical at diameters around 30 nm (Figure 5.12 A). In contrast to the native VLP, HBc-Ag expressing *Trichuris* MHC-II T-cell epitopes appeared to be heterogeneous (Figure 5.12 C–F). In addition, HBc-H₁₁₂₋₁₂₈ was aggregated (Figure 5.12 B). Table 5.3 summarises the VLP recombinant proteins expression trials.

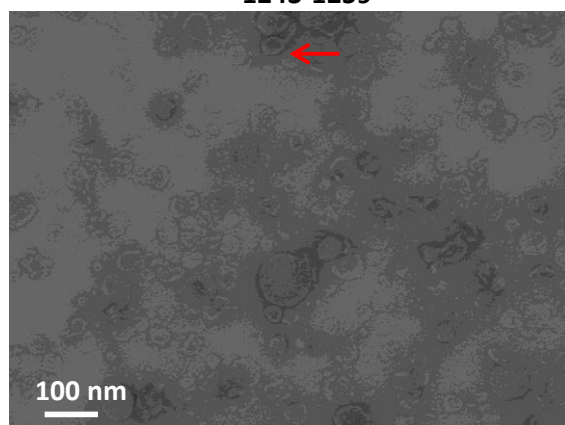
A: HBc-Ag VLP



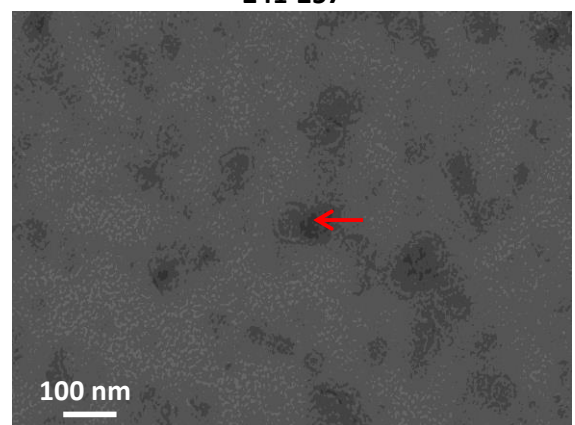
B: HBc-H₁₁₂₋₁₂₈



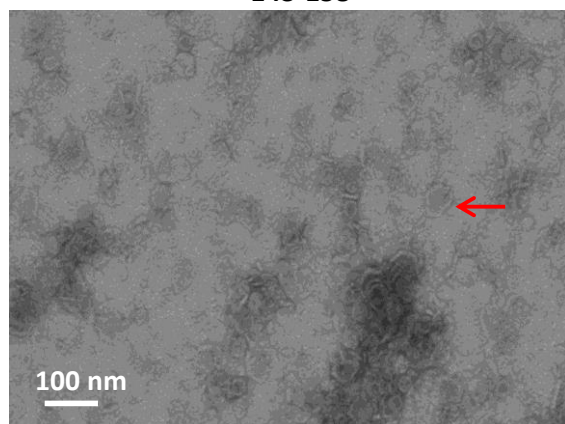
C: HBc-CBD₁₂₄₃₋₁₂₅₉



D: HBc-CBD₂₄₁₋₂₅₇



E: HBc-CLSP₁₄₃₋₁₅₈



F: HBc-CLSP₃₉₈₋₄₁₆

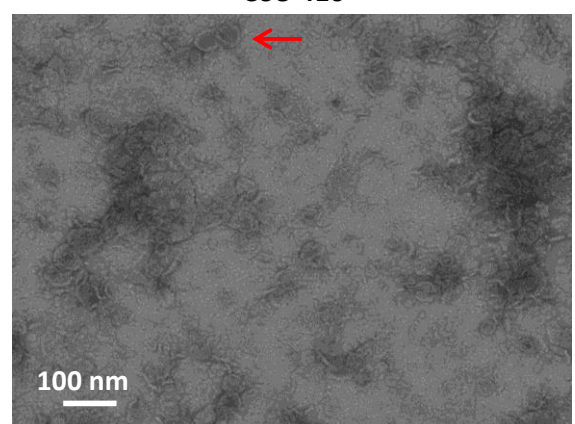


Figure 5.12 Electron microscopy of negatively stained VLP recombinant proteins. Purified VLPs at 0.5 mg/ml were negatively stained with 0.5% aqueous uranyl acetate and visualised by transmission electron microscopy. Bar=100 nm. The red arrow indicates an exemplar of the assembled spherical VLP recombinant particle.

Table 5.3 Summary of the VLP recombinant protein properties.

VLP recombinant protein name	Confirmed expression in <i>E. coli</i>	Average yield (mg) in 2L culture	EM analysis	Similar secondary structure composition to the native HBc-Ag
VLP (HBc-Ag)	Soluble	6	Uniform spherical particles	Folded
HBc-HP₁₋₅₁₂	insoluble	ND	ND	ND
HBc-mosaic	insoluble	ND	ND	ND
HBc-Pfam 256-273	insoluble	ND	ND	ND
HBc-H₁₁₂₋₁₂₈	Soluble	6	Aggregates	Yes
HBc-CLSP₄₃₃₋₄₅₀	Soluble	4	ND	ND
HBc-CLSP₂₂₂₋₂₃₇	Soluble	≤4	ND	ND
HBc-CLSP₁₄₃₋₁₅₈	Soluble	4	Heterogeneous particles	Yes
HBc-CLSP₄₂₄₋₄₄₃	Soluble	≤4	ND	ND
HBc-CLSP₃₉₈₋₄₁₆	Soluble	6	Heterogeneous particles	Yes
HBc-CBD₃₆₋₅₂	Soluble	4	ND	Notable difference in the composition of the secondary structure
HBc-CBD₁₂₄₃₋₁₂₅₉	Soluble	4	Heterogeneous particles	Yes
HBc-CBD₂₄₁₋₂₅₇	Soluble	6	Heterogeneous particles	Yes

ND: Not done.

5.4 Discussion

HBc-Ag was the first identified VLP carrier, and it remains one of the most flexible and promising VLP-based vaccine delivery systems for use in humans (Pumpens and Grens, 2001). HBc-Ag has several key features that make it suitable for vaccine delivery, such as its non-replicating, non-infective and self-assembled nature; the high efficiency with which foreign epitopes can be inserted; and its ability to induce a strong immune response without the need for an adjuvant (Pumpens and Grens, 1999; Qiao et al., 2016; Roose et al., 2013).

5.4.1 Selection of *E. coli* for expressing VLP recombinant proteins.

Major factors affecting VLP formulation are the safety and cost of the expression system to be scaled up for vaccine production (Kushnir et al., 2012). HBc-Ag VLP, as a vaccine carrier, has high levels of expression in several prokaryotic and eukaryotic expression systems, including bacteria (Bian et al., 2006; Wang et al., 2016; Zhang et al., 2007), yeast (Li et al., 2007; Rolland et al., 2001), insect (Brandenburg et al., 2005), and plant expression systems (Makarkov et al., 2019).

All the VLP recombinant proteins were expressed in *E. coli* because it is the most common expression system for industrial production due to its ease of use, cost-effectiveness and high level of expression of recombinant proteins compared to yeast and insect cells (Choi et al., 2006; Huang et al., 2017; Middelberg et al., 2011). However, there is a high risk of LPS or endotoxin contamination in the purified proteins (Grgacic and Anderson, 2006; Kushnir et al., 2012). Nevertheless, several recombinant proteins obtained from *E. coli* have been approved by the FDA and are widely used in therapy and vaccines. One example is the first recombinant human insulin (Humulin-US/Humuline-EU) to be used for treating diabetes (Altman, 1982) and the first VLP-based vaccine against hepatitis E virus (HEV) to be licensed in China (Wedemeyer and Pischke, 2011). In addition, two VLP-based vaccines against human papillomavirus (HPV), the causative agent of cervical cancer, are undergoing clinical trials (Wu et al., 2015). The level of endotoxin in the purified VLPs was unacceptably high; however, the method used to measure the LPS failed to differentiate between the modified and unmodified LPS. Future work may include quantifying LPS in the purified proteins using a more reliable assay such as the HEK-Blue™ hTLR4 cells detection assay (Govers et al., 2016).

Despite the success of the bacterial expression system in VLP production for many vaccines, it should be noted that yeast expression systems are effective alternatives that overcome the problem of endotoxin contamination during vaccine preparation. For example, the current HBV vaccine used in the US is composed of a hepatitis B surface antigen (HBsAg) VLP expressed on *Saccharomyces cerevisiae* yeast (McAlear et al., 1984). However, the expression of VLPs in yeast has several limitations compared to expression in bacteria (Freivalds et al., 2006; Zeltins, 2013). For instance, the VLP yield in yeast expression system is less than that in *E. coli*, and the yeast system is more suitable for production of non-enveloped VLPs than enveloped VLPs (Zeltins, 2013). A mammalian expression system has also been effectively utilised for VLP vaccine production, but it is not commonly used (Noad and Roy, 2003).

5.4.2 Insertion capacity and solubility of the native VLP (HBc-Ag)

A VLP's solubility and ability to assemble is highly dependent on its type, the site of insertion and the characteristics of the inserted peptides, such as their size, isoelectric point and hydrophobicity (Hill et al., 2018). Insertion of short peptides by genetic fusion into a VLP is often easier than insertion of larger antigens, and it usually does not interfere with VLP assembly. However, insertion of large proteins or mosaics (i.e. multiple epitopes) into one VLP carrier is more challenging (Pumpens and Grens, 2001). To overcome this problem, chemical conjugation, whereby VLPs and target antigens are expressed separately and brought together by means of chemical cross-linking to allow for more precise surface decoration of VLPs with large foreign antigens (Fogarty and Swartz, 2018; Patel and Swartz, 2011; Vogel and Bachmann, 2019). Chemical conjugation is primarily based on the modification of free amino group residues, such as lysine (Lys), carboxylic groups, sulfhydryl groups or hydroxyl groups, on the surface of VLPs using commercially available bifunctional cross-linker reagents (Mohsen et al., 2017b).

Previous studies have demonstrated the capacity of native VLP (HBc-Ag) to accommodate a whole protein by chemical coupling or genetic engineering (Akhras et al., 2017; Hill et al., 2018; Howarth and Brune, 2018; Peacey et al., 2007; Qi et al., 2015). In addition to the ability to insert a large target antigen at one site, a study of the MalariaVax vaccine demonstrated that, as carriers, HBc-Ag VLPs have the capacity to accommodate different foreign epitopes at different sites and elicit specific immunological responses to them (Gregson et al., 2008). HBc-HP₁₋₅₁₂ and the HBc-mosaic construct were insoluble when expressed in *E. coli*, and therefore, they were not further purified by SEC. Future work may include chemical coupling to solve this problem or use a different expression system to attempt expression of large proteins.

5.4.3 Assessing VLP recombinant proteins' structure, stability and assembly

It is well-established that VLP-based vaccines are often safer and more effective than conventional vaccines (Roldao et al., 2010). However, the VLPs must be correctly folded to induce a strong and long-lasting immune response (Frietze et al., 2016). Also, the native conformation of the fused foreign antigen within the native VLP should be maintained during vaccine formation, storage and administration to ensure a successful vaccine product (Josefsberg and Buckland, 2012). Therefore, identification of the physicochemical properties of the VLP in the early stages of vaccine formulation is essential to hasten identification of stable VLP antigen candidates (Cox and Onraedt, 2012; Jain et al., 2015; Volkin and Middaugh, 2010).

It is also important to assessing long-term stability while designing vaccines to overcome chemical and physical stresses that occur during and after development, such as changes in temperature and storage conditions (Brandau et al., 2003; Schumacher et al., 2018; Volkin and Middaugh, 2010). However, the thermal stability of the purified constructs was not addressed in this study because it is well-known that the complete icosahedral structure of the native VLP (HBc-Ag) is surprisingly stable and can withstand temperatures up to 80°C (Lee and Tan, 2008; Lu et al., 2015; Nath et al., 1992; Schumacher et al., 2018). For example, Li et al. (2018) investigated the use of the thermal stability of HBc particles to remove host cell proteins by heat treatment. They found

that the HBc particles were stable at 80°C for 30 min based on CD spectra, fluorescence spectra, EM, multi-angle laser light scattering and dynamic light scattering (Li et al., 2018). Although the thermal stability of the purified constructs was not considered, similar constructs that were designed and purified in our group were assessed using the ThermoFluor assay and proved to be highly stable (data not published) (Aston-Deaville, 2017).

Assessing the correct assembly of the VLP is critical to prevent the formation of protein aggregates that may affect the vaccine's stability, safety and efficacy (Mohr et al., 2013; Moussa et al., 2016). The secondary structure content of purified VLP recombinant proteins was measured by CD spectroscopy, and it was confirmed that inserting *Trichuris* epitopes into the MIR of the HBc-Ag VLP did not change the tertiary structure compared to native HBc-Ag VLP in which no epitopes were inserted.

TEM provided the final visual evidence that the native VLPs (HBc-Ag) perfectly self-assembled into uniform, spherical particles. However, the VLPs (HBc-Ag) expressing *Trichuris* epitopes appeared to have more heterogeneous particle composition than native VLP (HBc-Ag). Future work may include bioprocessing steps such as post-purification disassembly and reassembly treatment to further improve VLPs' homogeneity and stability in order to fulfil manufacturing requirements (Zhao et al., 2012a; Zhao et al., 2013; Zhao et al., 2012b).

Although characterising the structure and assembly of the VLPs is essential for development of vaccine candidates, few prior studies have monitored VLP assembly or reported whether fusing a target antigen to the VLP affects the assembly structure of the native VLP. For example, Milich et al. (2001) developed a V12.PF3.1 malaria vaccine based on HBc-Ag expressing T- and B-cell epitopes in the MIR and C-terminus. The vaccine elicited long-lasting sporozoite-specific antibodies and primed CSP-specific CD4+ T-cells (Milich et al., 2001). However, they did not report the physicochemical properties of VLPs or examine the structural assembly (Milich et al., 2001). Other studies assessed VLPs' assembly using TEM but did not compare the assembly of VLPs expressing foreign antigens to that of native VLPs or assess the physicochemical properties or structural composition of the VLPs (Lee et al., 2017; Lee et al., 2018; Lee et al., 2016). Table 5.4 summarises some examples in which VLP was used as a vaccine delivery system in the literature.

VLPs represent a step forward in vaccine development. However, like any new approach, there are still limitations to overcome related to the production of VLPs expressing foreign antigens and manufacturing processes. However, recent research on these topics is very promising, highlighting the flexibility of VLP-based technology for vaccine and immunotherapy development.

In conclusion, the current chapter focused on the initial development of VLPs (HBc-Ag) expressing *Trichuris* MHC-II T-cell epitopes. These *E. coli*-derived VLPs are expected to be efficacious and economical vaccine candidates to combat *Trichuris* infection.

5.5 Summary

- All the predicted *Trichuris* MHC-II T-cell epitopes identified in Chapter 4 were cloned and expressed in native VLPs (HBc-Ag) using the pET17b vector.

- Only soluble VLP recombinant proteins confirmed by SDS-PAGE analysis were purified with Strep-Tag affinity chromatography and SEC.
- Examination of VLPs by CD and TEM confirmed their structural assembly.
- Only soluble and highly purified HBc-Ag VLPs expressing *Trichuris* MHC-II T-cell epitopes (HBc-H₁₁₂₋₁₂₈, HBc-CBD₃₆₋₅₂, HBc-CBD₁₂₄₃₋₁₂₅₉, HBc-CBD₂₄₁₋₂₅₇, HBc-CLSP₁₄₃₋₁₅₈ and HBc-CLSP₃₉₈₋₄₁₆) will be used for the *in vivo* and *in vitro* assays to confirm antigenicity in the next chapters.

Table 5.4: Summary of biophysical analysis of VLP constructs reported in the literature.

VLP platform	Vaccine antigen	Measure endotoxin level	secondary structure analysis	VLP Assembly	Physicochemical properties	Evaluated <i>in vitro</i> or <i>in vivo</i>	Reference
HBc-Ag	Non	NR	✓	✓	NR	NR	(Suffian et al., 2017)
HBc-Ag	Ovalbumin	✓	NR	✓	✓	✓	(Akhras et al., 2017)
HBc-Ag	Porcine Reproductive and Respiratory Syndrome Virus	✓	NR	✓	NR	NR	(Murthy et al., 2015)
HBc-Ag	Influenza M2 protein (M2e)	NR	NR	NR	NR	✓	(Sun et al., 2015)
HBc-Ag	HBV and HCV Epitopes	NR	NR	✓	✓	✓	(Sominskaya et al., 2010)
HBc-Ag	Heat shock protein 65 (Hsp65)	NR	NR	NR	NR	✓	(Yang et al., 2007)
Influenza matrix protein (M1)	<i>C. sinensis</i> tegumental protein (22.3 kDa)	NR	NR	✓	NR	✓	(Lee et al., 2017)
Influenza matrix protein (M1)	Coronavirus (MERSCoV) spike (S) protein	NR	NR	✓	NR	✓	(Lan et al., 2018)
Dengue virus	Non	NR	NR	✓	NR	✓	(Boigard et al., 2018)
Bovine parvovirus	Foot-and-mouth virus conserved neutralizing epitope 8E8	NR	✓	✓	NR	✓	(Chang et al., 2018)

✓ Reported. NR: Not reported.

Chapter Six

In vitro evaluation of VLPs activating Antigen-Presenting Cells

6.1 Introduction

An ideal vaccine has to be highly immunogenic to promote the activation and orchestration of a specific immune response to produce protection against the target pathogen (Singha et al., 2018). However, one of the most challenging aspects of vaccine development is assessing the immunogenicity of new vaccine candidates.

The use of hepatitis B virus core antigen HBc-Ag (VLP) as a carrier of foreign epitopes has been well established as one of the most flexible and promising platforms in the construction of novel vaccines over the past several decades (Pumpens and Grens, 2001). As an antigen carrier, HBc-Ag derived VLP, either as a native VLP without an insert or with the fusion antigen, has unique immunologic features that distinguish it from other vaccine delivery systems. These features include the ability to (a) promote the uptake of antigens by different antigen-presenting cells (APCs) to activate T-helper and cytotoxic T-lymphocyte responses to foreign epitopes without the need for an adjuvant, (b) stimulate the innate immune response through toll-like receptors (TLRs) and other pattern-recognition receptors (PRRs), and (c) drive the production of potent, long-lasting antibodies via its dual role as a T-cell-dependent and independent antigen (Roose et al., 2013; Whitacre et al., 2009).

The self-adjuvanting effects of the highly immunogenic capsid shell of HBc-Ag (VLP) are inherent in their small size and surface geometry (Gamvrellis et al., 2004; Manolova et al., 2008; Vogel and Bachmann, 2019). These characteristics facilitate free entry into lymphatic vessels and direct drainage into local lymph nodes. Once in the lymph node, adaptive immune responses are induced. VLPs are preferentially taken up by lymph node-resident dendritic cells and macrophages, the two main APCs (Cubas et al., 2009; Gomes et al., 2017b; Manolova et al., 2008; Shirbaghaee and Bolhassani, 2016). Other studies have also suggested that the strong antibody immune response to HBc-Ag (VLP) is due to B-cells preferentially functioning as the primary APC rather than non-B cell professional APCs (dendritic cells or macrophages). Uptake is followed by antigen processing, MHC-I and MHC-II cross-presentation, and APC activation and maturation through the upregulation of costimulatory molecules and cytokine production, as well as the stimulation of a T-cell immune response (Cubas et al., 2009; Gomes et al., 2017b; Manolova et al., 2008; Shirbaghaee and Bolhassani, 2016).

In particular, the ability of HBc-Ag VLPs to target APCs is a critical advantage of VLP-based vaccines. Targeting APCs is now understood to represent potentially the most effective strategy of inducing strong humoral and cellular immune responses and immunological memory in vaccine development (Hill et al., 2018; Itano and Jenkins, 2003; Itano et al., 2003; McCullough and Sharma, 2017).

6.2 Aim and objectives

In an attempt to clarify our understanding of the interactions between VLPs and APCs, the overall aim of this chapter was to determine the ability of mouse bone marrow-derived dendritic cells (BMDCs) and mouse bone marrow-derived macrophages (BMDMs) to function as primary APCs for the native VLP (HBc-Ag) and for VLP expressing *Trichuris* MHC-II T-cell epitopes. This aim was addressed via four objectives:

- To address whether the native VLP (HBc-Ag) and VLP expressing *Trichuris* MHC-II T-cell epitope can activate APCs, BMDCs were stimulated with native VLP (HBc-Ag), VLP + T-cell epitopes (HBc-H₁₁₂₋₁₂₈, HBc-CBD₁₂₄₃₋₁₂₅₉, HBc-CBD₂₄₁₋₂₅₇, HBc-CLSP₁₄₃₋₁₅₈, and HBc-CLSP₃₉₈₋₄₁₆), ES or LPS for 24 hours. The cell surface markers, CD80, CD86, CD40, and MHC-II (I-a/I-b) were analysed using flow cytometry.
- To address the quality of immune responses to VLPs, BMDCs and BMDMs were stimulated with native VLP (HBc-Ag), VLP + T-cell epitopes (HBc-H₁₁₂₋₁₂₈, HBc-CBD₁₂₄₃₋₁₂₅₉, HBc-CBD₂₄₁₋₂₅₇, HBc-CLSP₁₄₃₋₁₅₈, and HBc-CLSP₃₉₈₋₄₁₆), ES or LPS for 24 hours. Supernatants were collected from stimulated BMDCs and BMDMs to measure the secretion of inflammatory cytokines using cytometric bead array (CBA).
- To address whether a native VLP (HBc-Ag) and VLP expressing *Trichuris* MHC-II T-cell epitope (HBc-H₁₁₂₋₁₂₈, HBc-CBD₂₄₁₋₂₅₇, and HBc-CLSP₃₉₈₋₄₁₆) are taken up by BMDCs, VLPs were labelled with fluorescein dye, and the fluorescent intensity was measured and compared to that of fluorescein-labelled bovine serum albumin (BSA) stimulated cells using flow cytometry.
- To confirm the internalisation and co-localization of fluorescein-conjugated VLPs (HBc-Ag, HBc-H₁₁₂₋₁₂₈, HBc-CBD₂₄₁₋₂₅₇, and HBc-CLSP₃₉₈₋₄₁₆) inside the APCs, BMDCs, and BMDMs were stained with LysoTracker dye, and intracellular lysosomal co-localization was assessed using Amnis ImageStreamX.

6.3 Results

6.3.1 Activation of BMDCs by VLPs

It is now well-known that cellular mediated immunity plays a central role in promoting potent immunity and protection. However, a fundamental step to mount an effective immune response to VLPs from naïve T-cells and later, the generation of memory cells is the activation of APCs (Gomes et al., 2017a). The state of activation of dendritic cells, in particular, is critical for priming potent T-cell responses. Activated dendritic cells (DCs) are generally characterised by up-regulation of cell surface costimulatory molecules (such as CD80 and CD86, MHC class I and II), and cytokine production (Banchereau et al., 2000). To assess whether the VLPs can activate the DCs APCs *in vitro*, were generated from murine bone marrow cells by incubation with 20 ng/ml of GM-CSF for 8 days. BMDCs on day 8 were stimulated with 10 µg/ml native VLP (HBc-Ag), VLP expressing *Trichuris* MHC-II T-cell epitope (HBc-H₁₁₂₋₁₂₈, HBc-CBD₁₂₄₃₋₁₂₅₉, HBc-CBD₂₄₁₋₂₅₇, HBc-CLSP₁₄₃₋₁₅₈, and HBc-CLSP₃₉₈₋₄₁₆) for 24 hours. It is known that *T. muris* ES and LPS activate BMDCs (D'elia and Else, 2009; Pooley et al., 2001); therefore, they were used as positive controls. As a negative control, BMDCs were left unstimulated.

BMDCs were then subsequently stained for DC surface markers (CD11b⁺, CD11c⁺, and F4/80⁻) prior to FACS analysis. Figure 6.1 represents the gating strategy used to identify the DC population. The DC population was negative for F4/80, excluding the presence of macrophages in the cell population. Single cell suspensions of DCs were gated for the high co-expression (>90%) of CD11b⁺CD11c⁺.

Stimulation of BMDCs with different VLPs, LPS and ES for 24 hours resulted in the activation of the DCs, as demonstrated by the upregulation in expression of co-stimulatory molecules including CD80 (Fig 6.2 A), CD86 (B), CD40 (C), and MHC class II (D) compared to the unstimulated DCs. All the VLPs had similar effectiveness in activating BMDCs *in vitro* and to the same extent as the LPS and ES positive controls. However, unstimulated DCs expressed variable levels of MHC-II across the three experiments (Fig 6.2 D). The high level of variation in expression of MHC-II may be due to the activation during harvesting. Overall, these results demonstrate that VLPs activate BMDCs.

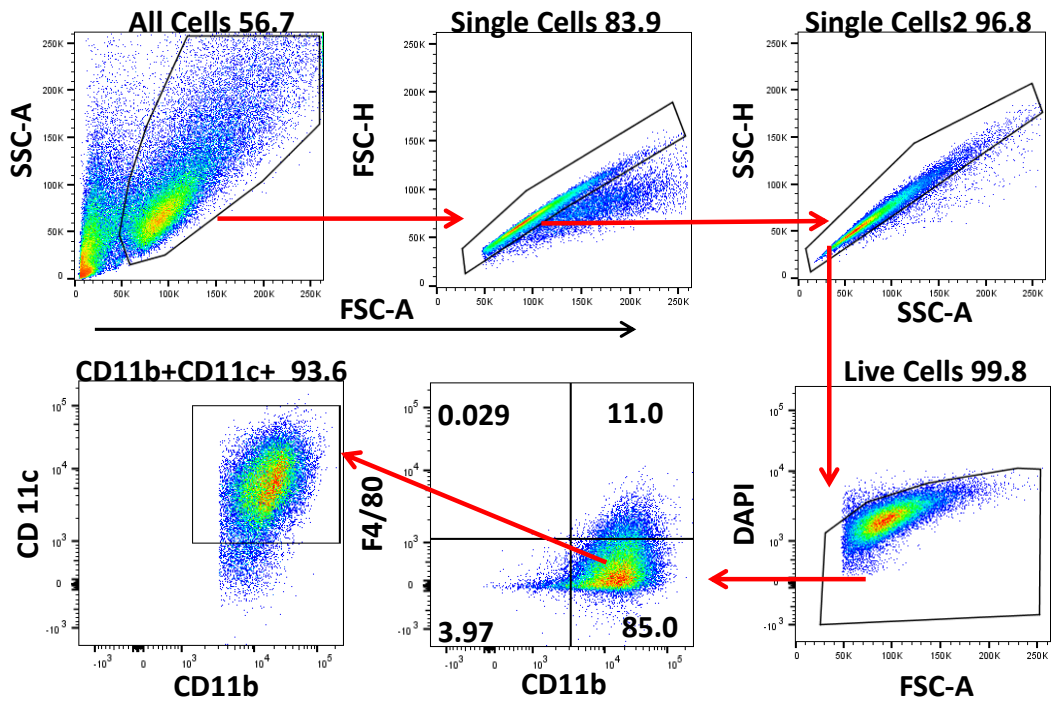


Figure 6.1 Representative gating strategy of mouse bone marrow-derived DCs (BMDCs) analysed by flow cytometry. BMDCs were gated first by size and granularity, doublets excluded, followed by gating on live cells. BMDCs were gated as CD11b+CD11c+ and F4/80-. Gates were set using respective Fluorescence Minus One (FMOs).

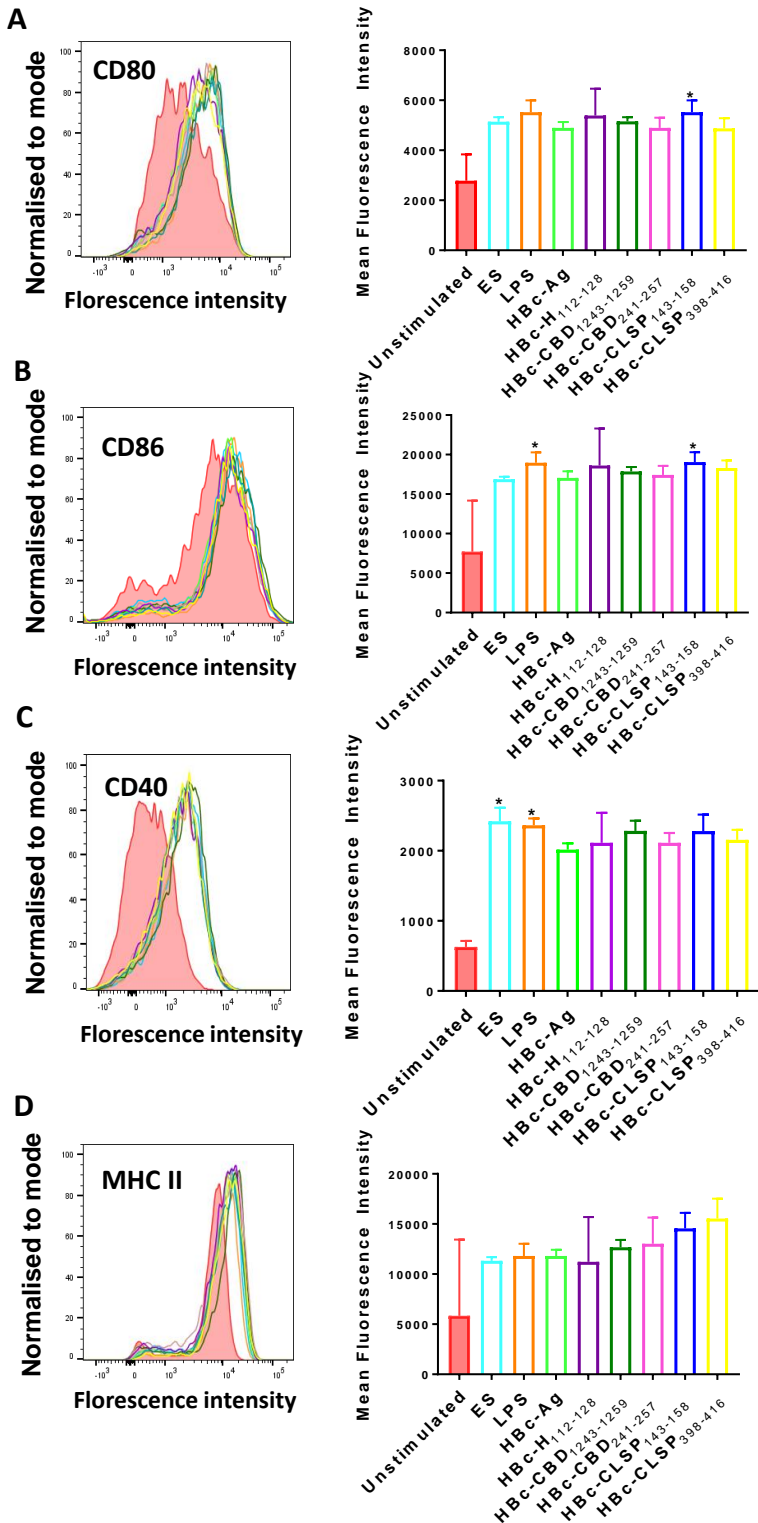


Figure 6.2 Phenotypic activation of BMDCs stimulated with VLPs compared to ES and LPS as positive controls. Day 8 BMDCs were incubated with either 0.1 µg/ml LPS, 50 µg/ml 4hr ES, or with 10 µg/ml VLPs (HBc-Ag, HBc-H₁₁₂₋₁₂₈, HBc-CBD₁₂₄₃₋₁₂₅₉, HBc-CBD₂₄₁₋₂₅₇, HBc-CLSP₁₄₃₋₁₅₈, and HBc-CLSP₃₉₈₋₄₁₆). After 24hrs of culture, mean fluorescent intensity (MFI) of the cell surface expression of (A) CD80, (B) CD86, (C) CD40, and (D) MHC-II (I-a/I-b) was determined by flow cytometry. Background unstimulated BMDCs are shown as a pink line. VLPs, LPS and ES stimulated the expression of high levels of all markers compared to unstimulated BMDCs. The bars represent mean ± SEM. Statistical analyses were carried out using the Kruskal-Wallis test against BMDCs unstimulated negative control. Significant differences are represented by (*P≤0.05) with a line. Chart bars represent the mean fluorescence intensity of BMDC grown from three individual mice from one representative experiment of two separate experiments. Histograms are the results of one representative mouse of two separate experiments.

6.3.2 Inflammatory cytokine production by BMDCs after stimulation with VLPs

As a next step, we focused on the immune responses of BMDCs to VLPs. BMDCs harvested on day 8 of culture with GM-CSF were stimulated at 1×10^6 /ml with 10 µg/ml VLPs (HBc-Ag, HBc-H₁₁₂₋₁₂₈, HBc-CBD₁₂₄₃₋₁₂₅₉, HBc-CBD₂₄₁₋₂₅₇, HBc-CLSP₁₄₃₋₁₅₈ and HBc-CLSP₃₉₈₋₄₁₆), and with 50 µg/ml ES and 0.1 µg/ml LPS as positive controls overnight at 37°C. Cells not exposed to any stimulant were used as a negative control. The concentration of the secreted cytokines (TNF-α, CCL2, IL-27, IL-1β, IL-10, IL-12p70, IL-6, and IL-17) in the culture supernatant of stimulated BMDCs was quantified by CBA.

The results showed that BMDCs stimulated with different VLPs, irrespective of whether they include CD4 T-cell epitopes produced high levels of IL-6 (Fig 6.3 A), TNF-α (B), IL-27 (E), and CCL2 (F). Levels were as high in general as the LPS and ES positive controls stimulants. However, the levels of IL-12p70 (Fig 6.3 C) were not significantly increased in BMDCs in response to VLPs, or LPS stimulation compared to the unstimulated group.

Interestingly, different VLPs induced the release of different levels of IL-10 and IL-27. For instance, BMDCs stimulated with the native VLP (HBc-Ag), HBc-H₁₁₂₋₁₂₈, HBc-CBD₁₂₄₃₋₁₂₅₉, and HBc-CLSP₁₄₃₋₁₅₈ produced high levels of IL-10 compared to the ES and LPS positive controls. In contrast, BMDCs stimulated with HBc-CBD₂₄₁₋₂₅₇ produced the lowest levels of IL-10 compared to the other VLP stimuli, as shown in Figure 6.3 (D). Moreover, BMDCs stimulated with HBc-CLSP₁₄₃₋₁₅₈ induced the release of significantly high levels of IL-27, equivalent to seen after exposure to ES, compared to the other VLP stimuli, as shown in Figure 6.3 (E).

Collectively, these results demonstrate that VLPs nanoparticles efficiently stimulated BMDCs to produce a broad range of pro-inflammatory and anti-inflammatory cytokines with the potential to polarise T-cells.

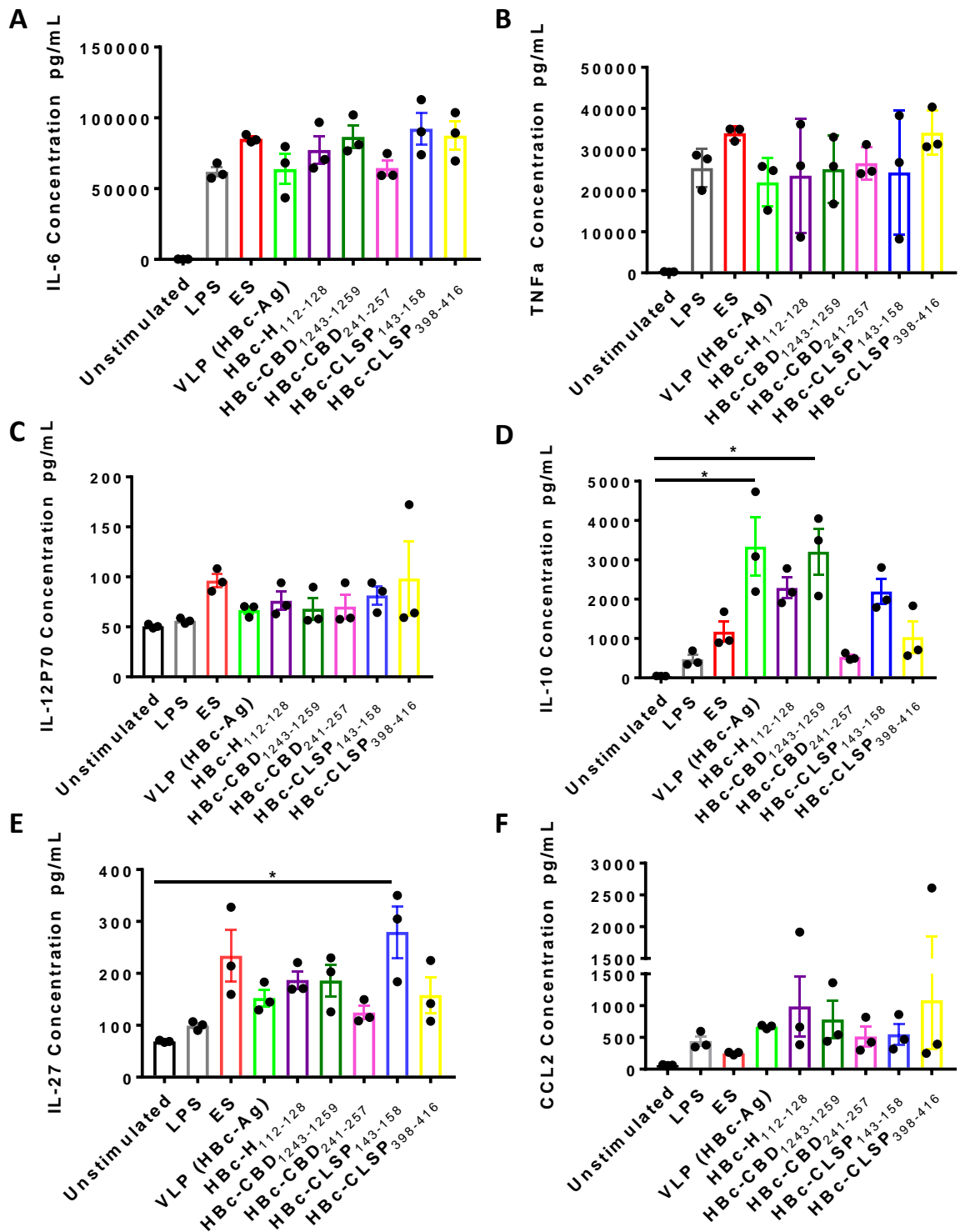


Figure 6.3 Inflammatory cytokines production by mouse bone marrow-derived DCs (BMDCs) in response to VLPs. BMDCs at 1×10^6 /ml were stimulated *in vitro* with 10 μ g/ml VLPs (HBc-Ag, HBc-H₁₁₂₋₁₂₈, HBc-CBD₁₂₄₃₋₁₂₅₉, HBc-CBD₂₄₁₋₂₅₇, HBc-CLSP₁₄₃₋₁₅₈ and HBc-CLSP₃₉₈₋₄₁₆) and with 50 μ g/ml ES and 0.1 μ g/ml LPS as positive controls. Unstimulated BMDCs served as negative controls. Supernatants were harvested after 24 hours for multiple cytokine analyses (A) IL-6, (B) TNF α , (C) IL-17p70, (D) IL-10, (E) IL-27, and (F) CCL2 measured by CBA. The bars represent mean \pm SEM. Statistical analyses were carried out using the Kruskal-Wallis test (multiple comparisons). Significant differences between groups are represented by (* $P \leq 0.05$) with a line. Chart bars represent BMDM grown from three individual mice from one representative experiment of two separate experiments.

6.3.3 Inflammatory cytokine production by BMDMs after stimulation with VLPs

Macrophages play a critical role in defending against various pathogens (Murray and Wynn, 2011). However, they can also regulate wound healing (Eming et al., 2007), and have an anti-inflammatory function (Shouval et al., 2014). To evaluate the macrophages activation upon exposure to various VLPs, BMDMs were generated from murine bone marrow cells and later stimulated with different VLPs.

BMDMs were generated from bone marrow cells by incubation with 0.1 mg/ml M-CSF for 8 days and were then subsequently stained for co-expression of cell surface markers, CD11b, CD11c, and F4/80 prior to FACS analysis. The BMDMs population were negative for CD11c, excluding the presence of BMDCs in the cell population (Data not shown). Figure 6.4 represents the gating strategy used to identify the macrophage population, revealing that CD11b⁺F4/80⁺ and CD11c⁻ BMDMs represented >90% of cells.

BMDMs on day 8 were stimulated at 1X10⁶/ml with 10 µg/ml VLPs (HBc-Ag, HBc-H₁₁₂₋₁₂₈, HBc-CBD₁₂₄₃₋₁₂₅₉, HBc-CBD₂₄₁₋₂₅₇, HBc-CLSP₁₄₃₋₁₅₈ and HBc-CLSP₃₉₈₋₄₁₆) for 24 hours at 37°C. 50 µg/ml ES and 0.1 µg/ml LPS were used as positive controls, and cells not exposed to any stimulant were used as a negative control. Cell supernatants were then harvested, and the concentration of secreted proinflammatory cytokines and chemokines in the culture supernatant were quantified by CBA.

All the different VLPs activated the BMDMs, inducing the secretion of high levels of MCP-1 (CCL2) (Fig 6.5 A), MIP-1α (CCL3) (B), and RANTES (CCL5) (C) chemokines, as did the LPS and ES compared to the unstimulated BMDMs. Furthermore, stimulation of BMDMs with different VLPs resulted in the induction of high levels of proinflammatory cytokines TNF-α (Fig 6.5 D), and IL-6 (E) and the anti-inflammatory cytokine, IL-10 (G). The levels of cytokines were, in general, higher than macrophages stimulated with ES and LPS controls, but statistical significance was not reached. The most noticeable difference in cytokine production by BMDMs in response to VLPs was for TNF and IL-1β, as shown in Figure 6.5 (D and F). BMDMs stimulated with HBc-CBD₁₂₄₃₋₁₂₅₉, and HBc-CLSP₁₄₃₋₁₅₈ produced consistently significantly high levels of TNF and IL-1β compared to unstimulated BMDMs. In contrast, the levels of IL-12P70, IL-13 and IL-17 were not detected in BMDMs in response to any of the VLPs, ES or LPS (Data not shown).

Collectively, these results demonstrate that the VLPs can stimulate macrophages to produce a broad range of both anti-inflammatory and pro-inflammatory cytokines.

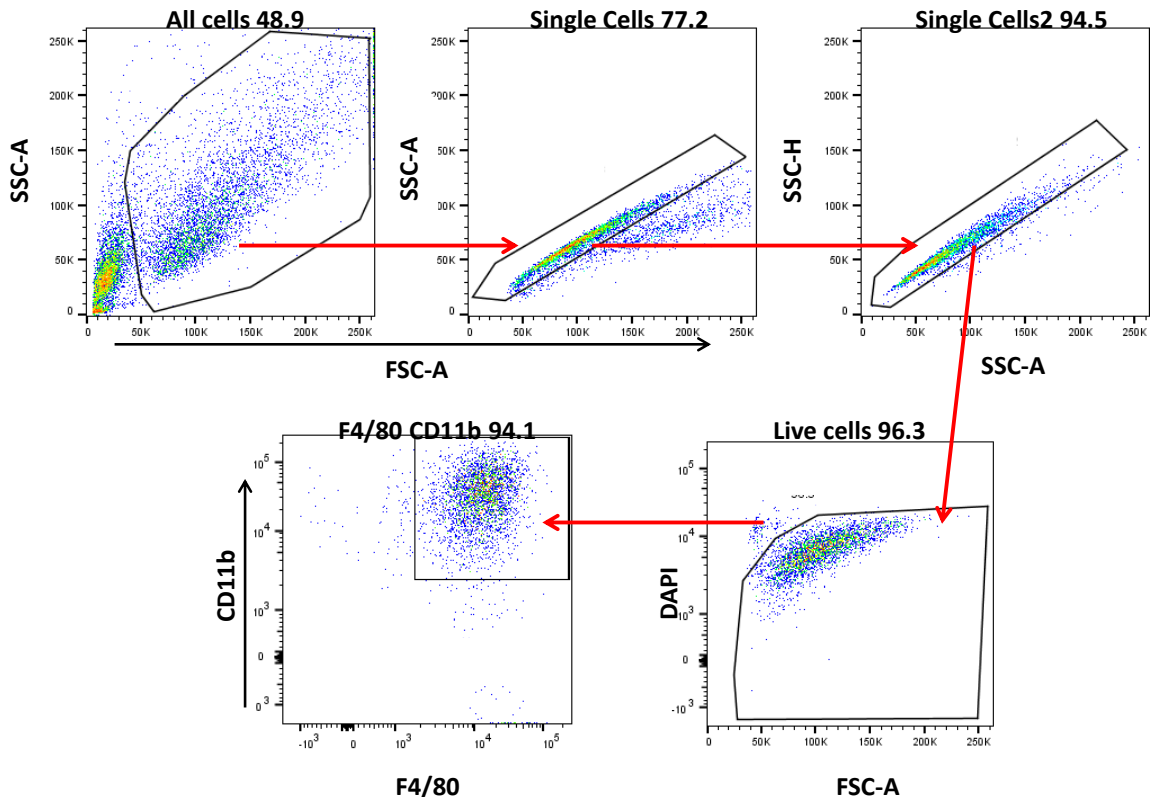


Figure 6.4 Representative gating strategy for mouse bone marrow-derived macrophages (BMDMs) purity. BMDMs analysed by flow cytometry. BMDMs cells were gated first by size to identify single cells followed by gating on live cells. BMDMs gated as F4/80⁺ CD11b⁺. Gates were set using respective Fluorescence minus one (FMOs).

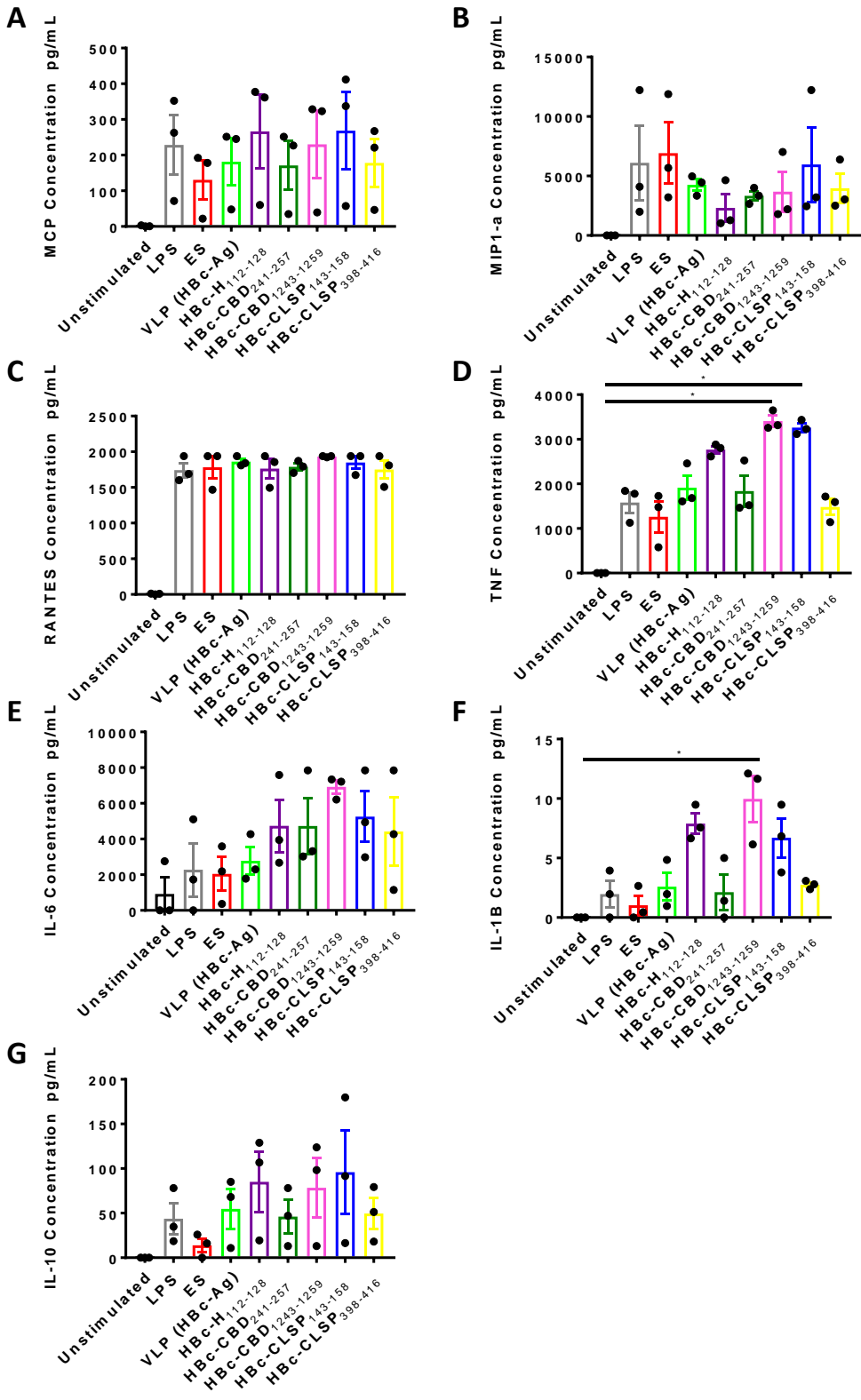


Figure 6.5 Inflammatory cytokines productions by mouse bone marrow-derived macrophages (BMDMs) in response to VLPs. BMDMs at 1×10^6 /ml were stimulated *in vitro* with 10 μ g/ml VLPs (HBc-Ag, HBc-H₁₁₂₋₁₂₈, HBc-CBD₁₂₄₃₋₁₂₅₉, HBc-CBD₂₄₁₋₂₅₇, HBc-CLSP₁₄₃₋₁₅₈ and HBc-CLSP₃₉₈₋₄₁₆) and with 50 μ g/ml ES and 0.1 μ g/ml LPS as positive controls. As a negative control, unstimulated BMDMs were examined. Supernatants were harvested after 24 hours for multiple chemokines and cytokine analyses (MCP-1 (CCL2), MIP (CCL3), RANTES (CCL5), TNF- α , IL-6, IL1 β , and IL-10) measured by LEGENDplex™. The bars represent mean \pm SEM. Statistical analyses were carried out using the Kruskal-Wallis test (multiple comparisons). Significant differences between groups are represented by (*P \leq 0.05) with a line. Chart bars represent BMDMs grown from three individual mice from one representative experiment of two separate experiments.

6.3.4 Uptake of fluorescein-conjugated VLPs by BMDCs

To further investigate whether the VLP can serve as a delivery tool to enhance antigen uptake by APCs, BMDCs were harvested on day 8, and cultured overnight at 37°C with 10 µg/ml fluorescein-conjugated VLPs (HBc-Ag, HBc-H₁₁₂₋₁₂₈, HBc-CLSP₃₉₈₋₄₁₆ and HBc-CBD₂₄₁₋₂₅₇) and with fluorescein-conjugated BSA as a control antigen. Antigen uptake by DCs was then examined by flow cytometry by gating for CD11b⁺CD11c⁺ cells also positive for FITC (Fig 6.6 A).

Figure 6.6 (B) reveals that all the fluorescent-labelled VLPs and control fluorescent-labelled BSA were successfully taken up by a proportion of DCs. However, the percentage of uptake varied between different VLPs, although no differences reached significance. Uptake of native VLP (HBc-Ag) and HBc-CLSP₃₉₈₋₄₁₆ was lower than uptake of BSA, while HBc-H₁₁₂₋₁₂₈ and HBc-CBD₂₄₁₋₂₅₇ were taken up by a higher % of DCs than BSA.

In order to assess whether the activation status of DCs that had taken up VLPs differed from the activation status of the overall DC population, CD86⁺ expression on FITC⁺ DCs was compared to the whole DC population. While around 80% of BMDCs were CD86⁺ (Fig 6.6 C), not all FITC⁺ BMDCs also expressed CD86⁺. Thus, of the BMDCs that took up the FITC labelled VLPs and FITC labelled BSA, only 50%-60% were activated DCs expressing CD86⁺, as shown in Figure 6.6 (D).

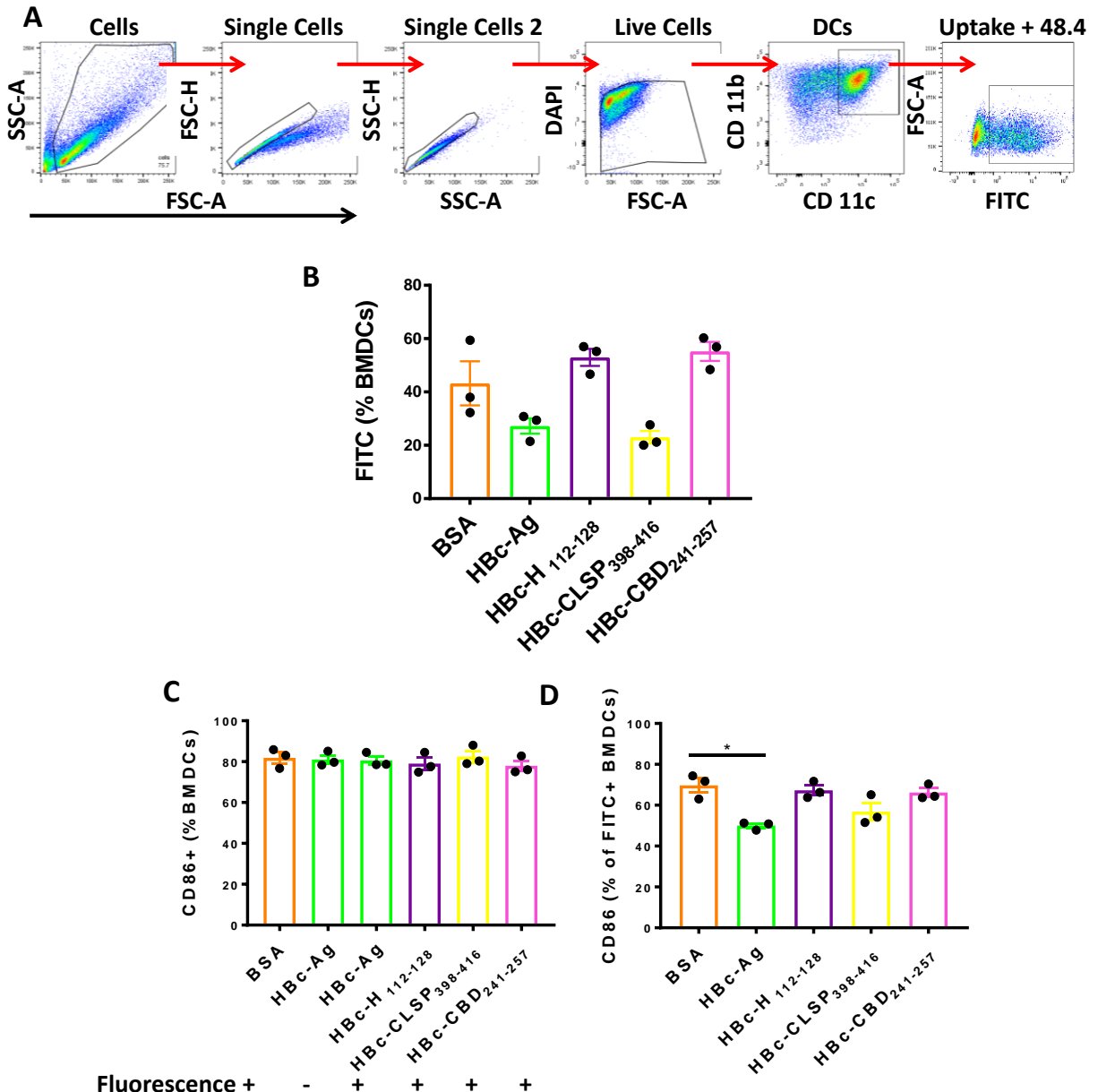


Figure 6.6 Uptake of VLPs by mouse bone marrow-derived DCs (BMDCs) analysed by flow cytometry. BMDCs on day 8 were stimulated with 10 µg/ml (HBC-Ag, HBC-H₁₁₂₋₁₂₈, HBC-CLSP₃₉₈₋₄₁₆ and HBC-CBD₂₄₁₋₂₅₇) and with fluorescein-conjugated BSA as a positive control for 24 hours. Cells were then subsequently stained for flow analysis (A) Representative gating strategy of VLP uptake by BMDCs. DCs were gated first by size and granularity, doublets excluded, followed by gating on live cells. DCs were gated as CD11b⁺CD11c⁺ and F4/80⁻ and VLP uptake by BMDCs was gated as FITC⁺. Gates were set using respective Fluorescence minus one (FMOs). (B) The percentage of uptake of different fluorescein-conjugated VLPs by BMDCs. (C) The percentage BMDCs expressing CD86⁺ stimulated with different VLPs and BSA. (D) The percentage of CD86⁺ BMDCs that took up fluorescein-conjugated VLPs. The bars represent as mean ± SEM. Statistical analyses were carried out using the Kruskal-Wallis test (multiple comparisons). Significant differences are represented by (*P≤0.05) with a line. Chart bars represent BMDC grown from three individual mice from one experiment.

6.3.5 Direct visualisation of VLP association and co-localization in APCs

From the flow-based analysis, it was uncertain whether fluorescein-conjugated VLPs remained exposed on the surface of the BMDCs or were subsequently internalised. Therefore we used Amnis ImageStreamX cytometer to confirm VLPs association and co-localization inside both BMDCs and BMDMs.

To visualise VLP association in DCs, BMDCs at $1 \times 10^6/\text{ml}$ were stimulated with 10 $\mu\text{g/ml}$ fluorescein-conjugated VLPs (HBc-Ag, HBc-H₁₁₂₋₁₂₈, HBc-CBD₂₄₁₋₂₅₇, and HBc-CLSP₃₉₈₋₄₁₆) for 24 hours. Fluorescein-conjugated BSA and fluorescein-conjugated dextran at 10 $\mu\text{g/ml}$ were used as positive controls, and cells not exposed to any stimulant were used as a negative control.

Similarly, to visualise VLP association in macrophages, BMDMs at $1 \times 10^6/\text{ml}$ were stained with Lysotracker to visualise the cellular lysosome compartment and were then subsequently stimulated with 10 $\mu\text{g/ml}$ fluorescein-conjugated VLPs (HBc-Ag, HBc-H₁₁₂₋₁₂₈, and HBc-CLSP₃₉₈₋₄₁₆) for 24 hours. Fluorescein-conjugated dextran at 10 $\mu\text{g/ml}$ was used as a positive control, and cells not exposed to any stimulant were used as a negative control.

The ImageStreamX captured digital images of each cell in 2 channels for the ‘internalisation’ analysis, which include brightfield (BF), and FITC (green) channels. It is necessary here to clarify that the ImageStreamX analysis tool uses the term ‘internalisation’. However, it is not clear at this stage if VLPs were truly internalised or were just exposed on the surface of the APCs. Images of individual cells taken by a merge of the two channels demonstrated that the fluorescein-conjugated VLPs were ‘internalised’ in both BMDCs and BMDMs, as shown in Figure 6.7 (A-D) and Figure 6.8 (A-C) compared to the unstimulated BMDCs (Fig 6.7 G) and unstimulated BMDMs (Fig 6.8 E).

The IDEAS software was then used to quantify the ‘internalisation’ by calculating the internalisation mean absolute deviation (MAD). The ‘Internalisation’ feature calculates the ratio of the intensity inside the cell to the intensity of the entire cell. Cells with a high level of ‘internalisation’ will have positive values while cells with no ‘internalisation’ will have negative values. The values are presented above each representative cell, as shown in Figure 6.7 (A-G) and Figure 6.8 (A-E).

Interestingly, BMDCs and BMDMs stimulated with different fluorescein-conjugated VLPs showed similar ‘internalisation’ MAD value around 1.3, which was higher than the fluorescein-conjugated BSA and fluorescein-conjugated dextran positive controls. In contrast, the unstimulated BMDCs and unstimulated BMDMs yielded a value of 0 indicating that the image pair had no association had taken place, as shown in Figure 6.7 (G) and Figure 6.8 (E).

To further confirm that the VLPs were co-localized within the lysosome of the APCs and not just associated on the cell surface, BMDCs and BMDMs at $1 \times 10^6/\text{ml}$ were stained with LysoTracker dye to stain the lysosomes within the cells. Cells were then subsequently stimulated with 10 $\mu\text{g/ml}$ fluorescein-conjugated VLPs (HBc-Ag, HBc-CBD₂₄₁₋₂₅₇, HBc-CLSP₃₉₈₋₄₁₆ and HBc-H₁₁₂₋₁₂₈) for 24 hours. Fluorescein-conjugated BSA and fluorescein-conjugated dextran at 10 $\mu\text{g/ml}$ were used as positive controls, and cells not exposed to any stimulant were used as a negative control.

The ImageStreamX captured digital images of each cell in 3 channels for the co-localization analysis, which include channels for brightfield (BF), FITC (green), and Lysotracker (red). Images of individual cells taken by a merge of the three channels revealed that the fluorescein-conjugated VLPs, fluorescein-conjugated BSA and fluorescein-conjugated dextran could be found accumulated in the lysosome compartment of the BMDCs (Fig 6.9 A-F) and BMDMs (Fig 6.10 A-D) and not just localised on the cell surface. In contrast, BMDCs (Fig 6.9 G) and BMDMs (Fig 6.10 E) not exposed to any stimulus showed no localisation.

Finally, the similarity feature on the IDEAS software was used to quantify the co-localization of the VLPs inside the APCs. The similarity feature utilises an algorithm developed to quantify the degree of co-localization to two images that are linearly correlated within a masked region. Poorly co-localized events will have similarity bright detail score (SBDS) of 0, and well co-localized events will have SBDS values around 1 (Ploppa et al., 2011). BMDCs and BMDMs stimulated with different fluorescein-conjugated VLPs yielded an SBDS value around 1, indicating that the image pair had a high degree of similarity which was equivalent to the fluorescein-conjugated BSA and fluorescein-conjugated dextran positive controls. In contrast, the SBDS values of the unstimulated BMDCs and the unstimulated BMDMs were 0, indicating that the image pair had no degree of similarity.

Collectively, these results indicate that fluorescein-conjugated VLPs were internalised and well co-localized in the lysosomes of both BMDCs and BMDMs.

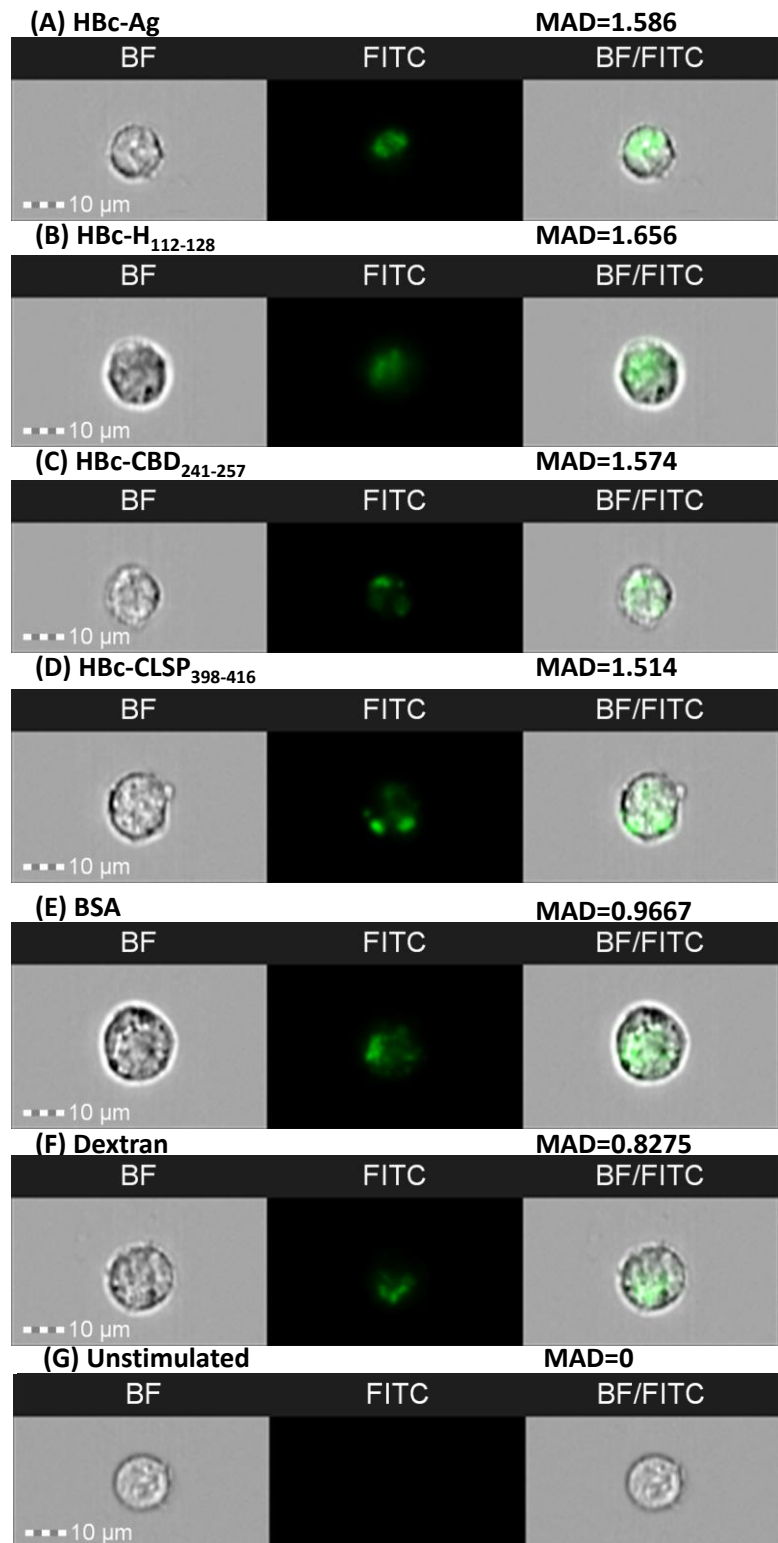


Figure 6.7 Representative images of fluorescein-conjugated VLPs internalisation in the BMDCs. BMDCs at $1 \times 10^6/\text{ml}$ were incubated with $10 \mu\text{g/ml}$ fluorescein-conjugated VLPs; (A) HBc-Ag, (B) HBc-H₁₁₂₋₁₂₈, (C) HBc-CBD₂₄₁₋₂₅₇, and (D) HBc-CLSP₃₉₈₋₄₁₆ for 24 hours. BMDMs were stimulated with $10 \mu\text{g/ml}$ fluorescein-conjugated BSA (E) and with $10 \mu\text{g/ml}$ fluorescein-conjugated dextran (F) as positive controls. As a negative control, unstimulated BMDMs were examined (G). Cell internalisation was determined by Amnis ImageStreamX cytometer compared to unstimulated BMDCs. Images shown, from left to right, show individual Brightfield images (BF) in the white channel, fluorescent-labelled stimulus (FITC) in the green channel and the combination of both BF/FITC merged channels. The internalisation mean absolute deviation (MAD) is included above its images. The positive MAD value represents internalisation, and negative values represent poor internalisation. Scale bars represent $10 \mu\text{m}$.

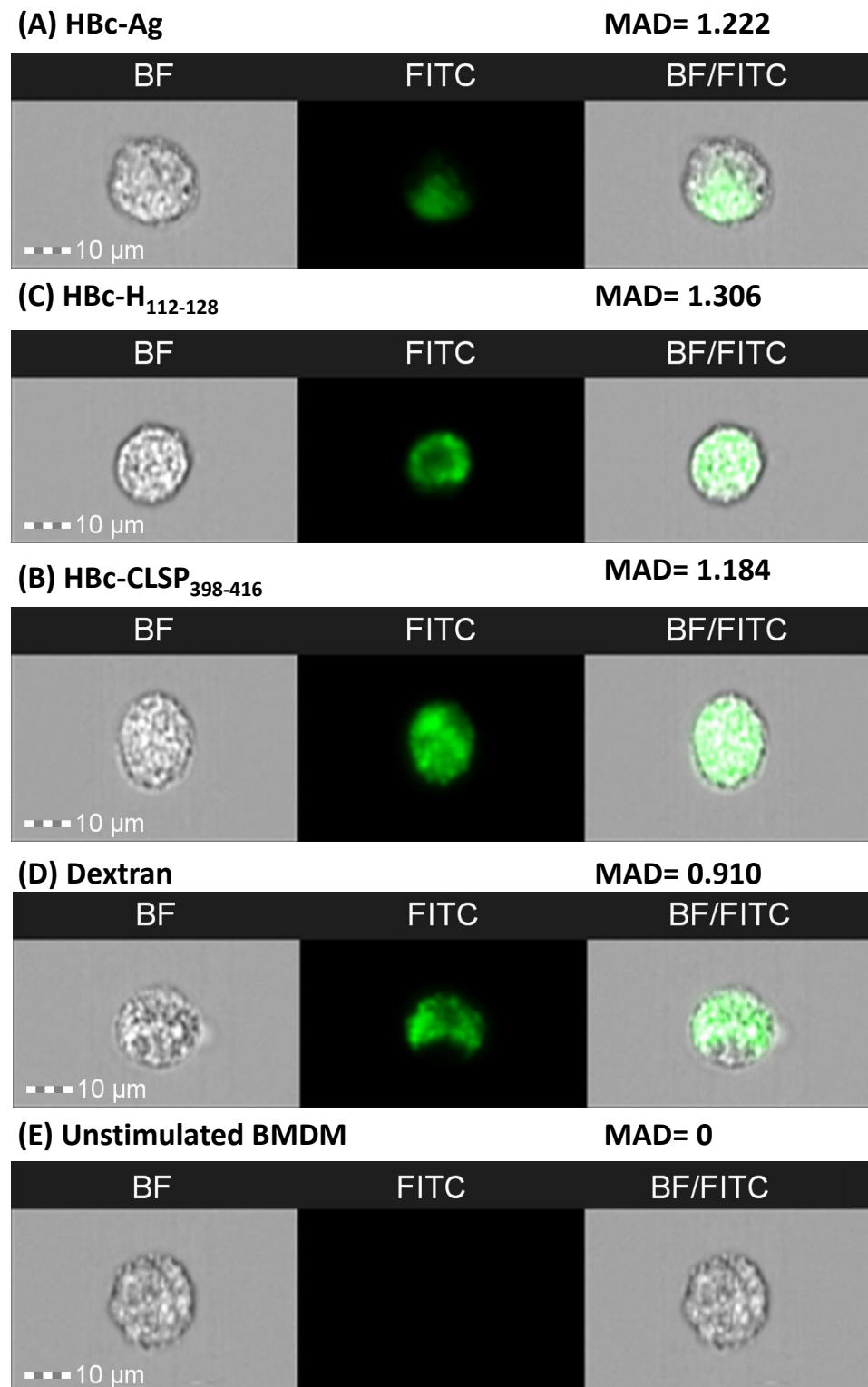


Figure 6.8 Representative images of fluorescein-conjugated VLPs internalisation in the BMDMs. BMDMs at $1 \times 10^6/\text{ml}$ were incubated with $10 \mu\text{g}/\text{ml}$ fluorescein-conjugated VLPs; (A) HBc-Ag, (B), and HBc-H₁₁₂₋₁₂₈, and (C) HBc-CLSP₃₉₈₋₄₁₆ for 24 hours. BMDMs were stimulated with $10 \mu\text{g}/\text{ml}$ fluorescein-conjugated Dextran as a positive control (D). As a negative control, unstimulated BMDMs were examined (E). Cell internalisation was determined by Amnis ImageStreamX cytometer compared to unstimulated BMDCs. Images shown, from left to right, show individual Brightfield images (BF) in the white channel, fluorescent-labelled stimulus (FITC) in the green channel and the combination of both BF/FITC merged channels. The internalisation mean absolute deviation (MAD) is included above its images. The positive MAD value represents internalisation, and negative values represent poor internalisation. Scale bars represent 10 µm.

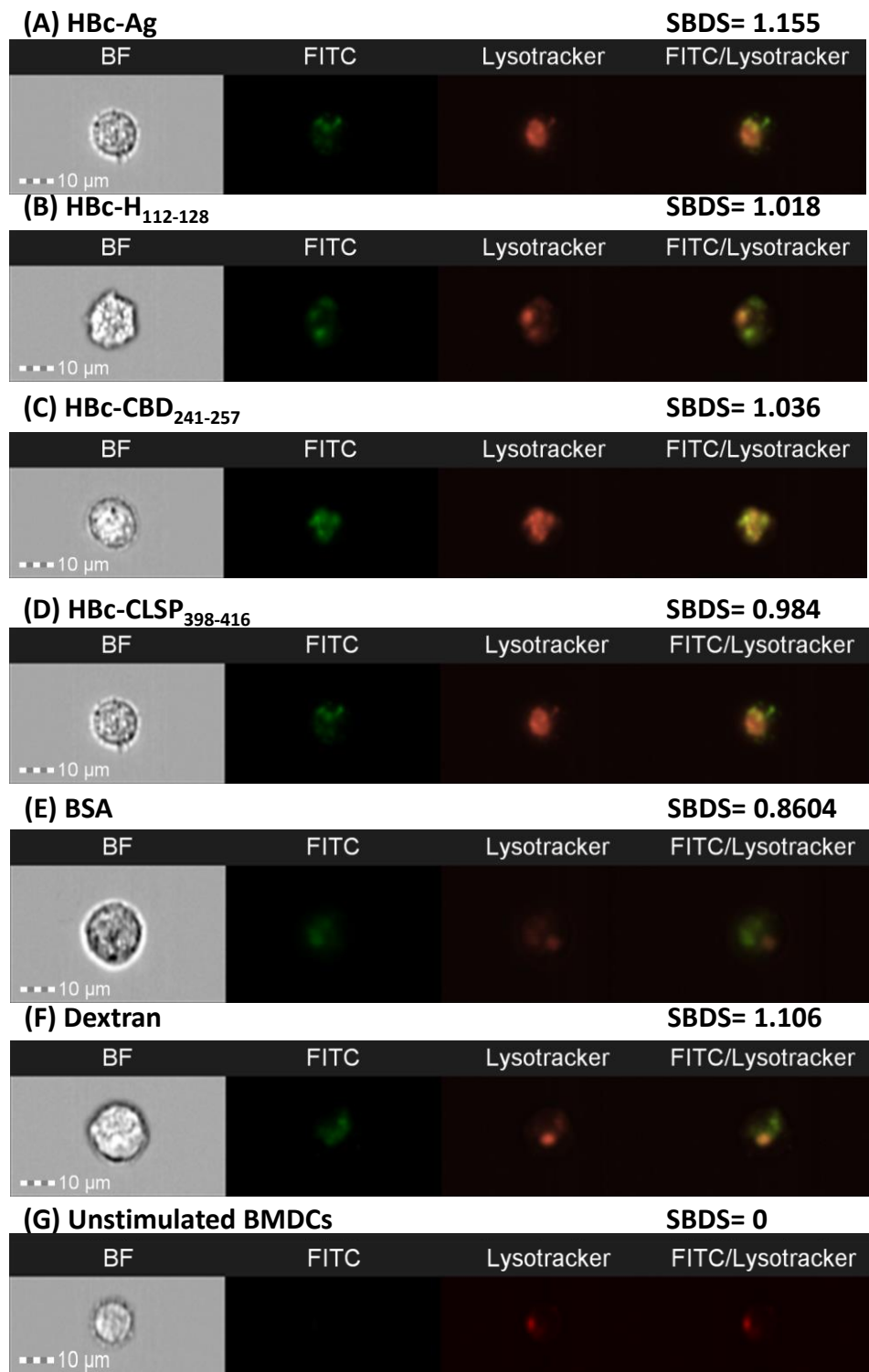


Figure 6.9 Representative images of fluorescein-conjugated VLPs co-localization in the BMDCs. BMDCs at $1 \times 10^6/\text{ml}$ were stained with Lysotracker to visualise the cellular lysosome compartment and subsequently stimulated with $10 \mu\text{g}/\text{ml}$ fluorescein-conjugated VLPs; (A) HBc-Ag, (B) HBc-H₁₁₂₋₁₂₈, (C) HBc-CBD₂₄₁₋₂₅₇, and (D) HBc-CLSP₃₉₈₋₄₁₆ for 24 hours. BMDCs were stimulated with $10 \mu\text{g}/\text{ml}$ fluorescein-conjugated BSA (E) and with $10 \mu\text{g}/\text{ml}$ fluorescein-conjugated dextran (F) as positive controls. As a negative control, unstimulated BMDCs were examined (G). Intracellular co-localization was determined by Amnis ImageStreamX cytometer. Images shown, from left to right, show individual Brightfield images (BF) in the white channel, fluorescent-labelled stimulus (FITC) in the green channel, stained lysosome (Lysotracker) in the red channel and the combination of both FITC/ Lysotracker merged channels. The Similarity bright detail score (SBDS) score from the IDEAS quantitative co-localization analysis is included above its image. SBDS values around 1 represent co-localization, and 0 values represent poor co-localization. Scale bars represent 10 µm.

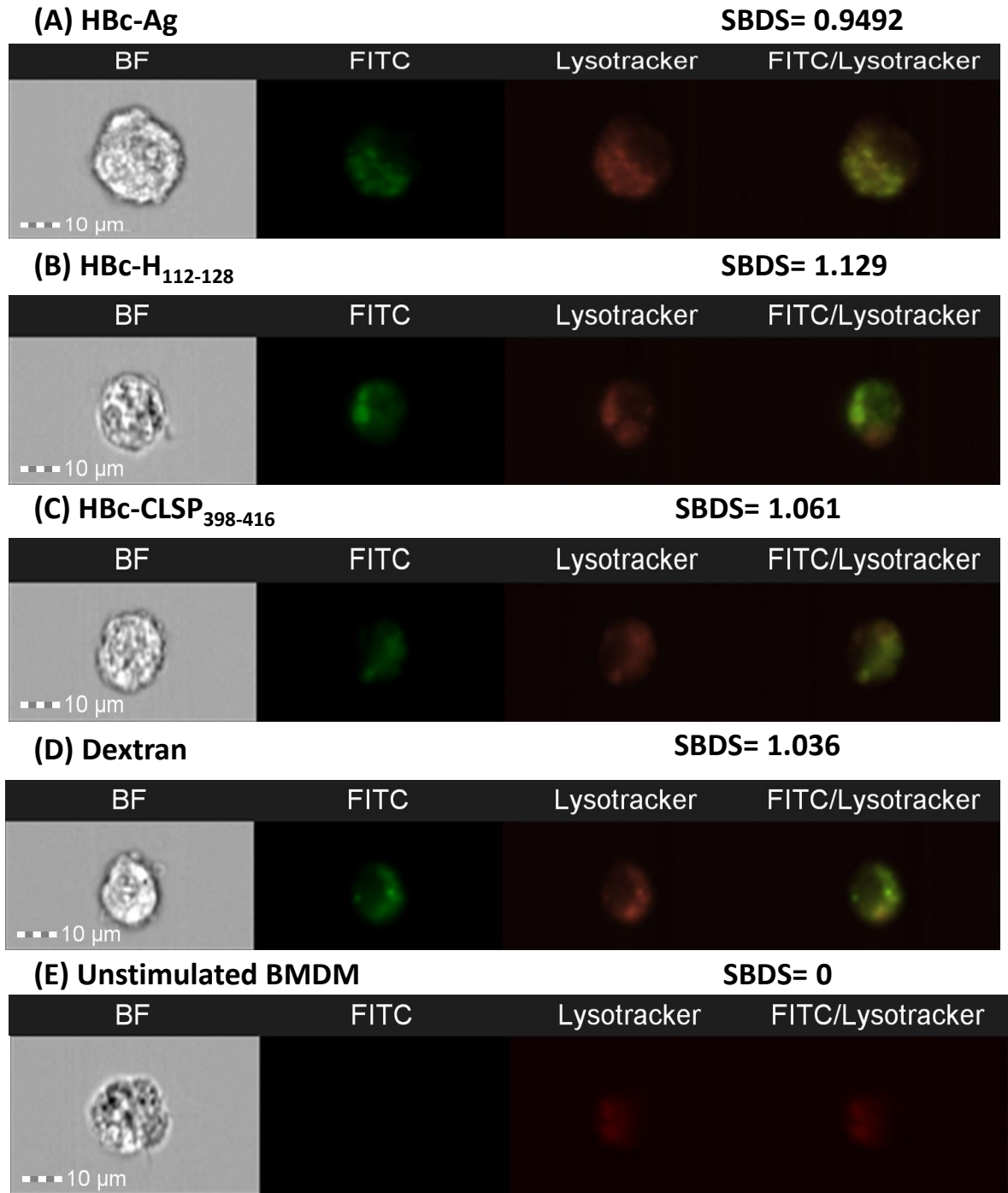


Figure 6.10 Representative images of fluorescein-conjugated VLPs co-localization in the BMDMs. BMDMs at $1 \times 10^6/\text{ml}$ were stained with Lysotracker to visualise the cellular lysosome compartment and subsequently stimulated with $10 \mu\text{g}/\text{ml}$ fluorescein-conjugated VLPs; (A) HBc-Ag, (B) HBc-H₁₁₂₋₁₂₈ and (C) HBc-CLSP₃₉₈₋₄₁₆ for 24 hours. BMDMs were stimulated with $10 \mu\text{g}/\text{ml}$ fluorescein-conjugated Dextran (D) as a positive control. As a negative control, unstimulated BMDMs were examined (E). Intracellular co-localization was determined by Amnis ImageStreamX cytometer. Images shown, from left to right, show individual Brightfield images (BF) in the white channel, fluorescent-labelled stimulus (FITC) in the green channel, stained lysosome (Lysotracker) in the red channel and the combination of both FITC/Lysotracker merged channels. The Similarity bright detail score (SBDS) score from the IDEAS quantitative co-localization analysis is included above its image. SBDS values around 1 represent co-localization, and 0 values represent poor co-localization. Scale bars represent 10 µm.

6.4 Discussion

The role of VLP as a vaccine delivery system has been a point of speculation since its discovery. VLPs have been proven to induce stronger protective immune responses against foreign carrier antigens when compared to other delivery systems (Vogel and Bachmann, 2019). However, the precise mechanism of how VLP activates the immune system and leads to an immune response against the antigen it carries is only partially understood. In particular, the uptake of HBc-Ag (VLP) by antigen-presenting cells has not been extensively studied compared to other VLPs obtained from other viruses such as the human papilloma virus-like particle (HPV-VLP).

The VLP as a vaccine platform can target both MHC-I and MHC-II processing and presentation pathways and generate cytokine production, which is essential to initiating a specific immune response (Cubas et al., 2009; Gomes et al., 2017b; Manolova et al., 2008; Shirbaghaee and Bolhassani, 2016). Most importantly, VLPs are advantageous vaccine delivery systems, as they can directly target the vaccine to different APCs. Among the APCs, DCs are the most potent APC that play crucial roles in delivering antigens from the site of exposure to the secondary lymphoid tissues for the initiation of specific T-cell (cytotoxic and helper) mediated immunity (Beyer et al., 2001; Steinman, 2001). In this study, we aimed to evaluate the innate stimulatory potential of the native VLP (HBc-Ag) that lacks C-terminal arginine and the VLPs expressing *Trichuris* MHC-II T-cell epitopes, by using two types of APCs, BMDCs and BMDMs. We also aimed to examine the ability of APCs to take up and internalise VLPs.

6.4.1 Dendritic cell activation by VLPs

It is now well established from a variety of studies, that VLPs derived from different viruses, such as human papillomavirus (HPV-16), Newcastle disease virus, murine polyomavirus, and SARS-Like coronavirus, can avidly bind and stimulate human and murine DCs (Bai et al., 2008; Bickert et al., 2007; Lenz et al., 2001; Lenz et al., 2003; McCullough and Sharma, 2017; Rudolf et al., 2001; Xu et al., 2019; Yang et al., 2004). The present chapter demonstrated that the VLPs used in this study provided two types of immunoregulator signals to BMDCs: (a) the upregulation of DC surface markers (CD40, CD80 and CD86) essential for the optimal activation of Ag-specific T-cells and (b) the mediation of inflammatory responses characterized by the secretion of high levels of cytokines, such as IL-6, IL-10 and TNF- α , which are involved in the immune regulation of B- and T-lymphocytes. Furthermore, VLPs were proven to be taken up by BMDCs efficiently and were not merely attached to the surface of APCs, suggesting that APCs will process and present the VLPs in the context of MHC molecules.

Interestingly, not all the BMDCs that took up the fluorescent-labelled VLPs expressed CD86 $^{+}$. For example, of the BMDCs that took up the fluorescent-labelled native VLP (HBc-Ag), only 50% were activated DCs expressing CD86 $^{+}$. This effect could be due to the enhanced ability of non-activated DCs to take up antigens compared to activated DCs (Sousa, 2006).

Collectively, these results suggest that VLPs are well placed to act as delivery systems to drive immune responses via DCs (Barth et al., 2005; Bosio et al., 2004; Da Silva et al., 2001; Lin et al., 2014; Rudolf et al., 2001; Warfield et al., 2003). In line with these observations, Ding et al. (2010)

demonstrated the phagocytosis of exogenous HBc-VLPs by BMDCs analysed by immunofluorescence and confocal laser scanning microscopy (CLSM). The phenotypic analysis also revealed that the HBc-VLP-pulsed BMDCs significantly increased the BMDC surface markers (CD80, CD86 and MHC-II) compared to the untreated BMDCs. Furthermore, the cytokine expression of HBc-VLP pulsed BMDCs identified by RT-PCR and electrophoresis on 1.2% agarose gel confirmed the secretion of IL-12 (p40) and IFN- γ compared to the control groups (Ding et al., 2010). The data are largely consistent with the results presented here although IL-12 (p40) and IFN- γ were not assessed and a broader profile of cytokines was measured, including IL-12p70.

More recently, Serradell et al. (2019) developed a (VLP-HA/VSP-G) vaccine composed of an influenza virus expressing influenza virus hemagglutinin (HA) antigen, coexpressed with the extracellular region of *Giardia lamblia* variant-specific surface proteins (VSPs) as an adjuvant. The recombinant protein (VLP-HA/VSP-G) significantly increased the expression of BMDC costimulatory molecules (CD40 and CD86) and induced the secretion of high levels of TNF- α , IL-10, and IL-6 cytokines *in vitro*. They also showed that oral vaccination with the recombinant protein protected mice from influenza infection and generated protective humoral and cellular immunity (Serradell et al., 2019). These data correlate well with the results presented here as the VLPs stimulated BMDCs to secrete high levels of IL-6 and TNF cytokines *in vitro* and increased the expression of BMDC costimulatory molecule (CD40).

Of the cytokines produced by DCs in response to VLP stimulation, IL-6, identified initially as a B-cell stimulatory factor 2, enhances antibody synthesis by activated B-cells (Kishimoto and Tanaka, 2015). IL-12, also produced by BMDCs activated by VLPs, plays an essential role as a bridge between the innate and adaptive immune systems. The secretion of IL-12 in response to infection polarises the immune system toward a primary Th-1 response by stimulating T-cells to produce IFN- γ (Fayette et al., 1998; Trinchieri, 1993). In the present study, the level of IL-12p70 produced by BMDCs in response to the native VLP (HBc-Ag) and VLPs expressing *Trichuris* epitopes stimulation was not significantly high. The native VLP (HBc-Ag) utilised in the current study is equivalent to the HBc-Ag lacking the C-terminal arginine (HBcAg-149). This finding is consistent with data on the Th1/ Th2 polarisation in immune responses to HBc-Ag (Chen et al., 2009; Milich et al., 1995). Thus, the full-length HBc-Ag, but neither of the HBc-Ag lacking the C-terminal arginine (HBcAg-144 and HBcAg-149), preferentially primed a Th1 immune response as measured by the production of IL-12p70 by dendritic cells from mice immunised with HBc-Ag and the subsequent release of IFN- γ by splenocytes (Riedl et al., 2002). Another study also showed that the full-length HBc-Ag induced the transcription and secretion of IL-18, a potent inductor of IFN- γ in peripheral blood mononuclear cells (PBMCs) in healthy controls and patients with chronic or acute hepatitis B infection, whereas the HBc-Ag lacking the C-terminal arginine-rich domain did not induce IL-18 in all groups (Manigold et al., 2003).

In all studies involving VLPs, it is essential to confirm that DC activation and the release of cytokines are in response to the interaction of DCs with the VLP protein structure and not due to endotoxin contamination whilst the VLPs were being made. For example, there were no alterations

in cytokine production when the DCs stimulated with VLPs were pretreated with polymyxin B, a compound that binds and inactivates LPS. Moreover, destroying the structure of the VLPs by boiling inhibited the cytokine production, while boiling LPS led to no alterations in the cytokines produced by VLP-stimulated DCs (Bosio et al., 2004; Lenz et al., 2001). Furthermore, when Ebola virus VLPs were depleted with specific antibodies and then incubated with DCs, cells did not upregulate cell-surface markers and failed to secrete cytokines (Bosio et al., 2004; Lenz et al., 2001). Although these types of studies were not undertaken in the current research, future analysis should include checks for endotoxin contamination.

Several studies have also addressed whether different APCs can take up VLPs. For example, electron microscopy and confocal imaging of mature DCs obtained from peripheral blood mononuclear cells (PBMCs) exposed to human immunodeficiency virus type 1 (HIV-VLPs) for 4 hours showed that VLPs were co-localized in the intracellular vesicular compartment. Further intracellular accumulation increased over time and in a dose-dependent manner (Izquierdo-Useros et al., 2009). Zhang et al. (2007) also showed that HBc-Ag expressing tumor epitopes bind and internalise to BMDCs efficiently *in vitro* when detected using immunofluorescence confocal microscopy. Furthermore, Link et al. (2012) suggested that a VLP's size and repetitive structure play an essential role in Ag presentation to B-cells. To analyse Ag trafficking, naïve wild-type mice were immunised with VLPs derived from the bacteriophage QB (QB-VLP), and Ag deposition on murine splenic follicular dendritic cells (FDCs) was determined 24 h after the challenge. The fluorescence images revealed the deposition of the VLP inside B-cell follicles (Link et al., 2012). In a second experiment, mice were passively immunised with anti-Qb IgM serum and then challenged with QB-VLPs to allow the formation of immune complexes (ICs) *in vivo*. Mice were then challenged with QB-VLPs, and Ag deposition was assessed 24 h after the challenge. The fluorescence images also revealed the accumulation of QB-VLPs inside the B-cell follicles as immune complexes via a process involving IgM antibodies and complement (Link et al., 2012).

Given that VLPs activate DCs and have the ability to interact with B-cells to facilitate Ab production after VLP vaccination without the need for an adjuvant, modifying a VLP using immunostimulatory adhesion molecules and cytokines co-displayed on the VLP to target APCs can enhance the activation of antigen-specific T lymphocytes responses (Akhras et al., 2017; Caminschi and Shortman, 2012; Hill et al., 2018; Gogesch et al., 2018; Gomes et al., 2017a; Mohsen et al., 2017b; Rohovie et al., 2017). For example, membrane-bound CD40 ligand (CD40L) expressed on the surface of simian immunodeficiency virus (SIV) VLPs and HIV-1 VLPs can be used to target CD40 receptor on DCs to enhance both CD4+ and CD8+ T-cell responses to HIV-1 glycosylphosphatidylinositol (GPI) protein (Franco et al., 2011; Skountzou et al., 2007; Zhang et al., 2010). The activity of CD40L-displaying HIV-1 VLPs significantly enhanced both humoral and cellular immune responses to HIV-1 Gag protein in immunised mice compared to the effect in immunised CD40-/- mice (Franco et al., 2011). In another study, the immunization of mice with a membrane-anchored granulocyte-macrophage colony stimulating factor (GM-CSF) expressed on SIV VLPs containing Gag, to target GM-CSF-receptor positive APCs significantly enhanced the production of SIV VLP-specific antibodies and activated both CD4+ and CD8+ T-cell responses

compared to the control immunized groups (SIV VLPs, SIV VLPs containing CD40L, or SIV VLPs mixed with soluble GM-CSF) (Skountzou et al., 2007).

6.4.2 Macrophage activation by VLPs

Macrophages, as APCs, play a role in promoting Th1 and Th2 immunity and controlling infection by producing proinflammatory and regulatory cytokines. However, the origin, size, and shape of exogenous stimuli influence the efficiency of phagocytosis, macrophage phenotype, and activation threshold (Daigneault et al., 2010; Dalgédiené et al., 2018; Murray and Wynn, 2011).

The present chapter carried out *in vitro* studies to determine the BMDMs activation upon exposure to the native VLP (HBc-Ag) and VLPs expressing different *Trichuris* T-cells epitopes. High levels of IL-10, TNF- α , IL-6, and IL1 β cytokines and MCP-1 (CCL2), MIP (CCL3), and RANTES (CCL5) chemokines were detected by BMDMs after treatment with different VLPs. The data suggest that the VLP is a potent inducer of proinflammatory cytokines. I further demonstrated that not only DCs, but also macrophages were able to take up the VLPs which co-localized in lysosomes.

These results are consistent with those of Lenz et al. (2003) and Wahl-Jensen et al. (2005) who examined the activation of macrophages in response to VLPs. For example, Lenz et al. (2003) found that bovine papillomavirus BPV VLPs labelled with green fluorescence protein (GFP) bind to the cell surface of human macrophages when analysed by flow cytometry. Furthermore, they found that human macrophages secreted the proinflammatory cytokines TNF- α , IL-6 and IL- 1 β in response to HPV16 VLPs, unlike the unstimulated DCs, as assessed by cytokine ELISA and intracellular cytokine staining. However, they did not assess the immune response to the native HPV VLP (Lenz et al., 2003). These results are consistent with Wahl-Jensen et al.'s work (2005), which found that VLPs with and without Ebola virus glycoproteins (GP) produced higher levels of proinflammatory cytokines (TNF- α , IL-6 and IL- 1 β) and IL-8 compared to the unstimulated cells when measured by real-time PCR. Also, VLP-GP induced higher levels of macrophage activation compared to the native VLP (Wahl-Jensen et al., 2005).

Furthermore, Cooper et al. (2005) examined the capacity of the HBc-Ag VLP (HBc-₁₄₄) which lacks the genetic material compared to the full-length HBc-Ag, to induce proinflammatory and regulatory cytokines in human macrophages. The full-length HBc capsid, but not the HBc-₁₄₄ capsid, efficiently bound differentiated THP-1 macrophages. However, both induced the production of proinflammatory and regulatory cytokines (TNF- α , IL-6, and IL-12p40) in a dose- and time-dependent manner (Cooper et al., 2005). The cytokine levels were lower in response to HBc-₁₄₄ compared to the full-length HBc-Ag. The recombinant full-length HBc-Ag and HBc-₁₄₄ were expressed and purified using *E. coli*. In order to rule out that the cytokines were induced in response to residual LPS contamination, the HBc-Ag, HBc-₁₄₄ and LPS control were preboiled before adding them to the THP-1 macrophages to measure cytokine induction using ELISA and RT-PCR. Both preboiled recombinant capsids but not the LPS control failed to induce cytokine production (Cooper et al., 2005).

It is also important to highlight the fact that there were differences in the responses of APCs after exposure to VLPs expressing different *Trichuris* T-cell epitopes. However, these changes could be

due to the nature of the inserted epitope or the structural assembly of the VLP. To further confirm and understand the differences in activation responses seen *in vitro*, future studies will need to focus on evaluating the VLPs *in vivo*. It will also be interesting to vaccinate mice with VLPs and then evaluate the activation responses to different DC subsets and to other APCs, including B-cells, *in vivo*.

Collectively, the findings reported in this chapter provide evidence that both APCs (dendritic cells and macrophages) effectively recognise and respond to VLPs expressing *Trichuris* MHC-II T-cell epitopes, supporting an orchestrated priming of both humoral and cellular immune responses in the development of VLP-mediated immunity even at low doses and in the absence of an adjuvant. Given the experimental explanation *in vitro* of the remarkable immunogenicity of HBc-Ag VLPs as a promising vaccine delivery system, I propose that HBc-VLPs expressing *Trichuris* MHC-II T-cell epitopes may drive strong *Trichuris* specific T-cell responses *in vivo* and, thus, could be used as a novel, effective vaccine against trichuriasis.

6.5 Summary

- The native VLP (HBc-Ag) and the VLP expressing *Trichuris* MHC-II T-cell epitopes (HBc-Ag, HBc-H₁₁₂₋₁₂₈, HBc-CBD₂₄₁₋₂₅₇, and HBc-CLSP₃₉₈₋₄₁₆) activated BMDCs as demonstrated by upregulation in the expression of costimulatory molecules CD80, CD86, CD40, and MHC-II.
- The native VLP (HBc-Ag) and the VLP expressing *Trichuris* MHC-II T-cell epitopes (HBc-Ag, HBc-H₁₁₂₋₁₂₈, HBc-CBD₁₂₄₃₋₁₂₅₉, HBc-CBD₂₄₁₋₂₅₇, HBc-CLSP₁₄₃₋₁₅₈, and HBc-CLSP₃₉₈₋₄₁₆) efficiently stimulated BMDCs and BMDMs to produce a broad range of pro-inflammatory and anti-inflammatory cytokines.
- The fluorescein-conjugated VLPs (HBc-Ag, HBc-H₁₁₂₋₁₂₈, HBc-CBD₂₄₁₋₂₅₇, and HBc-CLSP₃₉₈₋₄₁₆) were taken up by BMDCs. However, the percentage of uptake varied between different VLPs.
- The fluorescein-conjugated VLPs (HBc-Ag, HBc-H₁₁₂₋₁₂₈, HBc-CBD₂₄₁₋₂₅₇, and HBc-CLSP₃₉₈₋₄₁₆) were internalised and co-localized in the lysosomes of both BMDCs and BMDMs.

Chapter Seven

**VLPs expressing *Trichuris* T-cell
epitopes promote protective
immune responses *in vivo***

7.1 Introduction

Trichuriasis, caused by the whipworm *Trichuris trichiura*, is one of the most widespread soil-transmitted helminths in the world (Alexander and Blackburn, 2019). Global mass drug administration (MDA) programmes are being implemented, but repeated treatments are costly and may prevent the development of acquired immunity, and the existence of drug-resistant parasites is well established (Farrell et al., 2018; Speich et al., 2015; WHO, 2015). Thus, there is considerable interest in developing vaccines against these parasites (Becker et al., 2018; Dixon et al., 2008). A vaccine that protects against *Trichuris* infection was first demonstrated in mice immunised subcutaneously (s.c) with *Trichuris muris* excretory/secretory (ES) products (Jenkins and Wakelin, 1977), followed by fractions of ES (Shears et al., 2018b), and extracellular vesicles (EVs) (Shears et al., 2018a), and, more recently with *T. muris* whey acidic protein (Briggs et al., 2018).

It has been clearly demonstrated that susceptibility to infection and the development of chronic infection and colitis is driven by CD4+ Th1 immune responses, serum IgG2c, and the production of Th1 cytokines IL-12 and IFN- γ (Bancroft et al., 2001; Else et al., 1993b). In contrast, resistance to infection is driven by Th2 immune responses, serum IgG1, and the production of Th2 cytokines (IL-4, IL-9, and IL-13 (Dixon et al., 2010; Klementowicz et al., 2012). Th2 cytokines are known to stimulate different effector mechanisms critical to driving worm expulsion for the development of a protective immune response to *T. muris*. These effector mechanisms include epithelial cell turnover in the caecum and proximal colon (Cliffe et al., 2005), intestinal hyper-contractility (Khan et al., 2003), and the increased production of mucins by goblet cells (Artis et al., 2004b).

Despite the success of the previously mentioned vaccines, developing a vaccine for STHs based on native antigens has encountered many manufacturing complexities, such as cost, time consumption, as well as difficulty in purifying large quantities of the worm antigens, and controlling batch differences to develop a commercially stable vaccine (Geldhof et al., 2007; Hewitson and Maizels, 2014). An alternative is to develop a vaccine based on virus-like particles (VLPs) expressing *Trichuris* MHC-II T-cell epitopes to simplify the production challenges inherent in developing a safe, inexpensive vaccine that can induce an effective immune response (El-Sayed and Kamel, 2018; Geldhof et al., 2007; Jain et al., 2015).

The fast-growing knowledge of VLP-based vaccines against several parasites, including *Plasmodium* spp (Nardin et al., 2001; Salman et al., 2017), *Leishmania infantum* (Moura et al., 2017), *Toxoplasma gondii* (Guo et al., 2019), *Trichinella spiralis* (Lee et al., 2016), and *Clonorchis sinensis* (Lee et al., 2017) has escalated interest in developing a VLP-based vaccine against trichuriasis. To the best of our knowledge, this is the first study that has developed a vaccine against trichuriasis based on VLPs expressing novel *Trichuris* MHC-II T-cell epitopes.

7.2 Aim and objectives

The overall aim of this Chapter was to evaluate various VLPs expressing different *Trichuris* MHC-II T-cell epitopes as potential vaccine candidates *in vivo* in the murine model of *Trichuris* infection. This aim was addressed via three objectives:

- To test the immunogenic and protective immune response of a low-dose of a vaccine candidate, C57BL/6 mice were vaccinated with 25 µg of pre-mixed VLPs expressing *Trichuris* T-cell epitopes (HBc-H₁₁₂₋₁₂₈, HBc-CLSP₁₄₃₋₁₅₈, HBc-CBD₁₂₄₃₋₁₂₅₉, and HBc-CBD₂₄₁₋₂₅₇) at day -20 and boosted at day -10. As controls for susceptibility to infection, mice were injected with PBS and 25 µg native VLP (HBc-Ag). Mice were then challenged with a high-dose of *Trichuris* infection at day 0, and infection levels were assessed two weeks post infection (p.i.) for evidence of accelerated expulsion in vaccinated mice.
- To assess the potential of AddaVax adjuvant in enhancing the vaccine efficacy, C57BL/6 mice were vaccinated with 25 µg of pre-mixed VLPs expressing *Trichuris* T-cell epitopes (HBc-H₁₁₂₋₁₂₈, HBc-CLSP₁₄₃₋₁₅₈, HBc-CLSP₃₉₈₋₄₁₆, and HBc-CBD₂₄₁₋₂₅₇) formulated with AddaVax at day -35 and boosted at day -14. As a control for protective immunity, mice were vaccinated with 50 µg ES/AddaVax, and as controls for susceptibility to infection, mice were injected with PBS/AddaVax and 50 µg native VLP (HBc-Ag)/AddaVax. Mice were then challenged with a high-dose of *T. muris* infection at day 0, and infection levels were assessed at day 14 p.i.
- To test the immunogenic and protective immune response of a high-dose of a vaccine candidate, C57BL/6 mice were vaccinated with 50 µg of pre-mixed VLPs expressing *Trichuris* T-cell epitopes (HBc-CBD₁₂₄₃₋₁₂₅₉, HBc-CBD₂₄₁₋₂₅₇, HBc-CLSP₁₄₃₋₁₅₈, and HBc-CLSP₃₉₈₋₄₁₆) at day -20 and boosted at day -10. Control groups were injected with 50 µg ES/Alum, PBS or 50 µg native VLP (HBc-Ag) at day -20 and boosted at day -10. Mice were then challenged with a high-dose of *T. muris* infection at day 0, and infection levels were assessed at day 14 p.i.

7.3 Results

7.3.1 Experimental protocol for *in vivo* evaluation of vaccinating mice with 25 µg of pre-mixed VLPs expressing *Trichuris* MHC-II T-cell epitopes (HBc-H₁₁₂₋₁₂₈, HBc-CLSP₁₄₃₋₁₅₈, HBc-CBD₁₂₄₃₋₁₂₅₉, and HBc-CBD₂₄₁₋₂₅₇)

In order to investigate whether VLPs expressing *Trichuris* T-cell epitopes are capable of stimulating protective immunity, male C57BL/6 mice were subcutaneously vaccinated with 25 µg of pre-mixed VLPs+ T-cell epitopes (HBc-H₁₁₂₋₁₂₈, HBc-CLSP₁₄₃₋₁₅₈, HBc-CBD₁₂₄₃₋₁₂₅₉, and HBc-CBD₂₄₁₋₂₅₇) on day -20 and boosted on day -10. As controls for susceptibility to infection, mice were injected with PBS and 25 µg of native VLP (HBc-Ag). 5 mice from each group were immunised but were not infected with *T. muris*, and 5 mice from each group were immunised and then infected by oral gavage with approximately 150 infective *T. muris* eggs on day 0 and sacrificed at day 14 p.i. (Figure 7.1 A).

The protective efficacy of the vaccine was assessed two weeks p.i. by counting the worms from the proximal colon and caecum of each mouse. MLNs at day 14 p.i. were collected and re-stimulated *in vitro* with *Trichuris* ES for cytokine production, while blood was collected to measure serum parasite and VLP+ T-cell epitope-specific IgM, IgG1 and IgG2c antibodies levels. Proximal colon sections were collected to assess the pathology and count goblet cells.

7.3.1.1 25 µg of pre-mixed VLPs expressing *Trichuris* T-cell epitopes immunisation did not reduce the *T. muris* worm count following challenge infection

Previous studies have shown that the C57BL/6 mouse strain is normally resistant to infection when infected with a high-dose of *T. muris* eggs. Mice were able to expel the worms by day 21 p.i. and full protection was seen by day 28 p.i. (Bancroft et al., 2001; Cliffe et al., 2005; D'elia et al., 2009). However, no expulsion is normally seen two weeks p.i. unless the host has been previously infected or vaccinated. Based on these studies, all the vaccination studies conducted in this chapter used C57BL/6 mouse strain. Furthermore, only male C57BL/6 mice were subcutaneously vaccinated to ensure that expulsion and cytokine production was not subjective by gender differences (Else et al., 1994). The decision to administer the vaccine candidates subcutaneously was based on a previous study that showed that subcutaneous vaccination of NIH mice with ES not formulated with an adjuvant induced better protection (70%) than intraperitoneal vaccination (33%) at day 9 p.i. (Jenkins and Wakelin, 1983).

Caecum and colon worm loads following *T. muris* infection are the most prominent indicator to assess protective efficacy. In order to investigate whether the selected VLPs expressing *Trichuris* T-cell epitopes (HBc-H₁₁₂₋₁₂₈, HBc-CLSP₁₄₃₋₁₅₈, HBc-CBD₁₂₄₃₋₁₂₅₉, and HBc-CBD₂₄₁₋₂₅₇) are protective *in vivo*, worm burdens were assessed at day 14 p.i. and compared to those of mice injected with PBS and native VLP (HBc-Ag) control groups. This time point was chosen as resistance post vaccination will present as accelerated expulsion (Bancroft et al., 2001; Cliffe et al., 2005; D'elia et al., 2009).

As shown in Figure 7.1 (B), no reduction in worm burden was demonstrated in the VLPs+ T-cell epitopes vaccinated mouse group compared to the PBS and native VLP (HBc-Ag) control injected mice groups. However, one mouse expelled all the worms in the group immunised with VLPs+ T-cell epitopes.

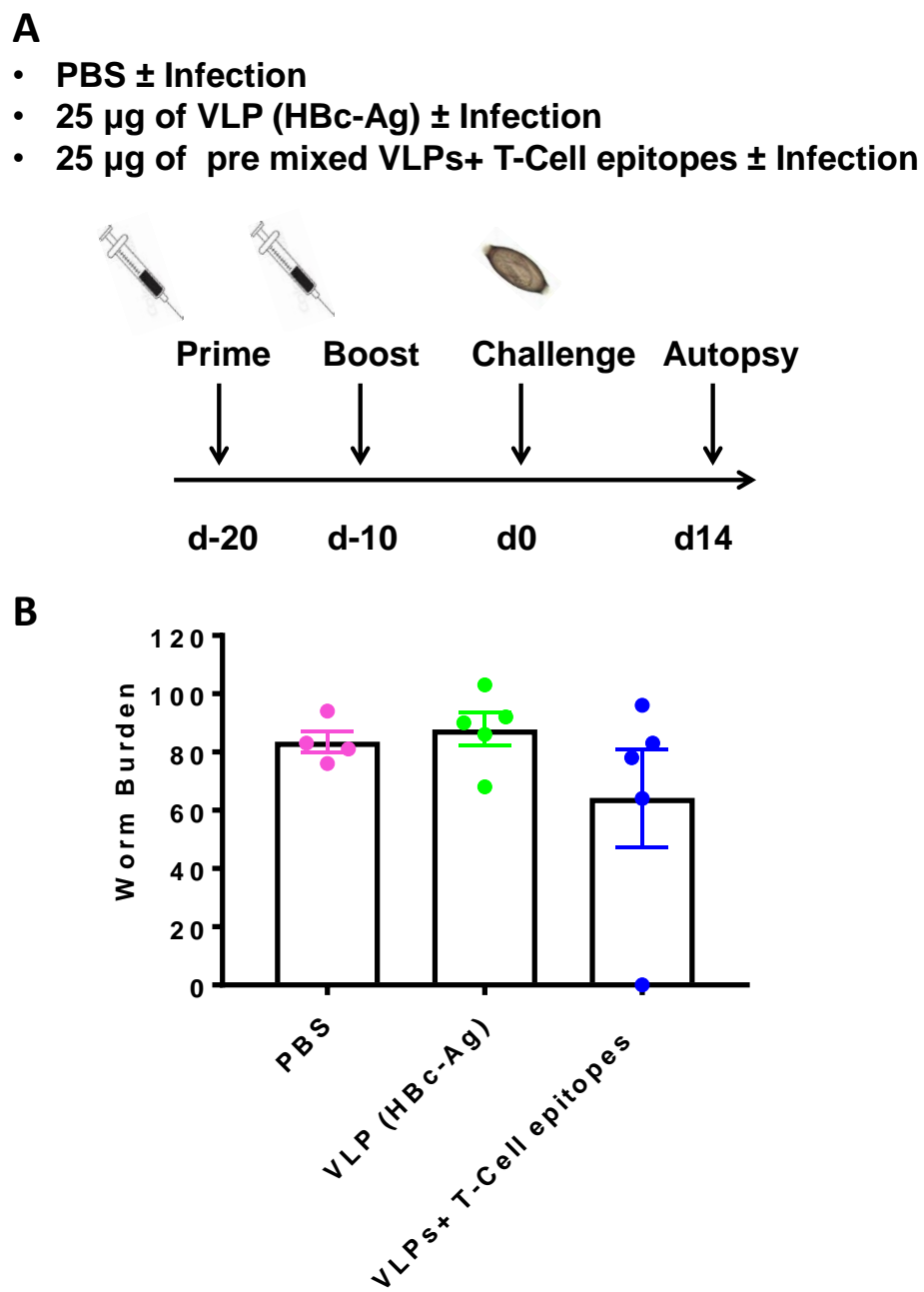


Figure 7.1 Experimental schedule and worm burden of mice vaccinated and challenged with a *T. muris* infection. (A) 6-week old male C57BL/6 mice were vaccinated subcutaneously with 25 µg of pre-mixed of VLPs + T-cell epitopes (HBc-H₁₁₂₋₁₂₈, HBc-CLSP₁₄₃₋₁₅₈, HBc-CBD₁₂₄₃₋₁₂₅₉, and HBc-CBD₂₄₁₋₂₅₇), 25 µg of native VLP (HBc-Ag), or PBS on day -20 and boosted on day -10. 5 mice from each group were infected by oral gavage with approximately 150 infective *T. muris* eggs on day 0 and sacrificed at day 14 post-infection. (B) Comparison of worm burden at day 14 p.i.. Statistical analyses were carried out using the Kruskal-Wallis test (multiple comparisons). Results are shown as mean ± SEM. n= 5 mice per group. The results presented are from one experiment.

7.3.1.2 Serum parasite-specific responses following vaccination of mice with VLPs expressing *Trichuris* T-cell epitopes

Parasite-specific IgG1 and IgG2c serum antibodies are often used as markers of resistance/susceptibility to *Trichuris* infection. The production of parasite-specific IgG1 is associated with Th2 protective immune response in mice resistant to infection. Whereas the production of parasite-specific IgG2c is associated with Th1 immune response in susceptible mice to infection (Else et al., 1993b). To analyse parasite-specific antibody responses of vaccinated mice, serial dilutions of sera were assessed using an ELISA-based assay with *Trichuris* excretory/secretory (ES) as a target antigen.

In general, IgM, IgG1 and IgG2ca isotype responses were similar in mice given a *T. muris* infection compared to those without challenge infection (Figure 7.2 A-C). There was a significant increase in parasite-specific IgM detected in the serum of mice vaccinated with VLPs+ T-cell epitopes compared to the native VLP (HBc-Ag) and PBS-injected mice with and without *T. muris* challenge (Fig 7.2 A). Importantly, significant levels of IgG1 (Fig 7.2 B) and IgG2c (Fig 7.2 C) were detected in the serum of mice vaccinated with VLPs+ T-cell epitopes compared to the native VLP (HBc-Ag), and PBS-injected mice.

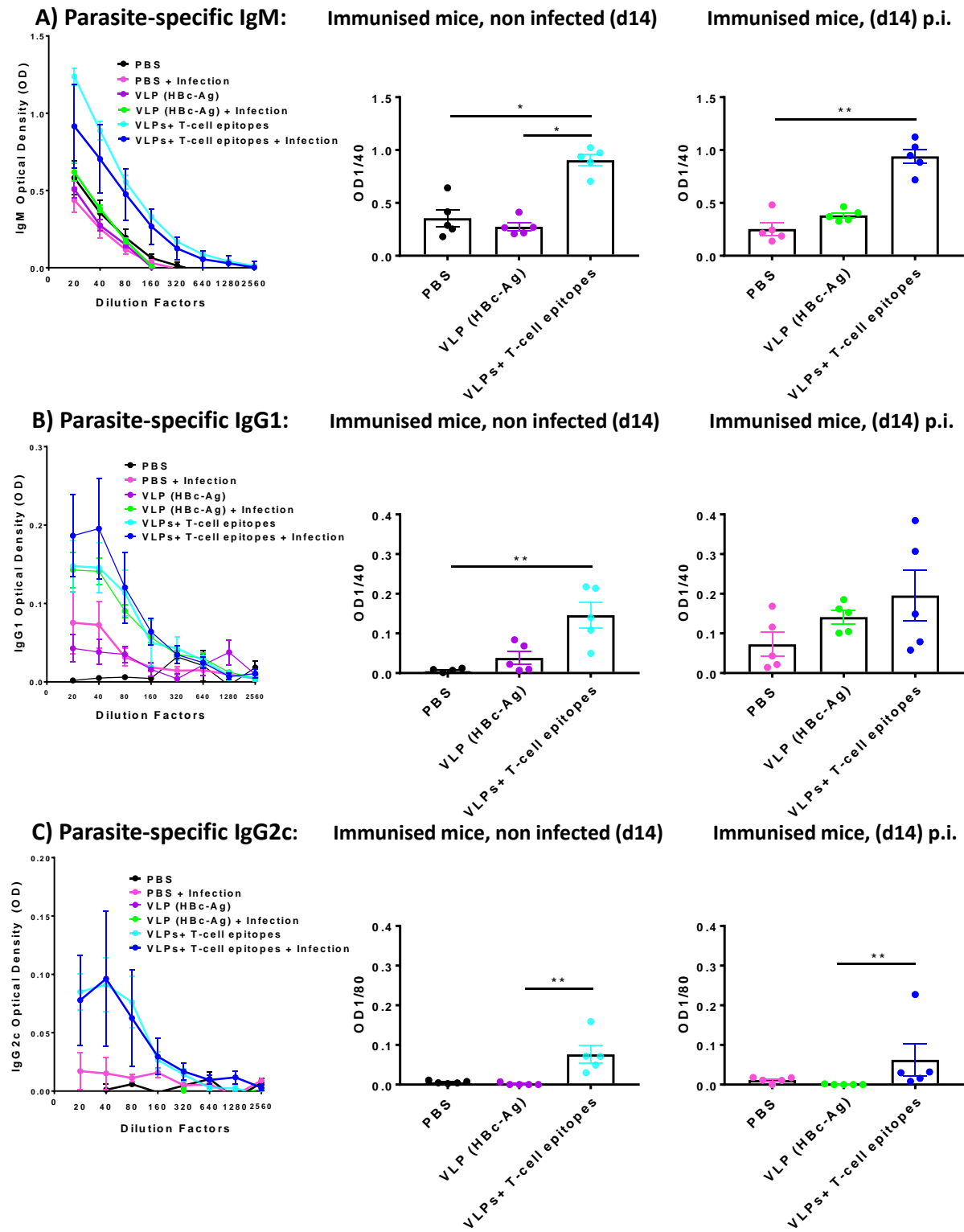


Figure 7.2 Parasite-specific IgM, IgG1 and IgG2c serum antibodies levels at day 14. 6 week old male C57BL/6 mice were vaccinated subcutaneously with 25 µg of pre-mixed VLPs+ T-cell epitopes (HBc-H₁₁₂₋₁₂₈, HBc-CLSP₁₄₃₋₁₅₈, HBc-CBD₁₂₄₃₋₁₂₅₉, and HBc-CBD₂₄₁₋₂₅₇), VLP (HBc-Ag), or PBS on day -20 and day -10 (10 mice per group). 5 mice from each of the three groups were infected by oral gavage with approximately 150 infective *T. muris* eggs and sacrificed at d14. 5 mice from each of the three groups were left uninfected. Day 14 sera were titrated against *T. muris* ES antigens to assess *T. muris* specific IgM levels by ELISA (A), IgG1 (B), and IgG2c (C) in the infected and uninfected mice groups with *Trichuris* eggs. Serum antibodies levels were measured for each mouse by ELISA (reading at 405 nm). Statistical analyses were carried out at 1:40 (IgM and IgG1) and 1:80 (IgG2c) serum dilutions using Kruskal-Wallis test (multiple comparisons). Significant differences between groups are represented by (*P≤0.05, **P≤0.01) with a line. Results are shown as mean ± SEM. n=5 mice per group. The results presented are from one experiment.

7.3.1.3 Serum VLP+ T-cell epitope-specific responses following vaccination of mice with VLPs expressing *Trichuris* T-cell epitopes

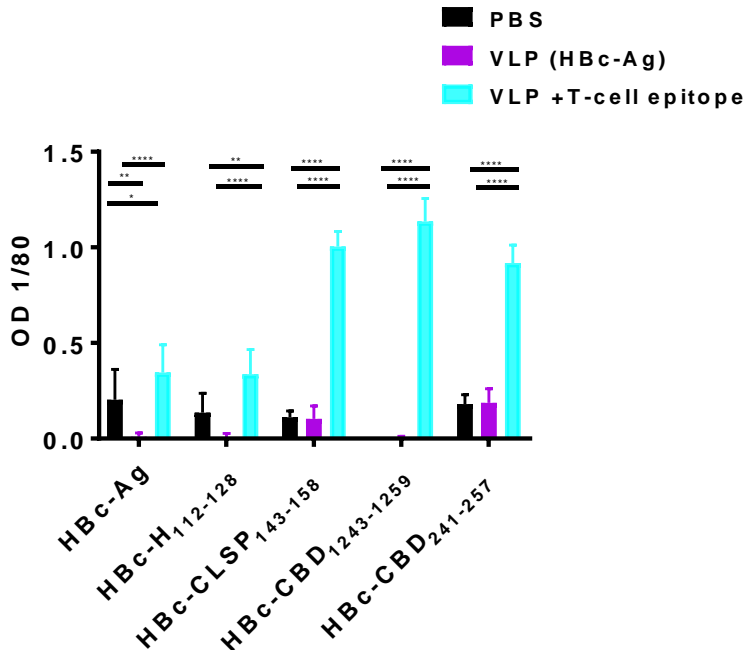
The strategy used in all the in vivo studies conducted in this chapter to identify potential vaccine candidate against trichuriasis was based on using a mixture of four VLPs expressing four different *Trichuris* MHC-II T-cell epitopes. Therefore, assessing VLPs+ T-cell epitope-specific antibody responses may provide valuable information about the most immunogenic ones amongst these epitopes.

To analyse VLP+ T-cell epitope specific-IgM antibody responses, serial dilutions of immunised mouse serum were assessed using an ELISA-based assay against individual VLP+ T-cell epitope recombinant protein (HBc-H₁₁₂₋₁₂₈, HBc-CLSP₁₄₃₋₁₅₈, HBc-CBD₁₂₄₃₋₁₂₅₉, and HBc-CBD₂₄₁₋₂₅₇), and native VLP (HBc-Ag) as target antigens.

The VLPs+ T-cell epitopes mouse sera reacted with their corresponding VLP+ T-cell epitope recombinant protein but not to the native VLP (HBc-Ag), as shown in Figure 7.3 (A) and (B). Interestingly, significantly higher levels of HBc-CLSP₁₄₃₋₁₅₈, HBc-CBD₁₂₄₃₋₁₂₅₉, and HBc-CBD₂₄₁₋₂₅₇ specific-IgM were detected in the serum of mice vaccinated with VLPs+ T-cell epitopes without (Fig 7.3 A) and after *Trichuris* infection (Fig 7.3 B) compared to the native VLP (HBc-Ag), and PBS-injected mice. However, only negligible levels of HBc-H₁₁₂₋₁₂₈ specific-IgM were detected in the serum of mice vaccinated with VLPs+ T-cell epitopes and with no significant production after fourteen days post *T. muris* infection challenge.

Collectively, these results demonstrate that vaccinating mice with a VLPs+ T-cell epitope vaccine induced strong VLPs+ T-cell epitopes-specific humoral immune responses to three VLPs+ T-cell epitopes recombinant proteins in the pre-mixed vaccine candidate.

A) VLPs-specific IgM levels in vaccinated, not infected mice with *Trichuris* infection



B) VLPs-specific IgM levels in vaccinated and infected mice with *Trichuris* infection

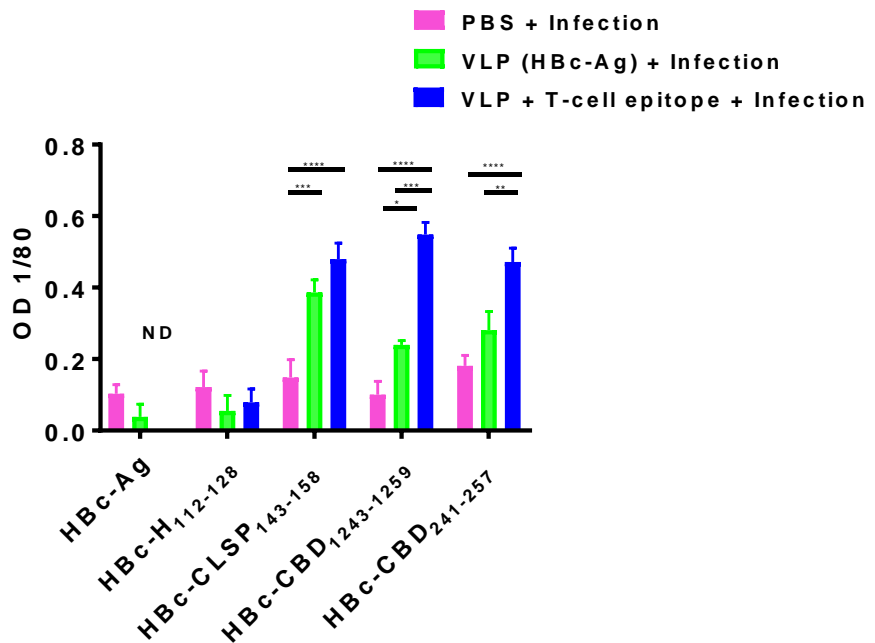


Figure 7.3 VLPs-specific IgM serum antibody levels at day 14 post-infection. 6 week old male C57BL/6 mice were vaccinated subcutaneously with 25 µg of pre-mixed VLPs+ T-cell epitopes (HBc-H₁₁₂₋₁₂₈, HBc-CLSP₁₄₃₋₁₅₈, HBc-CBD₁₂₄₃₋₁₂₅₉, and HBc-CBD₂₄₁₋₂₅₁), VLP (HBc-Ag), or PBS on day -20 and day -10. 5 mice from each of the three groups were infected by oral gavage with approximately 150 infective *T. muris* eggs and sacrificed at d14. 5 mice from each of the three groups were left uninfected. Day 14 sera were titrated against VLPs+ T-cell epitopes proteins (HBc-Ag, HBc-H₁₁₂₋₁₂₈, HBc-CLSP₁₄₃₋₁₅₈, HBc-CBD₁₂₄₃₋₁₂₅₉, and HBc-CBD₂₄₁₋₂₅₁) to assess VLPs specific IgM levels in the uninfected (A) and infected (B) mice groups with *Trichuris* eggs. Serum antibody levels were measured by ELISA (reading at 405 nm). Statistical analyses were carried out at 1:80 serum dilutions out using the Two-way ANOVA (multiple comparisons). Significant differences between groups are represented by (*P≤0.05, **P≤0.01, ***P≤0.001, ****P≤0.0001) with a line. ND: Not done. Results are shown as mean ± SEM. n= 5 mice per group. The results presented are from one experiment.

7.3.1.4 The cellular immune responses following vaccination of mice with VLPs expressing *Trichuris* T-cell epitopes and infection

It is already known that Th2 cytokines including IL-4, IL-5, IL-9 and IL-13 are produced during a protective immune response to *Trichuris*, while Th1 cytokines including IFN- γ are produced during an inappropriate immune response (Bancroft et al., 2001; Klementowicz et al., 2012). To analyse the cellular immune responses at the primary site of adaptive immune cell activation following *T. muris* infection (King et al., 2017), MLN cells of mice vaccinated with VLPs+ T-cell epitopes were re-stimulated *in vitro* at 5×10^6 /ml with 50 μ g/ml 4 hours ES for 48 hours. MLN cells were also re-stimulated *in vitro* at 5×10^6 /ml with 5 μ g/ml ConA for 24 hours. As a readout of cell activation, supernatants were analysed for the concentrations of a broad range of cytokines production by cytometric bead array (CBA) and compared to the PBS, and native VLP (HBc-Ag) injected mice and uninfected mice.

Re-stimulation of MLN cells taken from the VLPs+ T-cell epitopes vaccinated mice p.i. with *Trichuris* ES resulted in the induction of Th2 cytokines IL-4 (Fig 7.4 A), IL-5 (B), IL-9 (C) and IL-13 (D), while MLN cells taken from PBS and VLP (HBc-Ag) injected mice did not produce these cytokines at greater than uninfected levels.

Trichuris infection-primed MLN cells from mice immunised with VLPs+ T-cell epitopes, native VLP (HBc-Ag) and PBS groups produce significant high levels of Th1 cytokine IFN- γ (Fig 7.4 E), pro-inflammatory cytokines TNF (F), IL-6 (G), IL-17 (H), and anti-inflammatory cytokine IL-10 (I) in response to re-stimulation with worm ES antigens.

There were significant associations ($*p<0.05$) between increased cytokine production and worm burden. In particular, the mouse that expelled all the worms showed high levels of Th2 cytokines IL-4 (Figure 7.5 A), IL-5 (B), IL-9 (C), IL-13 (D) and the anti-inflammatory cytokine IL-10 (I) and low levels of Th1 cytokine IFN- γ (E). Furthermore, ConA re-stimulated MLN cells showed a slight but not significant ($P>0.05$) increase in production of Th2 cytokines IL-4 (Fig 7.6 A), IL-9 (C) and IL-13 (D) in all groups following *T. muris* infection. In contrast, ConA re-stimulated MLN cells showed significant production of Th1 cytokine IFN- γ (Fig 7.6 E), pro-inflammatory cytokine IL-6 (G) and anti-inflammatory cytokine IL-10 (I) in all groups following *T. muris* infection. However, ConA re-stimulated MLN cells showed no difference in the production of IL-5 (B) and pro-inflammatory cytokines TNF (G) and IL-17 (I) in all mice groups following *Trichuris* challenge.

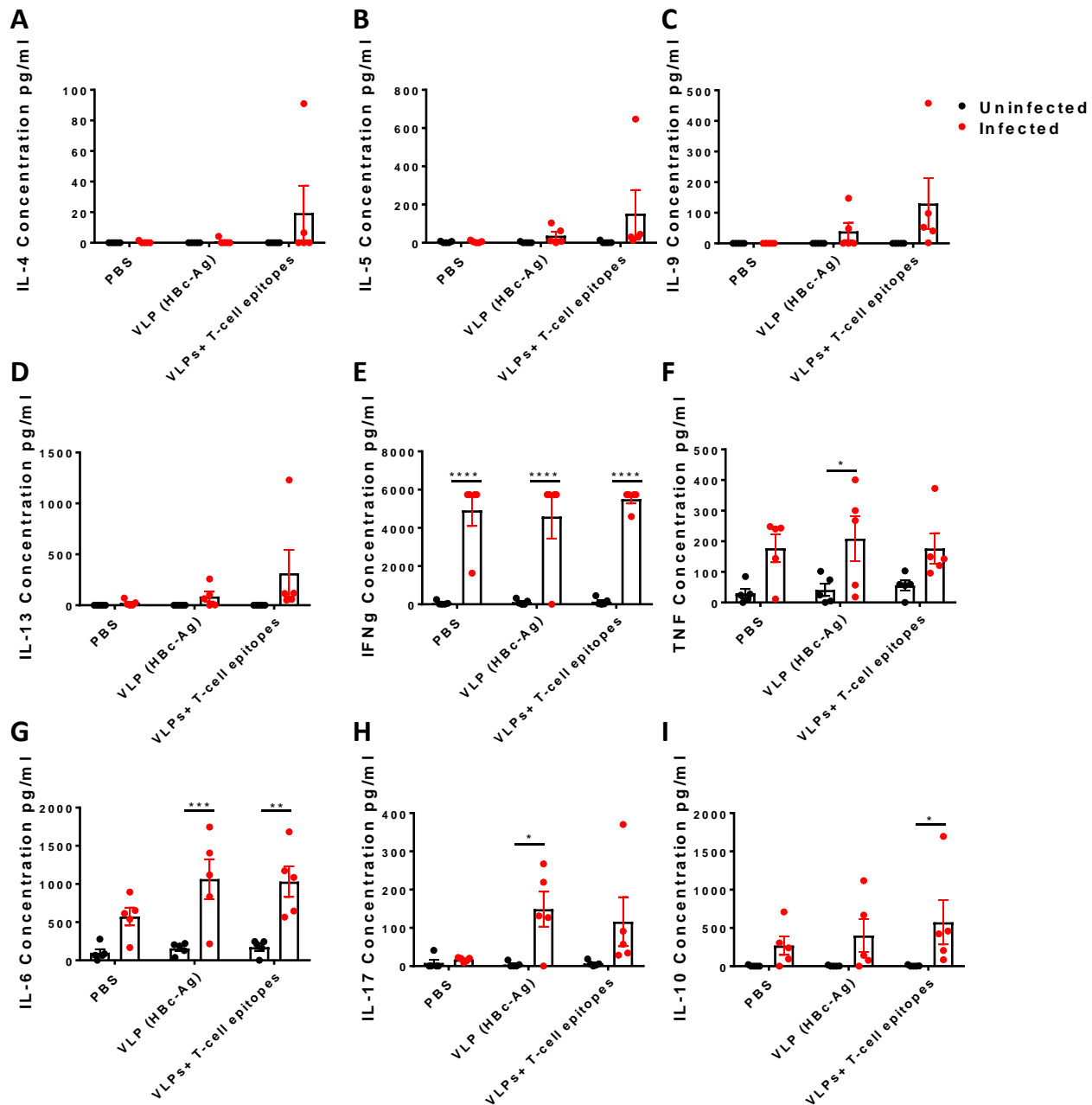


Figure 7.4 Parasite-specific cytokine production by mesenteric lymph node cells from mice vaccinated with VLPs+ T-cell epitopes and control mice. MLNs from mice vaccinated with 25 μ g of pre-mixed VLPs+ T-cell epitopes (HBC-H₁₁₂₋₁₂₈, HBC-CLSP₁₄₃₋₁₅₈, HBC-CBD₁₂₄₃₋₁₂₅₉, and HBC-CBD₂₄₁₋₂₅₇), PBS and 25 μ g VLP (HBC-Ag) groups, with and without *T. muris* infection were stimulated at 5×10^6 /ml with 50 μ g/ml *T. muris* ES. After 48 hours of stimulation, cell culture supernatants were harvested and assayed by cytometric bead array for IL-4 (A), IL-5 (B), IL-9 (C), IL-13 (D), IFN- γ (E), TNF (F), IL-6 (G), IL-17 (H) and IL-10 (I) production. Statistical analyses were carried out using the Two-way ANOVA (multiple comparisons). Significant differences between groups are represented by (* $P \leq 0.05$, ** $P \leq 0.01$, *** $P \leq 0.001$, **** $P \leq 0.0001$) with a line. Results are shown as mean \pm SEM. n= 5 mice per group. The results presented are from one experiment.

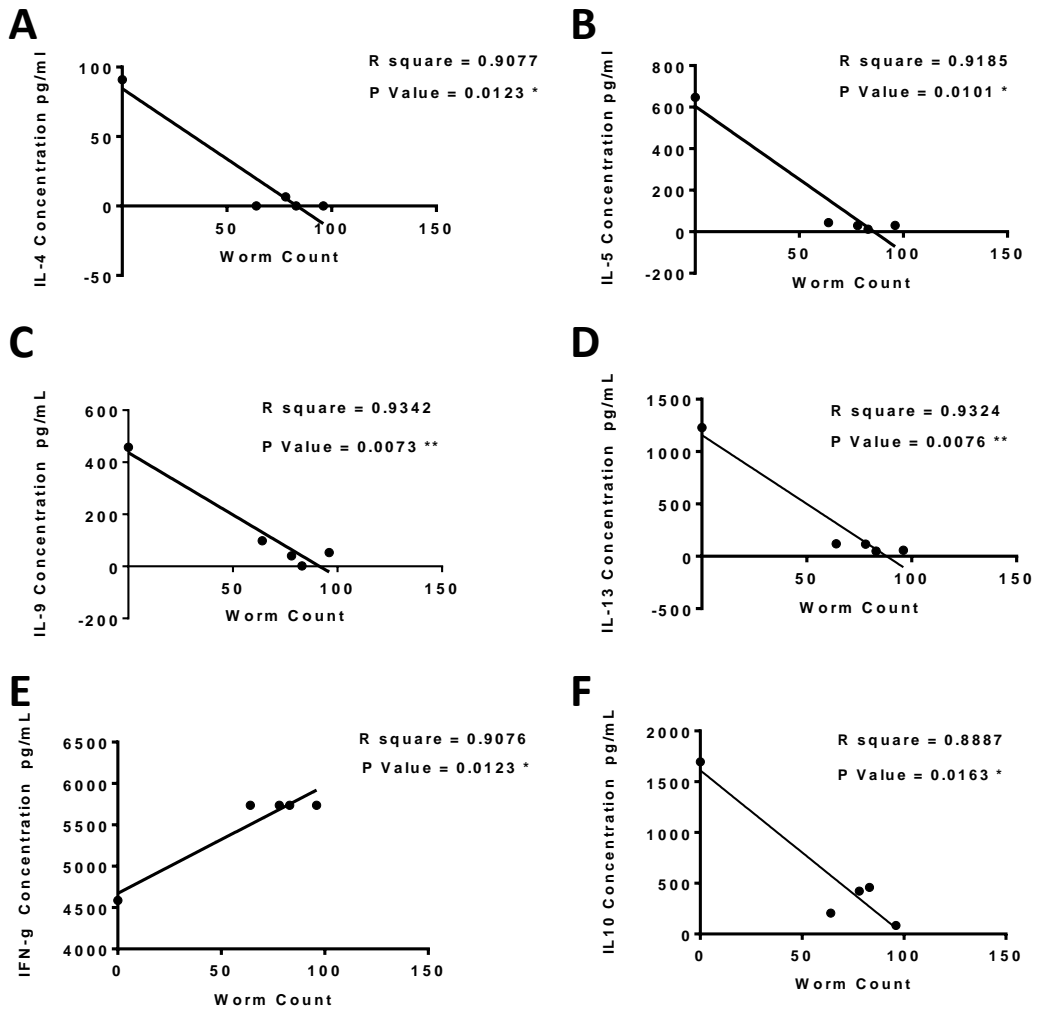


Figure 7.5 The correlation of worm burden with parasite-specific Th2 and anti-inflammatory cytokine production from mice vaccinated with VLPs+ T-cell epitopes. 6 week old male C57BL/6 mice were vaccinated subcutaneously with 25 µg of pre-mixed VLPs+ T-cell epitopes (HBc-H₁₁₂₋₁₂₈, HBc-CLSP₁₄₃₋₁₅₈, HBc-CBD₁₂₄₃₋₁₂₅₉, and HBc-CBD₂₄₁₋₂₅₇) on day -20 and day -10. Mice were then infected by oral gavage with approximately 150 infective *T. muris* eggs and sacrificed at d14. Worm burden were asses at day 14 p.i. by counting the worms from the cecum and colon. MLNs were re-stimulated *in vitro* at 5x10⁶/ml with 50 µg/ml *T. muris* ES. After 48 hours of stimulation, cell culture supernatants were harvested and assayed by cytometric bead array for IL-4 (A), IL-5 (B), IL-9 (C), IL-13 (D), and IFN-Y (E), and IL-10 (F) production. n= 5 mice per group. Significant correlations are represented by (*P≤0.05). The results presented are from one experiment.

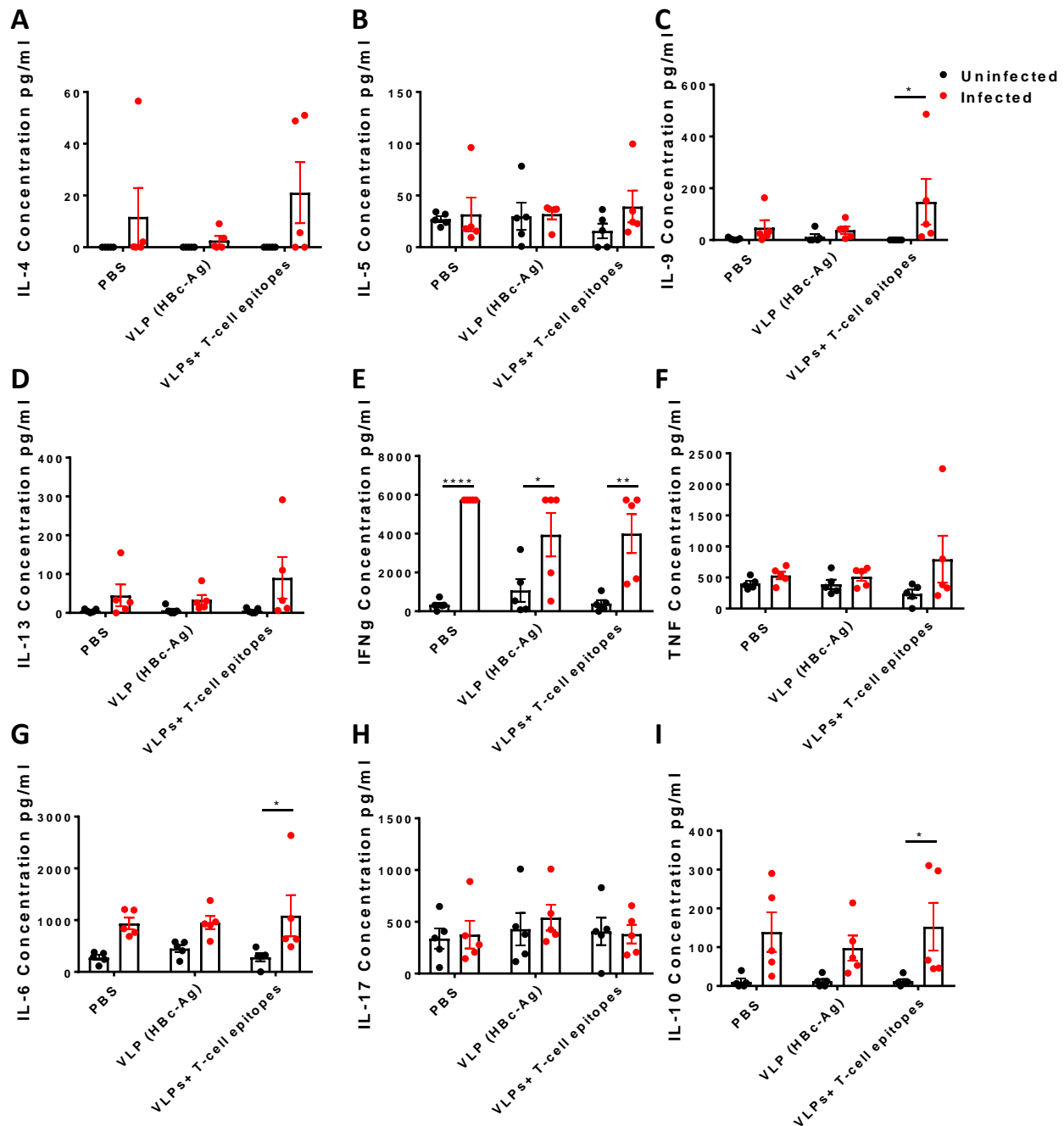


Figure 7.6 Cytokine production by mesenteric lymph node cells from mice vaccinated with VLPs+ T-cell epitopes and control mice. MLNs from mice vaccinated with 25 µg of pre-mixed VLPs+ T-cell epitopes (HBc-H₁₁₂₋₁₂₈, HBc-CLSP₁₄₃₋₁₅₈, HBc-CBD₁₂₄₃₋₁₂₅₉, and HBc-CBD₂₄₁₋₂₅₇), PBS and 25 µg VLP (HBc-Ag) groups, with and without *T. muris* infection. MLNs were stimulated at 5x10⁶/ml with 5 µg/ml ConA and after 24 hours of stimulation, cell culture supernatants were harvested and assayed by cytometric bead array for IL-4 (A), IL-5 (B), IL-9 (C), IL-13 (D), IFN-γ (E), TNF (F), IL-6 (G), IL-17 (H) and IL-10 (I) production. Statistical analyses were carried out using Two-way ANOVA (multiple comparisons). Significant differences between groups are represented by (*P≤0.05, **P≤0.01, ***P≤0.001, ****P≤0.0001) with a line. n= 5 mice per group. Results are shown as mean ± SEM. The results presented are from one experiment.

7.3.1.5 Crypt hyperplasia following vaccination of mice with VLPs expressing *Trichuris* T-cell epitopes

A variety of Th2-regulated effector mechanisms are involved in parasite clearance including epithelial cell turn over (Cliffe and Grencis, 2004; Cliffe et al., 2005), increased muscle hypercontractility (Khan et al., 2003), goblet cell hyperplasia and production of mucins (Artis et al., 2004b). It has been demonstrated that increased epithelial turnover resulting in short crypts is an important mechanism of expulsion in natural resistance BALB/c mice (Cliffe et al., 2005). In contrast, susceptible AKR mice with chronic infection are characterised by crypt hyperplasia under immune control by IFN- γ to regulate epithelial cell proliferation (Artis et al., 1999b; Cliffe et al., 2005). However, crypt hyperplasia was also seen in mice protected from infection by s.c immunisation with ES emulsified with Freund's incomplete adjuvant ES/FIA and PBS/FIA, followed by *Trichuris* infection (Dixon et al., 2010).

The length of colonic crypts was measured in VLPs+ T-cell epitopes, VLP (HBc-Ag) and PBS immunised mice with and without *Trichuris* infection as an index of crypt hyperplasia, as shown in Figure 7.7 (A). Prior to *Trichuris* infection, there was no difference in the average length of colonic crypts between VLPs+ T-cell epitopes, VLP (HBc-Ag), and PBS immunised mice. However, following a challenge infection, all mice groups exhibited crypt hyperplasia, with significant crypt hyperplasia ($P<0.05$) seen in mice vaccinated with VLPs+ T-cell epitopes compared to the PBS, and native VLP (HBc-Ag) injected mice, as shown in Figure 7.7 (B).

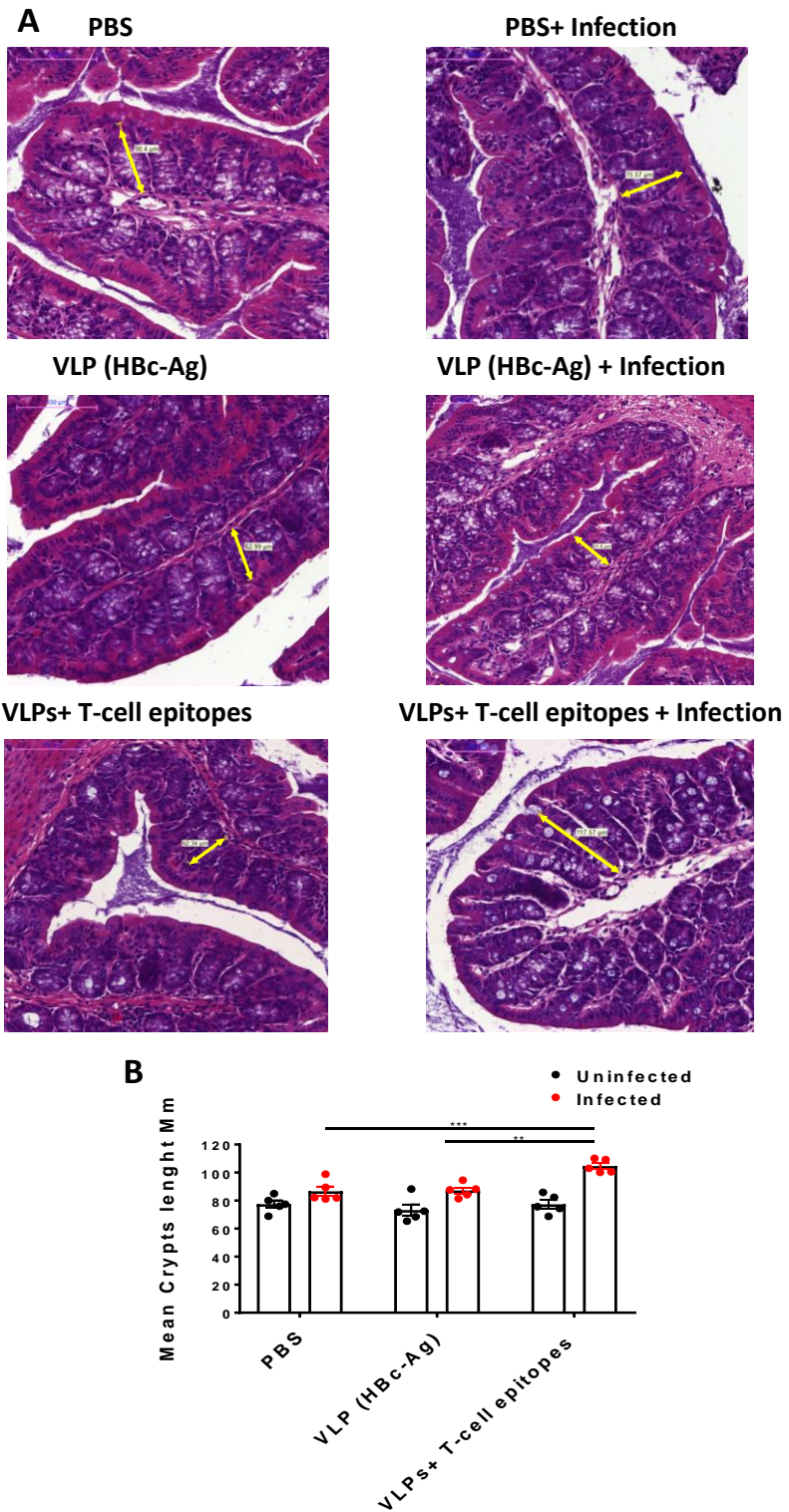


Figure 7.7 Changes in intestinal pathology in *T. muris* infected mice vaccinated with VLPs+ T-cell epitopes and control mice. (A) Representative photographs of gut sections stained with hematoxylin and eosin (H&E). Proximal colon was harvested from mice vaccinated with 25 µg of pre-mixed VLPs+ T-cell epitopes (HBc-H₁₁₂₋₁₂₈, HBc-CLSP₁₄₃₋₁₅₈, HBc-CBD₁₂₄₃₋₁₂₅₉, and HBc-CBD₂₄₁₋₂₅₇), 25 µg VLP (HBc-Ag) and PBS groups with and without *T. muris* infection. All photographs were taken with 20X magnification. Gut pathology assessed by measuring crypt lengths using Panoramic Viewer software. The yellow double-headed arrows show how the crypt lengths were measured. The Results are shown as mean crypt length from 20 crypts units per mouse and shown as the mean values per mouse ±SEM. Statistical analyses were carried out using the Two-way ANOVA (multiple comparisons). Significant differences between groups are represented by (**P≤0.01, ***P≤0.001) with a line. n= 5 mice per group. The results presented are from one experiment.

7.3.1.6 Goblet cells hyperplasia in mice vaccinated with VLPs expressing *Trichuris* T-cell epitopes

As mentioned before, goblet cells and the production of mucins are important in assisting parasite expulsion under the control of Th2 cytokines (IL-13 and IL-9) (Artis et al., 2004b). It has been demonstrated that a marked goblet cell hyperplasia is seen in both susceptible and resistant mice during *T. muris* infection compared to the uninfected naïve mice (Artis et al., 2004b; Cliffe and Grencis, 2004; Datta et al., 2005; Owyang et al., 2006). However, there is a difference in the type of mucin (the major protein component of mucus) produced by intestinal goblet cells between resistant and susceptible mice (Hasnain et al., 2011a; Hasnain et al., 2010).

PAS-stained goblet cells were measured in the mice vaccinated with VLPs+ T-cell epitopes compared to the native VLP (HBc-Ag), and PBS-injected mice with and without *T. muris* infection as an index of goblet cells hyperplasia, as shown in Figure 7.8 (A).

There was no significant increase ($P>0.05$) in the numbers of PAS-stained goblet cells in all the mouse groups prior to *T. muris* infection. However, following *Trichuris* challenge, significant ($P<0.05$) goblet cell hyperplasia was seen in the group vaccinated with VLPs+ T-cell epitopes compared to the native VLP (HBc-Ag) and PBS-injected mice (Figure 7.8 B).

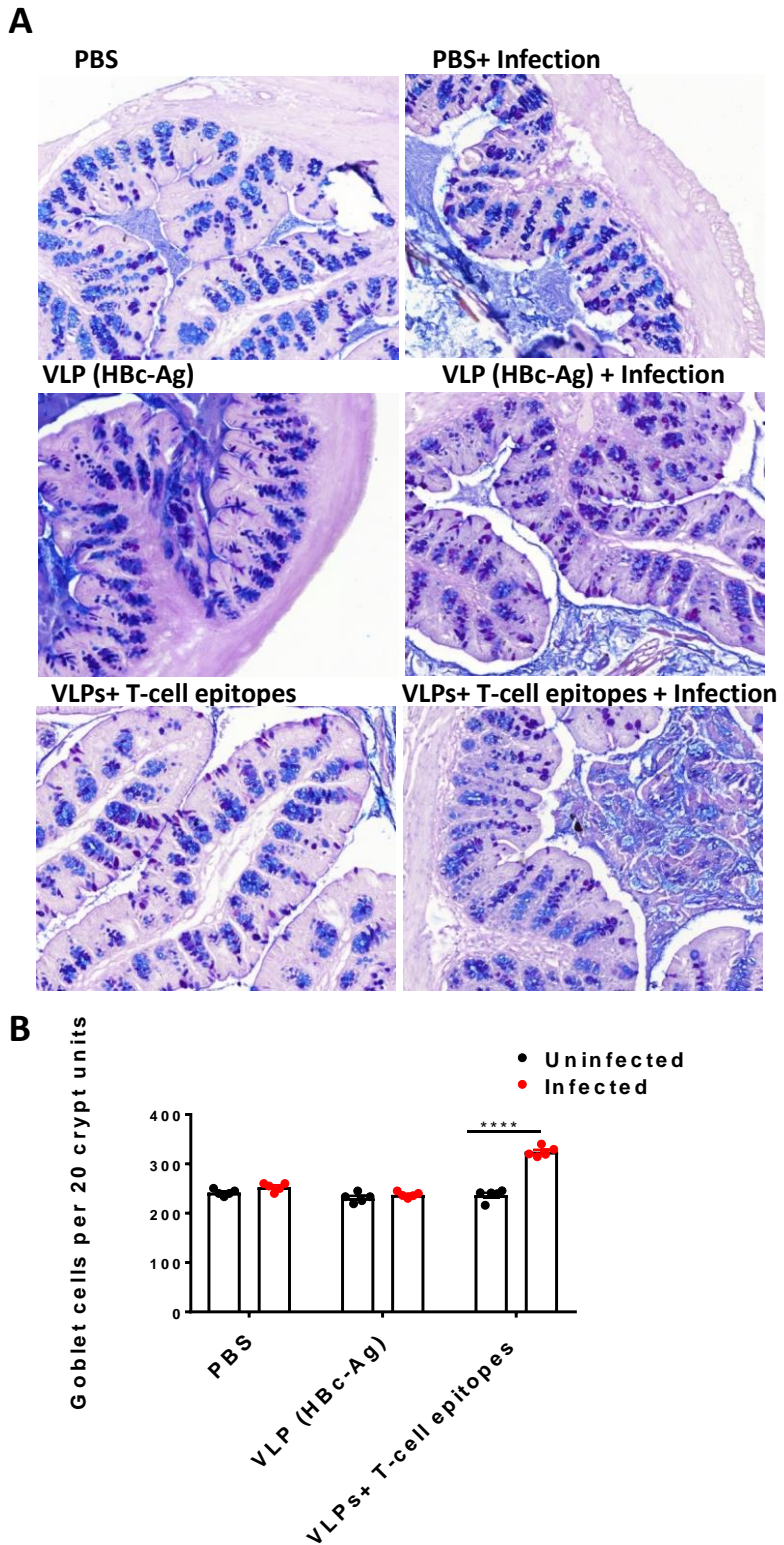


Figure 7.8 Quantification of goblet cell numbers in *T. muris* infected mice vaccinated with VLPs+ T-cell epitopes and control mice. (A) Representative photographs of gut sections stained with Periodic acid–Schiff staining (PAS). Proximal colon was harvested from mice vaccinated with 25 µg of pre-mixed VLPs+ T-cell epitopes (HBc-H₁₁₂₋₁₂₈, HBc-CLSP₁₄₃₋₁₅₈, HBc-CBD₁₂₄₃₋₁₂₅₉, and HBc-CBD₂₄₁₋₂₅₇), 25 µg VLP (HBc-Ag), and PBS groups with and without *T. muris* infection. All photographs were taken with 20X magnification. The slides were scanned, and the goblet cells were quantified using Panoramic Viewer software. All photographs were taken with 20X magnification. (B) Goblet cells were quantified by counting the number of alcian blue-stained cells per crypt unit in three fields of view from each section and are shown as mean cell numbers per 20 crypt units (cu) ±SEM. Statistical analyses were carried out using Two-way ANOVA (multiple comparisons). Significant differences between groups are represented by (*P≤0.05, **P≤0.01, ***P≤0.0001) with a line. n= 5 mice per group. The results presented are from one experiment.

7.3.2 Experimental protocol for *in vivo* evaluation of vaccinating mice with 25 µg of pre-mixed VLPs + *Trichuris* MHC-II T-cell epitopes (HBc-H₁₁₂₋₁₂₈, HBc-CLSP₁₄₃₋₁₅₈, HBc-CLSP₃₉₈₋₄₁₆, and HBc-CBD₂₄₁₋₂₅₇) formulated with AddaVax™ adjuvant

To determine if the addition of an AddaVax™ adjuvant can enhance the immune response to VLPs expressing *Trichuris* T-cell epitopes, 6-week old male C57BL/6 mice were vaccinated subcutaneously with 25 µg of pre-mixed VLPs+ T-cell epitopes (HBc-H₁₁₂₋₁₂₈, HBc-CLSP₁₄₃₋₁₅₈, HBc-CLSP₃₉₈₋₄₁₆, and HBc-CBD₂₄₁₋₂₅₇) formulated with an equal volume of AddaVax adjuvant on day -35 and boosted on day -14. As controls for susceptibility to infection, mice were injected with 25 µg of native VLP (HBc-Ag)/AddaVax, and PBS/AddaVax and as a control for protective immunity, mice were vaccinated with 50 µg ES/AddaVax. Two weeks after the last vaccination, mice were infected by oral gavage with approximately 150 infective *T. muris* eggs on day 0 and sacrificed at day 14 post-infection (Figure 7.9 A).

The vaccine dosing regime was changed to allow efficient time for antibody production and formation of memory immune response in response to the vaccine.

On day 14 p.i., the proximal colon and caecum were removed for worm burden estimation; colonic sections were also collected to assess the pathology and count goblet cells. MLNs were collected and were re-stimulated *in vitro* with *Trichuris* ES for cytokine analysis, while blood was collected to measure serum parasite and VLP+ T-cell epitope-specific IgM, IgG1 and IgG2c antibody levels.

7.3.2.1 25 µg of pre-mixed VLPs expressing *Trichuris* T-cell epitopes formulated with AddaVax adjuvant immunisation did not reduce the *T. muris* worm count following challenge infection

Activation of the innate immune system is essential for the successful induction of protective T-cell responses to control infection. Adjuvants have been traditionally used to stimulate the innate immune system efficiently to increase the magnitude of an adaptive response to a vaccine (Coffman et al., 2010). The AddaVax adjuvant, in particular, is a squalene-based oil-in-water emulsion with a formulation analogous to MF59 has been licensed in most of Europe for pandemic influenza vaccine (Ott et al., 2000; Podda, 2001). The AddaVax adjuvant has been demonstrated to stimulates potent cellular and humoral immune responses and generates marked memory responses (Calabro et al., 2013; Ott et al., 1995), with mixed Th1-Th2 immune responses (Knudsen et al., 2016; O'hagan et al., 2013). The success of AddaVax adjuvant is dependent on inducing the expression of genes involved in leukocyte migration, and antigen-presentation that are both larger and distinct from that induced by other adjuvants including Alum (Mosca et al., 2008).

A vaccine of VLPs expressing *Trichuris* T-cell epitopes (HBc-H₁₁₂₋₁₂₈, HBc-CLSP₁₄₃₋₁₅₈, HBc-CLSP₃₉₈₋₄₁₆, and HBc-CBD₂₄₁₋₂₅₇) formulated with AddaVax was evaluated against the protective vaccine ES/AddaVax and controls of native VLP (HBc-Ag)/AddaVax, and PBS/AddaVax. Choosing to vaccinate mice with 50 µg ES/AddaVax was based on a previous study that showed that vaccinating AKR susceptible mice with 50 µg ES/FIA significantly reduced worm burden at day 21 p.i. (Dixon, 2007). No significant differences were observed in the worm count at day 14 p.i. between VLPs+ T-cell epitopes/AddaVax and control groups. However, vaccinating mice with

ES/AddaVax led to a sterile immunity by day 14 p.i. with a statistically significant reduction in worm burden ($P \leq 0.01$) compared to the PBS/AddaVax and native VLP (HBc-Ag)/AddaVax injected mice (Figure 7.9 B).

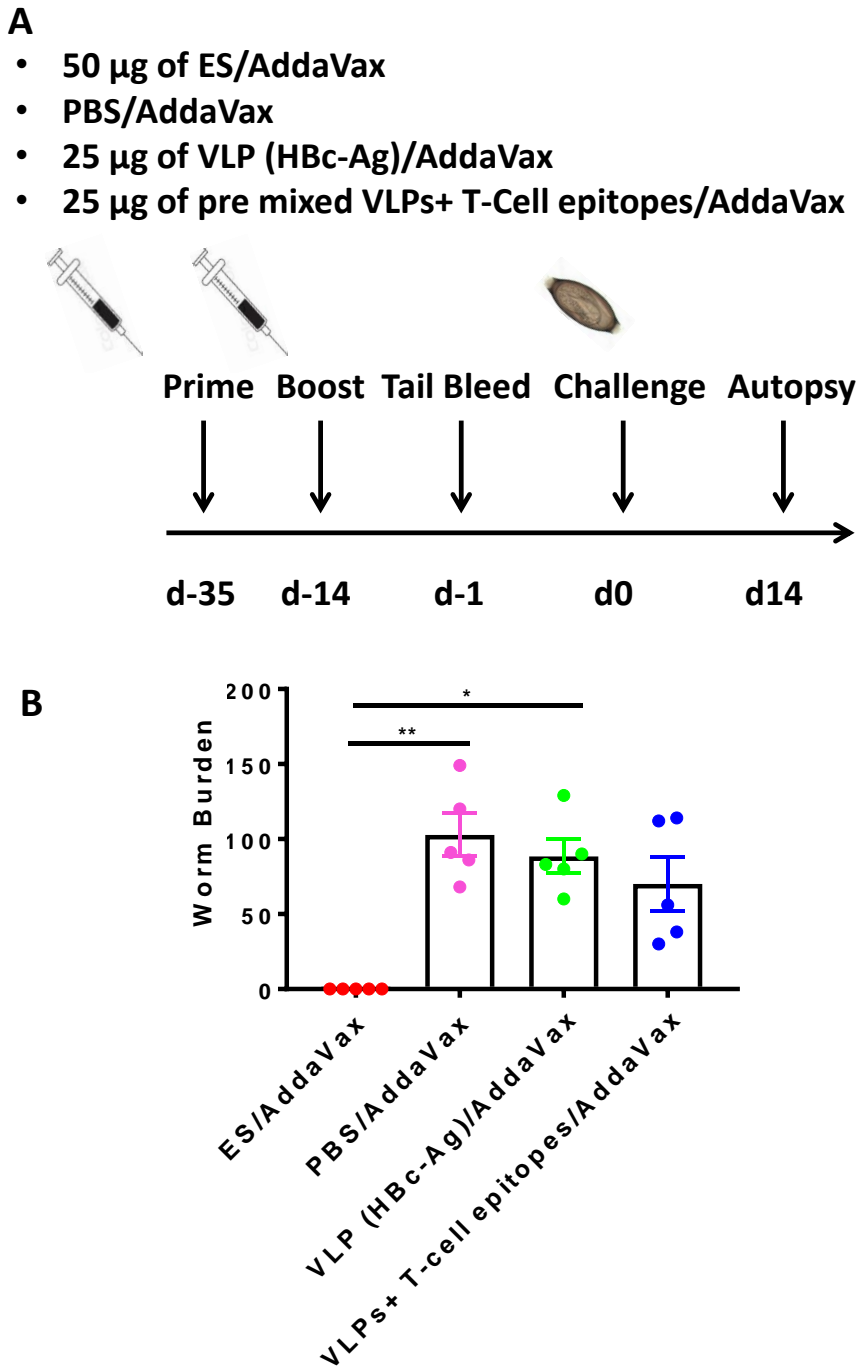


Figure 7.9 Experimental schedule and worm burden of mice vaccinated and challenged with a *T. muris* infection. (A) 6-week old male C57BL/6 mice were vaccinated subcutaneously with 25 µg of pre-mixed of VLPs+ T-cell epitopes (HBc-H₁₁₂₋₁₂₈, HBc-CLSP₁₄₃₋₁₅₈, HBc-CLSP₃₉₈₋₄₁₆, and HBc-CBD₂₄₁₋₂₅₇) formulated with AddaVax™ adjuvant, 25 µg of VLP (HBc-Ag)/AddaVax, 50 µg ES/AddaVax, or PBS/AddaVax on day -35 and boosted on day -14. Tail bleed was taken d-1 and mice were infected by oral gavage with approximately 150 infective *T. muris* eggs on day 0 and sacrificed at d14 post- infection. (B) Comparison of worm burden at day 14 post-infection. Results are shown as mean \pm SEM. Statistical analyses were carried out using the Kruskal-Wallis test (multiple comparisons). Significant differences between groups are represented by (* $P \leq 0.05$ and ** $P \leq 0.01$) with a line. n= 5 mice per group. The results presented are from one experiment.

7.3.2.2 Antigen profile in the sera of vaccinated mice

From the ELISA analysis (see Supplementary Figure 7.2), the serum of mice vaccinated with VLPs+ T-cell epitopes contains IgM antibody recognising *T. muris* ES. Therefore, serum samples from mice vaccinated with ES/AddaVax, and VLPs+ T-cell epitopes (HBc-H₁₁₂₋₁₂₈, HBc-CLSP₁₄₃₋₁₅₈, HBc-CLSP₃₉₈₋₄₁₆, and HBc-CBD₂₄₁₋₂₅₇)/AddaVax and mice injected with PBS/AddaVax, native VLP (HBc-Ag)/AddaVax were tested for their antibody recognition of *T. muris* ES antigens.

T. muris ES components were resolved by SDS-PAGE, transferred to nitrocellulose membrane and subsequently incubated with the serum of each vaccinated mouse separately. Previous work by Dixon et al. (2010) and Else et al. (1990) showed that resistance to *T. muris* infection correlated with serum antibody recognition of high molecular weight proteins in the *T. muris* adult and larval ES. Similarly, the immune serum of mice vaccinated with ES/AddaVax recognised a range of high molecular weight proteins from 37-250 kDa range. The banding pattern recognised by anti-IgM and anti-IgG in the immune serum appeared to reveal no qualitative difference in protein bands, as shown in Figure 7.10 (Lane 1 and 2). In contrast, the immune sera of mice injected with PBS/AddaVax and native VLP (HBc-Ag)/AddaVax did not recognise any protein in the *T. muris* ES. Importantly, serum from mice vaccinated with VLPs+ T-cell epitopes recognised high molecular weight proteins in the *T. muris* ES, suggesting that the H₁₁₂₋₁₂₈, CLSP₁₄₃₋₁₅₈, CBD₁₂₄₃₋₁₂₅₉, and CBD₂₄₁₋₂₅₇ are highly-conserved immunodominant epitopes expressed in several secretory proteins in the ES products of the *T. muris* worm (Fig 7.10 Lane 5).

Furthermore, the ELISA assay revealed that the serum from mice vaccinated with ES/AddaVax recognised the VLPs+ T-cell epitopes recombinant proteins (HBc-H₁₁₂₋₁₂₈, HBc-CLSP₁₄₃₋₁₅₈, and HBc-CBD₁₂₄₃₋₁₂₅₉) (see Supplementary Figure 7.3). Therefore, the presence of an antibody directed against the anti-VLPs+ T-cell epitopes in the serum of mice vaccinated with ES/AddaVax was assessed using western blot.

Moreover, in order to assess whether the antibody in the serum of the mice vaccinated with VLPs+ T-cell epitopes/AddaVax and infected with *T. muris* is specific to the vaccine candidate, the antigen profile in the serum of vaccinated mice was assessed using western blot. A mix of four VLPs+ T-cell epitope proteins was resolved by SDS-PAGE and then subsequently plotted against the serum of each vaccinated mouse separately. Anti-IgG in the serum of mice vaccinated with VLPs+ T-cell epitopes/AddaVax recognised a band around ~22 kDa corresponding to the size of the VLPs+ T-cell epitopes. Remarkably, the IgG in the serum of mice vaccinated with ES/AddaVax recognised the same 22 kDa band. In contrast, the immune sera of PBS/AddaVax-injected mice did not recognise any band, as shown in Figure 7.11.

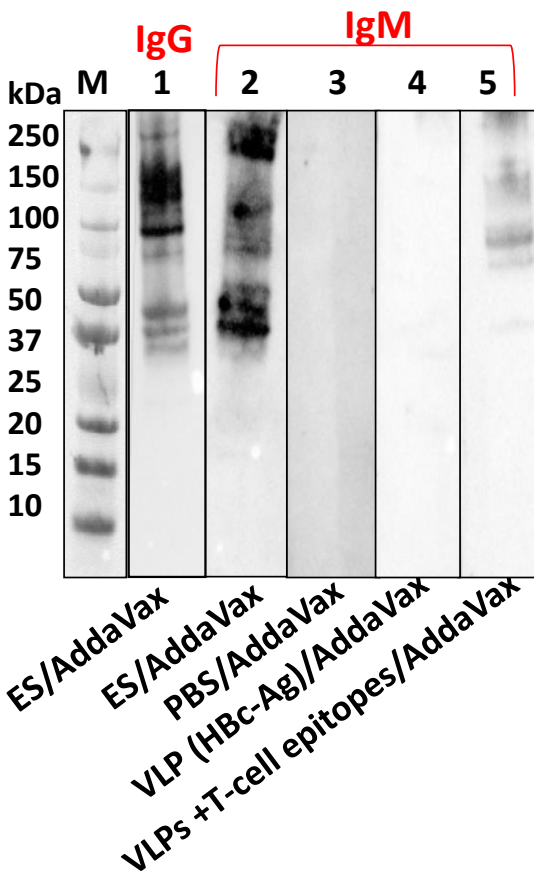


Figure 7.10 Western blots of serum of vaccinated mice and control groups against *T. muris* ES. (M) Precision plus protein all standard blue marker (BIO-RAD) was used as a reference. Mice were vaccinated subcutaneously with 50 µg ES/AddaVax, PBS, 25 µg native VLP (HBc-Ag), and 25 µg VLPs +T-cell epitopes (HBc-H₁₁₂₋₁₂₈, HBc-CLSP₁₄₃₋₁₅₈, HBc-CBD₁₂₄₃₋₁₂₅₉, and HBc-CBD₂₄₁₋₂₅₇), infected by oral gavage with approximately 150 infective *T. muris* eggs and sacrificed at d14. Day 14 sera were blotted against *T. muris* ES. Anti-mouse IgM and anti-IgG were used as secondary antibodies. WB was performed using (1:160) serum dilutions. One mouse per group was chosen to represent the result of its respective group. The results presented are from one experiment.

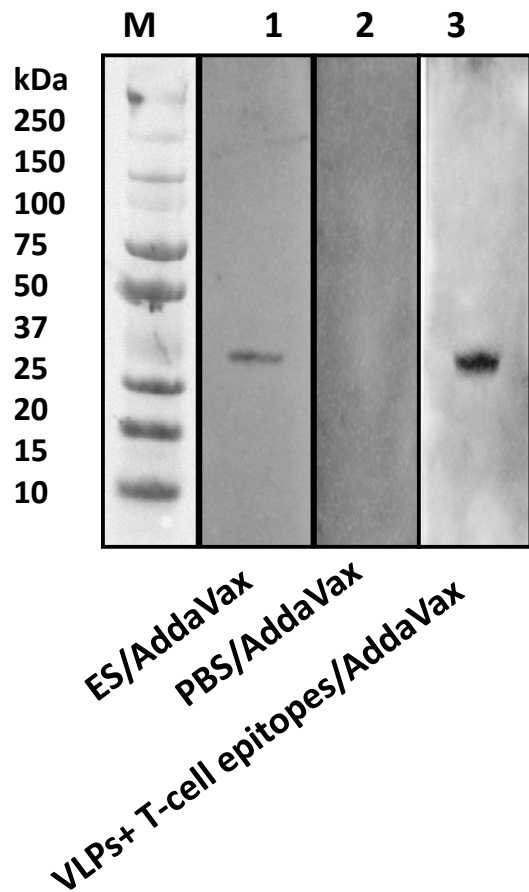


Figure 7.11 Western blots of serum IgG from vaccinated mice and control groups specific for VLPs+ T-cell epitopes proteins. (M) Precision plus protein all standard blue marker (BIO-RAD) was used as a reference. Mice were vaccinated subcutaneously with 50 µg ES/AddaVax, PBS/AddaVax and 25 µg VLPs+ T-cell epitopes (HBc-H₁₁₂₋₁₂₈, HBc-CLSP₁₄₃₋₁₅₈, HBc-CLSP₃₉₈₋₄₁₆, and HBc-CBD₂₄₁₋₂₅₇), on day -35 and boosted on day -14. Mice were infected by oral gavage with approximately 150 infective *T. muris* eggs and sacrificed at d14. Day 14 sera were blotted against pre-mixed VLPs+ T-cell epitopes proteins. Anti-mouse IgG was used as secondary antibodies. WB was performed using (1:160) serum dilutions. One mouse per group was chosen to represent the result of its respective group. The results presented are from one experiment.

7.3.3 Experimental protocol for *in vivo* evaluation of vaccinating mice with 50 µg of pre-mixed VLPs + *Trichuris* MHC-II T-cell epitopes (HBc-CBD₁₂₄₃₋₁₂₅₉, HBc-CBD₂₄₁₋₂₅₇, HBc-CLSP₁₄₃₋₁₅₈, and HBc-CLSP₃₉₈₋₄₁₆)

Based on the first *in vivo* study, immunisation of mice with 25 µg VLPs+ T-cell epitopes did not protect mice from *Trichuris* infection; however, one mouse expelled all the worms. Therefore, a decision was made to increase the dose of the VLPs+ T-cell epitopes vaccine candidate from 25 µg to 50 µg. Furthermore, based on the previous *in vivo* studies, no HBc-H₁₁₂₋₁₂₈-specific IgM antibodies were detected in the serum of mice vaccinated with pre-mixed VLPs+ T-cell epitopes. Therefore, a decision was made to replace this VLPs+ T-cell epitope recombinant protein with HBc-CLSP₃₉₈₋₄₁₆ in the pre-mixed VLPs+ T-cell epitopes vaccine candidate. As including an adjuvant and altering the vaccination regime did not result in protective immunity, the vaccination strategy used in the first experiment was followed.

To determine the protective efficacy of a high-dose of VLPs expressing *Trichuris* T-cell epitopes, C57BL/6 mice were vaccinated subcutaneously with 50 µg of pre-mixed VLPs+ T-cell epitopes (HBc-CBD₁₂₄₃₋₁₂₅₉, HBc-CBD₂₄₁₋₂₅₇, HBc-CLSP₁₄₃₋₁₅₈, and HBc-CLSP₃₉₈₋₄₁₆) on day -20 and boosted on day -10. As controls for susceptibility to infection, mice were injected with PBS and 50 µg of native VLP (HBc-Ag). As a control for protective immunity, mice were vaccinated with 50 µg ES (Dixon et al., 2010) formulated with an equal volume of Alum-aluminium salt adjuvant (Hogenesch, 2013). Ten days after the last vaccination, mice were infected by oral gavage with approximately 150 infective *T. muris* eggs on day 0 and sacrificed at day 14 p.i. (Figure 7.12 A).

The protective efficacy of the vaccine candidate was assessed two weeks post-infection by counting the worms from the proximal colon and caecum of each mouse. MLNs at day 14 p.i. were collected and re-stimulated *in vitro* with *Trichuris* ES for cytokine production, while blood was collected to measure serum parasite and VLP+ T-cell epitope-specific IgM, IgG1 and IgG2c antibody levels.

7.3.3.1 50 µg of pre-mixed VLPs expressing *Trichuris* T-cell epitopes immunisation reduced the *T. muris* worm count following challenge infection

Worm burden in mice immunised with pre-mixed VLPs+ T-cell epitopes (HBc-CBD₁₂₄₃₋₁₂₅₉, HBc-CBD₂₄₁₋₂₅₇, HBc-CLSP₁₄₃₋₁₅₈, and HBc-CLSP₃₉₈₋₄₁₆), ES/Alum, native VLP (HBc-Ag), and PBS at day 14 p.i. is shown in Figure 7.12 (B).

Worm count in susceptible control native VLP (HBc-Ag) group was then used to estimate the mean % reduction in infection as described previously by Chung et al. (2004) using the formula:

$$\% \text{ of reduction} = ((C-V)/C) \times 100$$

Where C is the worm count in mice immunised with native VLP (HBc-Ag), and V is the worm count in mice vaccinated with VLPs+ T-cell epitopes following *T. muris* infection.

Remarkably, vaccination with VLPs+ T-cell epitopes showed a statistically significant ($P<0.05$) reduction in worm burden (51.2%) by day 14 p.i.

A

- 50 µg ES/Alum
- PBS
- 50 µg VLP (HBc-Ag)
- 50 µg of pre mixed VLPs+ T-cell epitopes

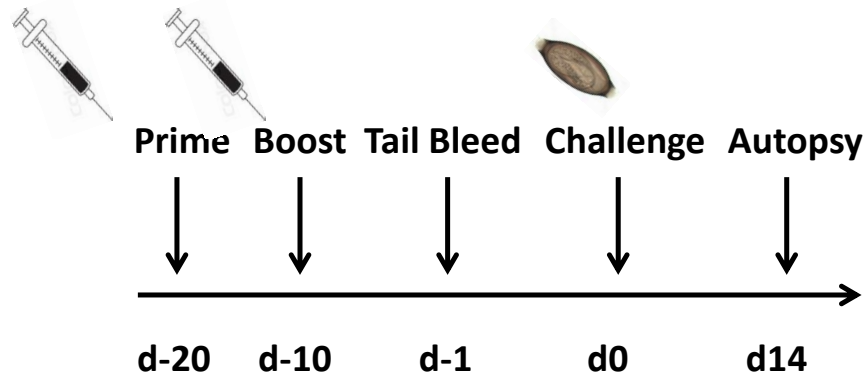
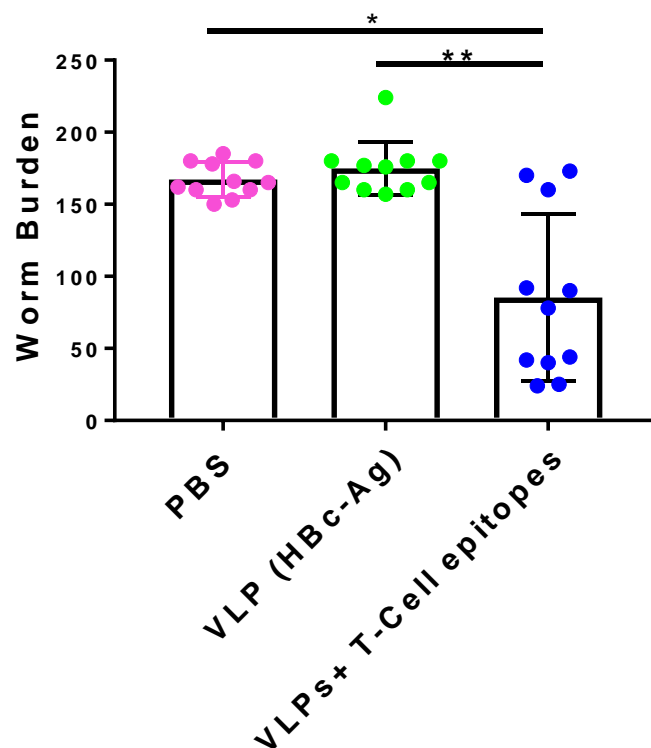
**B**

Figure 7.12 Experimental schedule and worm burden of mice vaccinated and challenged with a *T. muris* infection. 6-week old male C57BL/6 mice were vaccinated subcutaneously with 50 µg of pre-mixed of VLPs+ T-cell epitopes (HBc-CBD₁₂₄₃₋₁₂₅₉, HBc-CBD₂₄₁₋₂₅₇, HBc-CLSP₁₄₃₋₁₅₈, and HBc-CLSP₃₉₈₋₄₁₆), 50 µg of VLP (HBc-Ag), or PBS on day -20 and boosted on day -10. Tail bleed was taken d-1 and mice were infected by oral gavage with approximately 150 infective *T. muris* eggs on day 0 and sacrificed at d14 post-infection. (B) Comparison of worm burden at day 14 post-infection. Statistical analyses were carried out using the Kruskal-Wallis test (multiple comparisons). Significant differences between groups are represented by (****P≤0.0001) with a line. Results are shown as mean ± SEM. n= 11 mice per group. The results presented are from two separated experiments pooled together.

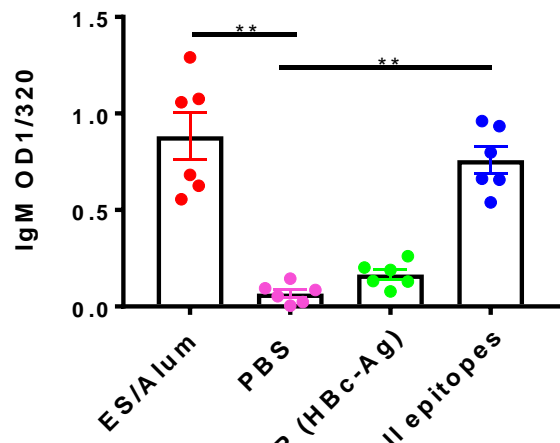
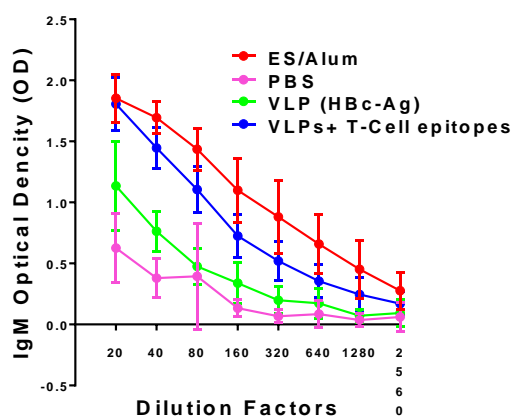
7.3.3.2 Serum parasite-specific responses following vaccination of mice with VLPs expressing *Trichuris* T-cell epitopes

To evaluate *T. muris*-specific serum antibody responses induced by vaccination with VLPs+ T-cell epitopes, parasite-specific IgM, IgG1, and IgG2c serum antibody levels were determined at d-1 and d14 p.i.. Notably, mice vaccinated with VLPs+ T-cell epitopes and ES/Alum produced similarly statistically significant higher levels of parasite-specific IgM serum antibody compared to the PBS, and native VLP (HBc-Ag) injected control groups prior to infection (Figure 7.13 A). In contrast, mice vaccinated with ES/Alum produced significantly higher levels of parasite-specific IgG1 prior to infection compared to the PBS, and native VLP (HBc-Ag) injected control groups. However, mice vaccinated with VLP+T cell epitopes produced only negligible levels of parasite-specific IgG1 prior to infection, as shown in Figure 7.13 (B).

Following vaccination and infection, VLPs+ T-cell epitopes and ES/Alum vaccinated mice had statistically significant higher levels parasite-specific IgM (Figure 7.14 A) and IgG2c (C) compared to the control PBS and native VLP (HBc-Ag) injected mice. However, high levels of parasite-specific IgG1 were only detected in the serum of mice vaccinated with ES/Alum following *Trichuris* infection (Figure 7.14 B). There was no or very low levels of parasite-specific IgM, IgG1, and IgG2c detected in the serum of native VLP (HBc-Ag) and PBS/FIA injected mice at day 14 p.i., as shown in Figure 7.14 (A-C).

Collectively, these results demonstrate that the VLPs+ T-cell epitopes vaccine candidate boosted parasite-specific humoral immune responses.

A) Parasite-specific IgM



B) Parasite-specific IgG1

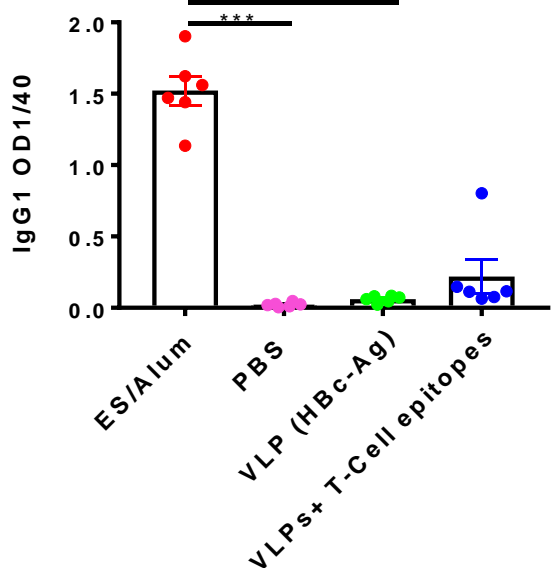
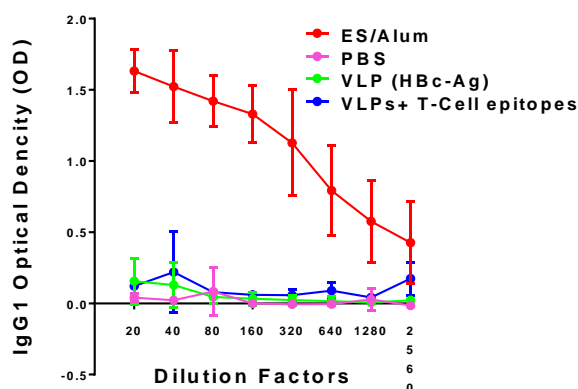


Figure 7.13 Parasite-specific IgM and IgG1 serum antibodies levels at day -1. 6-week old male C57BL/6 mice were vaccinated subcutaneously with 50 µg of pre-mixed of VLPs+ T-cell epitopes (HBc-CBD₁₂₄₃₋₁₂₅₉, HBc-CBD₂₄₁₋₂₅₇, HBc-CLSP₁₄₃₋₁₅₈, and HBc-CLSP₃₉₈₋₄₁₆), 50 µg of VLP (HBc-Ag), 50 µg ES/Alum, or PBS on day -20 and boosted on day -10. Tail bleed was taken d-1 and mice were infected by oral gavage with approximately 150 infective *T. muris* eggs on day 0 and sacrificed at d14 post-infection. Day -1 sera were titrated against *T. muris* ES antigens to assess parasite-specific IgM (A) IgG1, and IgG1 (B) levels in VLPs+ T-cell epitopes, VLP (HBc-Ag), PBS and in ES vaccinated mice by ELISA (reading at 405 nm). Statistical analyses were carried out at 1:320 (IgM) and 1:40 (IgG1) serum dilutions using the Kruskal-Wallis test (multiple comparisons). Significant differences between groups are represented by (*P≤0.05, **P≤0.01, ***P≤0.001, ****P≤0.0001) with a line. Results are shown as mean ± 1 SEM. n= 6 mice per group. This experiment was repeated two times, and the results shown here are representative of one experiment.

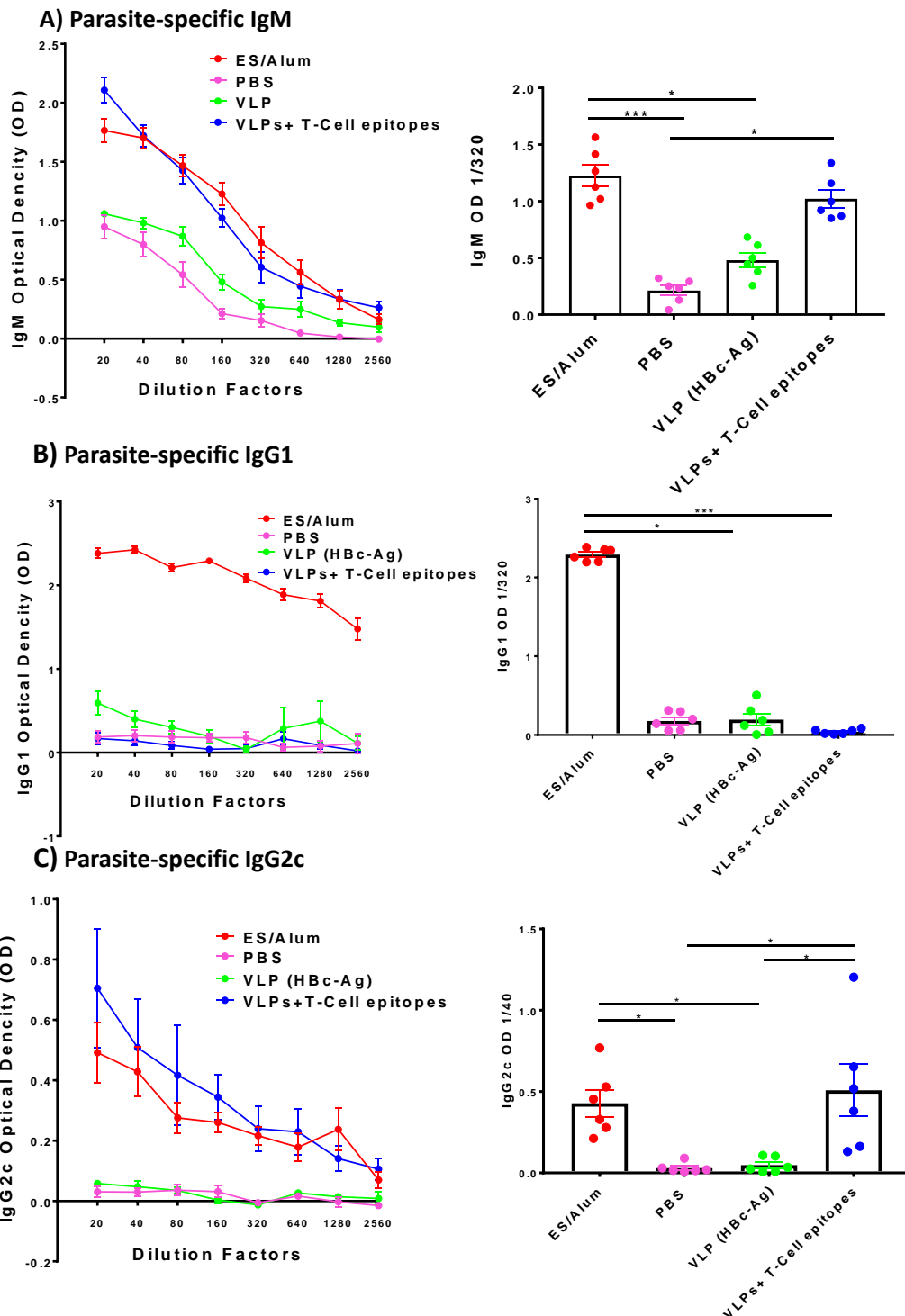


Figure 7.14 Parasite-specific IgM, IgG1 and IgG2c serum antibodies levels at day 14 post-infection. 6-week old male C57BL/6 mice were vaccinated subcutaneously with 50 µg of pre-mixed of VLPs+ T-cell epitopes (HBc-CBD₁₂₄₃₋₁₂₅₉, HBc-CBD₂₄₁₋₂₅₇, HBc-CLSP₁₄₃₋₁₅₈, and HBc-CLSP₃₉₈₋₄₁₆), 50 µg of VLP (HBc-Ag), 50 µg ES/Alum, or PBS on day -20 and boosted on day -10. Tail bleed was taken d-1 and mice were infected by oral gavage with approximately 150 infective *T. muris* eggs on day 0 and sacrificed at d14 post-infection. Day 14 p.i. sera were titrated against *T. muris* ES antigens to assess parasite-specific IgM (A) IgG1 (B), and IgG2c (C) levels in VLPs+ T-cell epitopes, VLP (HBc-Ag), PBS and in ES vaccinated mice by ELISA (reading at 405 nm). Statistical analyses were carried out at 1:320 (IgM and IgG1) and 1:40 (IgG2c) serum dilutions using Kruskal-Wallis test (multiple comparisons). Significant differences between groups are represented by (*P≤0.05, **P≤0.01, ***P≤0.001, ****P≤0.0001) with a line. Results are shown as mean ± SEM. n= 6 mice per group. This experiment was repeated two times, and the results shown here are representative of the two experiments.

7.3.3.3 Serum VLP+T cell epitope-specific responses following vaccination of mice with VLPs expressing *Trichuris* T-cell epitopes

The isotype profiles of antibodies elicited by VLPs+ T-cell epitopes were analysed using an ELISA-based assay at d-1 and d 14 p.i.. ELISA plates were coated with pre-mixed VLPs+ T-cell epitopes (HBc-CBD₁₂₄₃₋₁₂₅₉, HBc-CBD₂₄₁₋₂₅₇, HBc-CLSP₁₄₃₋₁₅₈, and HBc-CLSP₃₉₈₋₄₁₆) and with individual VLP+T cell epitope recombinant protein as detection antigens. All serum from mice vaccinated with VLPs+ T-cell epitopes displayed strong reactivity to the pre-mixed VLPs+ T-cell epitopes proteins. Statistically significant higher levels of VLPs+ T-cell epitopes-specific IgM (Figure 7. 15 A) and IgG1 (B) were measured at d-1 compared to the ES/Alum, PBS and VLP (HBc-Ag) immunised groups. Similarly, statistically significant higher levels of VLPs+ T-cell epitopes-specific IgM (Figure 7.16 A), IgG1 (B) and IgG2c (C) were produced following *Trichuris* infection. Notably, mice vaccinated with ES/Alum also produced high levels of VLPs+ T-cell epitopes-specific IgM following *Trichuris* infection, as shown in Figure 7.16 (A).

Furthermore, serum from mice vaccinated with the VLPs+ T-cell epitopes reacted with their corresponding VLP+T cell epitope recombinant protein but not the native VLP (HBc-Ag) protein. Significantly higher levels of VLP+ T-cell epitope specific-IgM (Figure 7.17 A-D), IgG1 (Figure 7.18 A-D), and IgG2c (Figure 7.19 A-D) were measured in the serum of mice vaccinated with VLPs+ T-cell epitopes compared to the ES/Alum, and PBS immunised mice groups. Furthermore, lower or background levels of native VLP (HBc-Ag) specific-IgM (Figure 7.17 A), and IgG2c (Figure 7.19 A) were detected in the sera of mice vaccinated with VLPs+ T-cell epitopes. However, low levels of native VLP (HBc-Ag) specific-IgG1 were detected in the sera of mice vaccinated with VLPs+ T-cell epitopes and native VLP (HBc-Ag) immunised group (Figure 7.18 A).

Collectively, these results demonstrate that vaccinating mice with VLPs+ T-cell epitopes induced strong humoral immune responses specific to the four VLPs+ T-cell epitopes recombinant proteins.

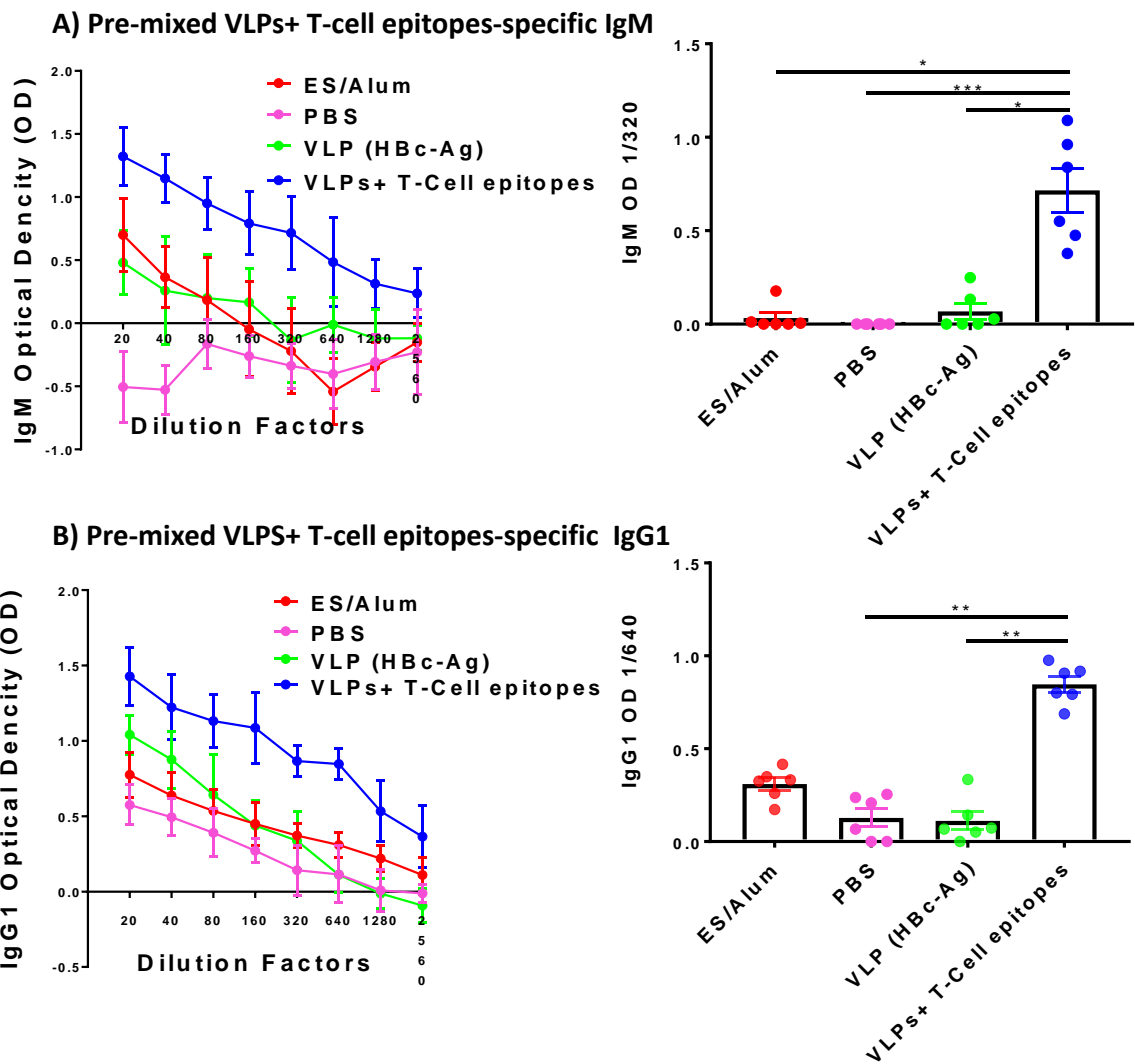


Figure 7.15 Pre-mixed VLPs+ T-cell epitopes-specific IgM and IgG1 serum antibodies levels at day -1. 6-week old male C57BL/6 mice were vaccinated subcutaneously with 50 µg of pre-mixed of VLPs+ T-cell epitopes (HBc-CBD₁₂₄₃₋₁₂₅₉, HBc-CBD₂₄₁₋₂₅₇, HBc-CLSP₁₄₃₋₁₅₈, and HBc-CLSP₃₉₈₋₄₁₆), 50 µg of VLP (HBc-Ag), 50 µg ES/Alum, or PBS on day -20 and boosted on day -10. Tail bleed was taken d-1 and mice were infected by oral gavage with approximately 150 infective *T. muris* eggs on day 0 and sacrificed at d14 post-infection. Day -1 sera were titrated against a cocktail of VLPs+ T-cell epitopes proteins (HBc-CBD₁₂₄₃₋₁₂₅₉, HBc-CBD₂₄₁₋₂₅₇, HBc-CLSP₁₄₃₋₁₅₈ and HBc-CLSP₃₉₈₋₄₁₆) to assess VLPs-specific IgM (A) and IgG1 (B) levels in VLPs+ T-cell epitopes, VLP (HBc-Ag), PBS and in ES vaccinated mice by ELISA (reading at 405 nm). Statistical analyses were carried out at 1:320 (IgM) and 1:640 (IgG1) serum dilutions using the Kruskal-Wallis test (multiple comparisons). Significant differences between groups are represented by (*P≤0.05, **P≤0.01, ***P≤0.001, ****P≤0.0001) with a line. Results are shown as mean ± SEM. n= 6 mice per group. This experiment was repeated two times, and the results shown here are representative of the two experiments.

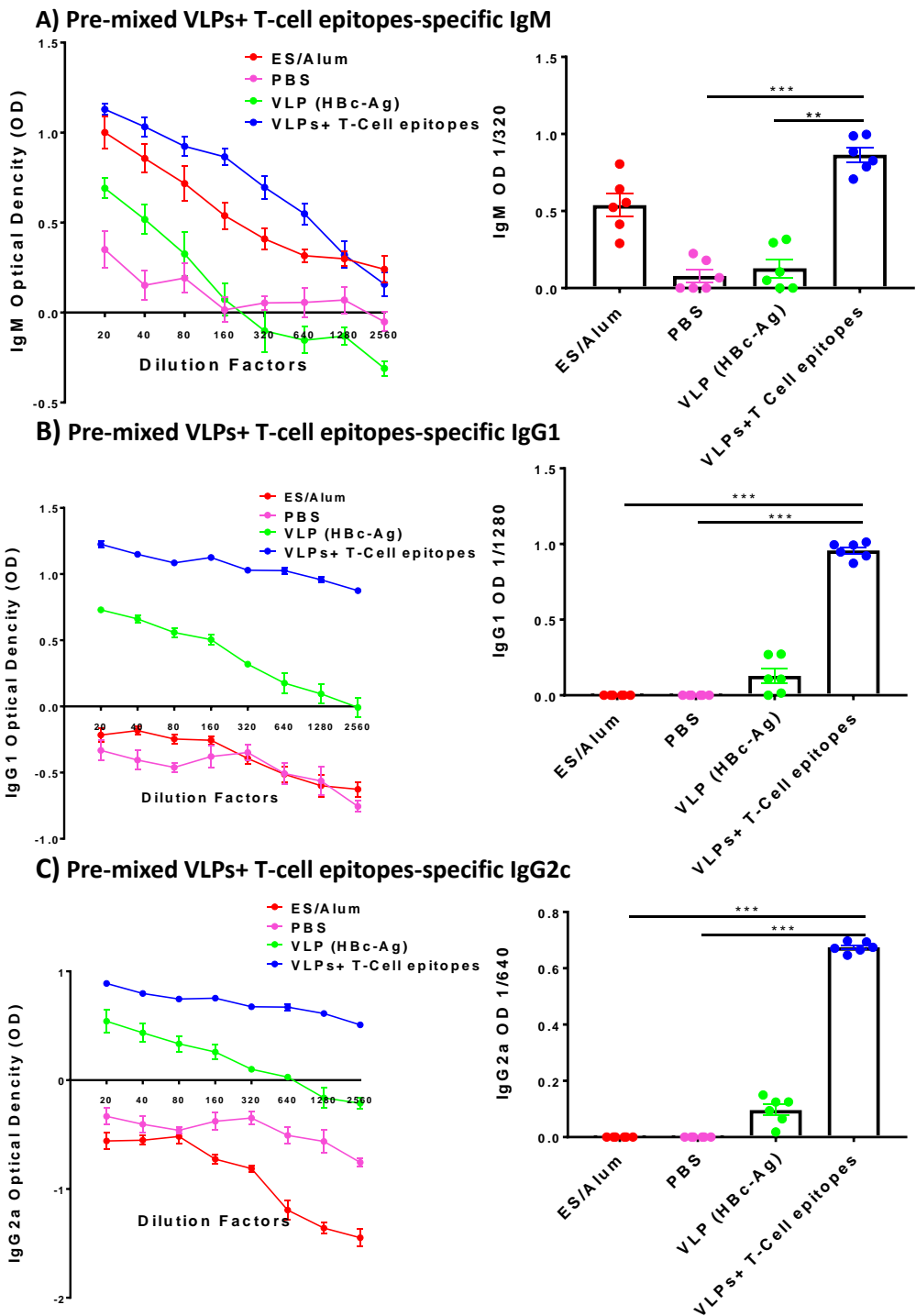
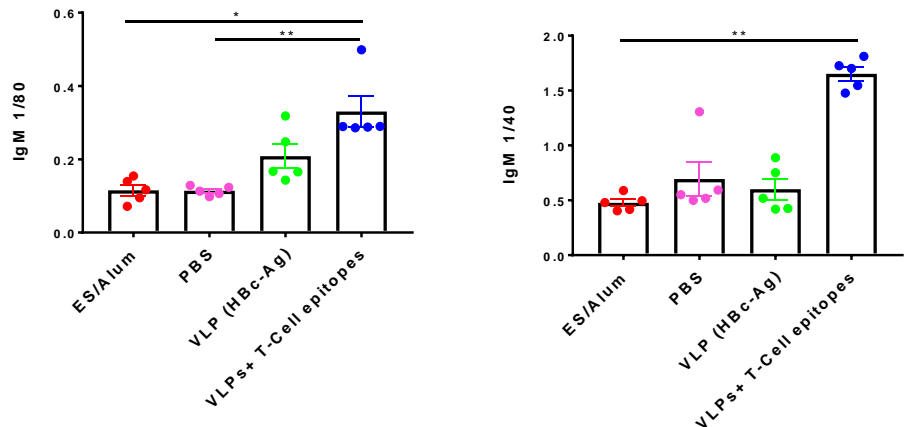
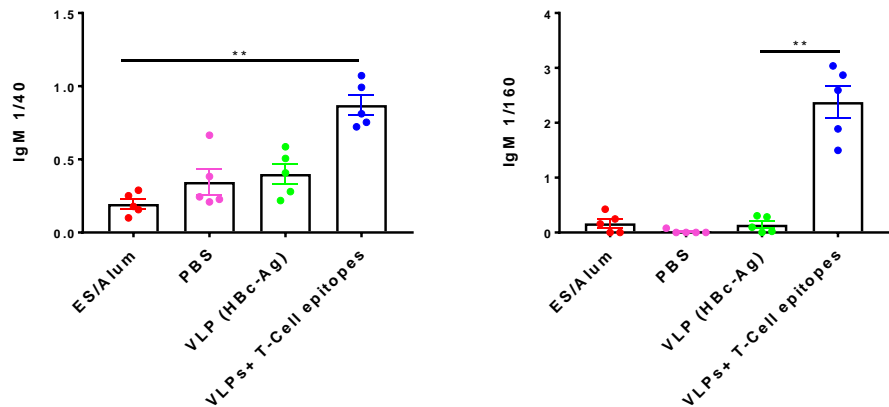


Figure 7.16 Pre-mixed VLP+ T-cell epitope-specific IgM, IgG1 and IgG2c levels at day 14 post-infection (p.i.). 6-week old male C57BL/6 mice were vaccinated subcutaneously with 50 µg of pre-mixed of VLPs+ T-cell epitopes (HBc-CBD₁₂₄₃₋₁₂₅₉, HBc-CBD₂₄₁₋₂₅₇, HBc-CLSP₁₄₃₋₁₅₈, and HBc-CLSP₃₉₈₋₄₁₆), 50 µg of VLP (HBc-Ag), 50 µg ES/Alum, or PBS on day -20 and boosted on day -10. Tail bleed was taken d-1 and mice were infected by oral gavage with approximately 150 infective *T. muris* eggs on day 0 and sacrificed at d14 post-infection. Day 14 p.i. sera were titrated against pre-mixed VLPs (HBc-CBD₁₂₄₃₋₁₂₅₉, HBc-CBD₂₄₁₋₂₅₇, HBc-CLSP₁₄₃₋₁₅₈ and HBc-CLSP₃₉₈₋₄₁₆) to assess VLPs-specific IgM (A), IgG1 (B), and IgG2c (C) levels in VLPs+ T-cell epitopes, VLP (HBc-Ag), PBS and in ES vaccinated mice by ELISA (reading at 405 nm). Statistical analyses were carried out at 1:320 (IgM) and 1:1280 (IgG1), 1:640 (IgG2c) serum dilutions using the Kruskal-Wallis test (multiple comparisons). Significant differences between groups are represented by (*P≤0.05, **P≤0.01, ***P≤0.001, ****P≤0.0001) with a line. Negative values were adjusted to 0. Results are shown as mean ± SEM. n= 6 mice per group. This experiment was repeated two times, and the results shown here are representative of the two experiments.

A) VLP (HBc-Ag)-specific IgM B) HBc-CBD₁₂₄₃₋₁₂₅₉-specific IgM



C) HBc-CBD₂₄₁₋₂₅₇-specific IgM D) HBc-CLSP₁₄₃₋₁₅₈-specific IgM



E) HBc-CLSP₃₉₈₋₄₁₆-specific IgM

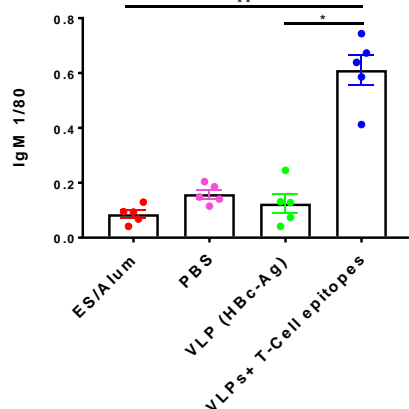
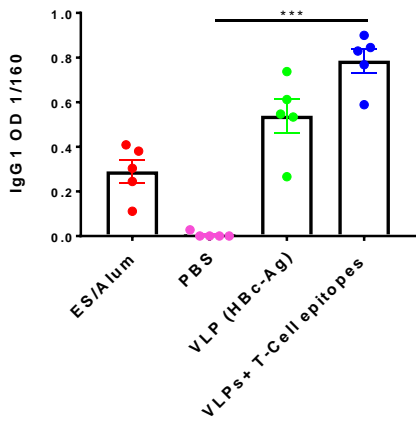
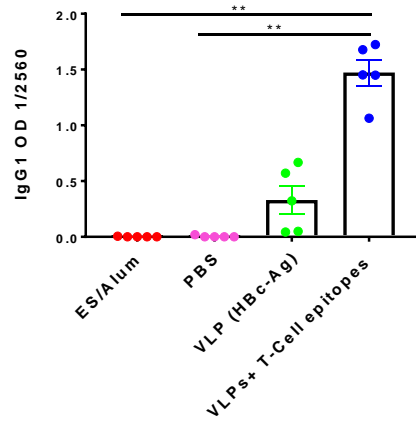


Figure 7.17 Native VLP (HBc-Ag) and VLP+ T-cell epitope-specific IgM levels at day 14 post-infection (p.i.). 6-week old male C57BL/6 mice were vaccinated subcutaneously with 50 µg of pre-mixed of VLPs+ T-cell epitopes (HBc-CBD₁₂₄₃₋₁₂₅₉, HBc-CBD₂₄₁₋₂₅₇, HBc-CLSP₁₄₃₋₁₅₈, and HBc-CLSP₃₉₈₋₄₁₆), 50 µg of VLP (HBc-Ag), 50 µg ES/Alum, or PBS on day -20 and boosted on day -10. Tail bleed was taken d-1 and mice were infected by oral gavage with approximately 150 infective *T. muris* eggs on day 0 and sacrificed at d14 post-infection. Day 14 p.i. sera were titrated against VLP (HBc-Ag) (A), HBc-CBD₁₂₄₃₋₁₂₅₉ (B), HBc-CBD₂₄₁₋₂₅₇ (C), HBc-CLSP₁₄₃₋₁₅₈ (D) and HBc-CLSP₃₉₈₋₄₁₆ (E) to assess VLPs-specific IgM by ELISA (reading at 405 nm). Statistical analyses were carried out at 1:40, 1:60 and 1:80 serum dilutions using the Kruskal-Wallis test (multiple comparisons). Significant differences between groups are represented by (*P≤0.05, **P≤0.01, ***P≤0.001, ****P≤0.0001) with a line. Negative values were adjusted to 0. Results are shown as mean ± SEM. n= 5 mice per group. This experiment was repeated two times, and the results shown here are representative of the two experiments.

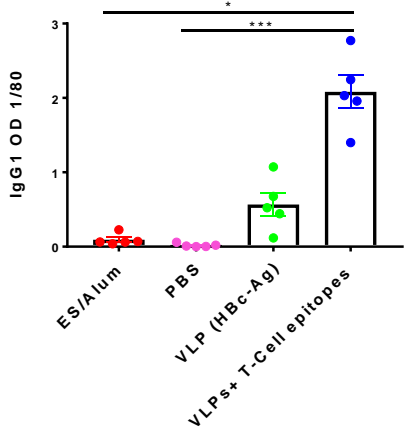
A) VLP (HBc-Ag)-specific IgG1



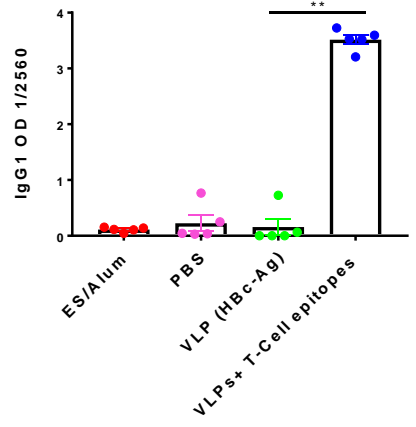
B) HBc-CBD₁₂₄₃₋₁₂₅₉-specific IgG1



C) HBc-CBD₂₄₁₋₂₅₇-specific IgG1



D) HBc-CLSP₁₄₃₋₁₅₈-specific IgG1



E) HBc-CLSP₃₉₈₋₄₁₆-specific IgG1

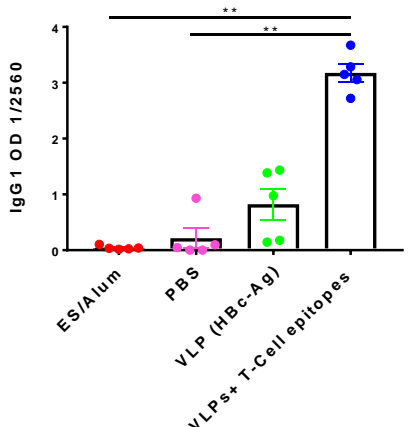
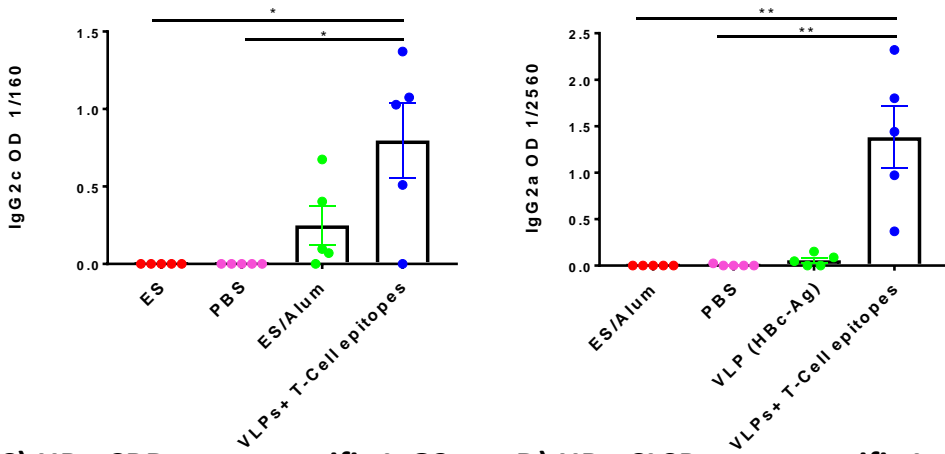
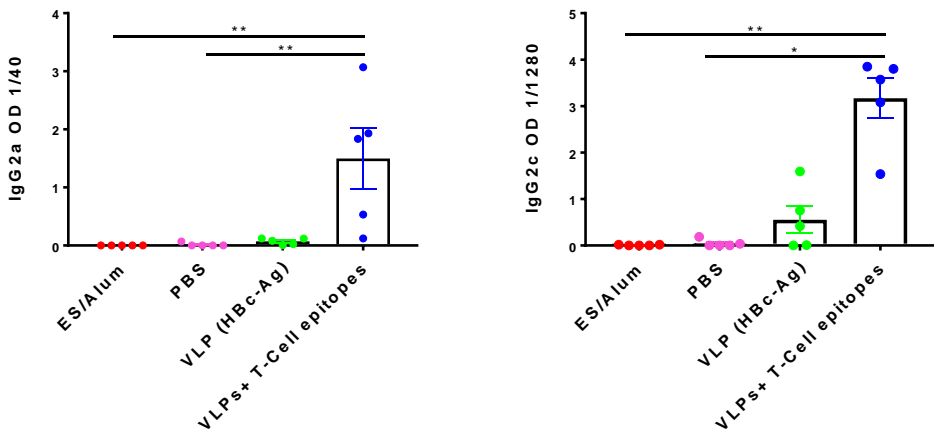


Figure 7.18 Native VLP (HBc-Ag) and VLP+ T-cell epitope-specific IgG1 levels at day 14 post-infection (p.i.). 6-week old male C57BL/6 mice were vaccinated subcutaneously with 50 µg of pre-mixed of VLPs+ T-cell epitopes (HBc-CBD₁₂₄₃₋₁₂₅₉, HBc-CBD₂₄₁₋₂₅₇, HBc-CLSP₁₄₃₋₁₅₈, and HBc-CLSP₃₉₈₋₄₁₆), 50 µg of VLP (HBc-Ag), 50 µg ES/ Alum, or PBS on day -20 and boosted on day -10. Tail bleed was taken d-1 and mice were infected by oral gavage with approximately 150 infective *T. muris* eggs on day 0 and sacrificed at d14 post-infection. Day 14 p.i. sera were titrated against VLP (HBc-Ag) (A), HBc-CBD₁₂₄₃₋₁₂₅₉ (B), HBc-CBD₂₄₁₋₂₅₇ (C), HBc-CLSP₁₄₃₋₁₅₈ (D) and HBc-CLSP₃₉₈₋₄₁₆ (E) to assess VLPs-specific IgG1 by ELISA (reading at 405 nm). Statistical analyses were carried out at 1:80, 1:160 and 1:2560 serum dilutions using the Kruskal-Wallis test (multiple comparisons). Significant differences between groups are represented by (*P≤0.05, **P≤0.01, ***P≤0.001, ****P≤0.0001) with a line. Negative values were adjusted to 0. Results are shown as mean ± SEM. n= 5 mice per group. This experiment was repeated two times, and the results shown here are representative of the two experiments.

A) VLP (HBc-Ag)-specific IgG2c B) HBc-CBD₁₂₄₃₋₁₂₅₉-specific IgG2c



C) HBc-CBD₂₄₁₋₂₅₇-specific IgG2c D) HBc-CLSP₁₄₃₋₁₅₈-specific IgG2c



E) HBc-CLSP₃₉₈₋₄₁₆-specific IgG2c

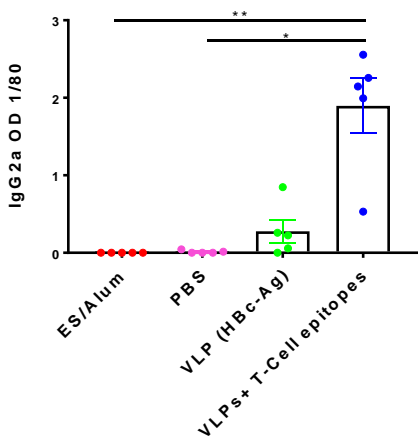


Figure 7.19 Native VLP (HBc-Ag) and VLP+ T-cell epitope-specific IgG2c levels at day 14 post-infection (p.i.). 6-week old male C57BL/6 mice were vaccinated subcutaneously with 50 µg of pre-mixed of VLPs+ T-cell epitopes (HBc-CBD₁₂₄₃₋₁₂₅₉, HBc-CBD₂₄₁₋₂₅₇, HBc-CLSP₁₄₃₋₁₅₈, and HBc-CLSP₃₉₈₋₄₁₆), 50 µg of VLP (HBc-Ag), 50 µg ES/Alum, or PBS on day -20 and boosted on day -10. Tail bleed was taken d-1 and mice were infected by oral gavage with approximately 150 infective *T. muris* eggs on day 0 and sacrificed at d14 post-infection. Day 14 p.i. sera were titrated against VLP (HBc-Ag) (A), HBc-CBD₁₂₄₃₋₁₂₅₉ (B), HBc-CBD₂₄₁₋₂₅₇ (C), HBc-CLSP₁₄₃₋₁₅₈ (D) and HBc-CLSP₃₉₈₋₄₁₆ (E) to assess VLPs-specific IgG2c by ELISA (reading at 405 nm). Statistical analyses were carried out at 1:40, 1:80, 1:1280 and 1:2560 serum dilutions using the Kruskal-Wallis test (multiple comparisons). Significant differences between groups are represented by (*P≤0.05, **P≤0.01, ***P≤0.001, ****P≤0.0001) with a line. Negative values were adjusted to 0. Results are shown as mean ± SEM. n= 5 mice per group. This experiment was repeated two times, and the results shown here are representative of the two experiments.

7.3.3.4 The cellular immune responses following vaccination of mice with VLPs expressing *Trichuris* T-cell epitopes

To analyze the cellular immune responses of mice vaccinated with VLPs+ T-cell epitopes compared to control ES/Alum, native VLP (HBc-Ag) and PBS immunised mice groups after *T. muris* infection, MLN cells were re-stimulated *in vitro* with *Trichuris* ES and with pre-mixed VLPs+ T-cell epitopes proteins (HBc-CBD₁₂₄₃₋₁₂₅₉, HBc-CBD₂₄₁₋₂₅₇, HBc-CLSP₁₄₃₋₁₅₈, and HBc-CLSP₃₉₈₋₄₁₆) for 48 hours and with ConA for 24 hours. Supernatants were assayed for Th2 cytokines (IL-4, IL-5, IL-9 and IL-13), Th1/Th17 cytokines (IL-2, IFN-γ and IL-17), proinflammatory cytokines (IL-6 and TNF-α), and the anti-inflammatory cytokine (IL-10) production by CBA. MLN cells from mice vaccinated with VLPs+ T-cell epitope produced higher levels of Th2 cytokines IL-4 (A), IL-5 (B), IL-9 (C), and IL-13 (D) compared to all immunised mice including ES/Alum group but statistical significance was not reached. Significantly higher levels of the proinflammatory cytokine IL-6 (Figure 7.20 H) were also detected in response to re-stimulation *in vitro* with ES compared to ES/Alum, and PBS immunised mice. Notably, re-stimulated MLN cells from mice vaccinated with VLPs+ T-cell epitope and ES/Alum produced similarly high levels of Th1 cytokine (IFN-γ) (Figure 7.20 F). In contrast, MLN cells from all vaccinated mice groups produced similar levels of IL-2 (Figure 7.20 E), TNF (G), IL-17 (I) cytokines and anti-inflammatory cytokine IL-10 (J) upon their re-stimulation *in vitro* with worm ES antigens.

The most noticeable difference in cytokine production in response to *in vitro* re-stimulation with VLPs+ T-cell epitopes was for IL-5, IL-6 and IL-10. Interestingly, re-stimulated MLN cells from mice vaccinated with VLPs+ T-cell epitopes and ES/Alum showed similarly higher levels of IL-5 (Figure 7.21 B), IL-6 (H) and IL-10 (J) compared to the PBS, and VLP (HBc-Ag) injected mice groups. Furthermore, MLN cells from mice vaccinated with ES/Alum produced significantly higher levels of IL-13 upon re-stimulation *in vitro* with VLPs+ T-cell epitopes proteins compared to all immunised groups (Figure 7.21D).

Furthermore, ConA re-stimulated MLN cells from mice vaccinated with VLPs+ T-cell epitopes and infected with *T. muris* showed a slight increase in the production of IL-5 (Figure 7.22 B), IL-9 (C) IL-13 (D), IL-2 (E), TNF (G) and IL-6 (H) compared to the three other immunised mouse groups.

Collectively, these results demonstrate that the VLPs+ T-cell epitopes vaccine candidate efficiently boosted the cellular immune response.

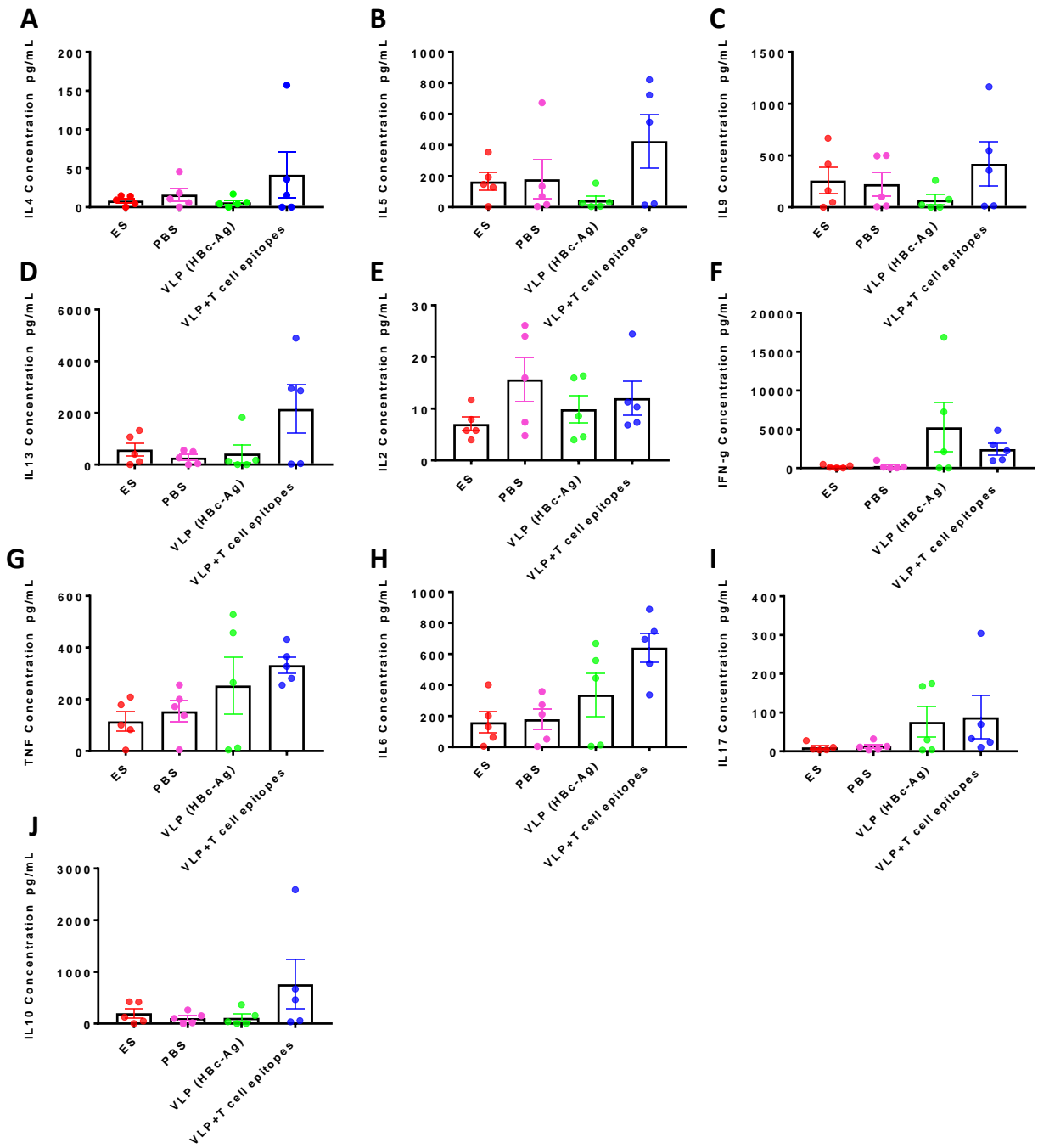


Figure 7.20 Parasite-specific cytokine productions by mesenteric lymph node cells from mice vaccinated with VLPs+ T-cell epitopes and control mice. MLNs from mice vaccinated with 50 µg of pre-mixed of VLPs+ T-cell epitopes epitopes (HBc-CBD₁₂₄₃₋₁₂₅₉, HBc-CBD₂₄₁₋₂₅₇, HBc-CLSP₁₄₃₋₁₅₈ and HBc-CLSP₃₉₈₋₄₁₆), 50 µg of VLP (HBc-Ag), 50 µg ES/Alum, or PBS on day -20 and boosted on day -10 were stimulated at 5x10⁶/ml with 50 µg/ml *T. muris* ES. After 48 hours of stimulation, cell culture supernatants were harvested and assayed by cytometric bead array for IL-4 (A), IL-5 (B), IL-9 (C), IL-13 (D), IL-2 (E), IFN-g (F), TNF (G), IL-6 (H), IL-17 (I) and IL-10 (J) production. Statistical analyses were carried out using the Kruskal-Wallis test (multiple comparisons). Significant differences between groups are represented by (*P≤0.05) with a line. Results are shown as mean ± SEM. n= 5 mice per group. This experiment was repeated two times, and the results shown here are representative of the two experiments.

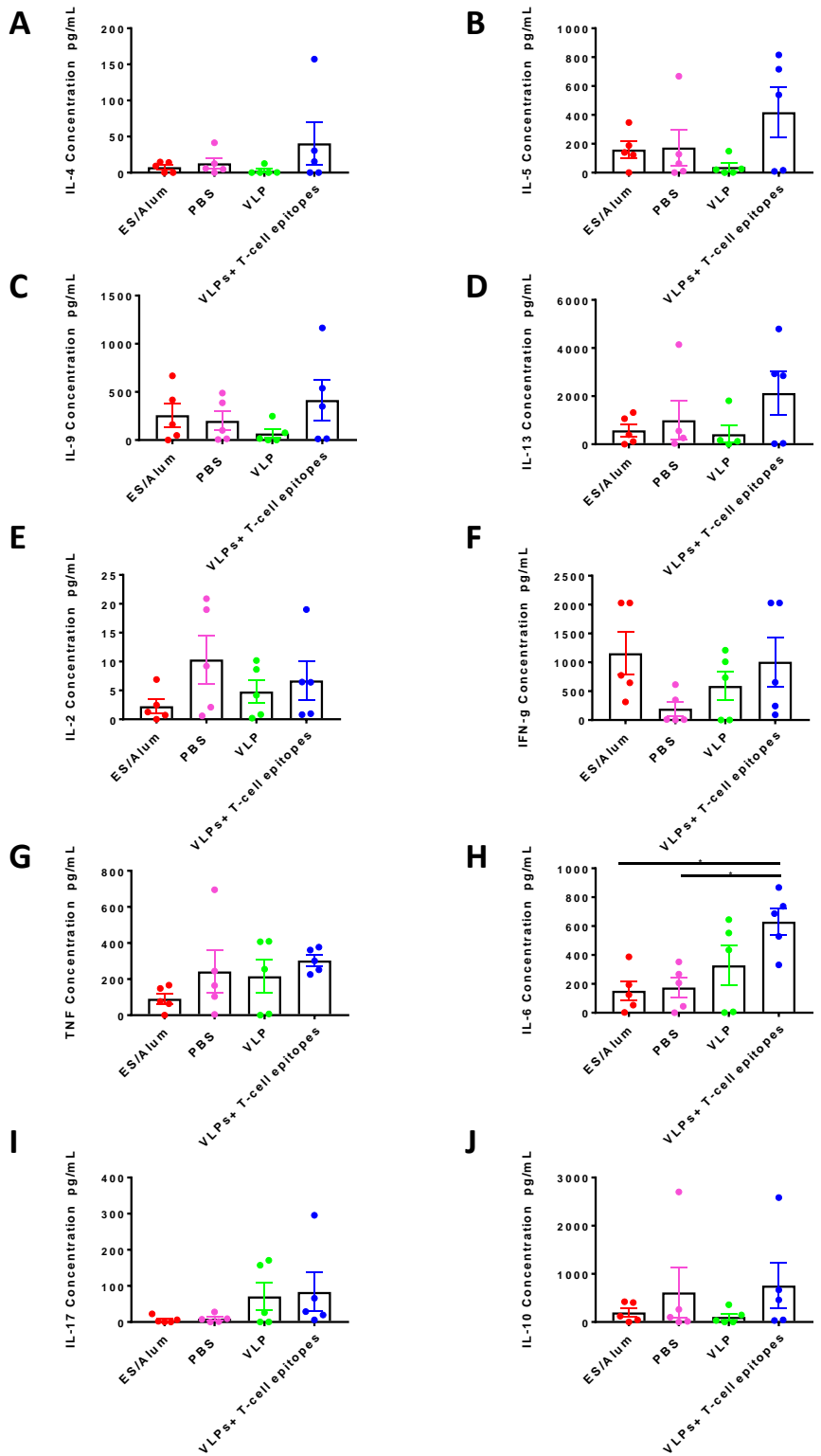


Figure 7.20 Parasite-specific cytokine production by mesenteric lymph node cells from mice vaccinated with VLPs+ T-cell epitopes and control mice. MLNs from mice vaccinated with 50 µg of pre-mixed of VLPs+ T-cell epitopes (HBc-CBD₁₂₄₃₋₁₂₅₉, HBc-CBD₂₄₁₋₂₅₇, HBc-CLSP₁₄₃₋₁₅₈ and HBc-CLSP₃₉₈₋₄₁₆), 50 µg of VLP (HBc-Ag), 50 µg ES/Alum, or PBS on day -20 and boosted on day -10 were stimulated at 5x10⁶/ml with 50 µg/ml *T. muris* ES. After 48 hours of stimulation, cell culture supernatants were harvested and assayed by cytometric bead array for IL-4 (A), IL-5 (B), IL-9 (C), IL-13 (D), IL-2 (E), IFN-g (F), TNF (G), IL-6 (H), IL-17 (I) and IL-10 (J) production. Statistical analyses were carried out using the Kruskal-Wallis test (multiple comparisons). Significant differences between groups are represented by (*P≤0.05) with a line. Results are shown as mean ± SEM. n= 5 mice per group. This experiment was repeated two times, and the results shown here are representative of the two experiments.

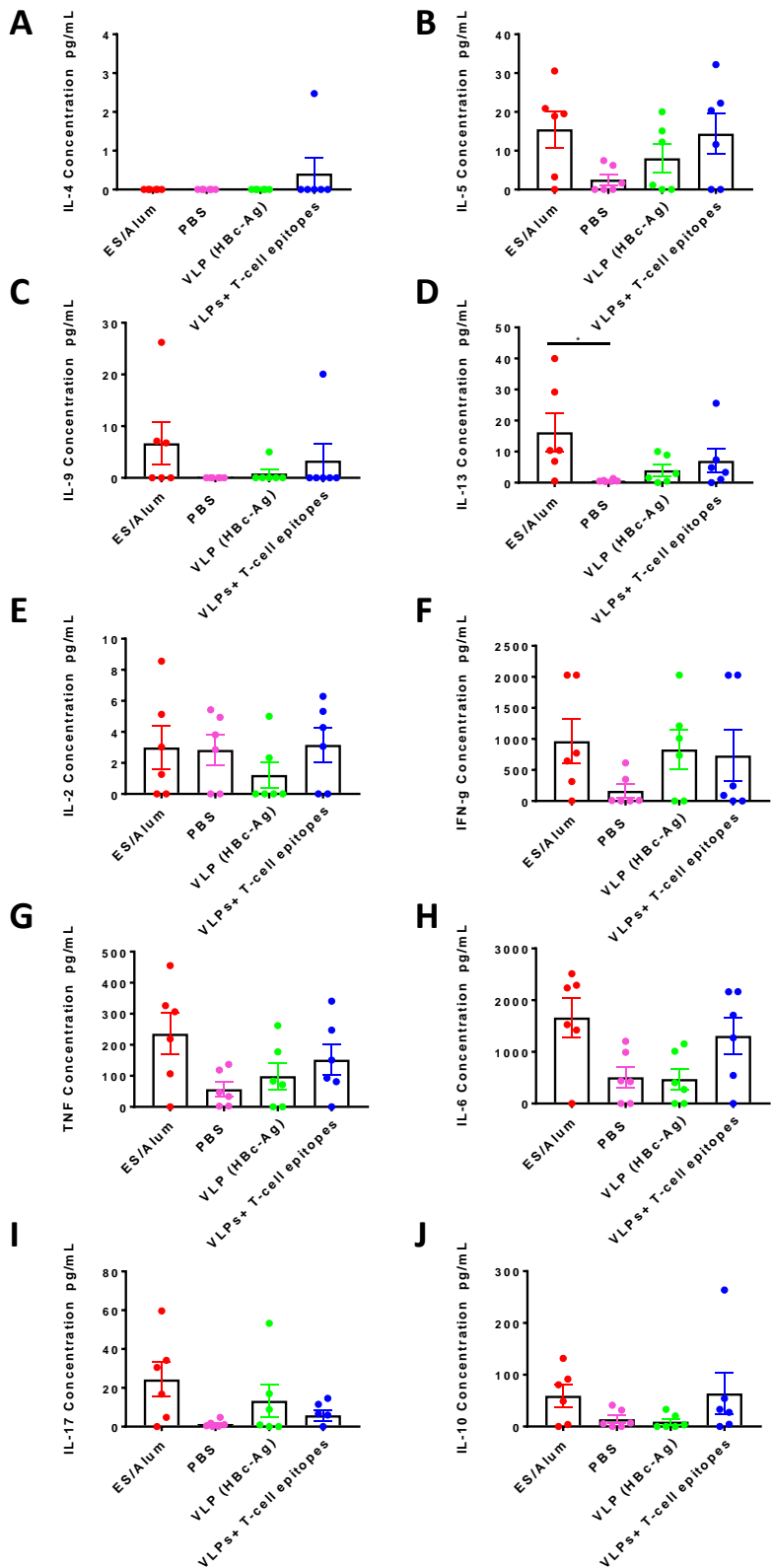


Figure 7.21 Cytokine production by mesenteric lymph node cells from mice vaccinated with VLPs+ T-cell epitopes and control mice. MLNs from mice vaccinated with 50 µg of pre-mixed of VLPs+ T-cell epitopes (HBc-CBD₁₂₄₃₋₁₂₅₉, HBc-CBD₂₄₁₋₂₅₇, HBc-CLSP₁₄₃₋₁₅₈ and HBc-CLSP₃₉₈₋₄₁₆), 50 µg of VLP (HBc-Ag), 50 µg ES/Alum, or PBS on day -20 and boosted on day -10. MLNs were stimulated at 5x10⁶/ml with 10 µg/ml pre-mixed of VLPs+ T-cell epitopes. After 48 hours of stimulation, cell culture supernatants were harvested and assayed by cytometric bead array for IL-4 (A), IL-5 (B), IL-9 (C), IL-13 (D), IL-2 (E), IFN- γ (F), TNF (G), IL-6 (H), IL-17 (I) and IL-10 (J) production. Statistical analyses were carried out using the Kruskal-Wallis test (multiple comparisons). Results are shown as mean ± SEM. n= 6 mice per group. This experiment was repeated two times, and the results shown here are representative of the two experiments.

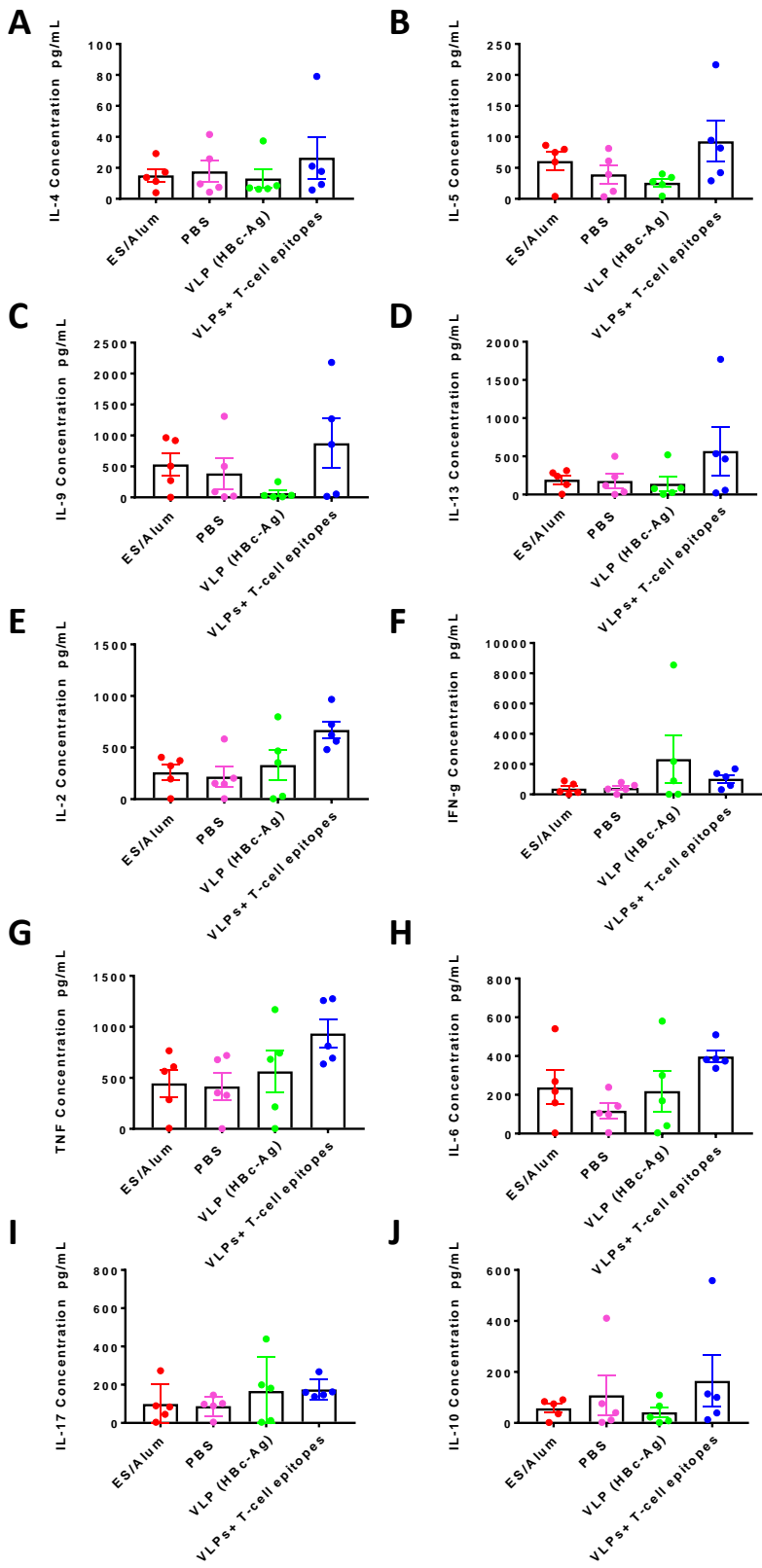


Figure 7.22 Cytokine production by mesenteric lymph node cells from mice vaccinated with VLPs+ T-cell epitopes and control mice. MLNs from mice vaccinated with 50 µg of pre-mixed of VLPs+ T-cell epitopes (HBc-CBD₁₂₄₃₋₁₂₅₉, HBc-CBD₂₄₁₋₂₅₇, HBc-CLSP₁₄₃₋₁₅₈ and HBc-CLSP₃₉₈₋₄₁₆), 50 µg of VLP (HBc-Ag), 50 µg ES/Alum, or PBS on day -20 and boosted on day -10. MLNs were stimulated at 5x10⁶/ml with 5 µg/ml ConA. After 24 of stimulation, cell culture supernatants were harvested and assayed by cytometric bead array for IL-4 (A), IL-5 (B), IL-9 (C), IL-13 (D), IL-2 (E), IFN-g (F), TNF (G), IL-6 (H), IL-17 (I) and IL-10 (J) production. Statistical analyses were carried out using the Kruskal-Wallis test (multiple comparisons). Results are shown as mean ± SEM. n= 5 mice per group. This experiment was repeated two times, and the results shown here are representative of the two experiments.

7.3.3.5 Crypt hyperplasia following vaccination of mice with VLPs expressing *Trichuris* T-cell epitopes

Figure 7.23 (A) shows colonic crypt lengths at day 14 p.i. in ES/Alum, PBS, native VLP (HBc-Ag), and VLPs+ T-cell epitopes vaccinated mice. VLPs+T-cell epitopes and ES/Alum vaccinated mice exhibited crypt hyperplasia with a significant difference compared to the PBS, and VLP (HBc-Ag) injected mice groups ($P<0.05$), as shown in Figure 7.23 (B).

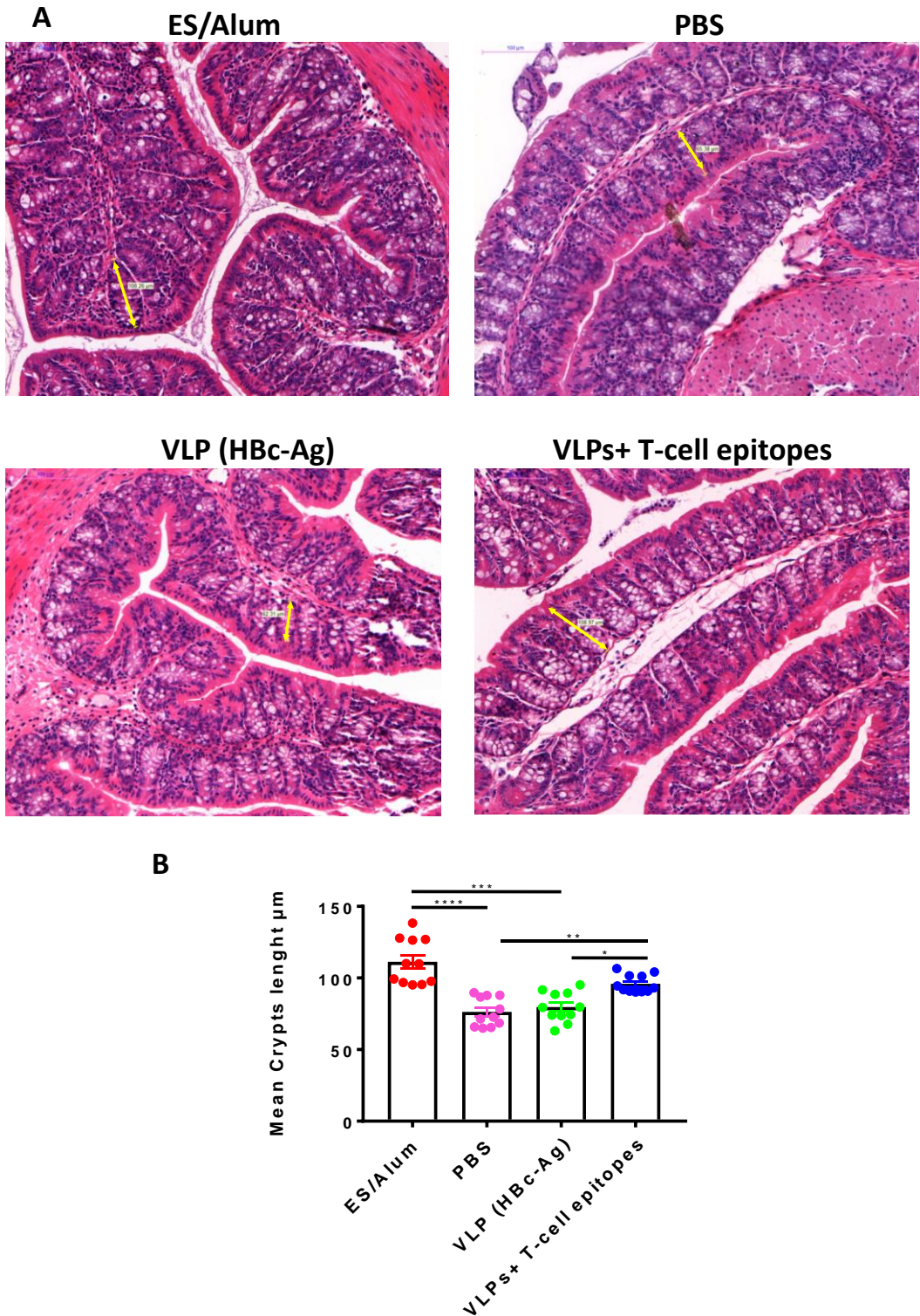


Figure 7.23 Changes in intestinal pathology in *T. muris* infected mice vaccinated with VLPs+ T-cell epitopes and control mice. (A) Representative photographs of gut sections stained with hematoxylin and eosin (H&E). Proximal colon was harvested from mice vaccinated with 50 µg of pre-mixed of VLPs+ T-cell epitopes (HBc-CBD₁₂₄₃₋₁₂₅₉, HBc-CBD₂₄₁₋₂₅₇, HBc-CLSP₁₄₃₋₁₅₈ and HBc-CLSP₃₉₈₋₄₁₆), 50 µg of VLP (HBc-Ag), 50 µg ES/Alum, or PBS on day -20 and boosted on day -10. All photographs were taken with 15X magnification. Gut pathology assessed by measuring crypt lengths using Panoramic Viewer software. The yellow double-headed arrows show how the crypt lengths were measured. Results are shown as mean crypt length from 20 crypts units per mouse and shown as the mean values per mouse ±SEM. Statistical analyses were carried out using the Kruskal-Wallis test (multiple comparisons). Significant differences between groups are represented by *P≤0.05, **P≤0.01, ***P≤0.001, ****P≤0.0001) with a line. n= 11 mice per group. The results presented are from two separated experiment pooled together.

7.3.3.6 Goblet cells hyperplasia in mice vaccinated with VLPs expressing *Trichuris* T-cell epitopes

PAS-stained goblet cells were measured in mice vaccinated with ES/Alum, PBS, VLP (HBc-Ag) and VLPs+ T-cell epitopes day 14 post *T. muris* infection as an index of goblet cell hyperplasia (Figure 7.24 A).

Interestingly, VLPs+T-cell epitopes and ES/Alum vaccinated mice exhibited goblet cells hyperplasia with a significant difference ($P<0.05$) compared to the PBS and native VLP (HBc-Ag) injected mice, as shown in Figure 7.24 (B). Isolated lymphoid follicle-like structures were found in the gut sections of mice immunised with VLPs+ T-cell epitopes and native VLP (HBc-Ag) following *Trichuris* challenge, as shown in Figure 7.25 (A and B).

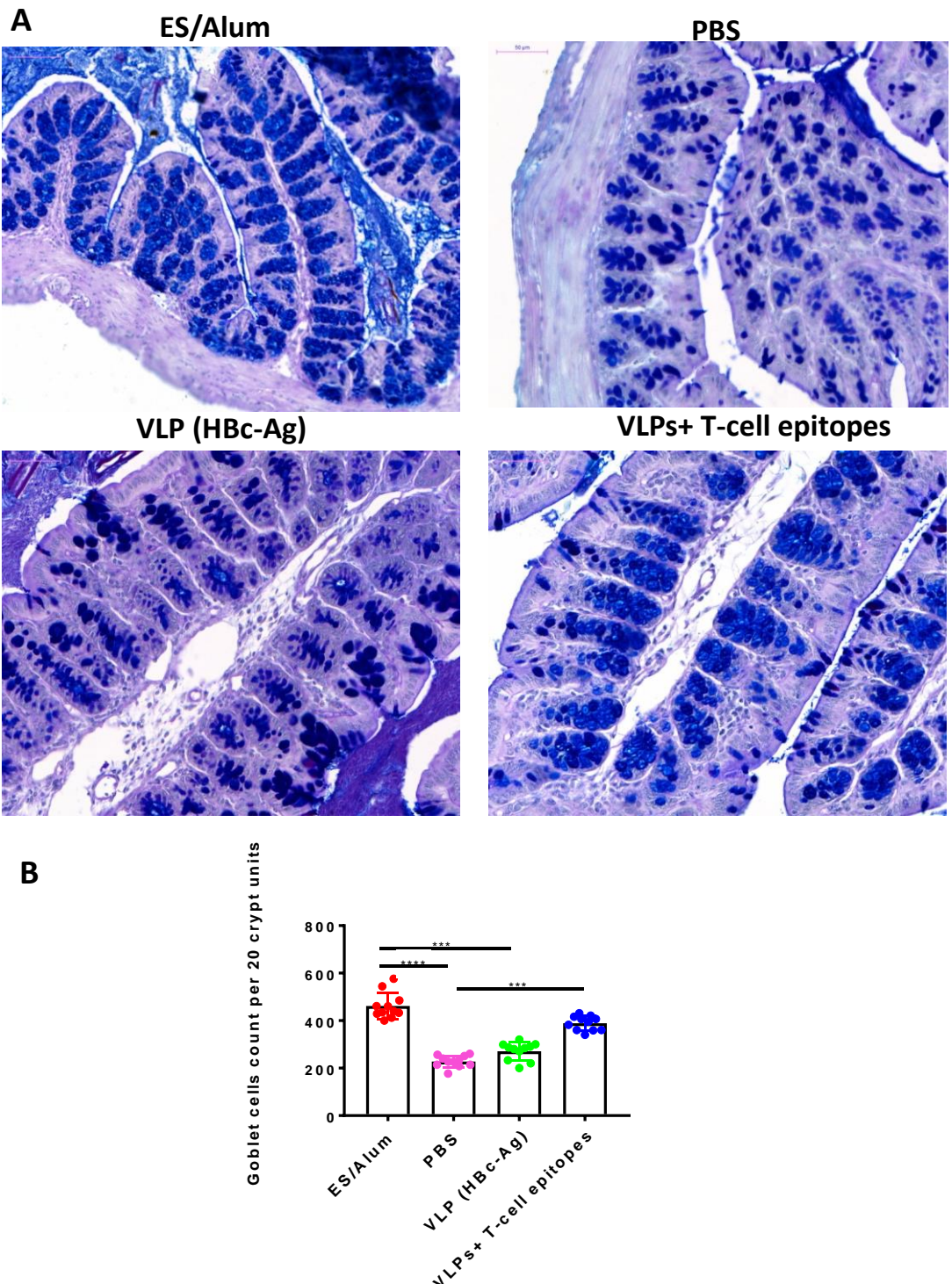


Figure 7.24 Quantification of goblet cell numbers in *T. muris* infected mice vaccinated with VLPs+ T-cell epitopes and control mice. (A) Representative photographs of gut sections stained with Periodic acid-Schiff staining (PAS). Proximal colon was harvested from mice vaccinated with 50 µg of pre-mixed of VLPs+ T-cell epitopes (HBc-CBD₁₂₄₃₋₁₂₅₉, HBc-CBD₂₄₁₋₂₅₇, HBc-CLSP₁₄₃₋₁₅₈ and HBc-CLSP₃₉₈₋₄₁₆), 50 µg of VLP (HBc-Ag), 50 µg *T. muris* ES formulated with Alum adjuvant, or PBS on day -20 and boosted on day -10. The slides were scanned, and the goblet cells were quantified using Panoramic Viewer software. All photographs were taken with 20X magnification. (B) Goblet cells were quantified by counting the number of alcian blue-stained cells per crypt unit in three fields of view from each section and are shown as mean cell numbers per 20 crypt units (cu) ±SEM. Statistical analyses were carried out using the Kruskal-Wallis test (multiple comparisons). Significant differences between groups are represented by (***P≤0.001, ****P≤0.0001) with a line. n= 11 mice per group. The results presented are from two separated experiment pooled together.

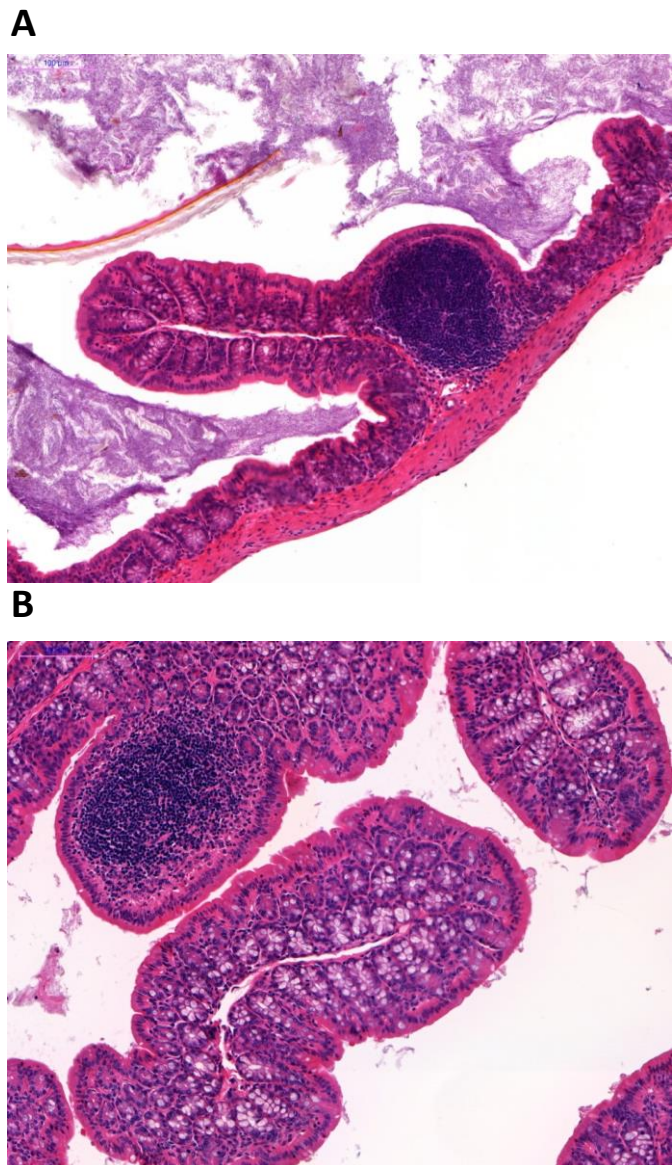


Figure 7.25 Isolated lymphoid follicle-like structures' in *T. muris* infected mice vaccinated with VLPs+ T-cell epitopes and control mice. Representative photographs of gut sections stained with hematoxylin and eosin (H&E). Proximal colon was harvested from mice immunised with 50 µg of pre-mixed of VLPs+ T-cell epitopes (A) or 50 µg of VLP (HBc-Ag) (B) on day -20 and boosted on day -10. The slides were scanned, and the pictures were taken using Panoramic Viewer software. All photographs were taken with 20X magnification. The results presented are from one of two separate experiments.

7.4 Discussion

Trichuris trichiura is one of the most common human soil-transmitted helminth (STH) parasites and remains a major health concern for humans worldwide (Alexander and Blackburn, 2019). Up to date, various pre-clinical vaccines against trichuriasis have been reported, containing ES/EVs products or fractions (Dixon et al., 2008; Shears et al., 2018a; Shears et al., 2018b). However, developing a vaccine for *Trichuris* based on native antigens has several limitations (Hewitson and Maizels, 2014). The current study investigated for the first time the protective efficacy of VLPs expressing novel *Trichuris* MHC-II T-cell epitopes that precisely target CD 4+ T-cells via antigen-presenting cells to elicit a *Trichuris*-specific immune response with minimal risks rather than using a whole *Trichuris* antigen. Based on the Foth et al.'s (2014) work, *Trichuris* MHC-II T-cell epitopes were predicted from different *Trichuris* proteins (chitin-binding domain-containing protein, chymotrypsin-like serine protease, and hypothetical protein) based on inclusion and exclusion criteria as discussed in Chapter 4.

7.4.1 Protection and immune responses to the VLPs+ T-cell epitopes vaccine candidates

Three *in vivo* experiments were conducted in this chapter to test the protective immune response of VLP-based vaccine candidates expressing different *Trichuris* T-cell epitopes prior to infection with *T. muris*. The first *in vivo* study in this chapter assessed the immunisation of mice with 25 µg of pre-mixed VLPs+ T-cell epitopes (HBc-H₁₁₂₋₁₂₈, HBc-CLSP₁₄₃₋₁₅₈, HBc-CBD₁₂₄₃₋₁₂₅₉, and HBc-CBD₂₄₁₋₂₅₇), followed by challenged infection. The vaccine candidate significantly boosted the immune response but was not sufficient to drive protection from *Trichuris* infection. High levels of parasite-specific IgM were detected in the serum of mice vaccinated with VLPs+ T-cell epitopes upon *T. muris* challenge infection, and to those without a challenge infection. These results suggest that these VLPs+ T-cell epitopes are antigenic and can boost strong antibody response enough to recognise specific small peptides in the *T. muris* ES. However, little or no parasite-specific IgG1 or IgG2c antibodies were measured in the serum of mice vaccinated with VLPs+ T-cell epitopes. These findings may suggest that the ability of the VLPs+ T-cell epitopes vaccine to drive a class-switched humoral immune response is different from that of the ES/Alum vaccine. Therefore, the antibody immune response was measured against the corresponding antigen rather than using ES as a detection antigen. High levels of VLPs+ T-cell epitopes-specific IgM, IgG1, and IgG2c were detected in the sera of mice vaccinated with VLPs+ T-cell epitopes. However, only negligible levels of HBc-H₁₁₂₋₁₂₈-specific-IgM were detected. These results suggest the H₁₁₂₋₁₂₈ epitope is not highly immunogenic compared to the other *Trichuris* epitopes in the vaccine cocktail, and therefore this VLP+T cell epitope recombinant protein was excluded from the vaccine cocktail in the third *in vivo* experiment.

Although VLPs are strong immunogens, several studies included an adjuvant in the VLP-based vaccine to induce stronger immune responses (Cimica and Galarza, 2017; Gomes et al., 2017a). Cimica et al. (2016) for example, developed a VLP-based vaccine for the human respiratory syncytial virus (RSV) based on a human metapneumovirus (hMPV) matrix protein (M) fused to an RSV glycoprotein formulated with AddaVax adjuvant. The VLP-based vaccine showed full protection against RSV infection and induced a mix of Th1/Th2 and Th17-mediated types of

immune responses (Cimica et al., 2016). However, this study did not assess the efficacy of the VLP-based vaccine without including the adjuvant.

Based on this study and others, a vaccination experiment was carried out using AddaVax adjuvant to improve the immunogenicity of the vaccine candidate. Surprisingly, immunisation of mice with VLPs+ T-cell epitopes (HBc-H₁₁₂₋₁₂₈, HBc-CLSP₁₄₃₋₁₅₈, HBc-CLSP₃₉₈₋₄₁₆, and HBc-CBD₂₄₁₋₂₅₇) formulated with AddaVax adjuvant followed by infection showed no enhanced potency of the VLPs+ T-cell epitopes vaccine compared to the control injected mice. However, antibody recognition in the serum of mice vaccinated with VLPs+ T-cell epitopes/AddaVax confirms that the antibodies in the serum were specific to the vaccine candidate. Importantly, antibodies in the serum of mice vaccinated with ES/AddaVax recognised a 22 kDa band corresponding to the size of the VLPs+ T-cell epitopes recombinant proteins, suggesting that antibodies induced by nature protective antigens recognised the *Trichuris* epitopes expressed in the VLPs. These results also explain the high levels of VLPs+ T-cell epitopes-specific IgM detected in the sera of mice vaccinated with ES.

Previous research conducted by Dixon et al., (2008) and Else et al., (1990) showed that antibody recognition of high molecular weight proteins in both adult and larval *T. muris* ES correlated with resistance to *T. muris* infection. Given that the serum of mice vaccinated with VLPs+ T-cell epitopes recognised a range of high molecular weight proteins in *T. muris* ES, suggests that H₁₁₂₋₁₂₈, CLSP₁₄₃₋₁₅₈, CBD₁₂₄₃₋₁₂₅₉, and CBD₂₄₁₋₂₅₇ are highly-conserved immunodominant epitopes and may be expressed in several *Trichuris* secretory proteins of high molecular weights, making them potential vaccine candidates.

After ruling out AddaVax adjuvant in the vaccine formula, it was logical to assess whether the vaccine dose may improve the efficacy of the vaccine. Remarkably, upon challenge infection, mice vaccinated with a high-dose of 50 µg of pre-mixed VLPs+ T-cell epitopes (HBc-CBD₁₂₄₃₋₁₂₅₉, HBc-CBD₂₄₁₋₂₅₇, HBc-CLSP₁₄₃₋₁₅₈, and HBc-CLSP₃₉₈₋₄₁₆) showed a significantly lower worm burden reduction of 51.2% in the caecum and colon. Furthermore, ES/Alum conferred as full protection as seen with ES/AddaVax. Replacing HBc-H₁₁₂₋₁₂₈ with HBc-CLSP₃₉₈₋₄₁₆ in the pre-mixed VLPs+ T-cell epitopes, with an optimal dose of 50 µg, may explain the improved vaccine efficacy.

It has been postulated that the role of B-cells in the immune response to *Trichuris* infection is context dependent (Sahputra et al., 2019; Sorobetea et al., 2018). For instance, B-cell-deficient µMT mice on a C57BL/6 background appeared to be susceptible to infection (Blackwell and Else, 2001). Earlier studies have also demonstrated that the adaptive transfer of CD4+ T-cells alone, purified from BALB/c donor mice into SCID mice, was sufficient to expel *T. muris* worms (Else and Grencis, 1996). However, the adoptive transfer of serum from resistant mice provided high levels of protection to susceptible strains of mice (Blackwell and Else, 2001; Selby and Wakelin, 1973). Early studies also showed that parasite-specific IgG1 is involved in the memory response of the adaptive immune system in resistant strains following primary infection (Else et al., 1993a).

In the third *in vivo* study presented here, parasite-specific IgM and IgG2c were detected in the sera of mice vaccinated with VLPs+ T-cell epitopes upon *T. muris* infection. Importantly, analysis of the

serum from immunised mice showed that the VLPs+ T-cell epitopes elicited the highest level of neutralising antibody to their corresponding VLP+T cell epitope recombinant protein (HBc-CBD₁₂₄₃₋₁₂₅₉, HBc-CBD₂₄₁₋₂₅₇, HBc-CLSP₁₄₃₋₁₅₈, and HBc-CLSP₃₉₈₋₄₁₆) but not the native VLP (HBc-Ag) protein. These results suggest that all four VLPs+ T-cell epitopes recombinant proteins had a similar effect on class switching and enhancing both Th1/Th2 mediated immune responses. These findings also suggest that the antibody-dependent mechanism may be crucial to the expulsion of *T. muris* in vaccinated mice. Thus, it would be instructive to vaccinate transgenic B-cell-deficient mice with a susceptible background to determine whether susceptible mice can be protected in the absence of antibodies.

Mice vaccinated with VLPs+ T-cell epitopes were also characterised by the production of MLN-derived Th2 cytokines. Remarkably, MLN cells from mice vaccinated with different VLP-based vaccine candidates produced high levels of Th2 (IL-4, IL-5, IL-9 and IL-13) cytokines and proinflammatory cytokines (IFN-γ and IL-6) in response to re-stimulation *in vitro* with ES. In contrast, mice immunised with native (HBc-Ag) and PBS showed similar MLN cytokine profiles to that documented for the susceptible mice strains during primary infection (Taylor et al., 2000).

These findings broadly support other studies linking Th2 cytokines and worm expulsion (Klementowicz et al., 2012). Of the Th2 cytokines produced in response to resistant to infection, IL-5, is involved in inducing eosinophilia during *T. muris* infection; however, IL-5 and eosinophils appeared not to be essential for worm expulsion in resistant BALB/k mice (Betts and Else, 1999; Svensson et al., 2011). In contrast, IL-9 is required to stimulate the intestinal muscle hypercontractility that drives *T. muris* expulsion (Khan et al., 2003; Richard et al., 2000). It has also been known that IL-13 plays essential roles in increasing epithelial cell turnover and increasing production of mucins in promoting worms expulsion (Bancroft et al., 2000; Bancroft et al., 1998). However, to test whether these Th2 cytokines induce similar responses in the VLPs+ T-cell epitopes vaccinated mice, future work may include using cytokine transgenic and knockout mice. Given the critical role played by Th2 cytokines in worm expulsion, our results demonstrating the protective immunity elicited by VLPs+ T-cell epitopes, strongly support their potential as vaccine candidates.

The results presented here are in agreement with those obtained by Dixon et al. (2010) who showed that vaccinating susceptible AKR mice with 100 µg ES in 100 µl FIA prior to infection with a high-dose of *T. muris* eggs induced sterile immunity when compared to the PBS/FIA injected mice. Protection was mediated in the presence of high levels of Th2 (IL-5, IL-9, and IL-13) cytokines and high levels of parasite-specific IgG1 and IgG2c. However, both immunised groups produced similar high levels of IFN-γ (Dixon et al., 2010). Other studies also showed that vaccinating C57BL/6 mice with either ES fractions or extracellular vesicles (EVs) isolated from *T. muris* without an adjuvant and prior to infection with a low-dose of *T. muris* eggs significantly induced a reduction in the worm burden compared to the PBS-injected group (Shears et al., 2018a; Shears et al., 2018b). High levels of both IgG1 and IgG2c anti-parasite antibodies against soluble ES antigens were detected in sera of mice vaccinated with *T. muris* EVs (Shears et al., 2018a). Notably, there was a significant increase in IL-13 and IL-9 production by infection-primed lymphocytes in response to the ES

fractions that induced a reduction in the worm burden (Shears et al., 2018b). The data are largely consistent with the results presented, here although the present study assessed the protective immune response of the vaccine candidates in an accelerated expulsion animal model and a broader profile of cytokines was measured. Although the ES/Alum vaccine led to full protection, the levels of Th2 cytokines in the re-stimulated MLNs were not dramatically high; however, this finding might be related to the accelerated expulsion and autopsy date (day 14 p.i.) being too late to detect peak cytokine production.

Furthermore, vaccinating AKR mice with either a *T. muris* whey acidic protein (rTm-WAP49) or a *T. muris* WAP fragment fusion protein (rTm-WAP-F8+Na-GST-1) formulated with Montanide ISA 720 adjuvant three times at two-week intervals prior to *T. muris* challenge induced a partial reduction in the worm burden by 48% and 38%, respectively (Briggs et al., 2018). The results showed that both humoral and cellular immune responses were induced, characterised by elevated antigen-specific IgG1 and IgG2c antibodies and Th2 (IL-4, IL-9, and IL-13) cytokines detected in the draining inguinal lymph nodes, draining mesenteric lymph nodes, and spleen of vaccinated mice (Briggs et al., 2018). These data correlate well with the results presented here; however, vaccinating mice with VLPs expressing *Trichuris* epitopes induced a reduction in the worm burden by 51.2%. Similarly, mice vaccinated with VLPs+ T-cell epitopes were characterised by the production of MLN-derived Th2 cytokines (IL-4, IL-9, and IL-13) in response to re-stimulation *in vitro* with *Trichuris* ES. High levels of VLP+T cell epitopes-specific IL-5, IL-6, and IL-10 cytokines were also detected in the re-stimulated MLNs of vaccinated mice.

Crypt hyperplasia is typically associated with chronic infection accompanied by both increased epithelial cell proliferation and apoptosis under the control of the IFN- γ pro-inflammatory cytokine (Artis et al., 1999b). In contrast, no such dramatic changes were observed in the gut of 'naturally resistant' mice. It has been demonstrated that resistant animals have accelerated epithelial cell turnover, resulting in short crypts, a mechanism that is functionally associated with *Trichuris* expulsion (Cliffe et al., 2005). However, the results described here are in good agreement with Dixon's (2010) findings, which showed that crypt hyperplasia was seen in both ES/FIA- and PBS/FIA-immunised mice groups following *Trichuris* infection. These results suggest that the increased rate of epithelial turnover, which appears to be an important mechanism to expel the worms in 'natural resistant' mice, is unlikely to be responsible for expulsion in 'vaccinated resistant' mice. The high levels of MLNs IFN- γ in VLPs+ T-cell epitopes and ES/Alum vaccinated mice may explain the crypt hyperplasia in both groups. These findings also suggest that epithelial cell proliferation is likely to occur at a similar rate in these mice compared to the PBS and VLP (HBC-Ag) injected mice.

The VLPs+ T-cell epitopes and ES/Alum vaccinated mice also showed marked goblet cell hyperplasia, which is a known IL-13-dependent mechanism of *Trichuris* expulsion in mice resistant to *Trichuris* infection (Datta et al., 2005). Goblet cells have been implicated in mucus production (Muc2 and Muc5ac) during Th2-mediated defence in resistant animals (Hasnain et al., 2010) by protecting the barrier from degradation by the worm-secreted serine proteases (Hasnain et al., 2012). Goblet cells also secrete several molecules other than mucins that contribute to *T. muris*

expulsion, including resistin-like molecule β (RELMβ) (Artis et al., 2004b). This putative mechanism of expulsion may also explain the vaccination-induced protection to challenge infection.

Interestingly, we also identified isolated lymphoid follicle-like structures in the large intestine of mice immunised with VLPs+ T-cell epitopes and native VLP (HBc-Ag). These follicular structures are filled mainly with B-cells interspersed by small clusters of CD4+/CD8+ T-cells and have been previously identified in the large intestine of both AKR and BALB/c mice infected with *T. muris* (Little et al., 2005). Similar structures have also been identified in the mouse small intestine in response to normal gut flora (Lorenz et al., 2003). The presence of these follicular structures may explain the strong antibody response in the mice vaccinated with VLPs+ T-cell epitopes, especially, that previous study has shown that IgG1 must be present in the mouse large intestine for effective larval clearance (Dixon et al., 2010). However, we are unsure, at this stage, whether these structures are isolated lymphoid follicles. Therefore, future work may include the immunohistochemical staining of B220+ cells to confirm lymphoid structures, and analyse the local tissue levels of antibodies post-infection.

7.4.2 VLP-based vaccines against parasite infections

The results presented here represent the first example of successful VLP-based vaccination against the *Trichuris* parasite using *Trichuris* MHC-II T-cell epitopes. However, there is a clear trend toward identifying and evaluating VLP-based vaccines expressing a whole protein or short peptides for the development of many anti-parasitic vaccines.

For example, Lee and co-workers (2016) developed a vaccine for human trichinellosis based on influenza matrix protein 1 (M1) VLP containing the whole 53 kDa ES protein of *T. spiralis* (T653K) with and without a cholera toxin (CT). Notably, BALB/c mice vaccinated twice with 25 µg of T653K VLP induced parasite-specific IgG, IgG1, and IgG2c antibody responses before and after an oral challenge with 100 *T. spiralis* larvae/mouse and showed a significant reduction in the worm burden upon infection. However, protective immune responses were significantly improved by vaccinating mice with T653K VLP/CT (Lee et al., 2016). Lee et al. (2017) also developed a vaccine for human clonorchiasis, based on the influenza matrix protein 1 (M1) VLP containing whole *C. sinensis* protein 22.3 kDa (CsTP 22.3). Rats vaccinated twice with 200 µg of CsTP VLP and challenged with *C. sinensis* metacercariae induced parasite-specific cellular and humoral immune responses. This result was confirmed with significant production of IgG, IgG1, and IgG2c in the serum and IgA in the faeces and intestines of the vaccinated group before and after challenge when compared to the naïve control. Moreover, vaccinated rats induced CD4+/CD8+ T-cell responses in the spleen compared to the native and the non-immunized control rats. Most importantly, a significant reduction in the worm burden was seen upon challenge infection without the need for an adjuvant in the vaccine formulation (Lee et al., 2017). The same group developed a VLP-based vaccine against *Toxoplasma gondii* based on the same VLP (influenza M1) containing *T. gondii* rhoptry protein 18 (ROP18) or microneme protein 8 (MIC8) (Lee et al., 2018). Mice vaccinated with a combination of ROP18 VLP or MIC8 VLP and challenged with *T. gondii* tachyzoites, induced a stronger immune response compared to the vaccinated groups with each VLP individually (Lee et al., 2018).

Hepatitis B VLP, in particular, has proved to be one of the most promising parasite delivery systems (Chisari and Ferrari, 1995; Qiao et al., 2016; Roose et al., 2013). The malaria (Malarivax ICC-1132) vaccine, for example, is composed of HBc-Ag expressing *P. falciparum* CS B-cell epitopes inserted into the MIR and T-cell epitopes in the C terminal expressed in *E. coli* and purified by gel filtration column chromatography. Mice and monkeys vaccinated with the Malarivax vaccine formulated in Freund's adjuvant developed long-lasting immunity and elicited an anti-CSP specific antibody and CD4+ immune response (Birkett et al., 2002; Birkett et al., 2001; Milich et al., 2001). Based on the strong experimental evidence *in vivo*, the vaccine was tested in human clinical trials. Healthy volunteers were vaccinated with the HBc-Ag containing *P. falciparum* CS T- and B-cell epitopes expressed in *E. coli* and purified by ammonium sulfate precipitation, size exclusion, hydrophobic interaction, and hydroxyapatite chromatography. The vaccine, formulated with alum or Montanide ISA 720 adjuvant, was found to be highly immunogenic and produced a specific antibody response to the CS and secretion of IFN- γ and IL-2 cytokines. Other than proving the immunogenicity of the vaccine, all the healthy volunteers showed no serious side effects from the vaccine (Gregson et al., 2008; Nardin et al., 2004; Oliveira et al., 2005).

The results of these studies support some critical insights into VLP-based vaccines, including confirming that an HBc virus-like particle, in particular, is an excellent delivery system for developing potential vaccine candidates for parasites. Besides, in order to enhance the immunity of the potential vaccine, it is recommended to include several antigens in the vaccine formula. Despite the promising results discussed in this chapter, it may be necessary to optimise vaccination schedules to prolong the exposure of antigens to the immune system or increase the dose to achieve an appropriate level of protection (Bachmann and Jennings, 2010; Johansen et al., 2008). Future work should also include investigating the efficacy of the vaccine candidate in a low-dose infection (25 eggs), which would ordinarily lead to chronic infection in C57BL/6 mice (Bancroft et al., 1994). To examine whether antibody production is required for vaccine-induced immunity, additional work could also investigate whether transferring serum from mice vaccinated with VLPs+ T-cell epitopes can protect against infection in naïve mice.

In summary, the current chapter identified a novel vaccine candidate against trichuriasis based on VLPs expressing different *Trichuris* MHC-II T-cell epitopes predicted from chitin-binding domain containing proteins and chymotrypsin-like serine proteases. Collectively, the data presented in this chapter further justify focussing on *Trichuris* epitopes predicted from the *Trichuris* genome that stimulate Th2 immune response rather than using whole or fractions of *Trichuris* ES antigens to identify potential vaccine candidates, as has been used for malaria vaccines (Gregson et al., 2008; Nardin et al., 2004; Oliveira et al., 2005).

7.5 Summary

- Vaccination of mice with 25 µg of pre-mixed VLPs expressing *Trichuris* MHC-II T-cell epitopes (HBc-H₁₁₂₋₁₂₈, HBc-CLSP₁₄₃₋₁₅₈, HBc-CBD₁₂₄₃₋₁₂₅₉, and HBc-CBD₂₄₁₋₂₅₇) was able to boost the immune response but was not sufficient to drive protection from a high-dose *Trichuris* infection.

- An oral challenge with *T. muris* infective eggs following vaccination with 25 µg of pre-mixed VLPs+ T-cell epitopes (HBc-H₁₁₂₋₁₂₈, HBc-CLSP₁₄₃₋₁₅₈, HBc-CLSP₃₉₈₋₄₁₆, and HBc-CBD₂₄₁₋₂₅₇) formulated with AddaVax adjuvant did not improve the efficacy of the vaccine candidate.
- Oral challenge with *T. muris* infective eggs following vaccination with 50 µg of pre-mixed VLPs+ T-cell epitopes (HBc-CBD₁₂₄₃₋₁₂₅₉, HBc-CBD₂₄₁₋₂₅₇, HBc-CLSP₁₄₃₋₁₅₈, and HBc-CLSP₃₉₈₋₄₁₆) led to a significant reduction in the worm burden (51.2%). Protective immunity was characterised by the production of MLN-derived Th1 and Th2 cytokines, high levels of serum antigen-specific IgM, IgG1, and IgG2c antibodies along with goblet cell hyperplasia.

Chapter Eight

Summary discussion

Trichuris trichiura infection remains a global public health issue, especially in the tropical and subtropical areas with poor hygiene and sanitation (Alexander and Blackburn, 2019). The ability to control such infection depends almost exclusively on administration of anthelmintic drugs to at-risk populations (Farrell et al., 2018; Freeman et al., 2019; WHO, 2015). However, the appearance of anthelmintic-resistant parasites has increased interest in developing a vaccine to provide a cost-effective, long-term immunological method to control helminth infection (Becker et al., 2018; Dixon et al., 2008; Doyle and Cotton, 2019). Despite research progress and significant early successes, there are no licensed vaccines for human STHs (Sacks et al., 2016). However, tremendous efforts toward state-of-the-art vaccine development have improved the understanding of the host-parasite interaction, parasite component isolation and characterisation and gene sequence analysis (Smith and Zarlenga, 2006).

The overall aim of this thesis was to develop an anti-*Trichuris* vaccine based on VLPs expressing *Trichuris* T-cell epitopes. This was done using an RV approach to overcome some of the challenges associated with developing helminth vaccines (Figure 8.1). To achieve this aim, first, a systematic review was performed to select the top MHC class II *in silico* prediction tools (Chapter 3). Second, the potential *Trichuris* MHC-II T-cell epitope vaccine candidates obtained from the *Trichuris* genome were identified using the selected *in silico* prediction tool (Chapter 4). Third, these epitopes were produced in a commercially viable manner by fusing epitopes in the MIR of the VLP (HBc-Ag) vaccine delivery system (Chapter 5). These VLPs + T-cell epitope vaccine candidates were then tested *in vitro* for their ability to activate APCs (Chapter 6). Finally, three *in vivo* experiments were conducted to test the protective immune response of VLPs expressing different *Trichuris* T-cell epitopes prior to infection with *T. muris* (Chapter 7). Collectively, the results of this research represent the first significant progress towards identifying a novel epitope-based vaccine for trichuriasis.

Chapter 3: Assessment of MHC-II restricted T-cell epitope prediction tools

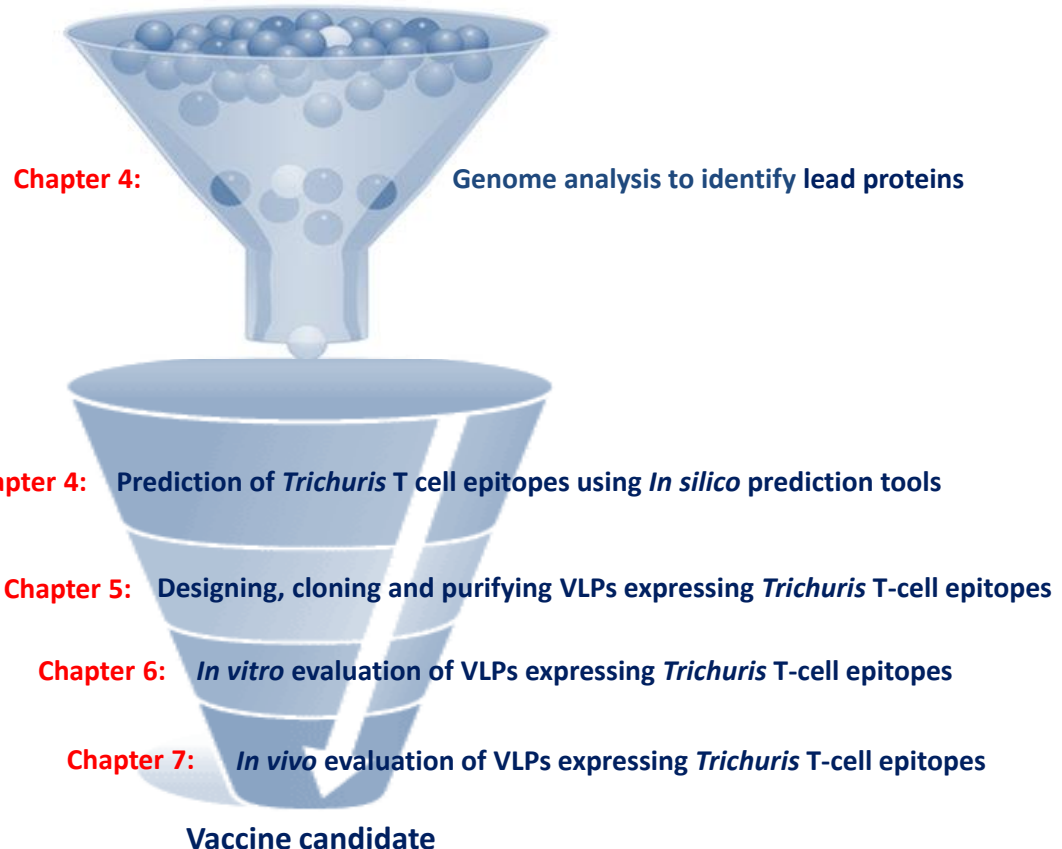


Figure 8.1 Reverse vaccinology strategy used to identify epitope-based vaccine against trichuriasis infection. Challenges begin with choosing the top MHC-II restricted T-cell epitope prediction tools (Chapter 3) followed by genome analysis to identify lead proteins with promising vaccine antigen properties from the whole genome of *T. trichiura* and *T. muris* (Chapter 4). *In silico* immunoinformatics tools were then used to predict *Trichuris* MHC-II T-cell epitopes by mapping protein sequence (Chapter 4). The selected *Trichuris* MHC-II T-cell epitopes were then cloned, expressed and purified in the VLP (HBc-Ag) delivery system (Chapter 5). *In vitro* assays were then conducted to evaluate the efficacy of the vaccine candidates to activate and stimulate APCs (Chapter 6). The vaccine candidates were then evaluated *in vivo* for immunogenicity and protection in mice (Chapter 7).

2.11 Identification of novel *Trichuris* MHC-II T-cell epitopes as promising vaccine candidates

There have been many attempts to develop vaccines for helminth parasites, but these parasites are relatively large multicellular organisms with a large genome (Noon and Aroian, 2017), which makes vaccine development challenging.

Over the past decade, considerable progress has been made in identification of candidate vaccine antigens for several important helminth parasites, such as the recombinant vaccine for the hookworm *N. americanus* based on Na-GST-1 and Na-APR-1 antigens (Diemert et al., 2018; Hotez et al., 2013). These parasite antigens are known to be involved in the breakdown of host haemoglobin and detoxification of haem, which is essential for parasite survival (Hotez et al.,

2013). The vaccine has been proven to be safe and highly immunogenic and is currently undergoing clinical trials in the United States, Brazil and Gabon (Diemert et al., 2017; Hotez et al., 2013).

T. muris excretory/secretory (ES) products (Jenkins and Wakelin, 1977), ES fractions (Shears et al., 2018b), extracellular vesicles (EVs) (Shears et al., 2018a), and, more recently, *T. muris* whey acidic protein (Briggs et al., 2018) have shown considerable potential in a number of pre-clinical protection trials. Despite these successes, developing a vaccine based on native antigens is associated with many manufacturing challenges, such as cost, time consumption, difficulties in purifying large quantities of worm antigens and control over differences between batches (Geldhof et al., 2007; Hewitson and Maizels, 2014). The current era of genome sequencing and the advent of immunoinformatics tools enable identification of potential vaccine parasite antigens *in silico* as an alternative to composing native antigens (Sousa and Doolan, 2016; Tordello et al., 2017). Such approaches may enable development of a safer and more reliable vaccine based on VLPs expressing *Trichuris* MHC-II T-cell epitopes.

Initiation of an antigen-specific immune response requires presentation of antigenic peptides to CD4+ T-cells in the context of MHC Class II molecules (Dhanda et al., 2017). Selection of appropriate MHC Class II binding peptides is therefore a critical first step in developing an epitope-based vaccine. Systematic review and evaluation of existing MHC-II restricted T-cell epitope prediction tools were carried out in Chapter 3 in order to select the top tools. The work described in Chapter 3 recommends the use of IE3DB (Zhang et al., 2008) and/or NETMHC-II 2.2 (Buus et al., 2015) prediction tools in any MHC class II epitope prediction study. However, the output results for these *in silico* prediction tools need to be carefully evaluated *in vitro* and *in vivo*.

To our knowledge, the data presented in Chapter 4 is the first to identify novel *Trichuris* MHC-II T-cell epitopes as potential vaccine antigen candidates. When designing an anti-*Trichuris* vaccine, one must remember that the end goal is development of a vaccine for humans, not mice. Thus, based on the work of Foth et al. (2014), a set of candidate proteins were selected from the *T. muris* and *T. trichiura* genomes using inclusion and exclusion criteria. Then, MHC-II T-cell epitopes were predicted using the IE3DB *in silico* prediction tool and were screened for allergenicity and conservancy. The framework used here to identify potential epitope vaccine candidates within the *T. muris* and *T. trichiura* genome could be used in the future to identify potential vaccine candidates within other parasite species.

The final set of *Trichuris* MHC-II T-cell epitopes vaccine candidates were identified from chitin-binding domain-containing proteins, chymotrypsin-like serine proteases, hypothetical protein, and from Pfam B domain-containing protein. Chitin-binding domains genes are highly expressed in different life stages in many parasites including *T. trichiura*, *Caenorhabditis elegans*, *Ascaris lumbricoides* and *Ancylostoma ceylanicum* (Foor, 1967; Santos et al., 2016; Veronico et al., 2001; Wei et al., 2016). In particular, these proteins are thought to be associated with eggshell formation and early development in the single-cell stage (Johnston et al., 2006, 2010). Furthermore, given that *T. muris* and more than 40 helminths species express a high level of chymotrypsin-like serine proteases, these proteases may be promising vaccine candidates (Cuesta-Astroz et al., 2017; Foth

et al., 2014). They seem to play a central role in either the invasion process or modulation of the host immune response to enhance the survival in the host (Balasubramanian et al., 2010; Santos et al., 2013; Toubarro et al., 2010; Yang et al., 2015).

Numerous publications have noted that the success of the most consistent vaccines against various helminth parasites has been achieved using helminth protease molecules (Dalton et al., 2003). For example, vaccinating BALB/c mice with the whole recombinant serine protease of *T. spiralis* prior to challenging them with *T. spiralis* infection led to a reduction in the worm burden and induced a mix of Th1 and Th2 immune responses (Feng et al., 2013; Wang et al., 2013; Xu et al., 2017). Furthermore, Shears et al. (2018b) showed that vaccinating mice with the ES fraction containing serine proteases induced high antibody responses. Remarkably, all the proteins selected in this study, except Pfam B domain-containing proteins, have been identified in most immunogenic fractions of *T. muris* ES following vaccination of mice (Shears et al., 2018b). Moreover, previous work by Dixon et al. (2008) and Else et al. (1990) showed that antibody recognition of high-molecular-weight proteins in both adult and larval *T. muris* ES was correlated with resistance to *T. muris* infection. Given that the serum of mice vaccinated with VLPs + T-cell epitopes recognised a range of high-molecular-weight proteins in *T. muris* ES, this suggests that the *Trichuris* epitopes predicted from chymotrypsin-like serine proteases and chitin-binding domains are highly conserved immunodominant epitopes that may be expressed in several *Trichuris* secretory proteins with high molecular weight. Collectively, the results of this study suggest that the selected *Trichuris* MHC-II T-cell epitopes are potential vaccine candidates and may explain the protective immune response developed in mice following vaccination (Chapter 7).

2.12 VLP (HBc-Ag) as a promising vaccine delivery system

Purified antigens can sometimes have poor immunogenicity. Therefore, choosing an economically viable antigen delivery system is critical, as this will have a tremendous impact on the immune pathways following vaccination (Cunningham et al., 2016; Wang, 2018). Numerous VLP-based vaccines have been engineered to exhibit foreign parasite antigens and have been proved to be highly immunogenic. Some of these VLP-based vaccines are in clinical development, such as the anti-malaria vaccine (RTS) (Dobano et al., 2019), and others are still under major research investigation, such as the vaccines against *Trichinella spiralis* (Lee et al., 2017), *Clonorchis sinensis* (Lee et al., 2017), and *Toxoplasma gondii* for example (Guo et al., 2019).

Chapter 5 highlighted the potential of native VLP (HBc-Ag) as a vaccine delivery system as it expresses *Trichuris* T-cell epitopes and simplifies the inherent production challenges associated with development of a safe and economical vaccine. All the predicted *Trichuris* MHC-II T-cell epitopes identified in Chapter 4 were successfully cloned in the MIR of the native VLP (HBc-Ag) and expressed using an *E. coli* expression system. Only the VLPs+ T-cell epitope recombinant proteins confirmed to be soluble by SDS-PAGE analysis were purified using Strep-Tag affinity chromatography and size-exclusion chromatography. Then, they were examined by CD and TEM to confirm their structural integrity and assembly.

The insertion of whole hypothetical protein (HBc-HP₁₋₅₁₂) and a mosaic construct (HBc-mosaic) providing a single expression system displaying multiple *Trichuris* epitopes (HBc-hypothetical protein (A0A0N5DRU5) + CLSP₃₉₈₋₄₁₆ epitope + chitin binding domain (A0A0N5DK22)) into HBc-Ag was successful. However, these two constructs were insoluble when expressed in *E. coli* and were not further purified by affinity chromatography. In future work aiming to develop these VLP recombinant proteins, chemical coupling may be used to solve this problem as this allows for more precise surface decoration of VLPs with large foreign antigens (Fogarty and Swartz, 2018; Patel and Swartz, 2011). Only soluble and highly purified VLPs expressing *Trichuris* MHC-II T-cell epitopes (HBc-H₁₁₂₋₁₂₈, HBc-CBD₃₆₋₅₂, HBc-CBD₁₂₄₃₋₁₂₅₉, HBc-CBD₂₄₁₋₂₅₇, HBc-CLSP₁₄₃₋₁₅₈ and HBc-CLSP₃₉₈₋₄₁₆) were used in the *in vitro* and *in vivo* assays performed to confirm antigenicity in Chapters 6 and 7.

The data presented in Chapter 6 demonstrated that the native VLP (HBc-Ag) and HBc-Ag expressing *Trichuris* MHC-II T-cell epitopes provided two types of immunoregulator signals to both APCs (DCs and macrophages). This can enable orchestrated priming of both humoral and cellular immune responses during the development of VLP-mediated immunity. First, the up-regulation of cell surface markers essential for optimal activation of Ag-specific T-cells. Second, stimulation of inflammatory responses characterised by the secretion of high levels of pro- and anti-inflammatory cytokines, which are involved in the immune regulation of B- and T-lymphocytes. Third, VLPs were proven to be taken up efficiently by both types APCs and were not merely attached to the surface of the APCs. These results suggest that the VLPs are well placed to act as delivery systems to drive immune responses via both APCs. Given that VLPs activate both APCs, future work may include evaluating the VLPs' activation responses to different DC subsets and other APCs including B-cells, *in vivo*. Additional work is also needed to modify the VLP using immunostimulatory adhesion molecules and cytokines co-displayed on the VLP to target APCs to enhance the activation of antigen-specific T-and B-cell effector cells.

2.13 Identification of a novel VLP-based vaccine against trichuriasis

One of the most important lessons learned from previous anti-parasite vaccines is that the use of multiple antigens induces more reliably high levels of protection than offered by a single antigen (Birkett et al., 2002; Cabrera-Mora et al., 2016). The work described in Chapter 7 evaluated the immunogenic and protective immune responses of a mixture of four VLPs expressing four different *Trichuris* MHC-II T-cell epitopes as a potential vaccine candidate *in vivo* in the murine model of *Trichuris* infection.

Mice vaccinated with 25 µg of pre-mixed VLPs expressing *Trichuris* MHC-II T-cell epitopes with and without an adjuvant boosted immune responses, but the responses were not sufficient to drive protection against a high-dose *Trichuris* infection. However, oral challenge with *T. muris* infective eggs following vaccination with a dose of 50 µg of pre-mixed VLPs+ T-cell epitopes (HBc-CBD₁₂₄₃₋₁₂₅₉, HBc-CBD₂₄₁₋₂₅₇, HBc-CLSP₁₄₃₋₁₅₈ and HBc-CLSP₃₉₈₋₄₁₆) led to a significant reduction in worm burden (51.2%). Also, mice vaccinated with VLPs+ T-cell epitopes produced MLN-derived Th1 (IFN-γ) and Th2 cytokines (IL-4, IL-5, IL-9, and IL-13), crypt hyperplasia and goblet cells hyperplasia. While it is known that goblet cell hyperplasia is an IL-13-dependent mechanism of

Trichuris expulsion in mice that are resistant to *Trichuris* infection (Datta et al., 2005), further work is required to elucidate whether goblet cell hyperplasia is a critical protective effector mechanism following vaccination of Muc2 KO mice with VLPs+ T-cell epitopes.

VLPs+ T-cell epitopes were found to elicit strong neutralising antibody responses involving isotype class-switching to IgG1 and IgG2c specific to their corresponding VLP+ T-cell epitope recombinant protein (HBc-CBD₁₂₄₃₋₁₂₅₉, HBc-CBD₂₄₁₋₂₅₇, HBc-CLSP₁₄₃₋₁₅₈ and HBc-CLSP₃₉₈₋₄₁₆). These results suggest that all four VLPs+ T-cell epitopes recombinant proteins had a similar effect on class switching and enhanced both Th1- and Th2-mediated immune responses. Although the significance of the follicular structures identified in the guts of some vaccinated mice is not yet clear, they may be related to the strong antibody response in mice vaccinated with VLPs+ T-cell epitopes. Collectively, these findings suggest that antibody-dependent mechanism may be crucial for expulsion of *T. muris* in vaccinated mice; yet, it is not an indicator of the degree of protection. Further studies placing greater focus on the role of B-cells as the primary APCs should be undertaken using B-cell KO mice.

This study supports the work of Dixon et al. (2010), who found that Th1 (IFN- γ) and Th2 (IL-5, IL-9, IL-13) cytokines, IgG1 and IgG2c antibodies, goblet cell hyperplasia and crypt hyperplasia are important elements of vaccine-induced resistance to *T. muris* following ES vaccination. Taken together, the results of this study suggest that there may be differences in the mechanisms of expulsion between those with natural resistance and those with vaccinated resistance. Thus, the correlation between immune response and protection offered by the VLPs+ T-cell epitope vaccine is a research priority. Also, despite the promising results of this study, additional technical issues need to be better explored. For example, the vaccine schedule and dose need to be optimised to achieve an appropriate level of protection.

2.14 Prospects and challenges for anti-*Trichuris* vaccine design

Development of new vaccines is a complex and multidisciplinary task that requires an understanding of host-pathogen interactions, epidemiology and manufacturing parameters (Cunningham et al., 2016). Most importantly, vaccine researchers must have an understanding of the immune mechanisms involved in diseases and protection in order to select appropriate antigenic targets and delivery systems to shape the immune response induced by the vaccine (Howarth and Brune, 2018; Knox et al., 2001). These factors determine the biomechanical requirements of production and the design of the laboratory and clinical trials (Howarth and Brune, 2018; Knox et al., 2001).

Recognition and understanding of a number of biological, socioeconomic and ethical factors are fundamental for developing long-lived protective vaccines (Ota et al., 2013). Clear knowledge of the risk groups and populations, age-specific infection rates and infection demographics is important as these factors are known to influence immune responses to vaccines (Cunningham et al., 2016). Additionally, political, ethical and socioeconomic issues such as education, behavioural and cultural factors affect not only vaccine selection but also evaluation of vaccine immune responses (Coughlin, 2006; Hotez, 2017).

Previous studies have demonstrated that most infants in endemic areas are infected with *T. trichiura* and school-aged children are at particularly high risk of *T. trichiura* infection (Awasthi et al., 2003; Bethony et al., 2006). Immunisation during the neonatal period may be a promising strategy as neonates are often capable of producing a Th2 response and antibody isotype switching to vaccine antigens (Adkins et al., 2001; Barrios et al., 1996). Thus, the ideal vaccine would be given to infants prior to risk as well as to older children and adults with ongoing infection. However, this strategy is problematic as an early study showed that vaccination could not protect susceptible mice with a pre-existing infection and subsequent challenge infection (Else and Wakelin, 1990a).

Considering the target populations that are most afflicted by trichuriasis infection, the administration route of the vaccine is another important factor that can influence the design of a vaccine and its accessibility to patients (Jain et al., 2015; Noon and Aroian, 2017). Adaptive immune responses are mainly induced in secondary lymphoid organs. Thus, it is critical for APCs to transport vaccine antigens through the lymphatic system from peripheral tissues to lymphoid organs (Bachmann and Jennings, 2010). Most currently approved vaccines are administered by intramuscular or subcutaneous injection. However, it has been suggested by many researchers that vaccine-induced protection against mucosal disease requires oral or nasal mucosal administration (Bachmann and Jennings, 2010). The particulate nature of VLPs enables them to be transported to lymph organs. In addition, they are very stable and can withstand adverse environments, such as those with acidic pH, making VLPs an attractive carrier for mucosally administered vaccines. Future work developing these vaccines should focus on assessing thermal stability and ensuring that vaccines can be stored without refrigeration to reduce delivery restrictions (Fogarty and Swartz, 2018).

It is also important to consider the epidemiology of infection during vaccine development. The viability of the vaccine candidates described in this thesis has been tested against one high-dose infection. A more realistic mouse model of human infection would involve chronic infection, as this would produce greater confidence that an anti-*Trichuris* vaccine could have a protective effect in the field. Future studies could vaccinate male C57BL/6 mice with the vaccine candidate, followed by a low-dose of *T. muris* infection to develop chronicity. The worm burdens should be assessed a number of weeks post-vaccination to determine how long vaccine-induced immunity to *Trichuris* lasts.

A key observation made during phase II of the clinical trial of the *N. americanus* vaccine was that pre-vaccination volunteers living in endemic areas experienced allergic reactions triggered by high IgE responses to infective larvae antigens (Diemert et al., 2012). Thus, it is critical to prevent allergic responses when developing a vaccine. Although the *Trichuris* T-cell epitopes selected for this study were screened for allergenicity *in silico*, future work must examine IgE responses in the sera from populations in countries with endemic STH infections.

Furthermore, all the pre-clinical vaccine evaluations of human STH infections used various laboratory infection models. Although there is no way of conducting these studies directly on humans, these models likely have limitations that could cause variation in the results, such as use

of different laboratory host species or strains; unnatural infection; and different reagents, equipment or researchers (Noon and Aroian, 2017; Zeng et al., 2016).

Coinfections with two or multiple soil-transmitted nematode infections including, *A. lumbricoides* and hookworms, mostly *Necator americanus*, are extremely common in young people (Alexander and Blackburn, 2019; Salim et al., 2015). Thus, researchers have proposed a single pan-anthelmintic vaccine against the three major human STHs to generate strong, lasting immunity with minimal side effects (Zhan et al., 2014). Although each of these STHs occupies a different location within the gastrointestinal tract and/or exhibits different feeding habits, which may present enormous obstacles for a single vaccine, these three helminths spp share highly conserved antigens that are likely to have very similar biological functions (Noon and Aroian, 2017). Thus, a Pan-anthelmintic vaccine based on protective epitopes from *Trichuris* and other cross-protective antigens may be achievable using the RV strategy.

2.15 Conclusions and future perspectives

Vaccines can serve as one of the most effective means to prevent trichuriasis. Approaches to anti-*Trichuris* vaccine development have focused mainly on *Trichuris* native antigens, limiting these vaccines' suitability for production and distribution in the developing world. Today, however, it may be prudent to consider alternatives to conventional thinking and appraise the available genetic information to develop an epitope-based vaccine to overcome these limitations.

The work presented in this thesis represents significant progress towards the development of a novel epitope-based vaccine against trichuriasis. We assert that VLPs (HBc-Ag) expressing *Trichuris* T-cell epitopes are potential vaccine candidates, as they meet the major vaccine design criteria: (1) self-assembly and display of the target antigens; (2) inexpensive production in *E. coli* expression systems; (3) stimulation of APCs for prompt activation of both humoral and cellular immune responses; (4) safety in a pre-clinical model; and (5) demonstration of efficacy in protecting against challenge infections without the need for an adjuvant.

There are multiple future works priorities in which to move forward. First, it is necessary to modify the VLP-based vaccine to target APCs in order to induce stronger humoral and cellular immune responses and immunological memory. Second, the protective efficacy and prolonged responses of these vaccine candidates must be tested in different animal models. Third, to determine the immune response that must be elicited by the VLP-based vaccine to develop protection. Finally, promising epitopes for *Trichuris* and other STH parasites must be identified to develop a pan-anthelmintic vaccine.

In conclusion, given the right combination of immunoinformatics and immunogenicity screening tools, epitope-based vaccines will undoubtedly limit the cost and effort associated with bringing a *Trichuris* vaccine to trial.

References

- Adkins, B., Bu, Y. & Guevara, P. (2001). 'The generation of Th memory in neonates versus adults: prolonged primary Th2 effector function and impaired development of Th1 memory effector function in murine neonates', *The Journal of Immunology*, 166(2), pp. 918-925.
- Agallou, M., Athanasiout, E., Koutsonit, O., Dotsika, E. & Karagouni, E. (2014). 'Experimental validation of multi-epitope peptides including promising MHC class I- and II-restricted epitopes of four known *Leishmania infantum* proteins', *Frontiers in Immunology*, 5.
- Agallou, M., Margaroni, M., Athanasiou, E., Toubanaki, D. K., Kontonikola, K., Karidi, K., Kammona, O., Kiparissides, C. & Karagouni, E. (2017). 'Identification of BALB/c Immune Markers Correlated with a Partial Protection to *Leishmania infantum* after Vaccination with a Rationally Designed Multi-epitope Cysteine Protease A Peptide-Based Nanovaccine', *PLoS Negl Trop Dis*, 11(1), p. e0005311.
- Ahlborg, N., Ling, I. T., Holder, A. A. & Riley, E. M. (2000). 'Linkage of exogenous T-cell epitopes to the 19-kilodalton region of Plasmodium yoelii merozoite surface protein 1 (MSP119) can enhance protective immunity against malaria and modulate the immunoglobulin subclass response to MSP119', *Infect Immun*, 68(4), pp. 2102-2109.
- Ahlborg, N., Sterky, F., Haddad, D., Perlmann, P., Nygren, P.-a., Andersson, R. & Berzins, K. (1997). 'Predominance of H-2 d-and H-2 k-restricted T-cell epitopes in the highly repetitive Plasmodium falciparum antigen Pf332', *Molecular immunology*, 34(5), pp. 379-389.
- Akache, B., Weeratna, R. D., Deora, A., Thorn, J. M., Champion, B., Merson, J. R., Davis, H. L. & McCluskie, M. J. (2016). 'Anti-IgE Qb-VLP conjugate vaccine self-adjuvants through activation of TLR7', *Vaccines*, 4(1), p. 3.
- Akhras, S., Toda, M., Boller, K., Himmelsbach, K., Elgner, F., Biehl, M., Scheurer, S., Gratz, M., Vieths, S. & Hildt, E. (2017). 'Cell-permeable capsids as universal antigen carrier for the induction of an antigen-specific CD8+ T-cell response', *Scientific reports*, 7(1), p. 9630.
- Akiho, H., Blennerhassett, P., Deng, Y. & Collins, S. M. (2002). 'Role of IL-4, IL-13, and STAT6 in inflammation-induced hypercontractility of murine smooth muscle cells', 282(2), pp. G226-G232.
- Albonico, M., Bickle, Q., Ramsan, M., Montresor, A., Savioli, L. & Taylor, M. (2003). 'Efficacy of mebendazole and levamisole alone or in combination against intestinal nematode infections after repeated targeted mebendazole treatment in Zanzibar', *Bulletin of the World Health Organization*, 81, pp. 343-352.
- Alexander, T. Y. & Blackburn, B. G. (2019). 'Soil-Transmitted Helminths: *Ascaris*, *Trichuris*, and Hookworm Infections', *Water and Sanitation-Related Diseases and the Environment: In the Age of Climate Change*, p. 95.
- Altman, D. G. & Bland, J. M. (1994). 'Diagnostic tests. 1: Sensitivity and specificity', *BMJ: British Medical Journal*, 308(6943), p. 1552.
- Altman, L. K. (1982). 'A new insulin given approval for use in US', *New York Times*, 30.
- Alves-Silva, M. V., Nico, D., Morrot, A., Palatnik, M. & Palatnik-de-Sousa, C. B. (2017). 'A Chimera Containing CD4+ and CD8+ T-Cell Epitopes of the *Leishmania donovani* Nucleoside Hydrolase (NH36) Optimizes Cross-Protection against *Leishmania amazonensis* Infection', *Front Immunol*, 8, p. 100.
- Ambühl, P. M., Tissot, A. C., Fulurija, A., Maurer, P., Nussberger, J., Sabat, R., Nieff, V., Schellekens, C., Sladko, K. & Roubicek, K. (2007). 'A vaccine for hypertension based on virus-like particles: preclinical efficacy and phase I safety and immunogenicity', *Journal of hypertension*, 25(1), pp. 63-72.
- Andersen, P., Andersen, A. B., Sørensen, A. & Nagai, S. (1995). 'Recall of long-lived immunity to *Mycobacterium tuberculosis* infection in mice', *The Journal of Immunology*, 154(7), pp. 3359-3372.
- Anderson, R. & May, R. (1985). 'Herd immunity to helminth infection and implications for parasite control'.

- Andreatta, M., Trolle, T., Yan, Z., Greenbaum, J. A., Peters, B. & Nielsen, M. (2018). 'An automated benchmarking platform for MHC class II binding prediction methods', *Bioinformatics*, 34(9), pp. 1522-1528.
- Anto, E. J. & Nugraha, S. E. J. O. A. M. J. o. M. S. (2019). 'Efficacy of Albendazole and Mebendazole With or Without Levamisole for Ascariasis and Trichuriasis', 7.
- Anzaghe, M., Schülke, S. & Scheurer, S. (2018). 'Virus-Like Particles as Carrier Systems to Enhance Immunomodulation in Allergen Immunotherapy', *Current allergy and asthma reports*, 18(12), p. 71.
- Arnon, R. & Ben-Yedidya, T. (2003). 'Old and new vaccine approaches', *International immunopharmacology*, 3(8), pp. 1195-1204.
- Artis, D., Humphreys, N. E., Bancroft, A. J., Rothwell, N. J., Potten, C. S. & Grencis, R. K. (1999a). 'Tumor Necrosis Factor α Is a Critical Component of Interleukin 13-Mediated Protective T Helper Cell Type 2 Responses during Helminth Infection', 190(7), pp. 953-962.
- Artis, D., Potten, C. S., Else, K. J., Finkelman, F. D. & Grencis, R. K. (1999b). 'Trichuris muris: host intestinal epithelial cell hyperproliferation during chronic infection is regulated by interferon- γ ', *Experimental parasitology*, 92(2), pp. 144-153.
- Artis, D., Villarino, A., Silverman, M., He, W., Thornton, E. M., Mu, S., Summer, S., Covey, T. M., Huang, E., Yoshida, H., Koretzky, G., Goldschmidt, M., Wu, G. D., de Sauvage, F., Miller, H. R. P., Saris, C. J. M., Scott, P. & Hunter, C. A. (2004a). 'The IL-27 Receptor (WSX-1) Is an Inhibitor of Innate and Adaptive Elements of Type 2 Immunity', *The Journal of Immunology*, 173(9), pp. 5626-5634.
- Artis, D., Wang, M. L., Keilbaugh, S. A., He, W., Brenes, M., Swain, G. P., Knight, P. A., Donaldson, D. D., Lazar, M. A. & Miller, H. R. (2004b). 'RELM β /FIZZ2 is a goblet cell-specific immune-effector molecule in the gastrointestinal tract', *Proceedings of the National Academy of Sciences*, 101(37), pp. 13596-13600.
- Aston-Deaville, S. J. (2017). *Development Of Improved Bioprocessing Methods For The Manufacture Of A Vaccine Against Meningococcal Meningitis*. PhD, The University of Manchester, Manchester.
- Astori, M. & Kraehenbuhl, J.-P. (1996). 'Recombinant fusion peptides containing single or multiple repeats of a ubiquitous T-helper epitope are highly immunogenic', *Molecular immunology*, 33(13), pp. 1017-1024.
- Awasthi, S., Bundy, D. A. & Savioli, L. (2003). 'Helminthic infections', *Bmj*, 327(7412), pp. 431-433.
- Bachmann, M. F. & Jennings, G. T. (2010). 'Vaccine delivery: a matter of size, geometry, kinetics and molecular patterns', *Nature Reviews Immunology*, 10(11), p. 787.
- Bachmann, M. F., Rohrer, U. H., Kundig, T. M., Burki, K., Hengartner, H. & Zinkernagel, R. M. (1993). 'The influence of antigen organization on B cell responsiveness', *Science*, 262(5138), pp. 1448-1451.
- Backert, L. & Kohlbacher, O. (2015). 'Immunoinformatics and epitope prediction in the age of genomic medicine', *Genome Med*, 7, p. 119.
- Bai, B., Hu, Q., Hu, H., Zhou, P., Shi, Z., Meng, J., Lu, B., Huang, Y., Mao, P. & Wang, H. (2008). 'Virus-like particles of SARS-like coronavirus formed by membrane proteins from different origins demonstrate stimulating activity in human dendritic cells', *PloS one*, 3(7), p. e2685.
- Bain, R. (1999). 'Irradiated vaccines for helminth control in livestock', *International journal for parasitology*, 29(1), pp. 185-191.
- Balasubramanian, N., Toubarro, D. & Simoes, N. (2010). 'Biochemical study and in vitro insect immune suppression by a trypsin-like secreted protease from the nematode Steinernema carpocapsae', *Parasite immunology*, 32(3), pp. 165-175.
- Bambini, S. & Rappuoli, R. J. D. d. t. (2009). 'The use of genomics in microbial vaccine development', 14(5-6), pp. 252-260.
- Banchereau, J., Briere, F., Caux, C., Davoust, J., Lebecque, S., Liu, Y.-J., Pulendran, B. & Palucka, K. (2000). 'Immunobiology of dendritic cells', *Annual review of immunology*, 18(1), pp. 767-811.

- Bancroft, A. J., Artis, D., Donaldson, D. D., Sypek, J. P. & Grencis, R. K. (2000). 'Gastrointestinal nematode expulsion in IL-4 knockout mice is IL-13 dependent', *European journal of immunology*, 30(7), pp. 2083-2091.
- Bancroft, A. J., Else, K. J. & Grencis, R. K. (1994). 'Low-level infection with *Trichuris muris* significantly affects the polarization of the CD4 response', *European journal of immunology*, 24(12), pp. 3113-3118.
- Bancroft, A. J., Else, K. J., Humphreys, N. E. & Grencis, R. K. (2001). 'The effect of challenge and trickle *Trichuris muris* infections on the polarisation of the immune response', *International journal for parasitology*, 31(14), pp. 1627-1637.
- Bancroft, A. J., Else, K. J., Sypek, J. P. & Grencis, R. K. (1997). 'Interleukin-12 promotes a chronic intestinal nematode infection', *Eur J Immunol*, 27(4), pp. 866-70.
- Bancroft, A. J., Humphreys, N. E., Worthington, J. J., Yoshida, H. & Grencis, R. K. (2004). 'WSX-1: a key role in induction of chronic intestinal nematode infection', *The Journal of Immunology*, 172(12), pp. 7635-7641.
- Bancroft, A. J., McKenzie, A. N. & Grencis, R. K. (1998). 'A critical role for IL-13 in resistance to intestinal nematode infection', *The Journal of Immunology*, 160(7), pp. 3453-3461.
- Barrios, C., Brawand, P., Berney, M., Brandt, C., Lambert, P. H. & Siegrist, C. A. (1996). 'Neonatal and early life immune responses to various forms of vaccine antigens qualitatively differ from adult responses: predominance of a Th2-biased pattern which persists after adult boosting', *European journal of immunology*, 26(7), pp. 1489-1496.
- Barth, H., Ulsenheimer, A., Pape, G. R., Diepolder, H. M., Hoffmann, M., Neumann-Haefelin, C., Thimme, R., Henneke, P., Klein, R. & Paranhos-Baccalà, G. (2005). 'Uptake and presentation of hepatitis C virus-like particles by human dendritic cells', *Blood*, 105(9), pp. 3605-3614.
- Becker, S. L., Liwanag, H. J., Snyder, J. S., Akogun, O., Belizario Jr, V., Freeman, M. C., Gyorkos, T. W., Imtiaz, R., Keiser, J. & Krolewiecki, A. (2018). 'Toward the 2020 goal of soil-transmitted helminthiasis control and elimination', *PLoS neglected tropical diseases*, 12(8), p. e0006606.
- Bell, L. V. & Else, K. J. (2011). 'Regulation of colonic epithelial cell turnover by IDO contributes to the innate susceptibility of SCID mice to *Trichuris muris* infection', 33(4), pp. 244-249.
- Bellaby, T., Robinson, K. & Wakelin, D. (1996). 'Induction of differential T-helper-cell responses in mice infected with variants of the parasitic nematode *Trichuris muris*', *Infection and immunity*, 64(3), pp. 791-795.
- Belladonna, M. L., Renaud, J.-C., Bianchi, R., Vacca, C., Fallarino, F., Orabona, C., Fioretti, M. C., Grohmann, U. & Puccetti, P. (2002). 'IL-23 and IL-12 have overlapping, but distinct, effects on murine dendritic cells', *The Journal of Immunology*, 168(11), pp. 5448-5454.
- Bénard, C. Y., Boyanov, A., Hall, D. H. & Hobert, O. (2006). 'DIG-1, a novel giant protein, non-autonomously mediates maintenance of nervous system architecture', *Development*, 133(17), pp. 3329-3340.
- Bergman, M. A., Cummings, L. A., Alaniz, R. C., Mayeda, L., Fellnerova, I. & Cookson, B. T. (2005). 'CD4+T-cell responses generated during murine *Salmonella enterica* serovar Typhimurium infection are directed towards multiple epitopes within the natural antigen FliC', *Infect Immun*, 73(11), pp. 7226-7235.
- Bessa, J., Zabel, F., Link, A., Jegerlehner, A., Hinton, H. J., Schmitz, N., Bauer, M., Kündig, T. M., Saudan, P. & Bachmann, M. F. (2012). 'Low-affinity B cells transport viral particles from the lung to the spleen to initiate antibody responses', *Proceedings of the National Academy of Sciences*, 109(50), pp. 20566-20571.
- Bethony, J., Brooker, S., Albonico, M., Geiger, S., Loukas, A., Diemert, D. & Hotez, P. (2006). 'Soil-transmitted helminth infections: ascariasis, trichuriasis, and hookworm', *Lancet*, 6(367), pp. 1521-32.
- Betts, C. & Else, K. (2000). '*Trichuris muris*: CD4+ T cell-mediated protection in reconstituted SCID mice', *Parasitology*, 121(6), pp. 631-637.
- Betts, C. J. & Else, K. J. (1999). 'Mast cells, eosinophils and antibody-mediated cellular cytotoxicity are not critical in resistance to *Trichuris muris*', *Parasite immunology*, 21(1), pp. 45-52.

- Beyer, T., Herrmann, M., Reiser, C., Bertling, W. & Hess, J. (2001). 'Bacterial carriers and virus-like-particles as antigen delivery devices: role of dendritic cells in antigen presentation', *Current Drug Targets-Infectious Disorders*, 1(3), pp. 287-302.
- Bian, Z., Hua, Z., Yan, W., Liu, M. & Zheng, Z. (2006). 'Expression in *Escherichia coli* of hepatitis B virus genes from minority nationality patients in Yunnan province with chronic hepatitis B and their antigenicity', *Zhonghua yi xue za zhi*, 86(14), pp. 983-986.
- Bickert, T., Wohlleben, G., Brinkman, M., Trujillo-Vargas, C. M., Ruehland, C., Reiser, C. O., Hess, J. & Erb, K. J. (2007). 'Murine polyomavirus-like particles induce maturation of bone marrow-derived dendritic cells and proliferation of T cells', *Medical microbiology and immunology*, 196(1), pp. 31-39.
- Birkett, A., Lyons, K., Schmidt, A., Boyd, D., Oliveira, G., Siddique, A., Nussenzweig, R., Calvo-Calle, J. & Nardin, E. (2002). 'A modified hepatitis B virus core particle containing multiple epitopes of the *Plasmodium falciparum* circumsporozoite protein provides a highly immunogenic malaria vaccine in preclinical analyses in rodent and primate hosts', *Infection and immunity*, 70(12), pp. 6860-6870.
- Birkett, A., Thornton, B., Milich, D., Oliveira, G., Siddique, A., Nussenzweig, R., Calvo-Calle, J. & Nardin, E. (2001). 'Hepatitis B virus core antigen particles containing minimal T and B cell epitopes of *Plasmodium falciparum* CS protein elicit high levels of malaria specific immune responses in mice and non-human primates', *Am. J. Trop. Med. Hyg*, 65, p. 258.
- Birnbaum, F. & Nassal, M. (1990). 'Hepatitis B virus nucleocapsid assembly: primary structure requirements in the core protein', *Journal of virology*, 64(7), pp. 3319-3330.
- Blackwell, N. M. & Else, K. J. (2001). 'B cells and antibodies are required for resistance to the parasitic gastrointestinal nematode *Trichuris muris*', *Infection and immunity*, 69(6), pp. 3860-3868.
- Blackwell, N. M. & Else, K. J. (2002). 'A comparison of local and peripheral parasite-specific antibody production in different strains of mice infected with *Trichuris muris*', *Parasite immunology*, 24(4), pp. 203-211.
- Blair, P. & Diemert, D. (2015). 'Update on prevention and treatment of intestinal helminth infections', *Current infectious disease reports*, 17(3), p. 12.
- Boigard, H., Cimica, V. & Galarza, J. M. (2018). 'Dengue-2 virus-like particle (VLP) based vaccine elicits the highest titers of neutralizing antibodies when produced at reduced temperature', *Vaccine*, 36(50), pp. 7728-7736.
- Borrás-Cuesta, F., Golvano, J.-J., García-Granero, M., Sarobe, P., Riezu-Boj, J.-I., Huarte, E. & Lasarte, J.-J. (2000). 'Specific and general HLA-DR binding motifs: comparison of algorithms', *Human immunology*, 61(3), pp. 266-278.
- Bosio, C. M., Moore, B. D., Warfield, K. L., Ruthel, G., Mohamadzadeh, M., Aman, M. J. & Bavari, S. (2004). 'Ebola and Marburg virus-like particles activate human myeloid dendritic cells', *Virology*, 326(2), pp. 280-287.
- Böttcher, B. & Nassal, M. (2018). 'Structure of Mutant Hepatitis B Core Protein Capsids with Premature Secretion Phenotype', *Journal of molecular biology*.
- Böttcher, B., Vogel, M., Ploss, M. & Nassal, M. (2006). 'High plasticity of the hepatitis B virus capsid revealed by conformational stress', *Journal of molecular biology*, 356(3), pp. 812-822.
- Böttcher, B., Wynne, S. & Crowther, R. (1997). 'Determination of the fold of the core protein of hepatitis B virus by electron cryomicroscopy', *Nature*, 386(6620), p. 88.
- Bouchery, T., Kyle, R., Ronchese, F. & Le Gros, G. (2014). 'The Differentiation of CD4(+) T-Helper Cell Subsets in the Context of Helminth Parasite Infection', *Front Immunol*, 5, p. 487.
- Bousarghin, L., Hubert, P., Franzen, E., Jacobs, N., Boniver, J. & Delvenne, P. (2005). 'Human papillomavirus 16 virus-like particles use heparan sulfates to bind dendritic cells and colocalize with langerin in Langerhans cells', *Journal of General Virology*, 86(5), pp. 1297-1305.
- Bowcutt, R., Bell, L., Little, M., Wilson, J., Booth, C., Murray, P., Else, K. & Cruickshank, S. J. P. i. (2011). 'Arginase-1-expressing macrophages are dispensable for resistance to infection with the gastrointestinal helminth *Trichuris muris*', 33(7), pp. 411-420.

- Bowcutt, R., Bramhall, M., Logunova, L., Wilson, J., Booth, C., Carding, S. R., Grencis, R. & Cruickshank, S. (2014). 'A role for the pattern recognition receptor Nod2 in promoting recruitment of CD103+ dendritic cells to the colon in response to *Trichuris muris* infection', *Mucosal Immunol*, 7(5), pp. 1094-105.
- Brandau, D. T., Jones, L. S., Wiethoff, C. M., Rexroad, J. & Middaugh, C. R. (2003). 'Thermal stability of vaccines', *Journal of pharmaceutical sciences*, 92(2), pp. 218-231.
- Brandenburg, B., Stockl, L., Gutzeit, C., Roos, M., Lupberger, J., Schwartlander, R., Gelderblom, H., Sauer, I. M., Hofschneider, P. H. & Hildt, E. (2005). 'A novel system for efficient gene transfer into primary human hepatocytes via cell-permeable hepatitis B virus-like particle', *Hepatology*, 42(6), pp. 1300-1309.
- Brandt, L., Oettinger, T., Holm, A., Andersen, A. B. & Andersen, P. (1996). 'Key epitopes on the ESAT-6 antigen recognized in mice during the recall of protective immunity to *Mycobacterium tuberculosis*', *The Journal of Immunology*, 157(8), pp. 3527-3533.
- Briggs, N., Wei, J., Versteeg, L., Zhan, B., Keegan, B., Damania, A., Pollet, J., Hayes, K. S., Beaumier, C. & Seid, C. A. (2018). 'Trichuris muris' whey acidic protein induces type 2 protective immunity against whipworm', *PLoS pathogens*, 14(8), p. e1007273.
- Brito, L. A. & Singh, M. (2011). 'Acceptable levels of endotoxin in vaccine formulations during preclinical research', *J Pharm Sci*, 100(1), pp. 34-7.
- Brooker, S., Clements, A. & Bundy, D. (2006). 'Global epidemiology, ecology and control of soil-transmitted helminth infections', *Advances in parasitology*, 62, pp. 221-261.
- Brown, J. H., Jardetzky, T. S., Gorga, J. C., Stern, L. J., Urban, R. G., Strominger, J. L. & Wiley, D. C. (1993). 'Three-dimensional structure of the human class II histocompatibility antigen HLA-DR1', *NATURE-LONDON-*, 364, pp. 33-33.
- Brusic, V., Bajic, V. B. & Petrovsky, N. (2004). 'Computational methods for prediction of T-cell epitopes—a framework for modelling, testing, and applications', *Methods*, 34(4), pp. 436-443.
- Brusic, V. & Petrovsky, N. (2005). 'Immunoinformatics and its relevance to understanding human immune disease'.
- Bui, H. H., Sidney, J., Li, W., Fusseder, N. & Sette, A. (2007). 'Development of an epitope conservancy analysis tool to facilitate the design of epitope-based diagnostics and vaccines', *BMC Bioinformatics*, 8, p. 361.
- Bundy, D. A., Cooper, E. S., Thompson, D. E., Anderson, R. M. & Didier, J. M. (1987). 'Age-related prevalence and intensity of *Trichuris trichiura* infection in a St. Lucian community', *Transactions of the Royal Society of Tropical Medicine and Hygiene*, 81(1), pp. 85-94.
- Bundy, D. A., Thompson, D. E., Golden, M. H., Cooper, E. S., Anderson, R. M. & Harland, P. S. (1985). 'Population distribution of *Trichuris trichiura* in a community of Jamaican children', *Transactions of the Royal Society of Tropical Medicine and Hygiene*, 79(2), pp. 232-237.
- Buus, S., Andreatta, M., Stryhn, A., Rasmussen, M., Karosiene, E. & Nielsen, M. (2015). Prediction of peptide-MHC class II binding affinity with improved binding core identification; implications for the interpretation of T cell cross-reactivity. In: 6th Argentinian Conference on Bioinformatics and Computational Biology, 2015. A2B2C.
- Cabrera-Mora, M., Fonseca, J. A., Singh, B., Zhao, C., Makarova, N., Dmitriev, I., Curiel, D. T., Blackwell, J. & Moreno, A. (2016). 'A recombinant chimeric Ad5/3 vector expressing a multistage *plasmodium* antigen induces protective immunity in mice using heterologous prime-boost immunization regimens', *The Journal of Immunology*, p. 1501926.
- Caffrey, C. R., Goupil, L., Rebello, K. M., Dalton, J. P. & Smith, D. (2018). 'Cysteine proteases as digestive enzymes in parasitic helminths', *PLoS neglected tropical diseases*, 12(8), p. e0005840.
- Calabro, S., Tritto, E., Pezzotti, A., Taccone, M., Muzzi, A., Bertholet, S., De Gregorio, E., O'Hagan, D. T., Baudner, B. & Seubert, A. (2013). 'The adjuvant effect of MF59 is due to the oil-in-water emulsion formulation, none of the individual components induce a comparable adjuvant effect', *Vaccine*, 31(33), pp. 3363-3369.
- Calvo-Calle, J., Hammer, J., Sinigaglia, F., Clavijo, P., Moya-Castro, Z. R. & Nardin, E. (1997). 'Binding of malaria T cell epitopes to DR and DQ molecules in vitro correlates with

- immunogenicity *in vivo*: identification of a universal T cell epitope in the *Plasmodium falciparum* circumsporozoite protein', *The Journal of Immunology*, 159(3), pp. 1362-1373.
- Caminschi, I. & Shortman, K. (2012). 'Boosting antibody responses by targeting antigens to dendritic cells', *Trends in immunology*, 33(2), pp. 71-77.
- Cantacessi, C., Mitreva, M., Jex, A. R., Young, N. D., Campbell, B. E., Hall, R. S., Doyle, M. A., Ralph, S. A., Rabelo, E. M., Ranganathan, S., Sternberg, P. W., Loukas, A. & Gasser, R. B. (2010). 'Massively parallel sequencing and analysis of the *Necator americanus* transcriptome', *PLoS Negl Trop Dis*, 4(5), p. e684.
- Cantacessi, C., Young, N. D., Nejsum, P., Jex, A. R., Campbell, B. E., Hall, R. S., Thamsborg, S. M., Scheerlinck, J.-P. & Gasser, R. B. (2011). 'The transcriptome of *Trichuris suis*-first molecular insights into a parasite with curative properties for key immune diseases of humans', *PLoS one*, 6(8), p. e23590.
- Cao, J., Zhang, J., Lu, Y., Luo, S., Zhang, J. & Zhu, P. (2019). 'Cryo-EM structure of native spherical subviral particles isolated from HBV carriers', *Virus research*, 259, pp. 90-96.
- Capecci, B., Serruto, D., Adu-Bobie, J., Rappuoli, R. & Pizza, M. (2004). 'The genome revolution in vaccine research', *Current issues in molecular biology*, 6, pp. 17-28.
- Chackerian, B. (2007). 'Virus-like particles: flexible platforms for vaccine development', *Expert review of vaccines*, 6(3), pp. 381-390.
- Chang, J., Zhang, Y., Yang, D., Jiang, Z., Wang, F. & Yu, L. (2018). 'Potent neutralization activity against type O foot-and-mouth disease virus elicited by a conserved type O neutralizing epitope displayed on bovine parvovirus virus-like particles', *Journal of General Virology*.
- Chanock, R. M., Lerner, R., Brown, F. & Ginsberg, H. (1987). 'Vaccines 87, modern approaches to new vaccines: Prevention of AIDS and other viral, bacterial and parasitic diseases'.
- Chaves, F. A., Lee, A. H., Nayak, J. L., Richards, K. A. & Sant, A. J. (2012). 'The utility and limitations of current Web-available algorithms to predict peptides recognized by CD4 T cells in response to pathogen infection', *J Immunol*, 188(9), pp. 4235-48.
- Cheever, A. W., Duvall, R. H., Hallack Jr, T. A., Minker, R. G., Malley, J. D. & Malley, K. G. (1987). 'Variation of hepatic fibrosis and granuloma size among mouse strains infected with *Schistosoma mansoni*', *The American journal of tropical medicine and hygiene*, 37(1), pp. 85-97.
- Chen, N., Yuan, Z. G., Xu, M. J., Zhou, D. H., Zhang, X. X., Zhang, Y. Z., Wang, X. W., Yan, C., Lin, R. Q. & Zhu, X. Q. (2012). 'Ascaris suum endolase is a potential vaccine candidate against ascariasis', *Vaccine*, 30(23), pp. 3478-3482.
- Chen, W., Shi, M., Shi, F., Mao, Y., Tang, Z., Zhang, B., Zhang, H., Chen, L., Chen, L. & Xin, S. (2009). 'HBcAg-pulsed dendritic cell vaccine induces Th1 polarization and production of hepatitis B virus-specific cytotoxic T lymphocytes', *Hepatology Research*, 39(4), pp. 355-365.
- Chen, X., Zaro, J. L. & Shen, W.-C. (2013). 'Fusion protein linkers: property, design and functionality', *Advanced drug delivery reviews*, 65(10), pp. 1357-1369.
- Chisari, F. V. & Ferrari, C. (1995). 'Hepatitis B virus immunopathogenesis', *Annu Rev Immunol*, 13(1), pp. 29-60.
- Choi, B., Kim, H., Choi, H. & Kang, S. (2018). 'Protein Cage Nanoparticles as Delivery Nanoplatforms', *Biomimetic Medical Materials*: Springerpp. 27-43.
- Choi, J. H., Keum, K. C. & Lee, S. Y. (2006). 'Production of recombinant proteins by high cell density culture of *Escherichia coli*', *Chemical Engineering Science*, 61(3), pp. 876-885.
- Chung, B.-S., Zhang, H., Choi, M.-H., Jeon, D., Li, S., Lee, M. & Hong, S.-T. (2004). 'Development of resistance to reinfection by *Clonorchis sinensis* in rats', *The Korean journal of parasitology*, 42(1), p. 19.
- Cielens, I., Ose, V., Petrovskis, I., Strelnikova, A., Renhofa, R., Kozlovska, T. & Pumpens, P. (2000). 'Mutilation of RNA phage Qbeta virus-like particles: from icosahedrons to rods', *FEBS Lett*, 482(3), pp. 261-4.
- Cimica, V., Boigard, H., Bhatia, B., Fallon, J. T., Alimova, A., Gottlieb, P. & Galarza, J. M. (2016). 'A novel respiratory syncytial virus-like particle (VLP) vaccine composed of the postfusion and prefusion conformations of the F glycoprotein', *Clinical and Vaccine Immunology*, pp. CVI. 00720-15.

- Cimica, V. & Galarza, J. M. (2017). 'Adjuvant formulations for virus-like particle (VLP) based vaccines', *Clinical immunology*, 183, pp. 99-108.
- Clarke, B., Newton, S., Carroll, A., Francis, M., Appleyard, G., Syred, A., Highfield, P., Rowlands, D. & Brown, F. (1987). 'Improved immunogenicity of a peptide epitope after fusion to hepatitis B core protein', *Nature*, 330(6146), p. 381.
- Clem, A. S. (2011). 'Fundamentals of vaccine immunology', *Journal of global infectious diseases*, 3(1), p. 73.
- Cliffe, L. J. & Grencis, R. K. (2004). 'The *Trichuris muris* system: a paradigm of resistance and susceptibility to intestinal nematode infection', *Advances in parasitology*, 57, pp. 255-307.
- Cliffe, L. J., Humphreys, N. E., Lane, T. E., Potten, C. S., Booth, C. & Grencis, R. K. (2005). 'Accelerated intestinal epithelial cell turnover: a new mechanism of parasite expulsion', *Science*, 308(5727), pp. 1463-1465.
- Clingan, J. M. & Matloubian, M. (2013). 'B Cell–Intrinsic TLR7 Signaling Is Required for Optimal B Cell Responses during Chronic Viral Infection', *The Journal of Immunology*, p. 1300244.
- Coakley, G., McCaskill, J. L., Borger, J. G., Simbari, F., Robertson, E., Millar, M., Harcus, Y., McSorley, H. J., Maizels, R. M. & Buck, A. H. (2017). 'Extracellular Vesicles from a Helminth Parasite Suppress Macrophage Activation and Constitute an Effective Vaccine for Protective Immunity', *Cell Reports*, 19(8), pp. 1545-1557.
- Coffman, R. L., Sher, A. & Seder, R. A. (2010). 'Vaccine adjuvants: putting innate immunity to work', *Immunity*, 33(4), pp. 492-503.
- Coler, R. N. & Reed, S. G. (2005). 'Second-generation vaccines against leishmaniasis', *Trends in parasitology*, 21(5), pp. 244-249.
- Collison, L. W., Chaturvedi, V., Henderson, A. L., Giacomin, P. R., Guy, C., Bankoti, J., Finkelstein, D., Forbes, K., Workman, C. J., Brown, S. A., Rehg, J. E., Jones, M. L., Ni, H. T., Artis, D., Turk, M. J. & Vignali, D. A. (2010). 'IL-35-mediated induction of a potent regulatory T cell population', *Nat Immunol*, 11(12), pp. 1093-101.
- Comber, J. D. & Philip, R. (2014). 'MHC class I antigen presentation and implications for developing a new generation of therapeutic vaccines', *Therapeutic advances in vaccines*, 2(3), pp. 77-89.
- Consortium, I. H. G. (2019). 'Comparative genomics of the major parasitic worms', *Nature genetics*, 51(1), p. 163.
- Conti-Fine, B. M. (1998). Diphtheria toxin epitopes. Google Patents.
- Cooper, A., Tal, G., Lider, O. & Shaul, Y. (2005). 'Cytokine induction by the hepatitis B virus capsid in macrophages is facilitated by membrane heparan sulfate and involves TLR2', *The Journal of Immunology*, 175(5), pp. 3165-3176.
- Costa, A. P. F., Gonçalves, A. K., Machado, P. R. L., de Souza, L. B., Sarmento, A., Cobucci, R. N. O., Giraldo, P. C. & Witkin, S. S. (2018). 'Immune response to human papillomavirus one year after prophylactic vaccination with AS04-adjuvanted HPV-16/18 vaccine: HPV-specific IgG and IgA antibodies in the circulation and the cervix', *Asian Pacific journal of cancer prevention: APJCP*, 19(8), p. 2313.
- Coughlin, S. S. (2006). 'Ethical issues in epidemiologic research and public health practice', *Emerging themes in epidemiology*, 3(1), p. 16.
- Cox, M. M. & Onraedt, A. (2012). 'Innovations in vaccine development: can regulatory authorities keep up?', *Expert review of vaccines*, 11(10), pp. 1171-1173.
- Crisci, E., Barcena, J. & Montoya, M. (2012). 'Virus-like particles: the new frontier of vaccines for animal viral infections', *Vet Immunol Immunopathol*, 148(3-4), pp. 211-25.
- Crisci, E., Bárcena, J. & Montoya, M. (2013). 'Virus-like particle-based vaccines for animal viral infections', *Inmunología*, 32(3), pp. 102-116.
- Crompton, D. & Savioli, L. (1993). 'Intestinal parasitic infections and urbanization', *Bulletin of the World Health Organization*, 71(1), p. 1.
- Crowther, R., Kiselev, N., Böttcher, B., Berriman, J., Borisova, G., Ose, V. & Pumpens, P. (1994). 'Three-dimensional structure of hepatitis B virus core particles determined by electron cryomicroscopy', *Cell*, 77(6), pp. 943-950.

- Cruickshank, S. M., Deschoolmeester, M. L., Svensson, M., Howell, G., Bazakou, A., Logunova, L., Little, M. C., English, N., Mack, M. & Grencis, R. K. (2009). 'Rapid dendritic cell mobilization to the large intestinal epithelium is associated with resistance to *Trichuris muris* infection', *The Journal of Immunology*, 182(5), pp. 3055-3062.
- Cubas, R., Zhang, S., Kwon, S., Sevick-Muraca, E. M., Li, M., Chen, C. & Yao, Q. (2009). 'Virus-like particle (VLP) lymphatic trafficking and immune response generation after immunization by different routes', *Journal of immunotherapy (Hagerstown, Md.: 1997)*, 32(2), p. 118.
- Cuesta-Astroz, Y., de Oliveira, F. S., Nahum, L. A. & Oliveira, G. (2017). 'Helminth secretomes reflect different lifestyles and parasitized hosts', *International journal for parasitology*, 47(9), pp. 529-544.
- Cunningham, A. L., Garçon, N., Leo, O., Friedland, L. R., Strugnell, R., Laupèze, B., Doherty, M. & Stern, P. (2016). 'Vaccine development: From concept to early clinical testing', *Vaccine*, 34(52), pp. 6655-6664.
- Curry, A. J., Jardim, A., Olobo, J. & Olafson, R. W. (1994). 'Cell-mediated responses of immunized vervet monkeys to defined *Leishmania* T-cell epitopes', *Infect Immun*, 62(5), pp. 1733-1741.
- D'argenio, D. A. & Wilson, C. B. (2010). 'A decade of vaccines: Integrating immunology and vaccinology for rational vaccine design', *Immunity*, 33(4), pp. 437-440.
- D'Elia, R., Behnke, J. M., Bradley, J. E. & Else, K. J. (2009). 'Regulatory T cells: a role in the control of helminth-driven intestinal pathology and worm survival', *The Journal of Immunology*, 182(4), pp. 2340-2348.
- D Hill, B., Zak, A., Khera, E. & Wen, F. (2018). 'Engineering virus-like particles for antigen and drug delivery', *Current Protein and Peptide Science*, 19(1), pp. 112-127.
- D'Elia, R. & Else, K. (2009). 'In vitro antigen presenting cell-derived IL-10 and IL-6 correlate with *Trichuris muris* isolate-specific survival', *Parasite immunology*, 31(3), pp. 123-131.
- Da Silva, D. M., Velders, M. P., Nieland, J. D., Schiller, J. T., Nickoloff, B. J. & Kast, W. M. (2001). 'Physical interaction of human papillomavirus virus-like particles with immune cells', *International immunology*, 13(5), pp. 633-641.
- Dabbagh, K., Takeyama, K., Lee, H. M., Ueki, I. F., Lausier, J. A. & Nadel, J. A. (1999). 'IL-4 induces mucin gene expression and goblet cell metaplasia *in vitro* and *in vivo*', *J Immunol*, 162(10), pp. 6233-7.
- Daigneault, M., Preston, J. A., Marriott, H. M., Whyte, M. K. & Dockrell, D. H. (2010). 'The identification of markers of macrophage differentiation in PMA-stimulated THP-1 cells and monocyte-derived macrophages', *PloS one*, 5(1), p. e8668.
- Dalgédienė, I., Lučiūnaitė, A. & Žvirblienė, A. (2018). 'Activation of Macrophages by Oligomeric Proteins of Different Size and Origin', *Mediators of inflammation*, 2018.
- Dalton, J. P., Brindley, P. J., Knox, D. P., Brady, C. P., Hotez, P. J., Donnelly, S., O'Neill, S. M., Mulcahy, G. & Loukas, A. (2003). 'Helminth vaccines: from mining genomic information for vaccine targets to systems used for protein expression', *International journal for parasitology*, 33(5-6), pp. 621-640.
- Datta, R., Hedeler, C., Paton, N., Brass, A. & Else, K. (2005). 'Identification of novel genes in intestinal tissue that are regulated after infection with an intestinal nematode parasite', *Infection and immunity*, 73(7), pp. 4025-4033.
- De Groot, A., Rayner, J. & Martin, W. (2002a). 'Modelling the immunogenicity of therapeutic proteins using T cell epitope mapping', *Developments in biologicals*, 112, pp. 71-80.
- De Groot, A. S. & Berzofsky, J. A. (2004). 'From genome to vaccine—new immunoinformatics tools for vaccine design', *Methods*, 34(4), pp. 425-428.
- De Groot, A. S. & Martin, W. (2009). 'Reducing risk, improving outcomes: bioengineering less immunogenic protein therapeutics', *Clinical Immunology*, 131(2), pp. 189-201.
- De Groot, A. S. & Moise, L. (2007). 'Prediction of immunogenicity for therapeutic proteins: state of the art', *Current Opinion in Drug Discovery and Development*, 10(3), p. 332.
- De Groot, A. S., Sbai, H., Saint Aubin, C., McMurry, J. & Martin, W. (2002b). 'Immuno-informatics: mining genomes for vaccine components', *Immunology and Cell Biology*, 80(3), pp. 255-269.

- De Sousa, K. P. & Doolan, D. L. (2016). 'Immunomics: a 21st century approach to vaccine development for complex pathogens', *Parasitology*, 143(2), pp. 236-44.
- Del Tordello, E., Rappuoli, R. & Delany, I. (2017). 'Reverse Vaccinology: Exploiting Genomes for Vaccine Design', *Human Vaccines: Emerging Technologies in Design and Development*, pp. 65-86.
- Demiri, M., Muller-Luda, K., Agace, W. W. & Svensson-Frej, M. (2017). 'Distinct DC subsets regulate adaptive Th1 and 2 responses during *Trichuris muris* infection', *Parasite Immunol*, 39(10).
- Demotz, S., Lanzavecchia, A., Eisel, U., Niemann, H., Widmann, C. & Corradin, G. (1989). 'Delineation of several DR-restricted tetanus toxin T cell epitopes', *The Journal of Immunology*, 142(2), pp. 394-402.
- Desjardins, C. A., Cerqueira, G. C., Goldberg, J. M., Hotopp, J. C. D., Haas, B. J., Zucker, J., Ribeiro, J. M., Saif, S., Levin, J. Z. & Fan, L. (2013). 'Genomics of *Loa loa*, a Wolbachia-free filarial parasite of humans', *Nature genetics*, 45(5), pp. 495-500.
- Dhanda, S. K., Gupta, S., Vir, P. & Raghava, G. P. (2013a). 'Prediction of IL4 inducing peptides', *Clin Dev Immunol*, 2013, p. 263952.
- Dhanda, S. K., Usmani, S. S., Agrawal, P., Nagpal, G., Gautam, A. & Raghava, G. P. S. (2017). 'Novel *in silico* tools for designing peptide-based subunit vaccines and immunotherapeutics', *Brief Bioinform*, 18(3), pp. 467-478.
- Dhanda, S. K., Vir, P. & Raghava, G. P. (2013b). 'Designing of interferon-gamma inducing MHC class-II binders', *Biol Direct*, 8, p. 30.
- Dias, D. S., Ribeiro, P. A., Martins, V. T., Lage, D. P., Costa, L. E., Chávez-Fumagalli, M. A., Ramos, F. F., Santos, T. T., Ludolf, F. & Oliveira, J. S. J. T. R. (2018). 'Vaccination with a CD4+ and CD8+ T-cell epitopes-based recombinant chimeric protein derived from *Leishmania infantum* proteins confers protective immunity against visceral leishmaniasis', 200, pp. 18-34.
- Diemert, D., Campbell, D., Brelsford, J., Leisure, C., Li, G., Peng, J., Zumer, M., Younes, N., Bottazzi, M. E. & Mejia, R. (2018). Controlled Human Hookworm Infection: Accelerating Human Hookworm Vaccine Development. In: Open Forum Infectious Diseases, 2018. Oxford University Press US. p. ofy083.
- Diemert, D. J., Freire, J., Valente, V., Fraga, C. G., Talles, F., Grahek, S., Campbell, D., Jariwala, A., Periago, M. V. & Enk, M. (2017). 'Safety and immunogenicity of the Na-GST-1 hookworm vaccine in Brazilian and American adults', *PLoS neglected tropical diseases*, 11(5), p. e0005574.
- Diemert, D. J., Pinto, A. G., Freire, J., Jariwala, A., Santiago, H., Hamilton, R. G., Periago, M. V., Loukas, A., Tribolet, L. & Mulvenna, J. (2012). 'Generalized urticaria induced by the Na-ASP-2 hookworm vaccine: implications for the development of vaccines against helminths', *Journal of Allergy and Clinical Immunology*, 130(1), pp. 169-176. e6.
- Diethylm-Okita, B. M., Okita, D. K., Banaszak, L. & Conti-Fine, B. M. (2000). 'Universal epitopes for human CD4+ cells on tetanus and diphtheria toxins', *Journal of Infectious Diseases*, 181(3), pp. 1001-1009.
- Diethylm-Okita, B. M., Raju, R., Okita, D. K. & Conti-Fine, B. M. (1997). 'Epitope repertoire of human CD4+ T cells on tetanus toxin: identification of immunodominant sequence segments', *Journal of Infectious Diseases*, 175(2), pp. 382-391.
- Dimitrov, I., Bangov, I., Flower, D. R. & Doytchinova, I. (2014). 'AllerTOP v. 2—a server for *in silico* prediction of allergens', *Journal of molecular modeling*, 20(6), pp. 1-6.
- Ding, F.-X., Xian, X., Guo, Y.-J., Liu, Y., Wang, Y., Yang, F., Wang, Y.-Z., Song, S.-X., Wang, F. & Sun, S.-H. (2010). 'A preliminary study on the activation and antigen presentation of hepatitis B virus core protein virus-like particle-pulsed bone marrow-derived dendritic cells', *Molecular bioSystems*, 6(11), pp. 2192-2199.
- Dixon, H. (2007). Vaccination and leukocyte homing in gastrointestinal nematode infection models. University of Manchester.
- Dixon, H., Blanchard, C., deschoolmeester, M. L., Yuill, N. C., Christie, J. W., Rothenberg, M. E. & Else, K. J. J. E. j. o. i. (2006). 'The role of Th2 cytokines, chemokines and parasite products

- in eosinophil recruitment to the gastrointestinal mucosa during helminth infection', 36(7), pp. 1753-1763.
- Dixon, H., Johnston, C. & Else, K. (2008). 'Antigen selection for future anti-*Trichuris* vaccines: a comparison of cytokine and antibody responses to larval and adult antigen in a primary infection', *Parasite immunology*, 30(9), pp. 454-461.
- Dixon, H., Little, M. C. & Else, K. J. (2010). 'Characterisation of the protective immune response following subcutaneous vaccination of susceptible mice against *Trichuris muris*', *International journal for parasitology*, 40(6), pp. 683-693.
- Dobano, C., Sanz, H., Sorgho, H., Dosoo, D., Mpina, M., Ubillos, I., Aguilar, R., Ford, T., Diez-Padrisa, N., Williams, N. A., Ayestaran, A., Traore, O., Nhabomba, A. J., Jairoce, C., Waitumbi, J., Agnandji, S. T., Kariuki, S., Abdulla, S., Aponte, J. J., Mordmuller, B., Asante, K. P., Owusu-Agyei, S., Tinto, H., Campo, J. J., Moncunill, G., Gyan, B., Valim, C. & Daubenberger, C. (2019). 'Concentration and avidity of antibodies to different circumsporozoite epitopes correlate with RTS,S/AS01E malaria vaccine efficacy', *Nat Commun*, 10(1), p. 2174.
- Dönnes, P. & Elofsson, A. (2002). 'Prediction of MHC class I binding peptides, using SVMHC', *BMC bioinformatics*, 3(1), p. 1.
- Doyle, S. R. & Cotton, J. A. (2019). 'Genome-wide Approaches to Investigate Anthelmintic Resistance', *Trends in parasitology*.
- Drake, L., Bianco, A., Bundy, D. & Ashall, F. (1994). 'Characterization of peptidases of adult *Trichuris muris*', *Parasitology*, 109(5), pp. 623-630.
- Drake, L., Jukes, M., Sternberg, R. & Bundy, D. (2000). Geohelminth infections (ascariasis, trichuriasis, and hookworm): cognitive and developmental impacts. In: Seminars in Pediatric Infectious Diseases, 2000. Elsevier. pp. 245-251.
- Dretler, A. W., Rouphael, N. G. & Stephens, D. S. (2018). 'Progress toward the global control of *Neisseria meningitidis*: 21st century vaccines, current guidelines, and challenges for future vaccine development', *Hum Vaccin Immunother*, 14(5), pp. 1146-1160.
- Dunn, J. C., Bettis, A. A., Wyine, N. Y., Lwin, A. M. M., Tun, A., Maung, N. S. & Anderson, R. M. (2019). 'Soil-transmitted helminth reinfection four and six months after mass drug administration: results from the delta region of Myanmar', *PLoS neglected tropical diseases*, 13(2), p. e0006591.
- e Sousa, C. R. (2006). 'Dendritic cells in a mature age', *Nature Reviews Immunology*, 6(6), p. 476.
- Eichenberger, R. M., Ryan, S., Jones, L., Buitrago, G., Polster, R., Montes de Oca, M., Zuvelek, J., Giacomin, P. R., Dent, L. A., Engwerda, C. R., Field, M. A., Sotillo, J. & Loukas, A. (2018a). 'Hookworm Secreted Extracellular Vesicles Interact With Host Cells and Prevent Inducible Colitis in Mice', *Front Immunol*, 9, p. 850.
- Eichenberger, R. M., Talukder, M. H., Field, M. A., Wangchuk, P., Giacomin, P., Loukas, A. & Sotillo, J. (2018b). 'Characterization of *Trichuris muris* secreted proteins and extracellular vesicles provides new insights into host-parasite communication', *Journal of extracellular vesicles*, 7(1), p. 1428004.
- El-Sayed, A. & Kamel, M. (2018). 'Advanced applications of nanotechnology in veterinary medicine', *Environmental Science and Pollution Research*, pp. 1-14.
- Elliott, T., Cerundolo, V., Elvin, J. & Townsend, A. (1991). 'Peptide-induced conformational change of the class I heavy chain'.
- Elliott, W. & Chan, J. J. I. M. A. (2018). 'Human Papillomavirus Vaccine (Gardasil 9)', 40(21).
- Else, K., Entwistle, G. & Grencis, R. (1993a). 'Correlations between worm burden and markers of Th1 and Th2 cell subset induction in an inbred strain of mouse infected with *Trichuris muris*', *Parasite immunology*, 15(10), pp. 595-600.
- Else, K., Finkelman, F., Maliszewski, C. & Grencis, R. (1994). 'Cytokine-mediated regulation of chronic intestinal helminth infection', *Journal of Experimental Medicine*, 179(1), pp. 347-351.
- Else, K. & Grencis, R. (1991). 'Cellular immune responses to the murine nematode parasite *Trichuris muris*. I. Differential cytokine production during acute or chronic infection', *Immunology*, 72(4), p. 508.

- Else, K., Hültner, L. & Grencis, R. (1992). 'Cellular immune responses to the murine nematode parasite *Trichuris muris*. II. Differential induction of TH-cell subsets in resistant versus susceptible mice', *Immunology*, 75(2), p. 232.
- Else, K. & Wakelin, D. (1988). 'The effects of H-2 and non-H-2 genes on the expulsion of the nematode *Trichuris muris* from inbred and congenic mice', *Parasitology*, 96(3), pp. 543-550.
- Else, K. & Wakelin, D. (1989). 'Genetic variation in the humoral immune responses of mice to the nematode *Trichuris muris*', *Parasite Immunology*, 11(1), pp. 77-90.
- Else, K. & Wakelin, D. (1990a). 'Genetically-determined influences on the ability of poor responder mice to respond to immunization against *Trichuris muris*', *Parasitology*, 100(3), pp. 479-489.
- Else, K., Wakelin, D., Wassom, D. & Hauda, K. (1990). 'MHC-restricted antibody responses to *Trichuris muris* excretory/secretory (E/S) antigen', *Parasite immunology*, 12(4-5), pp. 509-527.
- Else, K. J., Entwistle, G. M. & Grencis, R. K. (1993b). 'Correlations between worm burden and markers of Th1 and Th2 cell subset induction in an inbred strain of mouse infected with *Trichuris muris*', *Parasite Immunology*, 15(10), pp. 595-600.
- Else, K. J. & Grencis, R. K. (1996). 'Antibody-independent effector mechanisms in resistance to the intestinal nematode parasite *Trichuris muris*', *Infection and immunity*, 64(8), pp. 2950-2954.
- Else, K. J. & Wakelin, D. (1990b). 'Genetically-determined influences on the ability of poor responder mice to respond to immunization against *Trichuris muris*', *Parasitology*, 100(3), pp. 479-489.
- Else, K. J. J. o. h. (2003). 'Immunity to *Trichuris muris* in the laboratory mouse', 77(2), pp. 95-98.
- Eming, S. A., Krieg, T. & Davidson, J. M. (2007). 'Inflammation in wound repair: molecular and cellular mechanisms', *Journal of Investigative Dermatology*, 127(3), pp. 514-525.
- Fallon, P. G., Ballantyne, S. J., Mangan, N. E., Barlow, J. L., Dasvarma, A., Hewett, D. R., McIlgorm, A., Jolin, H. E. & McKenzie, A. N. J. (2006). 'Identification of an interleukin (IL)-25-dependent cell population that provides IL-4, IL-5, and IL-13 at the onset of helminth expulsion', 203(4), pp. 1105-1116.
- Farrell, S. H., Coffeng, L. E., Truscott, J. E., Werkman, M., Toor, J., de Vlas, S. J. & Anderson, R. M. (2018). 'Investigating the Effectiveness of Current and Modified World Health Organization Guidelines for the Control of Soil-Transmitted Helminth Infections', *Clinical Infectious Diseases*, 66(suppl_4), pp. S253-S259.
- Faulkner, H., Renauld, J.-C., Van Snick, J. & Grencis, R. (1998). 'Interleukin-9 enhances resistance to the intestinal nematode *Trichuris muris*', *Infection and immunity*, 66(8), pp. 3832-3840.
- Faulkner, H., Turner, J., Kamgno, J., Pion, S. D., Boussinesq, M. & Bradley, J. E. (2002). 'Age-and infection intensity-dependent cytokine and antibody production in human trichuriasis: the importance of IgE', *Journal of Infectious Diseases*, 185(5), pp. 665-674.
- Fausch, S. C., Da Silva, D. M. & Kast, W. M. (2003). 'Differential uptake and cross-presentation of human papillomavirus virus-like particles by dendritic cells and Langerhans cells', *Cancer Research*, 63(13), pp. 3478-3482.
- Fayette, J., Durand, I., Bridon, J., Arpin, C., Dubois, B., Caux, C., Liu, Y., Banchereau, J. & Briere, F. (1998). 'Dendritic cells enhance the differentiation of naive B cells into plasma cells in vitro', *Scandinavian journal of immunology*, 48(6), pp. 563-570.
- Faz-Lopez, B., Morales-Montor, J. & Terrazas, L. I. (2016). 'Role of Macrophages in the Repair Process during the Tissue Migrating and Resident Helminth Infections', *Biomed Res Int*, 2016, p. 8634603.
- Fehr, T., Skrastina, D., Pumpens, P. & Zinkernagel, R. M. (1998). 'T cell-independent type I antibody response against B cell epitopes expressed repetitively on recombinant virus particles', *Proceedings of the National Academy of Sciences*, 95(16), pp. 9477-9481.
- Feng, S., Wu, X., Wang, X., Bai, X., Shi, H., Tang, B., Liu, X., Song, Y., Boireau, P. & Wang, F. (2013). 'Vaccination of mice with an antigenic serine protease-like protein elicits a protective

- immune response against *Trichinella spiralis* infection', *The Journal of parasitology*, 99(3), pp. 426-432.
- Flohr, C., Tuyen, L. N., Lewis, S., Minh, T. T., Campbell, J., Britton, J., Williams, H., Hien, T. T., Farrar, J. & Quinnell, R. J. (2007). 'Low efficacy of mebendazole against hookworm in Vietnam: two randomized controlled trials', *The American journal of tropical medicine and hygiene*, 76(4), pp. 732-736.
- Fogarty, J. A. & Swartz, J. R. (2018). 'The exciting potential of modular nanoparticles for rapid development of highly effective vaccines', *Current Opinion in Chemical Engineering*, 19, pp. 1-8.
- Foor, W. E. (1967). 'Ultrastructural aspects of oocyte development and shell formation in *Ascaris lumbricoides*', *The Journal of parasitology*, pp. 1245-1261.
- Foth, B. J., Tsai, I. J., Reid, A. J., Bancroft, A. J., Nichol, S., Tracey, A., Holroyd, N., Cotton, J. A., Stanley, E. J. & Zarowiecki, M. (2014). 'Whipworm genome and dual-species transcriptome analyses provide molecular insights into an intimate host-parasite interaction', *Nature genetics*, 46(7), p. 693.
- Franco, D., Liu, W., Gardiner, D. F., Hahn, B. H. & Ho, D. D. (2011). 'CD40L-containing virus-like particle as a candidate HIV-1 vaccine targeting dendritic cells', *JAIDS Journal of Acquired Immune Deficiency Syndromes*, 56(5), pp. 393-400.
- Freeman, M. C., Akogun, O., Belizario, V., Jr., Brooker, S. J., Gyorkos, T. W., Imtiaz, R., Krolewiecki, A., Lee, S., Matendechero, S. H., Pullan, R. L. & Utzinger, J. (2019). 'Challenges and opportunities for control and elimination of soil-transmitted helminth infection beyond 2020', *PLoS Negl Trop Dis*, 13(4), p. e0007201.
- Freivalds, J., Dislers, A., Ose, V., Skrastina, D., Cielens, I., Pumpens, P., Sasnauskas, K. & Kazaks, A. (2006). 'Assembly of bacteriophage Q β virus-like particles in yeast *Saccharomyces cerevisiae* and *Pichia pastoris*', *Journal of biotechnology*, 123(3), pp. 297-303.
- Frietze, K. M., Peabody, D. S. & Chackerian, B. (2016). 'Engineering virus-like particles as vaccine platforms', *Current opinion in virology*, 18, pp. 44-49.
- Friscia, G., Vordermeier, H., Pasvol, G., Harris, D., Moreno, C. & Ivanyi, J. (1995). 'Human T cell responses to peptide epitopes of the 16-kD antigen in tuberculosis', *Clinical and experimental immunology*, 102(1), p. 53.
- Fuenmayor, J., Godia, F. & Cervera, L. (2017). 'Production of virus-like particles for vaccines', *N Biotechnol*, 39(Pt B), pp. 174-180.
- Gallina, A., Bonelli, F., Zentilin, L., Rindi, G., Muttini, M. & Milanesi, G. (1989). 'A recombinant hepatitis B core antigen polypeptide with the protamine-like domain deleted self-assembles into capsid particles but fails to bind nucleic acids', *Journal of virology*, 63(11), pp. 4645-4652.
- Gamvrellis, A., Leong, D., Hanley, J. C., Xiang, S. D., Mottram, P. & Plebanski, M. (2004). 'Vaccines that facilitate antigen entry into dendritic cells', *Immunology and cell biology*, 82(5), pp. 506-516.
- Gasteiger, E., Hoogland, C., Gattiker, A., Wilkins, M. R., Appel, R. D. & Bairoch, A. (2005). 'Protein identification and analysis tools on the ExPASy server', *The proteomics protocols handbook*: Springerpp. 571-607.
- Gause, K. T., Wheatley, A. K., Cui, J., Yan, Y., Kent, S. J. & Caruso, F. (2017). 'Immunological Principles Guiding the Rational Design of Particles for Vaccine Delivery', *ACS Nano*, 11(1), pp. 54-68.
- Gause, W. (2003). 'The immune response to parasitic helminths: insights from murine models', *Trends Immunol*, 24(5), pp. 269-277.
- Gazzinelli-Guimaraes, A. C., Gazzinelli-Guimaraes, P. H., Nogueira, D. S., Oliveira, F. M. S., Barbosa, F. S., Amorim, C. C. O., Cardoso, M. S., Kraemer, L., Caliari, M. V., Akamatsu, M. A., Ho, P. L., Jones, K. M., Weatherhead, J., Bottazzi, M. E., Hotez, P. J., Zhan, B., Bartholomeu, D. C., Russo, R. C., Bueno, L. L. & Fujiwara, R. T. (2018). 'IgG Induced by Vaccination With *Ascaris suum* Extracts Is Protective Against Infection', *Frontiers in Immunology*, 9.
- Geldhof, P., De Maere, V., Vercruyse, J. & Claerebout, E. (2007). 'Recombinant expression systems: the obstacle to helminth vaccines?', *Trends in parasitology*, 23(11), pp. 527-532.

- Geluk, A., Taneja, V., Van Meijgaarden, K. E., Zanelli, E., Abou-Zeid, C., Thole, J. E., De Vries, R. R., David, C. S. & Ottenhoff, T. H. (1998). 'Identification of HLA class II-restricted determinants of Mycobacterium tuberculosis-derived proteins by using HLA-transgenic, class II-deficient mice', *Proceedings of the National Academy of Sciences*, 95(18), pp. 10797-10802.
- Ghedin, E. (2014). 'Panning for molecular gold in whipworm genomes', *Nature genetics*, 46(7), p. 661.
- Ghedin, E., Wang, S., Spiro, D., Caler, E., Zhao, Q., Crabtree, J., Allen, J. E., Delcher, A. L., Giuliano, D. B. & Miranda-Saavedra, D. (2007). 'Draft genome of the filarial nematode parasite *Brugia malayi*', *Science*, 317(5845), pp. 1756-1760.
- Godkin, A. J., Smith, K. J., Willis, A., Tejada-Simon, M. V., Zhang, J., Elliott, T. & Hill, A. V. (2001). 'Naturally processed HLA class II peptides reveal highly conserved immunogenic flanking region sequence preferences that reflect antigen processing rather than peptide-MHC interactions', *The Journal of Immunology*, 166(11), pp. 6720-6727.
- Gogesch, P., Schülke, S., Scheurer, S., Mühlbach, M. D. & Waibler, Z. (2018). 'Modular MLV-VLPs co-displaying ovalbumin peptides and GM-CSF effectively induce expansion of CD11b+ APC and antigen-specific T cell responses in vitro', *Molecular immunology*, 101, pp. 19-28.
- Golias, C., Charalabopoulos, A., Stagikas, D., Charalabopoulos, K. & Batistatou, A. (2007). 'The kinin system-bradykinin: biological effects and clinical implications. Multiple role of the kinin system-bradykinin', *Hippokratia*, 11(3), p. 124.
- Gomes, A. C., Flace, A., Saudan, P., Zabel, F., Cabral-Miranda, G., Turabi, A. E., Manolova, V. & Bachmann, M. F. (2017a). 'adjusted Particle size eliminates the need of linkage of antigen and adjuvants for appropriated T cell responses in Virus-like Particle-Based Vaccines', *Frontiers in immunology*, 8, p. 226.
- Gomes, A. C., Mohsen, M. & Bachmann, M. F. (2017b). 'Harnessing nanoparticles for immunomodulation and vaccines', *Vaccines*, 5(1), p. 6.
- Gomez-Samblas, M., Garcia-Rodriguez, J. J., Treliis, M., Bernal, D., Lopez-Jaramillo, F. J., Santoyo-Gonzalez, F., Vilchez, S., Espino, A. M., Bolas-Fernandez, F. & Osuna, A. (2017). 'Self-adjuvanting C18 lipid vinyl sulfone-PP2A vaccine: study of the induced immunomodulation against *Trichuris muris* infection', *Open Biol*, 7(4).
- Gomez-Fuentes, S., Morales-Ruiz, V., López-Recinos, D., Guevara-Salinas, A., Arce-Sillas, A., Rodríguez, J., Parada-Colin, C. & Adalid-Peralta, L. J. J. o. H. (2019). 'Biological role of excretory-secretory proteins in endemic parasites of Latin America and the Caribbean', pp. 1-10.
- Govers, C., Tomassen, M. M., Rieder, A., Ballance, S., Knutsen, S. H., Mes, J. J. J. B. c. & fibre, d. (2016). 'Lipopolysaccharide quantification and alkali-based inactivation in polysaccharide preparations to enable in vitro immune modulatory studies', 8(1), pp. 15-25.
- Gowthaman, U. & Agrewala, J. N. (2007). 'In silico tools for predicting peptides binding to HLA-class II molecules: more confusion than conclusion', *Journal of proteome research*, 7(01), pp. 154-163.
- Grallert, H., Leopoldseder, S., Schuett, M., Kurze, P. & Buchberger, B. J. N. M. (2011). 'EndoLISA®: a novel and reliable method for endotoxin detection', 8(10).
- Greenfield, N. J. (2006). 'Using circular dichroism spectra to estimate protein secondary structure', *Nature protocols*, 1(6), p. 2876.
- Gregson, A. L., Oliveira, G., Othoro, C., Calvo-Calle, J. M., Thorton, G. B., Nardin, E. & Edelman, R. (2008). 'Phase I trial of an alhydrogel adjuvanted hepatitis B core virus-like particle containing epitopes of *Plasmodium falciparum* circumsporozoite protein', *PloS one*, 3(2), p. e1556.
- Grencis, R. (1993). 'Cytokine-mediated regulation of intestinal helminth infections: the *Trichuris muris* model', *Annals of Tropical Medicine & Parasitology*, 87(6), pp. 643-647.
- Grencis, R. (2001). 'Cytokine regulation of resistance and susceptibility to intestinal nematode infection—from host to parasite', *Veterinary parasitology*, 100(1-2), pp. 45-50.
- Grencis, R. K., Humphreys, N. E. & Bancroft, A. J. (2014). 'Immunity to gastrointestinal nematodes: mechanisms and myths', *Immunological reviews*, 260(1), pp. 183-205.

- Grgacic, E. V. & Anderson, D. A. (2006). 'Virus-like particles: passport to immune recognition', *Methods*, 40(1), pp. 60-65.
- Grover, A., Troutdt, J., Foster, C., Basaraba, R. & Izzo, A. (2014). 'High mobility group box 1 acts as an adjuvant for tuberculosis subunit vaccines', *Immunology*, 142(1), pp. 111-123.
- Gu, Y., Huang, J., Wang, X., Wang, L., Yang, J., Zhan, B. & Zhu, X. (2016). 'Identification and characterization of CD4+ T cell epitopes present in *Trichinella spiralis* paramyosin', *Veterinary parasitology*.
- Gu, Y., Sun, X., Li, B., Huang, J., Zhan, B. & Zhu, X. (2017). 'Vaccination with a Paramyosin-Based Multi-Epitope Vaccine Elicits Significant Protective Immunity against *Trichinella spiralis* Infection in Mice', *Front Microbiol*, 8, p. 1475.
- Guan, Q., Ma, Y., Hillman, C.-L., Ma, A., Zhou, G., Qing, G. & Peng, Z. (2009). 'Development of recombinant vaccines against IL-12/IL-23 p40 and *in vivo* evaluation of their effects in the downregulation of intestinal inflammation in murine colitis', *Vaccine*, 27(50), pp. 7096-7104.
- Guo, J., Zhou, A., Sun, X., Sha, W., Ai, K., Pan, G., Zhou, C., Zhou, H., Cong, H. & He, S. (2019). 'Immunogenicity of a Virus-Like-Particle Vaccine Containing Multiple Antigenic Epitopes of *Toxoplasma gondii* Against Acute and Chronic Toxoplasmosis in Mice', *Front Immunol*, 10, p. 592.
- Guo, L., Liu, K., Zhao, W., Li, X., Li, T., Tang, F., Zhang, R., Wu, W. & Xi, T. (2013). 'Immunological features and efficacy of the reconstructed epitope vaccine CtUBE against Helicobacter pylori infection in BALB/c mice model', *Applied microbiology and biotechnology*, 97(6), pp. 2367-2378.
- Gurunathan, S., Klinman, D. M. & Seder, R. A. (2000). 'DNA vaccines: immunology, application, and optimization', *Annual review of immunology*, 18(1), pp. 927-974.
- Haber, P., Moro, P. L., Ng, C., Lewis, P. W., Hibbs, B., Schillie, S. F., Nelson, N. P., Li, R., Stewart, B. & Cano, M. V. (2018). 'Safety of currently licensed hepatitis B surface antigen vaccines in the United States, Vaccine Adverse Event Reporting System (VAERS), 2005-2015', *Vaccine*, 36(4), pp. 559-564.
- Hansen, E. P., Kringel, H., Williams, A. R. & Nejsum, P. (2015). 'Secretion of RNA-Containing Extracellular Vesicles by the Porcine Whipworm, *Trichuris suis*', *J Parasitol*, 101(3), pp. 336-40.
- Harnett, M. M. & Harnett, W. J. T. i. p. (2017). 'Can parasitic worms cure the modern world's ills?', 33(9), pp. 694-705.
- Harrington, L. E., Hatton, R. D., Mangan, P. R., Turner, H., Murphy, T. L., Murphy, K. M. & Weaver, C. T. (2005). 'Interleukin 17-producing CD4+ effector T cells develop via a lineage distinct from the T helper type 1 and 2 lineages', *Nat Immunol*, 6(11), pp. 1123-32.
- Hasnain, S., Thornton, D. & Grencis, R. (2011a). 'Changes in the mucosal barrier during acute and chronic *Trichuris muris* infection', *Parasite immunology*, 33(1), pp. 45-55.
- Hasnain, S. Z., Evans, C. M., Roy, M., Gallagher, A. L., Kindrachuk, K. N., Barron, L., Dickey, B. F., Wilson, M. S., Wynn, T. A. & Grencis, R. K. (2011b). 'Muc5ac: a critical component mediating the rejection of enteric nematodes', *The Journal of experimental medicine*, 208(5), pp. 893-900.
- Hasnain, S. Z., McGuckin, M. A., Grencis, R. K. & Thornton, D. J. (2012). 'Serine protease (s) secreted by the nematode *Trichuris muris* degrade the mucus barrier', *PLoS neglected tropical diseases*, 6(10), p. e1856.
- Hasnain, S. Z., Wang, H., Ghia, J. E., Haq, N., Deng, Y., Velcich, A., Grencis, R. K., Thornton, D. J. & Khan, W. I. (2010). 'Mucin gene deficiency in mice impairs host resistance to an enteric parasitic infection', *Gastroenterology*, 138(5), pp. 1763-1771.e5.
- Hauet-Broere, F., Wieten, L., Guichelaar, T., Berlo, S., Van der Zee, R. & Van Eden, W. (2006). 'Heat shock proteins induce T cell regulation of chronic inflammation', *Annals of the rheumatic diseases*, 65(suppl 3), pp. iii65-iii68.

- Hawkes, N. (2015). 'European Medicines Agency approves first malaria vaccine', *BMJ*, 351, p. h4067.
- Hayes, K. S., Bancroft, A. J. & Grencis, R. K. (2007). 'The role of TNF-alpha in *Trichuris muris* infection I: influence of TNF-alpha receptor usage, gender and IL-13', *Parasite Immunol*, 29(11), pp. 575-82.
- Hayes, K. S., Hager, R. & Grencis, R. K. J. B. G. (2014). 'Sex-dependent genetic effects on immune responses to a parasitic nematode', 15(1), p. 193.
- He, L., De Groot, A. S., Gutierrez, A. H., Martin, W. D., Moise, L. & Bailey-Kellogg, C. (2014). 'Integrated assessment of predicted MHC binding and cross-conservation with self reveals patterns of viral camouflage', *BMC bioinformatics*, 15(4), p. S1.
- Hegde, N. R., Gauthami, S., Kumar, H. M. S. & Bayry, J. (2018). 'The use of databases, data mining and immunoinformatics in vaccinology: where are we?', *Expert Opinion on Drug Discovery*, 13(2), pp. 117-130.
- Hein, W. & Harrison, G. (2005). 'Vaccines against veterinary helminths', *Veterinary parasitology*, 132(3-4), pp. 217-222.
- Helmby, H., Takeda, K., Akira, S. & Grencis, R. K. (2001). 'Interleukin (IL)-18 promotes the development of chronic gastrointestinal helminth infection by downregulating IL-13', *J Exp Med*, 194(3), pp. 355-64.
- Hepworth, M. R., Danilowicz-Luebert, E., Rausch, S., Metz, M., Klotz, C., Maurer, M. & Hartmann, S. (2012). 'Mast cells orchestrate type 2 immunity to helminths through regulation of tissue-derived cytokines', *Proceedings of the National Academy of Sciences of the United States of America*, 109(17), pp. 6644-6649.
- Hepworth, M. R. & Grencis, R. K. (2009). 'Disruption of Th2 immunity results in a gender-specific expansion of IL-13 producing accessory NK cells during helminth infection', *The Journal of Immunology*, 183(6), pp. 3906-3914.
- Hepworth, M. R., Hardman, M. J. & Grencis, R. K. (2010). 'The role of sex hormones in the development of Th2 immunity in a gender-biased model of *Trichuris muris* infection', *European journal of immunology*, 40(2), pp. 406-416.
- Herbert, D. R., Yang, J. Q., Hogan, S. P., Groschwitz, K., Khodoun, M., Munitz, A., Orekov, T., Perkins, C., Wang, Q., Brombacher, F., Urban, J. F., Jr., Rothenberg, M. E. & Finkelman, F. D. (2009). 'Intestinal epithelial cell secretion of RELM-beta protects against gastrointestinal worm infection', *J Exp Med*, 206(13), pp. 2947-57.
- Hernandez, H. J., Edson, C. M., Harn, D. A., Ianelli, C. J. & Stadecker, M. J. (1998). '*Schistosoma mansoni*: genetic restriction and cytokine profile of the CD4+ T helper cell response to dominant epitope peptide of major egg antigen Sm-p40', *Experimental parasitology*, 90(1), pp. 122-130.
- Hernandez, H. J., Rutitzky, L. I., Lebens, M., Holmgren, J. & Stadecker, M. J. (2002). 'Diminished immunopathology in *Schistosoma mansoni* infection following intranasal administration of cholera toxin B-immunodominant peptide conjugate correlates with enhanced transforming growth factor-β production by CD4 T cells', *Parasite Immunol*, 24(8), pp. 423-427.
- Hernandez, H. J., Trzyna, W. C., Cordingley, J. S., Brodeur, P. H. & Stadecker, M. J. (1997). 'Differential antigen recognition by T cell populations from strains of mice developing polar forms of granulomatous inflammation in response to eggs of *Schistosoma mansoni*', *European journal of immunology*, 27(3), pp. 666-670.
- Hewitson, J. P. & Maizels, R. M. (2014). 'Vaccination against helminth parasite infections', *Expert review of vaccines*, 13(4), pp. 473-487.
- Hirota, K., Nagata, K., Norose, Y., Futagami, S., Nakagawa, Y., Senpuku, H., Kobayashi, M. & Takahashi, H. (2001). 'Identification of an Antigenic Epitope in *Helicobacter pylori* Urease That Induces Neutralizing Antibody Production', *Infect Immun*, 69(11), pp. 6597-6603.
- HogenEsch, H. (2013). 'Mechanism of immunopotentiation and safety of aluminum adjuvants', *Frontiers in immunology*, 3, p. 406.
- Homan, E. J. & Bremel, R. D. (2018). 'A role for epitope networking in immunomodulation by helminths', *Frontiers in immunology*, 9.

- Hong, S., Zhang, Z., Liu, H., Tian, M., Zhu, X., Zhang, Z., Wang, W., Zhou, X., Zhang, F. & Ge, Q. (2018). 'B Cells Are the Dominant Antigen-Presenting Cells that Activate Naive CD4+ T Cells upon Immunization with a Virus-Derived Nanoparticle Antigen', *Immunity*, 49(4), pp. 695-708. e4.
- Horsfall, A. C., Hay, F. C., Soltys, A. J. & Jones, M. G. (1991). 'Epitope mapping', *Immunology today*, 12(7), pp. 211-213.
- Horwitz, M. A., Harth, G., Dillon, B. J. & Masleša-Galić, S. (2005). 'Enhancing the protective efficacy of *Mycobacterium bovis* BCG vaccination against tuberculosis by boosting with the *Mycobacterium tuberculosis* major secretory protein', *Infection and immunity*, 73(8), pp. 4676-4683.
- Hotez, P. J. (2017). Ten failings in global neglected tropical diseases control. Public Library of Science.
- Hotez, P. J., Bottazzi, M. E., Bethony, J. & Diemert, D. D. (2019). 'Advancing the Development of a Human Schistosomiasis Vaccine', *Trends in parasitology*, 35(2), pp. 104-108.
- Hotez, P. J., Diemert, D., Bacon, K. M., Beaumier, C., Bethony, J. M., Bottazzi, M. E., Brooker, S., Couto, A. R., da Silva Freire, M. & Homma, A. (2013). 'The human hookworm vaccine', *Vaccine*, 31, pp. B227-B232.
- Hotez, P. J., Strych, U., Lustigman, S. & Bottazzi, M. E. (2016). 'Human anthelminthic vaccines: Rationale and challenges', *Vaccine*, 34(30), pp. 3549-3555.
- Howard, C. R. (1986). 'The biology of hepadnaviruses', *Journal of General Virology*, 67(7), pp. 1215-1235.
- Howarth, M. & Brune, K. D. (2018). 'New routes and opportunities for modular construction of particulate vaccines: stick, click and glue', *Frontiers in immunology*, 9, p. 1432.
- Howe, K. L., Bolt, B. J., Cain, S., Chan, J., Chen, W. J., Davis, P., Done, J., Down, T., Gao, S. & Grove, C. (2015). 'WormBase 2016: expanding to enable helminth genomic research', *Nucleic acids research*, p. gkv1217.
- Hu, J., Bae, Y.-K., Knobel, K. M. & Barr, M. M. (2006). 'Casein kinase II and calcineurin modulate TRPP function and ciliary localization', *Molecular biology of the cell*, 17(5), pp. 2200-2211.
- Huang, J. & Honda, W. (2006). 'CED: a conformational epitope database', *BMC immunology*, 7(1), p. 7.
- Huang, X., Wang, X., Zhang, J., Xia, N. & Zhao, Q. (2017). 'Escherichia coli-derived virus-like particles in vaccine development', *npj Vaccines*, 2(1), p. 3.
- Humphreys, N., Worthington, J. J., Little, M., Rice, E. & Grencis, R. K. (2004). 'The role of CD8+ cells in the establishment and maintenance of a *Trichuris muris* infection', *Parasite immunology*, 26(4), pp. 187-196.
- Humphreys, N. E. & Grencis, R. K. (2002). 'Effects of ageing on the immunoregulation of parasitic infection', *Infection and immunity*, 70(9), pp. 5148-5157.
- Humphreys, N. E., Xu, D., Hepworth, M. R., Liew, F. Y. & Grencis, R. K. (2008). 'IL-33, a potent inducer of adaptive immunity to intestinal nematodes', *The Journal of Immunology*, 180(4), pp. 2443-2449.
- Hunt, V. L., Tsai, I. J., Coghlan, A., Reid, A. J., Holroyd, N., Foth, B. J., Tracey, A., Cotton, J. A., Stanley, E. J. & Beasley, H. (2016). 'The genomic basis of parasitism in the *Strongyloides* clade of nematodes', *Nature genetics*, 48(3), p. 299.
- Huo, C., Yang, J., Lei, L., Qiao, L., Xin, J. & Pan, Z. (2017). 'Hepatitis B virus core particles containing multiple epitopes confer protection against enterovirus 71 and coxsackievirus A16 infection in mice', *Vaccine*, 35(52), pp. 7322-7330.
- Hurst, R. J. & Else, K. J. (2013). 'Trichuris muris research revisited: a journey through time', *Parasitology*, 140(11), pp. 1325-1339.
- Itano, A. A. & Jenkins, M. K. (2003). 'Antigen presentation to naive CD4 T cells in the lymph node', *Nature immunology*, 4(8), p. 733.
- Itano, A. A., McSorley, S. J., Reinhardt, R. L., Ehst, B. D., Ingulli, E., Rudensky, A. Y. & Jenkins, M. K. (2003). 'Distinct dendritic cell populations sequentially present antigen to CD4 T cells and stimulate different aspects of cell-mediated immunity', *Immunity*, 19(1), pp. 47-57.

- Ivan, D., Darren R, F. & Irini, D. (2011). 'Improving *in silico* prediction of epitope vaccine candidates by union and intersection of single predictors', *World Journal of Vaccines*, 2011.
- Izquierdo-Useros, N., Naranjo-Gómez, M., Archer, J., Hatch, S. C., Erkizia, I., Blanco, J., Borràs, F. E., Puertas, M. C., Connor, J. H. & Fernández-Figueras, M. T. (2009). 'Capture and transfer of HIV-1 particles by mature dendritic cells converges with the exosome-dissemination pathway', *Blood*, 113(12), pp. 2732-2741.
- Izvekova, G. & Frolova, T. (2017). 'Proteolytic enzymes and their inhibitors in cestodes', *Biology Bulletin Reviews*, 7(2), pp. 150-159.
- Jackson, J. A., Turner, J. D., Rentoul, L., Faulkner, H., Behnke, J. M., Hoyle, M., Grencis, R. K., Else, K. J., Kamgno, J., Boussinesq, M. & Bradley, J. E. (2004a). 'T helper cell type 2 responsiveness predicts future susceptibility to gastrointestinal nematodes in humans', *J Infect Dis*, 190(10), pp. 1804-11.
- Jackson, J. A., Turner, J. D., Rentoul, L., Faulkner, H., Behnke, J. M., Hoyle, M., Grencis, R. K., Else, K. J., Kamgno, J., Bradley, J. E. & Boussinesq, M. (2004b). 'Cytokine response profiles predict species-specific infection patterns in human GI nematodes', *Int J Parasitol*, 34(11), pp. 1237-44.
- Jain, N. K., Sahni, N., Kumru, O. S., Joshi, S. B., Volkin, D. B. & Middaugh, C. R. (2015). 'Formulation and stabilization of recombinant protein based virus-like particle vaccines', *Advanced drug delivery reviews*, 93, pp. 42-55.
- Janssens, M. E., Geysen, D., Broos, K., De Goeijse, I., Robbens, J., Van Petegem, F., Timmermans, J.-P. & Guisez, Y. (2010). 'Folding properties of the hepatitis B core as a carrier protein for vaccination research', *Amino acids*, 38(5), pp. 1617-1626.
- Jardim, A., Alexander, J., Teh, H. S., Ou, D. & Olafson, R. W. (1990). 'Immunoprotective *Leishmania major* synthetic T cell epitopes', *J Exp Med*, 172(2), pp. 645-648.
- Jegerlehner, A., Maurer, P., Bessa, J., Hinton, H. J., Kopf, M. & Bachmann, M. F. (2007). 'TLR9 signaling in B cells determines class switch recombination to IgG2a', *The Journal of Immunology*, 178(4), pp. 2415-2420.
- Jenkins, S. & Wakelin, D. (1983). 'Functional antigens of *Trichuris muris* released during in vitro maintenance: their immunogenicity and partial purification', *Parasitology*, 86(1), pp. 73-82.
- Jenkins, S. N. & Wakelin, D. (1977). 'The source and nature of some functional antigens of *Trichuris muris*', *Parasitology*, 74(2), pp. 153-161.
- Jennings, G. T. & Bachmann, M. F. (2008). 'The coming of age of virus-like particle vaccines', *Biological chemistry*, 389(5), pp. 521-536.
- Jensen, K. K., Andreatta, M., Marcatili, P., Buus, S., Greenbaum, J. A., Yan, Z., Sette, A., Peters, B. & Nielsen, M. (2018). 'Improved methods for predicting peptide binding affinity to MHC class II molecules', *Immunology*.
- Jeong, H. & Seong, B. L. (2017). 'Exploiting virus-like particles as innovative vaccines against emerging viral infections', *Journal of Microbiology*, 55(3), pp. 220-230.
- Jex, A. R., Gasser, R. B. & Schwarz, E. M. (2018). 'Transcriptomic Resources for Parasitic Nematodes of Veterinary Importance', *Trends in parasitology*.
- Jex, A. R., Nejsum, P., Schwarz, E. M., Hu, L., Young, N. D., Hall, R. S., Korhonen, P. K., Liao, S., Thamsborg, S. & Xia, J. (2014). 'Genome and transcriptome of the porcine whipworm *Trichuris suis*', *Nature genetics*, 46(7), p. 701.
- Joeris, T., Muller-Luda, K., Agace, W. W. & Mowat, A. M. (2017). 'Diversity and functions of intestinal mononuclear phagocytes', *Mucosal Immunol*, 10(4), pp. 845-864.
- Johansen, P., Storni, T., Rettig, L., Qiu, Z., Der-Sarkissian, A., Smith, K. A., Manolova, V., Lang, K. S., Senti, G. & Müllhaupt, B. (2008). 'Antigen kinetics determines immune reactivity', *Proceedings of the National Academy of Sciences*, 105(13), pp. 5189-5194.
- John, B. & Ralph, M. (1989). *Advances in Parasitology* (Vol. 28): Academic Press.
- John, L., John, G. J. & Kholia, T. (2012). 'A reverse vaccinology approach for the identification of potential vaccine candidates from *Leishmania* spp', *Applied biochemistry and biotechnology*, 167(5), pp. 1340-1350.

- Johnston, C., Bradley, J., Behnke, J., Matthews, K. & Else, K. (2005). 'Isolates of *Trichuris muris* elicit different adaptive immune responses in their murine host', *Parasite immunology*, 27(3), pp. 69-78.
- Johnston, W. L., Krizus, A. & Dennis, J. W. (2006). 'The eggshell is required for meiotic fidelity, polar-body extrusion and polarization of the *C. elegans* embryo', *BMC biology*, 4(1), p. 35.
- Johnston, W. L., Krizus, A. & Dennis, J. W. (2010). 'Eggshell chitin and chitin-interacting proteins prevent polyspermy in *C. elegans*', *Current Biology*, 20(21), pp. 1932-1937.
- Josefsberg, J. O. & Buckland, B. (2012). 'Vaccine process technology', *Biotechnology and bioengineering*, 109(6), pp. 1443-1460.
- Joshi, H., Lewis, K., Singharoy, A. & Ortoleva, P. J. (2013). 'Epitope engineering and molecular metrics of immunogenicity: A computational approach to VLP-based vaccine design', *Vaccine*, 31(42), pp. 4841-4847.
- Jourdan, P. M., Lamberton, P. H., Fenwick, A. & Addiss, D. G. (2018). 'Soil-transmitted helminth infections', *The Lancet*, 391(10117), pp. 252-265.
- Julia, V., Rassoulzadegan, M. & Glaichenhaus, N. (1996). 'Resistance to *Leishmania major* induced by tolerance to a single antigen', *Science*, 274(5286), pp. 421-423.
- Jurcevic, S., Hills, A., Pasvol, G., Davidson, R., Ivanyi, J. & Wilkinson, R. (1996). 'T cell responses to a mixture of *Mycobacterium tuberculosis* peptides with complementary HLA-DR binding profiles', *Clinical & Experimental Immunology*, 105(3), pp. 416-421.
- Jurtz, V., Paul, S., Andreatta, M., Marcatili, P., Peters, B. & Nielsen, M. J. T. J. o. I. (2017). 'NetMHCpan-4.0: improved peptide-MHC class I interaction predictions integrating eluted ligand and peptide binding affinity data', 199(9), pp. 3360-3368.
- Kanaujia, G., Motzel, S., Garcia, M., Andersen, P. & Gennaro, M. (2004). 'Recognition of ESAT-6 sequences by antibodies in sera of tuberculous nonhuman primates', *Clinical and diagnostic laboratory immunology*, 11(1), pp. 222-226.
- Kao, D. J. & Hodges, R. S. (2009). 'Advantages of a synthetic peptide immunogen over a protein immunogen in the development of an anti-pilus vaccine for *Pseudomonas aeruginosa*', *Chem Biol Drug Des*, 74(1), pp. 33-42.
- Kawano, M., Matsui, M. & Handa, H. (2018). 'Technologies that generate and modify virus-like particles for medical diagnostic and therapy purposes', *Design and Development of New Nanocarriers*: Elsevierpp. 555-594.
- KeatingGM, N. (2003). 'Recombinant hepatitisB vaccine (Engerix-B) A review of its immunogenicity and protective efficacy against hepatitis B', *Drugs*, 63, pp. 1021-1051.
- Keller, S. A., Bauer, M., Manolova, V., Muntwiler, S., Saudan, P. & Bachmann, M. F. (2010). 'Cutting edge: limited specialization of dendritic cell subsets for MHC class II-associated presentation of viral particles', *The Journal of Immunology*, 184(1), pp. 26-29.
- Kelly, B. L. & Locksley, R. M. (2004). 'The *Leishmania major* LACK antigen with an immunodominant epitope at amino acids 156 to 173 is not required for early Th2 development in BALB/c mice', *Infect Immun*, 72(12), pp. 6924-6931.
- Keshavarz, M., Mirzaei, H., Salemi, M., Momeni, F., Mousavi, M. J., Sadeghalvad, M., Arjeini, Y., Solaymani-Mohammadi, F., Nahand, J. S., Namdari, H., Mokhtari-Azad, T. & Rezaei, F. (2019). 'Influenza vaccine: Where are we and where do we go?', *Reviews in Medical Virology*, 29(1).
- Khalili, S., Jahangiri, A., Borna, H., Ahmadi Zanoos, K. & Amani, J. (2014). 'Computational vaccinology and epitope vaccine design by immunoinformatics', *Acta microbiologica et immunologica Hungarica*, 61(3), pp. 285-307.
- Khan, A. M., Miotto, O., Heiny, A., Salmon, J., Srinivasan, K., Nascimento, E. J., Marques, E. T., Brusic, V., Tan, T. W. & August, J. T. (2006). 'A systematic bioinformatics approach for selection of epitope-based vaccine targets', *Cellular immunology*, 244(2), pp. 141-147.
- Khan, W., Richard, M., Akiho, H., Blennerhasset, P., Humphreys, N., Grencis, R., Van Snick, J. & Collins, S. (2003). 'Modulation of intestinal muscle contraction by interleukin-9 (IL-9) or IL-9 neutralization: correlation with worm expulsion in murine nematode infections', *Infection and immunity*, 71(5), pp. 2430-2438.

- Khan, W. I., Motomura, Y., Blennerhassett, P. A., Kanbayashi, H., Varghese, A. K., El-Sharkawy, R. T., Gauldie, J. & Collins, S. M. (2005). 'Disruption of CD40-CD40 ligand pathway inhibits the development of intestinal muscle hypercontractility and protective immunity in in nematode infection', 288(1), pp. G15-G22.
- Khan, W. I., Vallance, B. A., Blennerhassett, P. A., Deng, Y., Verdu, E. F., Matthaei, K. I. & Collins, S. M. (2001). 'Critical Role for Signal Transducer and Activator of Transcription Factor 6 in Mediating Intestinal Muscle Hypercontractility and Worm Expulsion in Mediating Intestinal Muscle Hypercontractility and Worm Expulsion in *Trichinella spiralis*-Infected Mice', 69(2), pp. 838-844.
- Khuroo, M. S., Khuroo, M. S. & Khuroo, N. S. (2010). 'Trichuris dysentery syndrome: a common cause of chronic iron deficiency anemia in adults in an endemic area (with videos)', *Gastrointestinal Endoscopy*, 71(1), pp. 200-204.
- Kifle, D. W., Sotillo, J., Pearson, M. S. & Loukas, A. (2017). 'Extracellular vesicles as a target for the development of anti-helminth vaccines', 1(6), pp. 659-665.
- King, I. L., Mohrs, K., Meli, A. P., Downey, J., Lanthier, P., Tzelepis, F., Fritz, J. H., Tumanov, A. V., Divangahi, M. & Leadbetter, E. A. (2017). 'Intestinal helminth infection impacts the systemic distribution and function of the naive lymphocyte pool', *Mucosal immunology*, 10(5), p. 1160.
- Kironde, F., Rao, K., Shah, S., Kumar, A. & Sahoo, N. (1991). 'Towards the design of heterovalent anti-malaria vaccines: a hybrid immunogen capable of eliciting immune responses to epitopes of circumsporozoite antigens from two different species of the malaria parasite, *Plasmodium*', *Immunology*, 74(2), p. 323.
- Kishimoto, T. & Tanaka, T. (2015). 'Interleukin 6', *Encyclopedia of Inflammatory Diseases*, pp. 1-8.
- Klementowicz, J. E., Travis, M. A. & Grencis, R. K. (2012). *Trichuris muris*: a model of gastrointestinal parasite infection. In: Seminars in immunopathology, 2012. Springer. pp. 815-828.
- Klion, A. D. & Nutman, T. B. (2004). 'The role of eosinophils in host defense against helminth parasites', *J Allergy Clin Immunol*, 113(1), pp. 30-7.
- Knight, P. A., Wright, S. H., Lawrence, C. E., Paterson, Y. Y. & Miller, H. R. (2000). 'Delayed Expulsion of the Nematode *Trichinella spiralis* In Mice Lacking the Mucosal Mast Cell-Specific Granule Chymase, Mouse Mast Cell Protease-1', *The Journal of experimental medicine*, 192(12), pp. 1849-1856.
- Knox, D. P., Redmond, D. L., Skuce, P. J. & Newlands, G. F. (2001). 'The contribution of molecular biology to the development of vaccines against nematode and trematode parasites of domestic ruminants', *Veterinary parasitology*, 101(3-4), pp. 311-335.
- Knudsen, N. P. H., Olsen, A., Buonsanti, C., Follmann, F., Zhang, Y., Coler, R. N., Fox, C. B., Meinke, A., Casini, D. & Bonci, A. (2016). 'Different human vaccine adjuvants promote distinct antigen-independent immunological signatures tailored to different pathogens', *Scientific reports*, 6, p. 19570.
- Koletzki, D., Biel, S. S., Meisel, H., Nugel, E., Gelderblom, H. R., Krüger, D. H. & Ulrich, R. (1999). 'HBV core particles allow the insertion and surface exposure of the entire potentially protective region of Puumala hantavirus nucleocapsid protein', *Biological chemistry*, 380(3), pp. 325-333.
- Koyama, K. (2002). 'NK1. 1+ cell depletion *in vivo* fails to prevent protection against infection with the murine nematode parasite *Trichuris muris*', *Parasite immunology*, 24(11-12), pp. 527-533.
- Koyama, K. & Ito, Y. (1996). 'Comparative studies on immune responses to infection in susceptible B10. BR mice infected with different strains of the murine nematode parasite *Trichuris muris*', *Parasite immunology*, 18(5), pp. 257-263.
- Koyama, K., Tamachi, H. & Ito, Y. (1995). 'The role of CD4+ and CD8+ T cells in protective immunity to the murine nematode parasite *Trichuris muris*', *Parasite immunology*, 17(3), pp. 161-165.

- Koyama, K., Tamauchi, H., Tomita, M., Kitajima, T. & Ito, Y. (1999). 'B-cell activation in the mesenteric lymph nodes of resistant BALB/c mice infected with the murine nematode parasite *Trichuris muris*', *Parasitology research*, 85(3), pp. 194-199.
- Kratz, P. A., Böttcher, B. & Nassal, M. (1999). 'Native display of complete foreign protein domains on the surface of hepatitis B virus capsids', *Proceedings of the National Academy of Sciences*, 96(5), pp. 1915-1920.
- Kreider, T., Anthony, R. M., Urban, J. F., Jr. & Gause, W. C. (2007). 'Alternatively activated macrophages in helminth infections', *Curr Opin Immunol*, 19(4), pp. 448-53.
- Kuipers, G., Peschke, M., Ismail, N. B., Hjelm, A., Schlegel, S., Vikström, D., Luirink, J. & de Gier, J.-W. (2017). 'Optimizing *E. coli*-based membrane protein production using Lemo21 (DE3) or pReX and GFP-fusions', *Heterologous Gene Expression in E. coli: Methods and Protocols*, pp. 109-126.
- Kumar, M., Meenakshi, N., Sundaramurthi, J. C., Kaur, G., Mehra, N. K. & Raja, A. (2010). 'Immune response to *Mycobacterium tuberculosis* specific antigen ESAT-6 among south Indians', *Tuberculosis*, 90(1), pp. 60-69.
- Kumar, M. M. & Raja, A. (2010). 'Cytotoxicity responses to selected ESAT-6 and CFP-10 peptides in tuberculosis', *Cellular immunology*, 265(2), pp. 146-155.
- Kushnir, N., Streatfield, S. J. & Yusibov, V. (2012). 'Virus-like particles as a highly efficient vaccine platform: diversity of targets and production systems and advances in clinical development', *Vaccine*, 31(1), pp. 58-83.
- Kyriakopoulos, S. & Kontoravdi, C. (2013). 'Analysis of the landscape of biologically-derived pharmaceuticals in Europe: dominant production systems, molecule types on the rise and approval trends', *European Journal of Pharmaceutical Sciences*, 48(3), pp. 428-441.
- Kyte, J. & Doolittle, R. F. (1982). 'A simple method for displaying the hydropathic character of a protein', *Journal of molecular biology*, 157(1), pp. 105-132.
- Lafuente, E. M. & Reche, P. A. (2009). 'Prediction of MHC-peptide binding: a systematic and comprehensive overview', *Curr Pharm Des*, 15(28), pp. 3209-20.
- Lai, H.-J., Lo, S. J., Kage-Nakadai, E., Mitani, S. & Xue, D. (2009). 'The roles and acting mechanism of *Caenorhabditis elegans* DNase II genes in apoptotic DNA degradation and development', *PloS one*, 4(10), p. e7348.
- Lan, J., Deng, Y., Song, J., Huang, B., Wang, W. & Tan, W. (2018). 'Significant Spike-Specific IgG and Neutralizing Antibodies in Mice Induced by a Novel Chimeric Virus-Like Particle Vaccine Candidate for Middle East Respiratory Syndrome Coronavirus', *Virologica Sinica*, 33(5), pp. 453-455.
- Lazarski, C. A., Chaves, F. A., Jenks, S. A., Wu, S., Richards, K. A., Weaver, J. & Sant, A. J. (2005). 'The kinetic stability of MHC class II: peptide complexes is a key parameter that dictates immunodominance', *Immunity*, 23(1), pp. 29-40.
- Lee, B. O., Tucker, A., Frelin, L., Sallberg, M., Jones, J., Peters, C., Hughes, J., Whitacre, D., Darsow, B. & Peterson, D. L. (2009). 'Interaction of the hepatitis B core antigen and the innate immune system', *The Journal of Immunology*, 182(11), pp. 6670-6681.
- Lee, D.-H., Kim, A.-R., Lee, S.-H. & Quan, F.-S. (2017). 'Virus-like particles vaccine containing *Clonorchis sinensis* tegumental protein induces partial protection against *Clonorchis sinensis* infection', *Parasites & vectors*, 10(1), p. 626.
- Lee, K. W. & Tan, W. S. (2008). 'Recombinant hepatitis B virus core particles: association, dissociation and encapsidation of green fluorescent protein', *Journal of virological methods*, 151(2), pp. 172-180.
- Lee, S.-H., Kang, H.-J., Lee, D.-H., Kang, S.-M. & Quan, F.-S. (2018). 'Virus-like particle vaccines expressing *Toxoplasma gondii* rhoptry protein 18 and microneme protein 8 provide enhanced protection', *Vaccine*, 36(38), pp. 5692-5700.
- Lee, S.-H., Kim, S.-S., Lee, D.-H., Kim, A.-R. & Quan, F.-S. (2016). 'Evaluation of protective efficacy induced by virus-like particles containing a *Trichinella spiralis* excretory-secretory (ES) protein in mice', *Parasites & vectors*, 9(1), p. 384.
- Lee, T., Wakelin, D. & Grencis, R. (1983). 'Cellular mechanisms of immunity to the nematode *Trichuris muris*', *International journal for parasitology*, 13(4), pp. 349-353.

- Lenz, P., Day, P. M., Pang, Y.-Y. S., Frye, S. A., Jensen, P. N., Lowy, D. R. & Schiller, J. T. (2001). 'Papillomavirus-like particles induce acute activation of dendritic cells', *The Journal of Immunology*, 166(9), pp. 5346-5355.
- Lenz, P., Thompson, C. D., Day, P. M., Bacot, S. M., Lowy, D. R. & Schiller, J. T. (2003). 'Interaction of papillomavirus virus-like particles with human myeloid antigen-presenting cells', *Clinical immunology*, 106(3), pp. 231-237.
- Leroux, L.-P., Nasr, M., Valanparambil, R., Tam, M., Rosa, B. A., Siciliani, E., Hill, D. E., Zarlenga, D. S., Jaramillo, M. & Weinstock, J. V. (2018). 'Analysis of the *Trichuris suis* excretory/secretory proteins as a function of life cycle stage and their immunomodulatory properties', *Scientific reports*, 8(1), p. 15921.
- Leung, J. M. (2013). 'A role for IL-22 in the relationship between intestinal helminths, gut microbiota and mucosal immunity', *International journal for parasitology*, 43(3), pp. 253-257.
- Li, J., Chen, S., Xiao, X., Zhao, Y., Ding, W. & Li, X. C. (2017). 'IL-9 and Th9 cells in health and diseases-From tolerance to immunopathology', *Cytokine Growth Factor Rev*, 37, pp. 47-55.
- Li, Z.-X., Hong, G.-Q., Hu, B., Liang, M.-J., Xu, J. & Li, L. (2007). 'Suitability of yeast-and *Escherichia coli*-expressed hepatitis B virus core antigen derivatives for detection of anti-HBc antibodies in human sera', *Protein expression and purification*, 56(2), pp. 293-300.
- Li, Z., Wei, J., Yang, Y., Liu, L., Ma, G., Zhang, S. & Su, Z. (2018). 'A two-step heat treatment of cell disruption supernatant enables efficient removal of host cell proteins before chromatographic purification of HBc particles', *Journal of Chromatography A*, 1581, pp. 71-79.
- Licona-Limon, P., Arias-Rojas, A. & Olguin-Martinez, E. (2017). IL-9 and Th9 in parasite immunity. In: *Seminars in immunopathology*, 2017. Springer. pp. 29-38.
- Lightowlers, M. W. & Rickard, M. D. (1988). 'Excretory-secretory products of helminth parasites: effects on host immune responses', *Parasitology*, 96(S1), pp. S123-S166.
- Lin, H. H., Ray, S., Tongchusak, S., Reinherz, E. L. & Brusic, V. (2008). 'Evaluation of MHC-II peptide binding prediction servers: applications for vaccine research', *BMC bioinformatics*, 9((Suppl 12)), p. 10.
- Lin HH, Z. G., Tongchusak S, Reinherz EL, Brusic (2008). 'Evaluation of MHC-II peptide binding prediction servers: applications for vaccine research', *BMC Bioinformatics*, 9, p. Suppl 12.
- Lin, Y.-L., Hu, Y.-C., Liang, C.-C., Lin, S.-Y., Liang, Y.-C., Yuan, H.-P. & Chiang, B.-L. (2014). 'Enterovirus-71 virus-like particles induce the activation and maturation of human monocyte-derived dendritic cells through TLR4 signaling', *PLoS one*, 9(10), p. e111496.
- Link, A., Zabel, F., Schnetzler, Y., Titz, A., Brombacher, F. & Bachmann, M. F. (2012). 'Innate immunity mediates follicular transport of particulate but not soluble protein antigen', *The Journal of Immunology*, p. 1103312.
- Little, M. C., Bell, L. V., Cliffe, L. J. & Else, K. J. (2005). 'The characterization of intraepithelial lymphocytes, lamina propria leukocytes, and isolated lymphoid follicles in the large intestine of mice infected with the intestinal nematode parasite *Trichuris muris*', *The Journal of Immunology*, 175(10), pp. 6713-6722.
- Liu, F., Ge, S., Li, L., Wu, X., Liu, Z. & Wang, Z. (2012). 'Virus-like particles: potential veterinary vaccine immunogens', *Research in veterinary science*, 93(2), pp. 553-559.
- Liu, M. F., Wu, X. P., Wang, X. L., Yu, Y. L., Wang, W. F., Chen, Q. J., Boireau, P. & Liu, M. Y. (2008). 'The functions of Deoxyribonuclease II in immunity and development', *DNA Cell Biol*, 27(5), pp. 223-8.
- Liu, S., Tobias, R., McClure, S., Styba, G., Shi, Q. & Jackowski, G. (1997). 'Removal of endotoxin from recombinant protein preparations', *Clinical biochemistry*, 30(6), pp. 455-463.
- Lombard, M., Pastoret, P. & Moulin, A. (2007). 'A brief history of vaccines and vaccination', *Revue Scientifique et Technique-Office International des Epizooties*, 26(1), pp. 29-48.
- Lorentz, A., Schwengberg, S., Sellge, G., Manns, M. P. & Bischoff, S. C. (2000). 'Human intestinal mast cells are capable of producing different cytokine profiles: role of IgE receptor cross-linking and IL-4', *J Immunol*, 164(1), pp. 43-8.

- Lorenz, R. G., Chaplin, D. D., McDonald, K. G., McDonough, J. S. & Newberry, R. D. (2003). 'Isolated lymphoid follicle formation is inducible and dependent upon lymphotoxin-sufficient B lymphocytes, lymphotoxin β receptor, and TNF receptor I function', *The Journal of Immunology*, 170(11), pp. 5475-5482.
- Loukas, A. & Giacomin, P. (2016). 'Developments in the Design of Anti-helminth Vaccines', in Gause, W. C. & Artis, D. (eds.) *The Th2 Type Immune Response in Health and Disease: From Host Defense and Allergy to Metabolic Homeostasis and Beyond*. New York, NY: Springer New Yorkpp. 97-114.
- Lu, Y., Chan, W., Ko, B. Y., VanLang, C. C. & Swartz, J. R. (2015). 'Assessing sequence plasticity of a virus-like nanoparticle by evolution toward a versatile scaffold for vaccines and drug delivery', *Proceedings of the National Academy of Sciences*, 112(40), pp. 12360-12365.
- Luda, K. M., Joeris, T., Persson, E. K., Rivollier, A., Demiri, M., Sitnik, K. M., Pool, L., Holm, J. B., Melo-Gonzalez, F., Richter, L., Lambrecht, B. N., Kristiansen, K., Travis, M. A., Svensson-Frej, M., Kotarsky, K. & Agace, W. W. (2016). 'IRF8 Transcription-Factor-Dependent Classical Dendritic Cells Are Essential for Intestinal T Cell Homeostasis', *Immunity*, 44(4), pp. 860-74.
- Ludwig, C. & Wagner, R. (2007). 'Virus-like particles—universal molecular toolboxes', *Current opinion in biotechnology*, 18(6), pp. 537-545.
- Lund, O. (2005). *Immunological bioinformatics*: MIT press.
- Ma, X., Zhou, X., Zhu, Y., Li, Y., Wang, H., Mamuti, W., Li, Y., Wen, H. & Ding, J. (2013). 'The prediction of T-and B-combined epitope and tertiary structure of the Eg95 antigen of *Echinococcus granulosus*', *Experimental and therapeutic medicine*, 6(3), pp. 657-662.
- Ma, Y., Nolte, R. J. & Cornelissen, J. J. (2012). 'Virus-based nanocarriers for drug delivery', *Advanced drug delivery reviews*, 64(9), pp. 811-825.
- Madden, D. R. (1995). 'The three-dimensional structure of peptide-MHC complexes', *Annual review of immunology*, 13(1), pp. 587-622.
- Maizels, R. M. & Yazdanbakhsh, M. (2003). 'Immune regulation by helminth parasites: cellular and molecular mechanisms', *Nature Reviews Immunology*, 3(9), p. 733.
- Makarkov, A. I., Golizeh, M., Ruiz-Lancheros, E., Gopal, A. A., Costas-Cancelas, I. N., Chierzi, S., Pillet, S., Charland, N., Landry, N. & Rouiller, I. J. n. V. (2019). 'Plant-derived virus-like particle vaccines drive cross-presentation of influenza A hemagglutinin peptides by human monocyte-derived macrophages', 4(1), p. 17.
- Mamat, U., Woodard, R. W., Wilke, K., Souvignier, C., Mead, D., Steinmetz, E., Terry, K., Kovacich, C., Zegers, A. & Knox, C. J. N. M. (2013). 'Endotoxin-free protein production—ClearColi™ technology', 10(9).
- Manigold, T., Böcker, U., Chen, J., Gundt, J., Traber, P., Singer, M. V. & Rossol, S. (2003). 'Hepatitis B core antigen is a potent inductor of interleukin-18 in peripheral blood mononuclear cells of healthy controls and patients with hepatitis B infection', *Journal of medical virology*, 71(1), pp. 31-40.
- Manolova, V., Flace, A., Bauer, M., Schwarz, K., Saudan, P. & Bachmann, M. F. (2008). 'Nanoparticles target distinct dendritic cell populations according to their size', *European journal of immunology*, 38(5), pp. 1404-1413.
- Marcilla, A., Garg, G., Bernal, D., Ranganathan, S., Forment, J., Ortiz, J., Munoz-Antoli, C., Dominguez, M. V., Pedrola, L., Martinez-Blanch, J., Sotillo, J., Treliis, M., Toledo, R. & Esteban, J. G. (2012). 'The transcriptome analysis of *Strongyloides stercoralis* L3i larvae reveals targets for intervention in a neglected disease', *PLoS Negl Trop Dis*, 6(2), p. e1513.
- Marques, H. H., Zouain, C. S., Torres, C. B., Oliveira, J. S., Alves, J. B. & Goes, A. M. (2008). 'Protective effect and granuloma down-modulation promoted by RP44 antigen a fructose 1, 6 bisphosphate aldolase of *Schistosoma mansoni*', *Immunobiology*, 213(5), pp. 437-446.
- Martin, W., Sbai, H. & De Groot, A. S. (2003). 'Bioinformatics tools for identifying class I-restricted epitopes', *Methods*, 29(3), pp. 289-298.
- Mayer, J. U., Demiri, M., Agace, W. W., MacDonald, A. S., Svensson-Frej, M. & Milling, S. W. (2017). 'Different populations of CD11b(+) dendritic cells drive Th2 responses in the small intestine and colon', *Nat Commun*, 8, p. 15820.

- McAleer, W. J., Buynak, E. B., Maigetter, R. Z., Wampler, D. E., Miller, W. J. & Hilleman, M. R. (1984). 'Human hepatitis B vaccine from recombinant yeast', *Nature*, 307(5947), p. 178.
- McCullough, K. C. & Sharma, R. (2017). 'Dendritic Cell Endocytosis Essential for Viruses and Vaccines', *Biology of Myelomonocytic Cells*: InTech.
- McFarland, B. J., Sant, A. J., Lybrand, T. P. & Beeson, C. (1999). 'Ovalbumin (323-339) peptide binds to the major histocompatibility complex class II I-Ad protein using two functionally distinct registers', *Biochemistry*, 38(50), pp. 16663-16670.
- McGuckin, M. A., Linden, S. K., Sutton, P. & Florin, T. H. (2011). 'Mucin dynamics and enteric pathogens', *Nat Rev Microbiol*, 9(4), pp. 265-78.
- McKeage, K. & Romanowski, B. (2011). 'AS04-Adjuvanted Human Papillomavirus (HPV) Types 16 and 18 Vaccine (Cervarix®)', *Drugs*, 71(4), pp. 465-488.
- McSorley, H. J., Hewitson, J. P. & Maizels, R. M. (2013). 'Immunomodulation by helminth parasites: defining mechanisms and mediators', *Int J Parasitol*, 43(3-4), pp. 301-10.
- McSorley, S. J., Cookson, B. T. & Jenkins, M. K. (2000). 'Characterization of CD4+ T cell responses during natural infection with *Salmonella typhimurium*', *The Journal of Immunology*, 164(2), pp. 986-993.
- Mehta, P. N. (2013). 'Drugs for intestinal helminths', *Pediatric Infectious Disease*, 1(5), pp. 22-25.
- Meister, G. E., Roberts, C. G., Berzofsky, J. A. & De Groot, A. S. (1995). 'Two novel T cell epitope prediction algorithms based on MHC-binding motifs; comparison of predicted and published epitopes from *Mycobacterium tuberculosis* and HIV protein sequences', *Vaccine*, 13(6), pp. 581-591.
- Middelberg, A. P., Rivera-Hernandez, T., Wibowo, N., Lua, L. H., Fan, Y., Magor, G., Chang, C., Chuan, Y. P., Good, M. F. & Batzloff, M. R. (2011). 'A microbial platform for rapid and low-cost virus-like particle and capsomere vaccines', *Vaccine*, 29(41), pp. 7154-7162.
- Milich, D., McLachlan, A., Stahl, S., Wingfield, P., Thornton, G., Hughes, J. & Jones, J. (1988). 'Comparative immunogenicity of hepatitis B virus core and E antigens', *The Journal of Immunology*, 141(10), pp. 3617-3624.
- Milich, D. R. (1999). Do T cells "see" the hepatitis B core and e antigens differently? : Elsevier.
- Milich, D. R., Chen, M., Schödel, F., Peterson, D. L., Jones, J. E. & Hughes, J. L. (1997a). 'Role of B cells in antigen presentation of the hepatitis B core', *Proceedings of the National Academy of Sciences*, 94(26), pp. 14648-14653.
- Milich, D. R., Hughes, J., Jones, J., Sällberg, M. & Phillips, T. R. (2001). 'Conversion of poorly immunogenic malaria repeat sequences into a highly immunogenic vaccine candidate', *Vaccine*, 20(5-6), pp. 771-788.
- Milich, D. R. & McLachlan, A. (1986). 'The nucleocapsid of hepatitis B virus is both a T-cell-independent and a T-cell-dependent antigen', *Science*, 234(4782), pp. 1398-1401.
- Milich, D. R., McLACHLAN, A., Moriarty, A. & Thornton, G. B. (1987a). 'Immune response to hepatitis B virus core antigen (HBcAg): localization of T cell recognition sites within HBcAg/HBeAg', *The Journal of Immunology*, 139(4), pp. 1223-1231.
- Milich, D. R., McLachlan, A., Thornton, G. B. & Hughes, J. L. (1987b). 'Antibody production to the nucleocapsid and envelope of the hepatitis B virus primed by a single synthetic T cell site', *Nature*, 329(6139), p. 547.
- Milich, D. R., Peterson, D. L., Schödel, F., Jones, J. E. & Hughes, J. L. (1995). 'Preferential recognition of hepatitis B nucleocapsid antigens by Th1 or Th2 cells is epitope and major histocompatibility complex dependent', *Journal of virology*, 69(5), pp. 2776-2785.
- Milich, D. R., Schödel, F., Hughes, J. L., Jones, J. E. & Peterson, D. L. (1997b). 'The hepatitis B virus core and e antigens elicit different Th cell subsets: antigen structure can affect Th cell phenotype', *Journal of virology*, 71(3), pp. 2192-2201.
- Miller, T. A. (1978). 'Industrial development and field use of the canine hookworm vaccine', *Advances in parasitology*: Elsevierpp. 333-342.
- Minutti, C. M., Drube, S., Blair, N., Schwartz, C., McCrae, J. C., McKenzie, A. N., Kamradt, T., Mokry, M., Coffer, P. J. & Sibilia, M. J. I. (2017). 'Epidermal growth factor receptor expression licenses type-2 helper T cells to function in a T cell receptor-independent fashion', 47(4), pp. 710-722. e6.

- Miroux, B. & Walker, J. E. (1996). 'Over-production of proteins in *Escherichia coli*: mutant hosts that allow synthesis of some membrane proteins and globular proteins at high levels', *Journal of molecular biology*, 260(3), pp. 289-298.
- Mohamed Fawzi, E., Cruz Bustos, T., Gómez Samblas, M., González-González, G., Solano, J., González-Sánchez, M. E., De Pablos, L. M., Corral-Caridad, M. J., Cuquerella, M., Osuna, A. & Alunda, J. M. (2013). 'Intranasal Immunization of Lambs with Serine/Threonine Phosphatase 2A against Gastrointestinal Nematodes', 20(9), pp. 1352-1359.
- Moher, D., Liberati, A., Tetzlaff, J., Altman, D. G. & Group, P. (2010). 'Preferred reporting items for systematic reviews and meta-analyses: the PRISMA statement', *International journal of surgery*, 8(5), pp. 336-341.
- Mohr, J., Chuan, Y. P., Wu, Y., Lua, L. H. & Middelberg, A. P. (2013). 'Virus-like particle formulation optimization by miniaturized high-throughput screening', *Methods*, 60(3), pp. 248-256.
- Mohsen, M., Gomes, A., Vogel, M. & Bachmann, M. (2018). 'Interaction of viral capsid-derived virus-like particles (VLPs) with the innate immune system', *Vaccines*, 6(3), p. 37.
- Mohsen, M. O., Gomes, A. C., Cabral-Miranda, G., Krueger, C. C., Leoratti, F. M., Stein, J. V. & Bachmann, M. F. (2017a). 'Delivering adjuvants and antigens in separate nanoparticles eliminates the need of physical linkage for effective vaccination', *Journal of Controlled Release*, 251, pp. 92-100.
- Mohsen, M. O., Zha, L., Cabral-Miranda, G. & Bachmann, M. F. (2017b). Major findings and recent advances in virus-like particle (VLP)-based vaccines. In: Seminars in immunology, 2017b. Elsevier.
- Moise, L., Cousens, L., Fueyo, J. & De Groot, A. S. (2011). 'Harnessing the power of genomics and immunoinformatics to produce improved vaccines', *Expert opinion on drug discovery*, 6(1), pp. 9-15.
- Moise, L., Gutierrez, A. H., Bailey-Kellogg, C., Terry, F., Leng, Q., Abdel Hady, K. M., VerBerkmoes, N. C., Sztein, M. B., Losikoff, P. T., Martin, W. D., Rothman, A. L. & De Groot, A. S. (2013). 'The two-faced T cell epitope: examining the host-microbe interface with JanusMatrix', *Hum Vaccin Immunother*, 9(7), pp. 1577-86.
- Monie, A., Hung, C. F., Roden, R. & Wu, T. C. (2008). 'Cervarix: a vaccine for the prevention of HPV 16, 18-associated cervical cancer', *Biologics*, 2(1), pp. 97-105.
- Montresor, A., Crompton, D., Hall, A., Bundy, D. & Savioli, L. (1998). 'Guidelines for the evaluation of soil-transmitted helminthiasis and schistosomiasis at community level', Geneva: World Health Organization, pp. 1-49.
- Moon, J. J., Chu, H. H., Pepper, M., McSorley, S. J., Jameson, S. C., Kedl, R. M. & Jenkins, M. K. (2007). 'Naive CD4+ T cell frequency varies for different epitopes and predicts repertoire diversity and response magnitude', *Immunity*, 27(2), pp. 203-213.
- Mosavat, A., Soleimanpour, S., Farsiani, H., Sadeghian, H., Ghazvini, K., Sankian, M., Jamehdar, S. A. & Rezaee, S. A. (2016). 'Fused *Mycobacterium tuberculosis* multi-stage immunogens with an Fc-delivery system as a promising approach for the development of a tuberculosis vaccine', *Infection, Genetics and Evolution*, 39, pp. 163-172.
- Mosca, F., Tritto, E., Muzzi, A., Monaci, E., Bagnoli, F., Iavarone, C., O'Hagan, D., Rappuoli, R. & De Gregorio, E. (2008). 'Molecular and cellular signatures of human vaccine adjuvants', *Proceedings of the National Academy of Sciences*, 105(30), pp. 10501-10506.
- Moser, W., Ali, S. M., Ame, S. M., Speich, B., Puchkov, M., Huwyler, J., Albonico, M., Hattendorf, J. & Keiser, J. (2015). 'Efficacy and safety of oxantel pamoate in school-aged children infected with *Trichuris trichiura* on Pemba Island, Tanzania: a parallel, randomised, controlled, dose-ranging study', *The Lancet Infectious Diseases*.
- Motomura, Y., Khan, W. I., El-Sharkawy, R. T., Verma-Gandhu, M., Grencis, R. K. & Collins, S. M. (2010). 'Mechanisms underlying gut dysfunction in a murine model of chronic parasitic infection', 299(6), pp. G1354-G1360.
- Mougneau, E., Altare, F., Wakil, A. E., Zheng, S., Coppola, T., Wang, Z.-E., Waldmann, R., Locksley, R. M. & Glaichenhaus, N. (1995). 'Expression cloning of a protective *Leishmania* antigen', *Science*, 268(5210), pp. 563-566.

- Moura, A. P. V., Santos, L. C., Brito, C. R. N., Valencia, E., Junqueira, C., Filho, A. A., Sant'Anna, M. R., Gontijo, N. F., Bartholomeu, D. C. & Fujiwara, R. T. (2017). 'Virus-like particle display of the α -Gal carbohydrate for vaccination against *Leishmania* infection', *ACS central science*, 3(9), pp. 1026-1031.
- Moussa, E. M., Panchal, J. P., Moorthy, B. S., Blum, J. S., Joubert, M. K., Narhi, L. O. & Topp, E. M. (2016). 'Immunogenicity of therapeutic protein aggregates', *Journal of pharmaceutical sciences*, 105(2), pp. 417-430.
- Mrus, J., Baeten, B., Engelen, M. & Silber, S. (2018). 'Efficacy of single-dose 500 mg mebendazole in soil-transmitted helminth infections: a review', *Journal of helminthology*, 92(3), pp. 269-278.
- Mukai, K., Tsai, M., Starkl, P., Marichal, T. & Galli, S. J. (2016). 'IgE and mast cells in host defense against parasites and venoms', *Semin Immunopathol*, 38(5), pp. 581-603.
- Münz, C. (2012). 'Antigen processing for MHC class II presentation via autophagy', *Frontiers in immunology*, 3.
- Murray, P. J. & Wynn, T. A. (2011). 'Protective and pathogenic functions of macrophage subsets', *Nature Reviews Immunology*, 11(11), p. 723.
- Murthy, A. M. V., Ni, Y., Meng, X. & Zhang, C. (2015). 'Production and evaluation of virus-like particles displaying immunogenic epitopes of porcine reproductive and respiratory syndrome virus (PRRSV)', *International journal of molecular sciences*, 16(4), pp. 8382-8396.
- Murugan, N. & Dai, Y. (2005). 'Prediction of MHC class II binding peptides based on an iterative learning model', *Immunome research*, 1(1), p. 6.
- Myers, A. J., Marino, S., Kirschner, D. E. & Flynn, J. L. (2013). 'Inoculation dose of *Mycobacterium tuberculosis* does not influence priming of T cell responses in lymph nodes', *The Journal of Immunology*, 190(9), pp. 4707-4716.
- Nagel, E. & Diemert, D. (2018). 'Hookworm Vaccine Phase I Clinical Trial, Americaninhas, Brazil: The Faces Behind the Data'.
- Nagpal, G., Usmani, S. S., Dhanda, S. K., Kaur, H., Singh, S., Sharma, M. & Raghava, G. P. (2017). 'Computer-aided designing of immunosuppressive peptides based on IL-10 inducing potential', *Sci Rep*, 7, p. 42851.
- Nair, M. G., Guild, K. J., Du, Y., Zaph, C., Yancopoulos, G. D., Valenzuela, D. M., Murphy, A., Stevens, S., Karow, M. & Artis, D. (2008). 'Goblet Cell-Derived Resistin-Like Molecule β Augments CD4+ T Cell Production of IFN- γ and Infection-Induced Intestinal Inflammation', 181(7), pp. 4709-4715.
- Nance, J. (2005). 'PAR proteins and the establishment of cell polarity during *C. elegans* development', *Bioessays*, 27(2), pp. 126-135.
- Nardin, E. H., Calvo-Calle, J. M., Oliveira, G. A., Nussenzweig, R. S., Schneider, M., Tiercy, J.-M., Loutan, L., Hochstrasser, D. & Rose, K. (2001). 'A totally synthetic polyoxime malaria vaccine containing *Plasmodium falciparum* B cell and universal T cell epitopes elicits immune responses in volunteers of diverse HLA types', *The Journal of Immunology*, 166(1), pp. 481-489.
- Nardin, E. H., Oliveira, G. A., Calvo-Calle, J. M., Wetzel, K., Maier, C., Birkett, A. J., Sarpotdar, P., Corado, M. L., Thornton, G. B. & Schmidt, A. (2004). 'Phase I testing of a malaria vaccine composed of hepatitis B virus core particles expressing *Plasmodium falciparum* circumsporozoite epitopes', *Infection and immunity*, 72(11), pp. 6519-6527.
- Nassal, M. (1992). 'The arginine-rich domain of the hepatitis B virus core protein is required for pregenome encapsidation and productive viral positive-strand DNA synthesis but not for virus assembly', *Journal of virology*, 66(7), pp. 4107-4116.
- Nassal, M., Skamel, C., Vogel, M., Kratz, P. A., Stehle, T., Wallich, R. & Simon, M. M. (2008). 'Development of hepatitis B virus capsids into a whole-chain protein antigen display platform: new particulate Lyme disease vaccines', *International Journal of Medical Microbiology*, 298(1-2), pp. 135-142.

- Nath, N., Hickman, K., Nowlan, S., Shah, D., Phillips, J. & Babler, S. (1992). 'Stability of the recombinant hepatitis B core antigen', *Journal of clinical microbiology*, 30(6), pp. 1617-1619.
- Netter, H. J., Macnaughton, T. B., Woo, W.-P., Tindle, R. & Gowans, E. J. (2001). 'Antigenicity and immunogenicity of novel chimeric hepatitis B surface antigen particles with exposed hepatitis C virus epitopes', *Journal of virology*, 75(5), pp. 2130-2141.
- Nielsen, M., Justesen, S., Lund, O., Lundsgaard, C. & Buus, S. (2010a). 'NetMHCpan-2.0-Improved pan-specific HLA-DR predictions using a novel concurrent alignment and weight optimization training procedure', *Immunome Res*, 6(9), pp. 7580-6.
- Nielsen, M. & Lund, O. (2009). 'NN-align. An artificial neural network-based alignment algorithm for MHC class II peptide binding prediction', *BMC bioinformatics*, 10(1), p. 1.
- Nielsen, M., Lund, O., Buus, S. & Lundsgaard, C. (2010b). 'MHC class II epitope predictive algorithms', *Immunology*, 130(3), pp. 319-28.
- Nielsen, M., Lundsgaard, C., Worning, P., Hvid, C. S., Lamberth, K., Buus, S., Brunak, S. & Lund, O. (2004). 'Improved prediction of MHC class I and class II epitopes using a novel Gibbs sampling approach', *Bioinformatics*, 20(9), pp. 1388-1397.
- Noad, R. & Roy, P. (2003). 'Virus-like particles as immunogens', *Trends in microbiology*, 11(9), pp. 438-444.
- Noel, W., Raes, G., Hassanzadeh Ghassabeh, G., De Baetselier, P. & Beschin, A. (2004). 'Alternatively activated macrophages during parasite infections', *Trends Parasitol*, 20(3), pp. 126-33.
- Nokes, C., Cooper, E. S., Robinson, B. A. & Bundy, D. A. P. (1991). 'Geohelminth infection and academic assessment in Jamaican children', *Transactions of The Royal Society of Tropical Medicine and Hygiene*, 85(2), pp. 272-273.
- Noon, J. B. & Aroian, R. V. (2017). 'Recombinant subunit vaccines for soil-transmitted helminths', *Parasitology*, 144(14), pp. 1845-1870.
- Novitsky, T. J. J. A. o. t. N. Y. A. o. S. (1998). 'Limitations of the Limulus amebocyte lysate test in demonstrating circulating lipopolysaccharides', 851(1), pp. 416-421.
- O'Hagan, D. T., Ott, G. S., Nest, G. V., Rappuoli, R. & Giudice, G. D. (2013). 'The history of MF59® adjuvant: a phoenix that arose from the ashes', *Expert review of vaccines*, 12(1), pp. 13-30.
- Ogishi, M. & Yotsuyanagi, H. (2019). 'Quantitative Prediction of the Landscape of T Cell Epitope Immunogenicity in Sequence Space', *Frontiers in Immunology*, 10.
- Ohno, M., Kimura, M., Miyazaki, H., Okawa, K., Onuki, R., Nemoto, C., Tabata, E., Wakita, S., Kashimura, A. & Sakaguchi, M. J. S. r. (2016). 'Acidic mammalian chitinase is a proteases-resistant glycosidase in mouse digestive system', 6, p. 37756.
- Oliveira, G. A., Wetzel, K., Calvo-Calle, J. M., Nussenzweig, R., Schmidt, A., Birkett, A., Dubovsky, F., Tierney, E., Gleiter, C. H. & Boehmer, G. (2005). 'Safety and enhanced immunogenicity of a hepatitis B core particle *Plasmodium falciparum* malaria vaccine formulated in adjuvant Montanide ISA 720 in a phase I trial', *Infection and immunity*, 73(6), pp. 3587-3597.
- Olsen, A. W., Hansen, P. R., Holm, A. & Andersen, P. (2000). 'Efficient protection against *Mycobacterium tuberculosis* by vaccination with a single subdominant epitope from the ESAT-6 antigen', *European journal of immunology*, 30(6), pp. 1724-1732.
- Ota, M., Idoko, O., Ogundare, E. & Afolabi, M. (2013). 'Human immune responses to vaccines in the first year of life: Biological, socio-economic and ethical issues—A viewpoint', *Vaccine*, 31(21), pp. 2483-2488.
- Ott, G., Barchfeld, G. L., Chernoff, D., Radhakrishnan, R., van Hoogeveest, P. & Van Nest, G. (1995). 'MF59 design and evaluation of a safe and potent adjuvant for human vaccines', *Vaccine Design*: Springerpp. 277-296.
- Ott, G., Radhakrishnan, R., Fang, J.-H. & Hora, M. (2000). The adjuvant MF59: a 10-year perspective. Springer.
- Owyang, A. M., Zaph, C., Wilson, E. H., Guild, K. J., McClanahan, T., Miller, H. R., Cua, D. J., Goldschmidt, M., Hunter, C. A. & Kastelein, R. A. (2006). 'Interleukin 25 regulates type 2

- cytokine-dependent immunity and limits chronic inflammation in the gastrointestinal tract', *Journal of Experimental Medicine*, 203(4), pp. 843-849.
- Palatnik-de-Sousa, C. B., Soares, I. S. & Rosa, D. S. (2018). 'Editorial: Epitope Discovery and Synthetic Vaccine Design', *Front Immunol*, 9, p. 826.
- Pance, A. (2019). 'How elusive can a malaria vaccine be?', *Nature Reviews Microbiology*, p. 1.
- Pappalardo, F., Flower, D., Russo, G., Pennisi, M. & Motta, S. (2015). 'Computational modelling approaches to vaccinology', *Pharmacol Res*, 92, pp. 40-5.
- Patel, C., Hurlimann, E., Keller, L., Hattendorf, J., Sayasone, S., Ali, S. M., Ame, S. M., Coulibaly, J. T. & Keiser, J. (2019). 'Efficacy and safety of ivermectin and albendazole co-administration in school-aged children and adults infected with *Trichuris trichiura*: study protocol for a multi-country randomized controlled double-blind trial', *BMC Infect Dis*, 19(1), p. 262.
- Patel, K. G. & Swartz, J. R. (2011). 'Surface functionalization of virus-like particles by direct conjugation using azide- alkyne click chemistry', *Bioconjugate chemistry*, 22(3), pp. 376-387.
- Patronov, A. & Doytchinova, I. (2013). 'T-cell epitope vaccine design by immunoinformatics', *Open biology*, 3(1), p. 120139.
- Paul, S., Arlehamn, C. S. L., Scriba, T. J., Dillon, M. B., Oseroff, C., Hinz, D., McKinney, D. M., Pro, S. C., Sidney, J. & Peters, B. (2015). 'Development and validation of a broad scheme for prediction of HLA class II restricted T cell epitopes', *Journal of immunological methods*, 422, pp. 28-34.
- Paul, S., Sidney, J., Sette, A. & Peters, B. (2016). 'TepiTool: A Pipeline for Computational Prediction of T Cell Epitope Candidates', *Curr Protoc Immunol*, 114, pp. 18 19 1-18 19 24.
- Peacey, M., Wilson, S., Baird, M. A. & Ward, V. K. (2007). 'Versatile RHDV virus-like particles: Incorporation of antigens by genetic modification and chemical conjugation', *Biotechnology and bioengineering*, 98(5), pp. 968-977.
- Pelte, C., Cherepnev, G., Wang, Y., Schoenemann, C., Volk, H.-D. & Kern, F. (2004). 'Random screening of proteins for HLA-A* 0201-binding nine-amino acid peptides is not sufficient for identifying CD8 T cell epitopes recognized in the context of HLA-A* 0201', *The Journal of Immunology*, 172(11), pp. 6783-6789.
- Pennock, J. L. & Grencis, R. K. (2006). 'The mast cell and gut nematodes: damage and defence', *Chem Immunol Allergy*, 90, pp. 128-40.
- Percival-Alwyn, J. L., England, E., Kemp, B., Rapley, L., Davis, N. H., McCarthy, G. R., Majithiya, J. B., Corkill, D. J., Welsted, S. & Minton, K. (2015). Generation of potent mouse monoclonal antibodies to self-proteins using T-cell epitope "tags". In: MAbs, 2015. Taylor & Francis. pp. 129-137.
- Perrigoue, J. G., Saenz, S. A., Siracusa, M. C., Allenspach, E. J., Taylor, B. C., Giacomin, P. R., Nair, M. G., Du, Y., Zaph, C. & van Rooijen, N. (2009). 'MHC class II-dependent basophil-CD4+ T cell interactions promote TH2 cytokine-dependent immunity', *Nature immunology*, 10(7), pp. 697-705.
- Peters, B., Bui, H. H., Frankild, S., Nielson, M., Lundgaard, C., Kostem, E., Basch, D., Lamberth, K., Harndahl, M., Fleri, W., Wilson, S. S., Sidney, J., Lund, O., Buus, S. & Sette, A. (2006). 'A community resource benchmarking predictions of peptide binding to MHC-I molecules', *PLoS Comput Biol*, 2(6), p. e65.
- Petsch, D. & Anspach, F. B. (2000). 'Endotoxin removal from protein solutions', *Journal of biotechnology*, 76(2-3), pp. 97-119.
- Pizza, M., Scarlato, V., Masignani, V., Giuliani, M. M., Arico, B., Comanducci, M., Jennings, G. T., Baldi, L., Bartolini, E. & Capecchi, B. J. S. (2000). 'Identification of vaccine candidates against serogroup B meningococcus by whole-genome sequencing', 287(5459), pp. 1816-1820.
- Ploppa, A., George, T. C., Unertl, K. E., Nohe, B. & Durieux, M. E. (2011). 'ImageStream cytometry extends the analysis of phagocytosis and oxidative burst', *Scandinavian journal of clinical and laboratory investigation*, 71(5), pp. 362-369.

- Plummer, E. M. & Manchester, M. (2011). 'Viral nanoparticles and virus-like particles: platforms for contemporary vaccine design', *Wiley Interdisciplinary Reviews: Nanomedicine and Nanobiotechnology*, 3(2), pp. 174-196.
- Podda, A. (2001). 'The adjuvanted influenza vaccines with novel adjuvants: experience with the MF59-adjuvanted vaccine', *Vaccine*, 19(17-19), pp. 2673-2680.
- Ponomarenko, J. V. & Bourne, P. E. (2007). 'Antibody-protein interactions: benchmark datasets and prediction tools evaluation', *BMC Structural Biology*, 7(1), p. 64.
- Pooley, J. L., Heath, W. R. & Shortman, K. (2001). 'Cutting edge: intravenous soluble antigen is presented to CD4 T cells by CD8- dendritic cells, but cross-presented to CD8 T cells by CD8+ dendritic cells', *The Journal of Immunology*, 166(9), pp. 5327-5330.
- Pourseif, M. M., Moghaddam, G., Naghili, B., Saeedi, N., Parvizpour, S., Nematollahi, A. & Omidi, Y. (2018). 'A novel *in silico* minigene vaccine based on CD4(+) T-helper and B-cell epitopes of EG95 isolates for vaccination against *cystic echinococcosis*', *Comput Biol Chem*, 72, pp. 150-163.
- Pullan, R., Smith, J., Jasrasaria, R. & Brooker, S. (2014). 'Global numbers of infection and disease burden of soil transmitted helminth infections in 2010', *Parasites & Vectors*, 7(1), p. 37.
- Pumpens, P., Borisova, G., Crowther, R. & Grens, E. (1995). 'Hepatitis B virus core particles as epitope carriers', *Intervirology*, 38(1-2), pp. 63-74.
- Pumpens, P. & Grens, E. (1999). 'Hepatitis B core particles as a universal display model: a structure-function basis for development', *FEBS letters*, 442(1), pp. 1-6.
- Pumpens, P. & Grens, E. (2001). 'HBV core particles as a carrier for B cell/T cell epitopes', *Intervirology*, 44(2-3), pp. 98-114.
- Pumpens, P. & Grens, E. (2002). 'Artificial genes for chimeric virus-like particles', *Artificial DNA: Methods and applications*, pp. 249-327.
- Pushko, P., Tumpey, T. M., Bu, F., Knell, J., Robinson, R. & Smith, G. (2005). 'Influenza virus-like particles comprised of the HA, NA, and M1 proteins of H9N2 influenza virus induce protective immune responses in BALB/c mice', *Vaccine*, 23(50), pp. 5751-5759.
- Qi, Y., Kang, H., Zheng, X., Wang, H., Gao, Y., Yang, S. & Xia, X. (2015). 'Incorporation of membrane-anchored flagellin or *Escherichia coli* heat-labile enterotoxin B subunit enhances the immunogenicity of rabies virus-like particles in mice and dogs', *Frontiers in microbiology*, 6, p. 169.
- Qiao, L., Zhang, Y., Chai, F., Tan, Y., Huo, C. & Pan, Z. (2016). 'Chimeric virus-like particles containing a conserved region of the G protein in combination with a single peptide of the M2 protein confer protection against respiratory syncytial virus infection', *Antiviral research*, 131, pp. 131-140.
- Quihui, L., Valencia, M. E., Crompton, D. W., Phillips, S., Hagan, P., Morales, G. & Díaz-Camacho, S. P. (2006). 'Role of the employment status and education of mothers in the prevalence of intestinal parasitic infections in Mexican rural schoolchildren', *BMC Public Health*, 6(1), p. 225.
- Raetz, C. R. & Whitfield, C. (2002). 'Lipopolysaccharide endotoxins', *Annual review of biochemistry*, 71(1), pp. 635-700.
- Raju, R., Navaneetham, D., Okita, D., Diethelm-Okita, B., McCormick, D. & Conti-Fine, B. M. (1995). 'Epitopes for human CD4+ cells on diphtheria toxin: structural features of sequence segments forming epitopes recognized by most subjects', *European journal of immunology*, 25(12), pp. 3207-3214.
- Rammensee, H.-G., Bachmann, J., Emmerich, N. P. N., Bachor, O. A. & Stevanović, S. (1999). 'SYFPEITHI: database for MHC ligands and peptide motifs', *Immunogenetics*, 50(3-4), pp. 213-219.
- Rao, A. & Avni, O. J. B. m. b. (2000). 'Molecular aspects of T-cell differentiation', 56(4), pp. 969-984.
- Rapeah, S. & Norazmi, M. (2006). 'Immunogenicity of a recombinant *Mycobacterium bovis* bacille Calmette-Guérin expressing malarial and tuberculosis epitopes', *Vaccine*, 24(17), pp. 3646-3653.

- Rasmussen, M., Fenoy, E., Harndahl, M., Kristensen, A. B., Nielsen, I. K., Nielsen, M. & Buus, S. J. T. J. o. I. (2016). 'Pan-Specific Prediction of Peptide–MHC Class I Complex Stability, a Correlate of T Cell Immunogenicity', 197(4), pp. 1517-1524.
- Reche, P. A., Glutting, J.-P. & Reinherz, E. L. (2002). 'Prediction of MHC class I binding peptides using profile motifs', *Human immunology*, 63(9), pp. 701-709.
- Reichelt, P., Schwarz, C. & Donzeau, M. (2006). 'Single step protocol to purify recombinant proteins with low endotoxin contents', *Protein expression and purification*, 46(2), pp. 483-488.
- Reitmaier, R. (2007). 'Review of immunoinformatic approaches to *in-silico* B-cell epitope prediction', *Nature Precedings*.
- Ren, H. N., Guo, K. X., Zhang, Y., Sun, G. G., Liu, R. D., Jiang, P., Zhang, X., Wang, L., Cui, J. & Wang, Z. Q. (2018). 'Molecular characterization of a 31 kDa protein from *Trichinella spiralis* and its induced immune protection in BALB/c mice', *Parasites & vectors*, 11(1), p. 625.
- Richard AG, Thomas JK, K, J. & AO, B. (2002). *Immunolog* (Fifth Edition ed.). New York: W. H. Freeman.
- Richard, M., Gencis, R. K., Humphreys, N. E., Renauld, J.-C. & Van Snick, J. (2000). 'Anti-IL-9 vaccination prevents worm expulsion and blood eosinophilia in *Trichuris muris*-infected mice', *Proceedings of the National Academy of Sciences*, 97(2), pp. 767-772.
- Riedl, P., Stober, D., Oehninger, C., Melber, K., Reimann, J. & Schirmbeck, R. (2002). 'Priming Th1 immunity to viral core particles is facilitated by trace amounts of RNA bound to its arginine-rich domain', *The Journal of Immunology*, 168(10), pp. 4951-4959.
- Rizwan, M., Naz, A., Ahmad, J., Naz, K., Obaid, A., Parveen, T., Ahsan, M. & Ali, A. (2017). 'VacSol: a high throughput *in silico* pipeline to predict potential therapeutic targets in prokaryotic pathogens using subtractive reverse vaccinology', *BMC bioinformatics*, 18(1), p. 106.
- Roach, T., Wakelin, D., Else, K. & Bundy, D. (1988). 'Antigenic cross-reactivity between the human whipworm, *Trichuris trichiura*, and the mouse trichooids *Trichuris muris* and *Trichinella spiralis*', *Parasite immunology*, 10(3), pp. 279-291.
- Robertson, J. M., Jensen, P. E. & Evavold, B. D. (2000). 'DO11. 10 and OT-II T cells recognize a C-terminal ovalbumin 323–339 epitope', *The Journal of Immunology*, 164(9), pp. 4706-4712.
- Robinson, K., Bellaby, T. & Wakelin, D. (1995). 'Efficacy of oral vaccination against the murine intestinal parasite *Trichuris muris* is dependent upon host genetics', *Infection and immunity*, 63(5), pp. 1762-1766.
- Roden, R., Kirnbauer, R. & Schellenbacher, C. (2018). Papillomavirus-like particles (VLP) as broad spectrum human papillomavirus (HPV) vaccines. US Patent App. 14/875,374.
- Röhn, T. A., Jennings, G. T., Hernandez, M., Grest, P., Beck, M., Zou, Y., Kopf, M. & Bachmann, M. F. (2006). 'Vaccination against IL-17 suppresses autoimmune arthritis and encephalomyelitis', *European journal of immunology*, 36(11), pp. 2857-2867.
- Rohovie, M. J., Nagasawa, M. & Swartz, J. R. (2017). 'Virus-like particles: Next-generation nanoparticles for targeted therapeutic delivery', *Bioengineering & translational medicine*, 2(1), pp. 43-57.
- Roldao, A., Mellado, M. C. M., Castilho, L. R., Carrondo, M. J. & Alves, P. M. (2010). 'Virus-like particles in vaccine development', *Expert review of vaccines*, 9(10), pp. 1149-1176.
- Rolland, D., Gauthier, M., Dugua, J., Fournier, C., Delpech, L., Watelet, B., Letourneur, O., Arnaud, M. & Jolivet, M. (2001). 'Purification of recombinant HBc antigen expressed in *Escherichia coli* and *Pichia pastoris*: comparison of size-exclusion chromatography and ultracentrifugation', *Journal of Chromatography B: Biomedical Sciences and Applications*, 753(1), pp. 51-65.
- Roose, K., Baets, S. D., Schepens, B. & Saelens, X. (2013). 'Hepatitis B core-based virus-like particles to present heterologous epitopes', *Expert review of vaccines*, 12(2), pp. 183-198.
- Rosano, G. L. & Ceccarelli, E. A. (2014). 'Recombinant protein expression in *Escherichia coli*: advances and challenges', *Frontiers in microbiology*, 5, p. 172.
- Rötzschke, O., Falk, K., Stevanovic, S., Jung, G., Walden, P. & Rammensee, H. G. (1991). 'Exact prediction of a natural T cell epitope', *European journal of immunology*, 21(11), pp. 2891-2894.

- Rudolf, M. P., Fausch, S. C., Da Silva, D. M. & Kast, W. M. (2001). 'Human dendritic cells are activated by chimeric human papillomavirus type-16 virus-like particles and induce epitope-specific human T cell responses in vitro', *The Journal of Immunology*, 166(10), pp. 5917-5924.
- Ruedl, C., Storni, T., Lechner, F., Bächi, T. & Bachmann, M. F. (2002). 'Cross-presentation of virus-like particles by skin-derived CD8-dendritic cells: a dispensable role for TAP', *European journal of immunology*, 32(3), pp. 818-825.
- Russo, D. M., Jardim, A., Carvalho, E. M., Sleath, P. R., Armitage, R., Olafson, R. & Reed, S. (1993). 'Mapping human T cell epitopes in *Leishmania* gp63. Identification of cross-reactive and species-specific epitopes', *The Journal of Immunology*, 150(3), pp. 932-939.
- Ryadnov, M. G. (2012). 'Prescriptive peptide design', *Amino Acids, Peptides and Proteins*, 37, p. 190.
- Sacks, D. & Noben-Trauth, N. (2002). 'The immunology of susceptibility and resistance to *Leishmania major* in mice', *Nature Reviews Immunology*, 2(11), pp. 845-858.
- Sacks, D. L., Peters, N. C. & Bethony, J. M. (2016). 'Vaccines Against Parasites', *The Vaccine Book*: Elsevierpp. 331-360.
- Saenz, S. A., Siracusa, M. C., Perrigoue, J. G., Spencer, S. P., Urban Jr, J. F., Tocker, J. E., Budelsky, A. L., Kleinschek, M. A., Kastelein, R. A. & Kambayashi, T. (2010). 'IL25 elicits a multipotent progenitor cell population that promotes T H 2 cytokine responses', *Nature*, 464(7293), p. 1362.
- Sahputra, R., Ruckerl, D., Couper, K., Muller, W. & Else, K. (2019). 'The essential role played by B cells in supporting protective immunity against *Trichuris muris* infection is dependent on host genetic background and is independent of antibody', *BioRxiv*, p. 550434.
- Salim, N., Knopp, S., Lweno, O., Abdul, U., Mohamed, A., Schindler, T., Rothen, J., Masimba, J., Kwaba, D. & Mohammed, A. S. (2015). 'Distribution and risk factors for *Plasmodium* and helminth co-infections: a cross-sectional survey among children in Bagamoyo district, coastal region of Tanzania', *PLoS neglected tropical diseases*, 9(4), p. e0003660.
- Salimi, N., Fleri, W., Peters, B. & Sette, A. (2010). 'Design and utilization of epitope-based databases and predictive tools', *Immunogenetics*, 62(4), pp. 185-196.
- Salman, A. M., Montoya-Díaz, E., West, H., Lall, A., Atcheson, E., Lopez-Camacho, C., Ramesar, J., Bauza, K., Collins, K. A. & Brod, F. (2017). 'Rational development of a protective *P. vivax* vaccine evaluated with transgenic rodent parasite challenge models', *Scientific reports*, 7, p. 46482.
- Sanchez-Trincado, J. L., Gomez-Perosanz, M. & Reche, P. A. (2017). 'Fundamentals and Methods for T- and B-Cell Epitope Prediction', *J Immunol Res*, 2017, p. 2680160.
- Santarém, N., Silvestre, R., Tavares, J., Silva, M., Cabral, S., Maciel, J. & Cordeiro-da-Silva, A. (2007). 'Immune response regulation by *Leishmania* secreted and nonsecreted antigens', *BioMed Research International*, 2007.
- Santos, L. N., Gallo, M. B., Silva, E. S., Figueiredo, C. A. V., Cooper, P. J., Barreto, M. L., Loureiro, S., Pontes-de-Carvalho, L. C. & Alcantara-Neves, N. M. (2013). 'A proteomic approach to identify proteins from *Trichuris trichiura* extract with immunomodulatory effects', *Parasite immunology*, 35(5-6), pp. 188-193.
- Santos, L. N., Silva, E. S., Santos, A. S., De Sá, P. H., Ramos, R. T., Silva, A., Cooper, P. J., Barreto, M. L., Loureiro, S. & Pinheiro, C. S. (2016). 'De novo assembly and characterization of the *Trichuris trichiura* adult worm transcriptome using Ion Torrent sequencing', *Acta tropica*, 159, pp. 132-141.
- Schneider, B., Jariwala, A. R., Periago, M. V., Gazzinelli, M. F., Bose, S. N., Hotez, P. J., Diemert, D. J. & Bethony, J. M. (2011). 'A history of hookworm vaccine development', *Hum Vaccin*, 7(11), pp. 1234-44.
- Schneidman-Duhovny, D., Khuri, N., Dong, G. Q., Winter, M. B., Shifrut, E., Friedman, N., Craik, C. S., Pratt, K. P., Paz, P., Aswad, F. & Sali, A. (2018). 'Predicting CD4 T-cell epitopes based on antigen cleavage, MHCII presentation, and TCR recognition', *PLoS One*, 13(11), p. e0206654.

- Schödel, F., Milich, D. & Will, H. (1990). 'Hepatitis B virus nucleocapsid/pre-S2 fusion proteins expressed in attenuated *Salmonella* for oral vaccination', *The Journal of Immunology*, 145(12), pp. 4317-4321.
- Schödel, F., Moriarty, A., Peterson, D., Zheng, J., Hughes, J., Will, H., Leturcq, D., McGee, J. & Milich, D. (1992). 'The position of heterologous epitopes inserted in hepatitis B virus core particles determines their immunogenicity', *Journal of virology*, 66(1), pp. 106-114.
- Schödel, F., Wirtz, R., Peterson, D., Hughes, J., Warren, R., Sadoff, J. & Milich, D. (1994). 'Immunity to malaria elicited by hybrid hepatitis B virus core particles carrying circumsporozoite protein epitopes', *Journal of Experimental Medicine*, 180(3), pp. 1037-1046.
- Schopf, L. R., Hoffmann, K. F., Cheever, A. W., Urban, J. F. & Wynn, T. A. (2002). 'IL-10 is critical for host resistance and survival during gastrointestinal helminth infection', *The Journal of Immunology*, 168(5), pp. 2383-2392.
- Schröder, R., Maassen, A., Lippoldt, A., Börner, T., von Baehr, R. & Dobrowolski, P. (1991). 'Expression of the core antigen gene of hepatitis B virus (HBV) in *Acetobacter methanolicus* using broad-host-range vectors', *Applied microbiology and biotechnology*, 35(5), pp. 631-637.
- Schumacher, F. R., Delamarre, L., Jhunjhunwala, S., Modrusan, Z., Phung, Q. T., Elias, J. E. & Lill, J. R. (2017). 'Building proteomic tool boxes to monitor MHC class I and class II peptides', *Proteomics*, 17(1-2).
- Schumacher, J., Bacic, T., Staritzbichler, R., Daneschdar, M., Klamp, T., Arnold, P., Jägle, S., Türeci, Ö., Markl, J. & Sahin, U. (2018). 'Enhanced stability of a chimeric hepatitis B core antigen virus-like-particle (HBcAg-VLP) by a C-terminal linker-hexahistidine-peptide', *Journal of nanobiotechnology*, 16(1), p. 39.
- Schwarz, B., Uchida, M. & Douglas, T. (2017). 'Biomedical and catalytic opportunities of virus-like particles in nanotechnology', *Advances in virus research*: Elsevierpp. 1-60.
- Scott, P. & Kaufmann, S. H. (1991). 'The role of T-cell subsets and cytokines in the regulation of infection', *Immunology today*, 12(10), pp. 346-348.
- Seeger, C. & Mason, W. S. (2000). 'Hepatitis B virus biology', *Microbiology and molecular biology reviews*, 64(1), pp. 51-68.
- Selby, G. R. & Wakelin, D. (1973). 'Transfer of immunity against *Trichuris muris* in the mouse by serum and cells', *International journal for parasitology*, 3(6), pp. 717-721.
- Serradell, M. C., Rupil, L. L., Martino, R. A., Prucca, C. G., Carranza, P. G., Saura, A., Fernández, E. A., Gargantini, P. R., Tenaglia, A. H. & Petiti, J. P. (2019). 'Efficient oral vaccination by bioengineering virus-like particles with protozoan surface proteins', *Nature Communications*, 10(1), p. 361.
- Shears, R., Bancroft, A., Hughes, G., Grencis, R. & Thornton, D. (2018a). 'Extracellular vesicles induce protective immunity against *Trichuris muris*', *Parasite immunology*, p. e12536.
- Shears, R. K., Bancroft, A. J., Sharpe, C., Grencis, R. K. & Thornton, D. J. (2018b). 'Vaccination Against Whipworm: Identification of Potential Immunogenic Proteins in *Trichuris muris* Excretory/Secretory Material', *Scientific reports*, 8(1), p. 4508.
- Shen, Z. & Jacobs-Lorena, M. (1998). 'A Type I Peritrophic Matrix Protein from the Malaria Vector *Anopheles gambiae* Binds to Chitin Cloning, Expression, and Characterization ', *Journal of biological chemistry*, 273(28), pp. 17665-17670.
- Shey, R. A., Ghogomu, S. M., Esoh, K. K., Nebangwa, N. D., Shintouo, C. M., Nongley, N. F., Asa, B. F., Ngale, F. N., Vanhamme, L. & Souogui, J. (2019). '*In-silico* design of a multi-epitope vaccine candidate against onchocerciasis and related filarial diseases', *Sci Rep*, 9(1), p. 4409.
- Shimazu, R., Akashi, S., Ogata, H., Nagai, Y., Fukudome, K., Miyake, K. & Kimoto, M. (1999). 'MD-2, a molecule that confers lipopolysaccharide responsiveness on Toll-like receptor 4', *Journal of Experimental Medicine*, 189(11), pp. 1777-1782.
- Shirbaghaee, Z. & Bolhassani, A. (2016). 'Different applications of virus-like particles in biology and medicine: Vaccination and delivery systems', *Biopolymers*, 105(3), pp. 113-132.
- Shouval, D. S., Biswas, A., Goettel, J. A., McCann, K., Conaway, E., Redhu, N. S., Mascanfroni, I. D., Al Adham, Z., Lavoie, S. & Ibourk, M. (2014). 'Interleukin-10 receptor signaling in innate

- immune cells regulates mucosal immune tolerance and anti-inflammatory macrophage function', *Immunity*, 40(5), pp. 706-719.
- Sidhom, J.-W., Pardoll, D. & Baras, A. J. b. (2018). 'AI-MHC: an allele-integrated deep learning framework for improving Class I & Class II HLA-binding predictions', p. 318881.
- Sidney, J., Southwood, S., Moore, C., Oseroff, C., Pinilla, C., Grey, H. M. & Sette, A. (2013). 'Measurement of MHC/peptide interactions by gel filtration or monoclonal antibody capture', *Current protocols in immunology*, pp. 18.3. 1-18.3. 36.
- Siegrist, C.-A. & Aspinall, R. (2009). 'B-cell responses to vaccination at the extremes of age', *Nature Reviews Immunology*, 9(3), p. 185.
- Singh, S. P., Khan, F. & Mishra, B. N. (2010). 'Computational characterization of *Plasmodium falciparum* proteomic data for screening of potential vaccine candidates', *Human immunology*, 71(2), pp. 136-143.
- Singh, S. P. & Mishra, B. N. J. B. (2008). 'Prediction of MHC binding peptide using Gibbs motif sampler, weight matrix and artificial neural network', 3(4), p. 150.
- Singha, S., Shao, K., Ellestad, K. K., Yang, Y. & Santamaria, P. (2018). 'Nanoparticles for Immune Stimulation Against Infection, Cancer and Autoimmunity', *ACS Nano*.
- Sinha, J. & Bhattacharya, S. (2006). *A Text book of Immunology*: Academic Publishers.
- Sinigaglia, F. (1992). *P. falciparum* cs-peptides as universal t-cell epitope. Google Patents.
- Siracusa, M. C., Saenz, S. A., Hill, D. A., Kim, B. S., Headley, M. B., Doering, T. A., Wherry, E. J., Jessup, H. K., Siegel, L. A., Kambayashi, T., Dudek, E. C., Kubo, M., Cianferoni, A., Spergel, J. M., Ziegler, S. F., Comeau, M. R. & Artis, D. (2011). 'TSLP promotes interleukin-3-independent basophil haematopoiesis and type 2 inflammation', *Nature*, 477(7363), pp. 229-33.
- Skountzou, I., Quan, F.-S., Gangadhara, S., Ye, L., Vzorov, A., Selvaraj, P., Jacob, J., Compans, R. W. & Kang, S.-M. (2007). 'Incorporation of glycosylphosphatidylinositol-anchored granulocyte-macrophage colony-stimulating factor or CD40 ligand enhances immunogenicity of chimeric simian immunodeficiency virus-like particles', *Journal of virology*, 81(3), pp. 1083-1094.
- Smet, D. (1998). 'Human T-and B-Cell Reactivity to the 16 kDa α -Crystallin Protein of *Mycobacterium tuberculosis*', *Scandinavian journal of immunology*, 48(4), pp. 403-409.
- Smith, W. & Zarlenga, D. (2006). 'Developments and hurdles in generating vaccines for controlling helminth parasites of grazing ruminants', *Veterinary parasitology*, 139(4), pp. 347-359.
- Sokol, C. L., Chu, N.-Q., Yu, S., Nish, S. A., Laufer, T. M. & Medzhitov, R. (2009). 'Basophils function as antigen-presenting cells for an allergen-induced T helper type 2 response', *Nature immunology*, 10(7), pp. 713-720.
- Sollner, J., Grohmann, R., Rapberger, R., Perco, P., Lukas, A. & Mayer, B. (2008). 'Analysis and prediction of protective continuous B-cell epitopes on pathogen proteins', *Immunome Res*, 4(1).
- Sominskaya, I., Skrastina, D., Dislers, A., Vasiljev, D., Mihailova, M., Ose, V., Dreilina, D. & Pumpens, P. (2010). 'Construction and immunological evaluation of multivalent hepatitis B virus (HBV) core virus-like particles carrying HBV and HCV epitopes', *Clinical and Vaccine Immunology*, 17(6), pp. 1027-1033.
- Sominskaya, I., Skrastina, D., Petrovskis, I., Dishlers, A., Berza, I., Mihailova, M., Jansons, J., Akopjana, I., Stahovska, I. & Dreilina, D. (2013). 'A VLP library of C-terminally truncated Hepatitis B core proteins: correlation of RNA encapsidation with a Th1/Th2 switch in the immune responses of mice', *PloS one*, 8(9), p. e75938.
- Song, J.-M., Wang, B.-Z., Park, K.-M., Van Rooijen, N., Quan, F.-S., Kim, M.-C., Jin, H.-T., Pekosz, A., Compans, R. W. & Kang, S.-M. (2011). 'Influenza virus-like particles containing M2 induce broadly cross protective immunity', *PloS one*, 6(1), p. e14538.
- Sørensen, A. L., Nagai, S., Houen, G., Andersen, P. & Andersen, A. B. (1995). 'Purification and characterization of a low-molecular-mass T-cell antigen secreted by *Mycobacterium tuberculosis*', *Infect Immun*, 63(5), pp. 1710-1717.

- Soria-Guerra, R. E., Nieto-Gomez, R., Govea-Alonso, D. O. & Rosales-Mendoza, S. (2015). 'An overview of bioinformatics tools for epitope prediction: implications on vaccine development', *Journal of biomedical informatics*, 53, pp. 405-414.
- Sormanni, P., Amery, L., Ekizoglou, S., Vendruscolo, M. & Popovic, B. (2017). 'Rapid and accurate *in silico* solubility screening of a monoclonal antibody library', *Scientific Reports*, 7, p. 8200.
- Sormanni, P., Aprile, F. A. & Vendruscolo, M. (2015). 'The CamSol Method of Rational Design of Protein Mutants with Enhanced Solubility', *Journal of Molecular Biology*, 427(2), pp. 478-490.
- Sorobetea, D., Svensson-Frej, M. & Grencis, R. (2018). 'Immunity to gastrointestinal nematode infections', *Mucosal immunology*.
- Speich, B., Ali, S. M., Ame, S. M., Bogoch, I. I., Alles, R., Huwyler, J., Albonico, M., Hattendorf, J., Utzinger, J. & Keiser, J. (2015). 'Efficacy and safety of albendazole plus ivermectin, albendazole plus mebendazole, albendazole plus oxantel pamoate, and mebendazole alone against *Trichuris trichiura* and concomitant soil-transmitted helminth infections: a four-arm, randomised controlled trial', *The Lancet infectious diseases*, 15(3), pp. 277-284.
- Spencer, S., Wilhelm, C., Yang, Q., Hall, J., Bouladoux, N., Boyd, A., Nutman, T., Urban, J., Wang, J. & Ramalingam, T. (2014). 'Adaptation of innate lymphoid cells to a micronutrient deficiency promotes type 2 barrier immunity', *Science*, 343(6169), pp. 432-437.
- Speth, C., Bredl, S., Hagleitner, M., Wild, J., Dierich, M., Wolf, H., Schroeder, J., Wagner, R. & Deml, L. (2008). 'Human immunodeficiency virus type-1 (HIV-1) Pr55gag virus-like particles are potent activators of human monocytes', *Virology*, 382(1), pp. 46-58.
- Steinman, R. M. (2001). 'Dendritic cells and the control of immunity: enhancing the efficiency of antigen presentation', *The Mount Sinai journal of medicine, New York*, 68(3), pp. 160-166.
- Stephenson, L., Holland, C. & Cooper, E. (2000). 'The public health significance of *Trichuris trichiura*', *Parasitology*, 121(S1), pp. S73-S95.
- Storni, T. & Bachmann, M. F. (2004). 'Loading of MHC class I and II presentation pathways by exogenous antigens: a quantitative *in vivo* comparison', *The Journal of Immunology*, 172(10), pp. 6129-6135.
- Street, N. E. & Mosmann, T. R. (1991). 'Functional diversity of T lymphocytes due to secretion of different cytokine patterns', *The FASEB Journal*, 5(2), pp. 171-177.
- Suffian, I. F. B. M., Garcia-Maya, M., Brown, P., Bui, T., Nishimura, Y., Palermo, A. R. B. M. J., Ogino, C., Kondo, A. & Al-Jamal, K. T. (2017). 'Yield Optimisation of Hepatitis B Virus Core Particles in *E. coli* Expression System for Drug Delivery Applications', *Scientific reports*, 7, p. 43160.
- Sun, G. G., Lei, J. J., Ren, H. N., Zhang, Y., Guo, K. X., Long, S. R., Liu, R. D., Jiang, P., Wang, Z. Q. & Cui, J. (2019). 'Intranasal immunization with recombinant *Trichinella spiralis* serine protease elicits protective immunity in BALB/c mice', *Exp Parasitol*, 201, pp. 1-10.
- Sun, X., Wang, Y., Dong, C., Hu, J. & Yang, L. (2015). 'High copy numbers and N terminal insertion position of influenza A M2E fused with hepatitis B core antigen enhanced immunogenicity', *Bioscience trends*, 9(4), pp. 221-227.
- Svensson, M., Bell, L., Little, M. C., DeSchoolmeester, M., Locksley, R. & Else, K. (2011). 'Accumulation of eosinophils in intestine-draining mesenteric lymph nodes occurs after *Trichuris muris* infection', *Parasite immunology*, 33(1), pp. 1-11.
- Svensson, M., Russell, K., Mack, M. & Else, K. J. (2010). 'CD4+ T-cell localization to the large intestinal mucosa during *Trichuris muris* infection is mediated by Gαi-coupled receptors but is CCR6-and CXCR3-independent', *Immunology*, 129(2), pp. 257-267.
- Tao, P., Mahalingam, M., Kirtley, M. L., van Lier, C. J., Sha, J., Yeager, L. A., Chopra, A. K. & Rao, V. B. (2013). 'Mutated and Bacteriophage T4 Nanoparticle Arrayed F1-V Immunogens from *Yersinia pestis* as Next Generation Plague Vaccines', *Plos Pathogens*, 9(7).
- Tao, P., Zhu, J., Mahalingam, M., Batra, H. & Rao, V. B. (2018). 'Bacteriophage T4 nanoparticles for vaccine delivery against infectious diseases', *Adv Drug Deliv Rev*.
- Tarr, D. E. & Scott, A. L. (2005). 'MSP domain proteins', *TRENDS in Parasitology*, 21(5), pp. 224-231.

- Taylor, B. C., Zaph, C., Troy, A. E., Du, Y., Guild, K. J., Comeau, M. R. & Artis, D. (2009). 'TSLP regulates intestinal immunity and inflammation in mouse models of helminth infection and colitis', *J Exp Med*, 206(3), pp. 655-67.
- Taylor, M. D., Betts, C. J. & Else, K. J. (2000). 'Peripheral cytokine responses to *Trichuris muris* reflect those occurring locally at the site of infection', *Infection and immunity*, 68(4), pp. 1815-1819.
- Teh-Poot, C., Tzec-Arjona, E., Martínez-Vega, P., Ramirez-Sierra, M. J., Rosado-Vallado, M. & Dumonteil, E. J. T. J. o. i. d. (2014). 'From genome screening to creation of vaccine against *Trypanosoma cruzi* by use of immunoinformatics', *The Journal of Infectious Diseases*, 211(2), pp. 258-266.
- Terry, F. E., Moise, L., Martin, R. F., Torres, M., Pilotte, N., Williams, S. A. & De Groot, A. S. (2014). 'Time for T? Immunoinformatics addresses vaccine design for neglected tropical and emerging infectious diseases', *Expert review of vaccines*, 14(1), pp. 21-35.
- Thomas, S. & Luxon, B. A. (2013). 'Vaccines based on structure-based design provide protection against infectious diseases', *Expert review of vaccines*, 12(11), pp. 1301-1311.
- Tilney, L. G., Connelly, P. S., Guild, G. M., Vranich, K. A. & Artis, D. (2005). 'Adaptation of a nematode parasite to living within the mammalian epithelium', *Journal of Experimental Zoology Part a-Ecological and Integrative Physiology*, 303a(11), pp. 927-945.
- Tjoelker, L. W., Gosting, L., Frey, S., Hunter, C. L., Le Trong, H., Steiner, B., Brammer, H. & Gray, P. W. (2000). 'Structural and functional definition of the human chitinase chitin-binding domain', *Journal of biological chemistry*, 275(1), pp. 514-520.
- Toubarro, D., Lucena-Robles, M., Nascimento, G., Santos, R., Montiel, R., Veríssimo, P., Pires, E., Faro, C., Coelho, A. V. & Simões, N. (2010). 'Serine protease-mediated host invasion by the parasitic nematode *Steinernema carpocapsae*', *Journal of biological chemistry*, p. jbc. M110. 129346.
- Trinchieri, G. (1993). 'Interleukin-12 and its role in the generation of TH1 cells', *Immunology today*, 14(7), pp. 335-338.
- Tritten, L. & Geary, T. G. (2018). 'Helminth extracellular vesicles in host-parasite interactions', *Current opinion in microbiology*, 46, pp. 73-79.
- Tritten, L., Tam, M., Vargas, M., Jardim, A., Stevenson, M. M., Keiser, J. & Geary, T. G. (2017). 'Excretory/secretory products from the gastrointestinal nematode *Trichuris muris*', *Exp Parasitol*, 178, pp. 30-36.
- Tsuji, N., Miyoshi, T., Islam, M. K., Isobe, T., Yoshihara, S., Arakawa, T., Matsumoto, Y. & Yokomizo, Y. (2004). 'Recombinant Ascaris 16-Kilodalton protein-induced protection against *Ascaris suum* larval migration after intranasal vaccination in pigs', *The Journal of infectious diseases*, 190(10), pp. 1812-1820.
- Turner, H. C., Truscott, J. E., Bettis, A. A., Hollingsworth, T. D., Brooker, S. J. & Anderson, R. M. (2016). 'Analysis of the population-level impact of co-administering ivermectin with albendazole or mebendazole for the control and elimination of *Trichuris trichiura*', *Parasite epidemiology and control*, 1(2), pp. 177-187.
- Turner, J., Faulkner, H., Kamgno, J., Else, K., Boussinesq, M. & Bradley, J. E. (2002). 'A comparison of cellular and humoral immune responses to trichuroid derived antigens in human trichuriasis', *Parasite Immunol*, 24(2), pp. 83-93.
- Turner, J. E., Stockinger, B. & Helmy, H. (2013). 'IL-22 mediates goblet cell hyperplasia and worm expulsion in intestinal helminth infection', *PLoS Pathog*, 9(10), p. e1003698.
- Ulmer, J. B., Valley, U. & Rappuoli, R. (2006). 'Vaccine manufacturing: challenges and solutions', *Nature biotechnology*, 24(11), p. 1377.
- Urban, J. F., Steenhard, N. R., Solano-Aguilar, G. I., Dawson, H. D., Iweala, O. I., Nagler, C. R., Noland, G. S., Kumar, N., Anthony, R. M. & Shea-Donohue, T. (2007). 'Infection with parasitic nematodes confounds vaccination efficacy', *Veterinary parasitology*, 148(1), pp. 14-20.
- Usmani, S. S., Kumar, R., Bhalla, S., Kumar, V. & Raghava, G. P. S. (2018). 'In Silico Tools and Databases for Designing Peptide-Based Vaccine and Drugs', *Adv Protein Chem Struct Biol*, 112, pp. 221-263.

- Vaishnav, N., Gupta, A., Paul, S. & John, G. J. (2015). 'Overview of computational vaccinology: vaccine development through information technology', *Journal of applied genetics*, 56(3), pp. 381-391.
- Valmori, D., Pessi, A., Bianchi, E. & Corradin, G. (1992). 'Use of human universally antigenic tetanus toxin T cell epitopes as carriers for human vaccination', *The Journal of Immunology*, 149(2), pp. 717-721.
- Valmori, D., Sabbatini, A., Lanzavecchia, A., Corradin, G. & Matricardi, P. M. (1994). 'Functional analysis of two tetanus toxin universal T cell epitopes in their interaction with DR1101 and DR1104 alleles', *The Journal of Immunology*, 152(6), pp. 2921-2929.
- Vannella, K. M., Ramalingam, T. R., Hart, K. M., de Queiroz Prado, R., Sciurba, J., Barron, L., Borthwick, L. A., Smith, A. D., Mentink-Kane, M., White, S., Thompson, R. W., Cheever, A. A., Bock, K., Moore, I., Fitz, L. J., Urban, J. F., Jr. & Wynn, T. A. (2016). 'Acidic chitinase primes the protective immune response to gastrointestinal nematodes', *Nat Immunol*, 17(5), pp. 538-44.
- Varshavsky, A. (1997). 'The N-end rule pathway of protein degradation', *Genes to cells*, 2(1), pp. 13-28.
- Vasconcelos, N.-M., Siddique, A. B., Ahlborg, N. & Berzins, K. (2004). 'Differential antibody responses to *Plasmodium falciparum*-derived B-cell epitopes induced by diepitope multiple antigen peptides (MAP) containing different T-cell epitopes', *Vaccine*, 23(3), pp. 343-352.
- Veldhoen, M., Uyttenhove, C., Van Snick, J., Helmby, H., Westendorf, A., Buer, J., Martin, B., Wilhelm, C. & Stockinger, B. (2008). 'Transforming growth factor- β 'reprograms' the differentiation of T helper 2 cells and promotes an interleukin 9-producing subset', *Nature immunology*, 9(12), p. 1341.
- Veronica, P., Gray, L., Jones, J., Bazzicalupo, P., Arbucci, S., Cortese, M., Di Vito, M. & De Giorgi, C. (2001). 'Nematode chitin synthases: gene structure, expression and function in *Caenorhabditis elegans* and the plant parasitic nematode *Meloidogyne artiellia*', *Molecular Genetics and Genomics*, 266(1), pp. 28-34.
- Villegas-Mendez, A., Garin, M. I., Pineda-Molina, E., Veratti, E., Bueren, J. A., Fender, P. & Lenormand, J.-L. (2010). 'In vivo delivery of antigens by adenovirus dodecahedron induces cellular and humoral immune responses to elicit antitumor immunity', *Molecular Therapy*, 18(5), pp. 1046-1053.
- Viney, M. (2017). 'The genomic basis of nematode parasitism', *Briefings in functional genomics*, 17(1), pp. 8-14.
- Vivona, S., Gardy, J. L., Ramachandran, S., Brinkman, F. S., Raghava, G. P., Flower, D. R. & Filippini, F. (2008). 'Computer-aided biotechnology: from immuno-informatics to reverse vaccinology', *Trends Biotechnol*, 26(4), pp. 190-200.
- Vogel, M. & Bachmann, M. F. (2019). 'Immunogenicity and Immunodominance in Antibody Responses', *Curr Top Microbiol Immunol*.
- Vogelzang, A., Perdomo, C., Zedler, U., Kuhlmann, S., Hurwitz, R., Gengenbacher, M. & Kaufmann, S. H. (2014). 'Central memory CD4+ T cells are responsible for the recombinant Bacillus Calmette-Guérin ΔureC:: hly vaccine's superior protection against tuberculosis', *Journal of Infectious Diseases*, 210(12), pp. 1928-1937.
- Volkin, D. B. & Middaugh, C. R. (2010). 'Vaccines as physically and chemically well-defined pharmaceutical dosage forms', *Expert review of vaccines*, 9(7), pp. 689-691.
- Vordemeier, H., Harris, D., Roman, E., Lathigra, R., Moreno, C. & Ivanyi, J. (1991). 'Identification of T cell stimulatory peptides from the 38-kDa protein of *Mycobacterium tuberculosis*', *The Journal of Immunology*, 147(3), pp. 1023-1029.
- Vordermeier, H., Coombes, A., Jenkins, P., McGee, J., O'Hagan, D., Davis, S. & Singh, M. (1995). 'Synthetic delivery system for tuberculosis vaccines: immunological evaluation of the *M. tuberculosis* 38 kDa protein entrapped in biodegradable PLG microparticles', *Vaccine*, 13(16), pp. 1576-1582.

- Vordermeier, H., Harris, D., Lathigra, R., Roman, E., Moreno, C. & Ivanyi, J. (1993). 'Recognition of peptide epitopes of the 16,000 MW antigen of *Mycobacterium tuberculosis* by murine T cells', *Immunology*, 80(1), p. 6.
- Wahl-Jensen, V., Kurz, S. K., Hazelton, P. R., Schnittler, H.-J., Ströher, U., Burton, D. R. & Feldmann, H. (2005). 'Role of Ebola virus secreted glycoproteins and virus-like particles in activation of human macrophages', *Journal of virology*, 79(4), pp. 2413-2419.
- Wakelin, D. (1967). 'Acquired immunity to *Trichuris muris* in the albino laboratory mouse', *Parasitology*, 57(3), pp. 515-24.
- Wakelin, D. (1973). 'The stimulation of immunity to *Trichuris muris* in mice exposed to low-level infections', *Parasitology*, 66(1), pp. 181-189.
- Wakelin, D. & Selby, G. R. (1973). 'Functional antigens of *Trichuris muris*. The stimulation of immunity by vaccination of mice with somatic antigen preparations', *International journal for parasitology*, 3(6), pp. 711-715.
- Wang, B., Wang, Z. Q., Jin, J., Ren, H. J., Liu, L. N. & Cui, J. (2013). 'Cloning, expression and characterization of a *Trichinella spiralis* serine protease gene encoding a 35.5 kDa protein', *Experimental parasitology*, 134(2), pp. 148-154.
- Wang, P., Sidney, J., Dow, C., Mothe, B., Sette, A. & Peters, B. (2008). 'A systematic assessment of MHC class II peptide binding predictions and evaluation of a consensus approach', *PLoS Comput Biol*, 4(4), p. e1000048.
- Wang, P., Sidney, J., Kim, Y., Sette, A., Lund, O., Nielsen, M. & Peters, B. (2010). 'Peptide binding predictions for HLA DR, DP and DQ molecules', *BMC bioinformatics*, 11, p. 568.
- Wang, T. T. (2018). 'Immunity by Design', *Cell host & microbe*, 23(4), pp. 430-431.
- Wang, Y., Bai, X., Zhu, H., Wang, X., Shi, H., Tang, B., Boireau, P., Cai, X., Luo, X. & Liu, M. (2017). 'Immunoproteomic analysis of the excretory-secretory products of *Trichinella pseudospiralis* adult worms and newborn larvae', *Parasites & vectors*, 10(1), p. 579.
- Wang, Y., Wang, Y., Kang, N., Liu, Y., Shan, W., Bi, S., Ren, L. & Zhuang, G. (2016). 'Construction and immunological evaluation of CpG-Au@ HBc virus-like nanoparticles as a potential vaccine', *Nanoscale research letters*, 11(1), p. 338.
- Warfield, K. L., Bosio, C. M., Welcher, B. C., Deal, E. M., Mohamadzadeh, M., Schmaljohn, A., Aman, M. J. & Bavari, S. (2003). 'Ebola virus-like particles protect from lethal Ebola virus infection', *Proceedings of the National Academy of Sciences*, 100(26), pp. 15889-15894.
- Webb, L. M., Oyesola, O. O., Fruh, S. P., Kamynina, E., Still, K. M., Patel, R. K., Peng, S. A., Cubitt, R. L., Grimson, A., Grenier, J. K., Harris, T. H., Danko, C. G. & Tait Wojno, E. D. (2019). 'The Notch signaling pathway promotes basophil responses during helminth-induced type 2 inflammation', *J Exp Med*.
- Wedemeyer, H. & Pischke, S. (2011). 'Hepatitis: Hepatitis E vaccination—is HEV 239 the breakthrough?', *Nature Reviews Gastroenterology & Hepatology*, 8(1), p. 8.
- Wei, J., Damania, A., Gao, X., Liu, Z., Mejia, R., Mitreva, M., Strych, U., Bottazzi, M. E., Hotez, P. J. & Zhan, B. (2016). 'The hookworm *Ancylostoma ceylanicum* intestinal transcriptome provides a platform for selecting drug and vaccine candidates', *Parasites & vectors*, 9(1), p. 518.
- Wei, J., Gu, Y., Yang, J., Yang, Y., Wang, S., Cui, S. & Zhu, X. (2011). 'Identification and characterization of protective epitope of *Trichinella spiralis* paramyosin', *Vaccine*, 29(17), pp. 3162-3168.
- West, N. P., Thomson, S. A., Triccas, J. A., Medveczky, C. J., Ramshaw, I. A. & Britton, W. J. (2011). 'Delivery of a multivalent scrambled antigen vaccine induces broad spectrum immunity and protection against tuberculosis', *Vaccine*, 29(44), pp. 7759-7765.
- Whitacre, D. C., Lee, B. O. & Milich, D. R. (2009). 'Use of hepadnavirus core proteins as vaccine platforms', *Expert review of vaccines*, 8(11), pp. 1565-1573.
- Whitmore, L. & Wallace, B. (2009). 'Methods of analysis for circular dichroism spectroscopy of proteins and the DichroWeb server', *Modern Techniques for Circular Dichroism and Synchrotron Radiation Circular Dichroism Spectroscopy*, pp. 165-182.
- WHO, W. H. O. (2005). 'Deworming for health and development: report of the Third Global Meeting of the Partners for Parasite Control'.

- WHO, W. H. O. (2013). 'Weekly Epidemiological Record; 2006', *Schistosomiasis and soil-transmitted helminth infections-preliminary estimates of the number of children treated with albendazole or mebendazole*, pp. 145-164.
- WHO, W. h. O. (2015). 'Soil-transmitted helminthiasis: Deworming campaign improves child health, school attendance in Rwanda ', *Geneva: WHO Library*.
- Wieczorek, M., Abualrous, E. T., Sticht, J., Alvaro-Benito, M., Stolzenberg, S., Noe, F. & Freund, C. (2017). 'Major Histocompatibility Complex (MHC) Class I and MHC Class II Proteins: Conformational Plasticity in Antigen Presentation', *Frontiers in Immunology*, 8.
- Williams-Blangero, S., McGarvey, S. T., Subedi, J., Wiest, P. M., Upadhayay, R. P., Rai, D. R., Jha, B., Olds, G. R., Guanling, W. & Blangero, J. (2002). 'Genetic component to susceptibility to *Trichuris trichiura*: evidence from two Asian populations', *Genet Epidemiol*, 22(3), pp. 254-64.
- Williams, S. E., Brown, T. I., Roghanian, A. & Sallenave, J. M. (2006). 'SLPI and elafin: one glove, many fingers', *Clin Sci (Lond)*, 110(1), pp. 21-35.
- Winslow, G. M., Roberts, A. D., Blackman, M. A. & Woodland, D. L. (2003). 'Persistence and turnover of antigen-specific CD4 T cells during chronic tuberculosis infection in the mouse', *The Journal of Immunology*, 170(4), pp. 2046-2052.
- Woodworth, J. S., Aagaard, C. S., Hansen, P. R., Cassidy, J. P., Agger, E. M. & Andersen, P. (2014). 'Protective CD4 T cells targeting cryptic epitopes of *Mycobacterium tuberculosis* resist infection-driven terminal differentiation', *The Journal of Immunology*, 192(7), pp. 3247-3258.
- Worley, D. E., Meisenhelder, J. E., Sheffield, H. G. & Thompson, P. E. (1962). 'Experimental Studies on *Trichuris muris* in Mice with an Appraisal of Its Use for Evaluating Anthelmintics', *The Journal of Parasitology*, 48(3), pp. 433-437.
- Worthington, J. J., Klementowicz, J. E., Rahman, S., Czajkowska, B. I., Smedley, C., Waldmann, H., Sparwasser, T., Grencis, R. K. & Travis, M. A. (2013). 'Loss of the TGF β -activating integrin $\alpha v\beta 8$ on dendritic cells protects mice from chronic intestinal parasitic infection via control of type 2 immunity', *PLoS Pathog*, 9(10), p. e1003675.
- Wu, T., Hu, Y.-M., Li, J., Chu, K., Huang, S.-J., Zhao, H., Wang, Z.-Z., Yang, C.-L., Jiang, H.-M. & Wang, Y.-J. (2015). 'Immunogenicity and safety of an *E. coli*-produced bivalent human papillomavirus (type 16 and 18) vaccine: A randomized controlled phase 2 clinical trial', *Vaccine*, 33(32), pp. 3940-3946.
- Wykes, M., Pombo, A., Jenkins, C. & MacPherson, G. G. (1998). 'Dendritic cells interact directly with naive B lymphocytes to transfer antigen and initiate class switching in a primary T-dependent response', *The Journal of Immunology*, 161(3), pp. 1313-1319.
- Wynn, T. A. (2009). 'Basophils trump dendritic cells as APCs for TH2 responses', *Nature immunology*, 10(7), pp. 679-681.
- Xu, J., Bai, X., Wang, L. B., Shi, H. N., Van Der Giessen, J. W., Boireau, P., Liu, M. Y. & Liu, X. L. (2017). 'Immune responses in mice vaccinated with a DNA vaccine expressing serine protease-like protein from the new-born larval stage of *Trichinella spiralis*', *Parasitology*, 144(6), pp. 712-719.
- Xu, X., Ding, Z., Li, J., Liang, J., Bu, Z., Ding, J., Yang, Y., Lang, X., Wang, X. & Yin, R. (2019). 'Newcastle disease virus-like particles containing the Brucella BCSP31 protein induce dendritic cell activation and protect mice against virulent Brucella challenge', *Veterinary Microbiology*, 229, pp. 39-47.
- Yan, Q. (2010). 'Immunoinformatics and systems biology methods for personalized medicine', *Systems Biology in Drug Discovery and Development*: Springerpp. 203-220.
- Yang, B.-f., Zhao, H.-l., Xue, C., Xiong, X.-h., Zhang, W., Yao, X.-q. & Liu, Z.-m. (2007). 'Recombinant heat shock protein 65 carrying hepatitis B core antigen induces HBcAg-specific CTL response', *Vaccine*, 25(22), pp. 4478-4486.
- Yang, D., Rogers, M. & Liew, F. (1991). 'Identification and characterization of host-protective T-cell epitopes of a major surface glycoprotein (gp63) from *Leishmania major*', *Immunology*, 72(1), p. 3.

- Yang, J., Huston, L., Berger, D., Danke, N. A., Liu, A. W., Disis, M. L. & Kwok, W. W. (2005). 'Expression of HLA-DP0401 molecules for identification of DP0401 restricted antigen specific T cells', *Journal of clinical immunology*, 25(5), pp. 428-436.
- Yang, R., Murillo, F. M., Cui, H., Blosser, R., Uematsu, S., Takeda, K., Akira, S., Viscidi, R. P. & Roden, R. B. (2004). 'Papillomavirus-like particles stimulate murine bone marrow-derived dendritic cells to produce alpha interferon and Th1 immune responses via MyD88', *Journal of virology*, 78(20), pp. 11152-11160.
- Yang, X. & Yu, X. (2009). 'An introduction to epitope prediction methods and software', *Reviews in medical virology*, 19(2), pp. 77-96.
- Yang, Y., jun Wen, Y., Cai, Y. N., Vallée, I., Boireau, P., Liu, M. Y. & Cheng, S. P. (2015). 'Serine proteases of parasitic helminths', *The Korean journal of parasitology*, 53(1), p. 1.
- Yasser, E.-M., Dobbs, D. & Honavar, V. (2008). 'On evaluating MHC-II binding peptide prediction methods', *PLoS One*, 3(9), p. e3268.
- Yin, Y., Li, H., Wu, S., Dong, D., Zhang, J., Fu, L., Xu, J. & Chen, W. (2011). 'Hepatitis B virus core particles displaying *Mycobacterium tuberculosis* antigen ESAT-6 enhance ESAT-6-specific immune responses', *Vaccine*, 29(34), pp. 5645-5651.
- Yin, Y., Zhang, J., Dong, D., Liu, S., Guo, Q., Song, X., Li, G., Fu, L., Xu, J. & Chen, W. (2008). 'Chimeric hepatitis B virus core particles carrying an epitope of anthrax protective antigen induce protective immunity against *Bacillus anthracis*', *Vaccine*, 26(46), pp. 5814-5821.
- Yoichi, I. (1991). 'The absence of resistance in congenitally athymic nude mice toward infection with the intestinal nematode, *Trichuris muris*: resistance restored by lymphoid cell transfer', *International journal for parasitology*, 21(1), pp. 65-69.
- Yoshikawa, A., Tanaka, T., Hoshi, Y., Kato, N., Tachibana, K., Iizuka, H., Machida, A., Okamoto, H., Yamasaki, M. & Miyakawa, Y. (1993). 'Chimeric hepatitis B virus core particles with parts or copies of the hepatitis C virus core protein', *Journal of virology*, 67(10), pp. 6064-6070.
- Zaph, C., Troy, A. E., Taylor, B. C., Berman-Booty, L. D., Guild, K. J., Du, Y., Yost, E. A., Gruber, A. D., May, M. J., Greten, F. R., Eckmann, L., Karin, M. & Artis, D. (2007). 'Epithelial-cell-intrinsic IKK-beta expression regulates intestinal immune homeostasis', *Nature*, 446(7135), pp. 552-6.
- Zarowiecki, M. & Berriman, M. (2015). 'What helminth genomes have taught us about parasite evolution', *Parasitology*, 142(S1), pp. S85-S97.
- Zeltins, A. (2013). 'Construction and characterization of virus-like particles: a review', *Molecular biotechnology*, 53(1), pp. 92-107.
- Zeng, M., Nourishirazi, E., Guinet, E. & Nouri-Shirazi, M. (2016). 'The genetic background influences the cellular and humoral immune responses to vaccines', *Clinical & Experimental Immunology*, 186(2), pp. 190-204.
- Zhan, B., Beaumier, C. M., Briggs, N., Jones, K. M., Keegan, B. P., Bottazzi, M. E. & Hotez, P. J. (2014). 'Advancing a multivalent 'Pan-anthelmintic' vaccine against soil-transmitted nematode infections', *Expert review of vaccines*, 13(3), pp. 321-331.
- Zhan, B., Liu, Y., Badamchian, M., Williamson, A., Feng, J., Loukas, A., Hawdon, J. M. & Hotez, P. J. (2003). 'Molecular characterisation of the *Ancylostoma*-secreted protein family from the adult stage of *Ancylostoma caninum*', *International journal for parasitology*, 33(9), pp. 897-907.
- Zhang, L., Udaka, K., Mamitsuka, H. & Zhu, S. (2012). 'Toward more accurate pan-specific MHC-peptide binding prediction: a review of current methods and tools', *Briefings in bioinformatics*, 13(3), pp. 350-364.
- Zhang, Q., Wang, P., Kim, Y., Haste-Andersen, P., Beaver, J., Bourne, P. E., Bui, H.-H., Buus, S., Frankild, S. & Greenbaum, J. (2008). 'Immune epitope database analysis resource (IEDB-AR)', *Nucleic acids research*, 36(suppl 2), pp. W513-W518.
- Zhang, R., Zhang, S., Li, M., Chen, C. & Yao, Q. (2010). 'Incorporation of CD40 ligand into SHIV virus-like particles (VLP) enhances SHIV-VLP-induced dendritic cell activation and boosts immune responses against HIV', *Vaccine*, 28(31), pp. 5114-5127.

- Zhang, Y., Foster, J. M., Nelson, L. S., Ma, D. & Carlow, C. K. (2005). 'The chitin synthase genes chs-1 and chs-2 are essential for *C. elegans* development and responsible for chitin deposition in the eggshell and pharynx, respectively', *Developmental biology*, 285(2), pp. 330-339.
- Zhang, Y., Song, S., Liu, C., Wang, Y., Xian, X., He, Y., Wang, J., Liu, F. & Sun, S. (2007). 'Generation of chimeric HBc proteins with epitopes in *E. coli*: formation of virus-like particles and a potent inducer of antigen-specific cytotoxic immune response and anti-tumor effect *in vivo*', *Cellular immunology*, 247(1), pp. 18-27.
- Zhao, A., Urban, J. F., Jr., Anthony, R. M., Sun, R., Stiltz, J., van Rooijen, N., Wynn, T. A., Gause, W. C. & Shea-Donohue, T. (2008). 'Th2 cytokine-induced alterations in intestinal smooth muscle function depend on alternatively activated macrophages', *Gastroenterology*, 135(1), pp. 217-225 e1.
- Zhao, Q., Allen, M. J., Wang, Y., Wang, B., Wang, N., Shi, L. & Sitrin, R. D. (2012a). 'Disassembly and reassembly improves morphology and thermal stability of human papillomavirus type 16 virus-like particles', *Nanomedicine: Nanotechnology, Biology and Medicine*, 8(7), pp. 1182-1189.
- Zhao, Q., Li, S., Yu, H., Xia, N. & Modis, Y. (2013). 'Virus-like particle-based human vaccines: quality assessment based on structural and functional properties', *Trends in biotechnology*, 31(11), pp. 654-663.
- Zhao, Q., Modis, Y., High, K., Towne, V., Meng, Y., Wang, Y., Alexandroff, J., Brown, M., Carragher, B. & Potter, C. S. (2012b). 'Disassembly and reassembly of human papillomavirus virus-like particles produces more virion-like antibody reactivity', *Virology journal*, 9(1), p. 52.
- Zhao, W. & Sher, X. (2018). 'Systematically benchmarking peptide-MHC binding predictors: From synthetic to naturally processed epitopes', *PLoS Comput Biol*, 14(11), p. e1006457.
- Zhu, Z., Zheng, T., Homer, R. J., Kim, Y. K., Chen, N. Y., Cohn, L., Hamid, Q. & Elias, J. A. (2004). 'Acidic mammalian chitinase in asthmatic Th2 inflammation and IL-13 pathway activation', *Science*, 304(5677), pp. 1678-82.

Appendix

Appendices Chapter 3:

Supplementary Table 3.1 List of websites and sources used to screen for MHC class I and II *in silico* prediction tools.

Website sources
www.google.com
https://scholar.google.co.uk
http://www.ncbi.nlm.nih.gov/pubmed
http://europepmc.org/
http://tools.iedb.org/main/
http://omictools.com/
https://www.proimmune.com/ecommerce/index.php
http://rsob.royalsocietypublishing.org/
http://mba.biocuckoo.org/links.php
http://biorxiv.org/
http://www.biomedcentral.com/bmcbioinformatics/
http://www.researchgate.net/
http://www.mybiosoftware.com/about
http://www.immudex.com
http://www.imtech.res.in/raghava/vacci.html
http://osddlinux.osdd.net/vacci.php
http://www.mybiosoftware.com/about
http://www.epitope-informatics.com/
http://cancerimmunity.org/resources/webtools/
http://molbiol-tools.ca/Motifs.htm
http://www.hsls.pitt.edu/obrc/index.php?page=immunology
http://www.ebi.ac.uk/ipd/

Supplementary Table 3.2 MHC-II T-cell epitopes dataset used to evaluate the MHC-II *in silico* prediction tools used in this review.

Organism	Protein	Epitope origin residues	Amino acid sequence	Reference
<i>Clostridium tetani</i>	Tetanus Toxin (TT)	830–844	QYIKANSKFIGITEL	(Astori and Kraehenbuhl, 1996; Demotz et al., 1989; Diethelm-Okita et al., 2000; Diethelm-Okita et al., 1997; Valmori et al., 1992; Valmori et al., 1994; Vasconcelos et al., 2004; Yang et al., 2005)
		947–967	SFWLRLVPKVSASHLE VSFWLRLVPKVSASHL TVSFWLRVPKVSASH	
		634–653	DVSTIVPYIGPALNI VSTIVPYIGPALNIV IVPYIGPALNIVKQG	
		950–969	NNFTVSFWLRLVPKVS TVSFWLRVPKVSASH SFWLRLVPKVSASHL SFWLRLVPKVSASHLE	
		1273–1284	GQIGNDPNRDIL	
		271–290	PVFAGANYAAWAVNV AGANYAAWAVNVVAQV GANYAAWAVNVQAQVI ANYAAWAVNVQAQVID NYAAWAVNVQAQVIDS YAAWAVNVQAQVIDSE	
<i>Corynebacterium diphtheriae</i>	Diphtheria Toxin (DTX)	331–350	QSIALSSLMVAQAIPL LSSLMVAQAIPLVG ALSSLMVAQAIPLVG IALSSLMVAQAIPLVG SSLMVAQAIPLVGEL AQSIALSSLMVAQAI SIALSSLMVAQAIPL	(Conti-Fine, 1998; Diethelm-Okita et al., 2000; Percival-Alwyn et al., 2015; Raju et al., 1995)
		321–340	VHHNTTEEIVAQSIAL VAQSIALSSLMVAQA IVAQSIALSSLMVAQ	
		351–370	VDIGFAAYNFVESII DIGFAAYNFVEIIN	

			IGFAAYNFVESIINL GFAAYNFVESIINLF FAAYNFVESIINLFQ	
		411–430	QGESGHDIKITAENT GHDIKITAENTPLPI SGHDIKITAENTAEN ESGHDIKITAENTPL	
		431–450	GVLPTIPGKLDVNK TIPGKLDVNKS KTHI PTIPGKLDVNKS KTH	
<i>P. falciparum</i>	Erythrocyte binding proteins (EBP3)	12-27	LVSEEIVTEEGSVAQE VSEEIVTEEGSVAQE	(Ahlborg et al., 2000; Ahlborg et al., 1997; Calvo-Calle et al., 1997; Kironde et al., 1991; Sinigaglia, 1992; Vasconcelos et al., 2004)
	Circumsporozoite (CS)	379-398 326-345	AKMEKCSSVFNVVNS IEKKIAKMEKCSSVF EYLNKIQNLS STEWS NKIQNLS STEWSPCS	
<i>Mycobacterium tuberculosis</i>	6 kDa Early secretory antigenic target (ESAT-6)	1-20 71-90	QQWNFAGIEAAASAI EQQWNFAGIEAAASA TEQQWNFAGIEAAAS MTEQQWNFAGIEAAA QWNFAGIEAAASAIQ WNFAGIEAAASAIQG NLARTISEAGQAMAS LARTISEAGQAMAST ARTISEAGQAMASTE RTISEAGQAMASTEG	(Brandt et al., 1996; Grover et al., 2014; Kanaujia et al., 2004; Kumar et al., 2010; Kumar and Raja, 2010; Myers et al., 2013; Olsen et al., 2000; Rapeah and Norazmi, 2006; Sørensen et al., 1995; Vogelzang et al., 2014; West et al., 2011; Winslow et al., 2003; Woodworth et al., 2014)
	Antigen 85B (Ag85B)	240-254 154-173 164-183	FQDAYNAAGGHNAVF SAMILAAYHPQQFIYAGSLS AYHPQQFIYAGSLSA QQFIYAGSLSALLDP QFIYAGSLSALLDPS FIYAGSLSALLDPSQ IYAGSLSALLDPSQG	(Andersen et al., 1995; Brandt et al., 1996; Friscia et al., 1995; Geluk et al., 1998; Jurcevic et al., 1996; Smet, 1998; Vordermeier et al., 1995; Vordermeier et al., 1993)

		134-153 144-163 284-303	ANRAVKPTGSAAIGL NRAVKPTGSAAIGLS RAVKPTGSAAIGLSM AVKPTGSAAIGLSMA AAIGLSMAGSSAMILA AIGLSMAGSSAMILA IIGLSMAGSSAMILAA GLSMAGSSAMILAAY LSMAGSSAMILAAYH THSWEYWGAQLNAMK HSWEYWGAQLNAMKG	
	38 kDa	350-369	DQVFQPLPPAVVKL QVFQPLPPAVVKLS VHFQPLPPAVVKLSD HFQPLPPAVVKLSDA FQPLPPAVVKLSDAS	(Jurcevic et al., 1996; Vordemeier et al., 1991; Vordermeier et al., 1995)
<i>Leishmania major</i>	Surface proteinase of 63 kDa (GP63)	1-13 48-61 154-168 158-173 378-393 385-401 394-409 95-130 146-171	VRDVNWGALRIA LTNEKRDILVKHLIP YDQLVTRVVTHEMAH TRVVTHEMAHALGFS PFNVFSDAACR CIDGA AACR CIDGA FRPKATD RPKATDGIVKSYAGL DFVMYVASVPSEEGV PAANIASRYDQLVTR	(Curry et al., 1994; Jardim et al., 1990; Russo et al., 1993; Yang et al., 1991)
	Leishmania homologue of mammalian RACKs, the receptors for activated C kinase (LACK)	156-173 161-173	ICFSPSLEHPIVVSG SLEHPIVVSGSWD EHPIVVSGSWDNT	(Julia et al., 1996; Kelly and Locksley, 2004; Lazarski et al., 2005; Mougneau et al., 1995; Sacks and Noben-Trauth, 2002)

<i>Leishmania infantum</i>	Cysteine peptidase A (CPA)	149-163 246-260 114-128 257-271 32-46 312-326	MCGSCWAFATTGNIE PHDEEEIAAYVGKNG KDYKEHVHVDGSVR GKNGPVAVAVDATTW GVDDFIASAHYGRFK GSSWGEKGYIRLAMG	(Agallou et al., 2014; Coler and Reed, 2005)
	Histone 1 like protein (H1)	1-15 27-41 32-46 52-56 2-16 26-40 31-45 29-43 30-44 25-39 24-38 28-42 5-19 4-18 48-62 33-47 49-63 35-49	MSSDSAVAALSAAMT KTAAKKAAAKKAAAK KAAAKKAAAKKAGAK KAAAKKAAAKKAGAK SSDSAVAALSAAMTS KKTAAKKAAAKKAAA KKAAAKKAAAKKAGA AAKKAACAKKA AKKAACAKKA PKKTAACAKKA SPKKTAACAKKA TAAKKAACAKKA SAVAALSAAMTSPQK DSAVAALSAAMTSPQ AGAKKAVRKVATPKK AAAKKAACAKKAGAKK GAKKAVRKVATPKKP AKKAACAKKAGAKKAG AAKKAACAKKAGAKKA	
	Leishmania eukaryotic initiation factor (LeIF)	100-114 166-180 140-154 102-116 103-117 101-115 139-153 99-113 98-112 141-155	LSPTRELALQTAEVI ALRTESLRVLVLDEA DLRKLQAGVIVAVGT PTRELALQTAEVISR TRELALQTAEVISR SPTRELALQTAEVIS DDLRLQAGVIVAVG VLSPTRELALQTAEV LVLSPTRELALQTAE LRKLQAGVIVAVGTP PSSIQQRAIAPFTRG	

		49-63 48-62 50-64 97-111	KPSSIQQRAIAPFTR SSIQQRAIAPFTRGG GLVLSPTRELALQTA SNHTVSSMHAEMPKS	
<i>H. pylori</i>	Urease subunit beta	321-339 327-334	CHHLDKSIKEDVQFADSRI SIKEDVQFADSIRIP	(Guo et al., 2013; Hirota et al., 2001)
<i>Schistosoma mansoni</i>	Major egg antigen p40	234-246	PKSDNQIKAVPASQA	(Cheever et al., 1987; Hernandez et al., 1998; Hernandez et al., 2002; Hernandez et al., 1997)
<i>Salmonella typhimurium</i>	Flagellar filament protein (FliC)	427-441 428-442	GAVQNRFNSAITNLG AVQNRFNSAITNLGN	(Bergman et al., 2005; Mcsorley et al., 2000; Moon et al., 2007)
<i>T. muris</i>	Proteasome subunit beta	1-15 2-16 3-17 4-18 24-38 25-39 26-40 27-41	METYPVSRVNPakis ETYPVSRVNPakisQ TYPVSRVNPakisQS YPVSRVNPakisQSP SVVALMFDDGGVIIAA VVALMFDDGGVIIAAD VALMFDDGGVIIAADT ALMFDDGGVIIAADTM LMFDGGVIIAADTML	NA
Hen egg-white lysozyme	Ovalbumin	323-339	ISQAVHAAHAEINEAG SQAVHAAHAEINEAGR	(Mcfarland et al., 1999; Robertson et al., 2000)

Supplementary Table 3.3 List of MHC class I and II and HLA binders peptides *in silico* prediction tools.

Prediction tool	Website	Prediction Method	MHC Class
BIMAS	http://www-bimas.cit.nih.gov/molbio/hla_bind/	QM	I
BJTEpitope	http://www.biosun.org.cn/bjtepitope/	Naïve Bayes	I
CombiPRED	http://www.vaccinedesign.com/	A matrix-based tool that combines nHLAPred, BIMAS and SYFPEITHI	I
CTLPred	http://crdd.osdd.net/raghava/ctlpred/	QM, ANN and SVM	I
EpiJen	http://www.ddg-pharmfac.net/epijen/EpiJen/EpiJen.htm	Multistep algorithm (Proteasomal cleavage, TAP binders and MHC I binding)	I
Expitope	http://webclu.bio.wzw.tum.de/expitope/	NetChop, NetMHC and TAP affinity binding	I
HLA Binding MHC I peptide energy binding predictor	http://boson.research.microsoft.com/hlabinding/	Adaptive Double Threading. 3D structures based model (binding energy predictor).	I
HLArestrictor 1.2	http://www.cbs.dtu.dk/services/HLArestrictor/	Based on % rank score	I
IEDB Class I Immunogenicity	http://tools.iedb.org/immunogenicity/	This tool predicts the immunogenicity of MHC I (pMHC) complex using the amino acid properties and the position within the peptide.	I
IEDB MHC-I Binding Predictions	http://tools.iedb.org/mhci/	Framework including ANN, SMM, SMMPMBEC, Comblib, Consensus, NetMHCpan, NetMHCcons and PickPocket.	I
IEDB MHC-I processing predictions	http://tools.iedb.org/processing/	Framework including ANN, SMM, SMMPMBEC, Comblib, Consensus, NetMHCpan, NetMHCcons and PickPocket.	I
IEDB MHC-NP	http://tools.iedb.org/mhcnp/help/	Predict binding/nonbinding peptides for a given allele and predict naturally processed peptides.	I
KISS	http://cbio.ensmp.fr/kiss/	SVM using a multitask kernel	I
LpPep	http://zlab.bu.edu/zhiping/lppep.html	Linear programming (jack-knife procedure)	I
MAPPP	http://www.mpiib-berlin.mpg.de/MAPPP/binding.html	Based on a score calculated by BIMAS and SYFPEITHI for each subsequence. QM and Motifs	I
MMBPred	http://crdd.osdd.net/raghava/mmbpred/	QM	I

NetChop 3.1	http://www.cbs.dtu.dk/services/NetChop/	ANN	I
NetCTL 1.2	http://www.cbs.dtu.dk/services/NetCTL/	ANN	I
NetCTLpan 1.1	http://www.cbs.dtu.dk/services/NetCTLpan/	ANN	I
NetMHC 4.0	http://www.cbs.dtu.dk/services/NetMHC	ANN and weighted matrices	I
NetMHCcons 1.1	http://www.cbs.dtu.dk/services/NetMHCcons/	Integrating three methods: NetMHC (ANN), NetMHCpan (Pan specific ANN) and PickPocket (Matrix based)	I
NetMHCpan 2.8	http://www.cbs.dtu.dk/services/NetMHCpan/	Pan specific ANN	I
NetMHCstab 1.0	http://www.cbs.dtu.dk/services/NetMHCstab-1.0/	ANN	I
NetTepi 1.0	http://www.cbs.dtu.dk/services/NetTepi/	Integrates three methods: peptide-MHC binding affinity using NetMHCcons, peptide-MHC stability using the NetMHCstab and T-cell propensity.	I
Pcleavage	http://crdd.osdd.net/raghava/pcleavage/	SVM	I
PEPVAC	http://bio.dfci.harvard.edu/PEPVAC/	PSSM Profile-matrices	I
PREDEP	http://margalit.huji.ac.il/Teppred/mhc-bind/index.html	Threading and Motif.	I
PREDmafa	http://cvc.dfci.harvard.edu/mafa/	QM	I
ProPred1	http://www.imtech.res.in/raghava/propred1	Based on QM, proteasomal cleavage and promiscuous peptides.	I
SiIDER	http://modlab-cadd.ethz.ch/software/slider/	ANN and SVM	I
SMM	http://zlab.bu.edu/SMM/	linear programming (SMM)	I
SVMHC	http://www-bs.informatik.uniuebingen.de/Services/SVMHC http://svrmhc.biotead.org/	SVM	I
TAPpred	http://crdd.osdd.net/raghava/tapped/	SVM	I
T-EPIPOE Designer	http://www.bioinformation.net/ted/index.html	Structure modelling (Virtual pockets in 3D).	I
WAPP	http://abi.inf.uni-tuebingen.de/Services/WAPP/information	SVMHC	I
IFNepitope	http://crdd.osdd.net/raghava/ifnepitope/	Motif based SVM, and SVM hybrid.	IFN-gamma inducing epitope
EpiDOCK	http://epidock.ddg-pharmfac.net/	Structure molecular docking	II
EpiTOP	http://www.pharmfac.net/EpiTOP/	Proteochemometrics (QSAR) QM	II

FDR4	http://crdd.osdd.net/raghava/fdr4/	SVMOT	II
HLA-DR4Pred	http://www.imtech.res.in/raghava/hladr4pred/	SVM and ANN	II
IEDB MHC-II Binding Predictions	http://tools.iedb.org/mhcii/	Consensus, CombLib, NN-align (netMHCII-2.2), SMM-align (netMHCII-1.1), Sturniolo, and NetMHCIIpan.	II
IL4pred	http://crdd.osdd.net/raghava/il4pred/	SVM, Merci Motif based, Hybrid (SVM + Motif) based, and Swissprot based.	II
MetaMHCIIPan	http://www.biokdd.fudan.edu.cn/Service/MetaMHC.html	A pan-specific consensus	II
MHC	http://crdd.osdd.net/raghava/mhc/	Motifs Matrix Optimization Technique	II
MHC2MIL	http://datamining-iip.fudan.edu.cn/service/MHC2MIL/index.html	Pan-specific: PSSM, ANN, kernel based methods, and multiple instance learning based methods.	II
MHC2Pred	http://crdd.osdd.net/raghava/mhc2pred/	SVM	II
MHC2SKpan-1.0.	http://datamining-iip.fudan.edu.cn/service/MHC2SKpan/index.html	MHC-II String Kernel	II
MHCIIIMulti	http://etk.informatik.uni-tuebingen.de/acl_users/credentials_cookie_auth/require_login?came_from=http%3A//etk.informatik.uni-tuebingen.de/mhciiimulti/index_html/ddocument_view	Machine learning method	II
MHCMIIR 1.0	http://ailab.ist.psu.edu/mhcmir/	Multiple instance regression	II
MHC-Thread	http://www.csd.abdn.ac.uk/~qjlk/MHC-Thread/	Structure peptide threading	II
NetMHCII 2.2	http://www.cbs.dtu.dk/services/NetMHCII/	ANN	II
NetMHCIIpan 3.1	http://www.cbs.dtu.dk/services/NetMHCIIpan/	ANN	II
NNAlign	http://www.cbs.dtu.dk/services/NNAlign/	ANN	II
PREDIVAC	http://predivac.biosci.uq.edu.au/	PSSM	II
ProPred	http://crdd.osdd.net/raghava/propred/	QM	II
RTA	http://bordnerlab.org/RTA/	Regularized Thermodynamic Average	II
TEPITOPEpan	http://datamining-iip.fudan.edu.cn/service/TEPITOPEpan/TEPITOPEpan.html	PSSM	II
EpDis	http://bioinfo.matf.bg.ac.rs/home/downloads.waf!?cat=Software	NA	I and II
EpiMatrix	http://www.epivax.com/	Matrix-based and pocket Profile	I and II
EpiToolKit 2.0	http://epitoolkit.de/	Syfpeithi, BIMAS, SVMHC, SMM, SMMPMBEC, UniTope,	I and II

		NetMHC, NetMHCpan, NetMHCII, NetMHCIIpan, TEPITOPEpan.	
Epitopemap	http://dmnfarrell.github.io/epitopemap/	The Tepitope method is the Python implementation of TEPITOPEPan, NetMHCIIpan and IEDB MHCII	I and II
FRED	http://abi.inf.uni-tuebingen.de/Software/FRED/index.html	Machine learning method	I and II
HLAPRED	http://crdd.osdd.net/raghava/hlapred/	QM	I and II
Hotspot Hunter	http://antigen.i2r.a-star.edu.sg/hh/	ANN and SVM	I and II
MetaMHC	http://www.biokdd.fudan.edu.cn/Service/MetaMHC.html	Local Alignment (LA) kernel	I and II
MHCbench	http://crdd.osdd.net/raghava/mhcbench/	Evaluate and compare the performance of the old/new prediction methods in terms of the threshold dependent and independent parameters	I and II
MHC-BPS	http://bidd.cz3.nus.edu.sg/mhc/	SVM	I and II
MHCcluster 2.0	http://www.cbs.dtu.dk/services/MHCcluster/	Based on predicted binding specificity. MHC class I peptide binding predictions using NetMHCpan, and MHC class II peptide binding predictions using NetMHCIIpan	I and II
MHCpred	http://www.ddg-pharmfac.net/mhcpred/MHCpred/	QSAR	I and II
MOTIF SCAN	http://www.hiv.lanl.gov/content/immunology/motif_scan/	Sequence Motifs	I and II
MULTIPRED2	http://cvc.dfci.harvard.edu/multipred2/HTML/prediction2.php	netMHCpan and netMHCIIpan (ANN and HMM)	I and II
nHLApred	http://crdd.osdd.net/raghava/nhlapred/comp.html	ANN and QM	I and II
OptiTope	http://etk.informatik.uni-tuebingen.de/optitope	Designing epitope-based vaccines by assessing the immunogenicity	I and II
PepCrawler	http://bioinfo3d.cs.tau.ac.il/PepCrawler/about.html	Docking and structure modelling	I and II
PickPocket 1.1	http://www.cbs.dtu.dk/services/PickPocket/	Position specific weight matrix (SMM)	I and II
POPI2.0	http://iclab.life.nctu.edu.tw/POPI/	SVM	I and II
POPI2.0	http://iclab.life.nctu.edu.tw/POPI/	QM	I and II
PREDBALB/c	http://cvc.dfci.harvard.edu/balbc/	QM	I and II
Predict	http://research.i2r.a-star.edu.sg/fimm	ANN	I and II
RANKPEP	http://imed.med.ucm.es/Tools/rankpep_help.html	PSSM or profile	I and II
SNEPV2	http://etk.informatik.uni-tuebingen.de/snep	SYFPEITHI, Bimas/HLA_Bind, Epidemix, SVMHC, UniTope, TEPITOPE, MHCIIIMulti	I and II

SVMHC	http://abi.inf.uni-tuebingen.de/Services/SVMHC	SVM	I and II
SVRMHC	http://c1.accurascience.com/SVRMHCdb/	SVR	I and II
SYFPEITHI	http://www.syfpeithi.de/	MM	I and II
TEpredict	http://tepredict.sourceforge.net/index.html	QM	I and II
Tmhcpred	http://www.imtech.res.in/raghava/tmhcpred/index.html	Virtual and QM	I and II
Vaxign	http://www.violinet.org/vaxign/	PSSM	I and II

Abbreviations: SMM: stabilized matrix method, SMMPMBEC: SMM with a Peptide: MHC Binding Energy Covariance matrix (SMMPMBEC), CombLib: Scoring Matrices derived from Combinatorial Peptide Libraries, QM: quantitative matrix, ANN: artificial network, PSSM: position specific scoring matrix, SDR: specificity-determining residue, SVRM: support vector machine regression, SVMOT: Support Vector Machine Optimization Technique, MM: Motif Matrix, ARB: Average relative binding, QSAR: Quantitative Structure Activity Relationship, HLA Peptide Binding Predictions: The Bioinformatics and Molecular Analysis Section of the National Institutes of Health (BIMAS), KISS: Kernel-based Inter-allele peptide binding prediction system, WAPP: Whole Antigen Processing Pathway. NA: Not available.

Appendices Chapter 4:

Supplementary Table 4.1 Percentage conservation of the *T. muris* MHC-II T-cell epitopes ($\text{CLSP}_{222-237}$, $\text{CLSP}_{433-450}$, $\text{CLSP}_{143-158}$, $\text{CLSP}_{424-443}$) to homologous *T. trichiura* proteins.

Epitope	Peptide sequence	<i>T. trichiura</i> homology proteins											
		A0A07 7Z1C2	A0A07 7ZKH1	A0A07 7ZLU4	A0A07 7YXV1	A0A07 7Z5M9	A0A07 7ZGC 8	A0A07 7ZDL8	A0A07 7ZLQ9	A0A07 7Z2Z8	A0A07 7YX43	A0A07 7ZCD9	A0A07 7ZN47
$\text{CLSP}_{222-237}$	MEKKRKYLGSPLVCF	47	47	47	40	47	47	40	40	60	33	73	47
	EKKRKYLGSPLVCFV	53	53	53	47	47	53	47	40	60	40	80	53
$\text{CLSP}_{433-450}$	AKSKLRLVYAGSPRFS	80	33	33	33	80	80	47	40	47	27	33	80
	KSKLRLVYAGSPRFSR	80	40	33	33	87	87	47	33	47	27	33	87
	SKLRLVYAGSPRFSRI	73	33	27	33	87	87	40	33	47	27	33	87
	KLRVYAGSPRFSRIR	67	33	27	27	87	87	40	33	47	27	27	87
$\text{CLSP}_{143-158}$	AIIQLAKPVPSNTV	40	40	27	80	40	40	40	27	33	27	40	27
	ILQLAKPVPSNTVR	33	40	27	80	33	33	33	27	33	27	33	27
$\text{CLSP}_{398-416}$	SDHQEGYPVSPSVHI	27	27	33	87	33	33	33	33	40	27	33	33

	DHQEGYPVSPSVHIV	27	27	33	87	33	33	33	33	27	40	33
	HQEGLPVSPSVHIVS	27	27	33	87	33	33	33	33	27	40	33
	QEGYPVSPSVHIVSL	33	27	33	87	33	33	33	27	40	27	40
	EGYPVSPSVHIVSLA	33	27	33	93	27	33	33	27	40	27	33
CLSP ₄₂₄₋₄₄₃	CTGSLYASARANFTR	40	27	27	73	33	27	40	33	33	27	27
	TGSLYASARANFTRT	33	33	27	73	40	27	40	27	33	27	27
	GSLYASARANFTRTV	40	40	27	73	33	27	40	27	33	27	27
	YASARANFTRTVLTS	40	40	27	73	27	33	33	27	27	33	27

Supplementary Table 4.2 Percentage conservation of the *T. muris* MHC-II T-cell epitopes (CBD₃₆₋₅₂ and CBD₁₂₄₃₋₁₂₅₉) to homologous *T. trichiura* proteins.

Epitope	Peptide sequence	<i>T. trichiura</i> homology proteins					
		A0A077ZFY4	A0A077ZC62	A0A077Z8B3	A0A077Z3K5	A0A077Z111	A0A077ZFK2
CBD ₃₆₋₅₂	RPRLLKIKWSPTAAS	33	27	33	100	47	33
	PRLLKIKWSPTAAST	33	27	33	93	47	33
	RLLKIKWSPTAASTA	33	27	33	87	47	33
CBD ₁₂₄₃₋₁₂₅₉	PAGVVYQCTMPRYTL	87	33	27	33	33	33
	AGVVYQCTMPRYTLC	86	26	33	33	33	26
	GVVVYQCTMPRYTLCV	80	26	33	33	33	26

Supplementary Table 4.3 Percentage conservation of the *T. muris* MHC-II T-cell epitope (CBD₂₄₁₋₂₅₇) to homologous *T. trichiura* proteins.

Peptide sequence	<i>T. trichiura</i> homology proteins					
	O44397	Q27087	A0A077ZJX5	Q7KPx3	A0A077YWQ4	A0A077YYJ8
GRTTPVTSAPTTVTT	40.00	33.33	100.00	46.67	26.67	33.33
RTTPVTSAPTTVTTE	40.00	33.33	93.33	46.67	26.67	33.33
TPPVTSAPTTVTTER	33.33	33.33	86.67	46.67	26.67	33.33

Supplementary Table 4.4 Percentage conservation of the *T. muris* MHC-II T-cell epitope (Pfam₂₅₆₋₂₇₃) to homologous *T. trichiura* proteins.

Peptide sequence	<i>T. trichiura</i> homology proteins									
	A0A077 ZFC1	A0A077 ZQ60	A0A077 ZKA9	A0A077 ZEX9	A0A077 Z7Q4	A0A077 ZIP6	A0A077 ZF51	A0A077 ZGQ3	A0A077 ZIE1	A0A077 ZH26
NFGEYWFTKPVGSVS	73	73	73	80	73	73	73	73	73	60
FGEYWFTKPVGSVSY	73	73	73	80	80	80	80	80	80	67
GEYWFTKPVGSVSYK	67	67	67	73	73	73	73	73	73	60
EYWFTKPVGSVSYKV	67	67	67	73	67	67	67	67	67	53

Supplementary Table 4.5 Percentage conservation of the predicted *T. muris* MHC-II T-cell epitope (H₁₁₂₋₁₂₈) to homologous *T. trichiura* proteins.

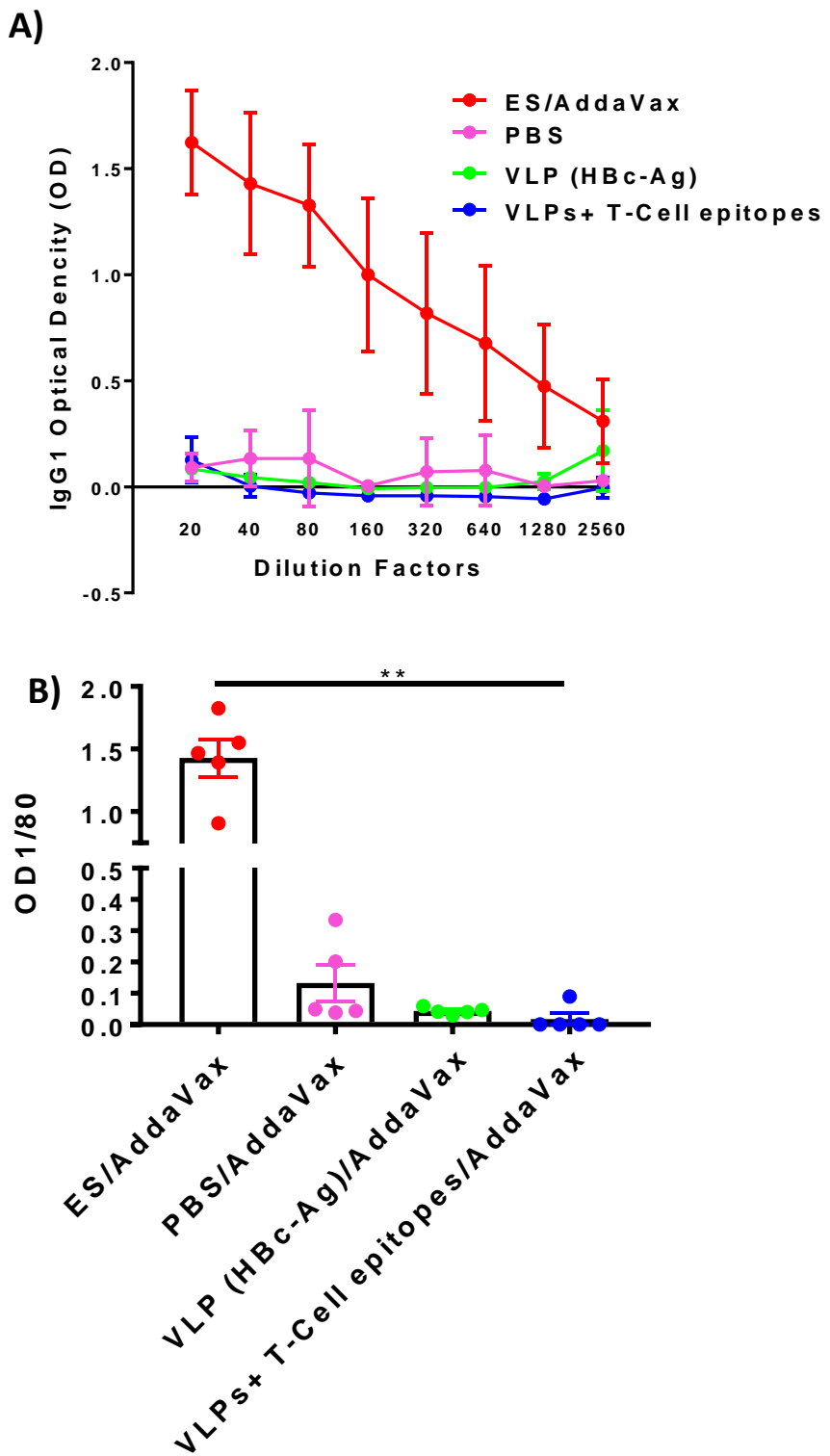
Peptide sequence	<i>T. trichiura</i> homology proteins							
	A0A077Z2Q3	A0A077YYY3	A0A077Z3K3	A0A077ZN82	A0A077ZDH0	A0A077ZE95	A0A077ZIB0	A0A077ZMB7
GARKFLPIYQKAVAE	87	87	87	87	87	87	87	87
ARKFLPIYQKAVAE	87	87	87	87	87	73	87	87
RKFLPIYQKAVAEK	86	86	86	86	86	73	86	86

Appendices Chapter 7:

Appendix 7.1 Serum parasite-specific responses following vaccination of mice with VLPs expressing *Trichuris* T-cell epitopes

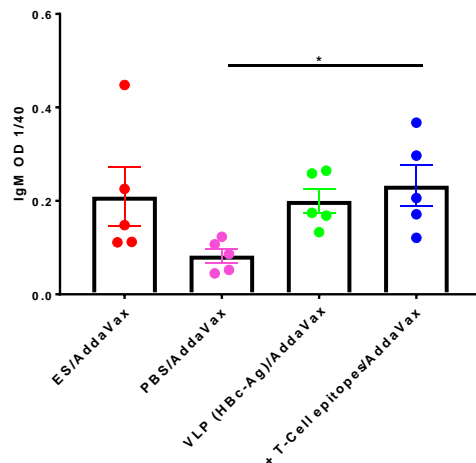
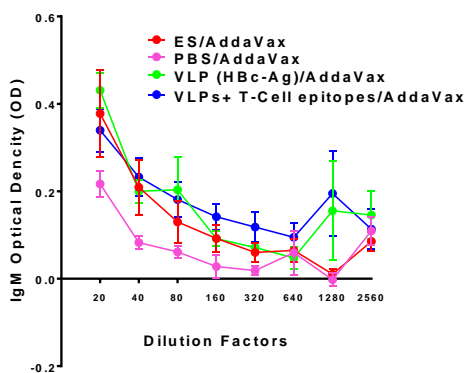
To analyse parasite-specific antibody (IgM, IgG1, and IgG2c) responses of mice vaccinated with (HBc-H₁₁₂₋₁₂₈, HBc-CLSP₁₄₃₋₁₅₈, HBc-CLSP₃₉₈₋₄₁₆ and HBc-CBD₂₄₁₋₂₅₇)/AddaVax, serial dilutions of mice serum were assessed using an ELISA-based assay with ES as a target antigen at day -1 and day 14 p.i. Parasite-specific IgG1 levels were only detected in the serum of mice vaccinated with ES/AddaVax prior to *Trichuris* infection, as shown in Supplementary Figure 7.1.

Following vaccination and *Trichuris* infection, negligible levels of parasite-specific IgM were detected in the serum of mice vaccinated with VLPs+ T-cell epitopes/AddaVax with a significant difference compared to the PBS/AddaVax injected mice (Supplementary Figure 7.2 A). Furthermore, ES vaccinated mice activated both Th1/Th2 immune responses as significant high levels of parasite-specific IgG2c/IgG1 were measured in mice sera (Supplementary Figure 7.2 B and C). However, no parasite-specific IgG1 and IgG2c antibodies were detected in the sera of mice vaccinated with PBS/AddaVax, VLP (HBc-Ag)/AddaVax and VLPs+ T-cell epitopes/AddaVax groups, as shown in Supplementary Figure 7.2 (B) and (C).

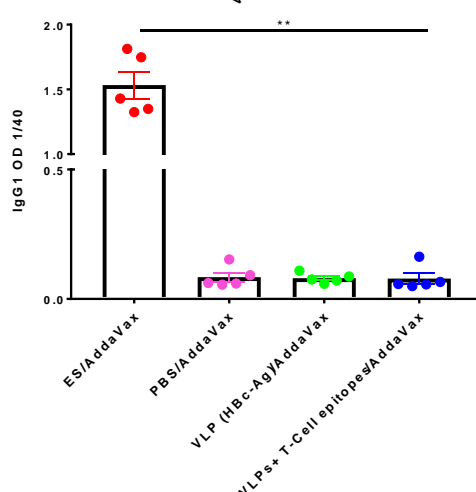
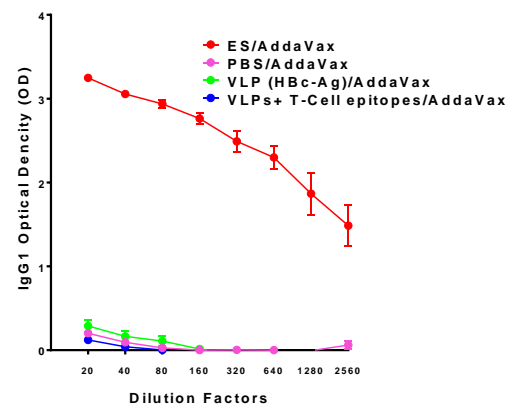


Supplementary Figure 7.1 Parasite-specific IgG1 serum antibody levels at day -1. 6-week old male C57BL/6 mice were vaccinated subcutaneously with 25 µg of pre-mixed of VLPs+ T-cell epitopes (HBc-H₁₁₂₋₁₂₈, HBc-CLSP₁₄₃₋₁₅₈, HBc-CLSP₃₉₈₋₄₁₆ and HBc-CBD₂₄₁₋₂₅₇) formulated with AddaVax™ adjuvant, 25 µg of VLP (HBc-Ag)/AddaVax, 50 µg ES/AddaVax, or PBS/AddaVax on day -35 and boosted on day -14. Mice were infected by oral gavage with approximately 150 infective *T. muris* eggs and sacrificed at d14. Day 14 sera were titrated against *T. muris* ES antigens to assess parasite-specific IgG1 Serum antibodies levels were measured for each mouse by ELISA (reading at 405 nm). Statistical analyses were carried out at 1:80 serum dilutions out using the Kruskal-Wallis test (multiple comparisons). Significant differences between groups are represented by (**P≤0.01) with a line. Results are shown as mean ± SEM. n= 5 mice per group. The results presented are from one experiment.

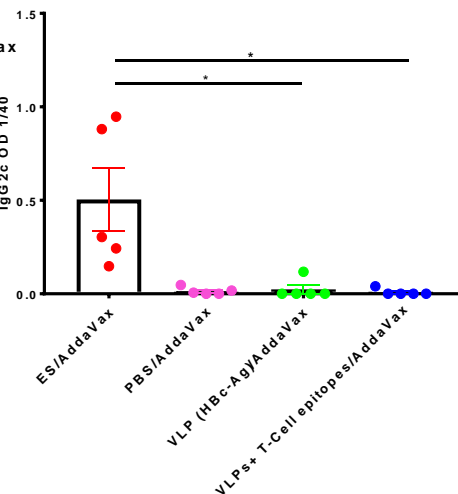
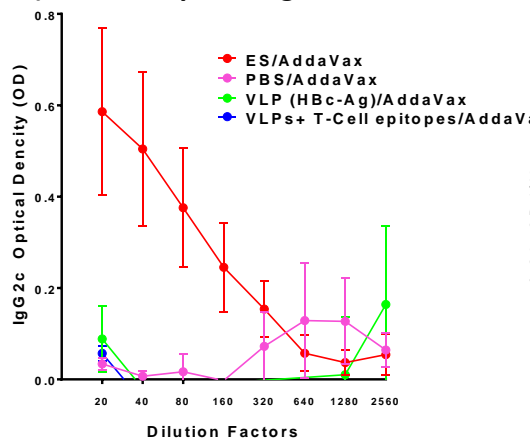
A) Parasite-specific IgM



B) Parasite-specific IgG1



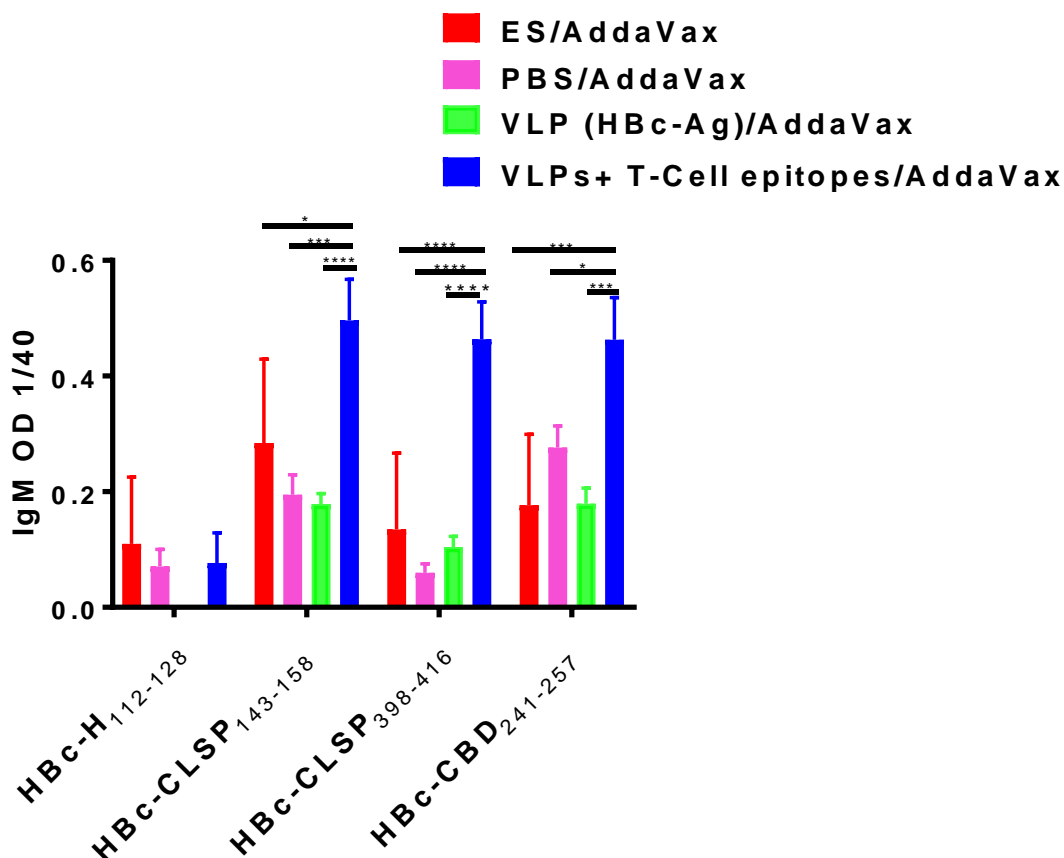
C) Parasite-specific IgG2c



Supplementary Figure 7.2 Parasite-specific IgM, IgG1 and IgG2c serum antibodies levels at day 14 post-infection. 6-week old male C57BL/6 mice were vaccinated subcutaneously with 25 µg of pre-mixed of VLPs+ T-cell epitopes (HBc-H₁₁₂₋₁₂₈, HBc-CLSP₁₄₃₋₁₅₈, HBc-CLSP₃₉₈₋₄₁₆ and HBc-CBD₂₄₁₋₂₅₇) formulated with AddaVax™ adjuvant, 25 µg of VLP (HBc-Ag)/AddaVax, 50 µg ES/AddaVax, or PBS/AddaVax on day -35 and boosted on day -14. Mice were infected by oral gavage with approximately 150 infective *T. muris* eggs and sacrificed at d14 post-infection. Day 14 sera were titrated against *T. muris* ES antigens to assess parasite-specific IgM (A), IgG1 (B), and IgG2c (C) by ELISA (reading at 405 nm). Statistical analyses were carried out at 1:20 (IgM and gG2c) and 1:40 (IgG1) serum dilutions using the Kruskal-Wallis test (multiple comparisons). Significant differences between groups are represented by (*P≤0.05, **P≤0.01) with a line. Results are shown as mean ± SEM. n= 5 mice per group. The results presented are from one experiment.

Appendix 7.2 Serum VLP+ T-cell epitope-specific responses following vaccination of mice with VLPs expressing *Trichuris* T-cell epitopes

To analyse VLPs+ T-cell epitopes specific-IgM antibody responses of vaccinated mice, serial dilutions of mice sera were assessed using an ELISA-based assay against pre-mixed VLPs+ T-cell epitopes (HBc-H₁₁₂₋₁₂₈, HBc-CLSP₁₄₃₋₁₅₈, HBc-CLSP₃₉₈₋₄₁₆ and HBc-CBD₂₄₁₋₂₅₇) as target antigens. Significantly higher levels of HBc-CLSP₁₄₃₋₁₅₈, HBc-CLSP₃₉₈₋₄₁₆ and HBc-CBD₂₄₁₋₂₅₇-specific IgM were measured in the sera of mice vaccinated with VLPs+ T-cell epitopes/AddaVax compared to the ES/AddaVax, PBS/AddaVax and VLP (HBc-Ag)/AddaVax immunised mice, groups, day 14 p.i. In contrast, only negligible levels of HBc-H₁₁₂₋₁₂₈-specific IgM were detected in the sera of vaccinated mice groups, as shown in Supplementary Figure 7.3. Furthermore, only background levels of VLPs+ T-cell epitopes-specific IgM levels were detected in the sera of mice immunised with ES/AddaVax, PBS/AddaVax and VLP (HBc-Ag)/AddaVax.



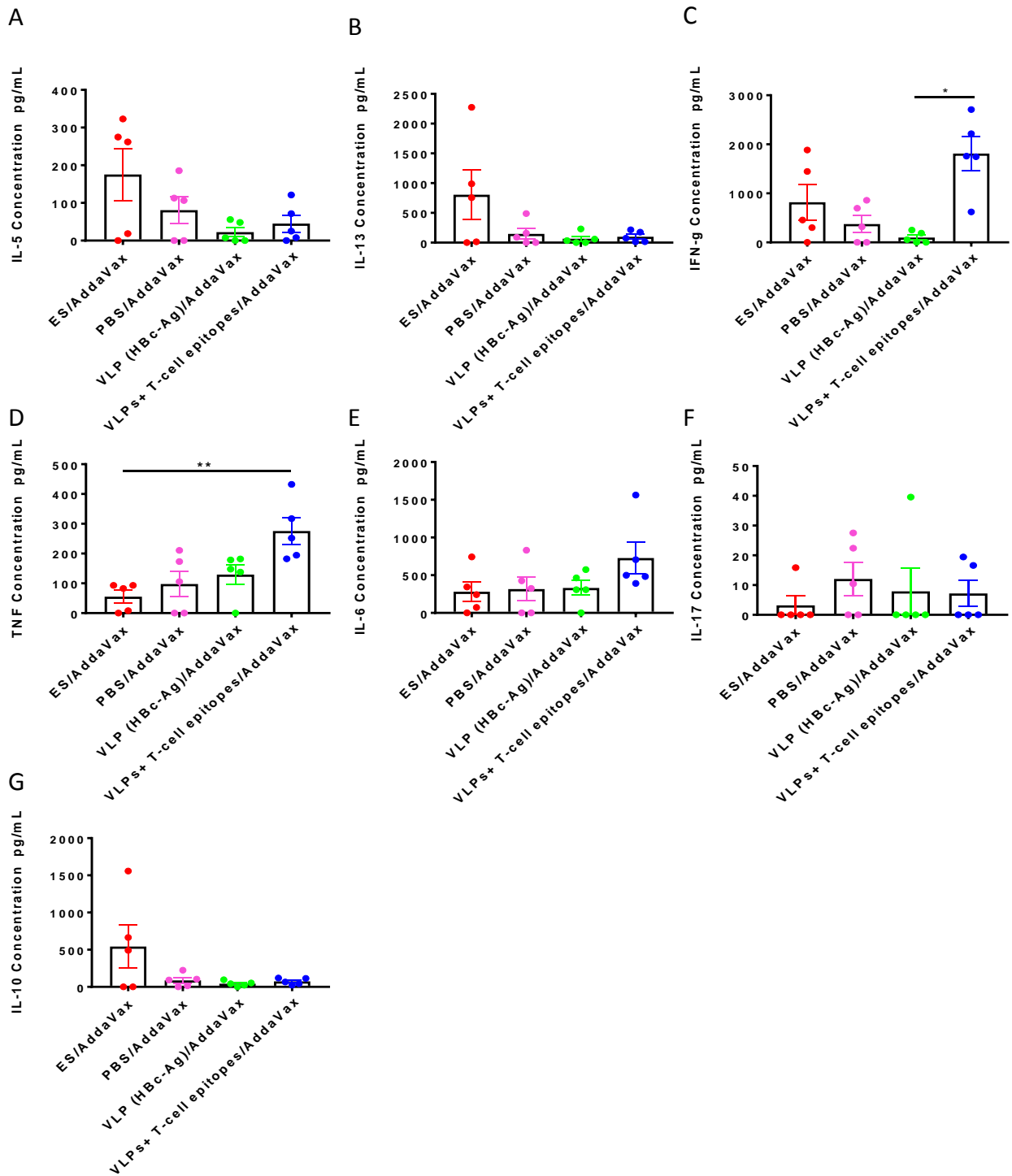
Supplementary Figure 7.3 VLPs-specific IgM serum antibody levels at day 14 post-infection. 6-week old male C57BL/6 mice were vaccinated subcutaneously with 25 µg of pre-mixed of VLP+ T cell epitopes (HBc-H₁₁₂₋₁₂₈, HBc-CLSP₁₄₃₋₁₅₈, HBc-CLSP₃₉₈₋₄₁₆ and HBc-CBD₂₄₁₋₂₅₇) formulated with AddaVax™ adjuvant, 25 µg of VLP (HBc-Ag)/AddaVax, 50 µg ES/AddaVax, or PBS/AddaVax on day -35 and boosted on day -14. Mice were infected by oral gavage with approximately 150 infective *T. muris* eggs and sacrificed at d14 post-infection. Day 14 sera were titrated against VLPs+ T-cell epitopes proteins (HBc-Ag, HBc-H₁₁₂₋₁₂₈, HBc-CLSP₁₄₃₋₁₅₈, HBc-CLSP₃₉₈₋₄₁₆ and HBc-CBD₂₄₁₋₂₅₇) to assess VLPs specific IgM levels measured by ELISA (reading at 405 nm). Statistical analyses were carried out at 1:40 serum dilutions using Two-way ANOVA (multiple comparisons). Significant differences between groups are represented by (*P≤0.05, **P≤0.01, ***P≤0.001, ****P≤0.0001) with a line. Results are shown as mean ± SEM. n= 5 mice per group. The results presented are from one experiment.

Appendix 7.3 The cellular immune responses following vaccination of mice with VLPs expressing *Trichuris* T-cell epitopes and infection

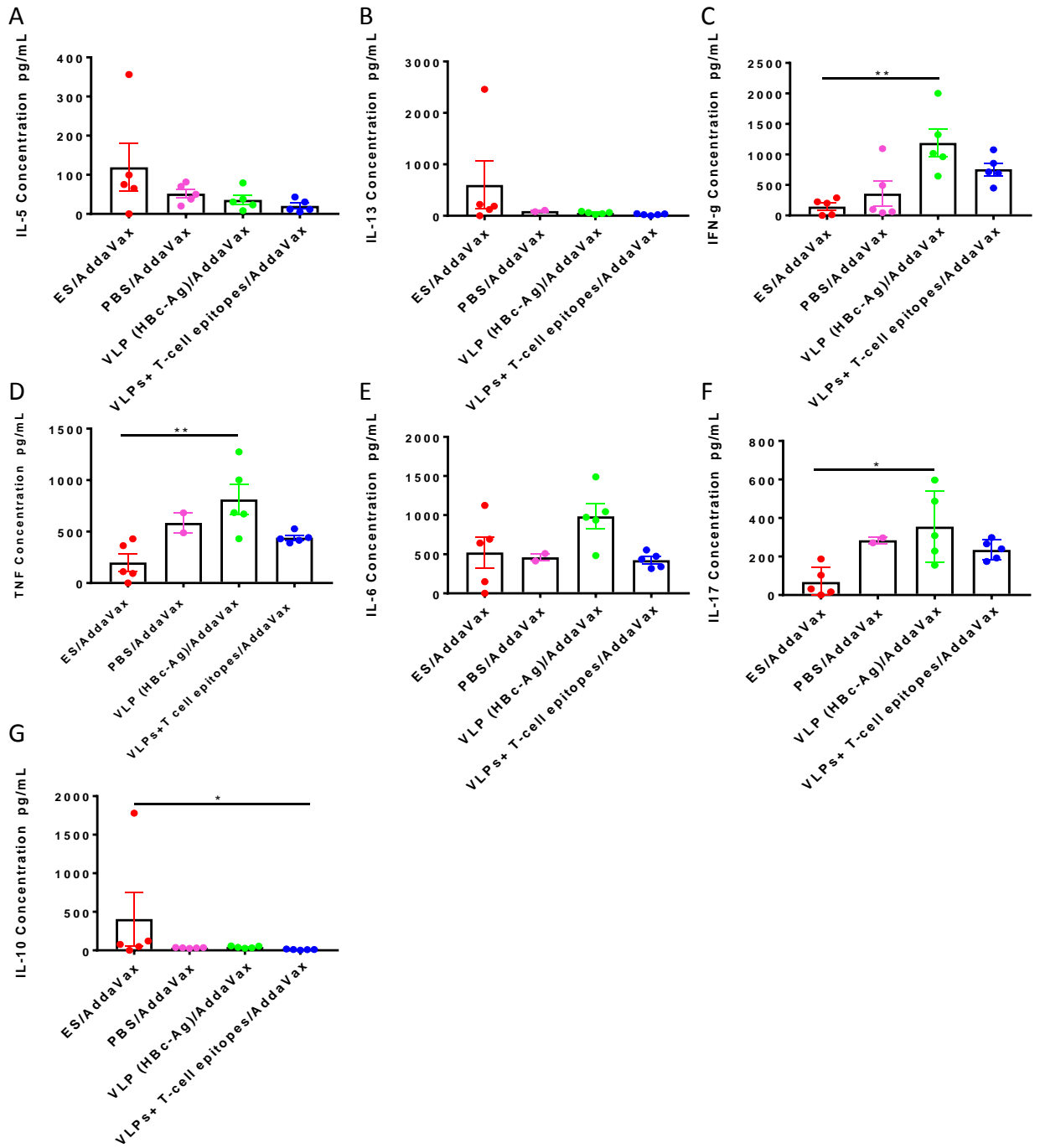
To analyse the cellular immune responses of mice vaccinated with VLPs+ T-cell epitopes/AddaVax compared to control ES/AddaVax, PBS/AddaVax and VLP (HBc-Ag)/AddaVax immunised mice groups after *T. muris* infection, MLN cells were re-stimulated *in vitro* with 4 hours ES for 48 hours and with ConA for 24 hours. As readout of cell activation, the supernatants were analysed for the concentrations of IL-5, IL-13, IFN- γ , TNF, IL-6, IL-17, and IL-10 cytokines production by CBA.

Only MLN cells from ES/AddaVax vaccinated mice released higher levels of IL-5 (Supplementary Figure 7.4 A), IL-13 (B) and IL-10 (G) compared to the VLPs+ T-cell epitopes/AddaVax, VLP (HBc-Ag)/AddaVax and PBS/AddaVax immunised mice upon their re-stimulation *in vitro* with ES antigens. In contrast, re-stimulated MLN cells taken from VLPs+ T-cell epitopes/AddaVax vaccinated mice day 14 p.i. produced significantly higher levels of IFN γ (Supplementary Figure 7.4 C), TNF (D) and IL-6 (E) compared to the ES/AddaVax, PBS/AddaVax, and VLP (HBc-Ag)/AddaVax immunised mice groups. Furthermore, there was no difference between the level of IL-17 in all immunised mice groups ($P>0.05$), as shown in Supplementary Figure 7.4 (F).

Similar results were seen when the MLN cells from all immunised mice groups were re-stimulated *in vitro* with ConA. Only MLN cells from ES/AddaVax vaccinated mice produced higher levels of Th2 cytokines (IL-5 and IL-13) and anti-inflammatory cytokine (IL-10) compared to the other immunised mice groups (Supplementary Figure 7.5 A, B and G). However, high levels of IFN- γ (Supplementary Figure 7.5 C), TNF (D), IL-6 (E) and IL-17 (F) were seen on the re-stimulated MLN cells taken from mice immunised with native VLP (HBc-Ag)/AddaVax compared to the other immunised mice groups.



Supplementary Figure 7.4 Parasite-specific cytokine production by mesenteric lymph node cells from mice vaccinated with VLPs+ T-cell epitopes and control mice. MLNs from mice vaccinated with 25 µg of pre-mixed of VLPs+ T-cell epitopes (HBc-H₁₁₂₋₁₂₈, HBc-CLSP₁₄₃₋₁₅₈, HBc-CLSP₃₉₈₋₄₁₆ and HBc-CBD₂₄₁₋₂₅₇) formulated with AddaVax™ adjuvant, 25 µg of VLP (HBc-Ag)/AddaVax, 50 µg ES/AddaVax, or PBS/AddaVax on day -35 and boosted on day -14 were stimulated at 5x10⁶/ml with 50 µg/ml *T. muris* ES. After 48 hours of stimulation, cell culture supernatants were harvested and assayed by cytometric bead array for IL-5 (A), IL-13 (B), IFN-g (C), TNF (D), IL-6 (E), IL-17 (F) and IL-10 (G) production. Statistical analyses were carried out using the Kruskal-Wallis test (multiple comparisons). Significant differences between groups are represented by (*P≤0.05, **P≤0.01) with a line. Results are shown as mean ± SEM. n= 5 mice per group. The results presented are from one experiment.

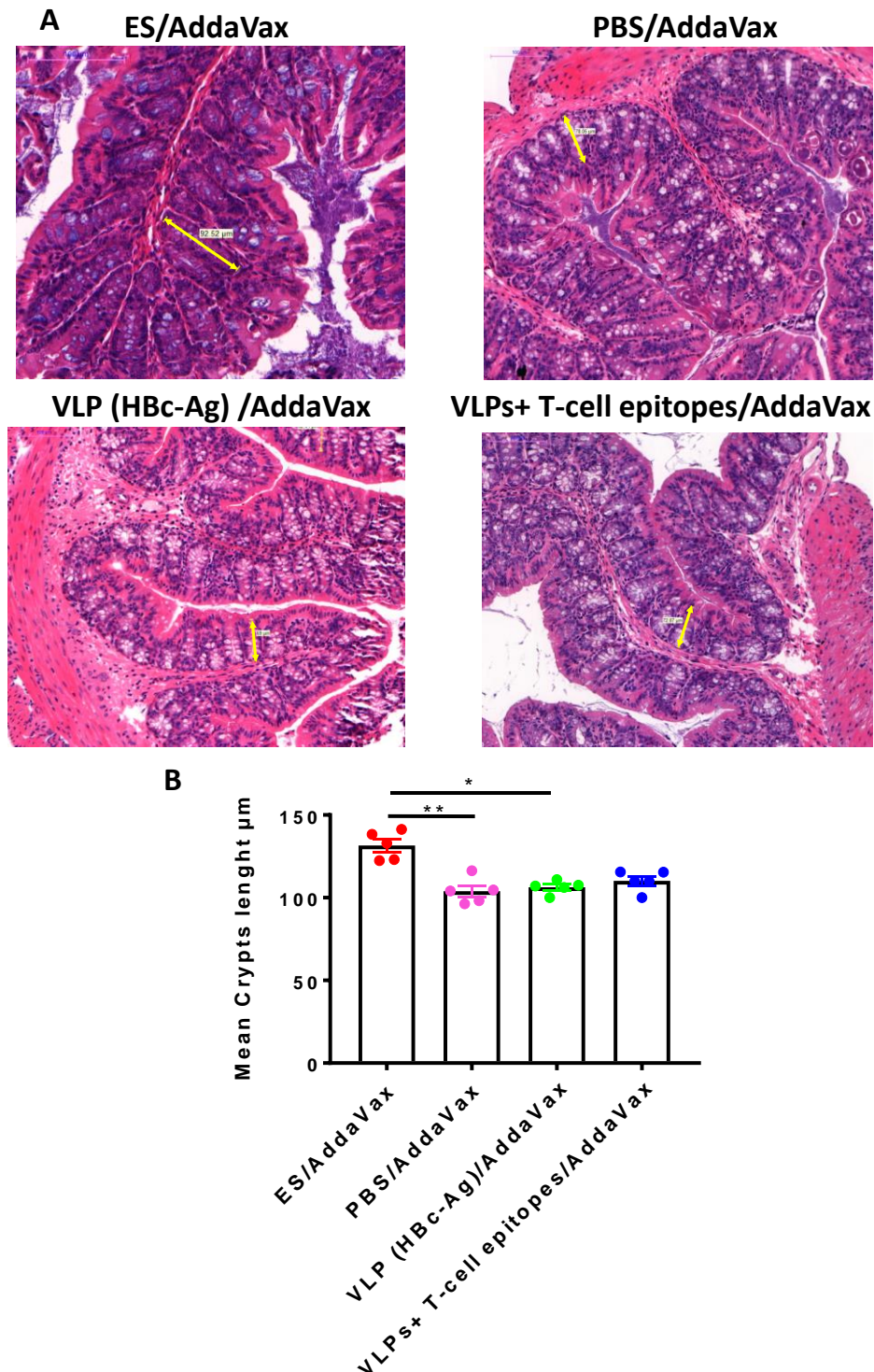


Supplementary Figure 7.5 Cytokine production by mesenteric lymph node cells from mice vaccinated with VLPs+ T-cell epitopes and control mice. MLNs from mice vaccinated with 25 µg of pre-mixed of VLPs+ T-cell epitopes (HBc-H₁₁₂₋₁₂₈, HBc-CLSP₁₄₃₋₁₅₈, HBc-CLSP₃₉₈₋₄₁₆ and HBc-CBD₂₄₁₋₂₅₇) formulated with AddaVax™ adjuvant, 25 µg of VLP (HBc-Ag)/AddaVax, 50 µg ES/AddaVax, or PBS/AddaVax on day -35 and boosted on day -14 were stimulated at 5x10⁶/ml with 5 µg/ml ConA. After 24 hours of stimulation, cell culture supernatants were harvested and assayed by cytometric bead array for IL-5 (A), IL-13 (B), IFN-g (C), TNF (D), IL-6 (E), IL-17 (F) and IL-10 (G) production. Statistical analyses were carried out using the Kruskal-Wallis test (multiple comparisons). Significant differences between groups are represented by (*P≤0.05, **P≤0.01) with a line. Results are shown as mean ± SEM. n= 5 mice per group. The results presented are from one experiment.

Appendix 7.4 Crypt hyperplasia following vaccination of mice with VLPs expressing *Trichuris* T-cell epitopes

The length of colonic crypts was measured day 14 p.i. in ES/AddaVax, PBS/AddaVax, VLP (HBc-Ag)/AddaVax and VLPs+ T-cell epitopes/AddaVax immunised mice groups following *Trichuris* infection as an index of crypt hyperplasia (Supplementary Figure 7.6 A).

Following a *Trichuris* infection, ES/AddaVax vaccinated mice exhibited crypt hyperplasia with a significant difference compared to the PBS/AddaVax, and VLP (HBc-Ag)/AddaVax injected mice groups ($P<0.05$), as shown in Supplementary Figure 7.6 (B).

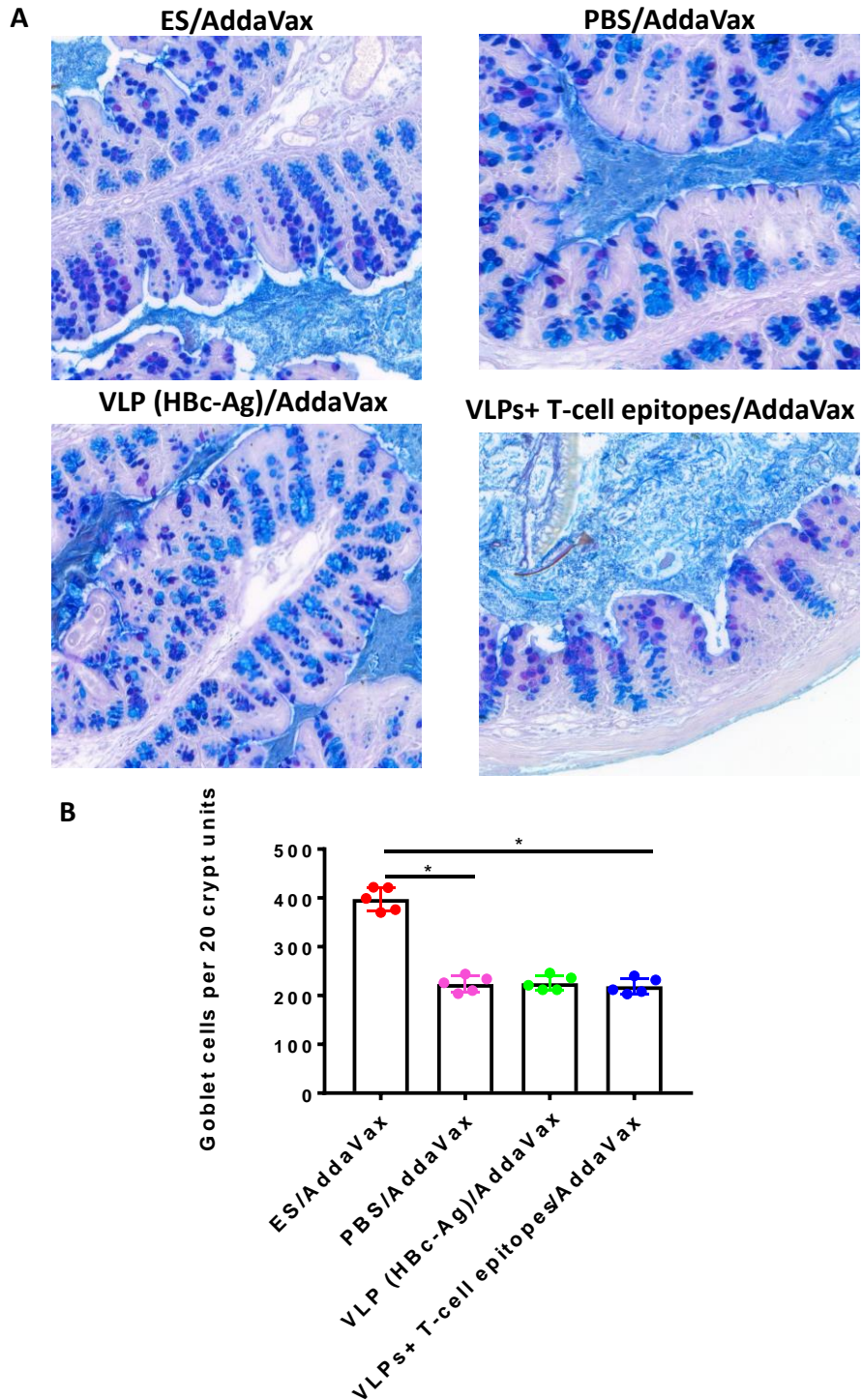


Supplementary Figure 7.6 Changes in intestinal pathology in *T. muris* infected mice vaccinated with VLPs+ T-cell epitopes and control mice. (A) Representative photographs of gut sections stained with hematoxylin and eosin (H&E). Proximal colon was harvested from mice vaccinated with 25 µg of pre-mixed VLPs+ T-cell epitopes (HBc-H₁₁₂₋₁₂₈, HBc-CLSP₁₄₃₋₁₅₈, HBc-CLSP₃₉₈₋₄₁₆ and HBc-CBD₂₄₁₋₂₅₇) formulated with AddaVax™ adjuvant, 25 µg of VLP (HBc-Ag)/AddaVax, 50 µg ES/AddaVax, or PBS/AddaVax on day -35 and boosted on day -14. All photographs were taken with 20X magnification. Gut pathology assessed by measuring crypt lengths using Panoramic Viewer software. The yellow double-headed arrows show how the crypt lengths were measured. Results are shown as mean crypt length from 20 crypts units per mouse and shown as the mean values per mouse ± SEM. Statistical analyses were carried out using the Kruskal-Wallis test (multiple comparisons). Significant differences between groups are represented by (**P≤0.01, ***P≤0.001) with a line. n= 5 mice per group. The results presented are from one experiment.

Appendix 7.5 Goblet cells hyperplasia in mice vaccinated with VLPs expressing *Trichuris* T-cell epitopes

PAS-stained goblet cells were measured in the mice vaccinated with ES/AddaVax, PBS/AddaVax, VLP (HBc-Ag)/AddaVax and VLPs+ T-cell epitopes/AddaVax day 14 p.i. as an index of goblet cells hyperplasia (Supplementary Figure 7.7 A).

Only ES/AddaVax vaccinated mice exhibited goblet cells hyperplasia with a significant difference ($P<0.05$) compared to the mice vaccinated with VLPs+ T-cell epitopes/AddaVax, and PBS/AddaVax injected mice, as shown in Supplementary Figure 7.7 (B).



Supplementary Figure 7.7 Quantification of goblet cell numbers in *T. muris* infected mice vaccinated with VLPs+ T-cell epitopes and control mice. (A) Representative photographs of gut sections stained with Periodic acid-Schiff staining (PAS). Proximal colon was harvested from mice vaccinated with 25 µg of pre-mixed of VLPs+ T-cell epitopes (HBc-H₁₁₂₋₁₂₈, HBc-CLSP₁₄₃₋₁₅₈, HBc-CLSP₃₉₈₋₄₁₆ and HBc-CBD₂₄₁₋₂₅₇) formulated with AddaVax™ adjuvant, 25 µg of VLP (HBc-Ag)/AddaVax, 50 µg ES/AddaVax, or PBS/AddaVax on day -35 and boosted on day -14. The slides were scanned, and the goblet cells were quantified using Panoramic Viewer software. All photographs were taken with 20X magnification. (B) Goblet cells were quantified by counting the number of alcian blue-stained cells per crypt unit in three fields of view from each section and are shown as mean cell numbers per 20 crypt units (cu) ±SEM. Statistical analyses were carried out using the Kruskal-Wallis test (multiple comparisons). Significant differences between groups are represented by (*P≤0.05) with a line. n= 5 mice per group. The results presented are from one experiment.